# FINITE ELEMENT ANALYSIS
OF
PILED FOUNDATIONS

A Thesis Submitted
In Partial Fulfilment of the Requirements
for the Degree of

DOCTOR OF PHILOSOPHY

by

S. L. NARASIMHAN

to the
DEPARTMENT OF CIVIL ENGINEERING
INDIAN INSTITUTE OF TECHNOLOGY KANPUR
SEPTEMBER, 1982
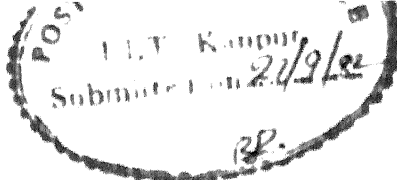
CERTIFICATE

This is to certify that the thesis 'Finite Element Analysis of Piled Foundations' submitted by Shri S.L. Narasimhan in partial fulfilment of the requirements for the Degree of Doctor of Philosophy of the Indian Institute of Technology, Kanpur is a record of bonafide research work carried out under my supervision and guidance. The work embodied in this thesis has not been submitted elsewhere for the award of a degree.

September, 1982

(N.S.V. KAMESWARA RAO)
PROFESSOR
DEPARTMENT OF CIVIL ENGINEERING
INDIAN INSTITUTE OF TECHNOLOGY
KANPUR

CE -1982-D-NAR

ACKNOWLEDGEMENTS

CONTENTS

LIST OF TABLES

LIST OF FIGURES

...

NOMENCLATURE

A - Area of annulus containing piles

A_p - Total area of cross section of piles in the annulus

a - Radius of footing/plate/raft. Also outer radius of superstructure

a' - Outer radius of raft (Chapter 6)

C, C_o - Cohesion

C_a - Adhesion between pile and soil

C_u - Undrained shear strength (cohesion)

C_{uo} - Undrained shear strength (cohesion) at ground level ($C_{uo} = C_u$ for homogeneous soil)

C_{uL} - Undrained shear strength (cohesion) at depth $= L$.

CPU   - Central processing unit in computer

CR   - This suffix denotes completely adhesive contact

CSS   - This suffix denotes completely smooth contact

d - Diameter of pile. Also dia.of loaded area for conc.load

d_b Diameter of enlarged base at tip of pile

d_c - Diameter of footing/raft. Also diameter of equivalent cap in pile-raft with square configuration.

E_p - Young's modulus of pile/plate material

E_{peq} - Young's modulus of annulus representing piles

E_R - Young's modulus of raft material

E_r - Young's modulus near pile due to the effect of installation

E_S, E_S' — Young's modulus of soil (undrained and drained)

E_{sa} — Young's modulus of soil at depth $Z = a$, below G.L.

E_{SH}, E_{SH}' — Young's modulus in the horizontal plane (undrained and drained).

E_{SL} — Young's modulus of soil at depth $Z = L$, below ground level

E_{SO} — Young's modulus of soil at ground level

E_{SS} — Young's modulus of superstructure material

E_{ST}, E_{SB} — Young's modulus of top and bottom soil layer

E_{SV}, E_{SV}' — Young's modulus of soil in vertical plane (undrained and drained)

f_R^* — Maximum radial in-plane stress in raft/footing

f_T^* — Maximum tangential in-plane stress in raft/footing

G_{SV}, G_{SV}' — Vertical shear modulus of soil (undrained and drained)

H — Total thickness of soil layer in finite element model.

h — Thickness of top soil layer in two layer soil medium.

I_{ij} — Settlement of ith unit due to load on jth unit

I_{max} — Maximum number of iterations specified

I_{MR} — Bending moment influence factors (radial)

I_{MT} — Bending moment influence factors (tangential)

I_R^* - Maximum settlement of circular raft under unit pressure

I_{RR} - Settlement of rigid circular footing under unit load.

I_S - Settlement influence factor

I_S^* - Maximum settlement influence factor

I_o - Case without considering effect of installation (homogeneous)

I_o^* - Settlement influence factor for in compressible pile in semiinfinite soil ($\nu_S = 0.5$)

I_1, I_4 - Case considering the effect of installation of bored pile in stiff clay.

I_2, I_5 - Case considering the effect of installation of driven pile in soft clay

I_3 - Case considering the effect of installation of driven pile in loose sand.

I_Δ - Differential settlement influence factor

$[I_i]$ - Interaction factor matrix (flexibility matrix) for ith linear portion

$[I_{PR}]$ - Flexibility matrix of the system for pile-raft action

$[I_R]$ - Flexibility matrix of the system for raft action

K - Pile stiffness factor (E_p/E_S)

K_B - Pile stiffness factor (E_p/E_{SB})

K_R - Relative rigidity of footing/raft/equivalent cap

K_T - Pile stiffness factor (E_p/E_{ST})

K_o - Coefficient of earth pressure at rest

k_n - Normal stiffness at interface

k_s — Shear stiffness at interface

L — Length of pile/piles/skirt

l/b — Aspect ratio (vertical dimension(1)/horizontal dimension (b))

M — Number of units in a pile group or pile-raft

M_H — Stress path gradient (σ'_V/σ'_H) from undrained triaxial tests on horizontal sample

M_R — Radial bending moment at distance r from centre

M^* — Maximum bending moment

$M^*_{I_n}$ — Maximum bending moment for Case I_n.

M^*_{PR} — Maximum bending moment in piled circular footing

M^*_R — Maximum bending moment in circular footing (Chapter 2). Also maximum radial bending moment (other Chapters)

M_T — Tangential bending moment at distance r from centre

M^*_T — Maximum tangential bending moment

M_V — Stress path gradient (σ'_V/σ'_H) from undrained triaxial tests on vertical sample

m — Vertical shear modulus (G_{SV})/Young's modulus in vertical direction (E_{SV})

m' — Drained vertical shear modulus (G'_{SV})/Drained Young's modulus in vertical direction(E'_{SV})

N — No. of linear portion in the idealisation of non-linear response

NT — Total No. of blocks into which mesh is divided

n, n' — E_{SH}/E_{SV} and E'_{SH}/E'_{SV} respectively for cross anisotropic soil.

P	— Total applied load
PPL	— Percentage load shared by pile/piles
PTL	— Percentage load transmitted by end bearing
P_1	— Load level upto which system acts as piled circular footing
P_{max}^1	— Maximum load for first portion in bilinear idealisation
P_{jmax}^i	— Maximum load for ith linear portion for jth unit
p	— Contact pressure blow footing/raft
$\{p^i\}$	— Load vector for ith linear portion containing loads carried by individual pile/pile-cap units.
$\{P_{PR}\}$	— Load vector for pile-raft action
$\{P_R\}$	— Load vector for raft action
Q	— Shear force/unit length
Q_{PR}^*	— Maximum shear force in pile-circular footing
Q_R^*	— Maximum shear force in circular footing
Q_{ult}	— Ultimate bearing capacity
q	— Applied uniform pressure over the entire footing area for u.d.l. or over pile area for central column loading (concentrated load).
q_u	— Collapse pressure
q_1	— u.d.l. over a circle of radius a
q_2	— u.d.l. over annulus of inner and outer radius equal to 0.9a and a respectively

q_3 — Linearly increasing lateral pressure magnitude at a depth of 0.1a below the top of the vertical portion of the superstructure

R_G — Group reduction factor for pile group and pile-raft.

R_S — Settlement factor for pile group and pile-raft

r — Radial distance from centre line

r_1 — Radius of disturbed zone due to the effect of installation in the case of clayey soils

r_p — Radius of the pile

R_k — Correction factor for compressibility (single pile)

R_h — Correction factor for finite layer (single pile)

R_ν — Correction factor for Poisson's ratio (single pile)

S — Settlement at distance r from centre line

S^* — Maximum settlement

S_{PR}^* — Maximum settlement-piled circular footing/pile-raft

S_R^* — Maximum settlement of circular footing/raft

S_{1P} — Settlement of single pile under unit load

SR — This suffix denotes the case with smooth raft/footing base

SPH — This suffix denotes the case with smooth pile head

S_o — Denotes the case without considering superstructure

S_1 — Denotes the case considering the effect of super-structure.

s — Spacing between piles/pile-cap units

t — Thickness of footing/raft/plate

t_R — Thickness of raft (Chapter 6).

UBC   – Ultimate bearing capacity of pile

udl   – Denotes uniformly distributed load over entire footing area

Z   – Depth below ground level

α – Interaction factor

α_a – Adhesion factor (Ca/Cu) for pile-soil interface

β – Non-homogeneity factor (E_{Sa}/E_{SO})

γ – Unit weight of soil

Δ – Differential settlement

Δ_{PR} – Differential settlement of piled circular footing

Δ_R – Differential settlement of circular footing

δ_o – Settlement of rigid cap (pile group or pile-raft)

$\{\delta\}$ – Settlement vector for pile group or pile raft

η – U.B.C. of free standing piles/Applied load on pile-raft

ν_p – Poisson's ratio of footing/pile/plate material

ν_S – Poisson's ratio of soil

ν_S' – Poisson's ratio of soil (drained)

ν_{SH}, ν_{SH}' – Poisson's ratio (undrained and drained) relating horizontal strains for cross-anisotropic soil

ν_{SV}, ν_{SV}' – Poisson's ratio (undrained and drained) for effect of vertical strains on horizontal strains in cross anisotropic soil.

σ_m – Mean normal stress (σ_{oct})

σ_R, σ_θ - Radial and tangential normal stress

σ_x, σ_y, σ_z - Normal stresses in **x, y, z** directions.

τ_{rz} - Shear stress

τ_{oct} - Octahedral shear stress

$\varnothing$ - Angle of internal friction

γ - Non-homogeneity coefficient

SYNOPSIS

Provision of a pile at the centre of a circular footing considerably reduces the settlement and hence it is a possible alternative under certain circumstances. Also such a 'piled circular footing' forms a typical unit of pile-raft systems, and a detailed study of such a unit would indicate the behaviour of a general pile-raft. So a detailed analysis of such unit has been taken up in this work. In addition, the analysis of pile group/pile raft of certain geometrical configurations under different soil conditions has also been carried out. Axisymmetric finite element programs were developed and have been used for most of the work reported. For the analysis of pile groups and pile-rafts of square arrangement 'interaction factor method' has been used.

A 'condensation procedure' similar to 'substructure technique' was developed and implemented in the program. This procedure does not require use of auxiliary storage like tape and large problems can be solved with small core. A study of the axisymmetrical, isoparametric 8 noded element with parabolic variation of displacements was carried out to assess its performance in bending with

different types of loading and single layer of elements has
been shown to be adequate for wide range of parameters.
The same parabolic isoparameteric elements have been used to
model soil, pile, footing and superstructure.

Parametric solutions for a piled circular footing of
finite rigidity set in deep homogeneous isotropic linearly
elastic foundation have been obtained for wide range of
geometric and material parameters, for two types of axi-
symmetrical loading. The effect of different parameters
on the behaviour is discussed. The results of settlement,
load transmitted by pile, raft bending moments etc., have
been tabulated in terms of non-dimensional parameters and
they can be used in the design of piled circular footing
which is shown to be a possible economical alternative by
an example. For certain cases the load shared by pile
may exceed its ultimate bearing capacity, even in working
load range. A simplified method of accounting for failure
of pile in such cases has been described.

Since soil often exhibits different types of
non-homogeneity, the effect of non-homogeneity on the behavi-
our of piled circular footing has been studied. The non-
homogeneities considered include, the soil stiffness increasing

linearly with depth, two layered soil medium in which there is a weaker soil below and non-homogeneities arising due to the installation of pile. The effects of these non-homogeneities on the behaviour of such unit have been discussed.

Cross anisotropy is an observed phenomenon in many soils. The effect of cross anisotropy on the behaviour of single pile and piled circular footing have been studied for wide range of parameters for in-compressible materials and certain cases of compressible materials. The effect of cross anisotropy on the behaviour of pile and piled footing, has been discussed. The distribution of stresses around the pile and piled circular footing have also been reported.

Most of the analyses reported in the literature assume smooth contact, satisfying vertical displacement compatibility only. Some analyses including the analyses described so far herein assume adhesive contact. So it is necessary to study the effect of smooth contact versus rough contact. For this study the use of 6 noded interface element along with 8 noded continuum elements was tested for circular raft of different rigidities and has been shown to model the contact between raft and soil adequately.

Using this interface element, the effect of smooth
contact between pile head and footing and also between
raft base and soil versus adhesive contact, on settlement,
percentage of pile load and raft bending moments have been
studied for a number of cases.

Progressive failure mechanism and bearing capacity
is another important aspect in any foundation problem.
These aspects have been studied for the piled circular
footing, circular footing and single pile, under undrained
soil condition assuming soil to be elastic-ideally plastic
obeying von Mises criterion, using 'initial stress' finite
element technique for computation and interface elements for
modelling the contact. Solutions have been obtained to
study the effect of footing flexibility, pile compressibility
and type of contact on the behaviour of circular footing,
single pile and piled circular footing under homogeneous and
non-homogeneous soil conditions.

From the elastic analysis of single pile and piled
circular footing, the 'interaction factors' were also
obtained. They have been used to study the settlement
behaviour of pile groups and pile-rafts of square arrange-
ment. Firstly the solutions so obtained are shown to be
in satisfactory agreement with available solutions for

homogeneous soil condition. Subsequently the method is used to study the settlement of such pile groups and pile-rafts in different types of non-homogeneous soil conditions mentioned earlier and in cross anisotropic soil. Solutions have been obtained assuming the cap or raft to be perfectly rigid or perfectly flexible. A 'non-linear interaction factor method' of analysis of pile group and pile raft is described and a bilinear analysis has been carried out in the case of pile-raft.

The effect of an axisymmetrical superstructure like those of some storage structures, nuclear containment structures etc. on the behaviour of circular raft and circular raft with an annular arrangement of piles near the edge has been studied. In this study the effect of superstructure rigidity on the behaviour of the foundation for different values of raft flexibility, pile length and Poisson's ratio of soil have been discussed and solutions are presented in non-dimensional form for use in design.

Some results pertaining to circular raft and single pile, taken for the purpose of checking and comparison from which conclusions of some importance were drawn have also been reported.

CHAPTER 1

INTRODUCTION

1.1 GENERAL

Piles are being used for transmitting the loads
from different kinds of structures like buildings, bridges
and retaining walls, to the soil strata, particularly when
the soil is weak, right from ancient times. One of the
methods of design of such piled foundations, is by using
empirical formulae obtained from experimental/field obser-
vations (Meyerhof (92), Burland et al (22)). Some such
empirical approaches have been discussed in review papers
by Meyerhof (92) and Cooke (35); in the latter's opinion such
empirical approaches are likely to remain for the foreseeable
future. Another approach is interactive theoretical analysis
using theory of elasticity/plasticity making certain ideal-
isations, regarding the material behaviour. This approach
is likely to be very useful in indicating the effects of
different geometric and material parameters on the behaviour
of piled foundations. Hence attention is focussed towards
this approach throughout this work.

Piled foundations may be free standing pile groups
(cap not in contact with ground) or pile-rafts (cap in
contact with ground). The latter type of foundation may be

useful in situations in which raft foundation itself has
adequate factor of safety; but the settlements are excessive.
Provision of pile may reduce the settlements substantially.
In such a pile-raft system, the cap or raft may also transfer
significant portion of the load to the soil. Hence inter-
action of pile-raft-soil system requires to be analysed
as against analysis of pile-soil system in the case of free
standing pile groups. Ofcourse, the effects of superstructure
and time also are to be included, to be more rigorous. The
number of investigations reported on the behaviour of pile
group have been quite many (Brief literature review is given
in Sec. 1.2).   Soil medium may exhibit non-homogeneity of
different kinds and anisotropy in stress-strain and strength
behaviour, due to its process of formation, and subsequent
changes in environment. However, reported studies on the
effect of such important aspects of soil on the behaviour
of pile group are inadequate.

Analysis of pile-raft systems has received still
less attention, probably due to the geometrical complexity
of the problem.   The effect of flexibility of the raft
and non-homogeneity and anisotropy of soil, on its behaviour
may be significant but the available literature on these

aspects are scanty. Pile-raft systems are not readily
amenable to general parametric studies, on the effect of
some of these aspects, particularly the flexibility of raft.
A piled circular footing forms a typical unit of a general
pile-raft system. A detailed analysis of this unit to study
the effect of different geometric and material parameters
would indicate the general trends that may be expected in the
case of general pile-raft system. Also, since piled circular
footing itself can be used as a foundation, solutions are
required for the design of the same.

Finite element method (FEM) has established itself
as a powerful numerical technique, for general engineering
analysis. In particular, geotechnical engineering problems
involving complicated geometry and material behaviour can
be solved by FEM, without much efforts, to handle such
complications. The literature contains innumerable references
using FEM particularly after late sixties. They mostly
pertain to some specific field problem or comparison of
numerical solutions with other analytical solutions or
experimental/field observations. However, it appears FEM has
not been fully exploited for presentation of solutions of
important geotechnical problems, like piled foundations,
particularly those involving non-homogeneity and anisotropy.

The interface conditions may influence the behaviour of piled foundations significantly. Such studies on the effect of interface conditions on the behaviour of systems involving two or more materials, have been made possible by the development of interface elements. Use of these interface elements would be very useful in the study of the influence of interface conditions on the behaviour of pile-raft/footing systems. .Such works are found to be rather few in the literature and more work is needed.

Pile foundation has certain advantages. Raft foundation or footing foundation has some merits. But a combination of these two essential foundation types may prove to be more effective and efficient, under certain circumstances. A study on the comparative performance of these types of foundation, may be useful in this regard.

The study of behaviour of piled foundation in the working load range is one important facet. Another euqally important aspect is the progressive failure mechanism upto collapse, a study of which would be very useful in understanding the behaviour of such foundations completely. Elasto-plastic finite element technique can be used for such problems involving complicated geometry.

However, these studies may be highly expensive in cases,
which require 3-dimensional treatment, when FEM is used.
For some cases involving simple geometry (e.g. single pile,
piled circular footing), which reduce to two dimensional
idealization, such studies can be made at reasonable cost.
Available literature even for the simple case of single pile
is too meagre and further work is required.

As pointed out above, analysis of problems requiring
3-dimensional finite element modelling, may be very expensive,
particularly when a number of cases of piled foundations are
to be analysed. Hence some simpler procedures like
'interaction factor method' require to be developed and
also such available procedures require to be extended/
improved, wherever possible and necessary.

In such interaction based method of analysis, the
response of individual pile and pile-pile interaction are
two important aspects. The non-linearity of response of
individual piles has been recognized and considered in many
analyses, as referred in Sec. 1.2. The pile-pile interaction
may reduce with increasing load, as the soil around the pile
in question fails, since the effect may be local and may
not be felt at locations away from the pile. Or in other
words, 'interaction' may be less at greater load levels.

This aspect does not appear to have been considered in the interaction based analyses of piled foundations. Hence a method is needed to be developed to account for this.

Nonlinear behaviour of foundation-soil system (although can be analysed in principle using FEM) may warrent some simplified procedures or simple approximate formulae, which can be used with hand calculations, for arriving at preliminary design.

Stiffness of the superstructure may significantly affect the behaviour of foundation-soil system. Although numerous works have been reported taking into account the super-structure in the analysis, available literature on the effect of superstructure on piled foundation is very meagre. Also, solutions assuming elastic connections between different components of the system are not found.

1.2 BRIEF LITERATURE REVIEW

1.2.1 Constitutive Models

For theoretical analyses of problems involving stress-strain response, first and fore most step is the selection of proper constitutive model defining stress-strain relations.

1.2.1.1 Linearly Elastic Model

Simplest model is linearly elastic one. The elasticity may be isotropic or anisotropic. The elastic soil continuum may be homogeneous or non-homogeneous. The non-homogeneity may be of different kinds, like layered, stiffness varying with depth, radial non-homogeneity etc. Even though soil is not an ideal elastic material, in the sense that stresses and strains are not linearly related, strains are not fully recoverable on reduction of stresses and strains are not independent of time, assumption of linearly elastic behaviour is expedient and should be sufficiently accurate for engineering purposes (Hooper (75) and Butterfield and Ghosh (25)). Hence these models may be highly useful for presenting general solutions. Such elastic solutions for a number of geotechnical problems including piled foundations have been given by Poulos and Davis (110, 111). In most of the cases soil exhibits cross anisotropy, with horizontal plane as plane of isotropy. Even though solutions for cross-anisotropic soil conditions have been presented for surface loading and footing (Hooper (74), Gerrard and Harrison (63), Gazetas (61), Gazetas (62), Wardle (139), no solutions for piled foundations appear to be available.

Even for linearly elastic soil model, exact mathematical solutions are possible only in some extremely simple situations. Though many exact solutions are available for surface loading, exact solutions do not appear to have been obtained even for an axially loaded single pile. (Recently some approximate expressions have been presented for settlement of single pile by Randolph (113)). However it is possible to solve almost all problems with any complicated boundary conditions and/or any complicated material model, by numerical methods like FEM.

1.2.1.2 Non-linear elastic models

It is well known that soil most often exhibits non-linear stress-strain behaviour. There are a variety of non-linear (Pseudo-elastic) elastic models available to model such behaviour. Simplest model of this kind may be bilinear or trilinear representation of stress-strain behaviour. These models have been used in the analysis of geotechnical problems by Ellison et al (58), D'appolonia et al (52) and Dunlop and Duncan (39). Another approach is to establish the non-linear stress strain relation from laboratory tests for any specific case and to use these results to define the value of soil modulus depending on

the state of strain (Girijavallaban et al (64) and Desai
and Reese (42)).

The most popular model of this kind is hyperbolic
stress-strain model developed by Duncan et al (41), based
on Kondner's (31) work, probably due to its simplicity
in application in FEM. Quite a few investigators have used
this model in the analysis of different geotechnical
problems (Chang and Duncan (27), Mitchell and Gardner (93),
clough and Duncan (33), Duncan and Clough (40), Kulhawy
et al (82), Desai (49), Desai et al (44), Varadarajan and
Yudhbir (137), Magid and Cunnell(87), Varadarajan and Arora
(134), Varadarajan and Arora (135),Ottaviani et al (99),
Law (83)). Improved modelling of stress-strain behaviour
can be made using spline function representation (Desai(50)),
which may fit with test results, in a better way. The
stress paths followed by different elements in the field
may be different. This aspect has been considered by using
stress path dependent soil parameters in such models by
Varadarajan and his associates (134, 135, 137). Semi-
empirical models have also been developed and implemented
in finite element analysis (Yudhbir et al (148), Rao (115)),
Higher order elasticity models may also be used; but this
approach requires determination of too many parameters
(Christian and Desai (30)).

These non-linear models may not predict the response near collapse satisfactorily (Chow and Smith (28), Arora (3)), Ozawa and Duncan (100). Nevertheless, these models have been shown to predict load-deformation response satisfactorily in most of the above references.

1.2.1.3 Elastic plastic models

Models of this category are in general better than pseudo-elastic ones, particularly in predicting the behaviour near collapse.

Here the stresses and strains are related entirely by their incremental behaviour arising from the theory of plasticity. Different ideal plasticity models like von-Mises, Drucker-Prager, Tresca and Mohr-Coulomb are available (Zienkiewicz (149)).

A general method of deriving the elastic-plastic matrix for these yield criteria, which can be used in finite element analyses, was presented by Nayak and Zienkiewicz (96). One of the efficient computation techniques called 'initial stress' approach which uses 'constant elastic matrix' for iterative solution has been described by Zienkiewicz et al (153). A further refinement of 'initial stress' method was proposed by Nayak and Zienkiewicz (95), in order to accelerate convergence of original 'initial stress' technique.

Tresca and von-Mises criteria are often used to study the undrained behaviour of clayey soils. A number of such works pertaining to strip footing (Hoeg et al (70), Fernandez and Christian (59), Davidson and Chen (54), Griffiths (66), Swamisaran and Pande (130), Toh and Sloan (132), Rowe et al (123), Zienkiewicz (150), Sloan and Randolph (127), Circular footing (Hoeg (69), Biondi et al (12), Das and Gangopadhyay (53), Vallippan et al (133), Sloan and Randalph (127), Rowe et al (123)) and single pile (Chaw and Smith (28), Balaam et al (5)) have been reported. The footings have been assumed to be very rigid or completely flexible in these works. Strain softening of soil was considered by (Hoeg (69), Biondi (12) and Sture and Ko (129). In most of these works 'small deformations' have been assumed. However, the geometric non-linearity arising from large deformations, have been considered by some investigators (Davidson and Chen (54), Toh and Sloan (132), Fernandez and Christian (59)). Anisotrophy was considered by Toh and Sloan (132).

Drucker-Prager or Mohr-Coulomb model has been used for studying the frictional behaviour of soils. A number of such studies pertaining to strip footing (Frank et al (60), Griffiths (66), Christian et al (31), Swamisaran and Pande (130), Rowe et al (123), Zienkiewicz (150), Desai et al (43)),

circular footing (Zienkiewicz (149)) and single pile
(Frank et al (60), Balaam et al (5)), have been reported.
The assumption that the plastic behaviour is 'associated'
gives rise to dilation much in excess of commonly observed
soil behaviour, when these yield models are used. Hence
'non-associated' plastic behaviour, usually with the
assumption of zero volume change, has been assumed by
many investigators. (Rowe et al (123), Zienkiewicz (150)
and Christian et al (31)).

The constitutive model developed by Roscoe and his
associates (117, 118, 119, 120, 124)), have been adopted and
used in the investigation of many geotechnical problems
(Zienkiewicz and Naylor (151), Hagmann (67), Zienkiewicz
et al (150)). Viscoplastic model (Zienkiewicz et al (150),
can also be used for studying elasto-plastic problems in
addition to time dependent problems (Zienkiewicz (149),
Griffiths (66) and Pande and Sharma (104)).

From the above review of literature on elasto-
plastic analyses of foundation problems it is found that
elasto-plastic analysis of piled foundations and that of
footings of finite flexibility reported are meagre.

The consitutive models are still in the developing
stage and a single model that can predict the behaviour

under a number of stress paths, that may occur in different
soil elements, in a realistic situation, is yet to emerge
(Desai (43)).

1.2.2 Analysis of Piled Foundations

1.2.2.1 Piled circular footing

An incompressible pile with an attached rigid circular
cap, in semi-infinite elastic continuum was studied and
parametric solutions were presented by Poulos (106), using
integral equation method, which uses Mindlin's solutions.
The pile compressibility was considered in the analysis of
some cases of piled footing with a square cap by Butterfield
and Banerjee (23), using Boundary element method.   Solutions
for piled strip foundation of finite strip flexibility, has
been presented by Brown et al (18), using integral equation
method.   Solutions taking into account the footing flexibility,
and non-homogeneity and anisotropy of soil are not available
for piled circular footing.   Also the influence of interface
conditions on the behaviour of such foundations has not been
studied.

1.2.2.2 Pile group

The analysis of pile group having complicated geometry
and/or material property, can be performed using 3-dimensional

finite element approach. (Ottaviani (98)). Another less
expensive approach is Boundary element method. This method
developed by Butterfield, Banerjee and their associates
(Butterfield and Banerjee (24), Banerjee and Butterfield
(8)), Can be used for the analysis of pile group subjected
to any general loading. The non-homogeneity of soil can
also be taken into account (Banerjee (7), Banerjee and
Davies (9). Recently this method has been extended to take
into account non-linearity of soil and slip at pile-soil
interface (Banerjee and Davies (10)). However, the limitation
of this method is that a point load solution is to be avail-
able.

Another approach for general analysis of pile group
is by using the pile response functions under different modes,
described by Reese et al (116). This approach can account
for non-linear response of pile heads in different modes.
It was developed without considering the pile-pile interaction
and latter it was extended to take into account such inter-
action (O'Neill et al (97)). But these interaction effects
were calculated based on elastic solutions.

Another approach to analyse the behaviour of pile
groups, is the 'interaction factor method' developed by

Poulos and his associates (Poulos and Davis (111)). The
interaction factors for any spacing between two piles are
computed from the analysis of two equally loaded similar
piles. For this purpose Mindlin's solutions are used.
This method has been recently extended to non-homogeneous
soil (modulus linearly increasing with depth), making
certain approximations (Poulos (109)). Approximate method
of calculating settlement for certain cases of layered
soil has also been presented (Poulos and Davis (111)).
However, for certain cases of non-homogeneous soil (e.g. a
layered soil medium in which top layers are stiffer),
these approximate methods are not satisfactory (Poulos and
Davis (111)). Recently another method of calculating the
'interaction factors' using some approximate solutions, which
can also be used to account for soil non-homogeneity, has
been reported by Randolph et al (114).

This method (interaction factor) is very economical
and attractive, if solutions for a number of pile group
configurations are required, since other methods require
seperate analysis for each individual case. Also, it would
be advantageous to combine such simpler methods with FEM
to obtain acceptable solutions at less cost, for problems
involving more complicated material model. The variation

of the interaction with load level does not appear to have been considered. Also the effect of anisotropy of soil on the behaviour of pile group has not been investigated.

1.2.2.3 Pile-raft systems

Very few analyses of pile-raft systems have been reported in the literature. For a general analysis, 3-dimensional finite element method is required to be used. Wherever possible the problem has been idealized as axisymmetrical or plane strain problem (Hooper (72), Knabe (80), Desai (44)).

Hain and Lee (68) have described a method of analysis of pile-raft systems, in which raft can be of finite flexibility. It is possible to include the bearing capacity failure of piles. This method has also been used by Weisner and Brown (144). This method requires determination of a number of interaction factors. Also, if this method is to be used for analysis of pile-raft in arbitrarily layered soil or anisotropic soil, 3-dimensional finite element representation of the continuum is required.

Knabe (80) has described a method of analysis of pile-raft. His method requires discretisation of piles and raft and uses the results of a number of finite element analyses

to generate the flexibility matrix of the system. However, this method can be used for any non-homogeneous or anisotropic soil situations.

The methods of analyses of pile-raft systems, discussed so far, require separate analysis for each individual case of pile-raft system. The method described by Davis and Poulos (56), based on interaction factors of pile-cap units may be economical and preferable, if a number of configuration of pile-raft systems are to b analysed. This method can be used for perfectly rigid or flexible cap/raft situations. This approach has been shown to give satisfactory results of settlement by Brown et al (17). An approximate method of accounting for bearing capacity failure of pile, if any, has also beendescribed by Davis and Poulos (56).

Other methods of analyses, which appear to be less popular are 'strip superposition method', 'plate on springs method' and 'plate on springs and continuum method' (Brown et al (17)).

The effect of non-homogeneity and anisotropy of soil on the behaviour of pile-raft system does not appear to have been studied in detail. Although the effect of superstructure on the behaviour of raft foundation has been investigated

by many investigators (Lee and Harison (86), Lee and Brown (85),
Wiberg (142), King and Chandrasekaran (77), Majid and Cunnell
(87), Wardle and Fraser (140)) the study of interaction of
superstructure with piled foundations is scanty (Buragohain
et al (19)).   Also, the effect of elastic connections
between superstructure and foundation (piled or unpiled)
soil system does not appear to have been considered.

1.3 OBJECT AND SCOPE

1.3.1 Object

Based on the literature review (Sec. 1.2), which also
indicates some of the areas in which work is needed, the
object of the present work is as follows.

1.   To study the effect of the following on the behaviour
      of piled foundations.
      (a) Flexibility of footing/cap/raft.
      (b) Interface conditions.
      (c) Soil non-homogeneity of different kinds.
      (d) The anisotropy of soil.

2.   To study the complete non-linear response of piled
      foundations upto failure.

3.   To develop a straight forward method to study the
      settlement behaviour of pile group and pile-raft systems,

set in any linearly elastic soil medium, combining axi-symmetric finite element analysis and the concept of 'interaction factor' method.

4. To develop a 'non-linear interaction factor' method, in which the interaction (factor) can also be varied depending on load level. (3) and (4) may be useful in **fulfilling** some of the objectives stated in (1), with less expensive computation.

5. To study the effect of superstructure on the behaviour of foundation (piled or unpiled) -soil system, with elastic connections between different components of the system.

6. To present the solutions in non-dimensional form, over wide range of parameters, whe-rever possible, so that they may be useful in the design.

7. To develop some simple formulae for hand calculations, for use in preliminary design.

8. To compare the preformance of pile-raft and pile-footing foundations, with those of free standing piles and unpiled raft/footing foundation.

1.3.2 Scope of the Present Work

1.3.2.1 Constitutive models used

For a general parametric study, to high light the effect of other parameters, a simpler constitutive model may be sufficient. Any assumptions other than a linearly elastic material for the soil and foundation/structure material, would lead to unduly complicated theory, which may lack useful generality, particularly when parametric solutions are attempted. Hence soil and other materials have been assumed to be linearly elastic in most of the work reported in this thesis. However, it must be stated that for these solutions to give realistic results, the elastic 'constants' that are used, have to be appropriate to the particular problem. That is, they may be determined for the actual field conditions, from appropriate field tests. These constants may not really be material constants; but merely constants of proportionality relating stress and strain, in a particular field situation.

For analysis of progressive deformation upto collapse, elastic- perfectly plastic model with associated flow rule obeying von-Mises yield criterion has been used for most of the work, to study the undrained behaviour. Some difficulties

that arise, when Tresca and Drucker-Prager yield criteria
are used, are indicated.

1.3.2.2. Numerical techniques used

For most of the work reported in this thesis axi-symm-
etric finite element displacement formulation has been used.
Quadratic isoparametric elements have been used to model
soil, pile, footing/raft and superstructure. These elements
are shown to model the flexture behaviour satisfactorily,
in addition to modelling general elastic behaviour. Standard
procedures for stiffness and load vector computation were
used (Zienkiewicz (152) and Bathe and Wilson (11). Desai
and Abel (45)). A 'Condensation procedure' was developed
and implemented in the Computer Program developed for elastic
analysis. This procedure does not require auxiliary storage
like tape, even for problems involving large number of
unknowns. Also, this procedure is particularly very
efficient, when a number of modifications in foundation/
interface/superstructure are to be analysed, for a given
soil profile, which is the case in most of the problems
taken up in the present work. 6 noded interface elements
of zero thickness were also (Buragohain (20)) included in the
computer program, so that interface behaviour can be simulated.

For elasto-plastic analysis also, quadratic iso-parametric elements and 6 noded interface elements were used. The non-linear problem was solved using 'initial stress' computation technique (Zienkiewicz et al (153)).

For analysis of pile group and pile-raft of square configuration, 'interaction factor method' (Poulos (107)), using the results of axi-symmetrical finite element analysis of single pile and piled circular footing, was used. A 'non-linear interaction factor method' of analysis is developed and 'a bilinear analysis' has been used for the analysis of pile-raft systems. This procedure can take into account the variation of interaction with load levels.

Approximate elasto-plastic analysis using excess load cut-off (Davis and Poulos (56)) was used in some cases of piled circular footing, for arriving at some approximate procedure to take into account the failure of pile in a piled circular footing.

Finite difference representation of circular plate and available elastic solutions to model the soil (Karamarkar (76)) have been used for approximate analysis of the effect of superstructure on the behaviour of circular raft, by making the raft slope zero at the raft-superstructure interface.

1.3.2.3 Problems solved

Piled Circular footing

A piled circular footing of finite rigidity, subjected
to two types of axi-symmetrical vertical loading has been
considered. Solutions have been obtained, over wide range
of geometric and material parameters. The effects of
different parameters on the behaviour of such piled circular
footing, have been discussed in detail. The solutions have
been presented in terms of non-dimensional parameters and
the same can be used in the design of such foundation.
The use of these solutions has been illustrated by examples,
which also bring out the comparison of piled circular footings
with circular footings and free standing pile foundation.
Based on the results of approximate elasto-plastic analyses,
a simplified procedure to take into account pile failure,
if any, has been described.

The effect of soil non-homogeneity of the following
kinds, on the behaviour of some typical cases of piled cir-
cular footings, was investigated.

(a) Young's modulus linearly increasing with depth.

(b) A two layer soil medium in which top soil layer
     is stiffer.

(c) Non-homogeneity arising due to the effect of
     installation of piles.

The effect of these non-homogeneities on the settlement, load taken by the pile, bending moments etc., are discussed in detail.

The effect of cross-anisotropy of the soil on the behaviour of piled circular footings and also **single** pile, have been investigated. The study has been performed over wide range of cross anisotropic parameters, in the case of incompressible material (saturated clay in undrained condition), as some simplification occurs in this case, in terms of number of anisotropic parameters. Few results have been reported for drained case, to indicate the trends. The effect of cross anisotropy on the behaviour of single pile and piled circular footing are discussed.

The above analyses of piled circular footing were carried out assuming fully adhesive elastic connections at the pile-footing-soil interfaces. Solutions were also obtained for perfectly smooth contact at pile-footing-soil interfaces. For this purpose interface elements were used in conjunction with quadratic isoparametric elements. Comparisons have been made between solutions for different interface conditions, to bring out the effect of smooth or rough contact, on the behaviour of piled circular footing.

Though Elasto-plastic analysis of a piled circular footing was the main objective, some cases of circular footing and single pile were also analysed. In these analyses the loading was assumed to be concentrated near the centre. The effect of interface conditions, compressibility of pile, flexibility of footing and variation of strength and stiffness with depth were studied. The effect of these parameters on the development of failure zones, collapse load behaviour and other design quantities like bending moment, load taken by pile etc., have been discussed. Interface elements were used in these analyses to simulate smooth or rough interface and also to permit slip, in case of skin friction failure, at pile-soil interface.

Pile-group and Pile-raft

An alternate method of computating 'interaction factors' using the results of axisymmetric finite element analysis of single pile or single pile-cap unit is proposed. The results obtained by this procedure are compared with available solutions for some cases. The proposed method has been used to study the behaviour of pile groups and pile-raft systems of square configuration, with perfectly rigid or flexible cap/raft conditions. The effect of different parameters has been discussed. The effect of different

kinds of non-homogeneities and cross-anisotropy of soil,
as considered in the analysis of piled circular footing, on
the behaviour of pile group and pile-raft, have been investi-
gated.

The reduction in the 'interaction' as the load on the
single pile-cap unit increases towards its ultimate value is
brought out, from elasto-plastic analysis results. A
'non-linear interaction factor method' in which
the effect of load level on interaction can be accounted for,
is described. The methods of obtaining these factors from
field tests or theoretical analysis, for use in the proposed
method have been explained. A particular case of non-linear
analysis, namely 'a bilinear analysis' has been carried out
for illustration, in the case of pile-raft systems.

The effect of superstructure rigidity

Some studies have been carried out using FEM, to study
the interaction of an axisymmetric superstructure with
circular raft-soil system and circular pile-raft-soil system.
Compatible elastic connections have been assumed between
different components of the system. In most of the cases
soil has been assumed to be homogeneous. A particular
case of soil non-homogeneity has also been considered. The

effect of flexibility of raft, length of piles, poisson's ratio of soil and variation in superstructure/soil stiffness on the behaviour of the system, has been discussed. Solutions have also been presented in non-dimensional form, for use in the design of certain cases of circular raft and pile-raft, considering the effect of superstructure rigidity. Comparison has also been made with an approximate method in which the raft slope is made zero at the raft-superstructure interface to account for superstructure rigidity.

Checks

The solutions obtained using numerical methods like FEM are 'approximate' ones. The accuracy depends essentially on the mesh layout in the case of elastic analysis, whereas the accuracy depends on several other factors in the case of elasto-plastic analysis. It must be shown that the results obtained may be acceptably accurate, so that the computed values may be relied upon. For this purpose the solutions obtained have been compared with available solutions wherever possible. Also, the accuracy of the results have been ascertained by mesh refinement studies in some cases. A static equilibrium check has been carried out in all the FEM analyses reported.

1.3.3 Organisation of the Thesis

The work done is divided into six Chapters as described below. In each chapter, the relevant literature is briefly reviewed, in the beginning. Since quantum of computer data generated during this investigation is quite large and parametric effects to be discussed are quite extensive, information available elsewhere is briefly mentioned in view of the volume of the thesis. However, relevant references are cited as far as possible. Analytical techniques are briefly explained. After formulating the problem, the computed results are discussed in detail. Salient conclusions drawn from the discussion of the results are presented at the end of each chapter.

In Chapter 2, elastic analysis of piled circular footing under different soil conditions is carried out. The results are presented in non-dimensional form for wide range of parameters, which may be used for design. Some examples have been worked out. The effect of various parameters are discussed in detail. A simplified procedure to account for pile failure is also described.

In Chapter 3, the effect of interface conditions on the behaviour of piled circular footing is studied. The

results for smooth contact and adhesive contact are compared.

In Chapter 4, elasto-plastic analysis of circular raft, single pile and piled circular footing has been carried out, using von-Mises yield criterion. The effect of smooth or rough contact, the compressibility of pile and flexibility of footing/raft are discussed. The progressive spread of failure zones are shown for most of the cases.

In Chapter 5, settlement analysis of pile group and pile-raft with square arrangement of piles has been carried out. The results of the proposed 'interaction factor method of analysis' are compared with available solutions to ascertain the accuracy. A non-linear interaction factor method is described. The results for different soil conditions are discussed in detail.

In Chapter 6, analysis of the interaction of a particular type of axisymmetrical superstructure with raft-soil and with pile-raft-soil systems are studied. Solutions are presented in non-dimensional form for some cases. Detailed discussion of parametric effects have been included.

In Chpater 7, the general conclusions and recommendations for further study are listed.

In Appendix A, the 'Condensation procedure' used for computation in the elastic analysis is described. The applicability of this method in geotechnical engineering analysis is high-lighted. Certain checks and observations, regarding the circular footing and single pile are presented.

In Appendix B and Appendix C, some studies made on the performance of quadratic isoparametric elements and six noded interface elements are presented respectively.

In Appendix D, some difficulties, met with in the conventional 'initial stress' elasto-plastic finite element analysis using Mohr-Coulomb and Drucker-Prager yield criteria, are described.

In Appendix E, details of computation for bilinear interaction factor method of analysis are presented.

In Appendix F, the salient features of computer program developed for elasto-plastic analysis are described and flow charts are also given.

Appendix G, contains the list of references.

CHAPTER 2

ELASTIC ANALYSIS OF PILED CIRCULAR FOOTING UNDER DIFFERENT SOIL CONDITIONS

2.1 INTRODUCTION

Addition of piles to raft foundation or independent footing significantly reduces the settlement of the foundation. Such foundations in which the cap or raft as well as the piles participate in transmitting the load to the soil, may be termed as piled foundation or pile-raft system. A simple type of 'piled foundation', is a piled circular footing, a detailed study of which would help in understanding the behaviour of a general pile-raft system. The piled circular footing as it is, can also be used as a foundation and it is shown herein subsequently to be a possible and economical alternative in many cases. So the solutions obtained for such a unit, would also be useful in the design of the same. Hence a detailed study of piled circular footing under different soil conditions, has been taken up in this chapter. Analysis of general pile-raft systems are discussed in chapters 5 and 6, subsequently.

Available literature on the analysis of 'piled foundation' or pile-raft systems is meagre. Parametric solutions for a rigid circular footing with an incompressible pile at the centre has been given by Poulos (106). Using these solutions

The solutions for a piled circular footing of finite
flexibility, appear to be not available. Also the influence of
non-homogeneity and cross-anisotropy does not appear to have
been studied. Hence solutions taking into account these aspects
are presented in this chapter. Completely adhesive contact
has been assumed between footing and soil and compatible elastic
connection has been assumed between pile head and footing in
this chapter. Solutions for smooth contacts have been presented
in chapter 3, subsequently.

Parametric solutions have been obtained for wide range
of geometric and material parameters for homogeneous soil
condition, by FEM, for two types of axi-symmetrical loadings.
Comparison is made with available solutions. The effect of
different parameters on the behaviour is discussed. The results
have been tabulated in terms of non-dimensional parameters
and they can be used in the design of piled circular footing.
Examples have been worked out for illustration, which also
bring out the comparison of behaviour of piled circular footing
with those of unpiled circular footing and free standing
piles. A simplified method of accounting for failure of pile
is described. Solutions have also been obtained for different
types of non-homogeneous and transversely isotropic soil
conditions. The effect of these non-homogeneities and

anisotropy have been discussed for a number of cases of piled circular footings.

2.2 DESCRIPTION OF THE PROBLEM

2.2.1 General

A typical piled circular footing is shown in Fig. 2.1. In this figure a flexible circular footing (of diameter d_c and thickness t) with a single compressible pile (of diameter d and length L) at the centre in a linearly elastic deep soil layer is shown. Two axi-symmetrical loadings have been considered namely vertical uniformly distributed load q, over entire footing area (denoted as **udl** in this thesis) and a uniformly distributed load q, distributed over a small circular area of diameter d at the centre (denoted as concentrated load in this thesis).

2.2.2 The Parameters Used

The following parameters were used in this work. Young's modulus of pile and footing material were assumed to be equal throughout (denoted as E_p).

Poisson's ratio of footing/pile material (ν_p) = 0.15.
Relative rigidity of footing (K_R) = 0.01, 0.1, 1, 10 and 100.
where

$$K_R = E_p (1 - \nu_S^2) t^3/E_S a^3 \qquad (2.1a)$$

in which E_S = Young's modulus of soil

$\quad\quad \nu_S$ = Poisson's ratio of soil

$\quad\quad$ t = thickness of footing

$\quad\quad$ a = radius of footing.

I. Homogeneous soil

Length of pile/diameter of pile (L/d) = 10, 25 and 40

Diameter of footing/diameter of pile (d_c/d) = 5,10 and 15.

Pile stiffness factor (K) = E_p/E_S = 200,500 and 1500.

ν_S = 0, 0.3 and 0.47.

II. Non-homogeneous soil

Three cases of soil non-homogeneity were considered as described below.

1. Modulus linearly increasing with depth:

L/d = 10 and 25

d_c/d = 5

Pile stiffness factor (K) = E_p/E_{S0} = 1500

where E_{S0} = Young's modulus at depth (Z) equal to zero.

Young's modulus is assumed to vary with depth as follows. (Fig. 2.19(a)).

$$E_{S\bar{Z}} = E_{S0} + (1 + \frac{(Z/d)}{\psi}) \quad\quad\quad (2.1b)$$

where Z = depth below ground level

E_Z = Young's modulus at depth Z.

ψ = a non-homogeneity coefficient.

When $\psi = \infty$, soil is homogeneous and when $\psi = 0$, the soil is infinitely stiff.

In the present work $\psi = 2.5$, 10 and ∞ were considered.

$\nu_S = 0.3$ (for all cases).

2. Layered soil:

A two layered soil medium (Fig. 2.28(a)) with a stiffer soil overlying a softer soil was considered, with parameters as follows in the present analysis.

$K = E_p/E_{ST} = 400$

where E_{ST} = Young's modulus of top soil layer.

ν_S = 0.3.

E_{ST}/E_{SB} = 5 (in most of the cases)

E_{ST}/E_{SB} = 3 and 10 (in some cases)

where E_{SB} = Young's modulus of bottom soil layer.

d_c/d = 5 and 10.

L/d = 10 and 25.

h/L = 0.1 to 1.5 where h is the thickness of the top soil layer (Fig. 2.28(a)).

3. Soil Non-homogeneity due to the effect of installation of pile:

The effect of installation of piles was considered by assuming a disturbed zone around the pile, where the Young's modulus may be different from the original value. A similar procedure has been used in the case of single free standing pile by Balaam et al (6). Three different cases were considered and they are listed below. In all the cases $d_c/d = 5$ and 10 and $L/d = 10$ and 40 were used.

(a)   Stiff clay soil whose modulus around the pile may decrease due to the installation of a bored pile. The assumed disturbed zone and modulus variation has been shown in Fig. 2.37(a).

Two cases, denoted as I_1 and I_4, were considered with parameters as follows (Fig. 2.37(a)).

I_1 - $r_1/r_p = 4$ $E_r/E_S = 0.5$ $E_p/E_S = 500$ $\nu_S = 0.47$

I_4 - $r_1/r_p = 4$ $E_r/E_S = 0.25$ $E_p/E_S = 500$ $\nu_S = 0.47$

(b)   Soft clay soil whose modulus around the pile may increase due to the installation of a driven pile. The assumed disturbed zone and modulus variation have been shown in Fig. 2.38(a). Two cases denoted as I_2 and I_5 were considered with parameters as follows (Fig. 2.38(a)).

$$I_2 - r_1/r_p = 4 \qquad E_r/E_S = 2 \qquad E_p/E_S = 1500 \qquad \nu_S = 0.47$$

$$I_5 - r_1/r_p = 4 \qquad E_r/E_S = 4 \qquad E_p/E_S = 1500 \qquad \nu_S = 0.47$$

For cases denoted as I_1, I_2, I_4 and I_5 the disturbed zone was assumed to extend upto radius r_1, from the centre and the modulus is E_r at the pile soil interface and varies linearly upto r_1 where the modulus is that of original soil. The disturbed zone has been assumed to extend upto 2.5d or 5 r_p below the pile tip, where r_p is the radius of the pile (Figs. 2.37(a) and 2.38(a)). r_1/r_p was kept equal to 4 in all the cases. Stiff and soft clay soils which are moderately sensitive to the installation of pile are represented by cases I_1 and I_2 respectively. Stiff and soft clay soils which are highly sensitive to the installation of piles are represented by cases I_4 and I_5 respectively. The assumed pattern of variation for the above cases is based on studies by DeMellow (51), Skempton (126) and D'Appolonia et al (52), the details of which have been explained by Balaam et al (6).

Loose sand whose modulus around the pile may be more in a disturbed zone due to the installation of a driven pile, as shown in Fig. 2.40(a): This case is denoted as I_3. The Poisson's ratio of soil was assumed to be equal to 0.3

in this case.   The pattern of variation of modulus assumed
in this case, is similar to the one assumed by Balaam et al (6),
which is based on the experimental results of Meyerhof (91).

More sophisticated analysis taking into account the
effect of installation and also the process of consolidation
is possible (Desai (47)); and such methods can be used in the
analysis of any specific field problem. But for a general
study attempted herein, the approximate method used in the
present work, is expected to indicate the general trends
satisfactorily.

I. Transversely Isotropic Soil

In the case of a general transversely isotropic or
cross-anisotropic soil the deformation behaviour is defined
by 5 independent material parameters. For a material having
a horizontal plane as the plane of isotropy, which is the
usual case in many soils, these parameters may be E_{SV}, n, ν_{SV},
ν_{SH} and m where

E_{SV} = Young's modulus in the vertical plane

E_{SH} = Young's modulus in the horizontal plane

n = E_{SH}/E_{SV} (n can take values   from 0 to 4)

ν_{SV} = Poisson's ratio for effect of vertical strain on
        horizontal strain

ν_{SH} = Poisson's ratio relating the strains in two horizontal
        directions

$$m \quad = \quad G_{SV}/E_{SV}$$

G_{SV} = shear modulus in the vertical plane.

A number of cases of incompressible (or undrained saturated clays) materials with cross-anisotropic properties and a particular case of fully drained cross anisotropic soil were considered with parameters as given below. In all the above cases the following geometric and material parameters were used.

$d_c/d = 5$, $L/d = 10$ and 25, $K = E_p/E_{SV} = 200$ and 1500.

(a)   In-compressible material:

In the case of incompressible cross anisotropic material the number of independent material constants reduces to three. They may be E_{SV}, n and m. The other two constants are already known ($\nu_{SV} = 0.5$ and $\nu_{SH} = 1 - n/2$ from Hooper (74)). The following cross anisotropic parameters were used in this work for computational purposes.

$E_{SV} = 0.5$, $m = 0.38$, $n = 1, 1.5, 2.5, 3.5$ and 3.98.

A constant value of m has been used in this work and this value is the average value reported for London clay (Ward et al (141)).

b. Fully drained parameters:

In the undrained case, once the value of m is kept constant, n becomes the only other parameter which can be varied to study the general effect of cross-anisotropy. Such simplification is not possible in the drained case, as there can be inumerable set of different combinations of these parameters. Hence a particular set of drained parameters which correspond approximately to undrained parameters with n = 2.5 was considered in this work. The method of computing these drained parameters has been given by Hooper (74) and it is based on theoretical considerations and observed values of stress path gradients (M_V and M_H). The drained parameters used in the present work were computed following the same procedure suggested by Hooper (74), and using the charts given by him.

The calculated values of these drained parameters assuming $\nu'_{SV} = 0$, $M_V = 1$ and $M_H = 0.38$ are as follows.

$$ n' = E'_{SH}/E'_{SV} = 3, \qquad \nu'_{SH} = -0.55, \; m' = 0.78 $$

(The primes denote drained parameters).

These parameters correspond to undrained case with n = 2.5 and m = 0.38, as stated earlier. The values of stress path gradients M_V and M_H assumed are the average values reported for London clay (Hooper (74)).

2.3 FINITE ELEMENT ANALYSIS

Footing pile and soil were modelled by 8 noded iso-
parametric elements, with quadratic variation of displacement
in axisymmetrical form. The details of finite element formul-
ation are available in a number of standard text books
(Zienkiewicz (152), Desai and Abel (45)). For numerical
integration 2 x 2 Gauss quadrature was used. A 'Condensation
procedure' was used so that problems with large number of
unknowns can be solved with small computer core. A detailed
description of this procedure is given in Appendix A. A
Computer Program 'PRELAN', developed incorporating this
procedure, can be used for elastic analysis of general axi-
symmetrical problems. Provision has been made in the program,
to compute and print settlements, differential settlement,
contact pressures, bending moments, shear forces, percentage
load taken by pile and percentage error from equilibrium
check, as discussed subsequently. Provision has also been
made to solve for anisotropic or non-homogeneous soil
conditions considered.

The description of meshes used, numerical techniques
for the computation of bending moments, shear force
and contact pressure, and checks performed to ascertain the
accuracy have been described in Appendix A. A study of

8 noded isoparametric elements used herein to model the footing also was carried out to assess its behaviour in bending. The results of this study are given in Appendix B. From this study, it is found that these quadratic elements model the bending behaviour satisfactorily even with one layer of elements, over wide range of aspect ratios as explained in Appendix B. The aspect ratio of elements used for representing the footing in the present work lied in this range, except for some stray cases of extremely thick or extremely thin footings.

The right hand side free boundary was kept at 50d, and the bottom rough rigid boundary was kept at 80 d. Three different meshes were used for different values of d_c/d. A typical mesh is shown in Appendix A. The other two meshes were similar to the one shown (Fig. A.1) in the vertical direction and it was altered in the horizontal direction for different values of d_c/d. The elements vertically down the centre were made pile elements or soil elements depending on the value of L/d. The thickness of the footing element was changed for different values of K_R. Deformation parameters of soil and pile/footing elements were assigned depending on the values of K and depdnding on the soil conditions (i.e. homogeneous, non-homogeneous or anisotropic). Hence using

these three meshes results have been computed and presented
in this chapter.   About 200 computer runs were made for the
analysis of piled circular footing and circular footing.   In
each run the results for eleven cases of piled footing/circular
footing were obtained as explained in Appendix A.   For each
case, the results of settlement, differential settlement,
contact pressure, footing bending moments, shear force and
percentage load transmitted by pile, were obtained.

The mesh was refined at the pile head by increasing
the number of elements by four times and also with two layers
of elements for representing the footing.   The results of
settlement, contact pressure and percentage pile load were
found to be affected by less than 0.5 percent by such
refinement.   The results of bending moment was found to be
affected by about 2 percent except at locations immediately
above the pile.   The adequacy of the mesh was also confirmed
by comparing the results with available solutions for circular
raft and single pile as discussed in Appendix A.

The load taken by the pile was computed as follows.
The load transferred to the soil is computed by integrating
the vertical stresses in the top most row of soil elements
immediately below the footing, over the entire horizontal
plane.   It is then substracted from the total applied load

to get the load taken by the pile. A static equilibrium check was also incorporated in the program, by integrating the stresses over the entire horizontal plane below the footing. Two point Gauss quadrature was found to be adequate, for such integration. The error observed from the said equilibrium check was less than 0.5 percent in all the cases considered and less than 0.1 percent in most of the cases. This error was found to be of smaller magnitude for piled footing and single pile (less than 0.1 %) than circular footing, (less than 0.5 %), for both loading cases considered. This is also a useful check on the accuracy of the results. The load taken by the pile may also be computed from the stresses in the top most pile element. The load obtained by such computation was compared with the load computed as explained earlier. The difference was found to be very small, as also seen from the equilibrium check reported above.

2.4 HOMOGENEOUS SOIL

2.4.1 General

The results for homogeneous soil condition are given in Figs. 2.1 to 2.18 and Tables 2.1 to 2.7. The maximum settlements reported **are** the maximum among the nodal displacements at ground level. Maximum bending moments

reported are the maximum among the Gauss point values, computed as explained in Appendix A. From the results a steep variation of bending moment along the footing radius, particularly in the case of flexible footing with pile, was observed. Hence for some cases (K_R = 1) coarse to fine technique (Desai and Abel (45)) was used to determine the bending moment at some intermediate points. The trends of settlement, percentage pile load, bending moment etc. are discussed below.

2.4.2 Settlement

Effect of L/d: From Fig. 2.3, it can be observed that the ratio of maximum settlement of piled footing (S_{PR}^*) to the maximum settlement of unpiled circular footing (S_R^*) reduces as L/d increases. But larger values of L/d beyond certain limit do not bring about appreciable further reduction in the settlement. For smaller values of d_c/d, there is more reduction and increasing L/d is less effective, particularly so, for smaller values of ν_S. For smaller values of L/d (upto L/d = 25), the effect of ν_S is more than the effect of K. For longer piles, the effect of K is more dominant than the effect of ν_S.

Effect of d_c/d: It was observed that rigid footing with shallow piles, subjected to both loadings and flexible footir

with shallow piles subjected to u.d.l. are not effective in reducing the settlement, for **larger** values of d_c/d (>12). However with concentrated loading, even shallow piles were found to be effective in the case of flexible piled footing, for larger values of d_c/d also.

Effect of K_R: The settlement ratio (S_{PR}^*/S_R^*), for some typical cases of piled circular footing is shown in Fig. 2.2. It can be observed that for K_R = 100 (a rigid footing with pile), the settlement becomes independent of the type of loading. For K_R = 10, the difference in settlement between those for u.d.l. and concentrated load, was found to range from 2.5 percent to 16 percent for the cases analysed. The minimum difference occurred for smaller values of L/d and larger values of d_c/d and the maximum difference occurred for larger values of L/d, smaller values of d_c/d and smaller values of ν_s. For K_R = 1.0 (fairly flexible footing) the difference in settlement ratios was found to vary over wide range (from 6 to 80 percent), depending on parameters as mentioned earlier.

It can be observed from Fig. 2.2, that while settlement ratio asymptotically increases to rigid footing with pile value in the case of concentrated loading, the pattern is different for u.d.l. No definite trend could be observed

in the case of u.d.l. This can be attributed to the difference in behaviour of free raft with u.d.l. and concentrated load. However it was observed in most of the cases (as also seen in Fig. 2.2), that there is an optimum K_R value (in the range of 0.1 to 1.0) at which the settlement ratio is minimum or in other wards provision of pile is most effective in reducing the settlement in the case of flexible footing subjected to u.d.l. The settlement ratio was found to be more sensitive to the values of ν_S in the case of concentrated loading for all values of K_R and less sensitive to ν_S in the case of flexible footing with pile subjected to u.d.l. This trend is also observed in Fig. 2.2.

Comparison of settlements of piled circular footing, single pile and circular footing: The portion of the load taken by the pile and the portion of the load transmitted by the footing was computed as explained earlier (Sec. 2.3). The settlement of circular footing and single pile for the example given below were calculated for the respective proportion of the load shared. The results are as follows.

Piled circular footing:

$(d_c/d = 4,\ L/d = 8,\ K = 1500,\ K_R = 100,\ \nu_S = 0.48.$
$d = 0.4m,\ E_S = 1000\ t/m^2.$ Applied pressure $= 15\ t).$

Load shared by pile   = 7.95t

Load shared by footing   = 7.05 t

Load transmitted by tip = 0.98 t

Max. settlement   = 0.47×10^{-3}m .

Circular footing: ($d_c/d = 4$, $K = 1500$, $K_R = 100$, $\nu_S = 0.48$)

Max. settlement (for a load of 7.05t) = 0.35×10^{-3}m.

Single pile: ($L/d = 8$, $K = 1500$, $\nu_S = 0.48$)

Max. settlement (for a load of 7.95 t) = 0.32×10^{-3}m

Load transmitted by tip = 0.69 t.

From the above calculated values the following observation can be made. The settlement of piled circular footing is 0.47×10^{-3} m where as the sum of the settlement of single pile and settlement of circular footing works out to be 0.67×10^{-3} m (i.e. 0.35 + 0.32). One of the reasons for this may be that in the case of piled circular footing the portion of the load transmitted by bottom portion of the pile is more than that of single pile as also indicated by the load transmitted by the tip of the pile. This example shows the effectiveness of piled circular footing in reducing the settlement. Some more examples are given in Sec. 2.4.11.

Comparison with available solutions:

The settlements computed from the present analysis
are compared with the solutions given by Poulos (106), for
rigid footing with incompressible pile in Figs. 2.14 to 2.16.
For smaller L/d (L/d = 10), the present solution for K = 1500
and K_R = 100 (rigid footing with fairly incompressible pile)
agrees closely with solution given by Poulos (106), for
rigid footing with pile (Fig. 2.14). It is also seen that the
pile compressibility does not affect the settlement appreciably.
The effect of fooring flexibility on settlements is significant
as seen in Fig. 2.14. For flexible footing with u.d.l., the
difference between rigid footing solution and present solution
is more for smaller values of d_c/d, whereas for concentrated
loading it is the other way.

For larger values L/d (e.g. L/d = 25) the effect of pile
compressibility is significant (Fig. 2.15). There is about
5 percent difference between present solution for K = 1500,
K_R = 100 and ν_S = 0.47 and incompressible pile solution
(Poulos (106)). The difference increases as pile compressibility
increases. The effect of flexibility of footing can also
be seen in Fig. 2.15.

The difference between present solution and Poulos (106)
solution is more for ν_S = 0 (Fig. 2.16) than for ν_S = 0.47

(Fig.2.15), for the same parameters. This indicates the effect of completely adhesive contact between footing and soil, which is likely to be minimum for $\nu_S = 0.5$ and maximum for $\nu_S = 0$ (Hooper (73)). Poulos (106) assumed smooth contact while adhesive contact has been assumed in the present work. The effect of adhesive contact increases as d_c/d increases. In general, the footing flexibility increases the normalised (normalised with the settlement of free standing pile) piled footing settlement (S_{PR}^*/S_P^*) whereas the pile compressibility decreases the same.

2.4.3 Percentage Pile Load (PPL)

For $K_R = 100$, the percentage load shared by pile (PPL), was found to be almost same irrespective of the type of loading, as also seen for some typical cases in Fig. 2.4. The values of PPL have been plotted against L/d for different parameters in Fig. 2.5. It can be observed that for less values of L/d the values of PPL, are found to be sensitive to the values of ν_S. For larger values of L/d, PPL is sensitive to the values of K. The sensitivity of the values of PPL to the values of ν_S can also be seen in results reported in Table 2.4. In Table 2.4, for $d_c/d = 5$, L/d = 10, $\nu = 100$ and K = 1500; PPL is 49 for $\nu_S = 0.47$ and PPL is 68,

for $\nu_S = 0$. It can be observed in Fig. 2.4, that the value of PPL is quite sensitive to the type of loading for flexible. Footing-pile (for example in the case when $K_R = 1$). For shallow piles with larger values of d_c/d, subjected to u.d.l., the effect of K_R on PPL was found to be small. In this case, it was found that there is a slight decrease in PPL with increasing K_R beyond $K_R = 1.0$. The reason for this reverse trend may be due to the difference in settlement profile for flexible and rigid footing with piles (for rigid footing-pile system, minimum settlement occurs near the centre and for flexible footing-pile minimum settlement occurs near the edge).

2.4.4 Differential Settlement

The ratio of differential settlement of piled circular footing (Δ_{PR}) to the differential settlement of unpiled circular footing.(Δ_R), has been plotted against K_R for some typical cases in Fig. 2.6. It can be observed that for concentrated loading the differential settlement substantially reduces by the provision of piles. This reduction is very large for flexible footing. For u.d.l. the reduction is marginal for flexible footing and there is some increase in the differential settlement compared to circular footing for rigid footing, in some cases (Fig.2.6).

It was observed that the settlement pattern is same for circular footing and piled circular footing for concentrated loading (maximum at the centre and minimum at the edge). In the case of u.d.l. it was observed that the maximum settlement occurs at the centre for free circular footing and maximum settlement occurs at the edge, for rigid footing with pile and at the middle, for flexible footing with pile. As d_c/d increases it was observed that the maximum settlement occurs in the middle even for more rigid footing with pile for u.d.l. The differential settlement was found to be more sensitive to ν_S for larger d_c/d and for larger values of K_R.

2.4.5 Bending Moment

The ratio of maximum bending moment for piled circular footing (M_{PR}^*) to the maximum bending moment for circular footing (M_R^*) has been shown for some typical cases in Fig. 2.7 (for concentrated loading) and Fig. 2.8 (for u.d.l.). In Fig. 2.7, it can be observed that the maximum bending moment substantially reduces in the case of concentrated loading and this reduction is very large for flexible footing with pile, compared to circular footing. This ratio was found to increase as K_R increases and was found to approach 1, for larger values of d_c/d with shallow piles. The effect

of compressibility of piles (K) was found to be in significant for smaller values of L/d. For larger values of L/d, the bending moment was found to decrease with increasing values of K. The bending moment was found to be quite sensitive to the values of ν_S. There is substantial reduction in positive bending moment for $\nu_S = 0$ compared to $\nu_S = 0.47$. (From Table 2.6 to 2.7 for L/d = 10 and K_R = 10, this reduction can be seen to be about 43 percent).

For u.d.l. the pattern is different. There is change in sign and also increase in the magnitude of maximum bending moment in general, compared to free circular footing, as seen in Fig. 2.8, for some typical cases. The bending moment ratio is found to be minimum for certain values of K_R, similar to the trend observed in the case of settlement ratio for this loading. The bending moment is positive for circular footing and in general negative for piled circular footing. As for concentrated load, the bending moment is sensitive to the value of ν_S in the case of u.d.l. also. When $\nu_S = 0$, the negative bending moment increases by large magnitude compared to $\nu_S = 0.47$, particularly for smaller values of L/d (from Tables 2.6 to 2.7 this increase can be seen to be about 35 percent for L/d = 10 and K_R = 10).

2.4.6 Shear Force

The ratio of maximum shear force for piled circular footing (Q_{HR}^{*}) to the maximum shear force for circular footing (Q_R^{*}), has been plotted for some typical cases of piled circular footing in Fig. 2.9 (for concentrated load) and 2.10 (for u.d.l.). It can be observed that this ratio is very small for flexible footing with pile subjected to concentrated loading, indicating large reduction in maximum shear force due to the provision of piles. This ratio increases as K_R increases and approaches unity for larger diameter footing with shallow pile. For smaller values of ν_S, there is greater reduction in shear force, compared to unpiled footing. For less compressible pile there is greater reduction.

In the case of u.d.l. (Fig. 2.10), there is large increase (as large as 10 to 20 times in some cases) in shear force compared to unpiled footing. But the maximum shear force occurs near the pile in the case of piled circular footing where as it occurs near the edge for circular footing, for this loading.

2.4.7 Contact Pressure

Uniformly distributed load: The computed values of contact pressure for this loading have been shown in Figs.2.11

to 2.12, for some typical cases. For rigid footing (K_R=100), and for smaller values of d_c/d, there is large reduction in contact pressure, compared to free circular footing and as d_c/d increases the contact pressure tends to that for free circular footing. Larger the value of K (less compressible pile), less is the contact pressure (Fig.2.12).For very flexible footing with pile, the contact pressure near the pile is considerably less than that for rigid footing with pile and steeply increases to applied pressure value at mid radius, particularly so for larger values of d_c/d (Fig. 2.11).

Concentrated loading: The computed values of contact pressure, have been shown for this type of loading in Fig. 2.13, for some typical cases. It can be observed that the general pattern of contact pressure distribution for piled circular footing is similar to that of circular footing for K_R = 1 as well as for K_R = 100. The magnitude of contact pressure reduces for piled circular footing. This reduction is more for larger values of K (stiff pile) and larger values of L/d.

2.4.8 In-Plane Stresses

The in-plane or membrane forces in radial and tangential direction were computed by integrating radial and tangential stresses over the entire thickness of the footing respectively.

The average values of the in-plane stresses were calculated
by dividing these forces by the thickness of the footing.
These in-plane stresses develop due to adhesive contact
assumed in the present work. The computed values of these
stresses have been summarised in Table 2.1 for some cases.
In the same table the computed values of maximum bending
stresses have also been given for comparison. It can be
observed that the maximum in-plane stresses are less than
10 percent of the maximum bending stresses in all the cases.
The in-plane(or membrane) stresses (average), were found to be
compressive in the radial direction and tensile in the tang-
ential direction, in general. The tensile in-plane stresses
were found to be in general small compared to compressive
in-plane stresses, for the case tabulated. The in-plane
stresses immediately above pile head, have not been considered
in the results reported in this section, as that cross section
might not be a critical cross section, due to the presence
of column and or pile.

2.4.9 Application in Design

-dimensional results have been presented in Tables
     . Complete results obtained have been tabulated
     ne the maximum settlement (Tables 2.2 to 2.3)
and load taken by pile (Tables 2.4 and 2.5). The results

have been presented for wide range of parameters and hence,
they can be used in the design of piled circular footing of
any flexibility, compressibility and for certain geometry
subjected to u.d.l. or concentrated load. Some results have
been tabulated to determine the bending moment distribution
(Tables 2.6 and 2.7). Knowing the load taken by the pile,
the maximum shear force which occurs near the pile, in most
of the cases, can also be calculated.

Even though the results presented apply directly to
piled circular footing, they may be used for square footing
with pile or square column loading, taking the equivalent
diameter for the same area.

2.4.10 Simplified Analysis in Case of Pile Failure

The elastic solutions presented are valid only if elastic
conditions prevail throughout the soil medium. In some cases,
particularly when a flexible footing is subjected to concentrated
loading, the pile load may exceed its ultimate bearing
capacity. Solution of this problem requires rigorous
elasto-plastic finite element analysis, for each individual
case, Such analysis has been carried out for some cases
and those results have been reported in Chapter 4.   A
simplified elasto-plastic analysis (excess load cut-off

method) described by Davis and Poulos (56) was carried out
for wide range of geometries assuming pile to be incompre-
ssible, footing to be rigid and soil to be cohesive (angle
of internal friction $(\emptyset)$ = 0 and Cohesion = C). A brief
description of the procedure of this simplified analysis
is given below.

The pile and the footing are devided into cylindrical
and annular elements respectively. The soil is modelled by
Boussenesq's or Mindlin's equations. The flexibility matrix
for soil is generated. The equations are solved using
the boundary conditions and satisfying the vertical displace-
ment compatibility to get the displacement and pressures at
the interfaces. In case the pressure at any interface
exceeds the yield value, at that point, the pressure is
kept constant at the yield value and resolved untill
pressures at all the interfaces are less than or equal
to the yield value. The analysis is carried out for incre-
ments of load to get the load-settlement response.

The results ofthe above analysis for four different
cases of piled circular footing have been shown in Figs. 2.17
and 2.18. It is observed that in all the cases (whether the
pile is dominant (i.e. L/d = 25, d_c/d = 5); or the footing
is dominant (i.e. L/d = 10, d_c/d = 10); or the pile and the
footing of equal dominance (i.e. L/d = 10, d_c/d = 5 and

L/d = 5, d_c/d = 10)), a bilinear approximation with limiting load (P_1), as given by equation 2.2, fits closely with the load-settlement curve, obtained by the simplified elasto-plastic analysis, over the normal working load ranges. It was found that the proposed bilinear approximation also fits well (except near collapse), with elasto-plastic finite element analysis using von Mises yield criterion, discussed in Chapter 5 and Sec. 5.2.2.3.

$$P_1 = (UBC + UBC \times 100/PPL)/2 \qquad (2.2)$$

where

P_1 = limiting load (as in Figs. 2.17 and 2.18).

UBC = ultimate bearing capacity of pile.

PPL = percentage load shared by pile (can be obtained from Table 2.4 and 2.5).

The essential features of the proposed bilinear approximation are,

1. Upto a load P_1, the system acts as piled footing. The slope of the load settlement curve for this portion corresponds to that of piled footing.

2. Beyond P_1, the system acts as unpiled footing. The slope of the load-settlement curve for this portion corresponds to that of unpiled footing.

A similar bilinear approximation has been described by Davis and Poulos (56), for a general pile-raft. But they have assumed $P_1 = UBC$, which can be seen to predict (Figs. 2.17 and 2.18) about 15 percent higher settlement, compared to the present procedure, for the cases considered.

As per the idealization suggested, the maximum settlement of piled footing taking into account the failure of pile can be computed as

$$S^* = I_S^* \, d \, P_1/E_S \, A + (P - P_1) \, I_R^*/A \qquad (2.3)$$

in which

S^* = maximum settlement of piled footing.

I_S^* = settlement influence factor for piled footing (from Tables 2.2. and 2.3)

d = diameter of pile

P_1 = limiting load as defined by eqation 2.2.

A = area of footing for u.d.l. or area of cross-section of pile for concentrated load.

E_S = Young's modulus of soil

P = total applied load

I_R^* = maximum settlement of unpiled footing under unit pressure acting over entire footing area for u.d.l. or over the pile area for concentrated load. (Can be obtained from Fig. A.5, Appendix A).

In Eqn. 2.3, P_1 is to be always less than or equal to P. If P_1 exceeds P, the behaviour is entirely in the first portion and the value of P_1 may be taken as equal to P.

The equation 2.3 can be conveniently used in the case of concentrated loading, for computing maximum settlement since the maximum settlement occurs at the centre for both unpiled footing and piled footing. However, for u.d.l., if pile failure occurs, computation of maximum settlement after superposition as in Eqn. 2.3 becomes difficult, since maximum settlement of piled footing may occur anywhere in the span depending on different parameters. In this case maximum settlement will have to be computed after superposing the settlement distribution due to piled footing action and unpiled footing action. Eqn. 2.3 can be used in this case for approximate assessment of maximum settlement.

2.4.11 Examples

2.4.11.1 Example 1

Calculations for piled circular footing and circular footing of different diameters and stiffnesses were carried out using the results of the present analysis, for the data given below .

Total applied load = 25 t

UBC of a pile 4 m long and 0.4 m diameter = 20 t.

Young's modulus of soil (undrained E_S) $= 200 t/m^2$

Pile stiffness factor $K = 1500$

Poisson's ratio of soil (undrained ν_S) $= 0.5$

Poisson's ratio of soil (drained ν_S') $= 0.3$

Young's modulus of soil (drained E_S') $= 173.4 \ t/m^2$
(Assuming shear modulus is constant)

Relative rigidity of footing K_R $= 1$ or 100

Dimeater of footing $= 2$ m or 4 m

Loading - A total load of 25 t may be distributed over
circular area of diameter $= 0.4$ m at the centre (concent-
rated load)or distributed over entire footing area (u.d.l.).
The maximum allowable settlement $= 4.5$ cm
A circular footing of 2m diameter may be assumed to have a
safe bearing capacity of 25 t.

The calculated values of settlement, maximum bending
moment, differential settlement, percent pile load, and
maximum shear force, have been tabulated in Table 2.8a, for
different cases of circular footing and piled circular footing
considered, for both drained and undrained conditions and for
both loading cases. From this table the following observat-
ions can be made.

Both rigid ($K_R = 100$) and fairly flexible ($K_R = 1$)
unpiled circular footing with a diameter of 2m, do not satisfy

the settlement restrictions. But provision of a 4 m long pile reduces the settlement to permissible limit. Unpiled footing 4 m diameter satisfies the settlement restriction but uneconomical in terms of volume of concrete. It appears that it may be economical to use a pile rather than increasing diameter or rigidity of footing to reduce the settlement. More rigorous cost analysis is required to ascertain the economical aspect. Further the following observations can be made from Table 2.8a.

In the case of concentrated loading there is large reduction in settlement and differential settlement for fairly flexible footing with pile and fair reduction in settlement for rigid footing with pile, compared to unpiled footing. There is substantial reduction in bending moment and shear force for both rigid and fairly flexible footing with pile, compared to plain footing. This would enable the design of thinner section and hence may be economical. In general there is increase in pile load as drainage occurs to a smaller extent for flexible piled footing (about 6 percent) than rigid piled footing (about 10 percent, comparing PPL for $\nu_S = 0.47$ and $\nu_S = 0.3$). The reduction in total settlement (drained) is more than the reduction in undrained settlement. The possible reasons for this are,

1. The load transmitted by pile is more for smaller value of ν_s.

2. The settlement of pile is less for less values of ν_s. The settlement of circular raft is more for smaller values of ν_s.

In the case of u.d.l., there is fair reduction in settlement and differential settlement. The bending moment and shear force increase, compared to unpiled footing. In general provision of pile is less advantageous for this loading than concentrated loading.

2.4.11.2 Example 2

The effectiveness of piled circular footing in reducing settlement, compared to unpiled circular footing was shown by a comparison in Example 1. Some more comparisons of settlement and bearing capacity are made with free standing piles and circular footing in Table 2.8b. It can be observed that the settlement of piled circular footing and that of two or three numbers of free standing piles are within permissible limits, indicating that provision of piles is effective in reducing the settlement. However, when free standing piles are used, they do not provide required bearing capacity, whereas piled circular footing satisfies bearing capacity

requirements also. Comparing the bearing capacity of single pile and circular footing, it can be noted that circular footing provides bulk of the bearing capacity in the piled circular footing.

It may be noted from expression for elastic settlement (Eq. 2.4) that the settlement of rigid circular raft reduces inversely with diameter, whereas the volume of the material increases as cube of the diameter (for same K_R) as in Eq. 2.5 for $K_R = 100$.

$$S_R^* = P(1 - \nu_S^2)/4\, d_c E_S \qquad (2.4)$$

$$\text{Volume} = 0.157\, d_c^3 \quad \text{(for data in Table 2.8b)} \qquad (2.5)$$

But undrained bearing capacity increases as square of the diameter. Further, it is shown in Sec. 4.4.2.2 that the bearing capacity of circular footing is fairly insensitive to K_R in the range of 1 to 100, whereas the settlements are quite sensitive to K_R values in this range (Fig. A.5). Hence the circular raft is efficient in providing the bearing capacity and less efficient in reducing the settlement. So it may be concluded that the pile reduces the settlement effectively and the footing provides the necessary bearing capacity in a piled circular footing. This makes this combination an efficient type of foundation for transmitting the load safely and without excessive deformation.

The comparison was made for undrained condition.
The efficiency is expected to increase further for drained
condition or sandy soil as observed in Example 1, regarding
settlement and as observed by Knabe (79), regarding bearing
capacity. This type of foundation with a pile with enlarged
base, is expected to be still more effective. It may be
expected that shallow piles may be more cost effective due
to less piling cost. However, model studies and detailed
cost analysis are required to further confirm the observat-
ions made herein.

2.4.12 Conclusions

From the elastic analysis of piled circular footing
set in homogeneous soil following conclusions can be drawn.

1.   The footing flexibility and pile compressibility
        for longer piles (L/d > 10) affect the behaviour
        of piled footing significantly and hence may affect
        the behaviour of pile-raft systems.

2.   For u.d.l. on a flexible piled footing, there is
        an optimum rigidity of the footing at which the
        system is most effective in reducing the settlement.

3.   Provision of pile significantly increases the
        magnitude of the bending moment and shear force in

the case of u.d.l. and substantially reduces bending moment and shear force in the case of concentrated loading.

4. As ν_S reduces to 0 from 0.5, there is large increase in the magnitude of bending moment in the case of u.d.l. and there is large reduction in bending moment in the case of concentrated loading.

5. In many cases piled footing may be economical compared to unpiled footing and free standing pile group, for a given permissible maximum settlement. Such piled footing of certain geometry can be designed using the non-dimensional charts presented herein and pile failure if any can also be taken into account by the method described in this chapter.

2.5 NON-HOMOGENEOUS SOIL

2.5.1 General

Often soil is found to be non-homogeneous. In actual cases it may be multilayered and (or) the stiffness may vary arbitrarily in the vertical and horizontal directions. For the purpose of this study, three types of non-homogeneities have been considered, the details of which have been given in Sec. 2.2.2. Case 1 refers to a soil for which the Young's

modulus linearly increases with depth. Case 2 refers to a two
layer soil medium in which a stiffer soil layer (with modulus
E_{ST}) overlies a softer soil (with modulus E_{SB}). Case 3
refers to the soil non-homogeneity due to the installation
of pile. The effects discussed herein -although directly
apply to a piled circular footing -they also indicate the
general trends that may be expected in the case of a general
pile-raft system.

2.5.2 Case 1 (Young's Modulus linearly increasing with depth)

The soil model assumed for this case has been given in
Fig. 2.19(a). The details of parameters defining non-homo-
geneity has been given in Sec. 2.2.2. The effect of this
type of non-homogeneity, on the behaviour of piled circular
footing are discussed.

Settlement: When subjected to both (u.d.l. and concentrated
load) loadings the non-homogeneity of this kind reduces the
settlement of piled circular footing substantially (as low
as one fourth of that for homogeneous soil in some cases),
the reduction being more for concentrated loading (Fig. 2.19(b)
and 2.20). It can also be observed that for concentrated
loading non-homogeneity reduces the sensitivity of settlement
to footing rigidity. The ratio S^{*}_{PR}/S^{*}_{R} has been tabulated

It can be observed for longer pile (L/d = 25), the
difference in PPL for ψ = 2.5 and ψ = 10, is very small.
On in other words, for longer piles the non-homogeneity
does not hav significant effect on PPL, after certain limit-
ing value of ψ .

In the case flexible footing subjected to u.d.l.,
the behaviour is different, For very flexible footing with
pile, there is a decrease in the value of PPL due to soil
non-homogeneity of this kind. The magnitude of this decrease
is more for L/d = 25 than L/d = 10. At K_R = 100, an increase
in PPL is noted (Figs.2.21 and 2.22). The value of K_R at
which the change from decrease to increase takes place, in-
creases with increasing value of L/d. From the limited
studies carried out herein, it appears that the load carried
by pile is sensitive to non-homogeneity if pile and footing
are of equal dominance.

Bending moment: The computed values of maximum bending
moments are shown in Fig. 2.23 (for u.d.l.) and Fig. 2.24
(for concentrated load), for different parameters. In
Fig. 2.24, it can be observed that for concentrated loading,
the maximum bending moment is reduced by the soil non-homo-
geneity for all values of K_R and both values of L/d. This
reduction is significantly more for L/d = 10 than L/d = 25,

for rigid footing with pile. However for flexible footing
with pile (K_R = 1.0), there is substantial reduction in
bending moment for both values of L/d, due to soil non-
homogeneity. The magnitude of this reduction is more than
50 percent, compared to homogeneous case.

In the case of u.d.l., the pattern is different, as
observed in the case of settlement and PPL previously. The
trends for flexible footing with pile is different from the
trend for rigid footing pile systems. For very rigid footing
with pile non-homogeneity increases the magnitude of the
bending moment for this loading. This increase is substantially
more for L/d = 10 than L/d = 25. For flexible footing with
pile, there is reduction in the magnitude of the bending
moment. The change from decrease to increase takes place at
a particular value of K_R depending on L/d and ψ . This
value of K_R at which the curves cross each other, is more
for L/d = 25 and less for L/d = 10.

Differential settlement: The computed values of differential
settlement have been presented for K_R = 0.1, 1 and 100 and
for both loading cases in Table 2.9b to indicate the effect
of non-homogeneity. For concentrated loading, it
can be observed that there is substantial reduction in
differential settlement as degree of non-homogeneity

increases (as ψ decreases). This reduction is more for more flexible footing-pile system than a rigid one. In the case of u.d.l. no definite trend could be observed. There is increase in differential settlement due to non-homogeneity in some cases and decrease of the same in some cases.

2.5.3 Case 2 (Two layer soil medium)

The two layered soil medium in which a stiffer layer over lies a softer layer was considered for the present analysis. The soil model is shown in Fig. 2.28(a) and the details have been given in Sec. 2.2.2. The effect of different parameters on the behaviour of piled circular footing in such soil medium are discussed below.

Settlement:

The computed results of settlement for piled circular footing and circular footing set in the two layer soil medium considered have been presented in Figs. 2.25(a) and 2.26. The settlement ratio (S_{PR}^* / S_R^*) has been plotted against h/L in Fig. 2.25 (b), where h is the thickness of the top stiff soil layer. From this figure it can be observed that the effectiveness of the pile in reducing the settlement is minimum (or S_{PR}^*/S_R^* is maximum), when h/L is between 0.4 and 0.7, in all the cases considered. As

h/L increases or decreases, settlement approaches the value, corresponding to homogeneous continuum (Fig. 2.25(b)). When h/L increases it approaches homogeneous continuum value gently whereas when h/L reduces, it approaches steeply. It can also be observed from Fig. 2.25(b), for concentrated loading, the value of h/L at which the settlement ratio is maximum, increases as K_R increases (comparing the peaks for different values of K_R). In the case of u.d.l., no such definite trend is observed. Another observation that can be made in the case of concentrated load is that, the sensitivity of the settlement ratio to the value of K_R, increases as h/L increases (comparing the settlement ratios for different values of h/L and K_R). In general, the piled circular footing is less effective for this type of non-homogeneous soil compared to homogeneous soil, in reducing the settlement.

Percentage pile load: The values of percentage load transmitted by pile (PPL) is shown in Figs. 2.27 to 2.30, for different parameters. It can be observed that if the pile is dominating (for example $d_c/d = 5$ and $L/d = 25$), the values of PPL are not significantly affected by the value of h/L (or in other wards by this type of non-homogeneity) as seen in Fig. 2.28. In this case, the maximum effect of

this type of non-homogeneity on PPL is about 15 percent. However if the footing is dominating (d_c/d = 10, L/d = 10, Fig. 2.29), the values of PPL, are quite sensitive to the values of h/L. In this case it is highly sensitive if the footing is rigid (K_R = 100), for which case the maximum effect of h/L on PPL is found to be more than 50 percent. However, for flexible footing-pile system, this effect is less (less than 20 percent). It can also be observed that there is a particular value of h/L at which PPL is minimum (Figs. 2.27 to 2.30). If the pile and footing are of more of less equal dominance (d_c/d = 5, L/d = 10 and d_c/d = 10, L/d = 25 in Fig. 2.27 and 2.30), the non-homogeneity has fairly significant effect on the value of PPL. In all the cases, the value of PPL is minimum for $h/L \div 0.6$. For more(or less)than this value, the value of PPL approaches homogeneous continuum value. If h/L is less, it approaches the homogeneous continuum value steeply and if h/L is more it approaches gently. The sensitivity of PPL to the values of E_{ST}/E_{SB}, is also shown in the Fig. 2.27, for a particular value of h/L.

Bending moment: The values of maximum bending moment have been plotted against K_R in Fig. 2.31(a) (for u.d.l.) and 2.31(b) (for concentrated load), for some cases. It can be

observed that the bending moment substantially reduces
as h/L reduces, in the case of u.d.l. (Fig. 2.31(a). In the
case of concentrated load, there is significant increase in
the value of bending moment due to this type of non-homogeneity
(Fig. 2.31(b)).

In Fig. 2.31(a), it can be observed that the value of
bending moment is minimum for h/L = 0.5 and 0.4 for L/d = 10
 and 25 respectively, for u.d.l. The effect of this type of
non-homogeneity on bending moment is less pronounced for
L/d = 25 than for L/d = 10. For h/L = 0.1, the behaviour is
sensitive to the value of K_R. For flexible footing-pile
systems the bending moment tends to be maximum for this value
of h/L, for L/d = 10.

In Fig. 2.31(b), it can be observed that there is in
general, increase in bending moment as h/L decreases, compared
to homogeneous soil case (h/L = 1.5). If the footing
is rigid (K_R = 100), the value of bending moment is less
sensitive to the presence of soft soil layer below (maximum
effect is less than 20 percent). However for flexible
footing-pile system, the value of bending moment increases
by more than 50 percent compared to homogeneous case (h/L = 1.5).
The value of bending moment is maximum for h/L = 0.1 for
flexible footing-pile system. For rigid footing-pile system,

the value of bending moment tends to be maximum when
h/L = 0.4 to 0.5.

When E_{ST}/E_{SB} = 10, (also shown in Fig. 2.31), there is
no significant change in bending moment compared to E_{ST}/E_{SB} = 5
for h/L = 1, except when footing is very flexible and subjected
to concentrated loading. For d_c/d = 10, L/d = 10 (footing
dominating), it was found that the effect of non-homogeneity
was substantially more than the case shown in Fig. 2.31a,
for u.d.l. In general, it may be stated that the bending
moment is quite sensitive to the presence of soft layer
below a top stiff layer, in the case of u.d.l. for all values
of K_R and in the case of concentrated load on fairly flexible
footing-pile system.

Differential settlement: The computed values of differential
settlement have been tabulated in Table 2.10, for some cases.
In the case of u.d.l., the differential settlement is found
to be minimum for h/L = 0.4 or 0.5, for both L/d = 10 and
L/d = 25, for all values of K_R. In the case of concentrated
loading, the trend for flexible footing-pile system is
different from the trend for rigid footing-pile system. For
a rigid footing-pile system, (K_R = 10), the differential
settlement is maximum for h/L = 0.4 or h/L = 0.5, where as

for a flexible footing-pile system, the values of differential settlement decrease with increasing h/L. In general from the computed values shown in Table 2.10, it can be inferred that the differential settlement is quite sensitive to this type of non-homogeneity.

2.5.4 Case 3 (Effect of installation of pile)

General: As mentioned in Sec. 2.2.2, Case 3 refers to the non-homogeneity arising due to the installation of pile. Different cases of such non-homogeneities considered have been designated as I_1, I_2, I_3, I_4 and I_5. I_0 refers to the homogeneous soil condition. I_1 and I_4 refers to a stiff clay, in which the installation of a bored pile is assumed to change the modulus around the pile as shown in Fig. 2.37(a) I_2 and I_5 refers to a soft clay, in which the installation of a driven pile is assumed to cause modulus variation as shown in Fig. 2.38(a). I_3 refers to a loose sandy soil in which installation of a driven pile is assumed to cause modulus variation around the pile, as shown in Fig. 2.40(a).

Percentage pile load: The computed values of percentage pile load (PPL) have been shown in Figs. 2.37 to 2.40, for different cases considered. It can be observed that the installation of pile increases the values of PPL in the case

of soft clay and reduces the values of PPL in the case of stiff clay, for all values of K_R, in the case of concentrated loading (Fig. 2.37 to 2.39). Such an increase or decrease is found to be maximum for $K_R = 100$. Percentage increase or decrease is more for shorter pile and larger value of d_c/d than longer pile and smaller value of d_c/d. Or in other wards the effect of installation is more significant if pile is less dominant. For the extreme case of I_4 and I_5 (for stiff clay and soft clay respectively), in which cases the soil is highly sensitive to the installation of pile, the pile load is affected by about 20 to 22 percent due to the installation of pile, for $L/d = 10$. When $L/d = 40$, the effect of installation is significantly reduced. The effect is roughly one fourth of that for $L/d = 10$.

When subjected to u.d.l., the effect of installation of pile in stiff clay or soft clay, shows some reverse trend, for flexible footing-pile system. There is some increase in pile load if the modulus around pile is less (stiff clay) and there is some decrease in pile load if the modulus around the pile is more (soft clay). (Fig. 2.37 to 2.39). This reverse trend is maximum when L/d is more and d_c/d is less. Such a reverse trend is not observed for $d_c/d = 10$ and $L/d = 10$ (footing dominating) as seen in Fig.2.39.

The value of K_R at which the reversal from increase to decrease (or decrease to increase) takes place shifts towards K_R = 100, as L/d increases and d_c/d decreases (i.e. as the pile becomes more and more dominant), as seen in Figs. 2.37 to 2.39.

The effect of installation of driven pile in loose sand can be seen in Fig. 2.40. In this case there is, in general an increase in pile load due to pile driving. The trends are similar to that of soft clay, discussed earlier. The reverse trend mentioned above are less pronounced, in this case than in the case of soft clay.

Settlement: The values of settlement ratio (S_{PR}^*/S_R^*), have been plotted against K_R, in Figs. 2.32 to 2.36, for different cases. In general, it is observed that the settlement increases or decreases due to the installation of pile depending on whether modulus reduces or increases respectively, compared to homogeneous soil condition (I_o). The effect of installation on settlement is maximum when the loading is concentrated and the footing is flexible. In the case of u.d.l., it is observed that the effect of installation is minimum for K_R = 0.1 to 1, where the settlement ratio itself is minimum (Figs. 2.32 to 2.35). The maximum effect

of installation observed is about 25 percent for $L/d = 10$, $d_c/d = 5$, I_5 and $K_R = 0.01$ (Fig. 2.33). For any practical case of K_R the effect is still less. For loose sand (I_3) trends similar to soft clay are observed (Fig. 2.36).

The effect of installation on the settlement of single free standing pile was also studied using the same method of analysis. The results have been tabulated in Table 2.11. It is observed that the effect of installation on settlement decreases as the length of pile increases. This effect for $L/d = 40$ is about one half of that for $L/d = 10$, in all the cases. The reason for this may be that the proportion of the disturbed zone in the pressure bulb, reduces as the length of pile increases. It may also be observed from Table 2.11, that the effect of installation on settlement for cases I_4 and I_5 are approximately double of those for I_1 and I_2, which indicates that when E_I/E_S is doubled or halved, the percent difference roughly gets doubled.

Bending Moment: The ratio of the maximum bending moment taking into account the effect of installation to the maximum bending moment for homogeneous soil (M_I^*/M_{IO}^*), has been plotted against K_R, for different cases in Figs. 2.41 to 2.43. The following general trends can be observed from these figures.

The effect of installation on bending moment is less for larger values of L/d and smaller value of d_c/d. In

other wards, the effect is less if the pile is dominating.
For concentrated loading, the effect of installation is
minimum when the footing is rigid whereas for u.d.l. the
effect of installation is maximum for such rigid footing-pile
system.

From Figs. 2.41 and 2.42 it was observed that maximum
increase or decrease in bending moment due to installation
is about 60 percent. Maximum decrease is for the case I_5
with K_R = 0.1 and maximum increase is for case I_4 with
K_R = 0.1, both for L/d = 10 and for concentrated load. For
u.d.l. the maximum change in bending moment due to install-
ation of pile, observed is 40 percent, for rigid footing-
pile system, for the cases I_4 and I_5. In the case of u.d.l.
in some cases (Figs. 2.41 and .2.42) there is some change
from decrease to increase or increase to decrease in the
values of bending moment compared to those for the case I_0,
as K_R changes from 0.1 to 100. This trend is similar
to the trends observed earlier in the case of PPL..

Differential settlement: The effect of installation of
pile on differential settlement is shown in Table 2.12,
for d_c/d = 5 and L/d = 10, which indicates the effects for
bored-pile in stiff clay, driven pile in soft clay and
driven pile in loose sand. It can be observed in Table 2.12,

that for stiff clay the differential settlement substantially
increases when subjected to concentrated loading and this
increase is more for $K_R = 0.1$ than $K_R = 1$. When subjected to
u.d.l., there is significant reduction in differential settlement
due to the installation of a bored pile, and this reduction
is more for $K_R = 1$ than $K_R = 0.1$. In the case of soft clay,
the trends are reverse of the trends observed in the case
of stiff clay. In the case of loose sand, the effect of
installation of driven pile is to increase the differential
settlement for u.d.l. and reduce the differential settlement
for concentrated loading, as observed in the case of soft
clay. In general the magnitude of these effects is
upto about 30 percent, except for cases I_4 and I_5 in which
cases soil is highly sensitive to installation.

2.5.5 Conclusions

From the elastic analysis of piled circular footing,
set in soil exhibiting different types of non-homogeneities,
the conclusions that may be drawn are listed below.

Case 1: (Soil stiffness linearly increasing with depth)

1.   Provision of pile to reduce the settlement of circular
        footing is significantly more effective for this
        case of nonhomogeneous soil than homogeneous soil,
        particularly when the footing is fairly flexible and

loading is concentrated. In the case of flexible footing
with pile, subjected to u.d.l., there is some optimum
value of non-homogeneity coefficient ψ , at which provision
of pile is most effective in reducing the settlement of
circular footing.

The load shared by pile is fairly sensitive to this type of
non-homogeneity, the sensitivity being more for rigid footing-
pile system.

The values of maximum bending moment and differential settle-
ment substantially reduce compared to those of homogeneous
soil condition, in the case of concentrated loading. When
subjected to u.d.l., the trends of moment and differential
settlement observed for rigid and flexible footing-pile system
are different.

e 2: (A two layered soil medium)

In general, provision of pile is less effective in reducing
the settlement of circular footing, for this type of non-
homogeneity and its effectiveness is observed to be minimum
in the range of values of h/L between 0.4 and 0.7.

The percentage load shared by pile, is minimum for h/L in
the range of 0.4 to 0.7. If the footing is flexible, the
value of percentage pile load, is less sensitive to this type
of non-homogeneity.

3. The values of bending moment and differential settlement
    are quite sensitive to this type of soil non-homogeneity.
    In general, maximum bending moment and differential
    settlement reduce in the case of u.d.l. and increase in
    the case of concentrated load for fairly rigid footing-
    pile system.

Case 3 (Effect of Installation of piles)

The values of settlement and load shared by pile are
not very sensitive to this type of non-homogeneity,
except when soil is highly sensitive to installation of
pile (cases I_4 and I_5). However the values of bending
moment and differential settlement are fairly sensitive
to this type of non-homogeneity even if soil is moder-
ately sensitive to installation of pile (cases I_1, I_2
and I_3).

The effect of installation of single free standing
pile, on the settlement decreases with increasing values
of L/d. This trend is reflected in the behaviour of
piled circular footing.

2.6 TRANSVERSELY ISOTROPIC SOIL

2.6.1 General

The cross-anisotropic parameters used in the
present analysis have been explained in Sec. 2.2.2.

For a cross anisotropic incompressible material, a number of cases were considered covering the possible range (n = 1 to 4). For the drained case a particular set of anisotropic parameters were used, as explained in Sec. 2.2.2. Results were obtained for free standing single pile also, as no information appears to be available about the effect of cross-anisotropy on the behaviour of single pile. As in the previous cases, solutions were obtained for a number of cases of piled circular footing and circular footing. The computed results are discussed below.

2.6.2 Single Pile

Incompressible Material: The results of surface settlement of single pile has been plotted against 'n' (E_{SH}/E_{SV}) for different values of L/d and K, in Fig 2.44, for incompressible material. It can be observed that the effect of cross anisotropy for values of n > 1, is to reduce the settlement compared to isotropic soil condition.(n=1). The rate of change of settlement with respect to n is found to reduce upto n $\simeq$ 2.5 and then increases.   It appears that for the limiting value of n equal to 4, the settlement tends to zero, for all values of L/d, as in the case of surface loading (Hooper (74)). For shallow piles (L/d = 10), the reduction in settlement due to cross anisotropy is more,

than that for longer piles (L/d = 25). For n = 2.5, K = 20
the reduction in settlement compared to homogeneous soil
(n = 1), is 33 percent, 19 percent and 13 percent for
L/d = 0, 10 and 25 respectively, showing that the effect o
cross anisotropy decreases with increasing length of pile.
It can be observed that for values of n upto about 3.5, the
curves for K = 1500 and K = 200, are almost parallel to
each other, for both L/d = 10 and L/d = 25. This shows
that the reduction settlement due to such anisotropy is not
sensitive to pile compressibility for the values of n in
the range of 1 to 3.5. The theoretical solution given by
Hooper (74), for surface circular loading (L/d = 0) on
elastic continuum has also been shown in Fig. 2.44, for
comparison.

For larger values of n (> 2.5), it was found that the
numerical solution was more sensitive to the type of right
hand side boundary and the value of ν_{SV} used. Hence
for these values of n, ν_{SV} = 0.499 was used. (In most of the
cases analysed a value of ν_{SV} = 0.47 has been used).
The results obtained with restricted right hand side
boundary, has also been shown in Fig. 2.44, for L/d = 25 and
K = 200.

Drained condition: A particular set of drained cross anisotropic parameters corresponding to undraihed parameters with n = 2.5, was considered as explained in Sec. 2.2.2. The relation between undrained and drained parameters for isotropic and cross anisotropic soil, is as follows Hooper (74).

For isotropy: (Prime denotes drained parameter)

$$E'_S = \frac{(1 + \nu'_S) E_S}{(1 + \nu_S)} \qquad (2.6)$$

For cross anisotropy (Hooper (74)):

$$E'_{SV} = \frac{n E'_{SH} E_{SV}}{n' E_{SH}} \qquad (2.7)$$

$$E_{SH} = \frac{(4 - n) E'_{SH}}{2(1 + \nu_{SH})} \qquad (2.8)$$

From the above expressions for the parameters used in the present analysis (n = 2.5, n' = 3, ν'_{SH} = -0.55, ν_S (isotropic) $\simeq$ 0.5). The following relation is obtained.

For isotropic soil: $E'_{SV} = E_{SV}/1.5$

For cross anisotropic soil considered: $E'_{SV} = E_{SV}/2$.

The computed values of settlement using these values of modulii for undrained and drained conditions, are compared in Table 2.13, for some cases of cross-anisotropic soil. From this table it can be seen that reduction in total

(drained) settlement due to cross anisotropy is considerably less than the corresponding reduction in undrained settlement, for the cases considered. Or in other words cross-anisotropy increases the proportion of consolidation part of settlement. Similar observations have been made in the case of circular raft on similar soil by Hooper (74), in his analytical study.

Stress distribution around pile: The results of stress distribution around the pile were obtained for incompressible material having different degrees of anisotropy using mesh 1 (Fig. 4.1 in Chapter 4). The mean normal stress ($\sigma_m = (\sigma_x + \sigma_y + \sigma_z)/3$) around the pile has been plotted against depth (Z), in Fig. 2.45 for different values of cross-anisotropic parameter n, for a pile with $L/d = 8$ and $K = 500$. It can be observed that the values of σ_m are quite sensitive to the value of n, near the tip of the pile and top region of the pile. When n approaches the limiting value of 4, the value of σ_m increases to very large values. The magnitude of σ_m would have some significance in non-linear analysis in which the deformation parameters depend on σ_m. Hence, in such analysis, the anisotropy of the kind considered herein, might have some significant effect on the behaviour of pile.

The variation of octahedral shear stress (τ_{oct}) with depth (Z), has been plotted for different values of n, in Fig. 2.46. It can be observed that the values of τ_{oct} are less sensitive to cross anisotropy (or the values of n) in comparison to the effect on σ_m except for n = 3.99. Earlier it was observed that the settlement is affected by cross-anisotropy marginally upto n = 2.5. The reason for this may be that shear stress distribution around the pile is not very sensitive to the value of n upto 2.5, which is indicated by the study of stresses now.

2.6.3 Piled Circular Footing

Settlement: The results of settlement computed for different cases of cross-anisotropy considered have been presented in non-dimensional form for different parameters in Figs. 2.47 to 2.50. It can be observed, for u.d.l. (Figs. 2.47 and 2.48), as well as concentrated load (Figs. 2.49 and 2.50), the general effect of cross-anisotropy for the cases considered herein, is to reduce the settlement. The magnitude of this reduction increases with increasing n values.

In Fig. 2.48 (b), it can be observed that the $S^* - n$ curves for $K_R = 0.1$ and $K_R = 100$ and for K = 1500 and K = 200 are parallel to each other, indicating that the reduction in settlement due to cross anisotropy (for u.d.l. and $d_c/d = 5$ and L/d = 10) is fairly independent of the values

of K and also K_R. In Fig. 2.48(a) such curves for $K_R = 0.1$ and $K_R = 100$ are fairly parallel for $K = 200$ and the curves are not parallel for $K = 1500$, indicating that if pile is fairly dominant the reduction in settlement is sensitive to the values of K_R. In Fig. 2.47 and 2.48, it can be observed that when n approaches the limiting value of 4, the settlement reduces by very large amount and these settlements are almost independent of K and L/d. It is also observed for n $\cong$ 4., the settlement is insensitive to values of K_R.

For concentrated loading the results of settlement have been presented in Figs. 2.49(a) and 2.50. In Fig. 2.49(b), the values of settlement have been plotted against the value of n. For this loading it can be observed that for n in the range of 1.5, the effect of K_R is slightly less pronounced than other value of n, for both L/d = 10 and L/d = 25 (Fig.2.49(b)). As n approaches the limiting value of 4, the settlement becomes almost independent of L/d for $K_R = 100$; but for $K_R = 0.01$, the value of L/d still has significant effect on settlement even for n $\cong$ 4.

It can be observed that the reduction in drained non-dimensional settlement ($S^* E_S/qa$) due to the cross-anisotropy is slightly more than the reduction in undrained case (comparing the difference in settlement for R_0 and R_2 with that for R_0' and R_2' in Figs. 2.47 to 2.50). But

it is to be noted that the relation between drained and undrained modulii are different for isotropic and aniso-tropic cases as discussed in previous section. If the modulus is substituted and the actual settlement compared, the reduction in total or drained settlement due to cross anisotropy is found to be significantly less than the corresponding reduction in undrained case (referring to Table 2.14 - for undrained case the reduction in S^*/qd is about 20 percent and the corresponding reduction for drained case is about 6 percent).

In table 2.14, the settlement ratio (S^*_{PR}/S^*_R), has been compared for different values of n between 1 and 2.5. It can be observed that the effect of cross-anisotropy on the settlement ratio for undrained as well as drained cases is small (less than 10 percent in most of the cases), for both L/d = 10 and 25 and for both K_R = 0.1 and 10 for both cases of loading. In the drained case the effect of cross anisotropy is to reduce the settlement ratio and in the undrained case it is the reverse. However, for n = 3.5, it was observed that the settlement ratio was significantly different from that for isotropic soil and when n approaches the limiting value of 4, the piles become completely in-effective in reducing the settlement (In this case the settlement ratio approaches unity).

Percentage pile load: The computed values of percentage pile
load (PPL), have been presented in Figs. 2.51 to 2.53, for
different parameters. For incompressible material the values
of PPL reduce with increasing n, in all the cases. This
reduction is small for n upto about 2.5, and for n greater
than 2.5 the values of PPL reduce by large amount as can
be seen in the Fig. 2.51(b). It can also be observed in
Fig. 2.51 that the value of PPL is less sensitive to
anisotropy (or the value of n), for concentrated loading
than u.d.l. (For K_R = 1, PPL is 82 and 77 for n = 1 and 3.5
respectively for concentrated load, whereas PPL is 54 and 36
for u.d.l., for the same n values, in Fig. 2.51). Another
observation that can be made in the Fig. 2.51(b) is that
for both K_R = 100 and K_R = 1, and for both cases of loading
the PPL – n curves for L/d = 10 and 25 are almost parallel
to each other in the range of n between 1 and 2.5, indicating
that the reduction in PPL is fairly independent of L/d, in
this range of n-values.

In Fig. 2.53, for drained condition, it can be
observed that there is increase in the value of PPL for
concentrated loading for all values K_R and a mixed trend
in the case of u.d.l. depending on K_R values. However,
the effect is small for the parameters considered herein.

Bending moment: The values of maximum footing bending moments (Maximum among the values computed at Gauss points), have been plotted against K_R in Fig. 2.54 (for u.d.l.) and Fig. 2.55 (for concentrated load), for a particular piled ($L/d = 10$, $d_c/d = 5$ and $K = 1500$) circular footing, for different values of anisotropic parameters. It can be observed from Fig. 2.54 that the values of maximum bending moments reduce with increasing values of n and this reduction is small (less than 20 percent) for n upto 2.5. For n = 3.5, there is large change in bending moment. The effect of cross anisotropy for fully drained case is also to reduce the value of bending moment for flexible footing-pile system the reduction being more for very flexible footing-pile. However, if the footing is rigid ($K_R \geq 10$), the cross anisotropy tends to increase the value of bending moment for drained case.

In the case of concentrated loading and incompressible material, the cross-anisotropy increase the value of bending moment. The effect is insignificant for flexible footing-pile system (Fig. 2.55) and for fairly rigid footing-pile ($K_R = 10$) also, the effect is small (about 13 percent for n = 2.5). This trend is consistant with the trend of PPL observed earlier. For fully drained condition the effect is

slightly more than undrained condition and the effect is significant for both flexible and rigid footing-pile system in contrast to undrained case. (Fig. 2.55).

Stress distribution around pile: The distribution of σ_m with depth is shown in Fig. 2.56, for different cross-anisotropic parameters, for a particular piled circular footing. It is observed that the effect of cross-anisotropy is to increase the value of σ_m, as previously observed in the case of single pile (Sec. 2.6.2), but to a smaller extent in this case than the previous case.

The distribution of τ_{oct} is shown in Fig. 2.57 for piled circular footing considered. It can be observed that the effect of cross-anisotropy is to reduce the value of τ_{oct} in general as previously observed in the case of single pile. However in the top onefourth length of the pile, no definite trend is observed. Comparison of τ_{oct} distribution around the pile for piled circular footing (Fig. 2.57) and single pile (Fig. 2.46) reveals that the shear stresses in the top region are very small in the former case compared to latter case, for both isotropic and cross anisotropic soil conditions.

The contact pressure distribution has been shown in the Fig. 2.57(b). It can be observed that the contact

pressure increases with increasing value of n, particularly near the edge. For n = 3.99, the contact pressure increases to a large value, indicating that almost the entire load is transmitted by footing. This is consistant with the trend observed in the values of PPL earlier.

2.6.4 Conclusions

From the analysis of piled circular footing and single pile set in cross anisotropic soil the following general conclusions can be drawn.

1. In the case of single piles, the effect of cross anisotropy is to reduce the settlement for the range of parameters considered. This reduction reduces with increasing values of L/d. The reduction in settlement compared to isotropic case is fairly independent of the values of K, for n in the range of 1 to 3.5. For the limiting value of n = 4, the settlements appear to tend to zero. The reduction in total (fully drained) settlement due to cross anisotropy is significantly less, compared to undrained settlement for the range of parameters considered. The distribution of σ_m near the tip is found to be quite sensitive to cross-anisotropy in the case of incompressible material.

2. The settlement of piled circular footing significantly reduces due to the cross anisotropy, in the range of parameters considered herein. This reduction is considerably more in the case of undrained condition than drained condition. The settlement ratio (S_{PR}^*/S_R^*) is not affected much (less than about 10 percent), by the cross anisotropy, for n upto 2.5. Hence the effectiveness of provision of pile in reducing the settlement of circular footing is not very much different from that for isotropic case, in this range of n.

3. The percentage load shared by pile in a piled circular footing reduces with increasing values of n for incompressible material. The reduction is small upto n = 2.5. For the limiting value of n = 4, almost entire load is transmitted by footing.

4. The values of bending moment in a piled circular footing subjected to concentrated loading, increase by a small amount (less than 15 percent) due to the cross anisotropy, in the undrained case. There is some reduction in the bending moment due to cross-anisotropy when subjected to u.d.l., except for rigid footing-pile system, in which case there is some increase in bending moment.

5. The shear stress distribution in the top region of pile is significantly less in the case of piled circular footing, compared to single free standing pile, for both isotropic and cross-ansisotropic incompressible material. The effect of cross-anisotropy is less pronounced on the distribution of σ_m, in the case of piled circular footing than single pile. The contact pressure increases due to cross anisotropy in the case of incompressible material, particularly so near the edge of the piled circular footing.

TABLE 2.1 IN-PLANE STRESSES AND BENDING STRESSES

Diameter of footing/diameter of pile = 5
Pile stiffness factor   (K)   = 1500

/d	K_R	$\nu_S = 0.47$		$\nu_S = 0$	
		Maximum Bending stress	Max.inplane stress	Max.bending stress	Max. inplane stress
)	10	18.33[a]	1.51	37.60	2.93
		1.22[b]	0.02	0.82	0.04
	1	69.82	4.60	123.44	7.98
		4.31	0.18	2.84	0.13
25	10	31.73	2.14	48.19	3.24
		0.66	0.04	0.48	0.05
	1	111.48	6.32	154.96	8.88
		2.32	0.08	1.39	0.05

a - For Unit uniform pressure over entire footing area.

b - For Unit uniform pressure over pile area.

TABLE 2.2 SETTLEMENT INFLUENCE FACTORS

(Piled Circular Footing—$d_c/d = 5$)

$I_S^* = S^* \dfrac{E_S}{qd}$, where I_S^* = maximum settlement influence factor, S^* = maximum settlem...

E_S = Young's modulus of soil, d = diameter of pile, and

q = applied uniform pressure over the entire footing area for u.d.l. or over the pile area for concentrated load.

Poisson's Ratio γ_S	Length/Dia. of pile L/d	Pile Stiffness Factor K	$K_R = 0.01$		$K_R = 0.1$		$K_R = 1.0$		$K_R = 10$		$K_R = 100$	
			I_S^* udl	$I_S^* \times 100$ Conc. Load	I_S^* udl.	$I_S^* \times 100$ Conc. Load	I_S^* udl.	$I_S^* \times 100$ Conc. Load	I_S^* udl.	$I_S^* \times 100$ Conc. Load	I_S^* udl.	$I_S^* \times 100$ Conc. Load
1	2	3	4	5	6	7	8	9	10	11	12	13
0.47	10	1500	2.712	10.630	2.331	10.280	2.255	9.385	2.151	8.665	2.125	8.495
		500	2.734	11.130	2.422	10.730	2.291	9.730	2.197	8.878	2.175	8.678
		200	2.777	12.180	2.482	11.660	2.348	10.370	2.281	9.265	2.268	9.093
	25	1500	2.283	6.055	1.938	5.370	1.708	5.725	1.434	5.495	1.370	5.435
		500	2.356	7.158	2.015	7.012	1.828	6.619	1.602	6.237	1.551	6.135
		200	2.475	9.183	2.156	8.898	2.008	8.123	1.863	7.438	1.835	7.348
	40	1500	2.117	4.644	1.780	4.596	1.493	4.454	1.160	4.316	1.083	4.275
		500	2.239	6.186	1.896	6.074	1.682	5.769	1.424	5.465	1.364	5.380
		200	2.412	8.693	2.090	8.433	1.935	7.715	1.779	7.080	1.748	7.001

Cont⁴. Table 2.2

1	2	3	4	5	6	7	8	9	10	11	12	13
0.30	10	1500	2.937	10.160	2.596	9.940	2.430	9.330	2.228	8.305	2.179	8.685
		500	2.972	10.700	2.628	10.410	2.481	9.702	2.291	9.071	2.244	8.915
		200	3.008	11.750	2.685	11.370	2.558	10.410	2.404	9.565	2.371	9.463
	25	1500	2.484	5.745	2.146	5.695	1.830	5.535	1.446	5.390	1.354	5.350
		500	2.570	6.854	2.223	6.755	1.973	6.488	1.641	6.219	1.561	6.141
		200	2.701	8.880	2.363	8.673	2.188	8.106	1.947	7.588	1.895	7.548
	40	1500	2.316	4.423	1.979	4.392	1.612	4.304	1.171	4.214	1.067	4.187
		500	2.451	5.960	2.108	5.884	1.826	5.674	1.462	5.456	1.375	5.391
		200	2.638	8.445	2.301	8.253	2.117	7.718	1.864	7.240	1.810	7.205
0.00	10	1500	2.860	8.723	2.586	8.587	2.381	8.279	2.074	7.990	1.994	7.927
	25	1500	2.404	4.928	2.144	4.904	1.793	4.831	1.324	4.755	1.206	4.731
		500	2.491	6.045	2.244	5.984	1.955	5.832	1.543	5.668	1.437	5.614
		200	2.640	8.028	2.402	7.833	2.199	7.503	1.884	7.165	1.811	7.164

TABLE 2.3 SETTLEMENT INFLUENCE FACTORS

(Piled Circular Footing d_c/d = 10 and 15)

$$I_S^* = s^* \cdot E_S/qd \quad \text{(Notations as given in Table 2.2)}$$

ν_s	L/d	K	K_R = 0.01		K_R = 0.1		K_R = 1.0		K_R = 10		K_R = 100	
			I_S^* udl. Load	I_S^* x100 Conc. Load	I_S^* udl.	I_S^* x100 Conc. Load	I_S^* udl.	I_S^* x100 Conc. Load	I_S^* udl.	I_S^* x100 Conc. Load	I_S^* udl.	I_S^* x100 Conc. Load
1	2	3	4	5	6	7	8	9	10	11	12	13
Diameter of footing/diameter of pile = 10												
0.47	10	1500	6.480	10.090	5.925	9.090	5.850	7.090	5.500	5.755	5.485	5.515
		500	6.496	10.550	5.993	9.442	5.632	7.222	5.541	5.803	5.525	5.558
		200	6.548	11.510	6.080	10.060	5.725	7.435	5.610	5.903	5.595	5.670
	25	1500	5.635	5.896	4.904	5.615	4.549	4.937	4.309	4.368	4.253	5.250
		500	5.747	6.933	5.082	6.498	4.720	5.474	4.582	4.692	4.555	4.556
		200	5.953	8.828	5.362	7.960	5.013	6.258	4.960	5.185	4.957	4.998
	40	1500	5.245	4.554	4.462	4.392	4.049	3.976	3.635	3.607	3.544	3.526
		500	5.459	6.025	4.759	5.688	4.391	4.872	4.170	4.228	4.128	4.140
		200	5.787	8.378	5.182	7.575	4.828	5.988	4.770	4.980	4.765	4.805
0.30	10	1500	7.035	9.651	6.351	8.885	5.971	7.303	5.923	6.141	5.922	5.935
		500	7.049	10.120	6.411	9.249	6.031	7.451	5.984	6.205	5.978	5.988
		200	7.095	11.090	6.495	9.920	6.133	7.713	6.088	6.352	6.088	6.132

Contd. Table 2.3

1	2	3	4	5	6	7	8	9	10	11	12	13
0.30	25	1500	6.155	5.601	5.340	5.402	4.937	4.904	4.487	4.458	4.389	4.369
		500	6.266	6.646	5.516	6.309	5.159	5.515	4.853	4.873	4.786	4.754
		200	6.480	8.535	5.803	7.840	5.478	6.423	5.348	5.503	5.335	5.352
	40	1500	5.745	4.339	4.904	4.226	4.405	3.908	3.758	3.642	3.617	3.602
		500	5.962	5.310	5.198	5.545	4.812	4.910	4.411	4.381	4.328	4.323
		200	6.320	8.135	5.633	7.488	5.308	6.158	5.153	5.293	5.135	5.152
0.0	25	1500	5.962	4.789	5.311	4.666	4.891	4.369	4.225	4.086	4.062	4.029
		500	6.087	5.834	5.487	5.607	5.175	5.064	4.689	4.601	4.576	4.515
		200	6.323	7.670	5.768	7.140	5.565	6.063	5.303	5.355	5.278	5.258

Diameter of footing/diameter of pile = 15

1	2	3	4	5	6	7	8	9	10	11	12	13
0.47	10	1500	10.250	9.560	9.725	7.965	9.076	5.410	8.705	4.079	8.650	3.875
0.47	25	1500	9.135	5.725	8.220	5.240	7.586	4.185	7.496	3.464	7.485	3.344
0.00	25	1500	9.626	4.644	8.665	4.399	8.221	3.863	7.690	3.434	7.550	3.356

TABLE 2.4   PERCENTAGE LOAD SHARED BY PILE
(Piled Circular Footing—$d_c/d = 5$)

s	L/d	K	$K_R = 0.01$		$K_R = 0.1$		$K_R = 1.0$		$K_R = 10.0$		$K_R = 100.0$	
			udl.	Conc. Load	udl.	Conc. Load	udl.	Conc. Load	udl.	Conc. Load	udl.	Conc. Load
1	2	3	4	5	6	7	8	9	10	11	12	13
0.47	10	1500	18.38	92.37	30.39	83.71	41.15	66.76	47.41	52.81	48.87	49.64
		500	17.29	91.73	28.68	82.95	38.50	65.34	44.44	50.31	45.79	46.54
		200	16.08	90.32	26.16	80.67	34.48	61.47	39.14	45.01	40.07	40.61
	25	1500	20.76	96.06	35.89	91.46	53.74	81.75	66.92	73.02	70.00	70.86
		500	19.25	94.77	33.05	89.16	48.53	77.33	59.94	66.39	62.55	63.37
		200	17.44	92.42	29.16	84.90	41.14	69.40	49.08	55.32	50.70	51.26
	40	1500	21.37	96.95	37.40	93.43	57.35	85.89	72.68	78.94	76.28	77.16
		500	19.62	95.33	34.00	90.40	50.76	79.87	63.42	69.97	66.33	67.16
		200	17.65	92.69	29.57	85.42	42.07	70.45	50.47	56.74	52.18	52.75
0.30	10	1500	21.69	94.02	33.87	86.87	47.16	73.15	56.24	61.74	58.36	59.11
		500	20.38	93.01	32.25	85.87	44.45	71.45	53.18	59.04	55.23	55.95
		200	19.27	91.61	29.79	83.51	40.32	67.48	47.67	53.50	49.26	49.76
	25	1500	23.66	97.00	38.59	93.33	58.10	85.95	73.27	79.32	76.84	77.66
		500	22.13	95.65	36.13	91.19	53.27	81.80	66.83	73.15	69.99	70.77
		200	20.53	93.47	32.49	87.18	46.22	74.39	56.52	62.64	58.73	59.25

Contd. Table 2.4

<div style="page-break-after:always"></div>

1	2	3	4	5	6	7	8	9	10	11	12	13
0.30	40	1500	24.10	97.67	39.83	94.89	60.96	89.17	77.80	83.96	81.76	82.60
		500	22.49	96.12	36.89	92.14	55.03	83.77	69.56	75.95	72.93	73.72
		200	20.69	93.67	32.82	87.59	46.94	75.19	57.59	63.73	59.87	60.39
0.00	10	1500	22.61	94.95	35.76	89.84	51.79	79.49	64.44	70.56	67.56	68.38
	25	1500	24.46	97.52	39.65	94.92	60.65	89.63	78.33	84.83	82.67	83.54
		500	23.36	96.29	37.17	92.63	55.95	85.44	71.81	78.57	75.73	76.53
		200	21.81	94.12	33.56	88.68	48.83	77.93	61.39	67.90	64.34	64.86

TABLE 2.5 PERCENTAGE LOAD SHARED BY PILE
(Piled Circular Footing d_c/d = 10 and 15)

| | | | K_R = 0.01 | | K_R = 0.1 | | K_R = 1.0 | | K_R = 10.0 | | K_R = 100.0 | |
| | | | udl. | Conc. Load | udl. | Conc. Load | udl. | Conc. Load | udl. | Conc. Load | udl. | Conc. Load |
γ_s	L/d	K										
1	2	3	4	5	6	7	8	9	10	11	12	13
Diameter of Footing/Diameter of Pile = 10												
0.47	10	1500	8.97	85.37	15.70	68.26	19.54	40.77	19.40	23.20	19.40	19.87
		500	8.27	84.58	15.19	66.77	17.96	39.04	17.63	21.38	17.61	17.98
		200	7.35	82.34	13.40	62.84	15.29	34.82	14.63	17.89	14.43	14.68
	25	1500	11.99	92.32	24.03	82.37	35.54	62.90	41.98	47.26	43.30	43.91
		500	10.68	90.12	21.05	77.97	30.20	55.91	34.38	39.20	35.09	35.57
		200	8.97	86.03	17.27	70.11	22.77	44.96	24.23	28.05	24.30	24.59
	40	1500	12.98	94.09	26.48	86.79	41.50	70.43	51.20	56.91	53.22	53.87
		500	11.31	91.21	22.56	80.34	33.61	60.16	39.32	44.36	40.32	40.82
		200	9.24	86.49	17.92	71.08	24.06	46.51	25.94	29.82	26.10	26.40
0.30	10	1500	10.88	87.87	19.70	73.28	25.19	48.52	27.02	31.25	27.26	27.74
		500	10.27	86.83	18.27	71.47	23.34	46.13	24.74	28.86	25.05	25.43
		200	9.46	84.72	16.35	67.62	20.06	41.22	20.86	24.42	21.01	21.22

Contd. Table 2.5

1	2	3	4	5	6	7	8	9	10	11	12	13
0.30	25	1500	13.62	93.78	26.31	85.59	40.53	69.39	49.94	55.58	51.85	52.49
		500	12.49	91.71	23.70	81.44	35.15	62.26	41.81	46.96	43.12	43.59
		200	10.96	87.97	19.97	74.16	27.43	51.03	30.72	34.82	31.28	31.52
	40	1500	14.47	95.23	28.42	28.84	45.71	75.83	58.22	64.21	60.81	61.49
		500	13.02	92.59	24.99	83.40	38.14	65.91	46.26	51.58	47.84	48.33
		200	11.20	88.34	20.50	74.92	28.55	52.36	32.23	36.38	32.85	33.09
0.00	25	1500	14.15	94.94	27.22	88.36	41.23	75.25	57.12	63.50	60.00	60.71
		500	13.26	92.87	24.46	84.03	38.26	67.42	47.74	53.49	49.78	50.29
		200	11.64	89.07	20.70	76.55	29.92	55.29	35.21	39.73	36.34	36.58

Diameter of Footing/Diameter of pile = 15

1	2	3	4	5	6	7	8	9	10	11	12	13
0.47	10	1500	6.25	78.27	10.42	54.02	10.57	25.69	9.20	11.63	8.93	9.20
0.47	25	1500	9.44	88.44	13.33	72.91	25.16	47.98	27.18	31.17	27.47	27.91
0.00	25	1500	11.23	92.21	22.13	81.40	34.10	61.98	41.36	46.61	42.94	43.47

Contd. Table 2.6

1	2	3	4	5	6	7	8	9	10
25	0.2211	-222.3	-181.7	4.642	4.494	-283.9	-220.0	2.276	2.434
	0.2789	-150.2	-165.5	3.492	4.147	-195.0	-204.1	1.670	2.212
	0.3211	-112.9	-152.6	2.868	3.885	-150.0	-190.1	1.344	2.048
	0.3789	-75.62	-139.1	2.213	3.583	-104.9	-175.0	0.997	1.856
	0.4423	-46.48	-122.3	1.665	3.237	-69.41	-155.7	0.702	1.649
	0.5577	-13.32	-96.07	0.956	2.687	-28.57	-125.0	0.322	1.331
	0.6423	0.073	-80.47	0.571	2.341	-10.79	-106.4	0.126	1.135
	0.7577	8.941	-64.45	0.240	1.965	1.111	-87.20	-0.046	0.923
	0.8423	7.207	-56.43	0.020	1.716	3.461	-76.57	-0.114	0.796
	0.9577	—	-48.90	—	1.461	—	-66.56	—	0.665

TABLE 2.7 FOOTING BENDING MOMENTS
(Piled Circular Footing - $K_R = 1$)

$d_c/d = 5$ $K = 1500$ $I_{MR} = M_R/qa^2$ $I_{MT} = M_T/qa^2$

(Notations as given in Table 2.6)

Length/ Dia. of pile L/d	Radial Distance from centre/ Radius of footing r/a	Poisson's ratio $\nu_s = 0.47$				Poisson's ratio $\nu_s = 0.00$			
		udl.		Conc. Load		udl.		Conc. Load	
		$I_{MR}\times1000$	$I_{MT}\times1000$	$I_{MR}\times1000$	$I_{MT}\times1000$	$I_{MR}\times1000$	$I_{MT}\times1000$	$I_{MR}\times1000$	$I_{MT}\times1000$
10	0.2106	-112.60	-56.56	6.787	3.374	-167.90	-78.45	3.818	1.8
	0.2394	- 89.53	-57.72	5.823	3.557	-137.40	-82.60	3.251	1.9
	0.2606	- 72.89	-56.69	5.127	3.595	-114.80	-82.37	2.830	1.9
	0.2894	- 50.60	-53.65	4.198	3.563	- 84.03	-73.99	2.253	1.9
	0.3211	- 37.10	-50.61	3.599	3.515	- 65.88	-75.47	1.894	1.9
	0.3789	- 15.76	-43.98	2.641	3.339	- 37.58	-63.11	1.327	1.7
	0.4423	- 0.22	-35.76	1.888	3.054	- 16.80	-58.30	0.882	1.6
	0.5577	14.87	-23.62	0.979	2.550	3.81	-43.37	0.358	1.3
	0.6423	18.43	-16.91	0.545	2.215	10.20	-34.70	0.119	1.1
	0.7577	17.67	-10.90	0.130	1.846	10.87	-26.76	-0.064	0.8
	0.8423	11.40	- 8.92	0.014	1.619	7.36	-23.13	-0.120	0.7
	0.9577	3.742	- 7.84	—	1.380	—	-20.60	—	0.6

Contd. Table 111

Contd. Table 2.7

1	2	3	4	5	6	7	8	9	10
25	0.2106	-178.10	-87.95	3.657	1.874	-210.30	-97.97	1.875	0.964
	0.2394	-145.80	-91.04	3.135	1.966	-173.50	-103.60	1.595	1.015
	0.2606	-122.50	-90.47	2.758	1.982	-146.30	-103.60	1.387	1.020
	0.2894	-91.29	-87.24	2.255	1.958	-109.10	-99.91	1.102	0.995
	0.3211	-72.00	-83.86	1.932	1.928	-87.01	-95.95	0.924	0.966
	0.3789	-41.47	-75.68	1.414	1.825	-52.47	-87.44	0.644	0.902
	0.4423	-18.68	-64.85	1.007	1.665	-26.79	-75.79	0.423	0.809
	0.5577	5.20	-47.99	0.517	1.387	-0.04	-57.63	0.165	0.653
	0.6423	12.97	-38.11	0.285	1.203	8.65	-46.85	0.048	0.553
	0.7577	15.80	-28.58	0.090	1.001	11.40	-36.61	-0.040	0.446
	0.8423	11.18	-24.43	0.003	0.878	8.56	-31.64	-0.065	0.385
	0.9577	-	-21.07	-	0.748	-	-27.79	-	0.325

TABLE 2.8a   COMPARISON OF PILED FOOTING AND UNPILED FOOTING

a - $\nu_S = 0.47$ (undrained)   b - $\nu_S = 0.30$ (drained)

Description	Type of loading	Raft 1 $K_R=1$	Piled raft 1 $K_R=1$	Raft 1 $K_R=100$	Piled raft 1 $K_R=100$	Raft 2 $K_R=1$	Raft 2 $K_R=100$
Maximum Settlement S^* cm.	udl.	5.28[a] / 6.59[b]	3.61 / 4.48	4.90 / 6.13	3.40 / 4.01	2.64 / 3.30	2.45 / 3.07
	Conc. Load	7.20 / 8.60	3.75 / 4.35	4.90 / 6.13	3.40 / 4.01	3.67 / 4.39	2.45 / 3.07
Differential Settlement Δ cm	udl.	0.62 / 0.59	0.34 / 0.57	– / –	– / –	0.31 / 0.30	– / –
	Conc. Load	3.2 / 3.5	0.93 / 0.88	– / –	– / –	1.60 / 1.75	– / –
Maximum Bending Moment M^* t m/m	udl.	0.42 / 0.41	−0.90 / −1.10	0.58 / 0.48	−1.11 / −1.35	0.42 / 0.41	0.58 / 0.48
	Conc. Load	4.00 / 4.00	1.36 / 1.07	5.20 / 4.96	2.22 / 1.80	– / –	– / –
Maximum Shear Force Q^* t/m	udl.	0.98 / 0.97	4.52 / 5.42	1.32 / 1.24	9.17 / 10.20	0.98 / 0.97	1.32 / 1.24
	Conc. Load	18.8 / 18.9	3.12 / 2.83	20.00 / 20.00	10.40 / 8.60	18.80 / 18.90	20.00 / 20.00
Percent Load Taken by Pile % PPL %	udl.	0.00 / 0.00	41.0 / 47.0	0.00 / 0.00	49.00 / 59.00	0.00 / 0.00	0.00 / 0.00
	Conc. Load	0.00 / 0.00	67.0 / 73.0	0.00 / 0.00	49.00 / 59.00	0.00 / 0.00	0.00 / 0.00
Thickness of footing cm	–	9.50	9.50	44.00	44.00	19.00	88.00
Diameter of footing d_c cm	–	200	200	200	200	400	400
Length of pile L m	–	0	4.00	0	4.00	0	0
Volume of concrete m^3		0.30	0.80	1.40	1.88	2.38	11.1

TABLE 2.8b COMPARISON OF PILED FOOTING WITH OTHER TYPES
OF FOUNDATIONS

Data: $c_u = 10 t/m^2$, $d = 1m$, $E_S = 500 \ t/m^2$

$\nu_S = 0.5$, $K = 1500$, $L/d = 10$, $K_R = 100$

$d_c/d = 5$, $q = 1000 \ t/m^2$, Factor of safety against
shear failure = 2

Permissible settlement = 4.5 cm.

Conc. load - q over circle of dia. d at centre.

Description	Single Pile	Circular Footing	Piled Circular Footing	3 Free Standing Piles
Settlement cm	5.50	6.00	4.25	1.83
Bearing Capacity[a] t/m^2	490	1575	2002	1470
Volume of material[b] m^3	7.85	19.63	27.48	43.18

a - calculated as sum of bearing capacity of pile and footing
   area in contact with soil, for piled circular footing, as
   discussed in Sec. 4.4.4.1.

b - Calculated assuming uniform thickness for footing or cap.

TABLE 2.9a SETTLEMENT RATIO (S^*_{PR}/S^*_R) NON-HOMOGENEOUS SOIL CASE 1

$d_c/d = 5$ $\nu_S = 0.3$, $K = 1500$

L/d	ψ	$K_R = 1$		$K_R = 10$		$K_R = 100$ Both Load
		udl.	Conc.Load	udl.	Conc.Load	
10	∞	0.666	0.465	0.658	0.616	0.646
	10	0.577	0.324	0.527	0.467	0.500
	2.5	0.543	0.209	0.430	0.337	0.377
25	∞	0.500	0.276	0.427	0.377	0.400
	10	0.434	0.157	0.302	0.234	0.257
	2.5	0.463	0.114	0.287	0.188	0.215

TABLE 2.9b DIFFERENTIAL SETTLEMENT (Δ_{PR})
NON-HOMOGENEOUS SOIL - CASE 1

$d_c/d = 5$ $\nu_S = 0.3$ $K = 1500$ $I_\Delta = \dfrac{\Delta_{PR} E_{SO}}{qa}$

L/d	ψ	$K_R = 0.1$		$K_R = 1.0$		$K_R = 10$	
		udl.	Conc. Load	udl.	Conc. Load	udl.	Conc. Load
10	∞	13.79	77.40	7.86	41.50	1.78	7.20
	10	15.05	52.57	9.28	30.26	2.16	6.43
	2.5	13.94	29.97	9.60	19.33	2.48	4.66
25	∞	20.32	38.61	12.08	21.64	2.70	4.40
	10	19.91	23.48	12.63	14.08	2.96	3.11
	2.5	15.98	16.19	11.30	10.74	2.95	2.67

For udl. the values tabulated are I_Δ x 50

For Conc. load the values tabulated are I_Δ x 5000.

TABLE 2.10   DIFFERENTIAL SETTLEMENT (Δ_{PR}) LAYERED SOIL

$d_c/d = 5$ $L/d = 10$ and 25 $E_{ST}/E_{SB} = 5$ $E_P/E_{ST} = 400$

$\nu_S = 0.3$ $I_\Delta = (\Delta E_{ST})/qd$

L/d	h/L	$K_R = 0.1$		$K_R = 1.0$		$K_R = 10.0$	
		udl	Conc. Load	udl.	Conc.Load	udl.	Conc. Load
		I_Δ	$I_\Delta \times 100$	I_Δ	$I_\Delta \times 100$	I_Δ	$I_\Delta \times 100$
10	0.1	0.676	10.852	0.269	4.127	0.067	0.624
	0.5	0.352	7.145	0.149	3.590	0.048	0.663
	1.0	0.545	5.111	0.308	2.732	0.081	0.525
	1.5	0.630	4.526	0.367	2.452	0.093	0.475
25	0.1	0.931	5.069	0.499	2.410	0.114	0.409
	0.4	0.718	3.995	0.431	2.175	0.107	0.417
	1.0	0.873	2.977	0.535	1.669	0.130	0.322
	1.5	0.902	2.832	0.552	1.592	0.133	0.308

TABLE 2.11   EFFECT OF INSTALLATION ON SETTLEMENT OF SINGLE FREE STANDING PILE

$$I_S^* = S^* E_S / qd$$

Maximum settlement influence factors (I_S^*) have been given in Table

Description		L/d	Considering effect of installation	Homogeneous soil (I_o)	Percent Difference
$K = 500$ $\nu_S = 0.47$	I_1	10 40	0.137 0.0693	0.116 0.0630	+18.1 +10.0
$K = 1500$ $\nu_S = 0.47$	I_2	10 40	0.0935 0.0426	0.1110 0.0471	−15.4 − 9.7
$K = 1500$ $\nu_S = 0.3$	I_3	10 40	0.0915 0.0414	0.1070 0.0449	−14.1 − 8.8
$K = 500$, $\nu_S = 0.47$	I_4	10	0.162	0.116	+39.7
$K=1500$, $\nu_S = 0.47$	I_5	10	0.0815	0.111	−26.2

TABLE 2.12   EFFECT OF INSTALLATION OF PILE ON DIFFERENTIAL
SETTLEMENT (Δ)

$d_c/d = 5$ $L/d = 10$ $I_\Delta = \Delta E_S/qd$

Description of soil	Installation	$K_R = 0.1$		$K_R = 1$	
		udl.	Conc.Load	udl.	Conc. Load
		I_Δ	I_Δ x100	I_Δ	I_Δ x 100
Stiff clay (Bored pile) $K = 500$ $s = 0.47$	I_0	0.474	4.840	0.232	2.551
	I_1	0.435	6.311	0.168	3.102
	I_4	0.369	7.822	0.104	3.611
Soft clay (Driven pile) $K = 1500$ $s = 0.47$	I_0	0.483	4.491	0.238	2.332
	I_2	0.498	3.240	0.289	1.815
	I_5	0.457	2.291	0.309	1.382
Loose sand (Driven pile) $K = 1500$ $s = 0.3$	I_0	0.690	3.870	0.393	2.075
	I_3	0.771	3.025	0.461	1.672

TABLE 2.13   COMPARISION OF SETTLEMENT OF SINGLE PILE - CROSS
ANISOTROPIC SOIL

$E_{SV} = 1$

The computed values of S^*/qd are given in Table

L/d	Undrained $\nu_{SV} = 0.5$			Drained $\nu_{SV} = 0$		
	n=1	n = 2.5	% reduction	n=1	n=3	reduction%
10	0.110	0.086	23	0.137	0.127	7.3
25	0.062	0.051	18	0.075	0.074	1.5

Undrained parameters - m = 0.38   Drained Parameters - m'=0.76

$\nu_{SV} \simeq 0.5$, $\nu_{SH} = 1-n/2$, n = 2.5   (Corresponding to above undrained parameters) $n'=3$, $\nu'_{SH} = -0.55$

$\nu'_{SV} = 0, E'_{SV} = E_S$ / 2

TABLE 2.14   COMPARISON OF SETTLEMENT – EFFECT OF CROSS-ANISOTROPY

$d_c/d = 5$, $K = 1500$

Cross anisotropic parameters:
Undrained   – $\nu_{SV} = 0.47$, $\nu_{SH} = 1-n/2$, $m = 0.38$

Drained   – $\nu'_{SV} = 0.00$, $\nu'_{SH} = -0.55$, $m' = 0.76$

(a)   Settlement Ratio $= (S^*_{PR}/S^*_R)$

L/d	n or n'	$K_R = 0.1$		$K_R = 10.0$	
		udl.	Conc. Load	udl.	Conc. Load
10 (undrained)	1.0	0.633	0.309	0.715	0.683
	1.5	0.638 (1)	0.304 (2)	0.721 (1)	0.686 (0)
	2.5	0.675 (7)	0.323 (5)	0.764 (7)	0.725 (6)
25 (undrained)	1.0	0.513	0.179	0.477	0.433
	1.5	0.519 (1)	0.179 (0)	0.489 (3)	0.441 (2)
	2.5	0.554 (8)	0.196 (9)	0.542 (14)	0.489 (13)
10 (Drained)	1.0	0.640	0.245	0.600	0.548
	3.0	0.622 (3)	0.223 (9)	0.560 (7)	0.503 (8)

(b) S^*/qd for $E_{SV} = 1$

L/d	n or n'	$K_R = 0.1$		$K_R = 10.0$	
10 (undrained)	1.0	2.391	0.103	2.151	0.087
	2.5	1.863 (22)	0.084 (19)	1.687 (22)	0.069 (21)
10 (drained)	1.0	3.901	0.129	3.227	0.120
	3.0	3.900 (0)	0.122 (5)	3.033 (6)	0.115 (4)

Figures in bracket is the percent change due to cross anisotropy.
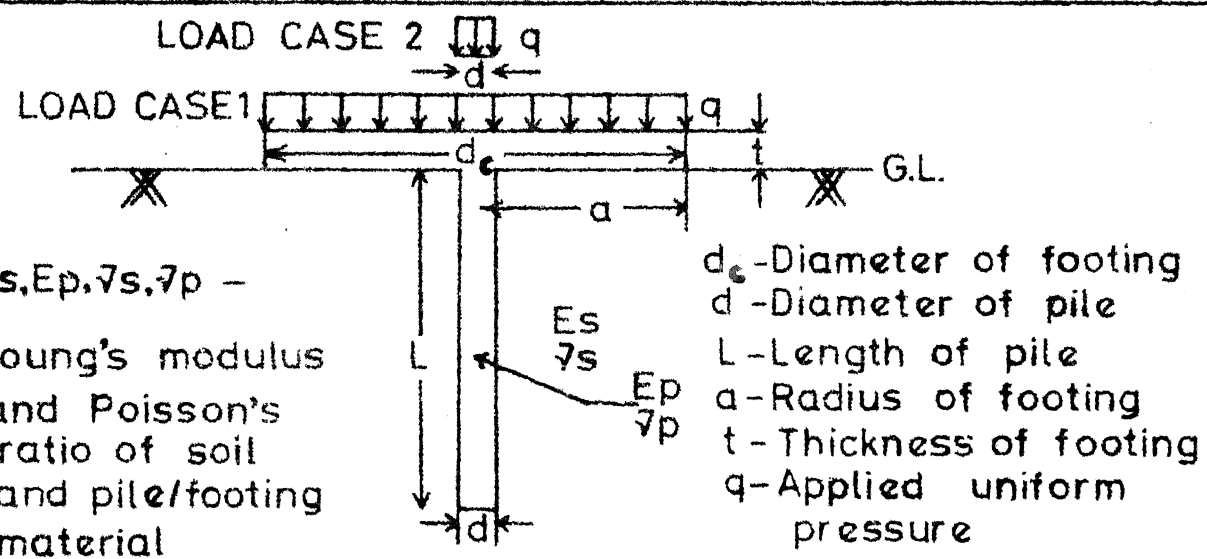
Fig 2·1 The Problem
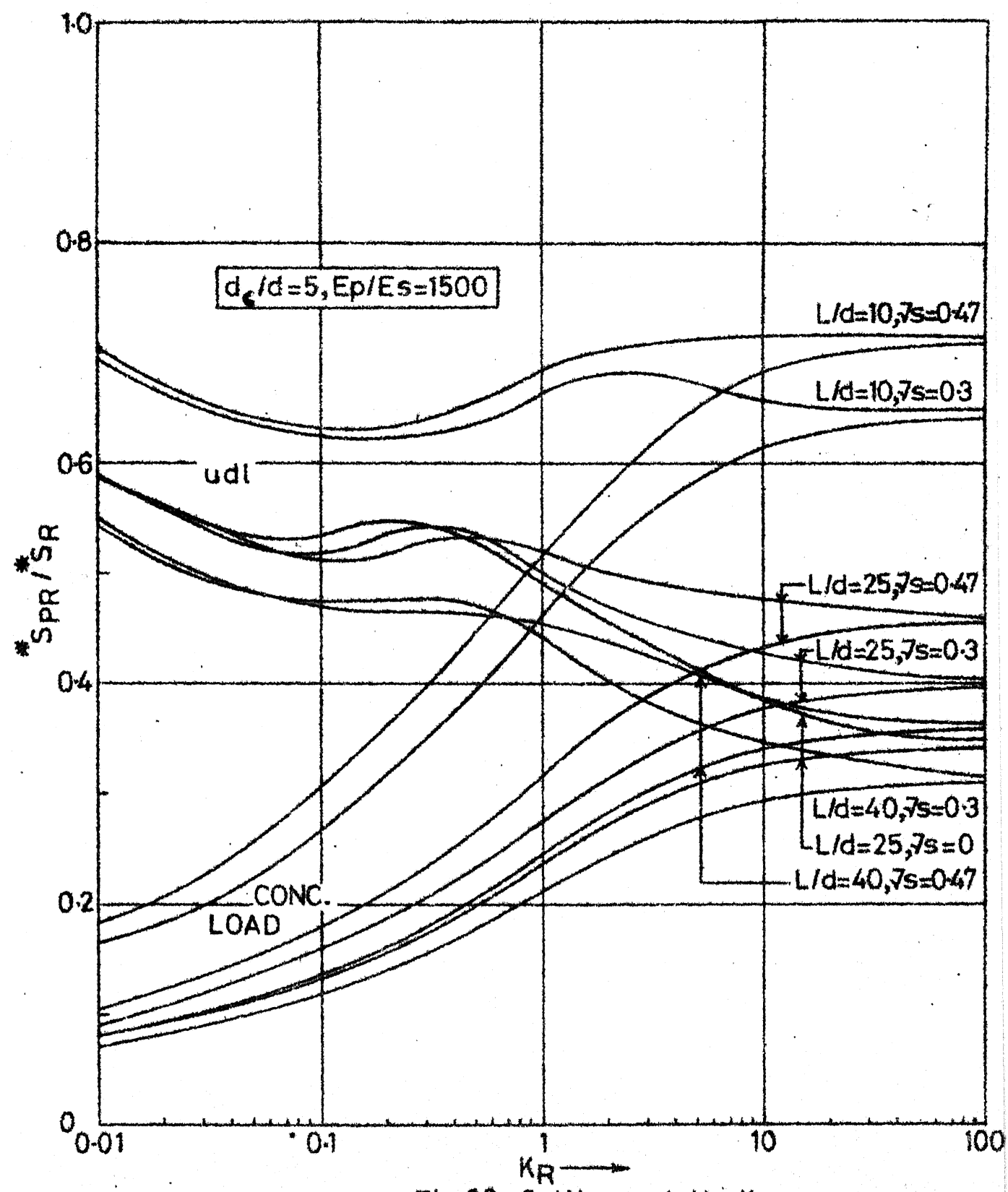
Fig.2·2 Settlement Vs K_R
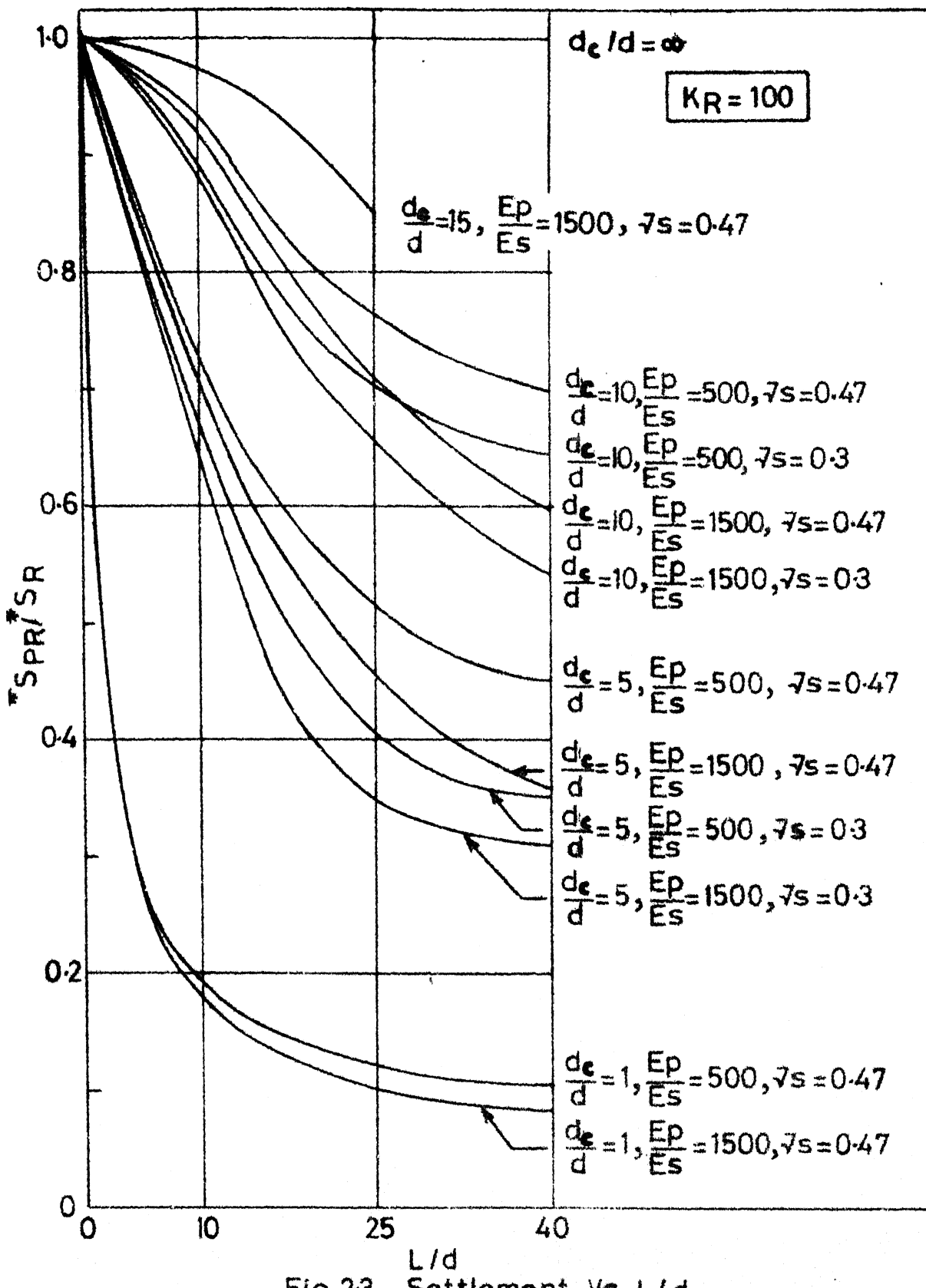
Fig.2·3 Settlement Vs L/d
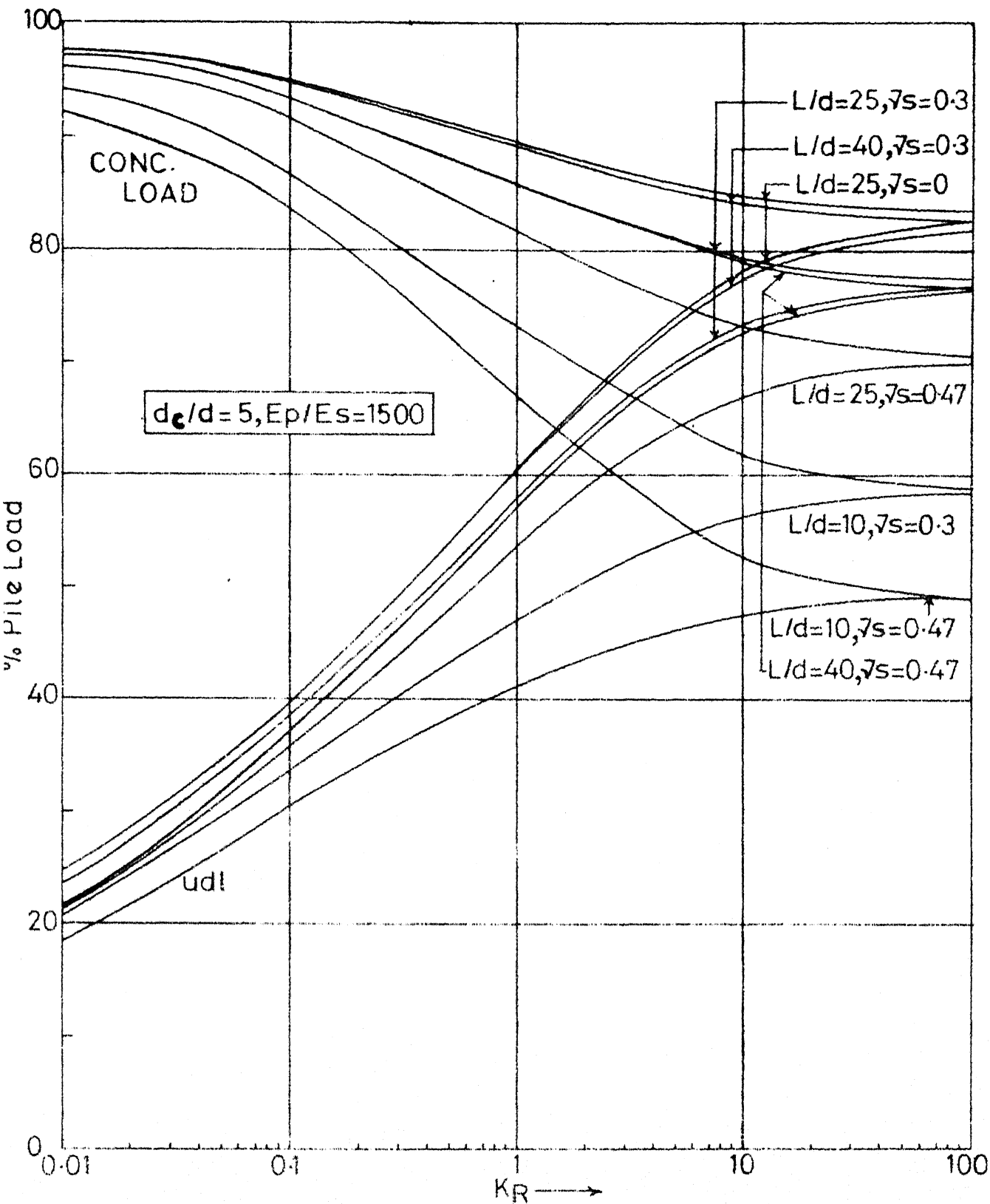
Fig.24   Percent Pile Load Vs K_R
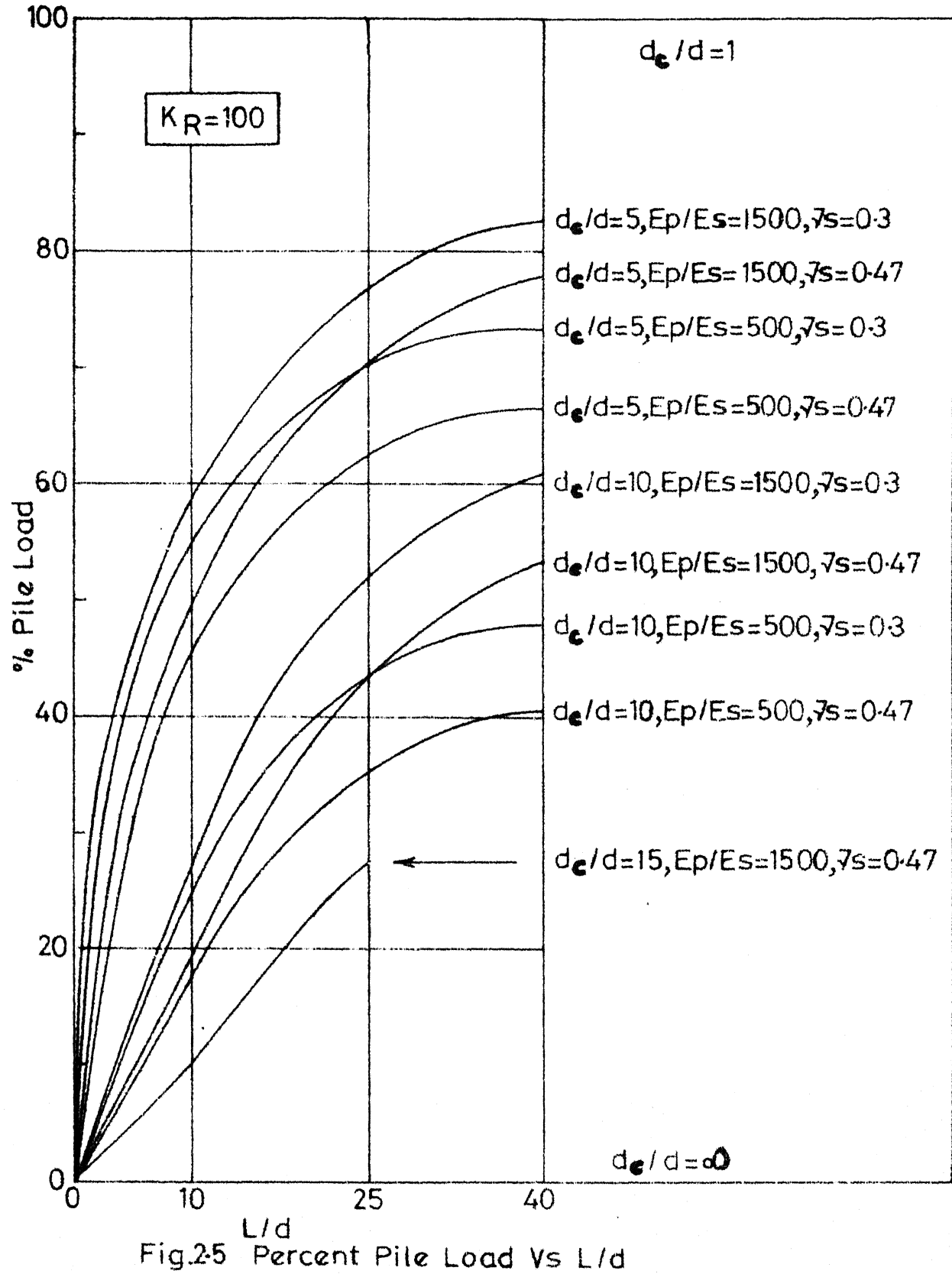
Fig.2·5 Percent Pile Load Vs L/d

L/d=40,Ep/Es=500,⅂s=0·3
L/d=40,Ep/Es=1500,⅂s=0·3
L/d=40,Ep/Es=500,⅂s=0·47
L/d=10,Ep/Es=500,⅂s=0·3
L/d=10,Ep/Es=1500,⅂s=0·3

L/d=10,Ep/Es=500,⅂s=0·47

L/d=10,Ep/Es=1500,⅂s=0·47

L/d=40,Ep/Es=1500,
⅂s=0·47

udl

L/d=10,Ep/Es=500,⅂s=0·47
L/d=10,Ep/Es=1500,⅂s=0·47
L/d=10 Ep/Es=500 ⅂s=0·3

L/d=10,Ep/Es=1500,⅂s=0·3
L/d=40,Ep/Es=500,⅂s=0·47

L/d=40,Ep/Es=500,⅂s=0·3
L/d=40,Ep/Es=1500,⅂s=0·47

L/d=40,Ep/Es=1500,⅂s=0·3

CONC.LOAD

$d_c/d=5$

K_R ⟶
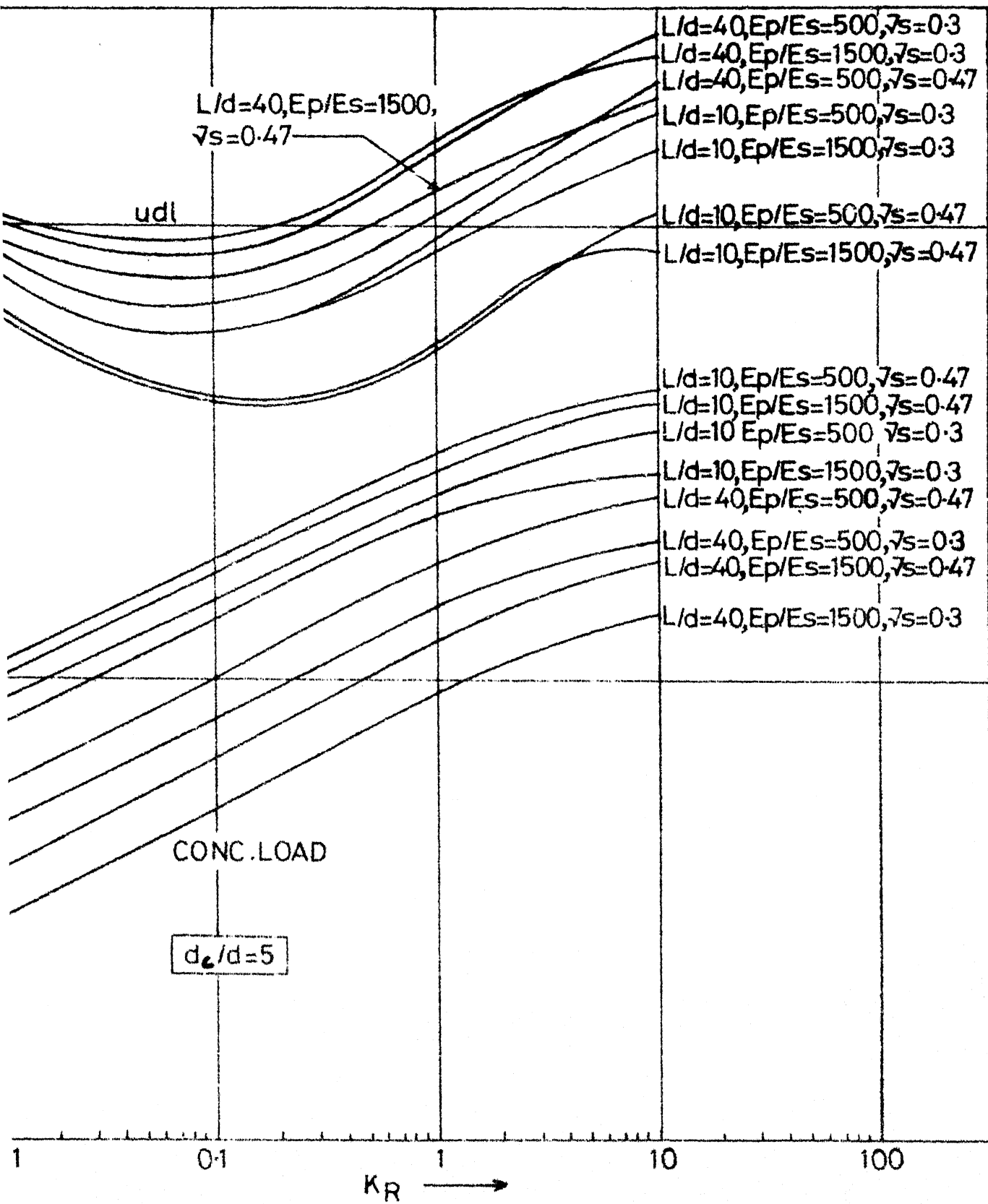
Fig. 2·6   Differential Settlement
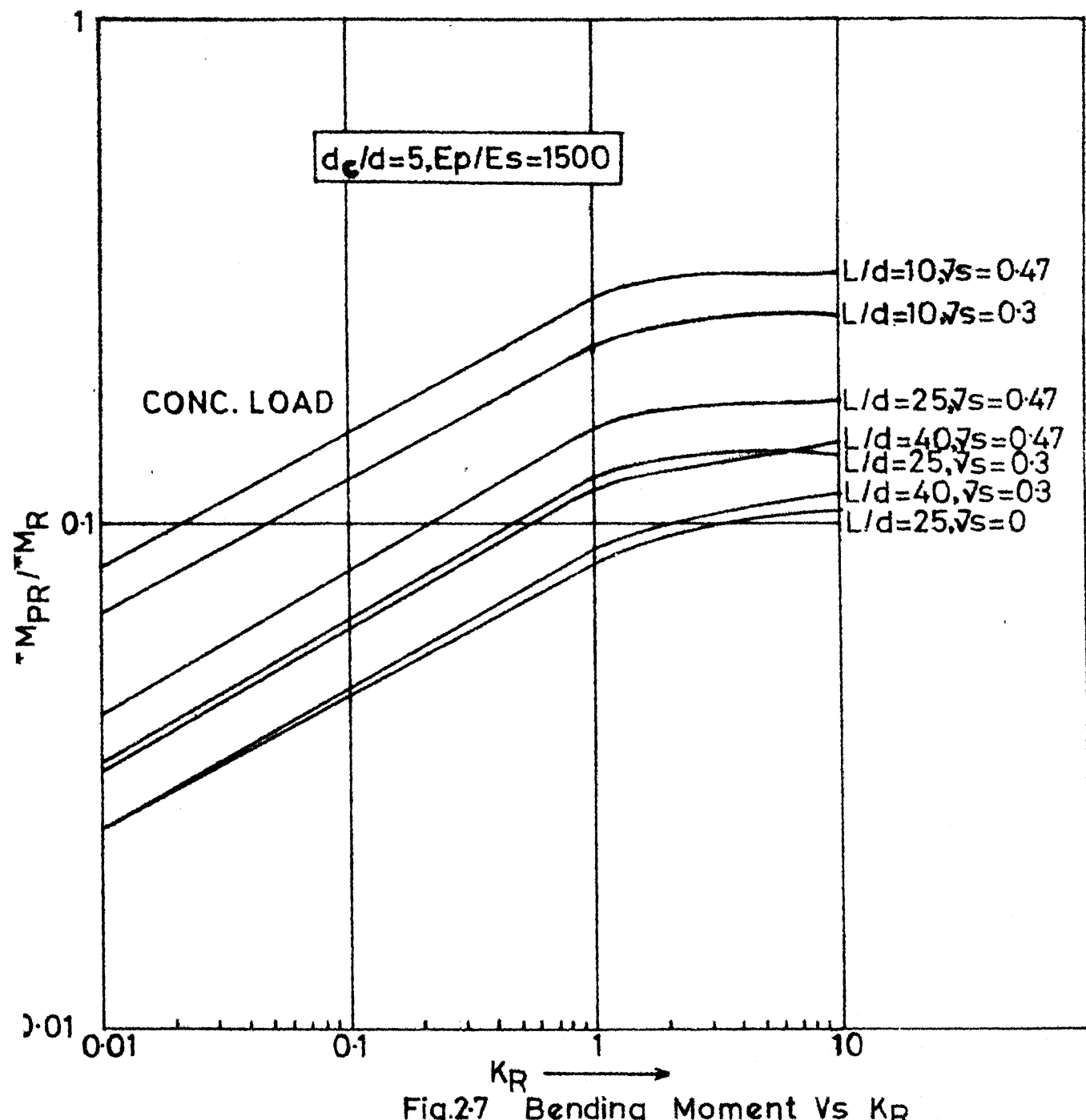
Fig.2·7   Bending   Moment   Vs K_R
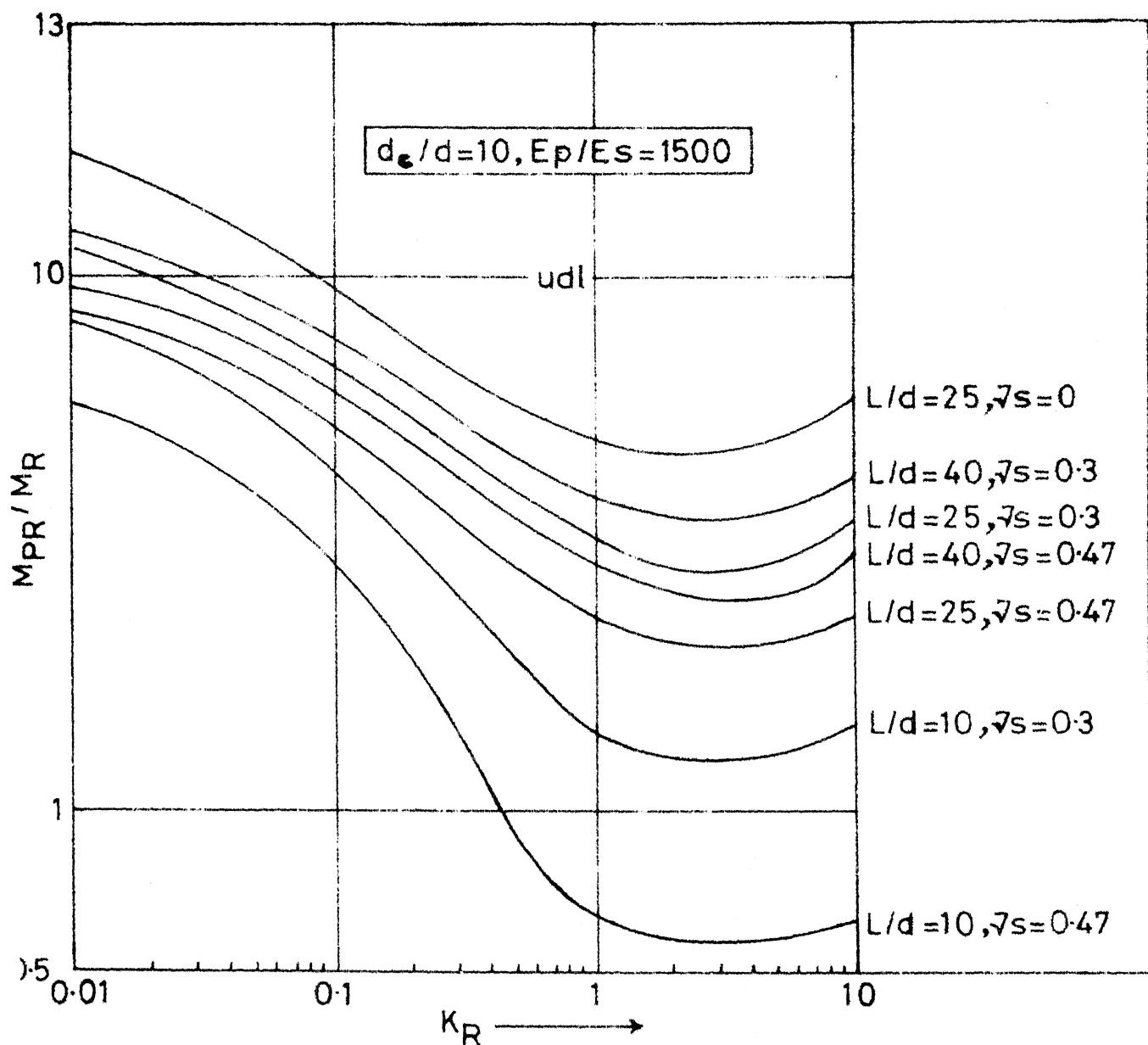
Fig.2·8 Bending Moment
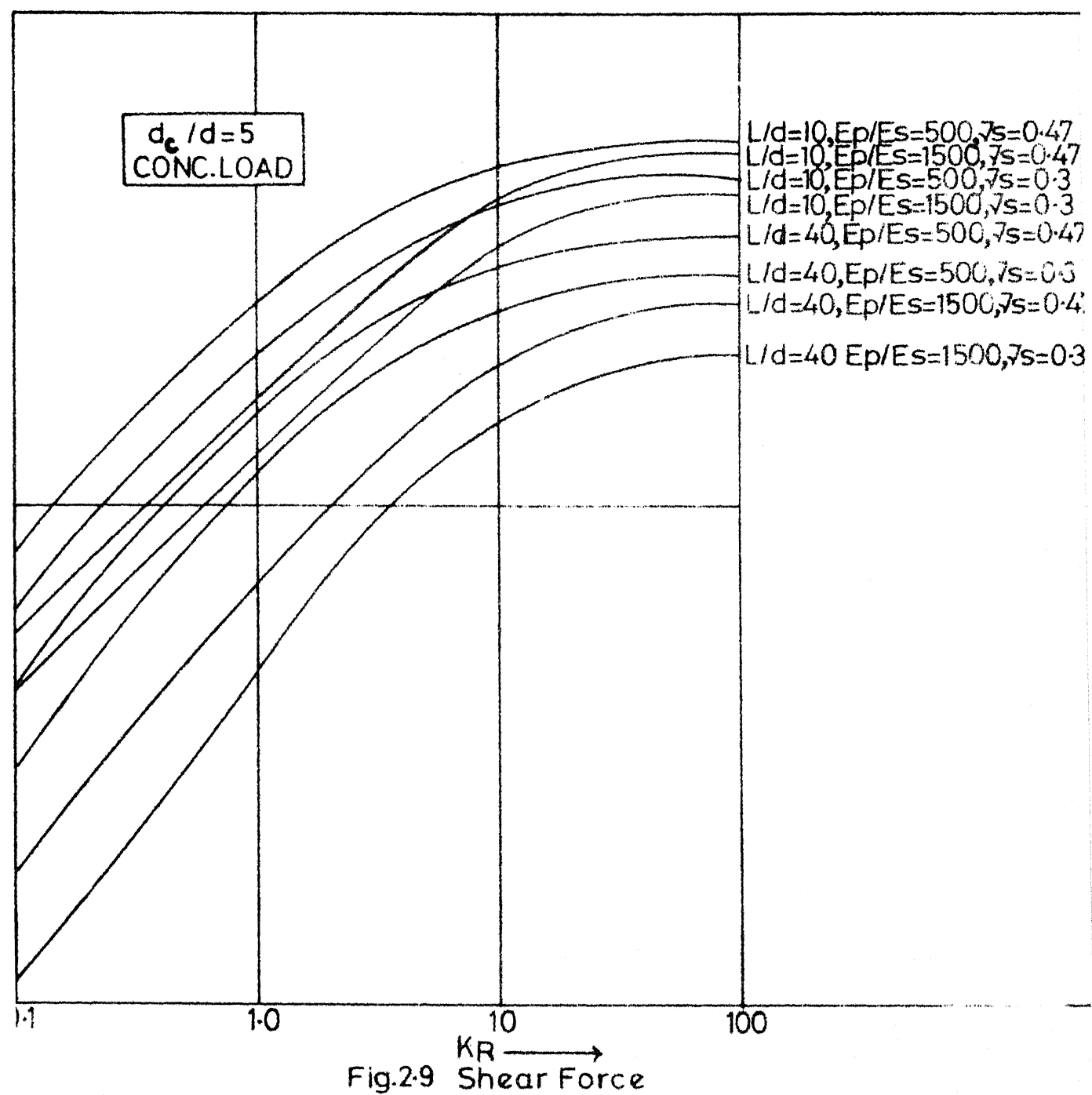
Fig.2.9 Shear Force
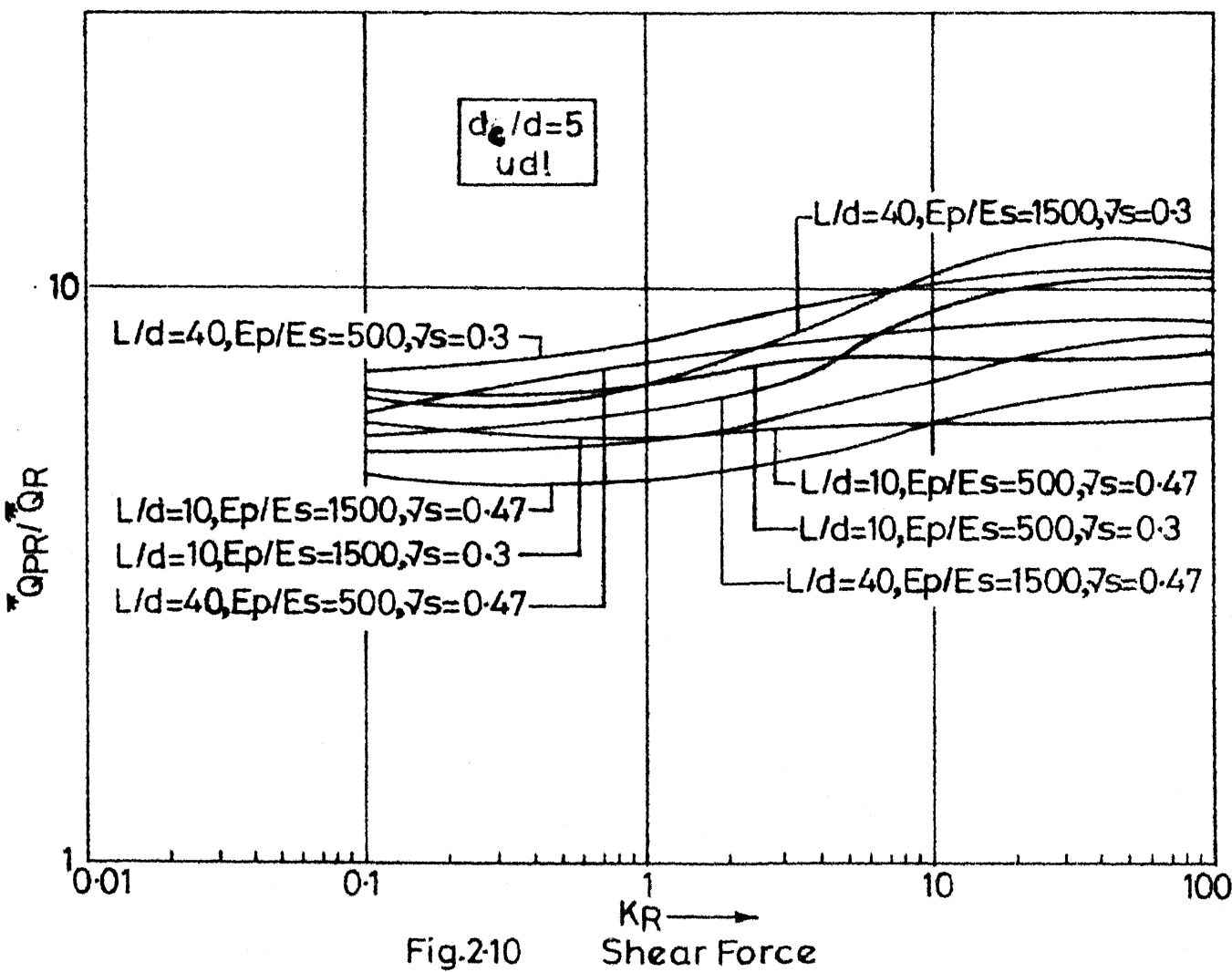
Fig. 2.10   Shear Force
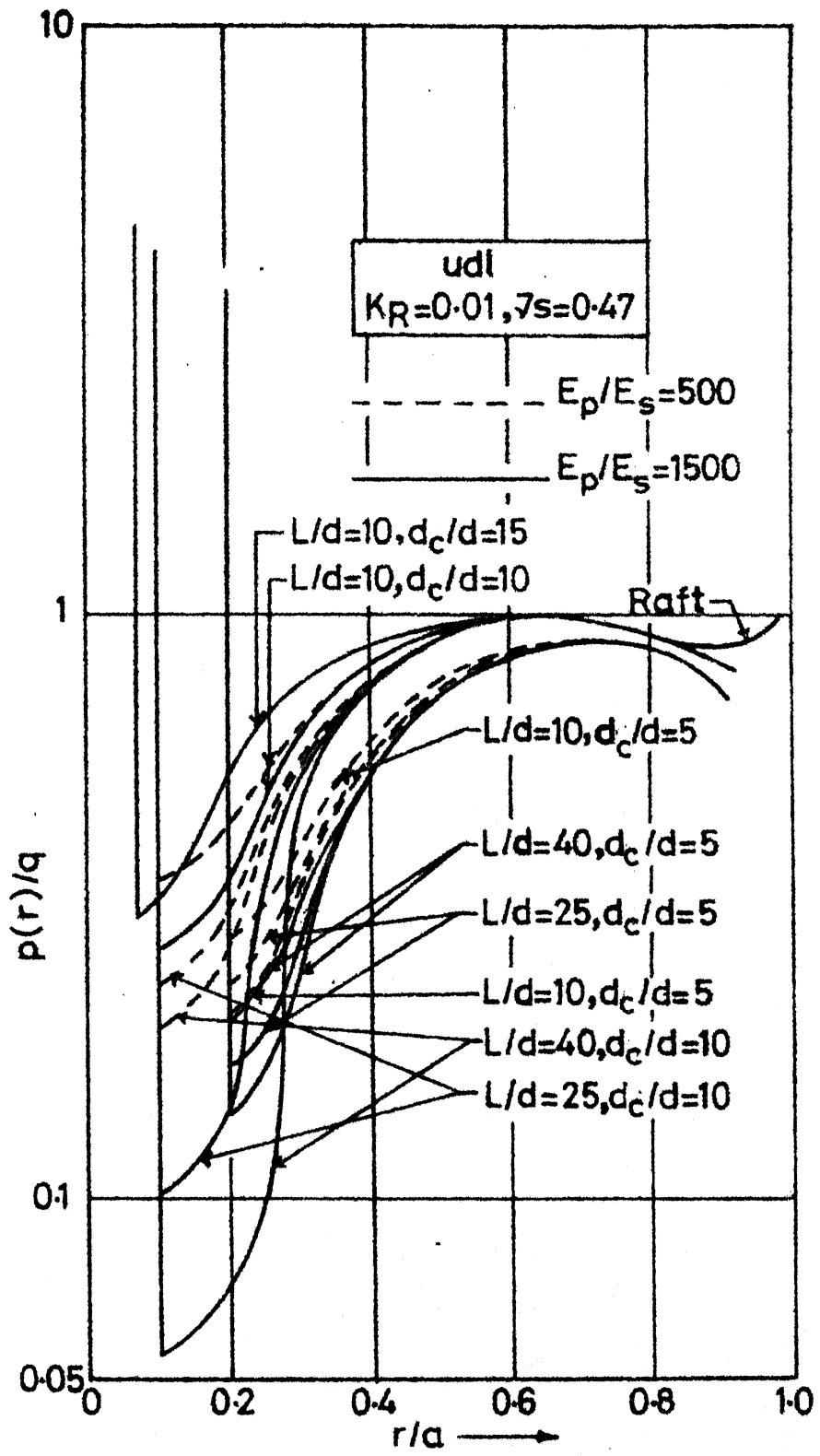
Fig.2·11   Contact pressure distribution (udl)
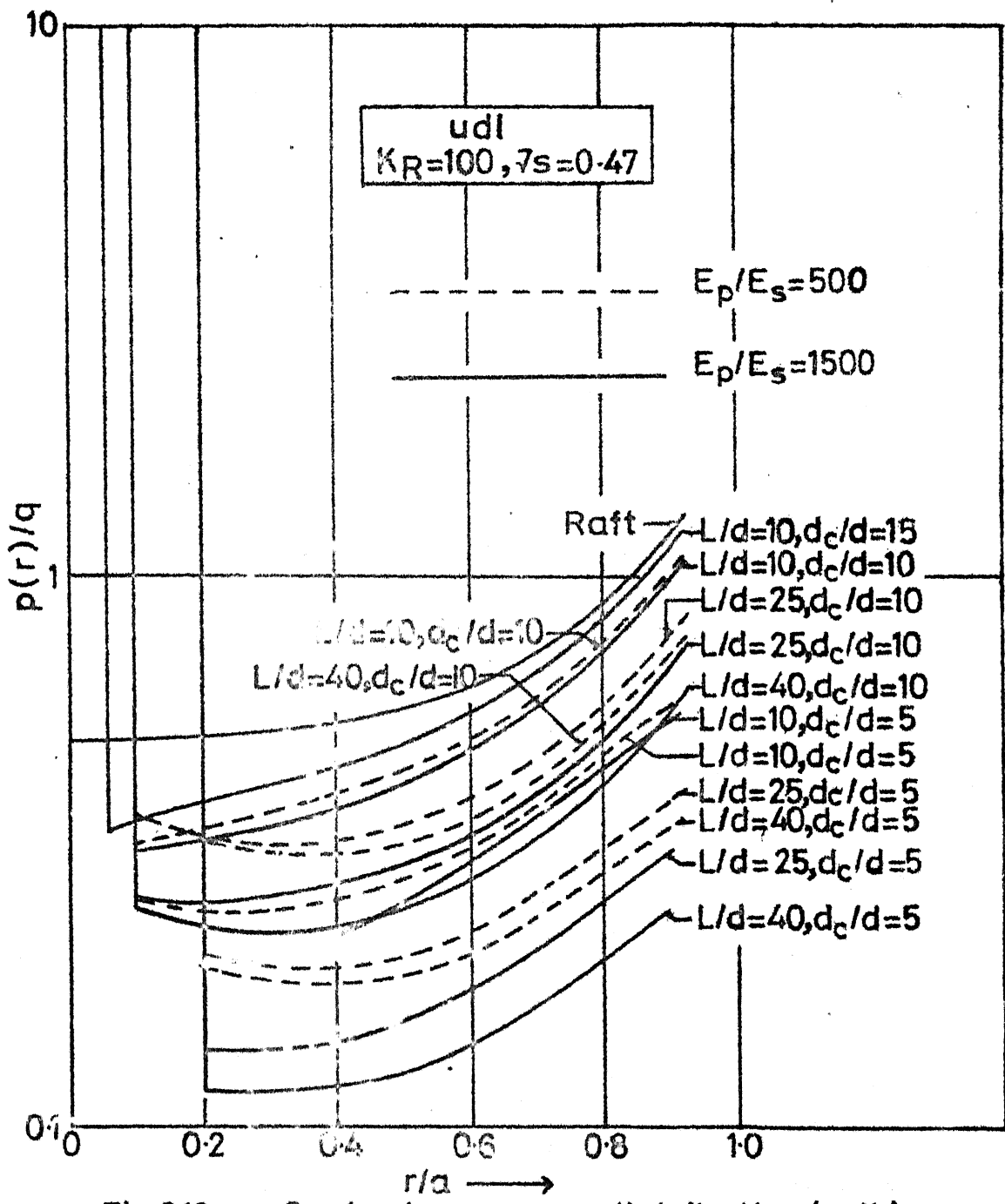
Fig. 2·12   Contact pressure distribution (udl)
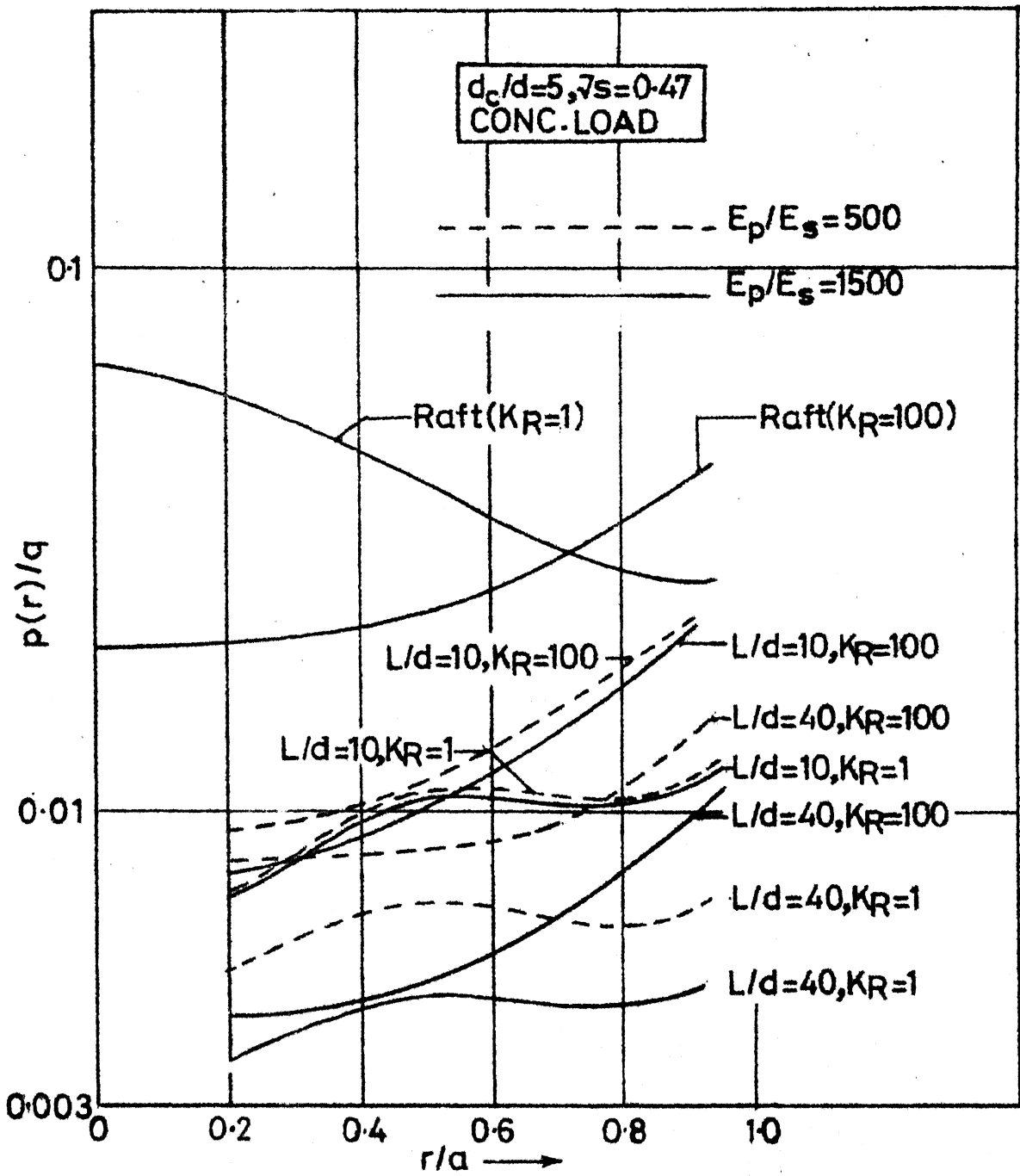
Fig.2·13   Contact pressure distribution
(CONC. LOAD)
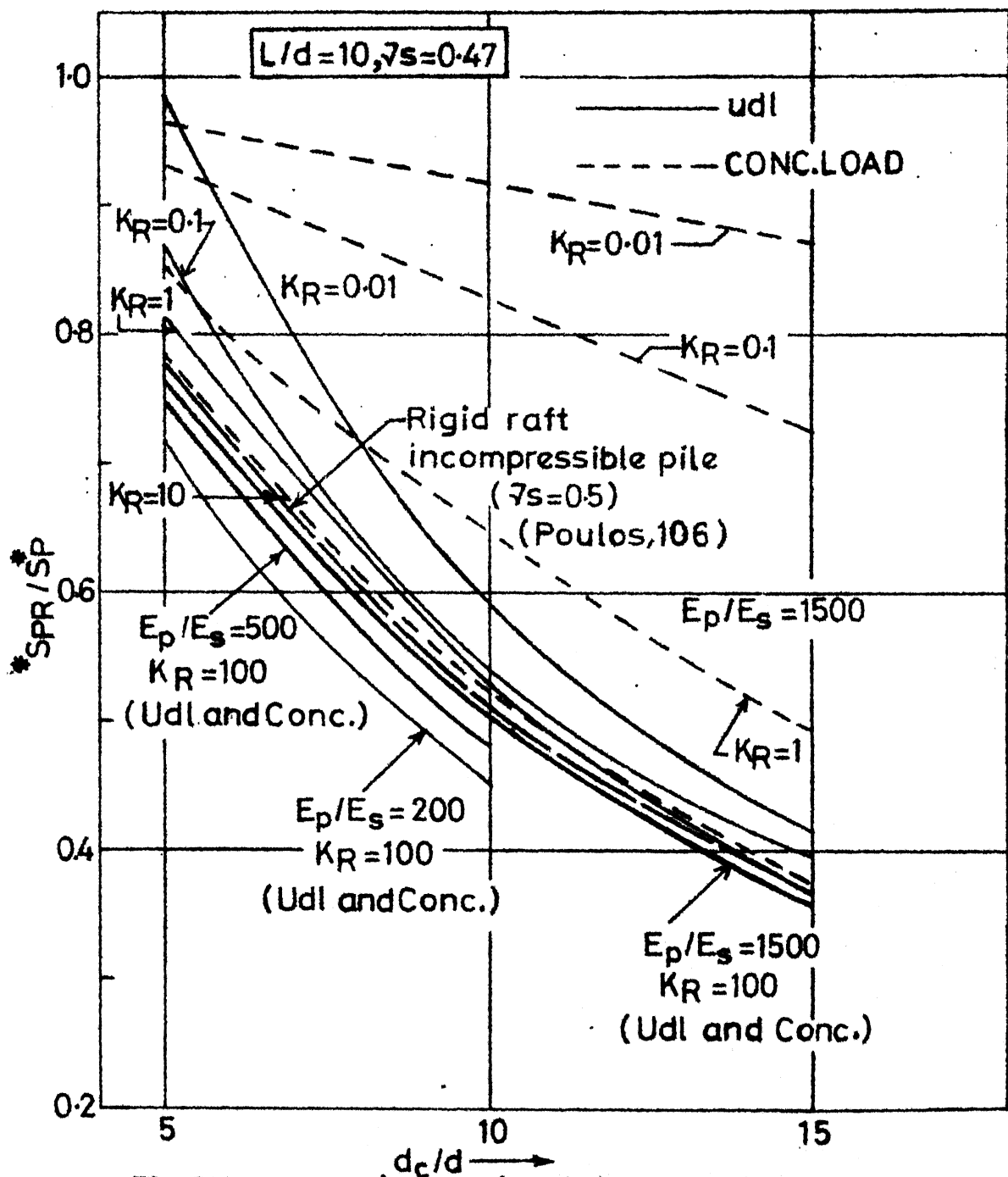
Fig.214 Comparison with rigid raft incompressible pile solution
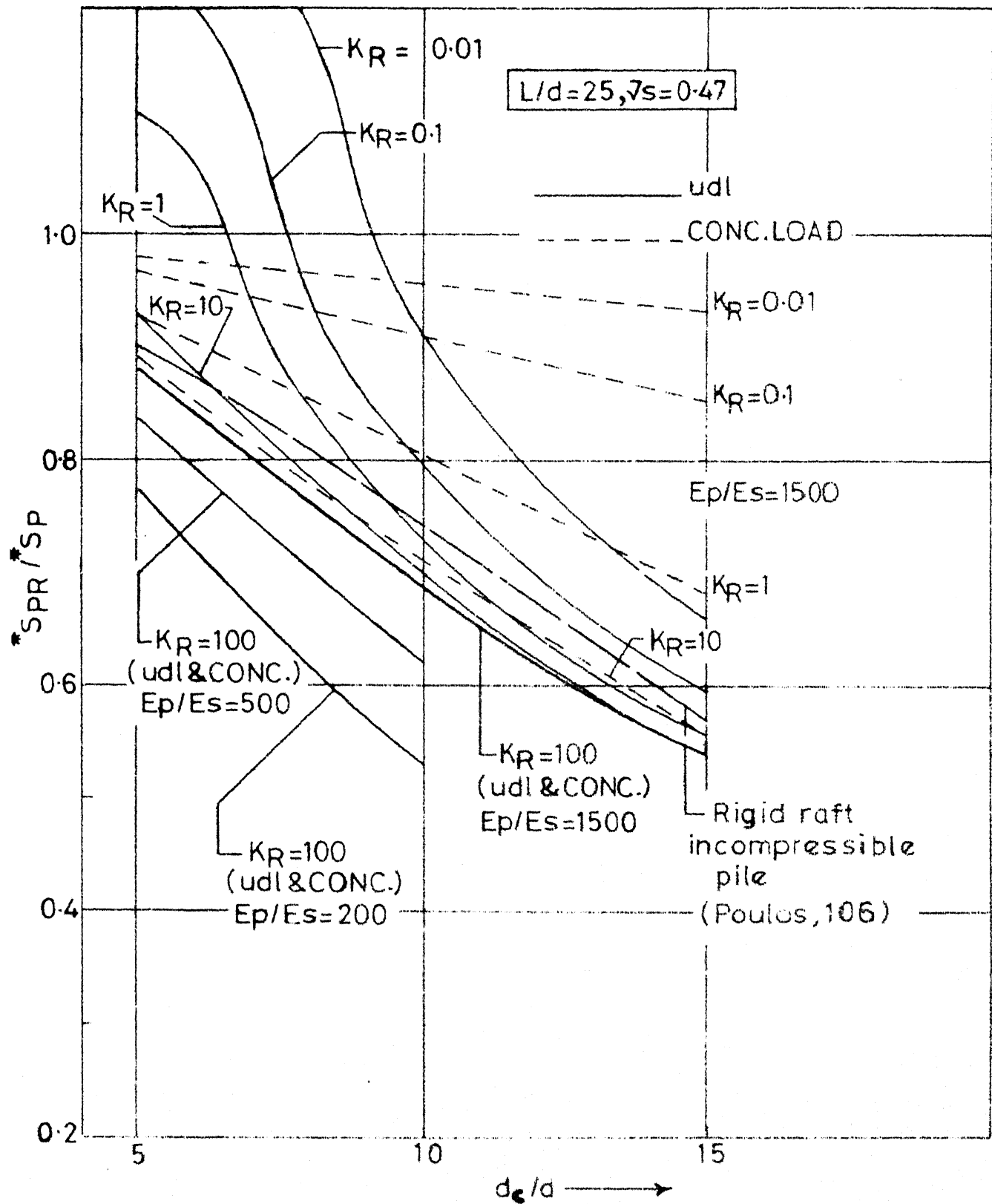
Fig.2.15 Comparison with rigid raft
incompressible pile solution
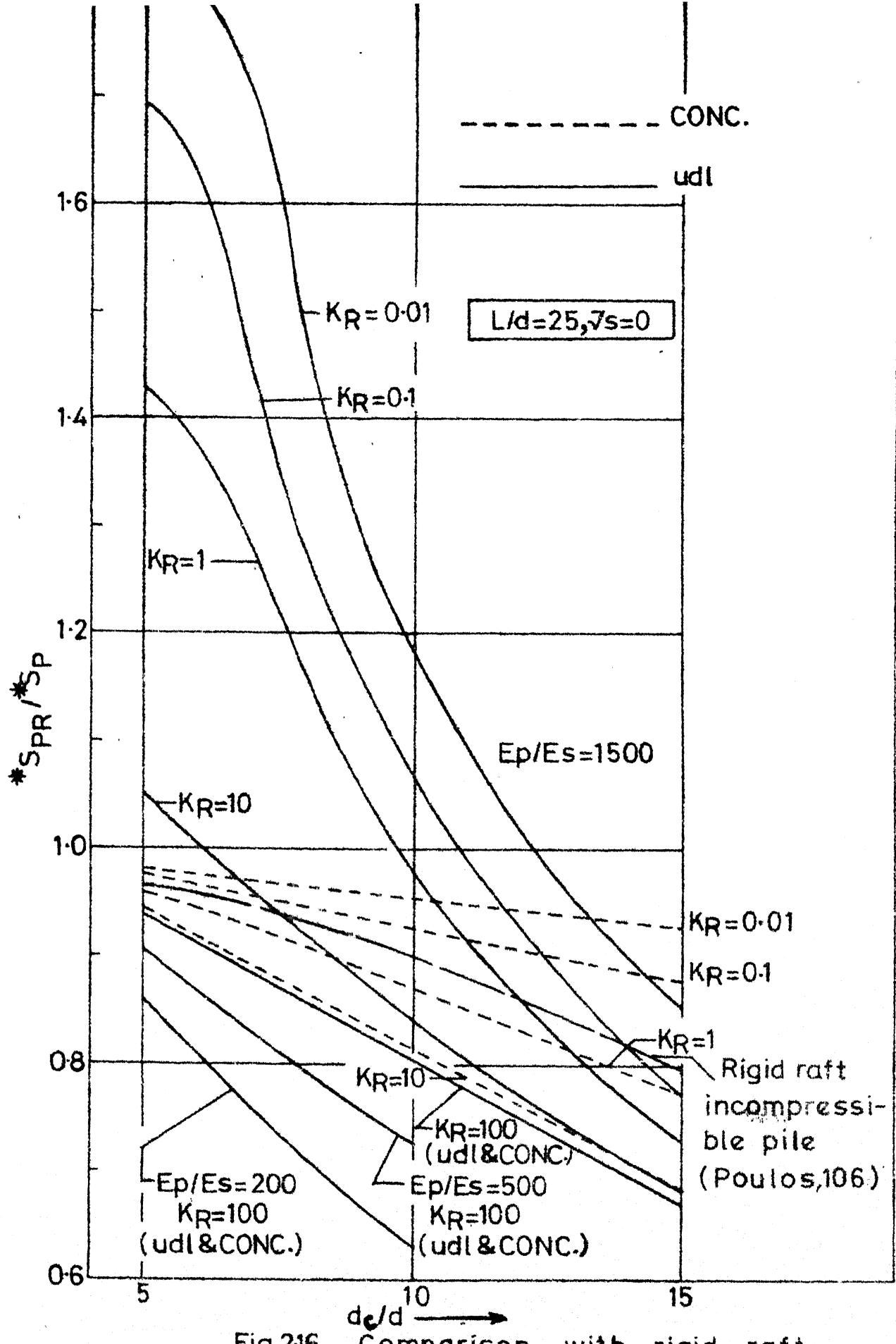
Fig.2.16 Comparison with rigid raft

Fig.2·18 Assumption to account for pile failure.
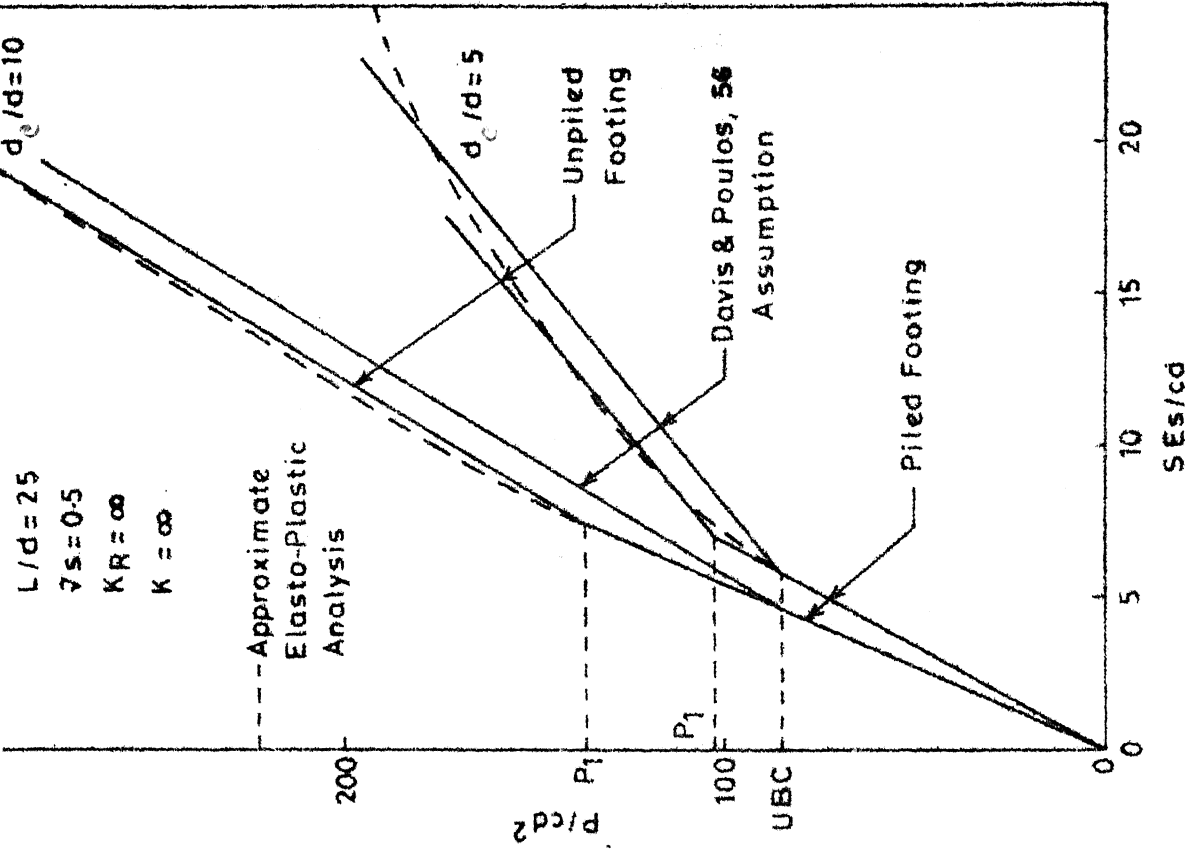
Fig.2·17 Assumption to account for pile failure.

(a) Non-homogeneous soil medium (case 1)

(b) Settlement Vs K_R

$\nu_s = 0.3$
$d_c / d = 5$
$E_p / E_{SO} = 1500$
udl

$E_Z = E_{SO}(1 + \dfrac{Z/d}{\psi})$

$G_0 - \psi = \infty$
$G_2 - \psi = 10$
$G_1 - \psi = 2.5$
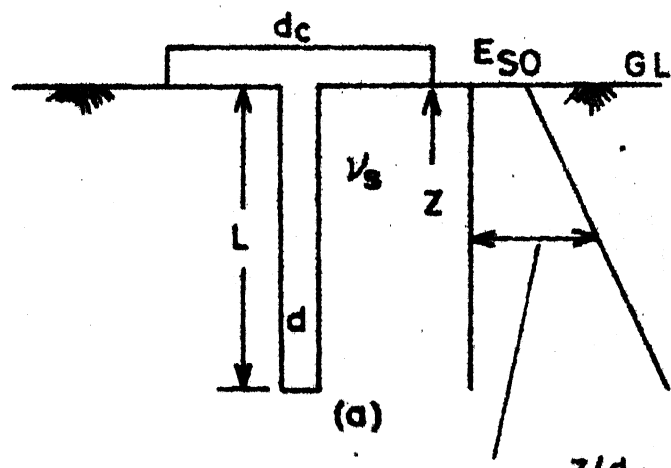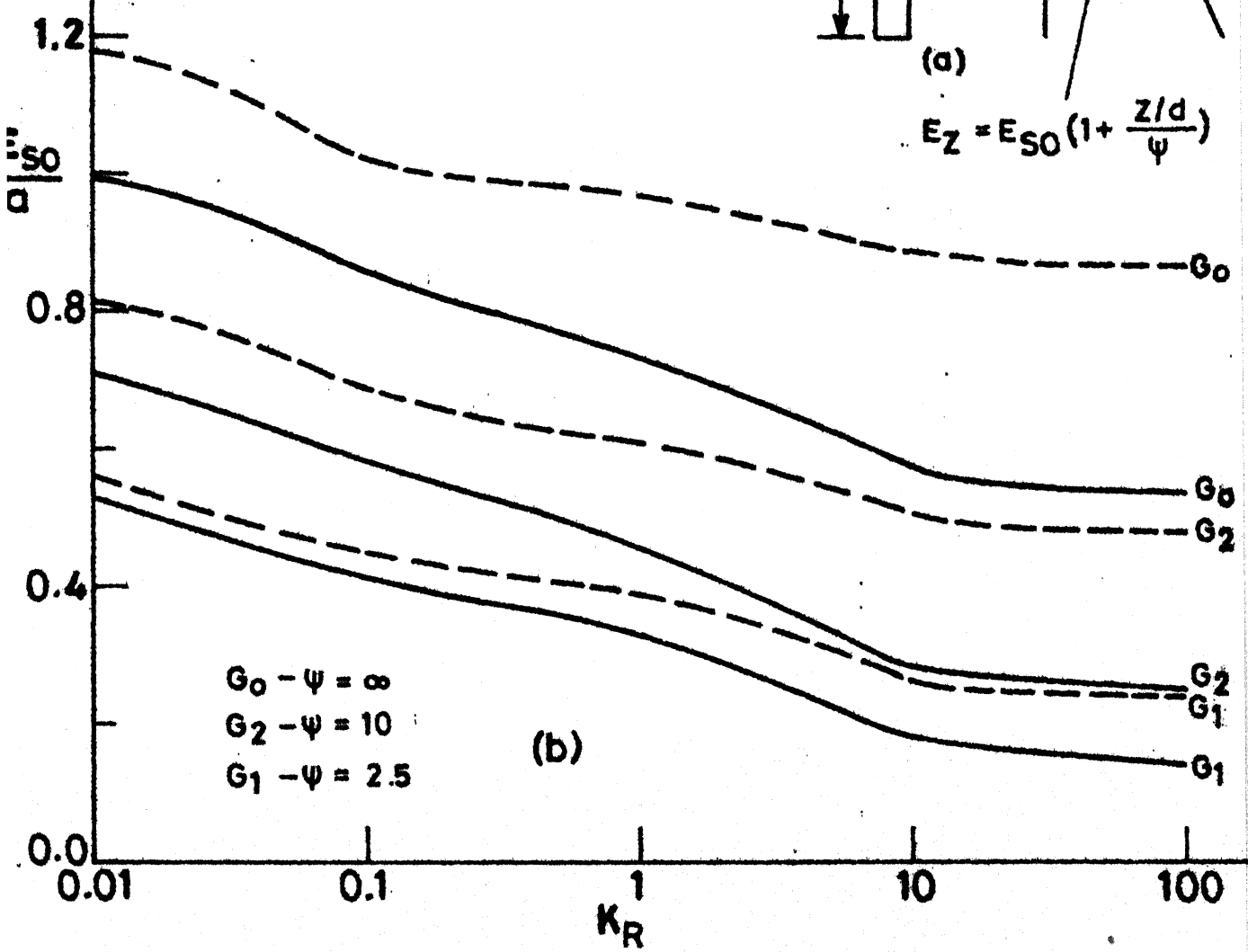
L/d = 10

L/d = 25

Non-homogeneous soil as in Fig. 2.19 (a).

$\nu_s = 0.3$

$d_c / d = 5$

$E_p / E_{so} = 1500$

conc. load

$L/d = 10$

$L/d = 25$

$G_0 - \psi = \infty$

$G_2 - \psi = 10$

$G_1 - \psi = 2.5$

K_R
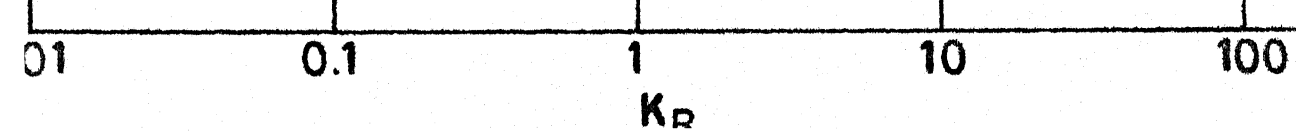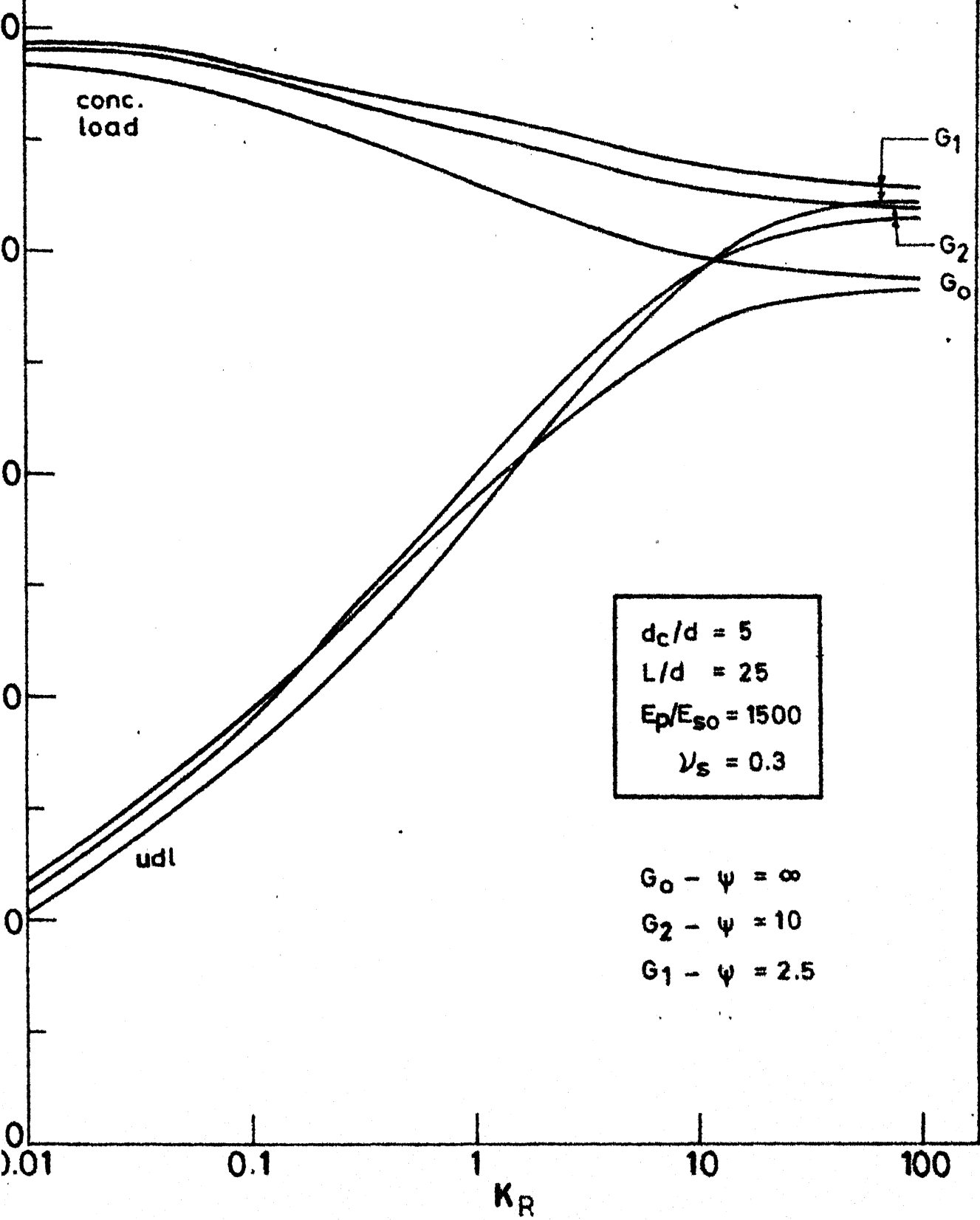
Non-homogeneous soil as in Fig. 2.19(a)

Non-homogeneous soil as in Fig.2.19(a)

conc.
load

udl

$d_c/d = 5$

$\nu_s = 0.3$

$L/d = 10$

$E_p/E_{so} = 1500$

G_1

G_2

G_0

$G_0 - \psi = \infty$

$G_2 - \psi = 10$

$G_1 - \psi = 2.5$

0.01   0.1   1   10   100

K_R

Non-homogeneous soil as in Fig.2.19(a)

$d_c/d = 5$
$\nu_S = 0.3$
$E_P/E_{SO} = 1500$
udl

L/d = 25
L/d = 10

$G_0 - \psi = \infty$
$G_2 - \psi = 10$
$G_1 - \psi = 2.5$
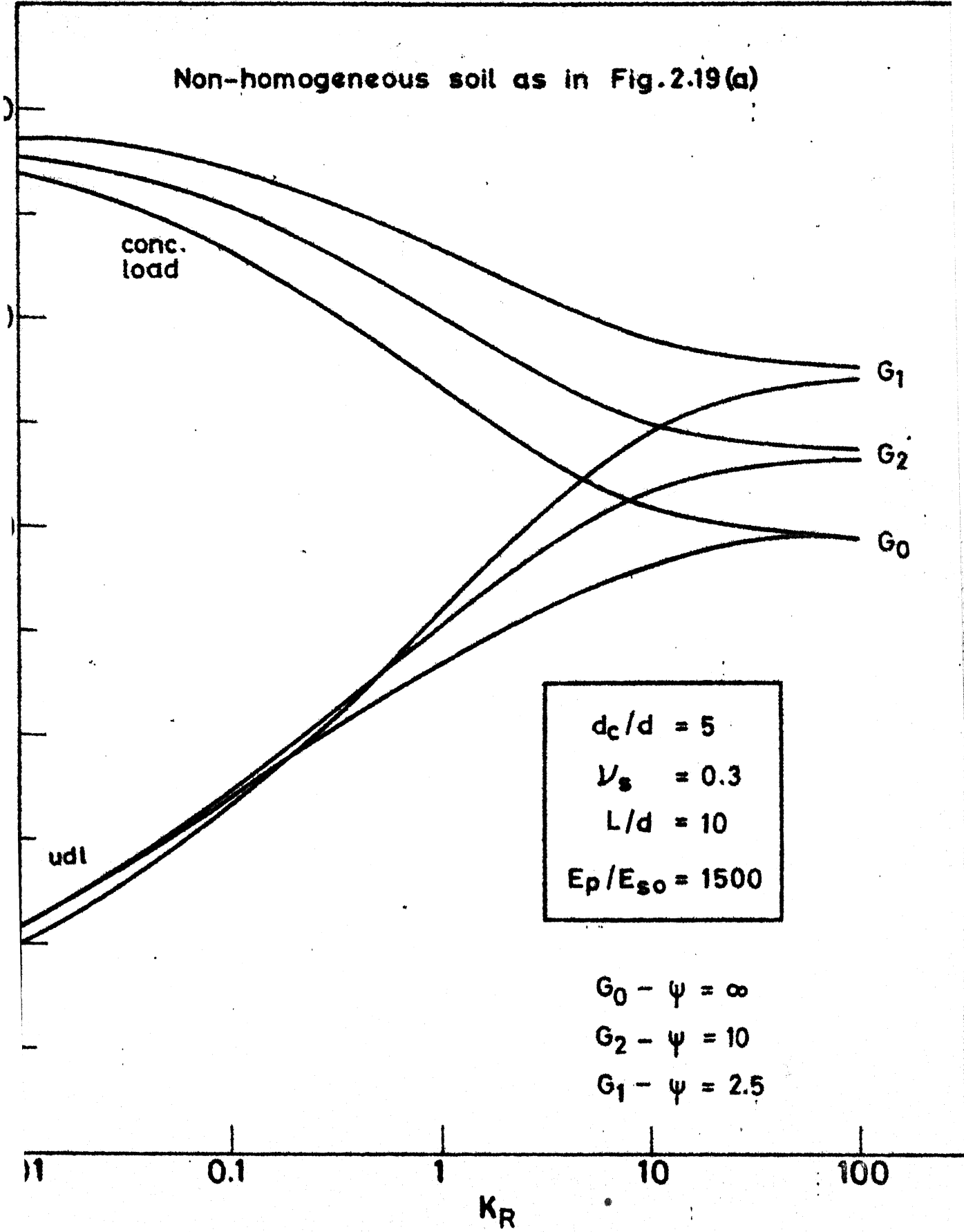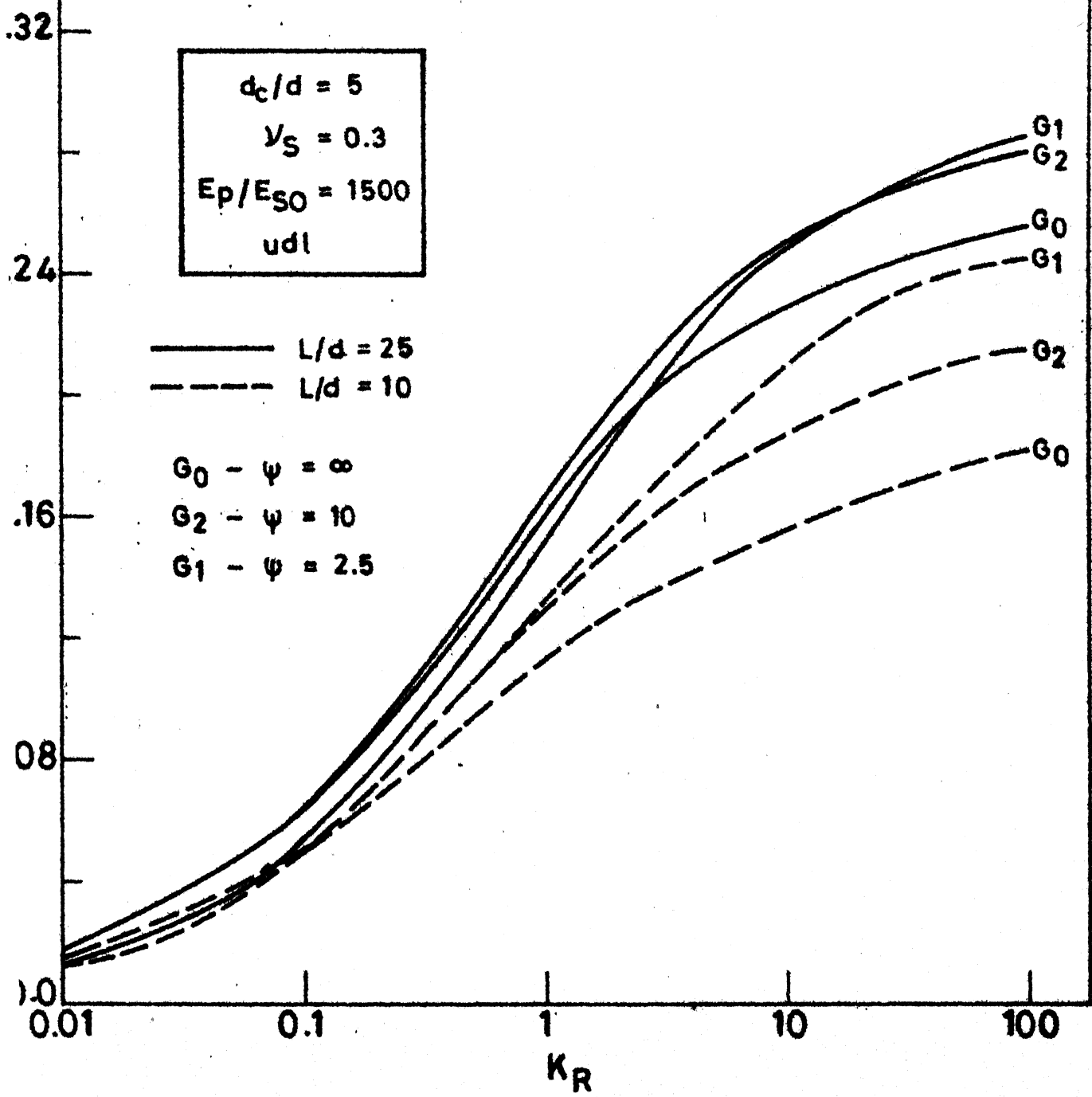
Fig. 2.23   Max. bending moment Vs K_R (non-homo. soil).
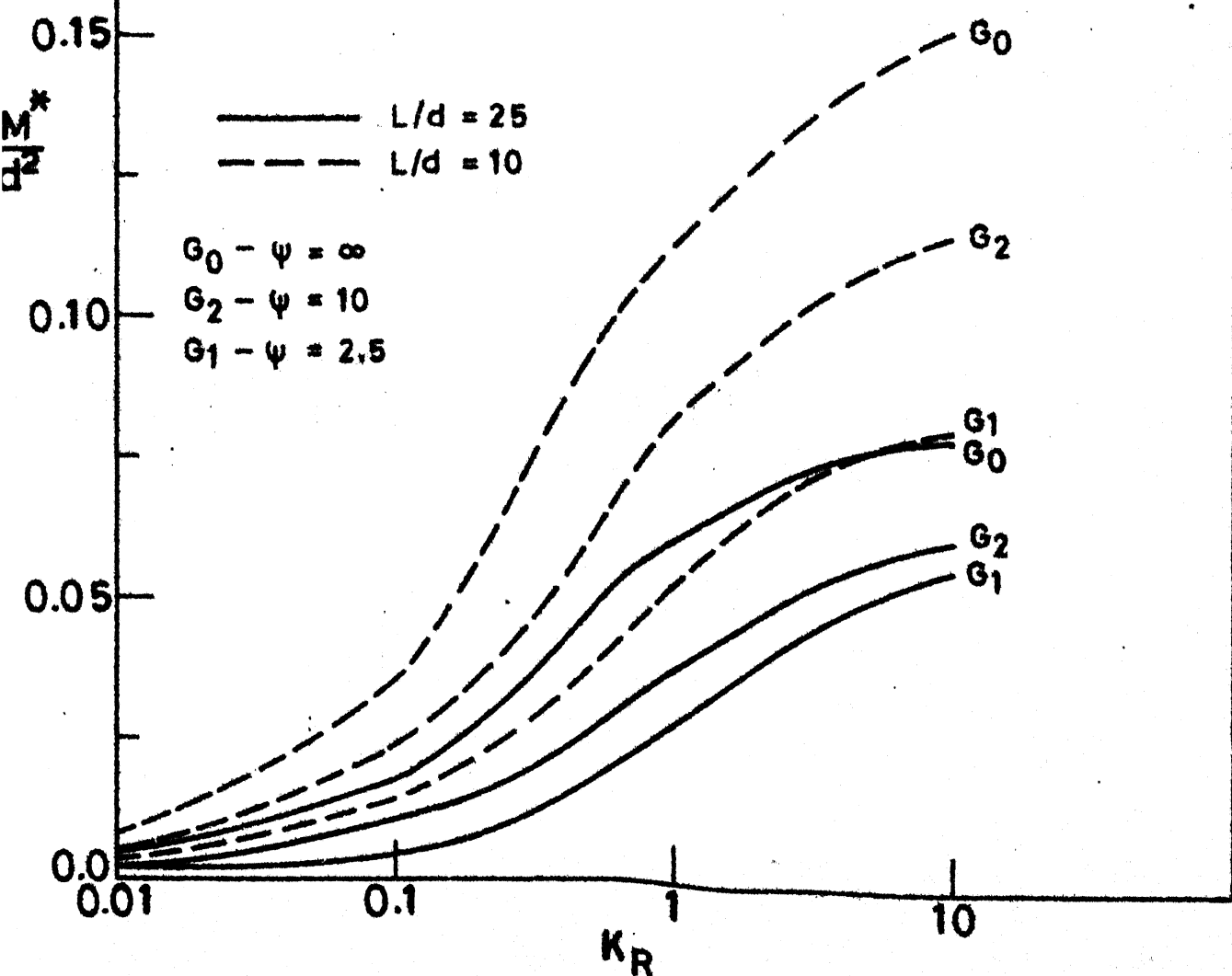
Fig. 2.24 Max. bending moment Vs K_R (non-homo. soil)
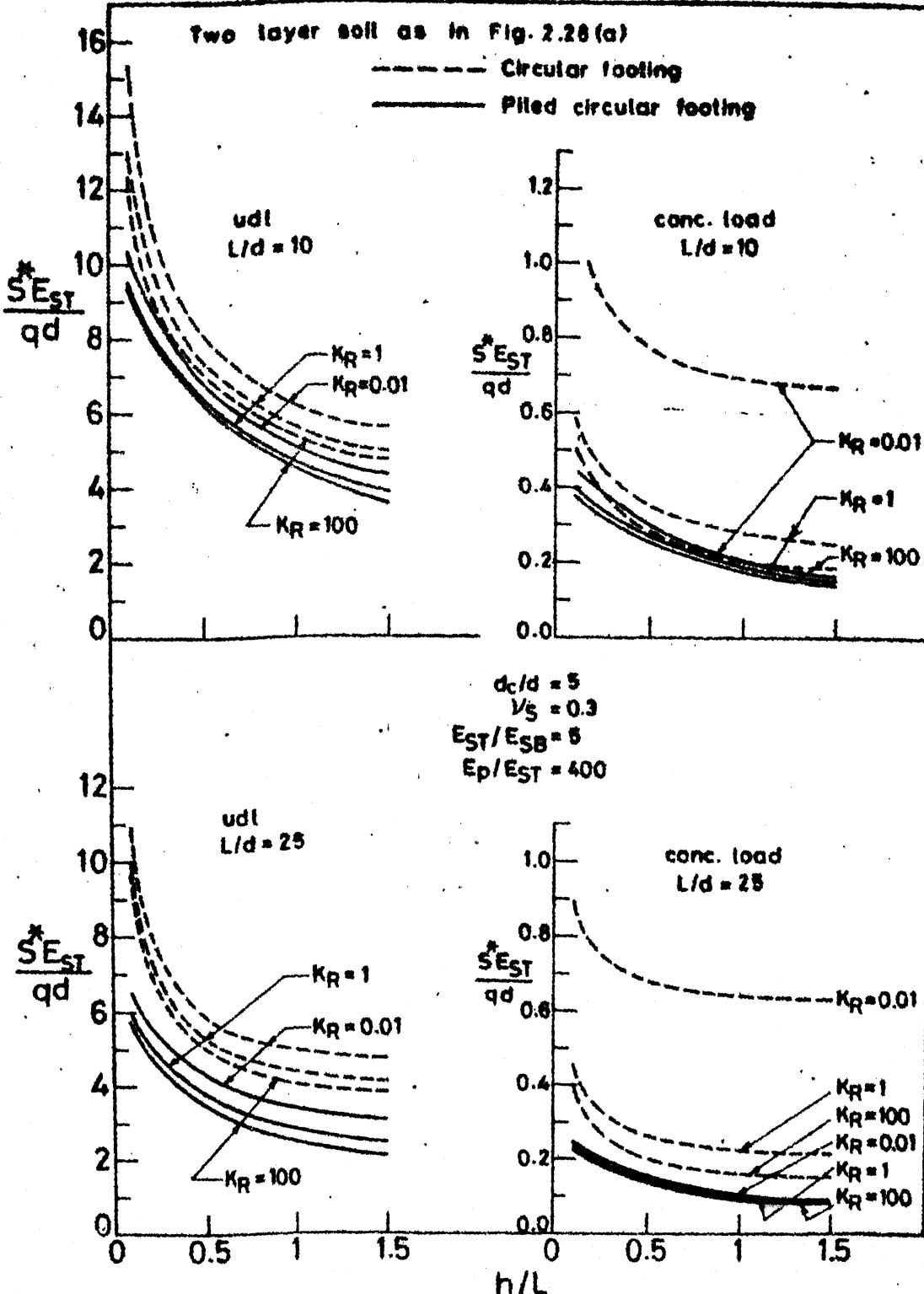
Fig. 2.25(a) Settlement Vs h/L (Layered soil).

Two layer soil as in Fig. 2.28(a)

$d_c/d = 5$
$\nu_s = 0.3$
$E_{ST}/E_{SB} = 5$
$E_P/E_{ST} = 400$
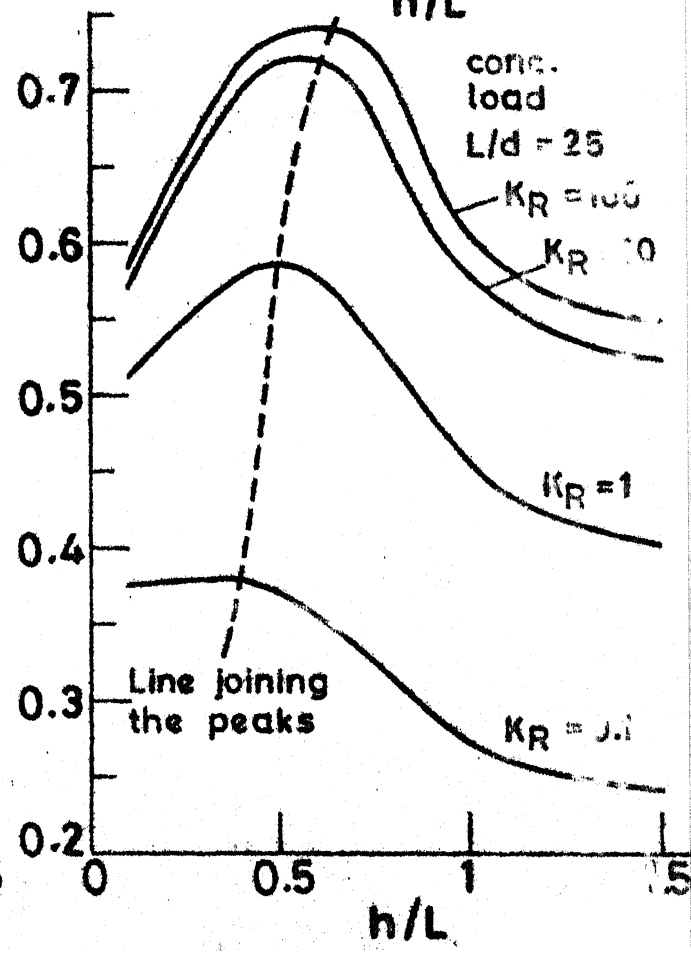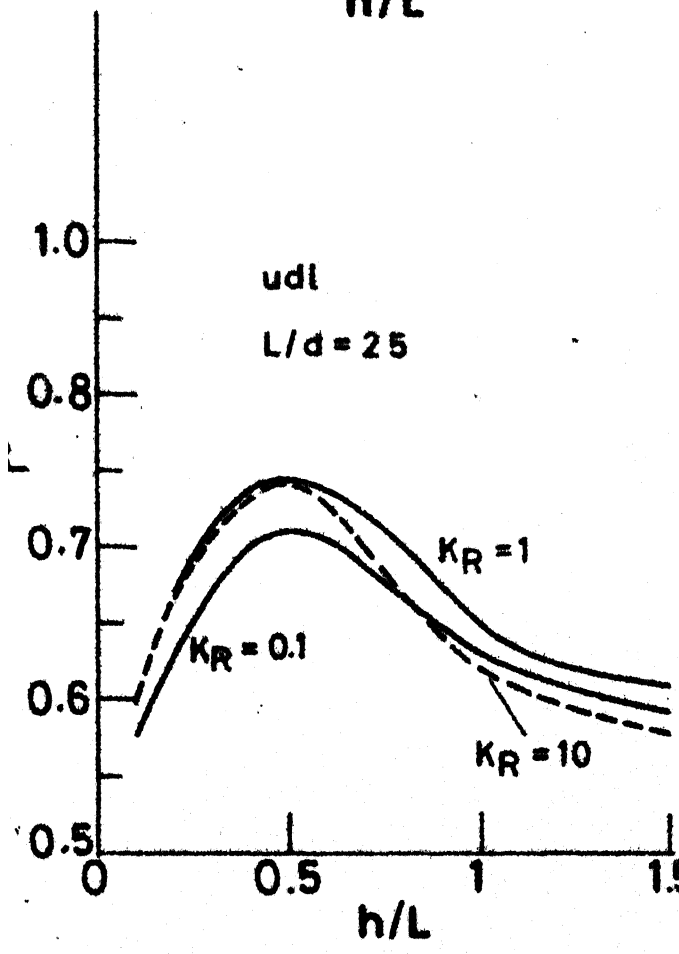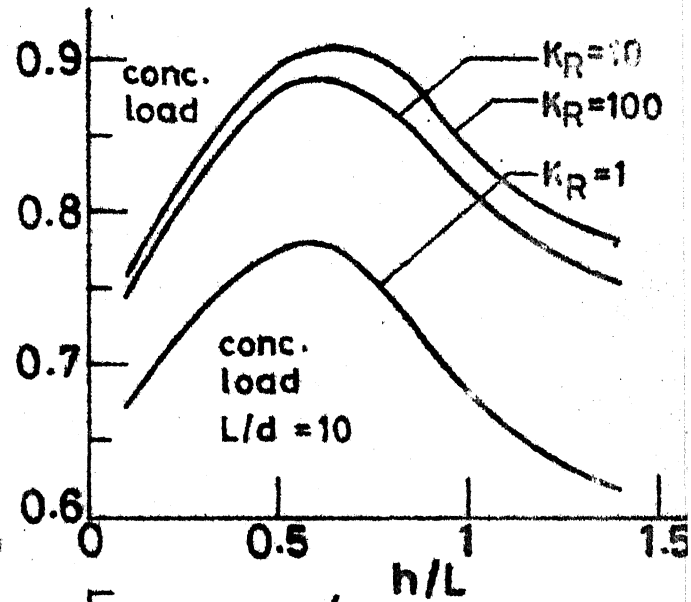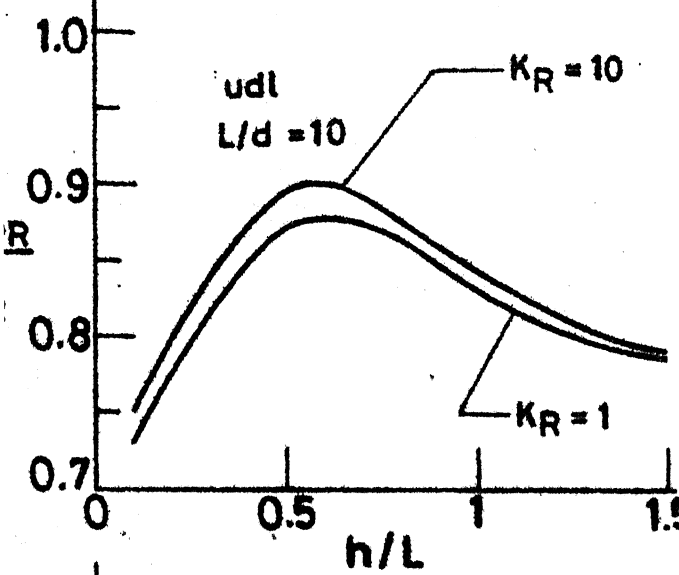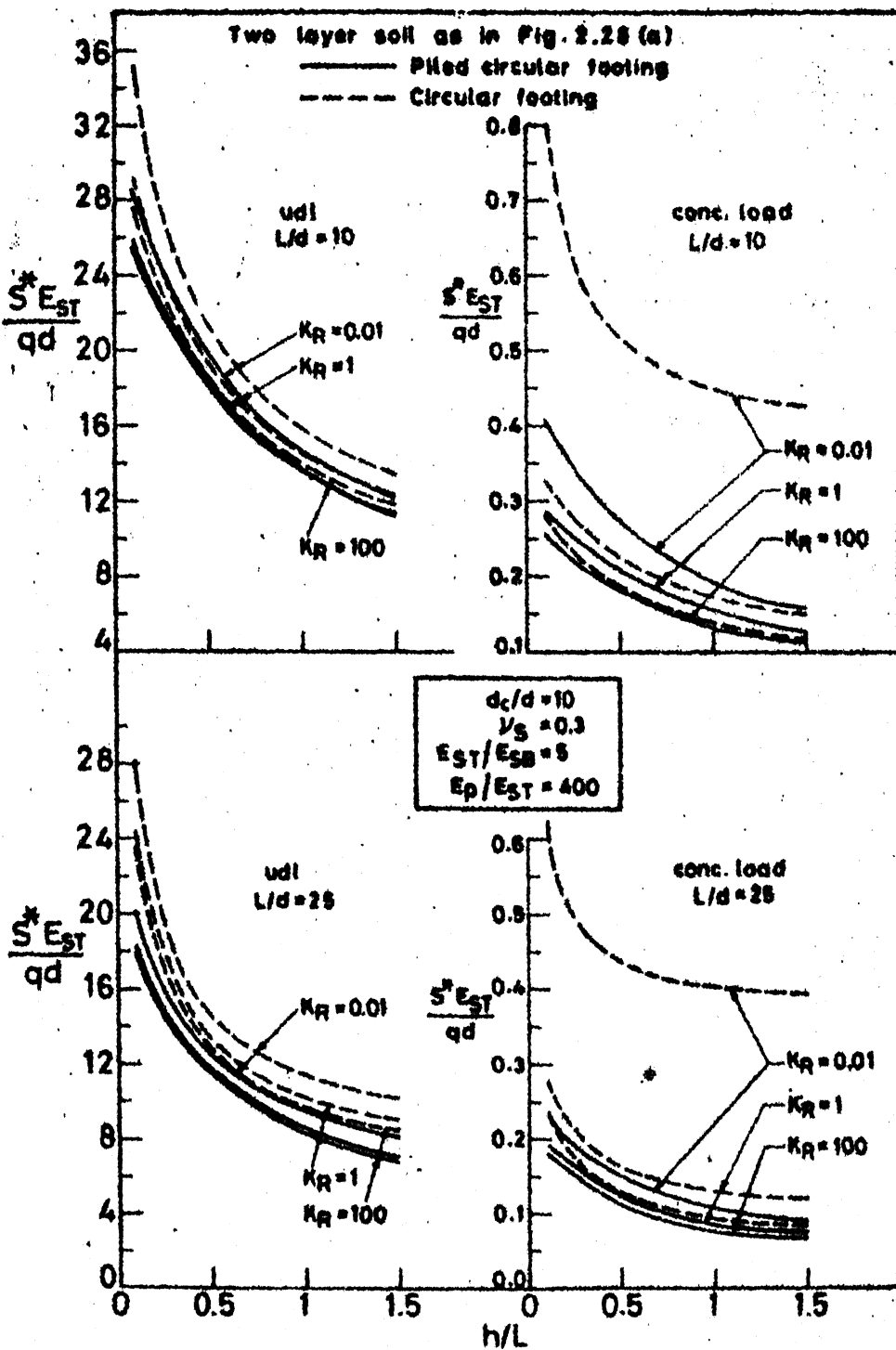
Fig. 2.26 Settlement Vs h/L (Layered soil).
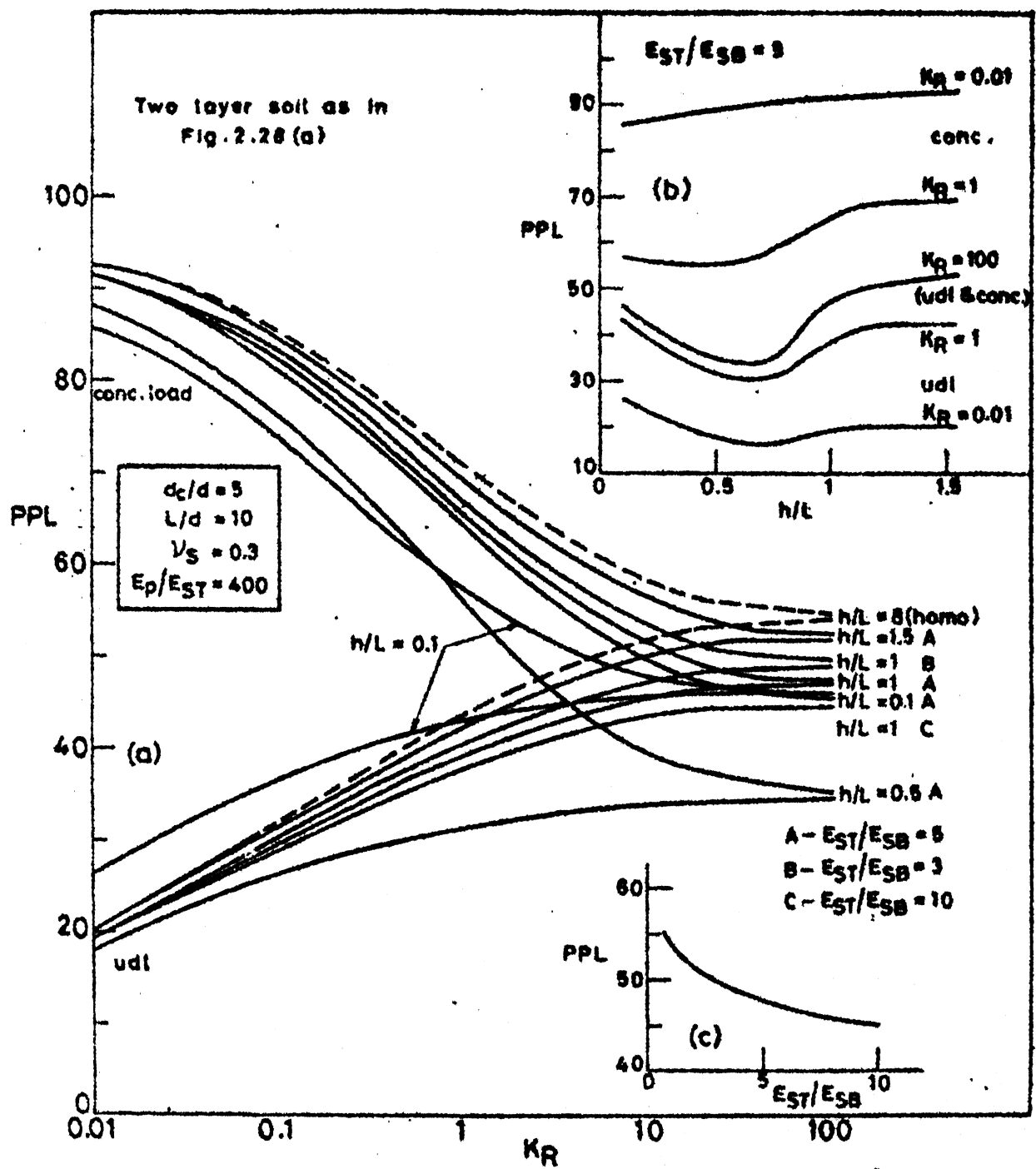
Fig.2.27   Percent pile load   (layered soil).
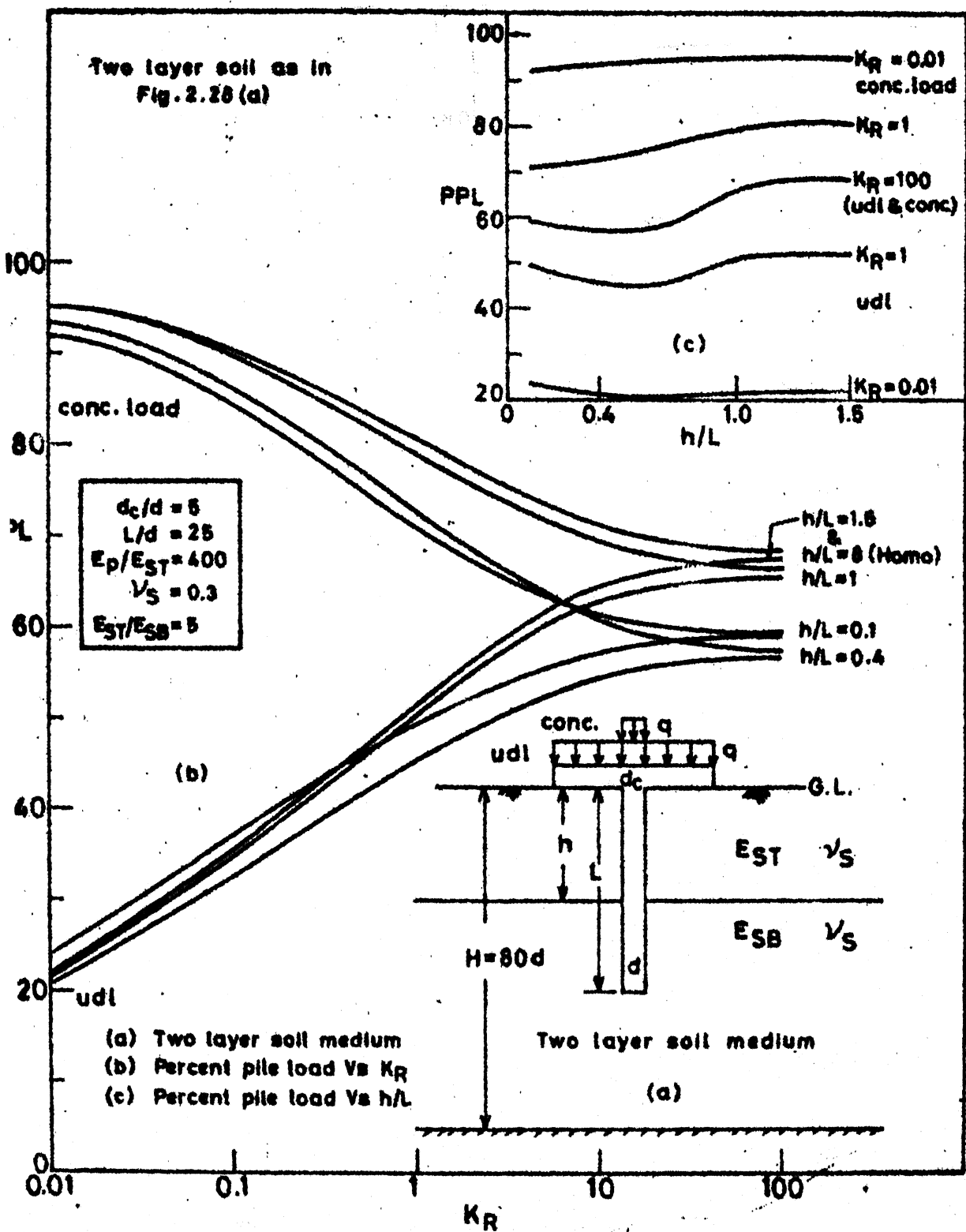
Fig. 2.28 Piled circular footing in two layer soil medium.
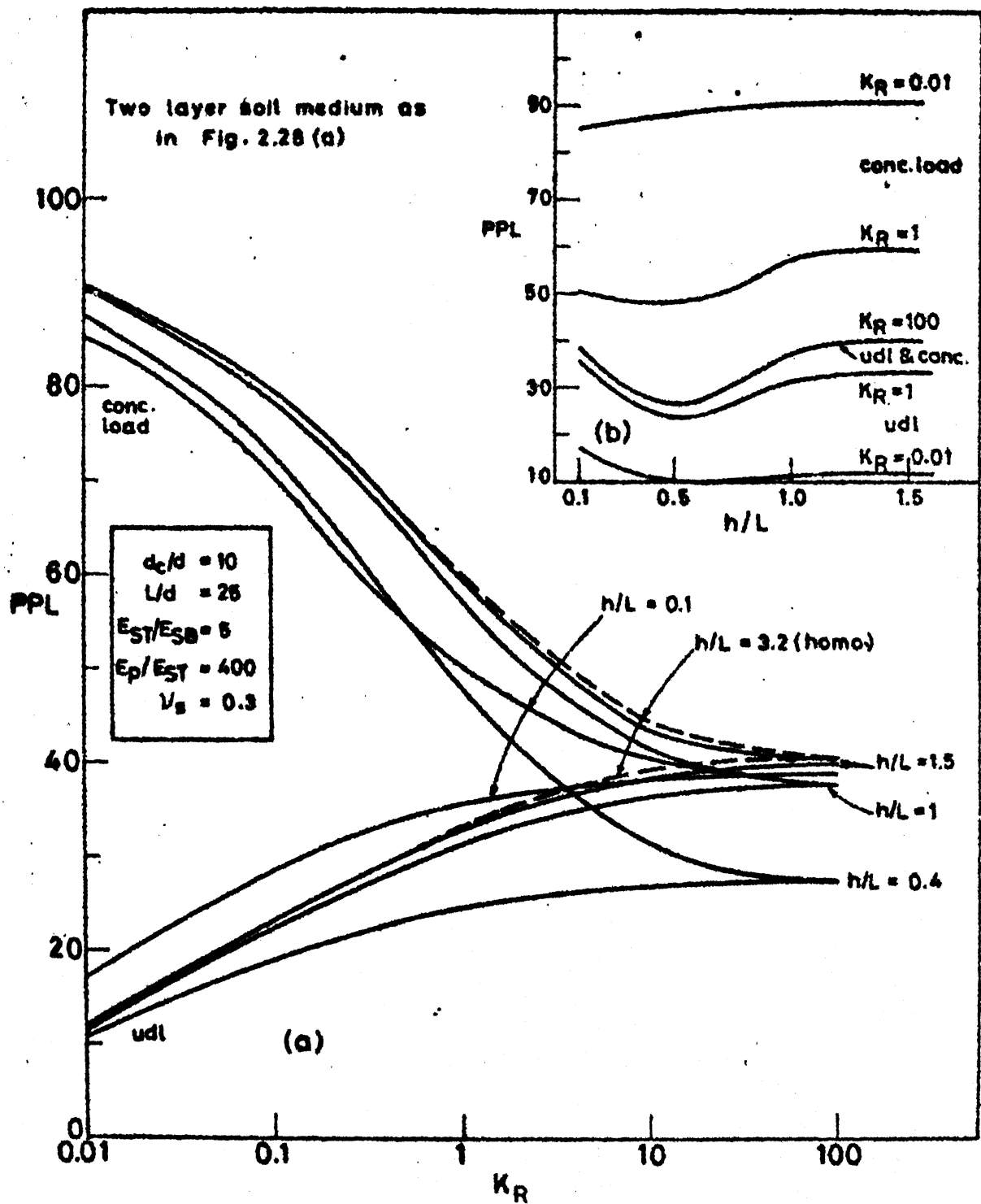
Fig. 2.30   Percent pile load (layered soil).

Two layer soil as in
Fig.2.28(a)

$d_c/d = 5$
$\nu_S = 0.3$
$E_p/E_{ST} = 400$

$\left.\begin{array}{l} L/d = 25 \\ L/d = 10 \end{array}\right\} \dfrac{E_{ST}}{E_{SB}} = 5$

$\bullet \quad E_{ST}/E_{SB}=10, L/d=10, h/L=1$

(a) udl

$h/L=1.5$
$h/L=1.0$
$h/L=0.1$
$h/L=0.4$
$h/L=1.5$
$h/L=1.0$
$h/L=0.1$
$h/L=0.5$

$\dfrac{M^*}{qa^2}$

K_R

(b) conc. load

$h/L=0.5$
$h/L=0.1$
$h/L=1.0$
$h/L=1.5$
$h/L=0.1$
$h/L=0.4$
$h/L=1.5$

$\dfrac{M^*}{qa^2}$

K_R
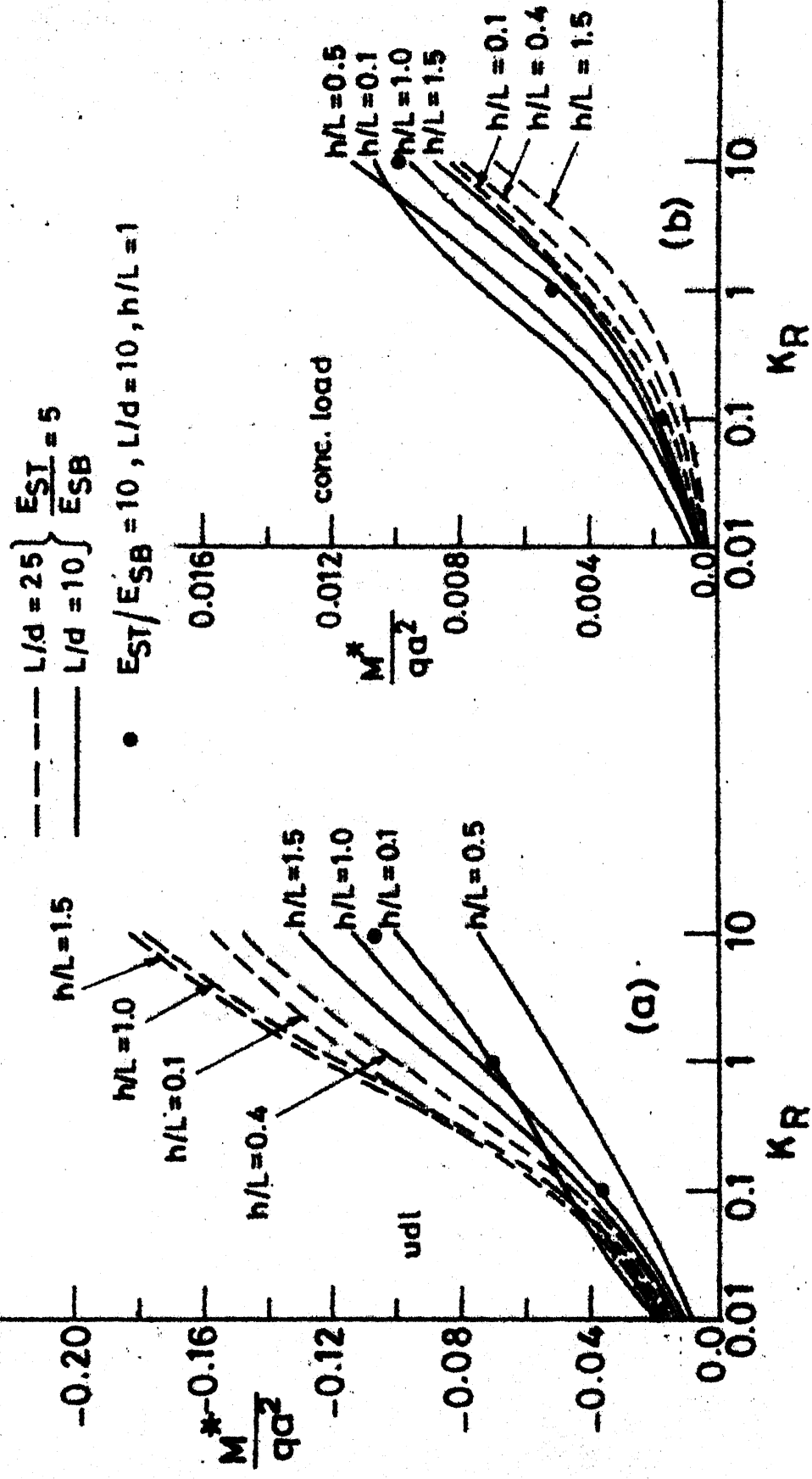
Fig. 2.31 Max. bending moment Vs K_R (layered soil)
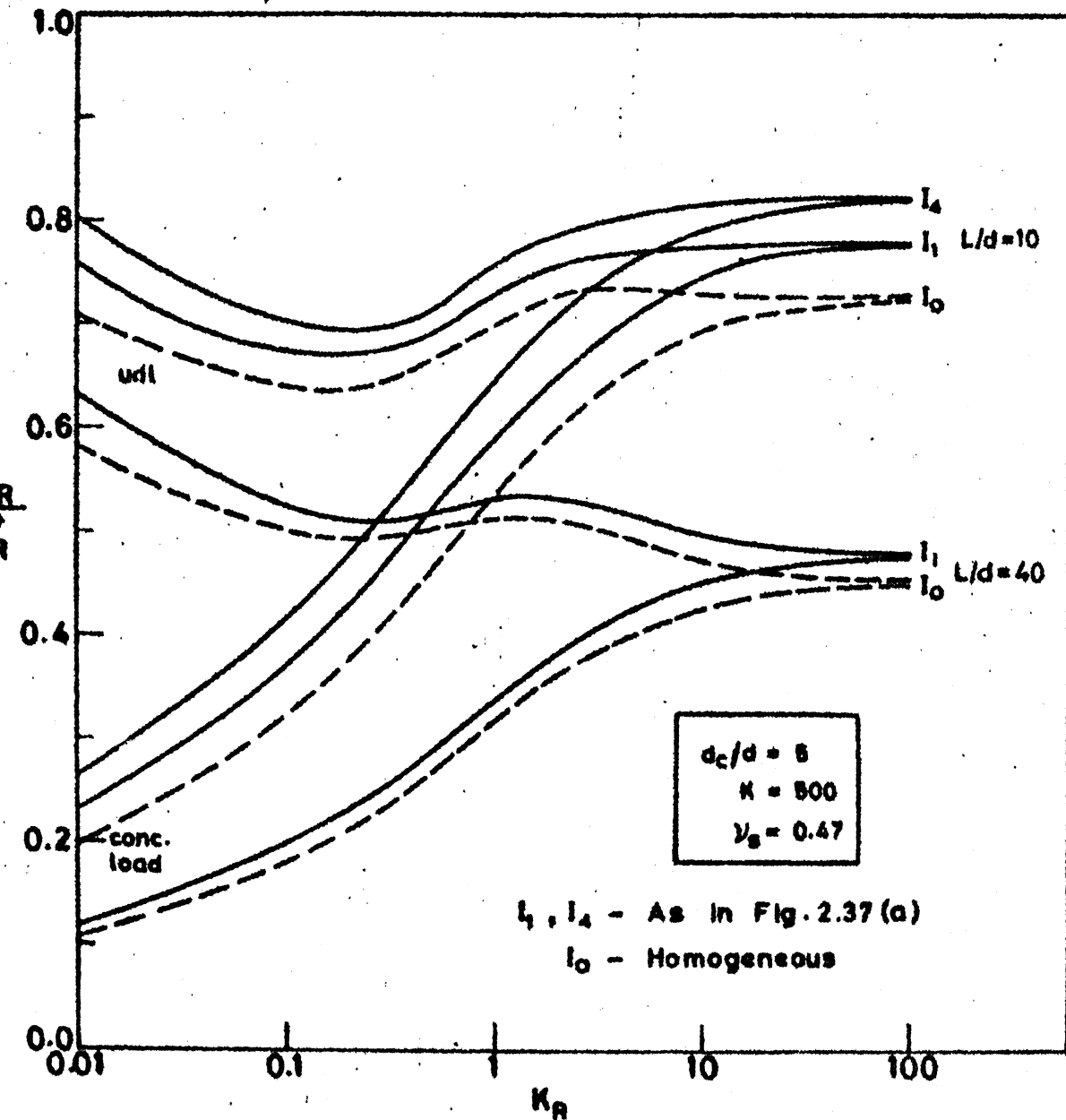
Fig. 2.32 Settlement ratio Vs K_R (effect of installation).

150
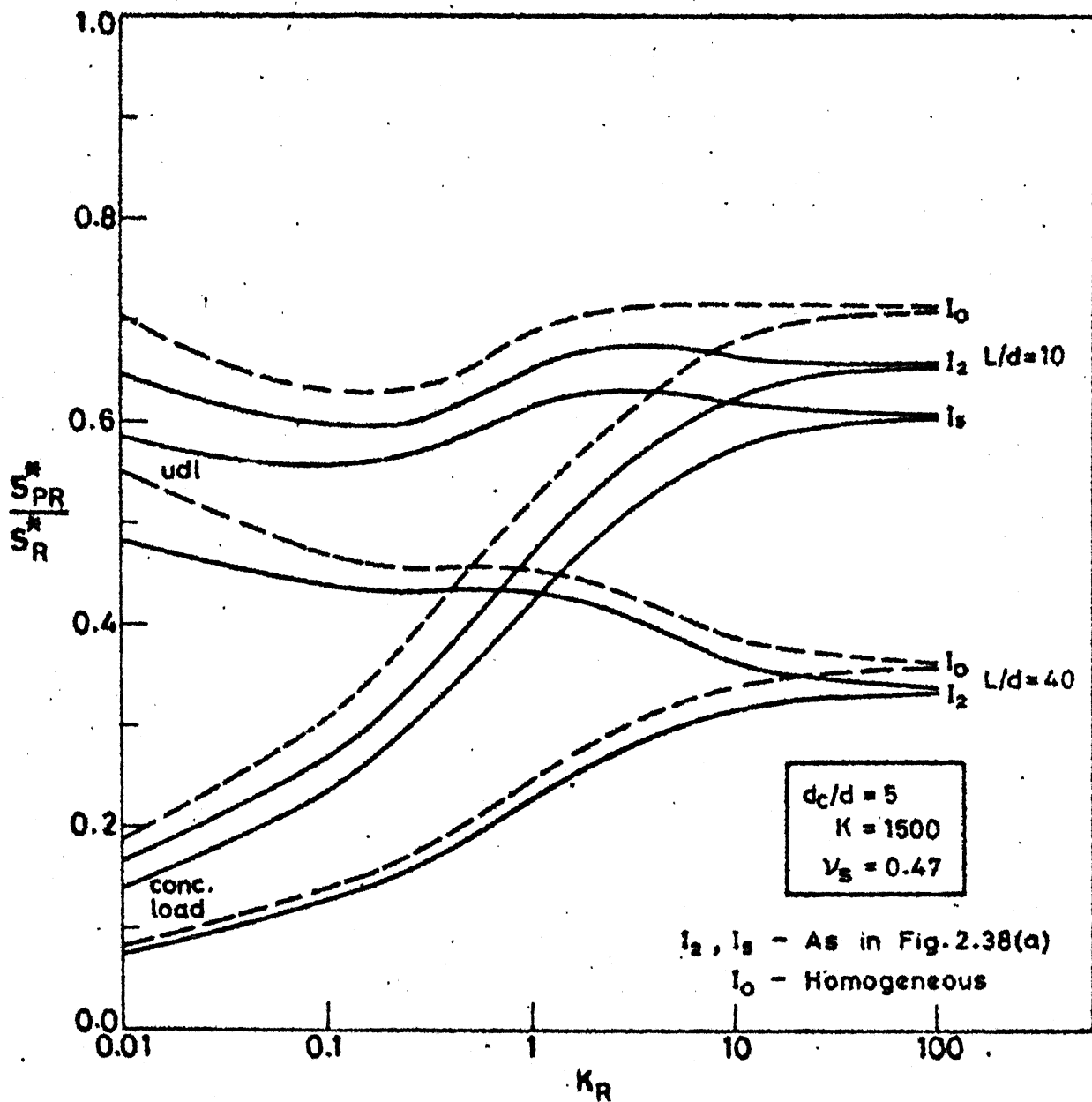
Fig. 2.33 Settlement ratio Vs K_R (effect of installation).
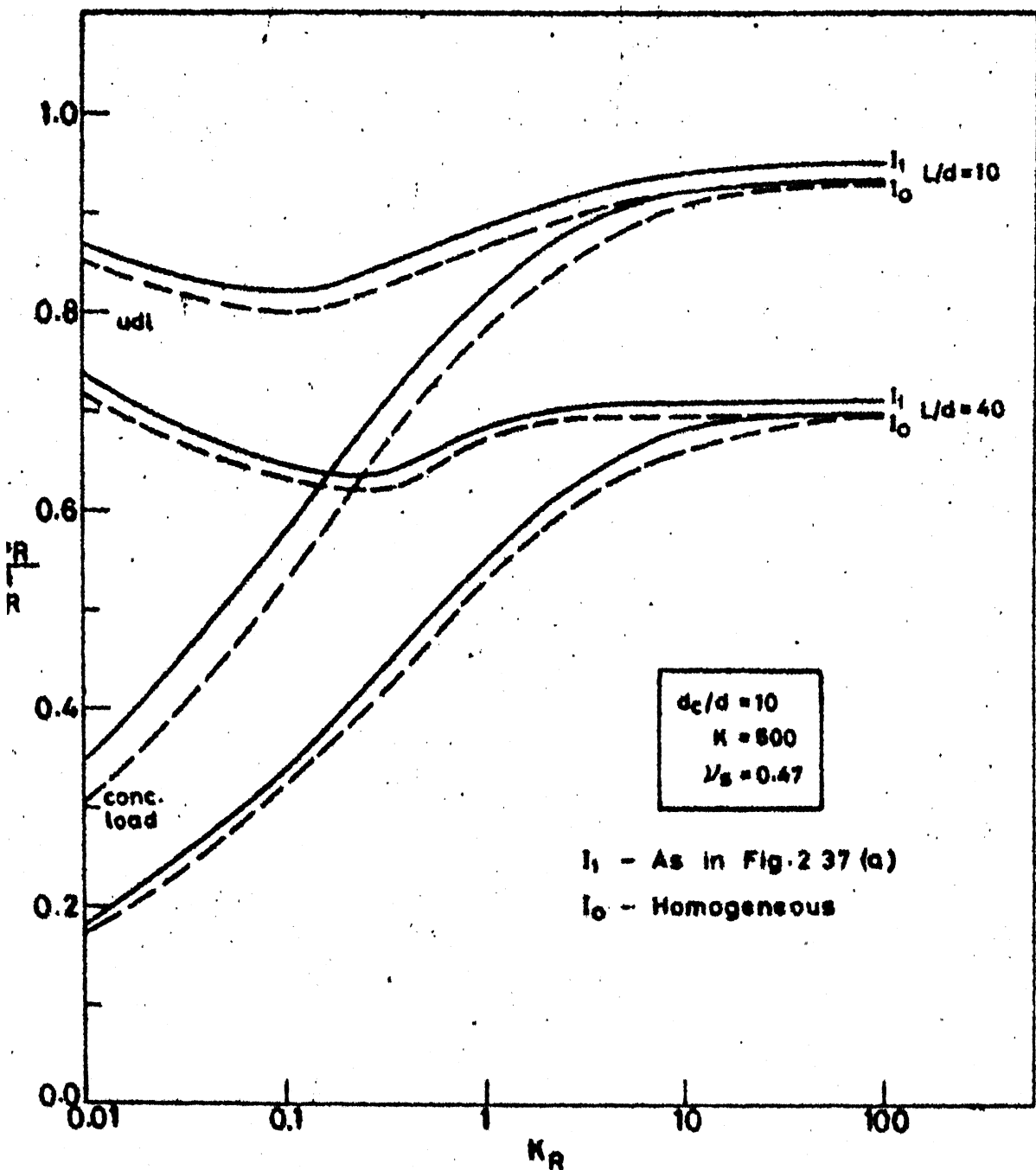
Fig. 2.34 Settlement ratio Vs K_R (effect of installation).
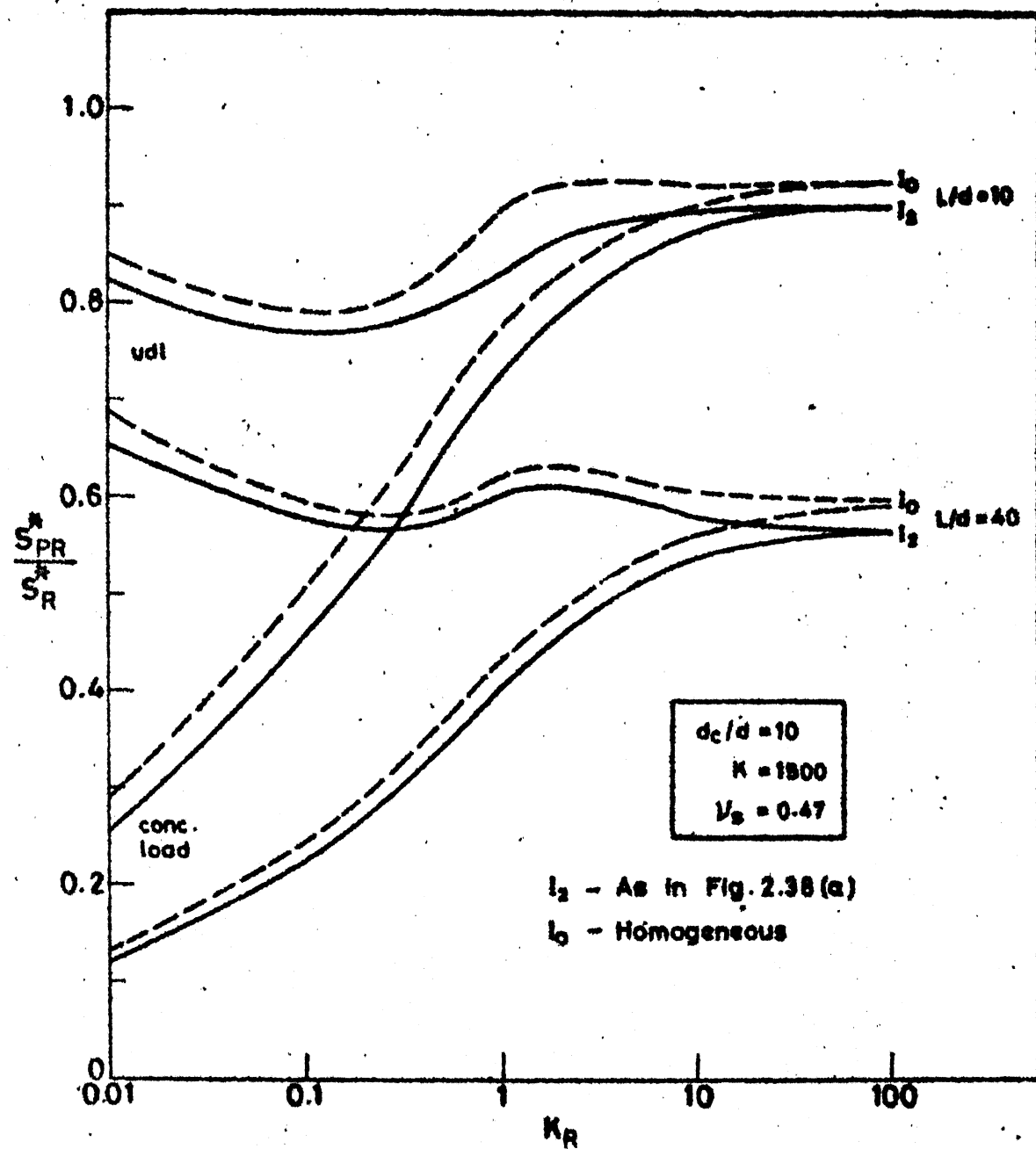
Fig. 2.35   Settlement ratio Vs K_R (effect of installation).
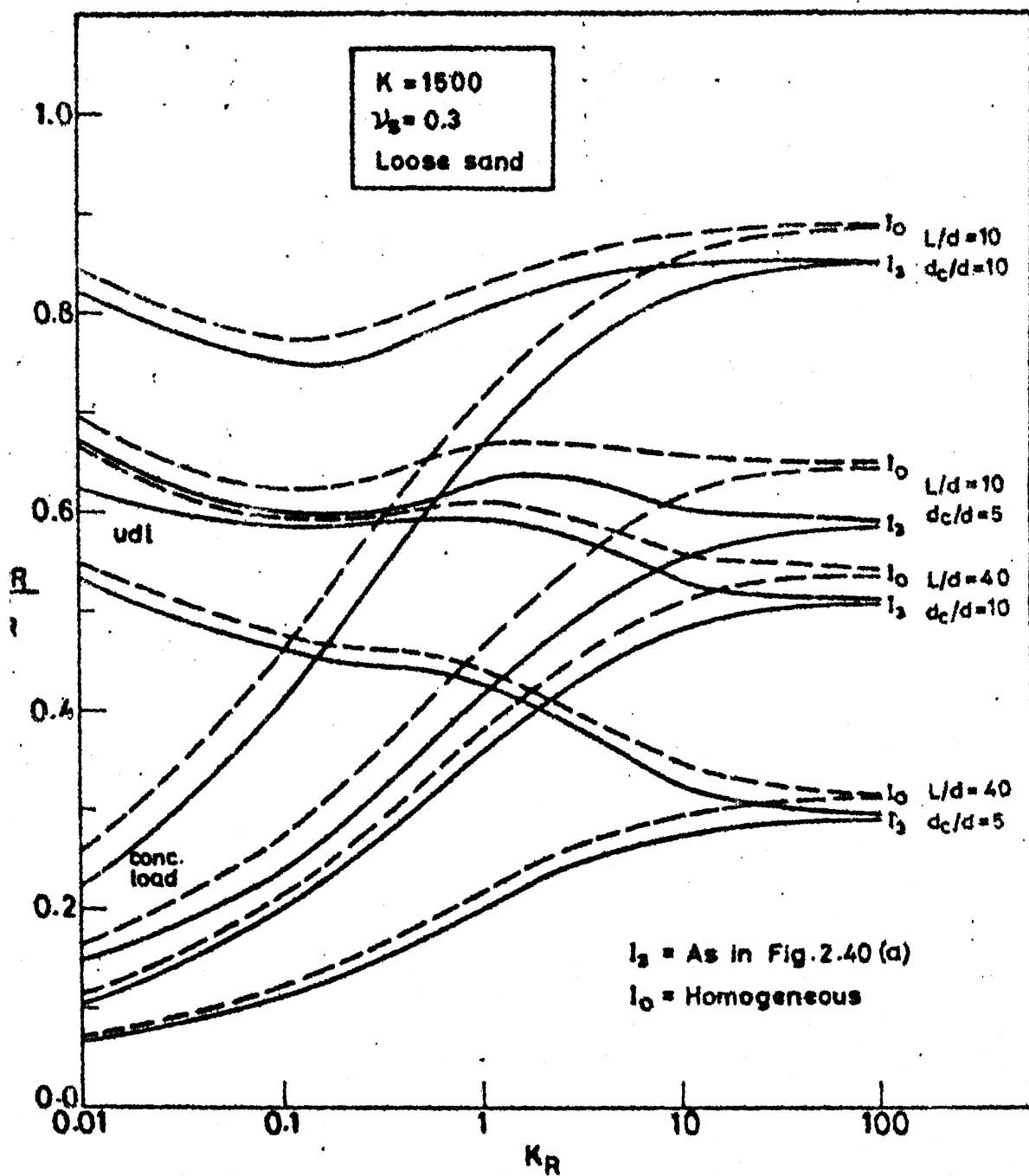
Fig. 2.36 Settlement ratio Vs K_R (effect of installation).
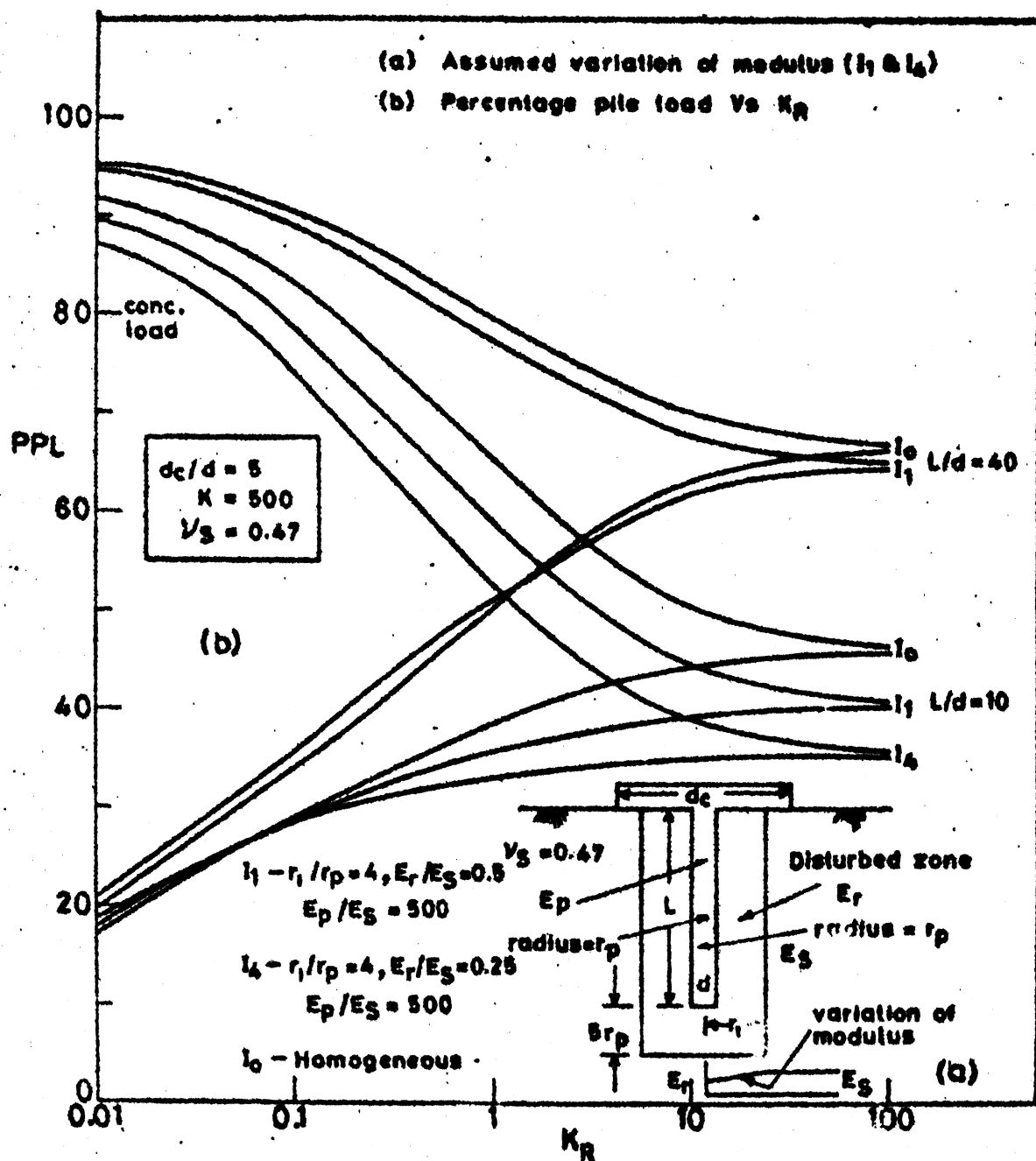
Fig. 2.37 Effect of installation of pile.
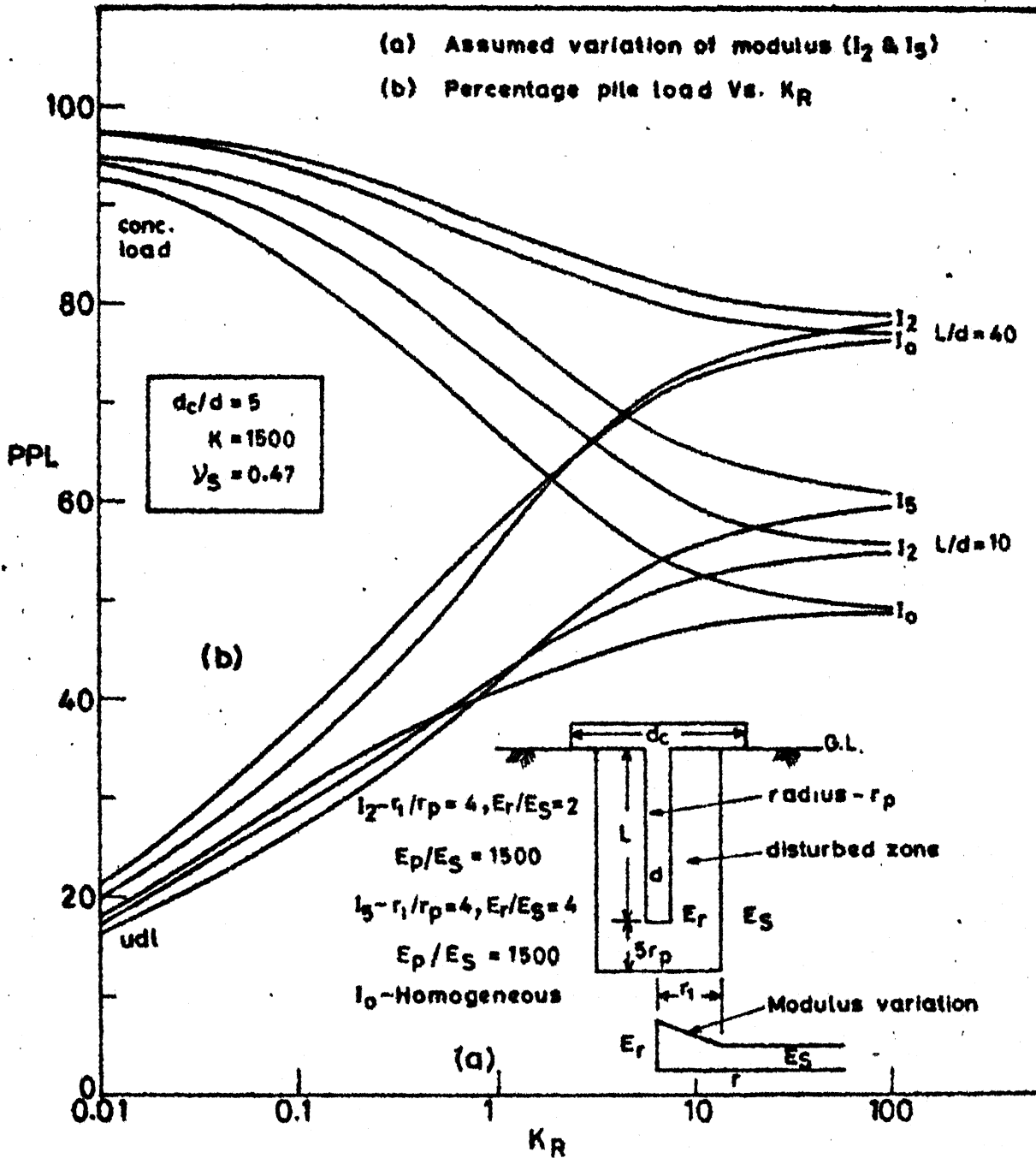
Fig.2.38 Effect of installation of pile.
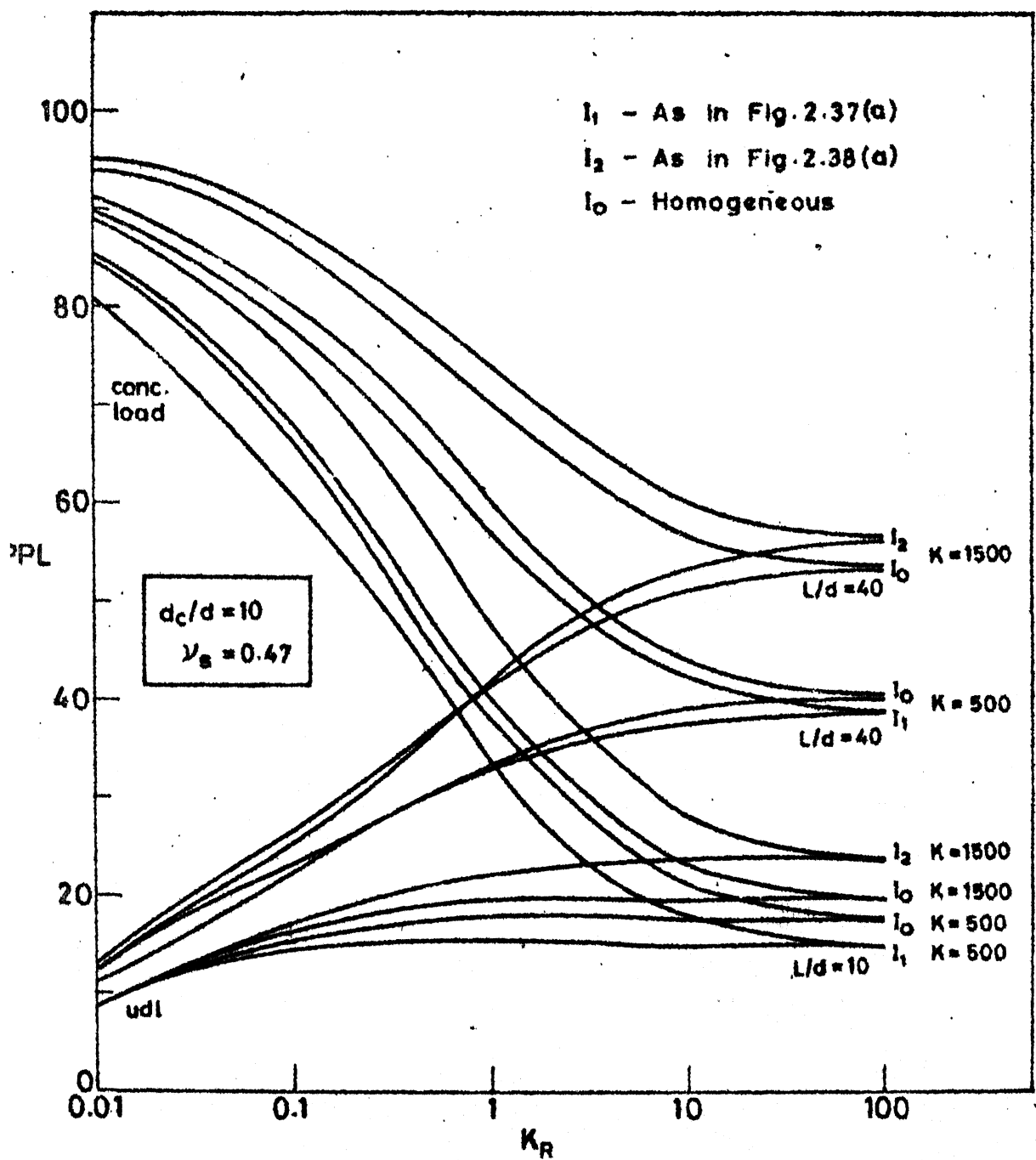
Fig. 2.39   Percent pile load Vs K_R (effect of installation).
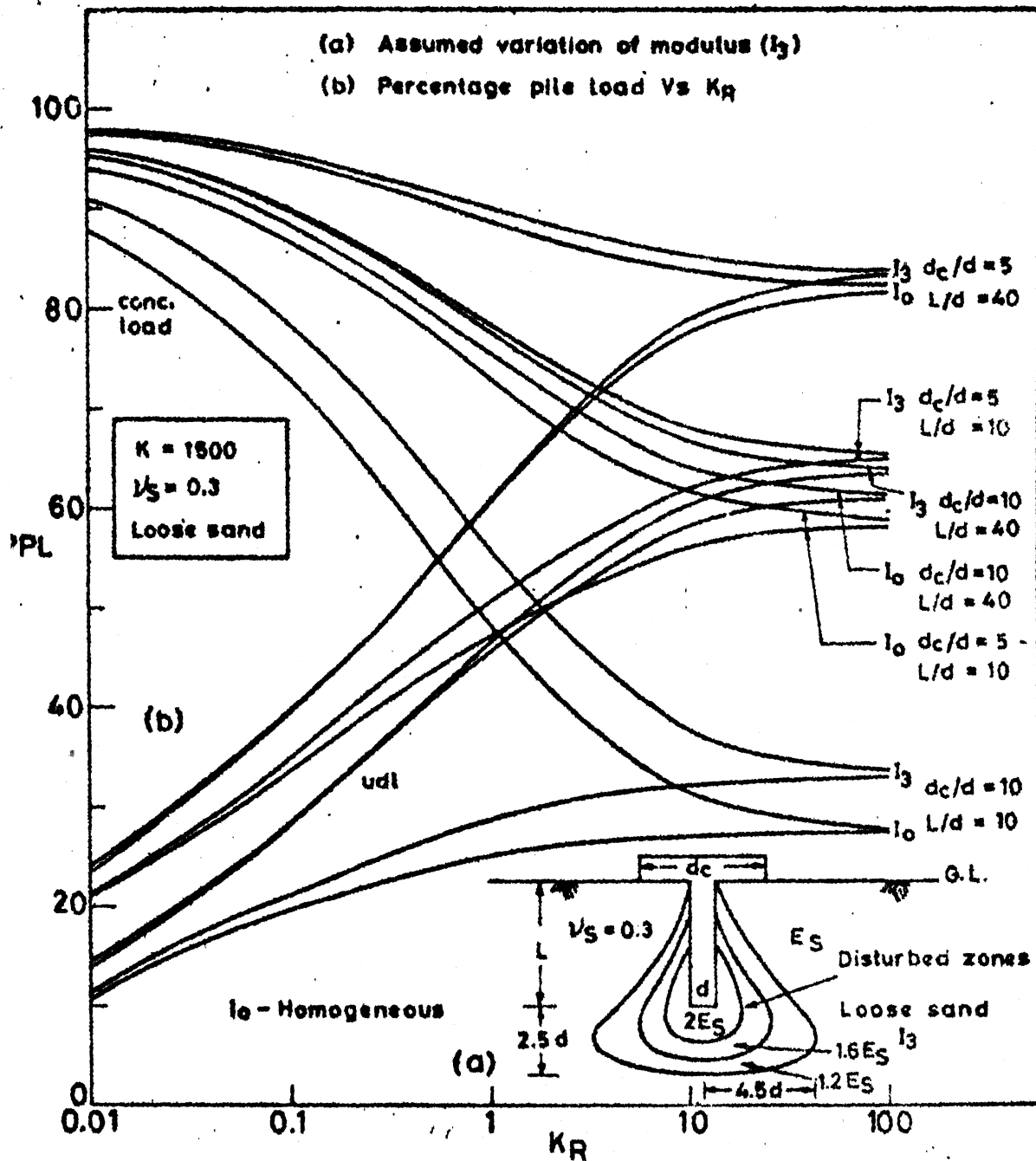
Fig. 2.40 Effect of installation of pile (loose sand).
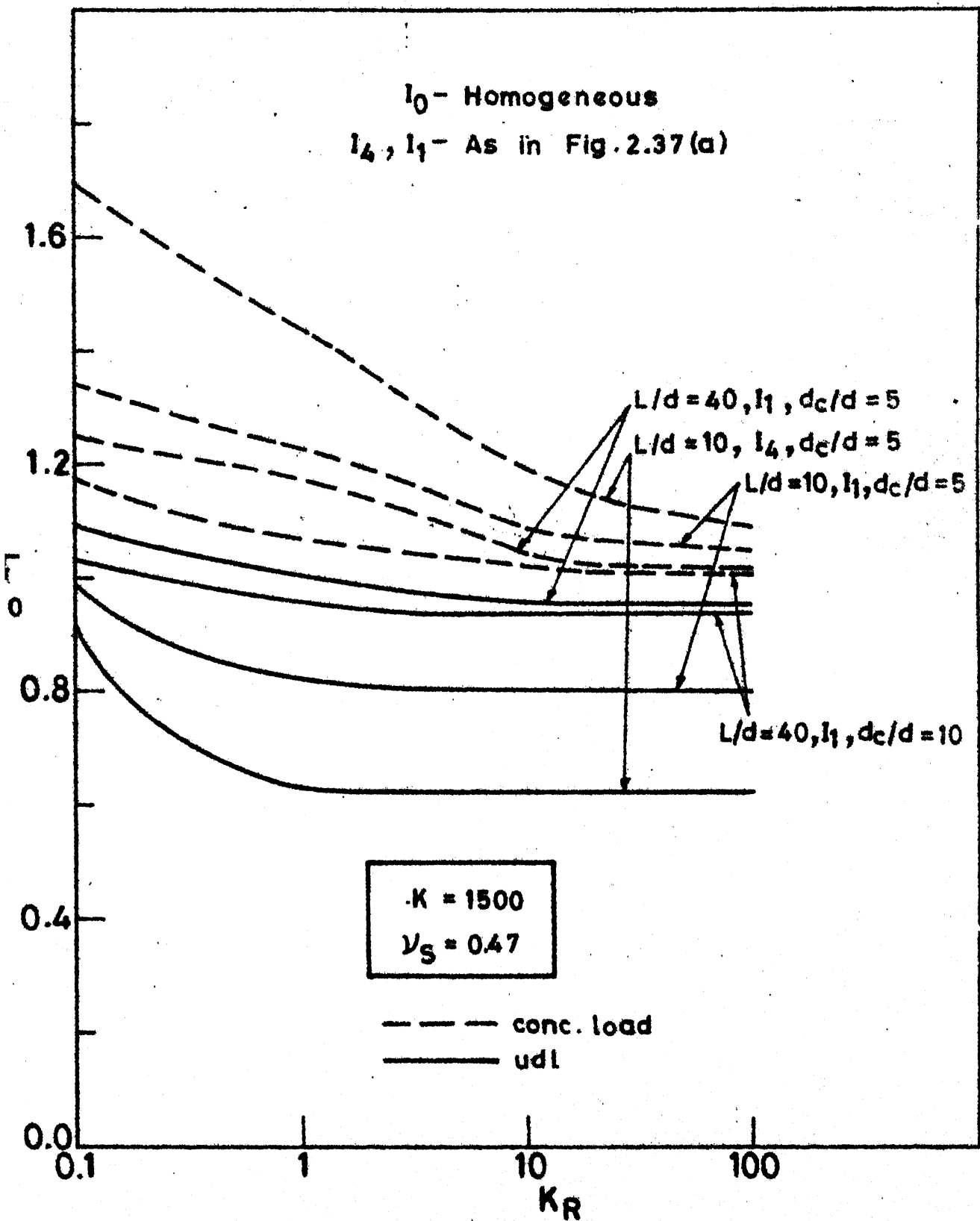
Fig. 2.41   Effect of installation on bending moment

I_0 = Homogeneous

I_2, I_5 = As in Fig. 2.38(a)

L/d = 10, I_5, d_c/d = 5

L/d = 10, I_2, d_c/d = 5

L/d = 40, I_2, d_c/d = 10

L/d = 40, I_2, d_c/d = 5

K = 500
ν_s = 0.47

– – – – conc. load

———— udl

Fig. 2.42 Effect of installation on bending moment.
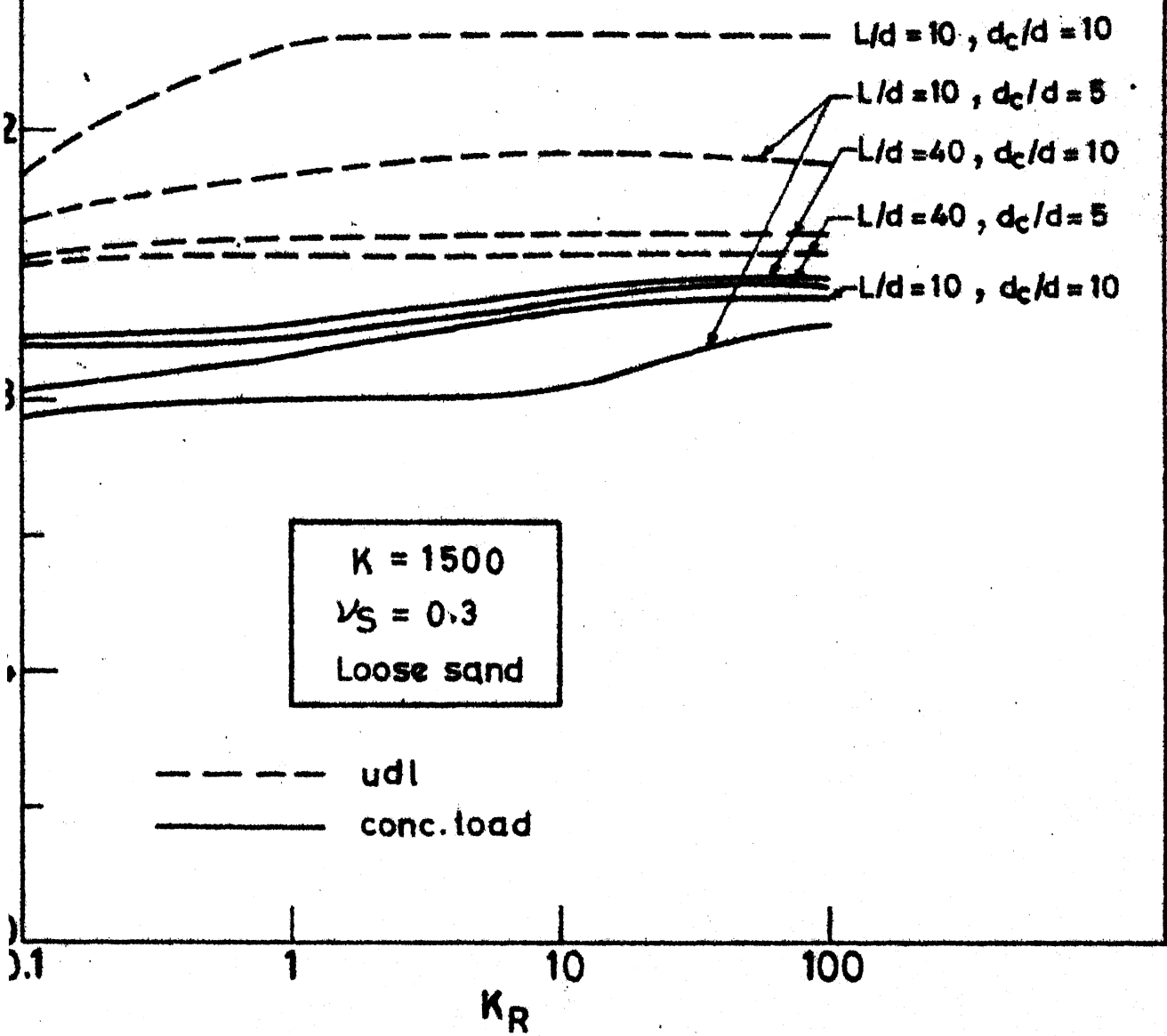
Fig. 2.43 Effect of installation on bending moment.
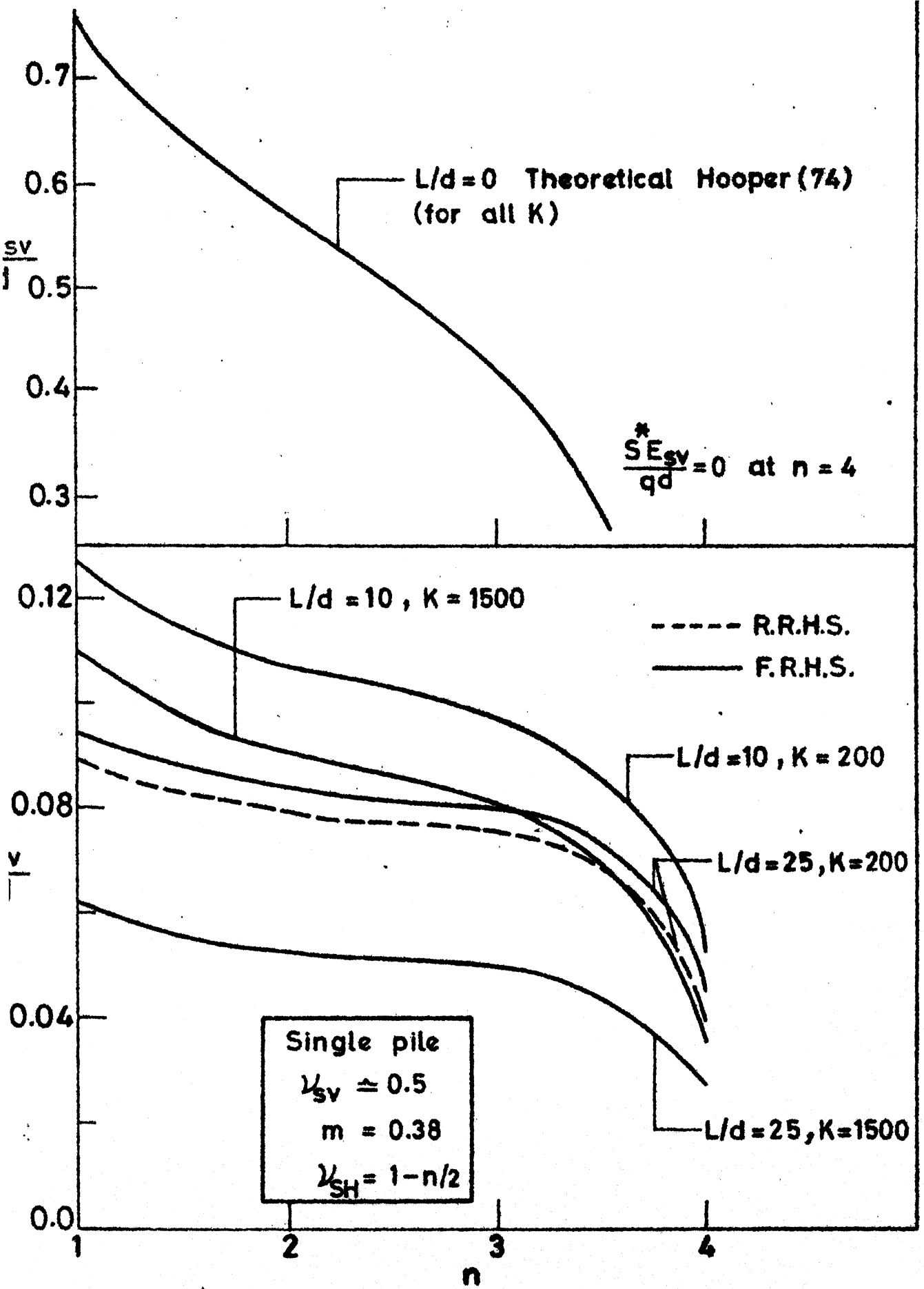
Fig. 2.44 Settlement Vs n (cross anisotropic soil).
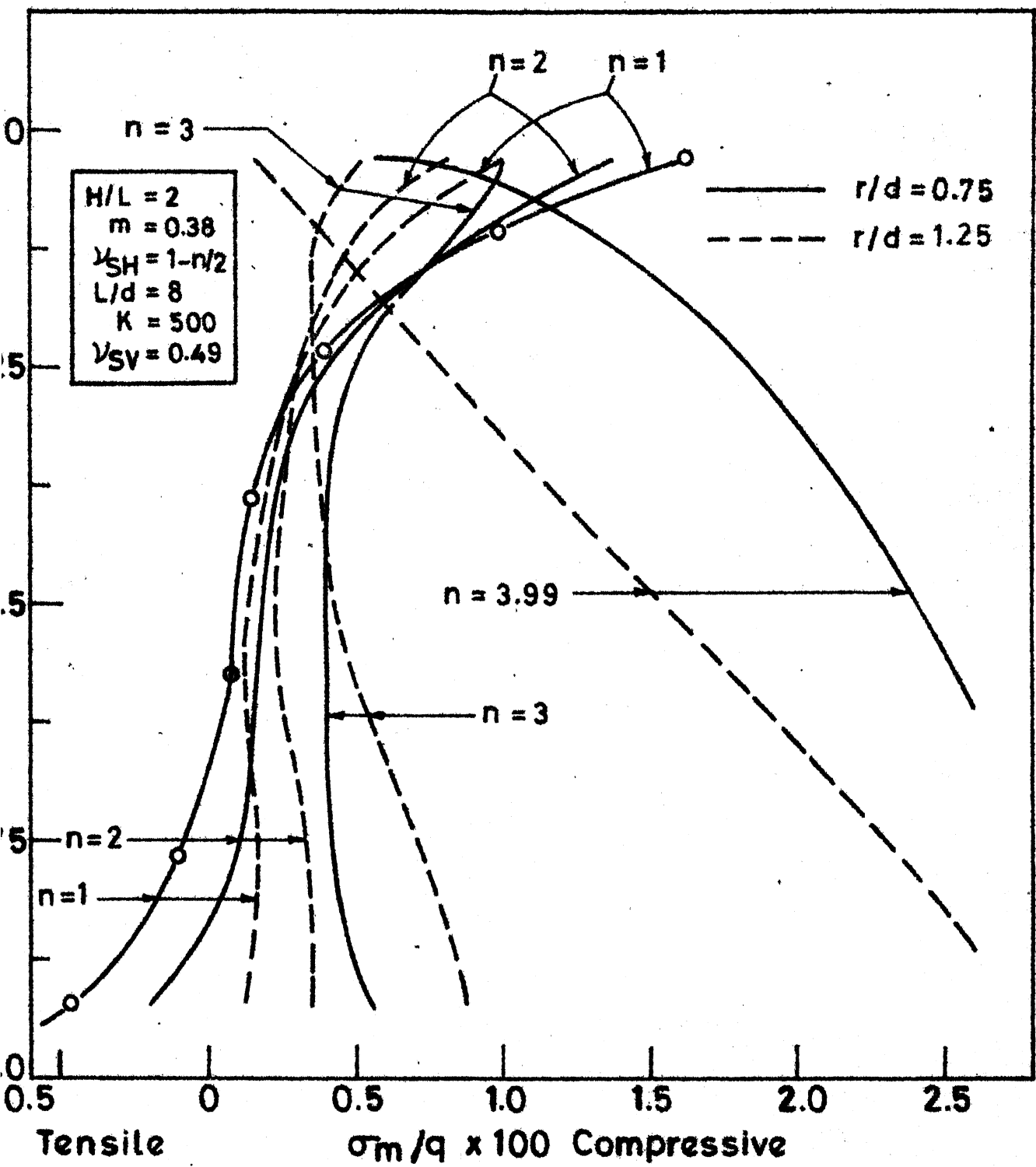
Fig. 2·45 Mean normal stress(σ_m) around single pile.
(cross-anisotropic soil).
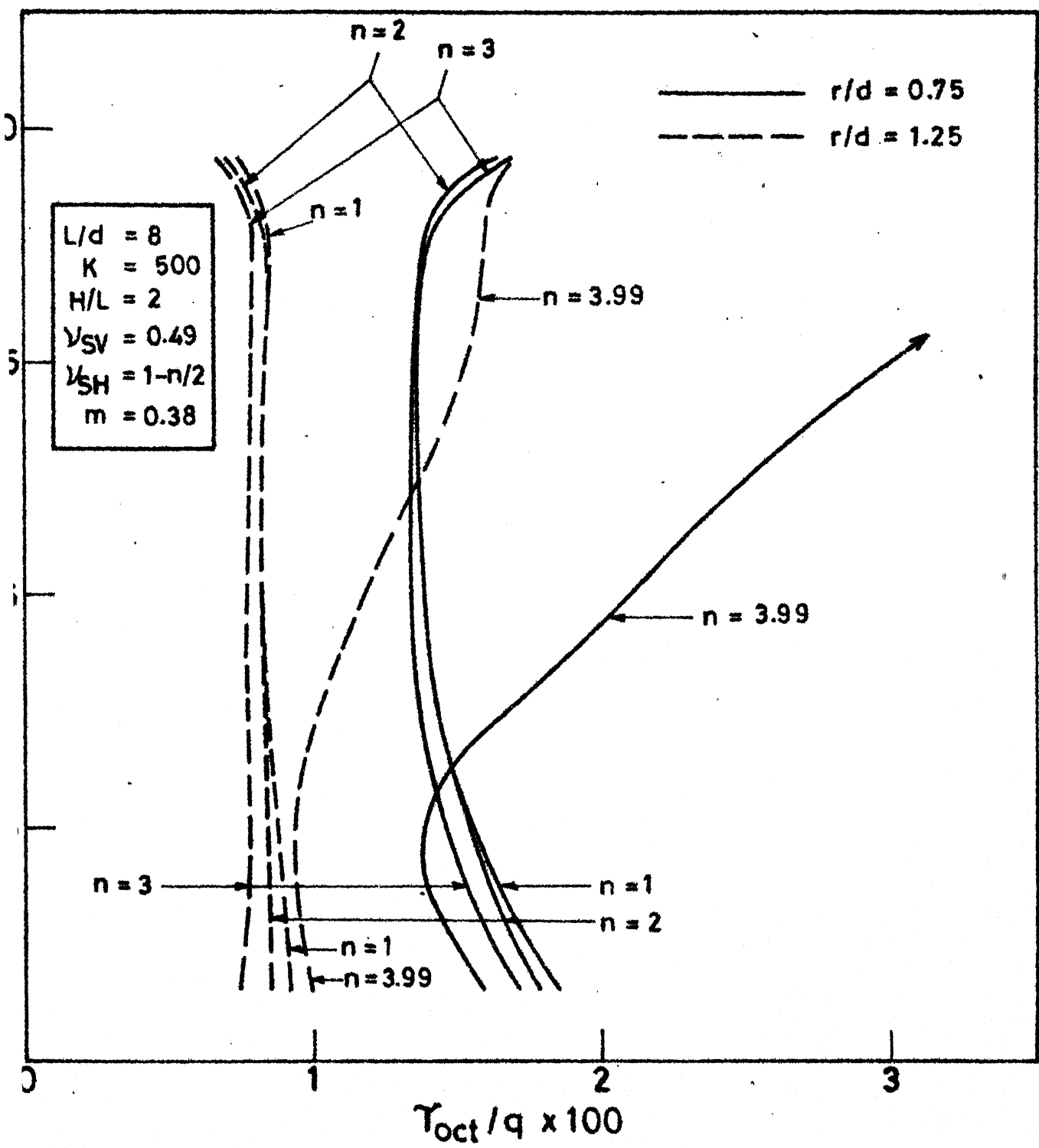
Fig. 2.46 τ_{oct} distribution around pile (cross anisotropic soil).

Fig. 2.47 Settlement Vs K_R (cross anisotropic soil).
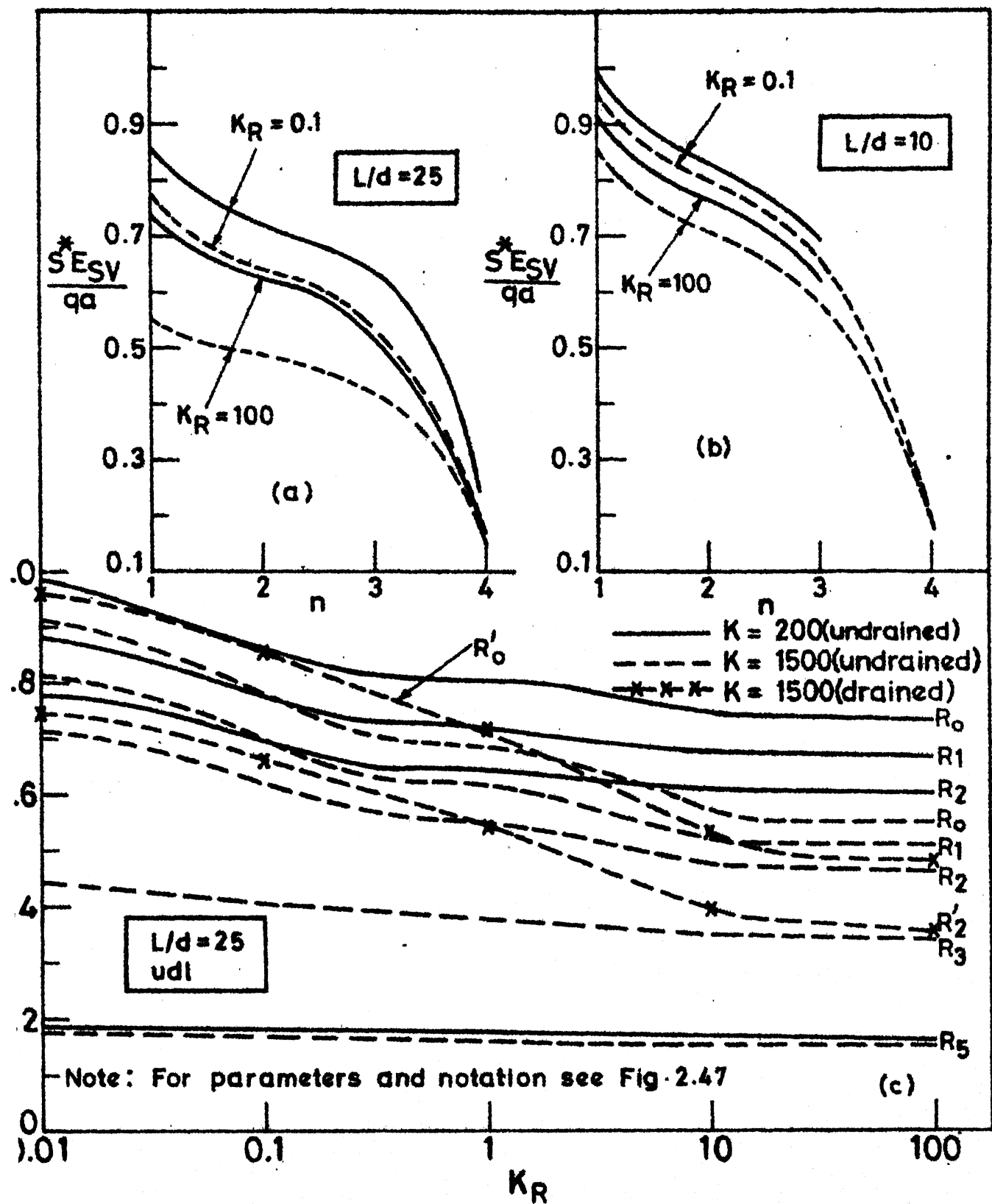
Fig. 2.48 Settlement Vs K_R (cross-anisotropic soil).
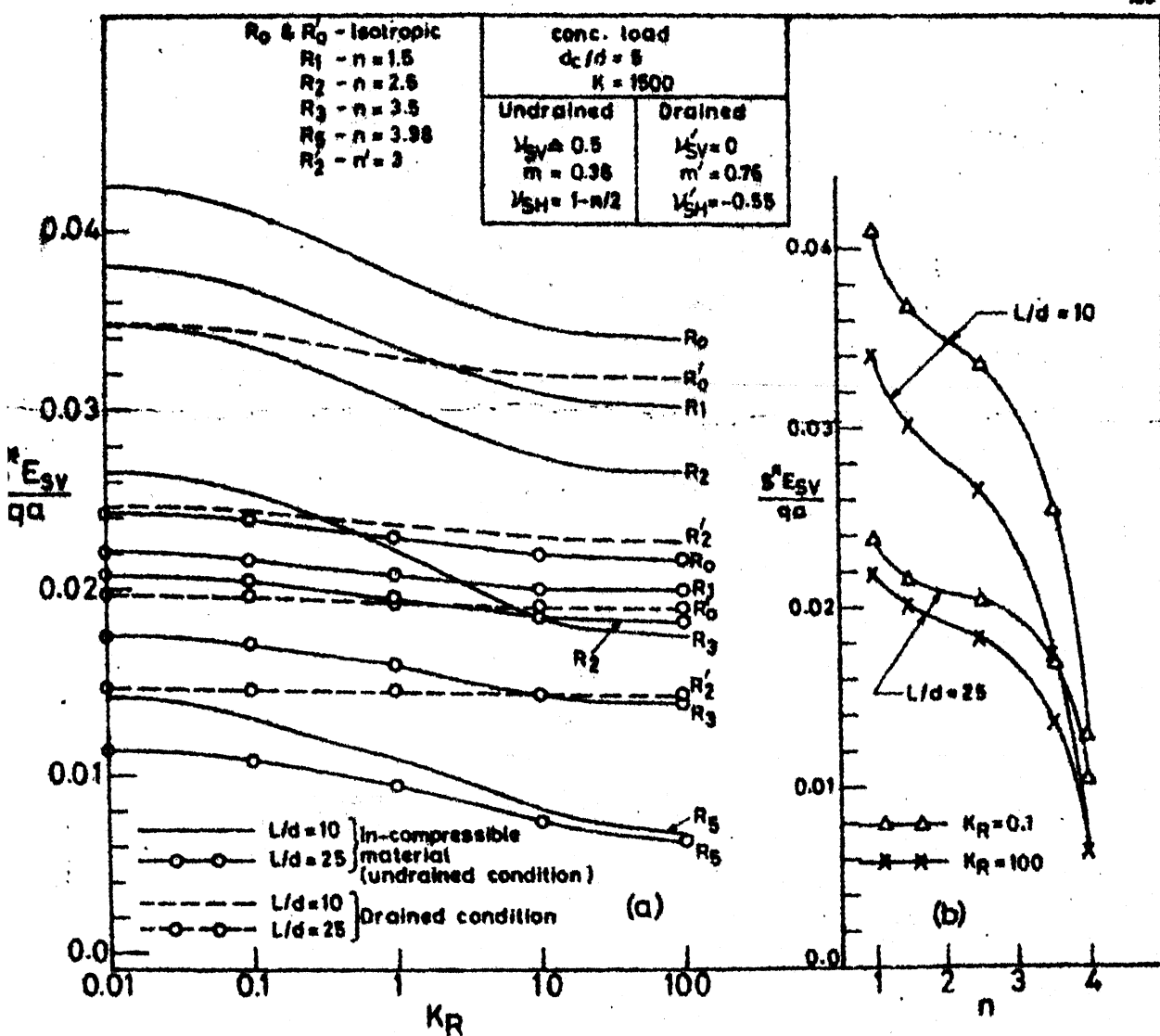
Fig. 2.49 Settlement Vs K_R and n (cross anisotropic soil).
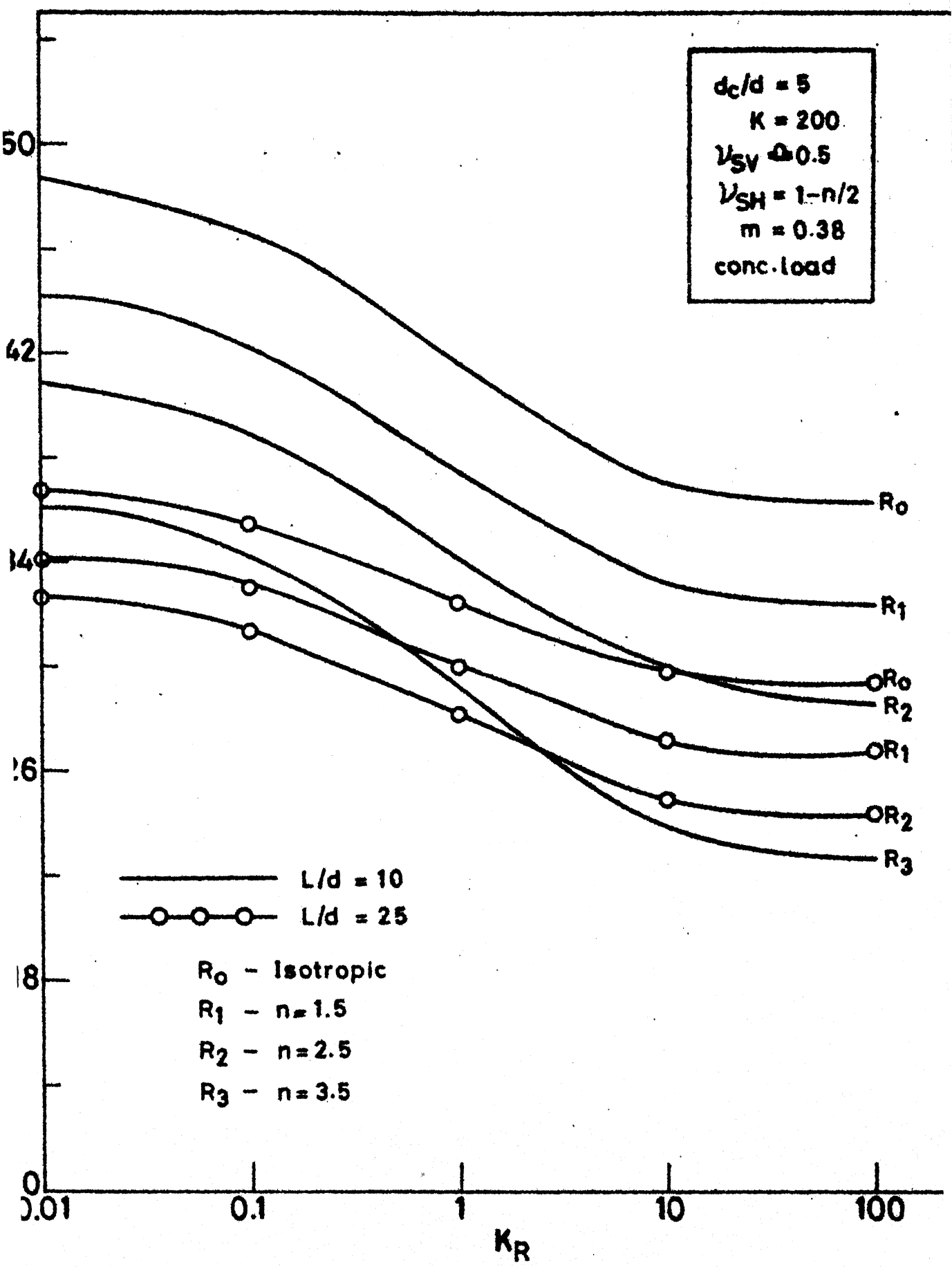
Fig. 2·50. Settlement Vs K_R (cross-anisotropic soil).
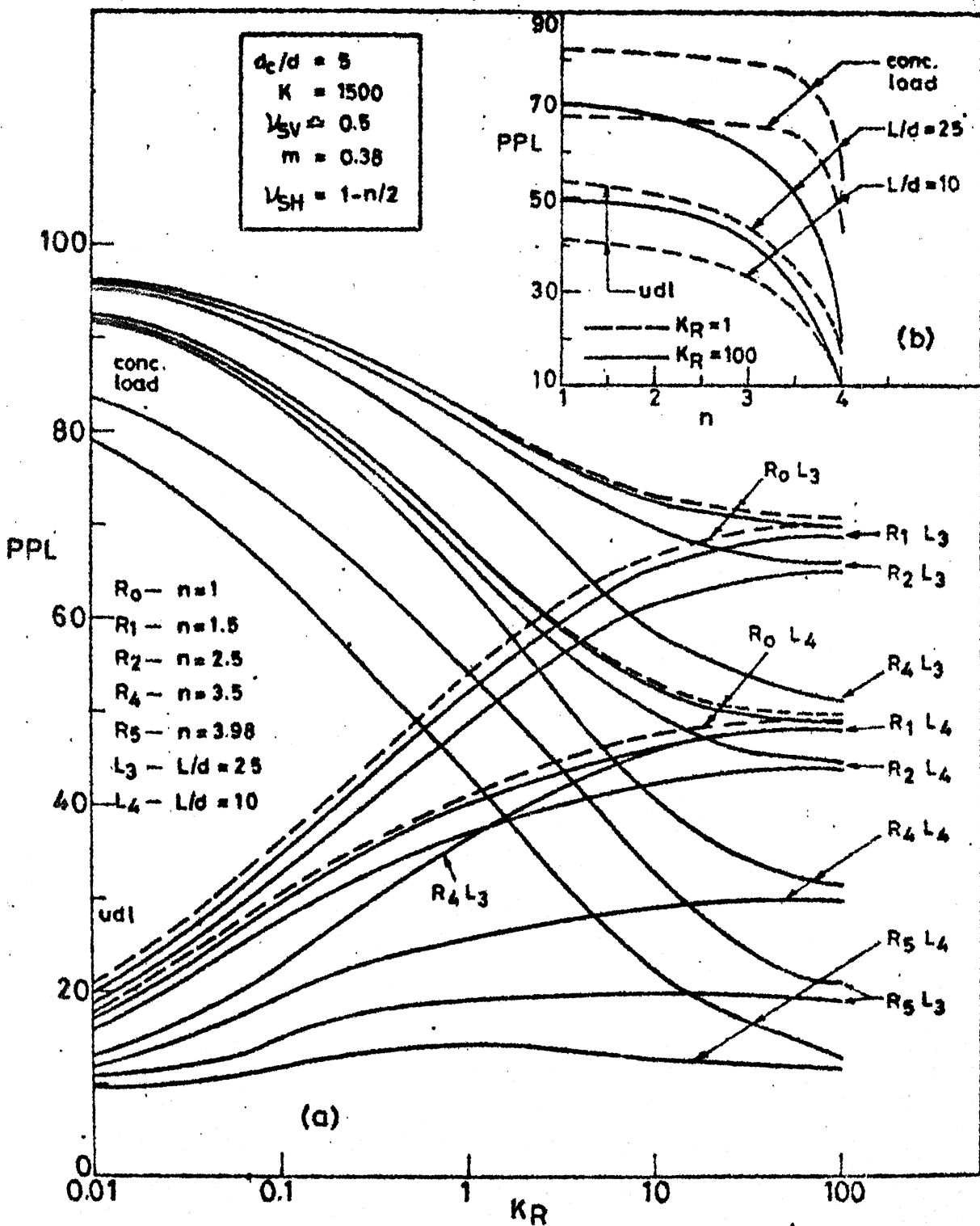
Fig. 2.51 Percent pile load Vs K_R (cross anisotropic soil).

169
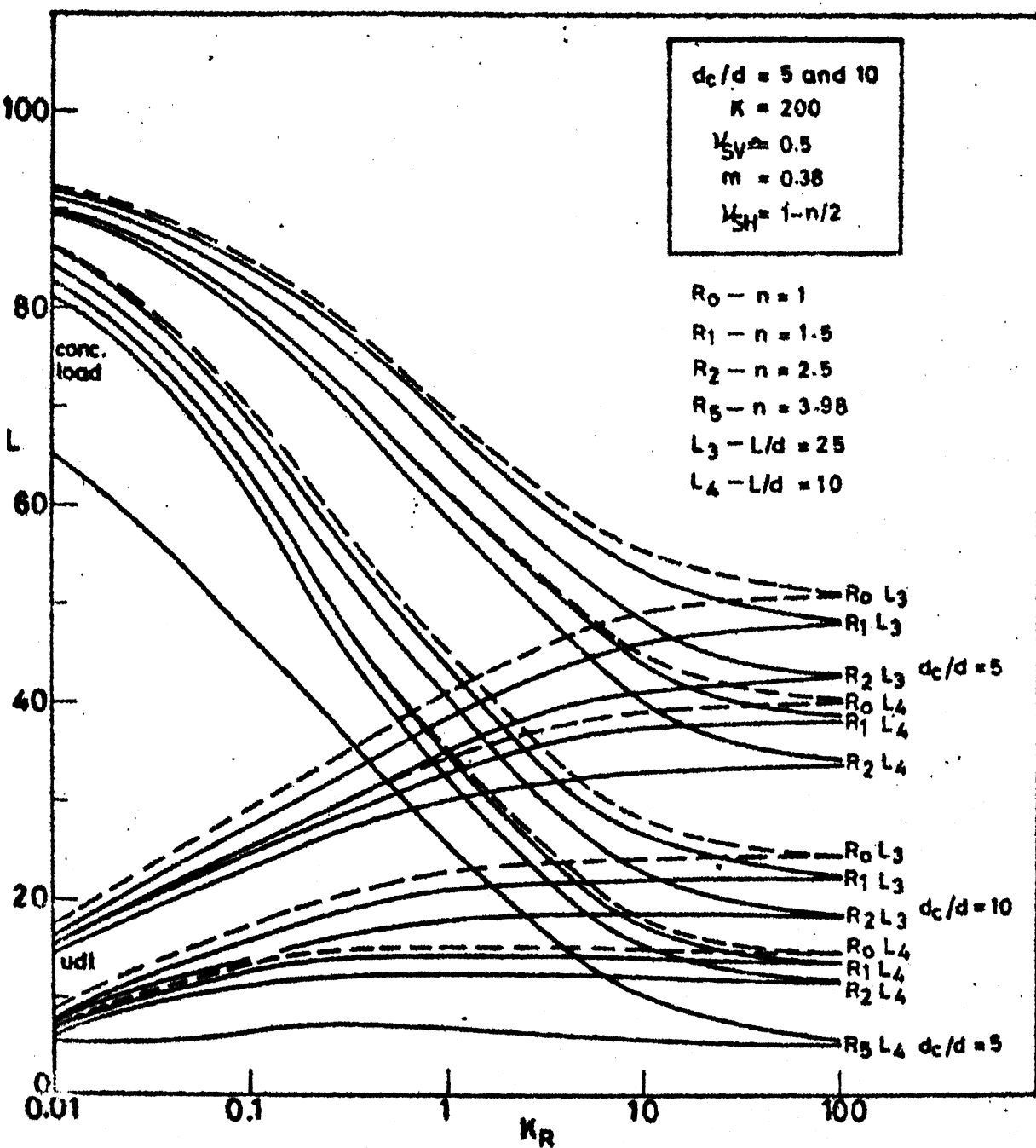
Fig. 2.52 Percent pile load vs K_R (cross anisotropic soil).

conc. load

R_O
R_2
$L/d = 25$
R_2
R_O

R_2
$L/d = 10$
R_O

R_O – Isotropic
R_2 – $\nu'_{SH} = -0.55$
$\qquad m' = 0.78$
$\qquad n' = 3$

$d_c/d = 5$
$K = 1500$
$\nu'_{SV} = 0$

udl

K_R

01   0.1   1   10   100
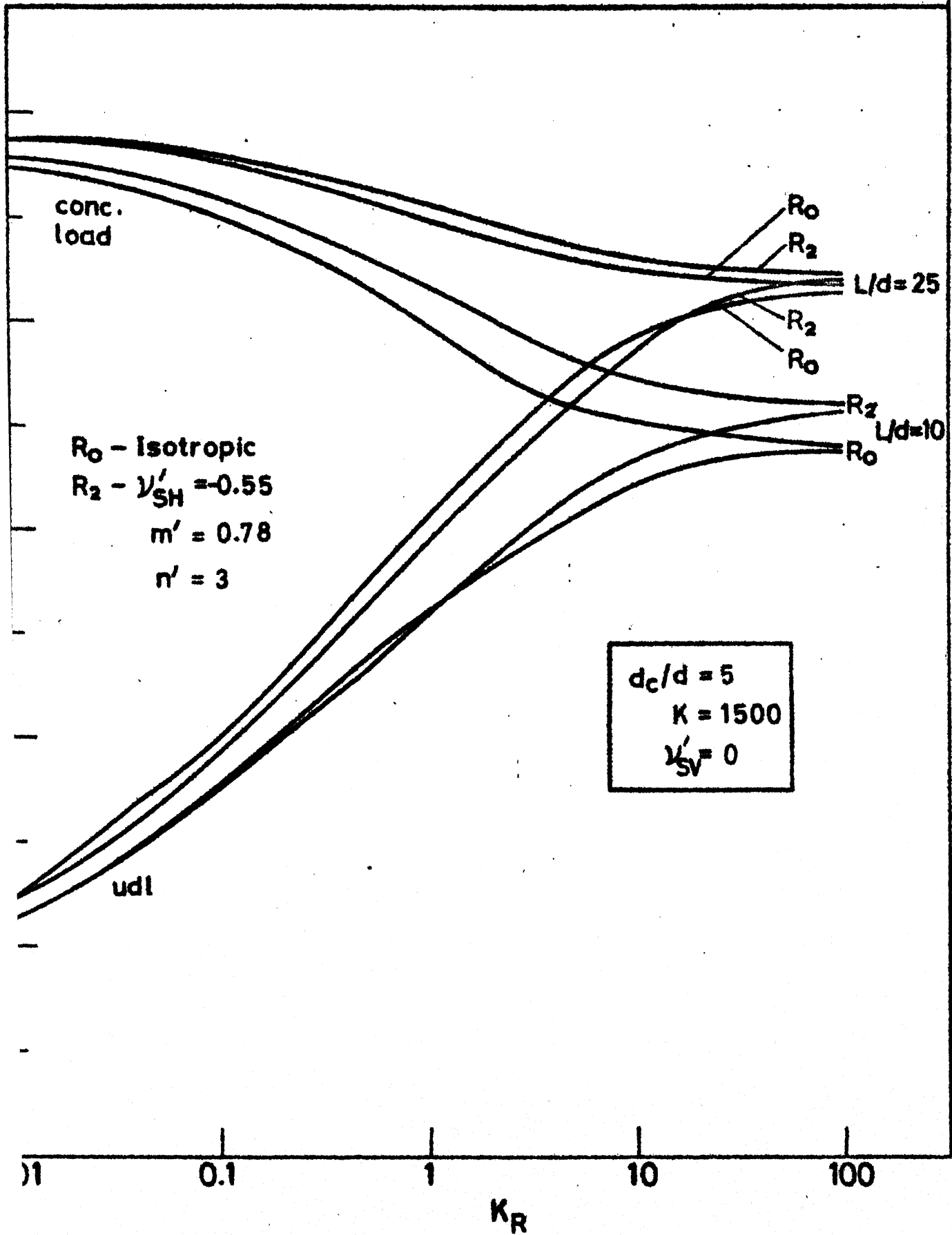
Fig. 2.53   PPL   Vs K_R (cross-anisotropic soil).

Figure with annotations:

Box (upper left):
L/d = 10
$d_c/d = 5$
K = 1500
udl

Drained
$\nu'_{SV} = 0$
$\nu'_{SH} = -0.55$
$m' = 0.76$
$R'_2 - n' = 3$
$R'_0 -$ Isotropic

Undrained
(Incompressible)
$\nu_{SV} \doteq 0.5$
$m = 0.38$
$\nu_{SH} = 1-n/2$
$R_0 -$ Isotropic
$R_1 - n = 1.5$
$R_2 - n = 2.5$
$R_3 - n = 3.5$

Curve labels: R'_2, R'_0, R_0, R_1, R_2, R_3

* Greater positive moment develops

x-axis: K_R (values: 01, 0.1, 1, 10, 100)
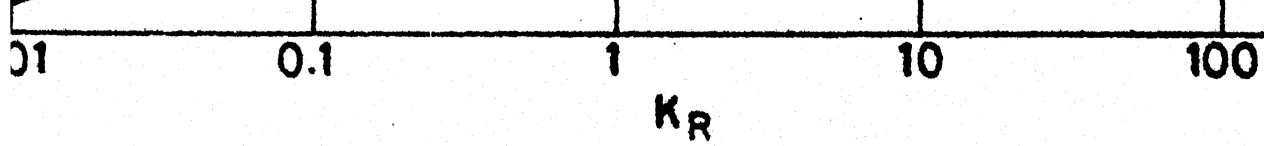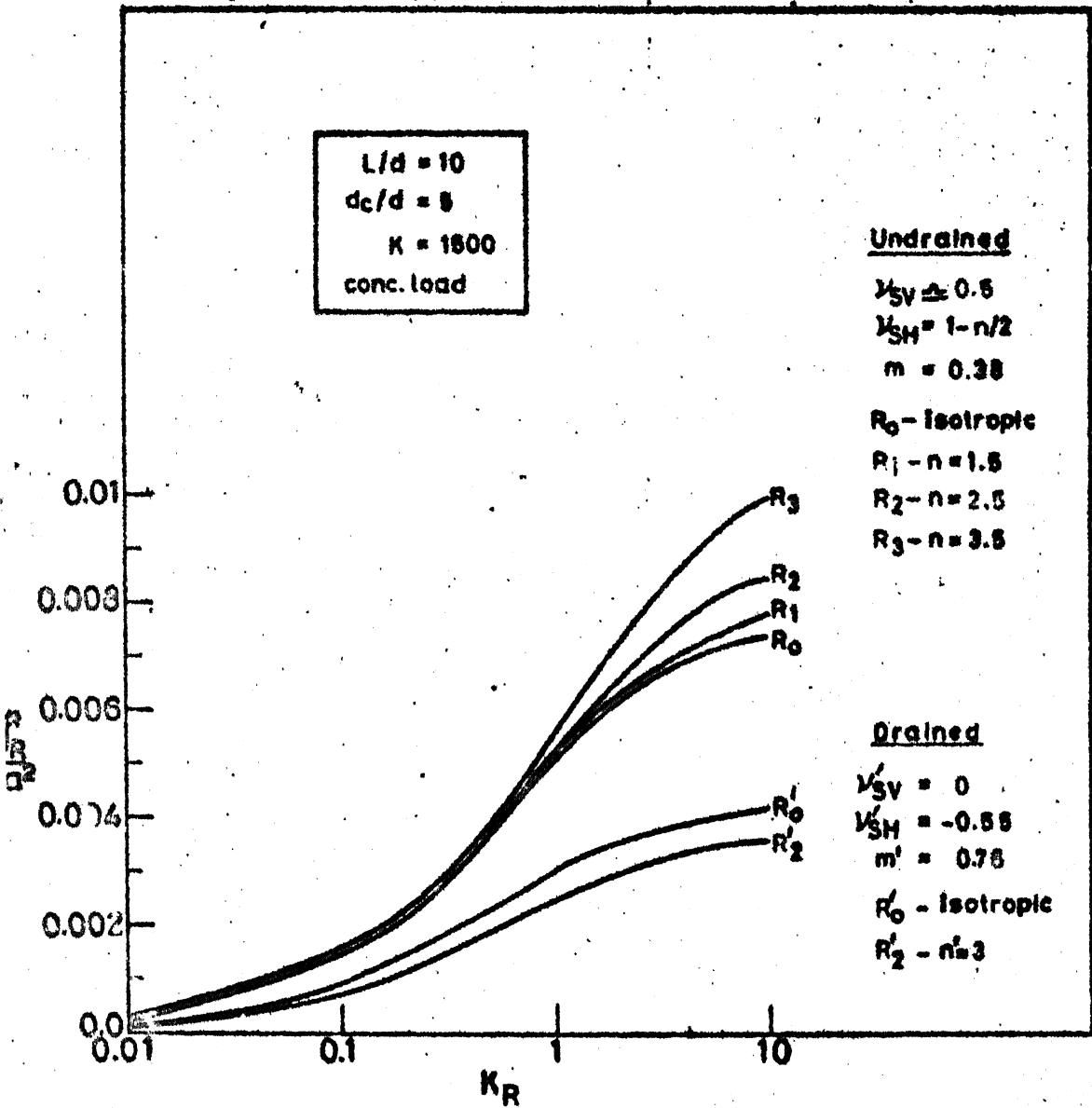
Fig.2.55 Bending moment Vs K_R (cross-anisotropic soil).
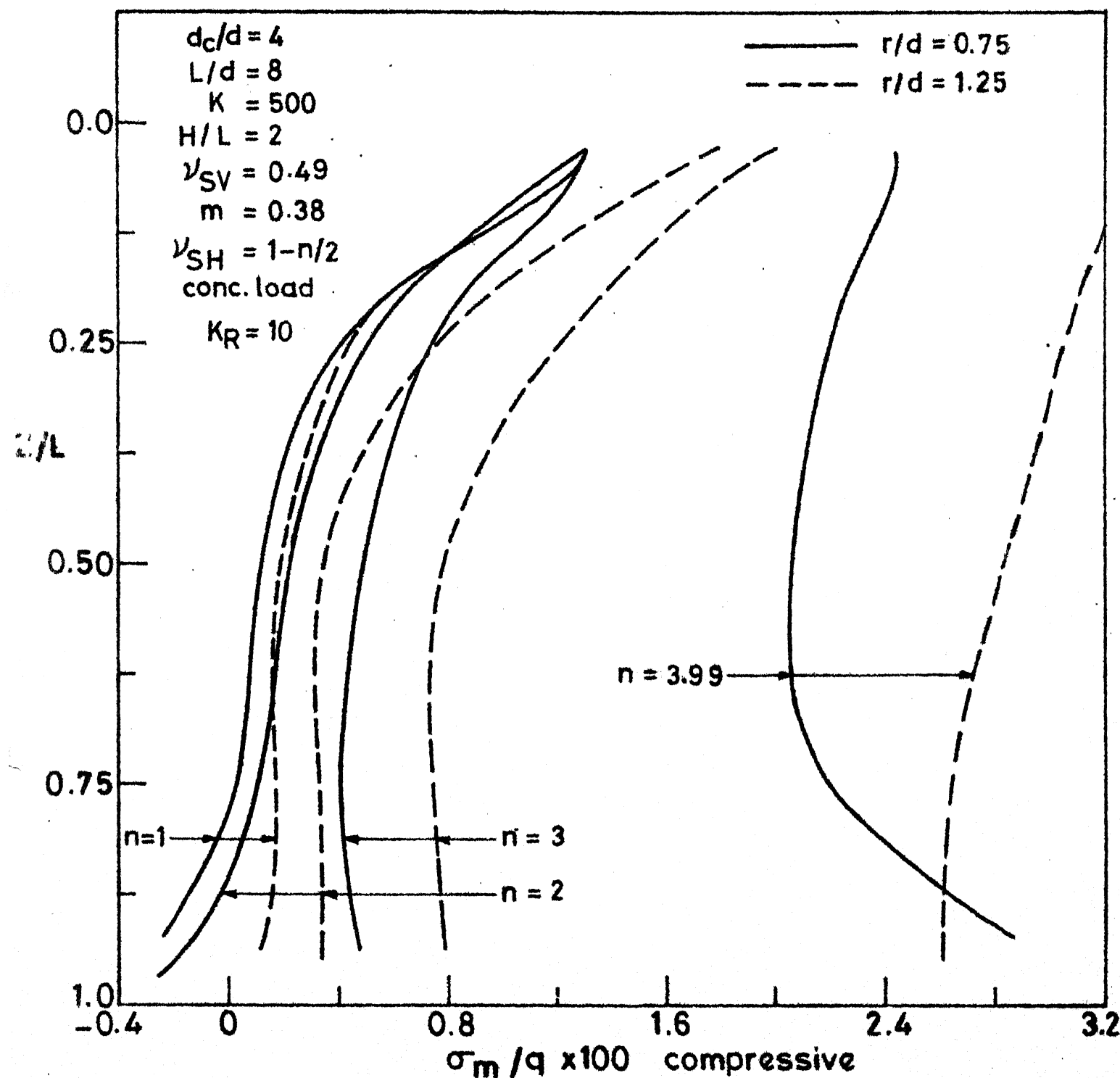
Fig.2.56 σ_m distribution around piled circular footing.
(cross anisotropic soil)
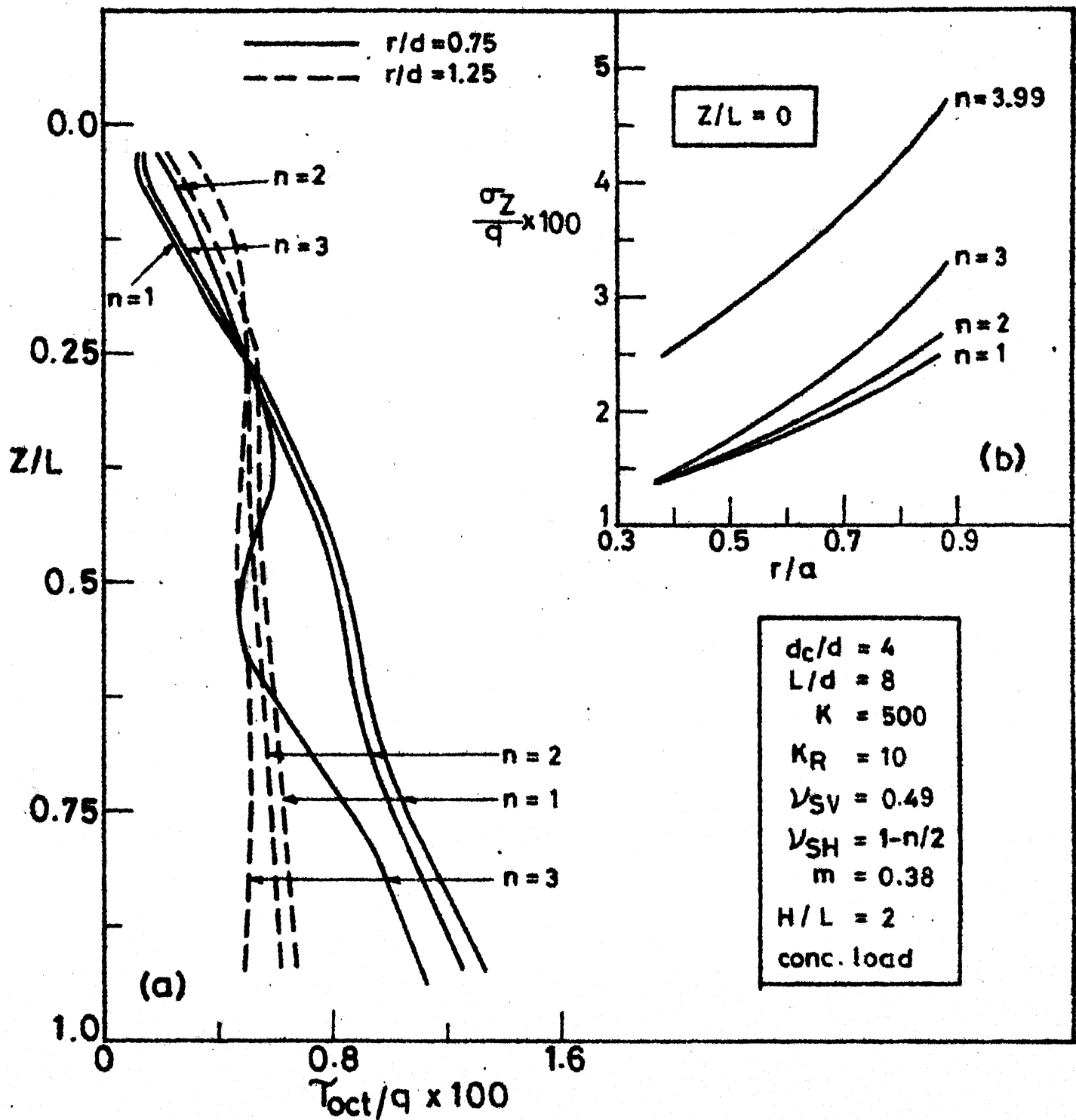
Fig. 2.57 τ_{oct} and $\sigma_{\bar{z}}$ distribution for piled circular footing (cross-anisotropic soil).

CHAPTER 3

THE EFFECT OF SMOOTH INTERFACE ON THE BEHAVIOUR OF

PILED CIRCULAR FOOTINGS

3.1 INTRODUCTION

Most of the analyses of pile-raft reported (Davis and Poulos (56), Hain and Lee (68), Butterfield and Banerjee (23) and Brown et al (18)) assume smooth contact between soil and raft. They have assumed sliding ball type connection between pile head and raft satisfying only vertical displacement compatibility. Hooper (72) has analysed a particular case of pile-raft system assuming completely adhesive contact. Comparison between smooth contact and adhesive contact would indicate the implications of these assumptions. A general pile-raft system is not amenable to such a comparitive study, as the number of parameters become too many. Since a compressible pile with an attached circular cap of finite rigidity forms a typical unit of a general pile-raft system, a study of such unit would indicate the general trends that may be expected in a pile-raft system. Also, it was shown in Chapter 2, that such a unit by itself is a possible alternative type of foundation and solutions for adhesive contact were presented therein. In this chapter, some solutions have been obtained for smooth contact between soil

and raft and also between pile head and raft, for this unit.
Comparison is made with solutions with adhesive contact
assumption. Few solutions for pile-raft systems using the
interaction factors for smooth contact also, have been
presented in Chapter 5 (Sec. 5.6.1.3). The adhesive contacts
referred may also be termed as compatible elastic connections
between different components of the system.

3.2 FINITE ELEMENT ANALYSIS

Initial trials were made with 4 noded axisymmetric
linear continuum elements to represent circular raft and
soil and 4 noded interface elements (Goodman et al (65)) in
axisymmetric mode (Desai (49)), to model the raft-soil
interface. The number of elements representing raft was double
the number of 8 noded elements used in the analysis reported
in Appendix A. It was found that bending moments were over
predicted by about 18 percent when 4 noded elements were used,
compared to those obtained using 8 noded elements, which
agreed well with Brown's (15) solution (Appendix A). Hence,
it was decided that it is preferable to use 8 noded elements,
to model the behaviour of different components, namely soil,
raft and pile and 6 noded interface elements to model the
interface behaviour. Desai (48) has also suggested the use
of such higher order elements, when flexibility of structure

is to be considered. Pande et al (105) have also stressed
the superior performance of these parabolic elements.

The 6 noded interface elements used, has been described
by Buragohain et al (20). This element is isoparametric and
of zero thickness with parabolic variation of displacements
in the direction of interface. Buragohain et al (20) had
used numerical intergration for the computation of stiffness
matrix of these joint elements. In the present work the
integrations were performed in closed form for straight sided
joint elements (Vijayan (138)), which can be used along with
straight sided continuum elements. Another possible and pro-
mising alternative to the zero thickness interface elements
used, is 8 noded 'thin elements', described by Desai (46) and
Pande and Sharma (105).

The computation procedure, checks performed and method
of computation of bending moments, contact pressure, percent
pile load etc. have been described in Appendix A. A study
carried out on the performance of these interface elements,
has been discussed in Appendix C, wherein it is shown that
the use of 6 noded joint elements gives satisfactory
results, including the stresses in the vicinity of the
interface, and also the values of normal and shear stiffness
for getting satisfactory results have been obtained therein.

The mesh used is similar to one given in Fig. A.1, in Appendix A. The mesh was refined near the pile head so as to model the pile head-raft interface in a better way (Fig.3.5). However, it was found that this refinement brought about negligible difference in the values of settlement and percentage pile load (PPL), and small difference (about 2 percent) in the values of bending moments (except immediately above the pile head), compared to original mesh, for adhesive contact. This refined mesh was used for the study reported in this chapter.

Smooth contact was simulated by assigning a low value of shear stiffness (10^{-4} F/L^3), keeping the value of normal stiffness large (10^7 F/L^3), for the interface elements. These stiffness values were obtained from the study presented in Appendix C. The objective of this parametric study is limited to obtain   solutions for smooth contact and compare with adhesive contact solutions. However, the interface element can be used for modelling any non-linear interface behaviour, if desired in any specific case or for modelling joint slip depending on the stresses at the interface. The same element has been used for the latter purpose in the elasto-plastic analysis in Chapter 4.

3.3 PARAMETERS AND CASES CONSIDERED

Parameters used:

Poisson's ratio of soil (ν_S) = 0.47 and 0

Relative rigidity of footing (K_R - Eq. 2.1a, in Chap.2)

= 1, 10 and 100

Diameter of footing/length of pile (d_c/L)

= 0.2, 0.5, 1 and 2.

(If d_c/L is equal to 0.2, the pile may be dominating in the system and if d_c/L is equal to 2, the footing may be dominating in the system. If d_c/L is equal to 0.5, the pile and footing may be of equal dominance).

In all the cases, the ratio d_c/d was kept equal to 5, pile stiffness factor (K) was equal to 1500, and the Poisson's ratio of footing/pile material was equal to 0.15. Two different loadings were used namely a uniformly distributed load over the entire footing area and udl over the pile area, at the centre. The latter case is termed as concentrated load in this work.

Cases considered:

Solutions were obtained for the following four types of interface conditions.

1. Perfectly adhesive contact at all interfaces (pile-footing and footing-soil):

This case was simulated by analysis without

introducing any joint element (Fig. 3.5(a)) and the solutions are same as those obtained in Chapter 2. This case is denoted as CR or a subscript CR.

2. Smooth contact between footing and soil and perfect adhesion between pile head and footing: This condition was simulated by introducing joint elements between footing and soil only (Fig. 3.5(b)) and by assigning high value of normal stiffness and low value of shear stiffness for them. This case is denoted as SR or by subscript SR.

3. Smooth contact between pile head and footing and perfect adhesion between footing and soil: This condition was simulated by introducing joint elements between pile head and footing only (Fig.3.5(c)) and by assigning low value of shear stiffness and high value of normal stiffness for them. This case is denoted as SPH or by subscript SPH.

4. Completely smooth contact between pile head and footing and also between footing base and soil: This condition was simulated by introducing joint elements both at pile-footing interface and footing-soil interface (Fig. 3.5(d)) and by assigning

stiffness values as before, for them. This case

is denoted as CSS or by subscript CSS.

The solutions for case 4 were obtained for $d_c/L = 0.5$

only.

3.4 DISCUSSION OF RESULTS

3.4.1 General

The results have been presented in Figs. 3.1 to 3.10.

Fig. 3.1(a) shows the variation of ratio of percentage pile

load (PPL) for different values of L/d and for different

cases considered. As mentioned earlier the subscripts CR,

SPH and SR denote different contact conditions. Fig.3.1(b)

shows the variation of ratio of maximum settlements (S^*)

for different values of L/d and for different cases

considered. The subscripts have the same meaning. Figs.3.2

to 3.4 show the bending moments near the pile (which is

maximum in most of the cases) for different parameters.

Figs. 3.5 to 3.10 show the variation of bending moment,

along the footing, for different values of parameters.

In these figures symbols M_R, M_T and M*, represent radial,

tangential and maximum bending moment respectively. 'q'

is the applied uniformly distributed load over the entire

footing area, which case is denoted as 'udl' or

applied uniform pressure (q) over pile area, which case is

denoted as 'concentrated load', 'r' is the radial distance
from the centre and 'a' is the radius of the footing.

3.4.2 Settlement

It can be observed in Fig. 3.1(b) that S^*_{SPH}/S^*_{CR} is
almost equal to 1, for all the cases, indicating that the
settlements are not significantly affected by the type of
contact between pile head and footing. The type of contact
between footing and soil, also does not affect the settlements
much (less than 3 percent), for $\nu_S = 0.47$, for all the cases
(from the values of S^*_{SR}/S^*_{CR}). However, for $\nu_S = 0$, the
effect of adhesive contact is significant. It can be seen
that the effect of adhesive contact between footing and
soil, reduces the settlement and this reduction increases
as footing becomes more dominant in the system (i.e. as
d_c/L increases). For $L/d = 10$, which is an average case
in which pile carries about 50 percent of the load, adhesive
contact reduces the settlement by 7 percent (From Fig.3.1(b)
S^*_{SR}/S^*_{CR} = 1.07, for $d_c/L = 0.5$ and $\nu_S = 0$). Due to
interfacial slip the actual reduction may be still less,
and hence it may be concluded that the type of contact
does not influence the settlement appreciably.

3.4.3 Pile Load

It can be seen in Fig. 3.1(a) that the smooth or
adhesive connection at pile head, slightly increases (less
than 5 percent) PPL, for u.d.l. and slightly reduces
(less than 5 percent) PPL for concentrated load, except
for $d_c/L = 2$ ($L/d = 2.5$), in which case footing is very
dominant (PPL_{SPH}/PPL_{CR} values in Fig. 3.1(a) are between 0.95
to 1.05). This increase or decrease is more for $K_R = 1$
than $K_R = 100$ and 10. Again, interfacial slip would
reduce this effect to some extent. Accordingly, it may be
concluded that the type of contact at pile-footing
interface does not influence the value of PPL significantly
for practical cases (unless the raft is very dominant).

It can be seen in Fig. 3.1(a), that PPL_{SR}/PPL_{CR} is
more than 1 for $\nu_S = 0$ and less than 1 for $\nu_S = 0.47$,
indicating that smooth contact between raft and soil
increases the value of PPL in the former case and decreases
the value of PPL in the latter case. Again this effect
is small (less than 8 percent) for practical cases. As
before, the effect is more for $K_R = 1$ than $K_R = 10$ and 100.
It is to be noted that the effect of drainage (i.e. change
of ν_S from 0.5 to 0) on PPL, predicted from smooth
contact assumption and adhesive contact assumption may

moments and smaller magnitudes of radial bending moments, compared to adhesive contact, except for $K_R = 100$, in which case no definite trends could be observed (Figs. 3.2 to 3.4). This increase or decrease is of the order of 20 to 30 percent and this effect is found to be slightly more for $L/d = 10$ than $L/d = 25$ and $L/d = 5$. For $K_R = 100$, and for concentrated loading, the adhesive contact between pile head and footing, reduces the radial bending moment significantly and it is interesting to note that these values are less than those for $K_R = 10$ and 1, in many cases, (Figs. 3.2 to 3.4). This is because for $K_R = 100$, the value of bending moment is maximum near the centre and reduces rapidly at 0.221a where the values are reported, and it is not so, far $K_R = 10$ and $K_R = 1$. For smooth pile head assumption, the value of bending moment increases as K_R increases, as would be expected. In general, the effect of smooth contact between pile head and raft on maximum bending moment is found to be significantly more than the effect of smooth contact between footing and soil, for $K_R = 1$ and $K_R = 10$. In the case of concentrated loading, for $K_R = 1$ and 10, the effect of smooth contact between footing and soil on M_R^* is very small, compared to the effect of smooth contact between pile head and footing.

Bending moment distribution:

The distribution of M_T and M_R (for some cases), has been plotted against r/a, in Figs. 3.5 to 3.10, for K_R = 10 and for different contact conditions. Poisson's ratio of soil and L/d, In general the following observations can be made from these figures.

1. The magnitudes of bending moments immediately above pile (r/a < 0.2), are substantially affected by the type of contact between pile and raft. Even though this effect is large, this may not be of much concern, as this section may not be critical section.

2. The bending moments adjacent to pile have already been discussed in previous paragraph. The values of bending moment for smooth pile head and completely adhesive contact, approach each other as r/a approaches 1, which indicates that this effect is maximum near the pile head and vanishes near the edge.

3. The effect of smooth footing-soil interface, (compared to adhesive contact on footing bending moments, is small for ν_S = 0.47 and quite significant for ν_S = 0. For ν_S = 0, for concentrated loading, the values of M_{SR} (for smooth footing-soil

interface) are consistantly more than the values
of M_{CR} (for completely adhesive interface), along the
entires footing radius. Since the values of bending
moments are small near the raft edge, the effect of
smooth contact is quite large near the edge; here
M_{SR} is upto about 40 percent more than M_{CR}. For
u.d.l., for this value of ν_S ($\nu_S = 0$), M_{SR} is
less than M_{CR} near the edge by large amount (upto
about 50 percent) and near the centre the value of
M_{SR} becomes more than M_{CR}. They cross each other
near the pile for $L/d = 5$ and near the edge for
$L/d = 25$.

3.4.5 Differential Settlement

Differential settlement was found to be more for
different types of smooth contact than completely adhesive
contact, in general. Such increase in differential settle-
ment was found to be more for $\nu_S = 0$ than for $\nu_S = 0.47$
and it was also found that this effect was more for shorter
pile than for longer pile. For $L/d = 10$, the maximum
increase in differential settlement due to smooth contact
between footing-soil interface was about 20 percent and it
was found to increase as L/d decreases and vice versa.
In this connection it is worth noting that the effect of

adhesive contact on the differential settlement of circular raft, subjected to u.d.l. is about 44 percent for $\nu_s = 0$ (Hooper (73)).

3.5 CONCLUSIONS

1. The settlement and percentage of load shared by piles are not significantly affected by the type of contact between footing and soil and also between pile head and footing, in general, except when the footing is dominating in the system, which may not be a practical case. This is likely to be true for pile-raft systems also, as the problem considered is a typical unit of such a system.

2. The maximum bending moments, which occur adjacent to pile in most of the cases, are affected by 20 to 30 percent by the type of contact between different components of the system. In general, tangential moment increases and radial moment decreases due to smooth contact compared to adhesive contact, except for $K_R = 100$, in which case no general conclusions could be drawn.

3. The effect of type of contact at pile-footing interface, becomes insignificant near the edge of footing. The effect of the type of footing soil interface, is

maximum for $\nu_S = 0$ and this effect is maximum near footing edge, and decreases and/or changes sign near the pile.

4. The differential settlement, increases for smooth contact compared to adhesive contact. This effect is about 20 percent for an average case ($L/d = 10$, $d_c/d = 5$).
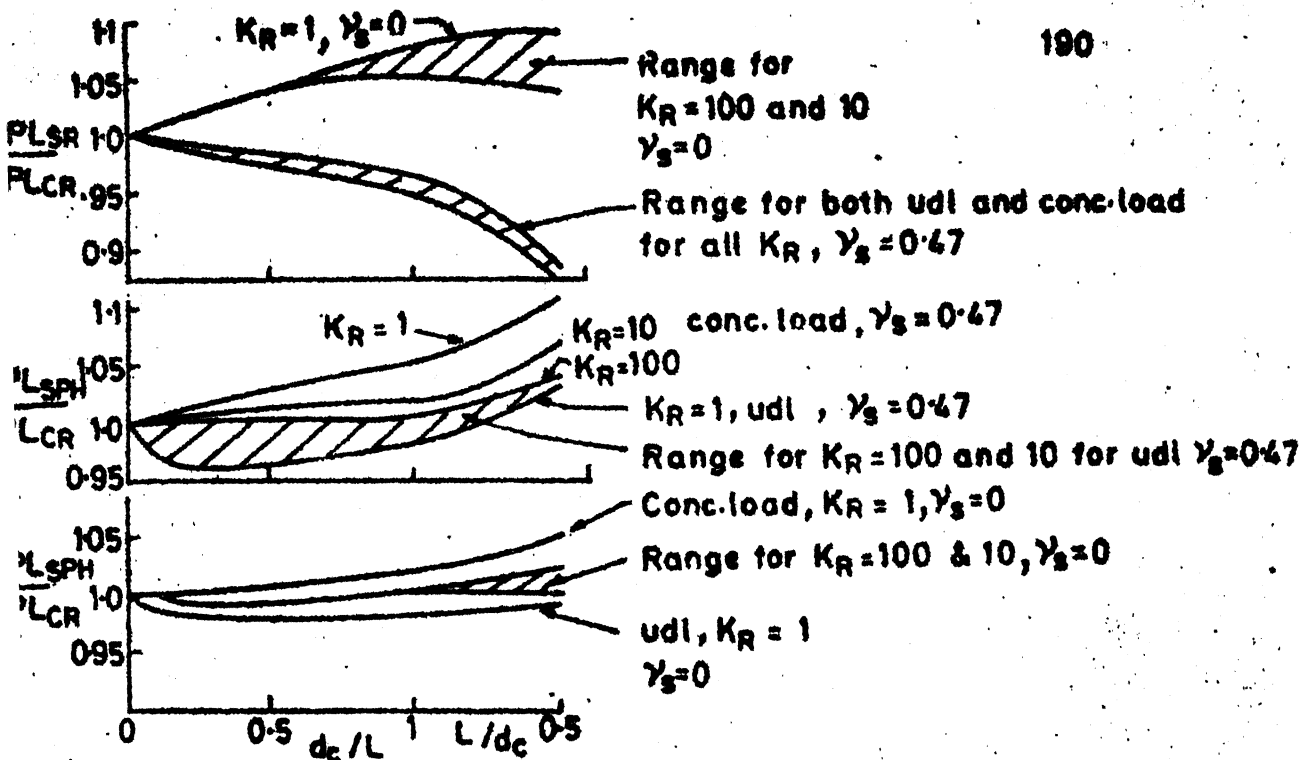
Fig.3·1(a) PPL Vs d_c/L
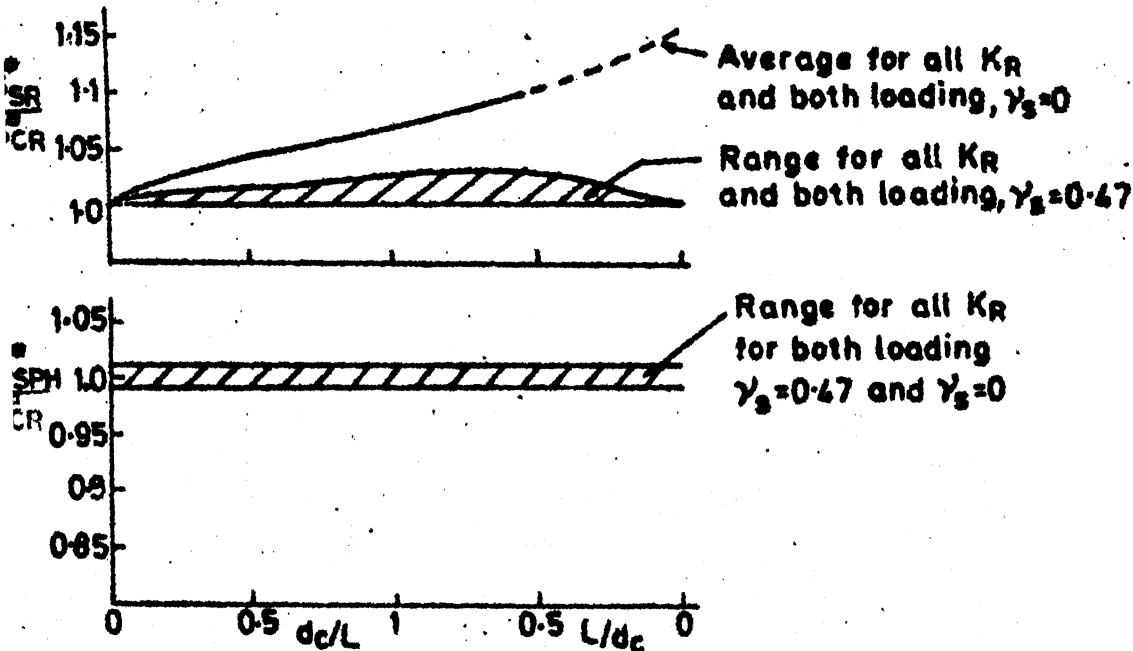
Fig.3·1(b) Settlement Vs d_c/L

190
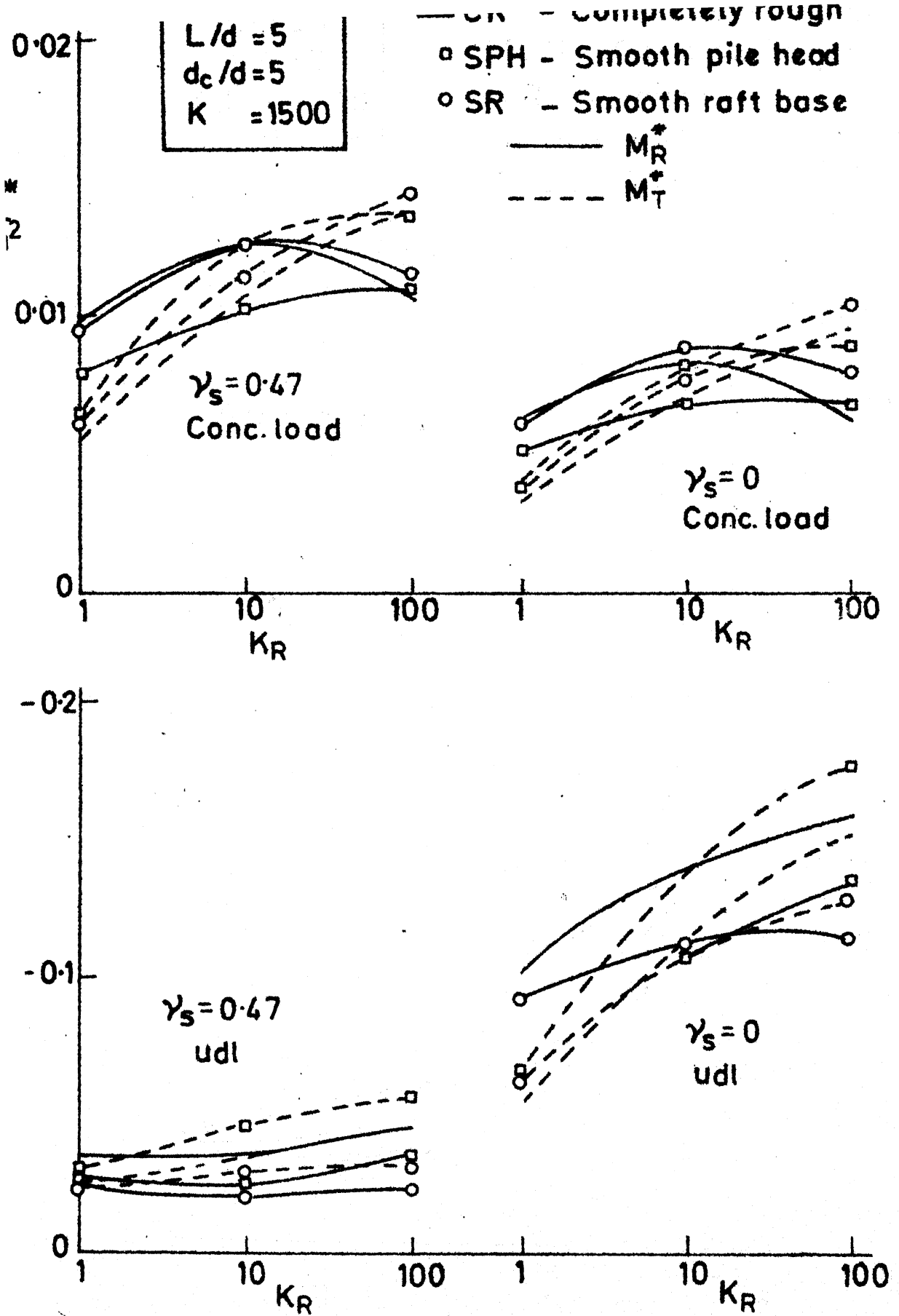
Fig. 3·2 Max. Bending Moment (raft) Vs K_R

Legend:
- CR (Completely rough)
- SPH (Smooth pile head)
- SR (Smooth raft base)
- CSS (Completely smooth)
- M_R^*
- M_T

Top left panel: $\gamma_s = 0.47$, Conc. load

Top right panel: $\gamma_s = 0$, Conc. load

Bottom left panel: $\gamma_s = 0.47$, udl

Bottom right panel: $\gamma_s = 0$, udl
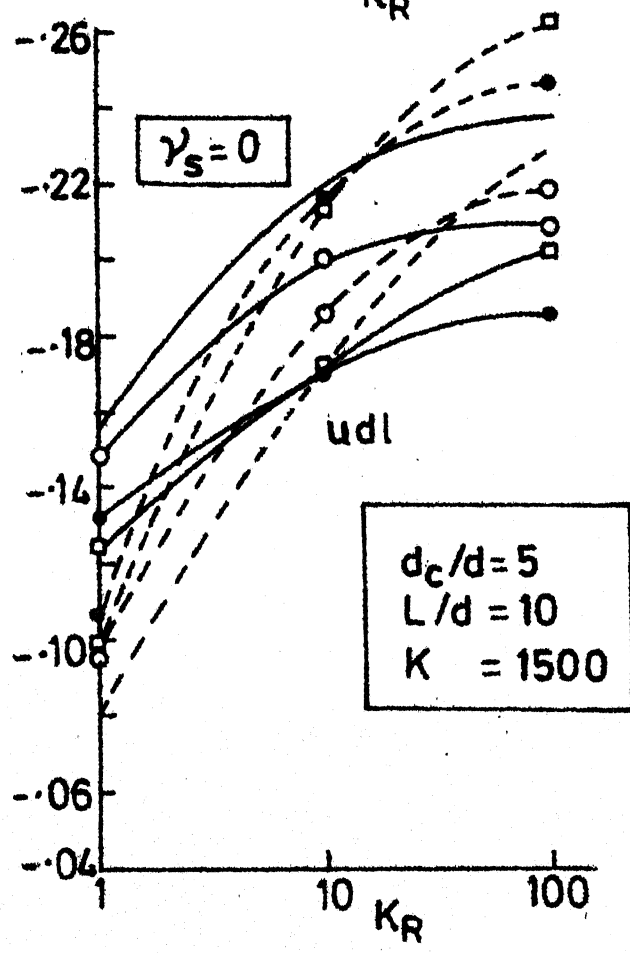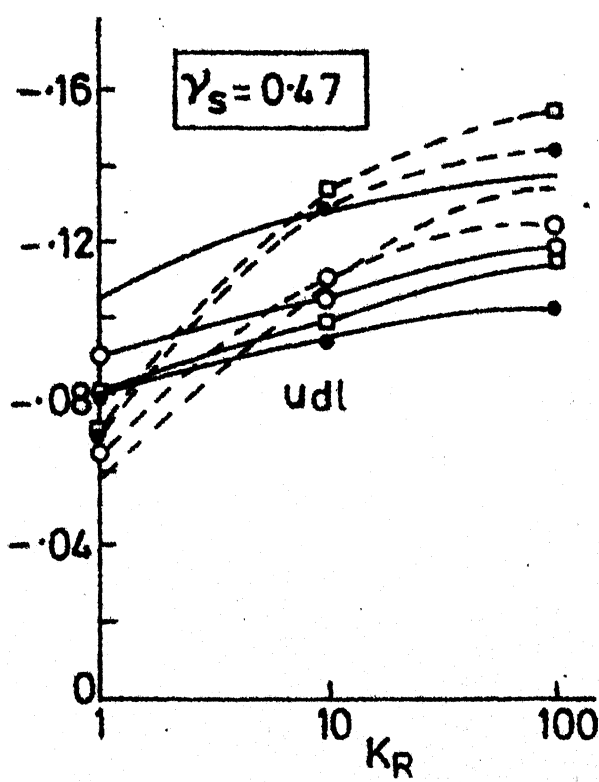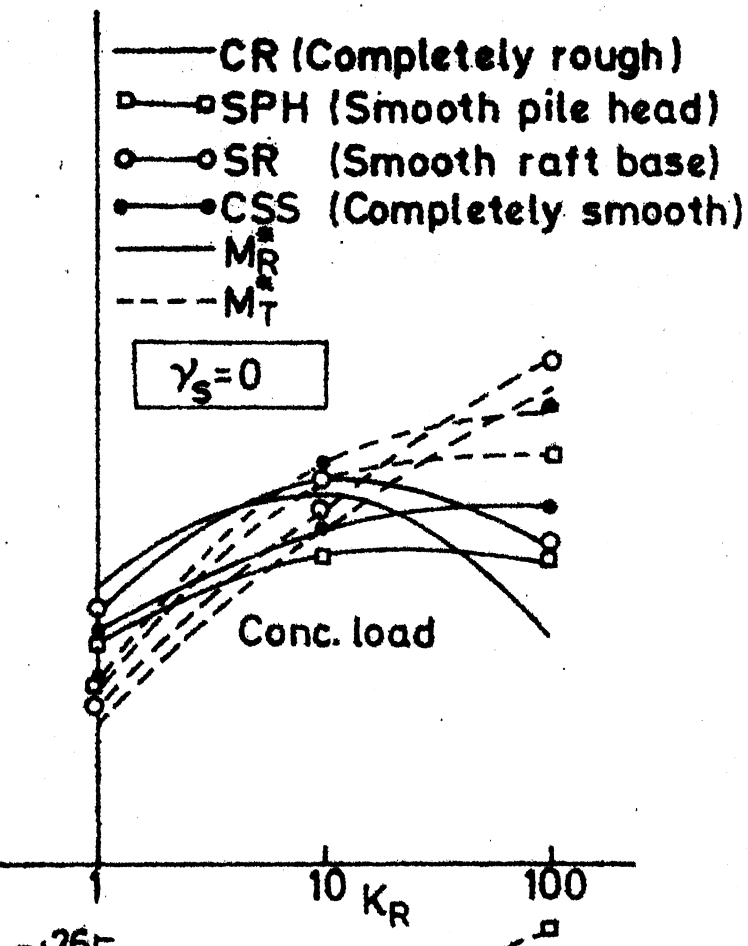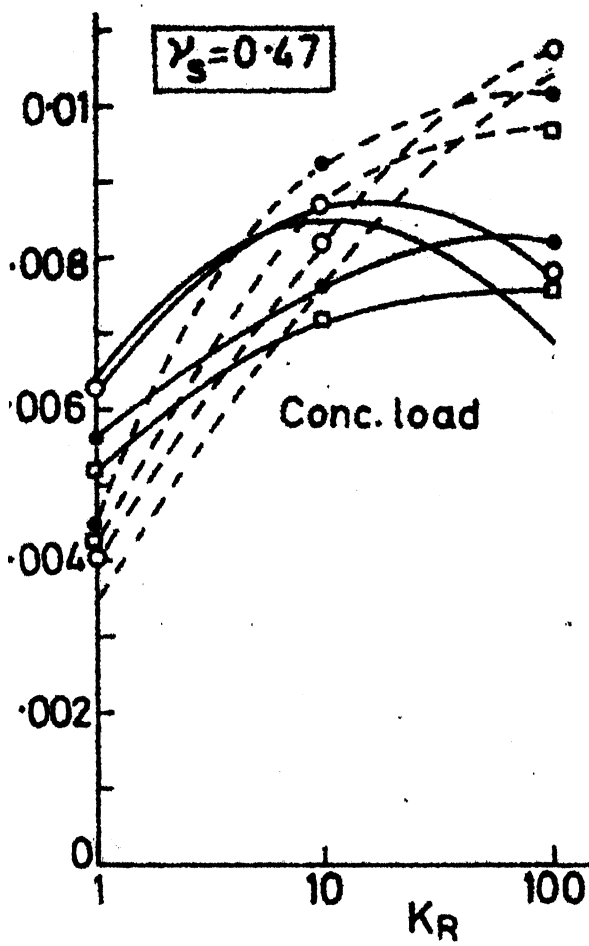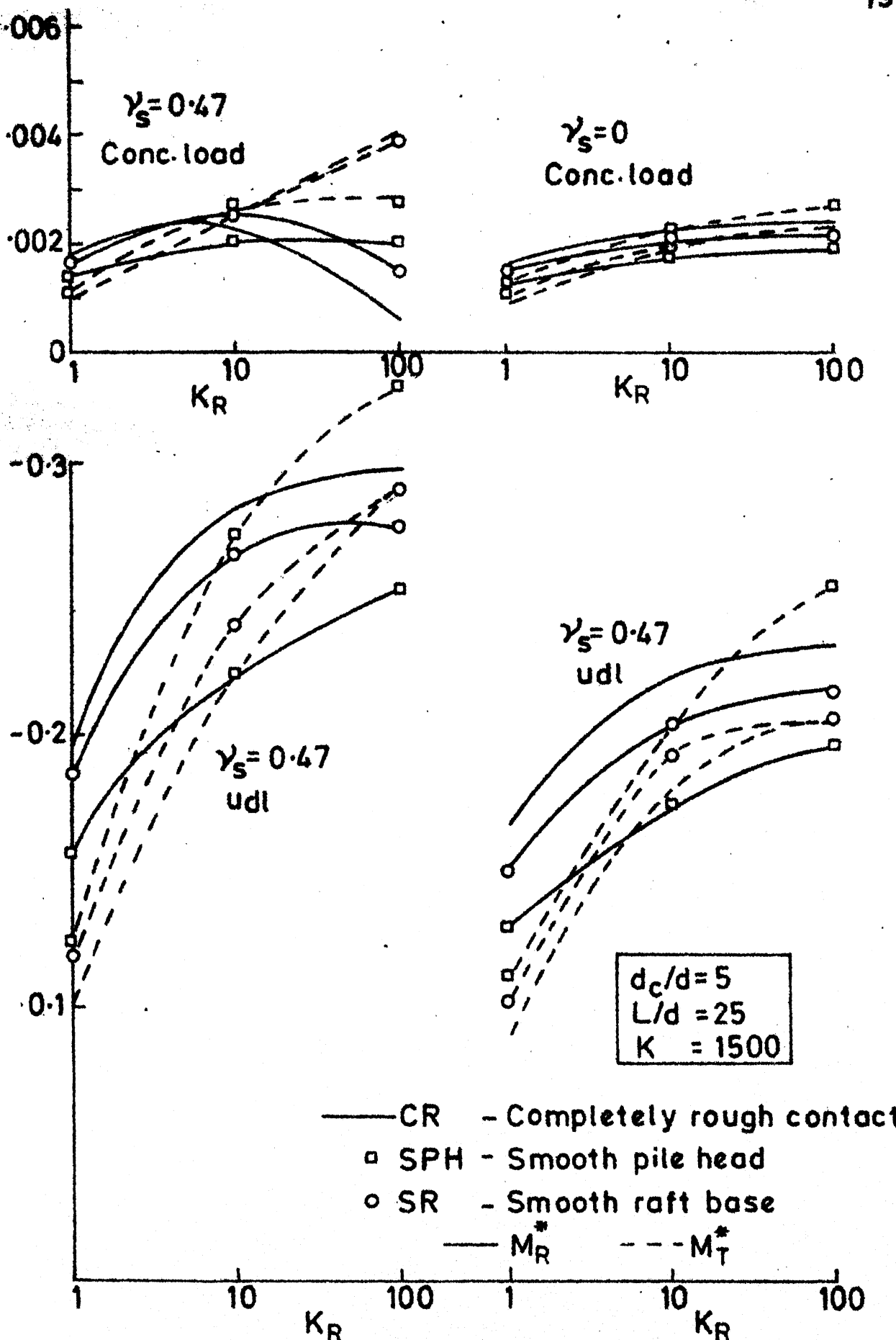
$d_c/d = 5$
$L/d = 10$
$K = 1500$

Fig.3·4 Max·(raft) Bending Moment Vs K_R
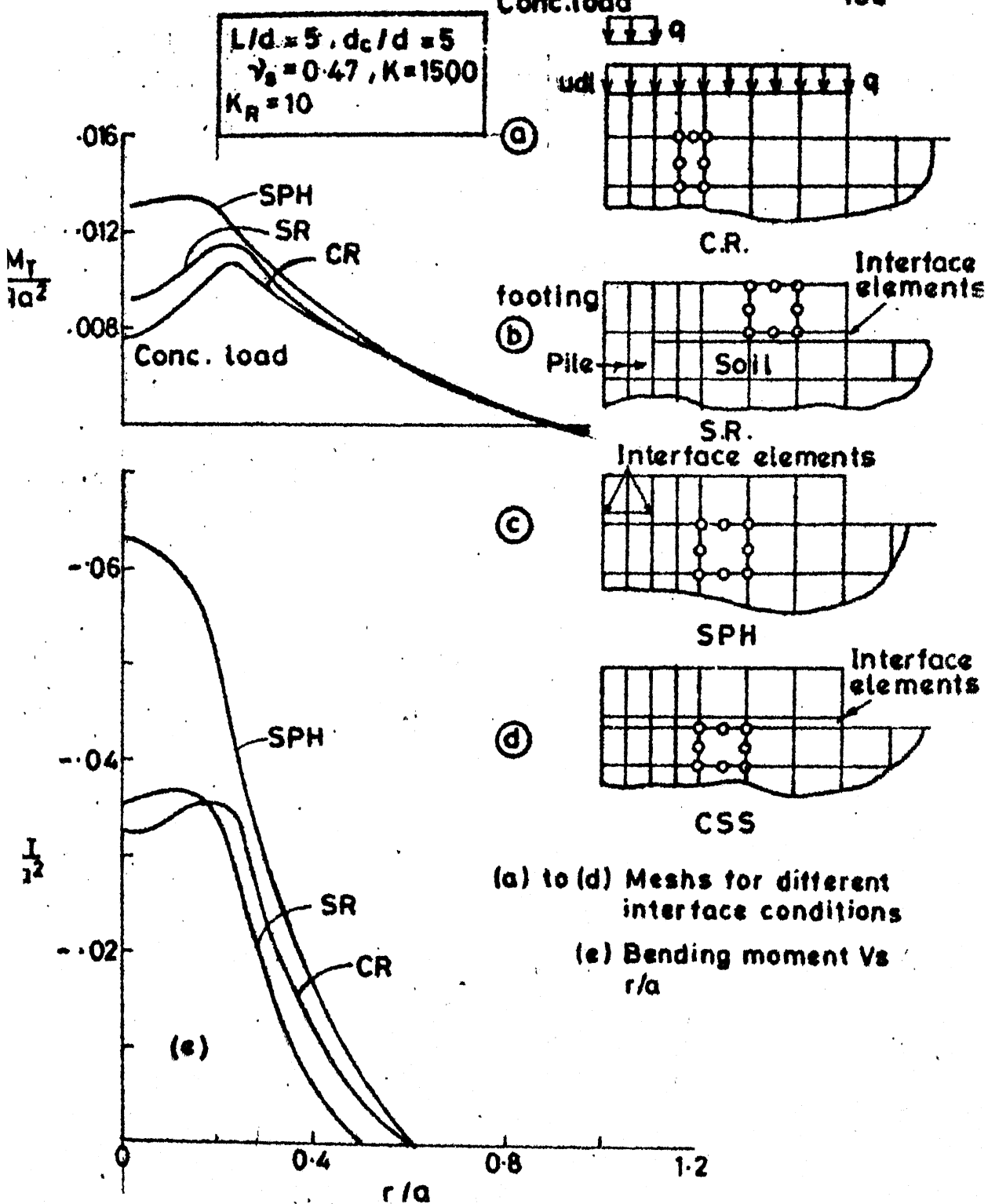
Fig. 3.5. Piled circular footing with different interface conditions

$L/d=5, d_c/d=5$
$\gamma_s=0, K=1500$
$K_R=10$

CR - Completely rough
SR - Smooth raft base
SPH - Smooth pile head
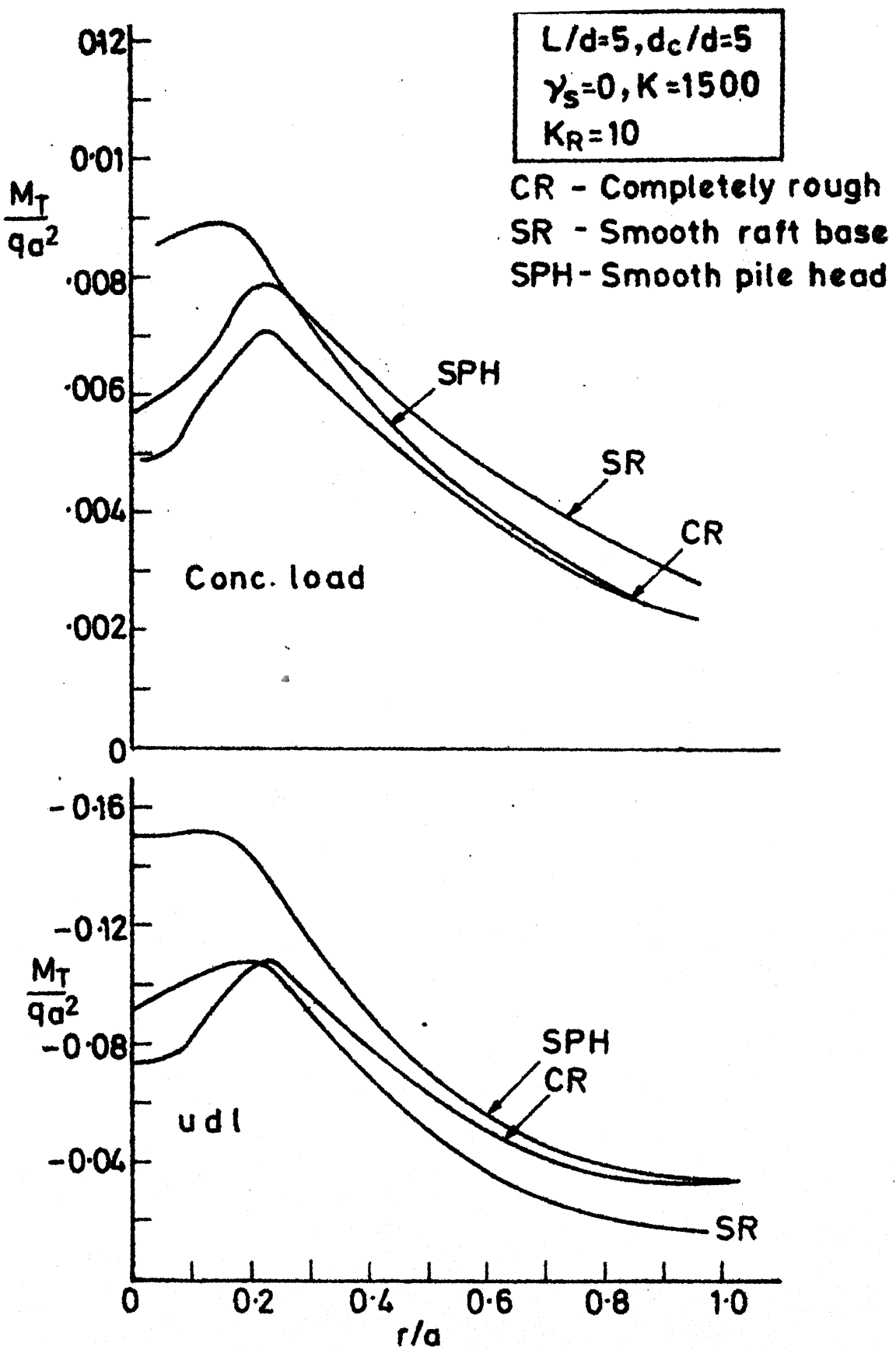
Fig. 3.6 Bending Moment Vs r/a

Fig.3.7 Bending Moment Vs r/a

Top graph: $\frac{M}{qa^2}$ versus r/a, "Conc. load"

Legend:
$L/d=10$, $d_c/d=5$
$\gamma_s=0$, $K=1500$
$K_R=10$

M_T/qa^2 (solid line)
M_R/qa^2 (dashed line)

Curves labelled: SPH, CR, SR

Bottom graph: versus r/a, "udl"

Curves labelled: SR, SPH, SR, CR

CR — Completely rough
SR — Smooth raft base
SPH — Smooth pile head

$\dfrac{M_T}{qa^2}$

·005

·003

·001

Conc. load

SPH

SR

CR

SR
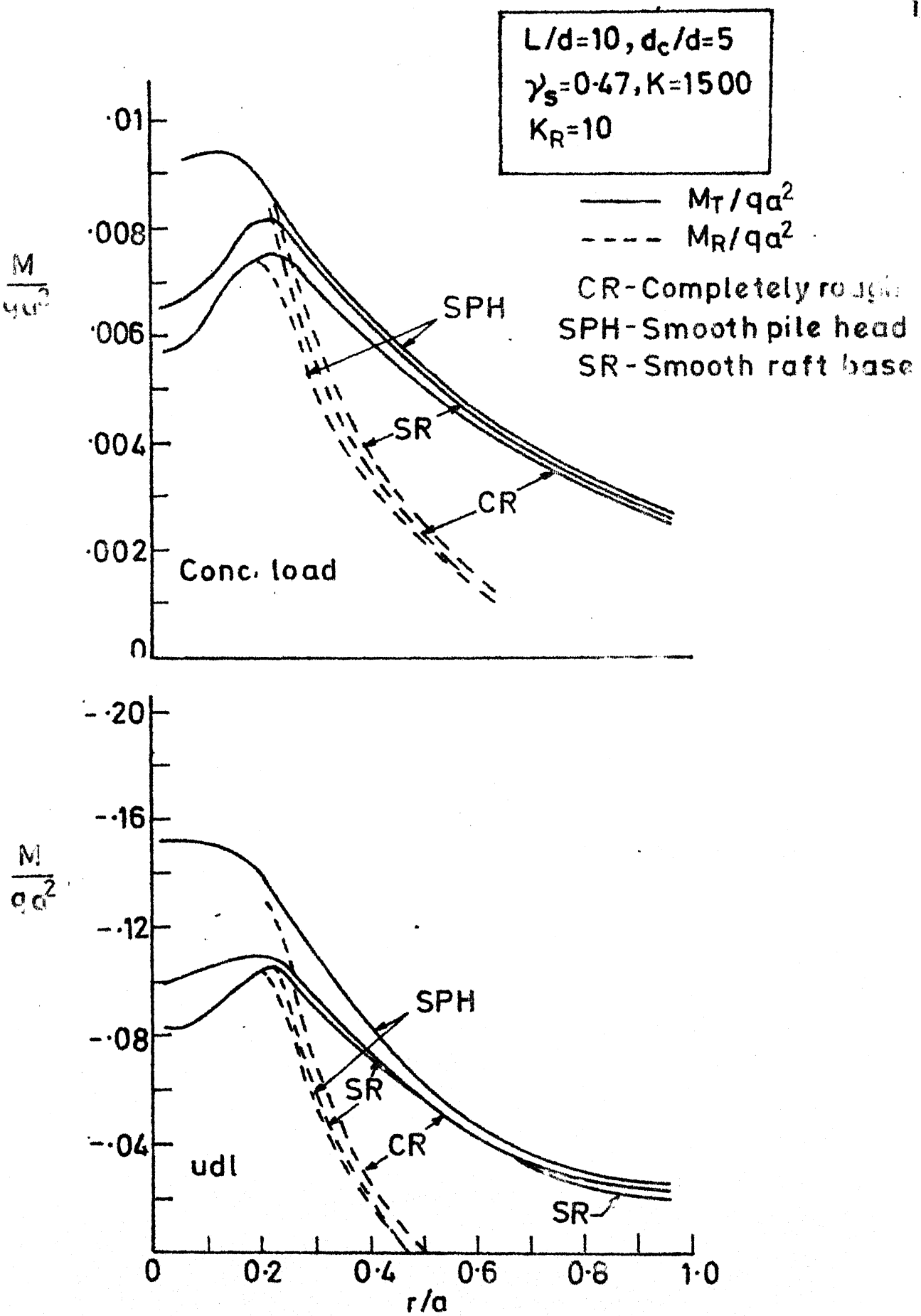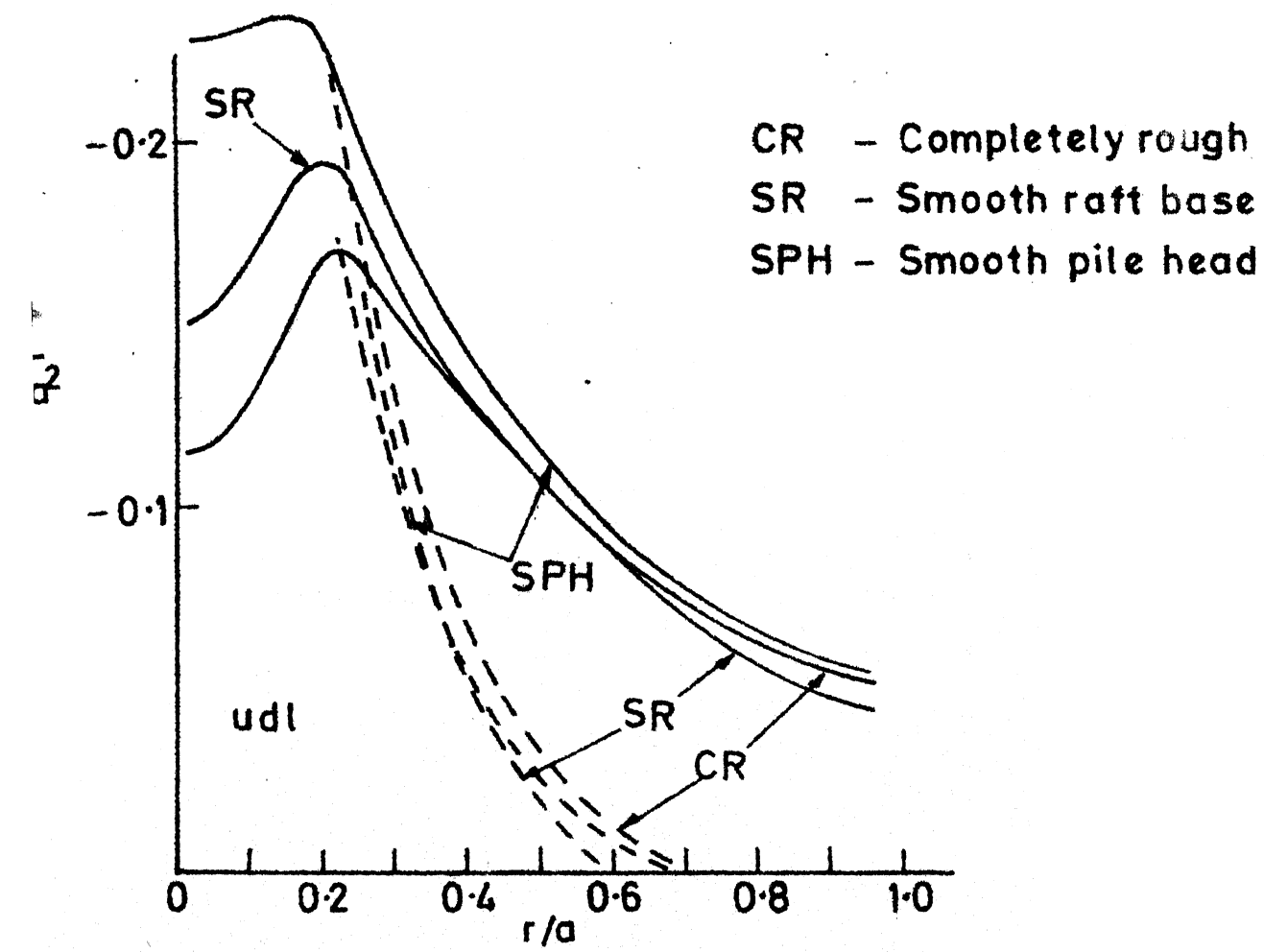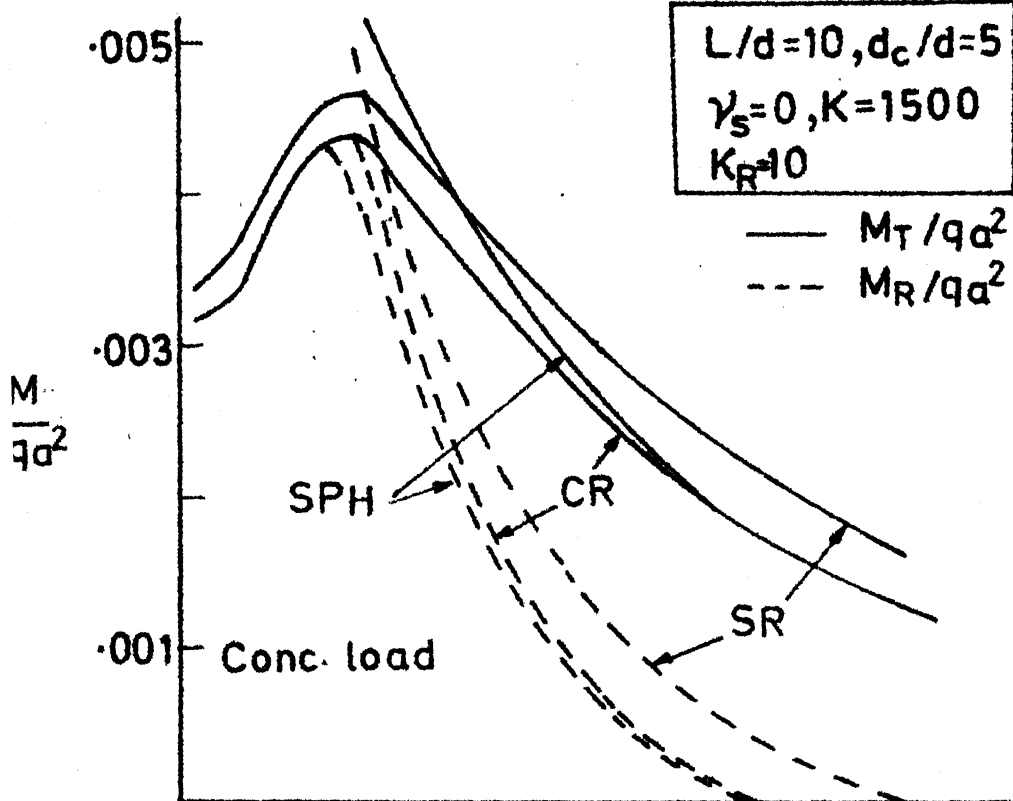
L/d=25, d_c/d=5
$\gamma_s = 0.47$, K=1500
$K_R = 10$

CR – Completely rough
SPH–Smooth pile head
SR – Smooth raft base

$\dfrac{M_T}{qa^2}$

−0·2

−0·1

SPH

SR

CR

udl
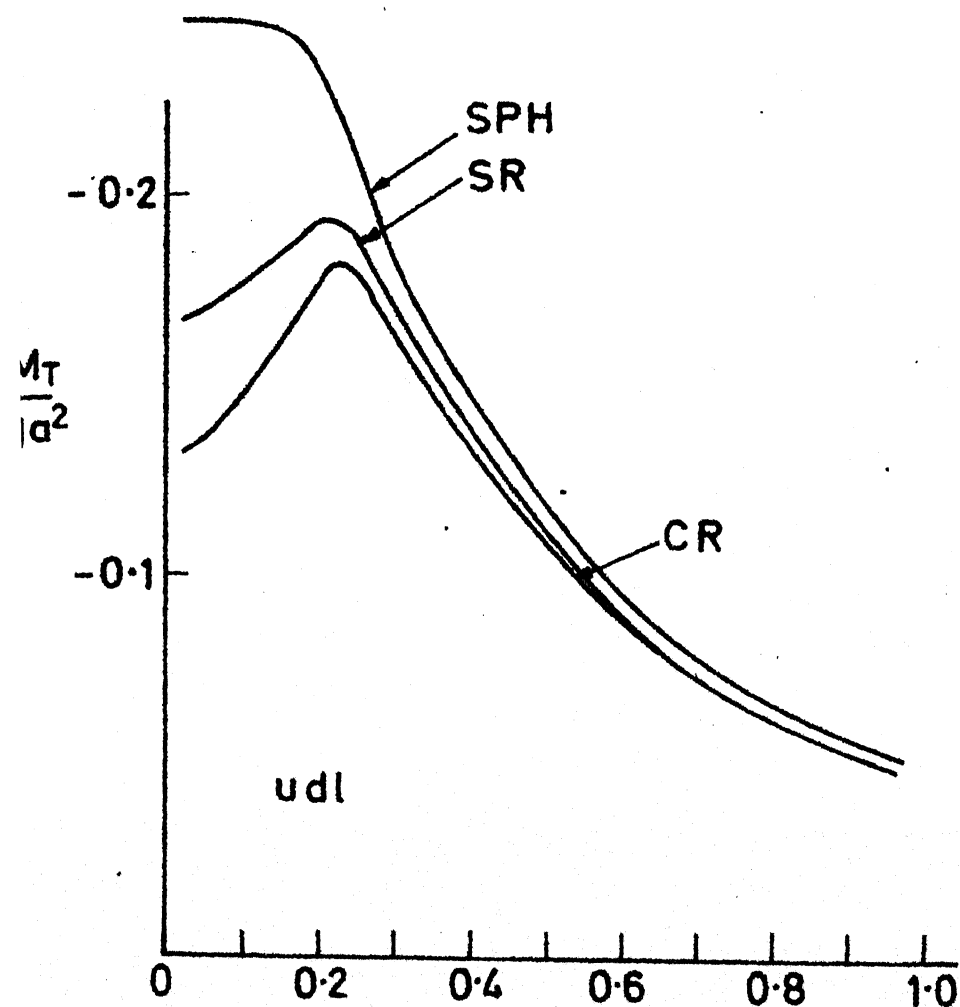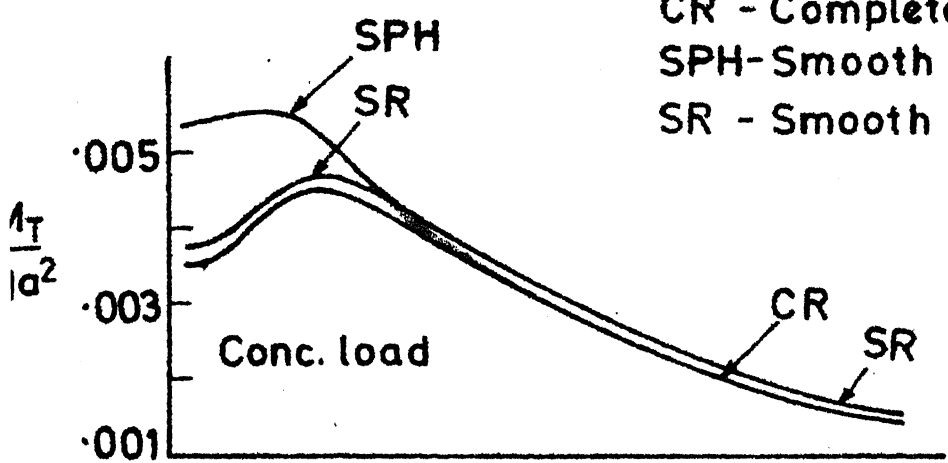
0   0·2   0·4   0·6   0·8   1·0
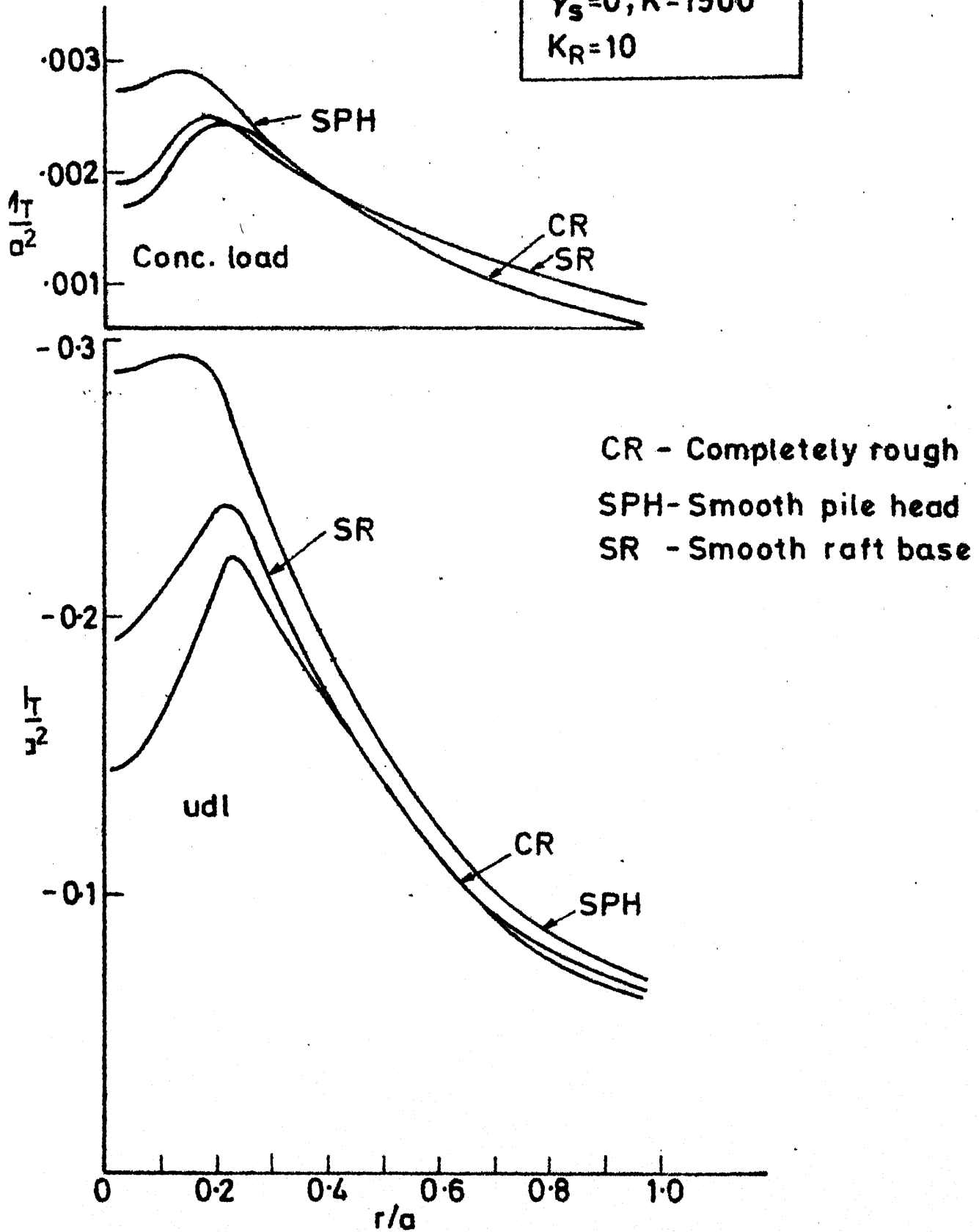
Fig. 3·10 Bending Moment Vs r/a

CHAPTER 4

ELASTO-PLASTIC ANALYSIS OF CIRCULAR FOOTING, SINGLE PILE AND PILED CIRCULAR FOOTING

4.1 INTRODUCTION

Deformation within permissible limit and adequate factor of safety against complete collapse are two essential requirements to be satisfied in any foundation design. The work reported in Chapters 2,3,5 and 6 are devoted to the analysis of behaviour of different types of foundation under working load ranges, which may be useful in the design satisfying the first requirement. In those chapters, soil has been modelled as linearly elastic and homogeneous in some cases and non-homogeneous or transversely isotropic in some cases. For some situations, (e.g. pile raft, pile group and piled circular footing)wherein nonlinear behaviour may be significant even in the working load ranges, certain approximate procedures have been described to account for such non-linearity. The design satisfying the second requirement, requires the assessment of collapse load or bearing capacity of the foundation proposed. By using elasto-plastic finite element technique, it is possible to determine collapse load, in addition to tracing the complete progressive failure mechanism. So this technique has been used in this chapter to study the progressive

failure of certain types of foundations under different soil and interface conditions. Though the essential aim of this part of the work is to study the behaviour upto collapse of piled circular footing which cannot be studied by other methods like slip line method, some cases of circular footing and single pile have also been studied.

Due to its immense capacity to handle any non-linear situation, finite element method is extensively used for solving variety of non-linear problems. There are quite a few publications wherein different types of 'non-linear elastic' finite element techniques have been used for the analysis of circular footing (Withiam et al (147), Desai et al (42), Girijavallabhan et al (64), and Varadarajan and Arora (135)) and for the analysis of single pile (Ellison et al (58), Desai (49), Balaam et al (6), Ottaviani et al (99), and Law (83)*). These non-linear elastic analyses may be mainly useful for the study of deformation behaviour, although the bearing capacity can be assessed for a given limiting deformation. Elasto-plastic analysis would indicate the collapse load straight away. Non-linear elastic-plastic analysis is also possible and has been reported for

*This reference appeared after the completion of the present work and during preparation of this thesis.

the plane strain problem of a strip footing by Pande
et al (104) and Fernandez and Christian (59). Such an
analysis may be very useful in the study of any specific
field problem; but for a study of general nature linearly
elastic-perfectly plastic analysis may be sufficient. A
number of investigators have carried out elasto-plastic
finite element analysis of circular footing (Hoeg (69),
Das et al (53), Zienkiewicz (149), Rowe et al (123),
Biondi et al (12), and Matsumoto and Ko (89)*). The
influence of smooth or rough interface has not been reported
for circular footing although a study of this aspect has been
reported for strip footing (Davidson et al (54) and
Griffiths (66)*). Also, footing of finite rigidity subjected
to central column loading has not been studied. These
aspects are studied herein, for circular footing.

Very few results of elasto-plastic analysis of
piled foundation are available in the literature. For
example, Balaam et al (5) have studied the behaviour of
granular pile. Their work is limited to deformation
behaviour and analysis upto collapse has not been carried
out. Frank et al (60)* have reported elasto-plastic

- -

*reference appeared after the completion of present
work and during the preparation of this thesis.

analysis of single pile using Mohr-Coulomb yield criterion.
Chaw and Smith (28)* have used the same type of elements,
same 'initial stress' finite element technique and same
yield criterion (von-Mises), as used in the present work
for static and dynamic analysis of single pile. They have
concluded that the analytical results compare well with
observed field data. However, comparison with conventional
bearing capacity formulae and investigation of some of the
aspects like the effect of tensile stresses that develop
near the tip, soil non-homogeneity and mesh refinement on
the progressive deformation behaviour and collapse load, has
not been reported. Hence some of these aspects have been
studied for single pile. In addition, analysis of piled
circular footing has also been carried out for different
parameters.

For the analyses discussed in this chapter von-Mises
yield criterion and associated flow rule have been used to
study the undrained response under different material,
geometric and interface conditions. Some studies carried out
using other yield criteria have been discussed in Appendix D.

4.2 FINITE ELEMENT ANALYSIS

Soil, pile and footing have been modelled by
axisymmetric parabolic, isoparametric elements with (2x2)

reduced integration. Use of such higher order elements with reduced integration and with stress sampling at these integration points, has been recommended by Zienkiewicz (152), for von-Mises type criterion, which does not permit volume change. This is required because as the extent of plastic zone spreads, the deformation becomes nearly incompressible, and with conventional exactly integrated elements the system 'locks' and a true collapse load cannot be obtained (Zienkievicz (152)). To model the footing-soil interface and pile-soil interface, 6 noded interface elements of zero thickness, which have been discussed in Chapter 3, have been used. Here, these elements permit slip in case shear stresses at the interface exceed the shear strength, in addition to modelling of completely smooth or adhesive interface.

The computation was carried out using 'initial stress' technique (Zienkiewicz et al (153)). The computer program developed at I.I.T., Kanpur (Vijayan (138)) for elasto-plastic analysis of anchors was checked, corrected wherever necessary and modified to incorporate the following additional capabilities.

Six noded interface element with straight sides and of zero thickness referred in Chapter 3, was modified

and implemented so as to model both vertical and horizontal interfaces. During the loading process, the interface behaviour was simulated as follows.

Initially both joint stiffnesses (k_n and k_s) are assigned large values by input data. (By a seperate parametric study a value of 10^8 F/L^3 was found to give satisfactory results for the parameters used in this analysis). After each load increment, the stresses at the interfaces are computed. In case stresses exceed tthe strength prescribed, the corresponding joint stiffness is made very small (10^{-3} F/L^3) and the stiffness matrix is reassembled and inverted for the computation in the next load increment. Only the joint stiffness is modified and the original elastic stiffness of other solid elements are retained. Modification of stiffness of solid elements also, for the current state of these elements, would be economical and reduce the number of iterations required (Zienkiewicz (152)), for convergence. But in the present analysis, there is already large difference between the stiffness of elements representing soil and footing/pile. So in the present analysis, such a modification might introduce severe ill-conditioning and involve large round off errors in the system, when a number of elements become plastic.

(An alternate computation procedure to overcome this
difficulty has been presented by Rowe et al (121). How-
ever, this procedure was not used in the present analysis)
Hence the initial elastic stiffness matrix with modifications,
if any, for joint stiffness only, was inverted and used for
the resolution in the 'initial stress' iterative computation
process. Also, this procedure would be more efficient
if non-associated flow rule is to be used, in which case
the stiffness matrix would become unsymmetrical and pose
some other computation problems if such modifications of
stiffness matrix at intermediate stage is used.

A static equilibrium check was introduced by
integrating the vertical stresses in the joint elements.
It was observed that the error was less than 0.2 percent
in all the cases analysed herein, with joint stiffness
values assigned as discussed earlier.

Provision was also made to handle the cases in which
modulus and shear strength vary linearly with depth.
Computation of bending moment (as explained in Appendix A),
percentage pile load (as explained in Chapter 2, Sec. 2.3),
contact pressure and percentage load transmitted by end
bearing, was also included. Provision was also made to
reduce the modulus to an arbitrary small value at any

integration point, where tensile mean normal stress ($\overline{\sigma_m}$) exceeds the prescribed tensile strength.

The details of computer program developed are given in Appendix F.

4.3 CASES CONSIDERED

4.3.1 Parameters Used

Poisson's ratio of soil has been assumed to be 0.48 and angle of internal friction ($\emptyset$) has been assumed to be zero throughout, as study of undrained behaviour is attempted herein. The right hand side smooth boundary and bottom rough rigid boundary were kept at 16d (Figs. 4.1 to 4.5) from the centre and ground level respectively, where d is the diameter of the pile ('d' is also the diameter of the loaded area for central column loading). The ratio of diameter of the footing (d_c) to the diameter of pile (d) has been assumed to be 4, in all the cases considered. The ratio of length (L) to diameter of the pile (d) has been assumed to be 8 for all the cases of pile and piled circular footing. The enlarged diameter (d_b) has been assumed to be twice the diameter of pile in a few analyses of pile and piled circular footing with enlarged base.

The values of E_P/E_{SO} and E_R/E_{SO} have been assumed to be equal and this value denoted as 'K', has been kept

at 1500 or 100. (E_P and E_R denote Young's modulus of pile and footing material and E_{SO} denotes the Young's modulus of soil at ground level). The value of relative rigidity (K_R - as defined in equation 2.1, in Chapter 2) of footing/ raft, has been assumed to be 100 or 1. For non-homogeneous soil considered, the values of Young's modulus (E_S) and undrained shear strength (C_u) are assumed to vary linearly with depth such that

$$E_{SL} = 2\ E_{SO} \quad \text{and} \quad C_{UL} = 2C_{UO}$$

where E_{SL} and C_{UL} are the values of Young's modulus and shear strength at a depth equal to length of pile (or 8d in the present analysis), from the ground level respectively. C_{UO} is the shear strength at ground level. The value of Poisson's ratio of pile and footing material was assumed to be 0.15 throughout. The shear strength of pile and footing material has been assumed to be large compared to soil.

The soil, pile and footing have been assumed to be weightless in most of the cases. In some cases (Run P6 and P10), the weight of the soil has been considered and in such cases the value of earth pressure coefficient at rest (K_o) has been assumed to be unity and γ/C_u has been assumed to be 1.8. (γ = unit weight of soil). Since von-Mises yield

criterion has been used, the weight of soil (for $K_o = 1$) does not affect the results expect when tension failure is considered.

4.3.2 Meshes Used

For the analyses reported a number of meshes were used. These are shown in Figs. 4.1 to 4.5.

Mesh 2S (Fig. 4.2) is a very coarse mesh containing only 13 elements, used for circular flexible uniformly distributed load. Mesh 2R, also shown in Fig. 4.2, is another mesh used for the same loading.

Mesh 1 (Fig. 4.1) has been used for analysis without interface elements in the case of circular footing, single pile and piled circular footing, subjected to central column loading. Mesh 1P and Mesh 1PJ (Fig. 4.1) were used for analysis of single pile, without and with interface elements respectively. Mesh 1, has been used for analysis of circular footing and piled circular footing.

Mesh 2R (Fig. 4.2) with interface elements, has been used for the analysis of circular footing. Mesh 2 RM (Fig. 4.2) is a refined mesh used for the same analysis. Mesh 2P (Fig. 4.4) has been used for the analysis of single pile. This is a refined mesh with interface elements.

Mesh 2 (Fig. 4.3) with interface elements was used for the analysis of piled circular footing. Mesh 2M (Fig. 4.5) is a refined version of Mesh 2.

Among these meshes mesh 2R(u.d.l.), 2RM, 2P and 2M are the refined meshes for the study of circular flexible raft subjected to uniformly distributed load, circular footing subjected to central column loading, single pile and piled circular footing respectively. The studies using other meshes are useful in indicating the effect of mesh refinement and associated parameters. Details of different computer runs have been tabulated in Tables 4.1 to 4.3, at the end of this chapter.

4.4 RESULTS AND DISCUSSION

4.4.1 Convergence Criterion and Maximum Number of Iterations

The value of collapse load obtained by numerical method like one used herein, depends on factors listed below.

1.   The fineness of the mesh used.

2.   The size of each load increment

3.   Maximum number of iterations specified (I_{max}).

4.   Convergence criterion adopted.

It is usually presumed that collapse has occured, if for any load increment, the numerical process fails to

converge as per the convergence criterion adopted, even after I_{max} number of iterations. Obviously best results can be obtained by using very fine mesh, with small load increments, adopting strict convergence criterion and specifying large value of I_{max}; but such an analysis would be very expensive, for the problems attempted herein. The results are found to be not very sensitive to increment size in the case of 'initial stress' technique, as shown by Zinkiewicz (152) and also as observed subsequently herein. All the runs were made such that the collapse load is approached in about 15 to 30 equal increments. The convergence criterion used here is based on the absolute maximum magnitude of correction load, in the correction load vector. This criterion was fixed at 0.1 percent of the total applied load in each increment for all the runs. Since the convergence criterion adopted is rather strict, the load-deformation response and intermediate failure mechanism are likely to be quite satisfactory. But it would require very large number of iterations to capture the 'exact' collapse load. So, for certain cases, large values (400 and 600) of I_{max} were specified and it was found that by using I_{max} equal to 200 or 300, satisfactory values of collapse load can be obtained. Hence, in all the subsequent work maximum number of iterations was specified as 200 or

300, to make a trade off between cost and accuracy.
Implications of this are further discussed subsequently.

In the case of single pile when interface elements
are used it was found that once skin friction is completely
mobilized, the failure is sudden. So in these cases the
run was stopped when the stiffness of the system computed
on the basis of the displacements between successive
increments is less than about 1/20 of the initial elastic
stiffness of the system.

Rowe and Davis (123), Marti et al (88), and
Toh et al (132), have also recognised the difficulty in
predicting the 'exact' collapse load and have presented
certain techniques to get better results. However, these
techniques were not tried in this work.

4.4.2 Circular Footing

Details of computer runs made for circular footing
are given in Table 4.1.

4.4.2.1 Uniformly distributed load on the surface of the soil:

The results for circular uniformly distributed load,
are shown in Fig. 4.6. The run R1 was made, using a
very coarse mesh of only 13 elements, specifying I_{max}
equal to 600. At the termination of the run, the stiffness
of the system had already become less than 1/40 of initial

elastic stiffness and still had not converged. Hence it
may be deemed to have failed. The failure pressure for
I_{max} = 600 is 6.6 C_{uo}. If I_{max} had been fixed at 200,
it would have predicted 6.3 C_{uo} as collapse load, involving
only less than 5 percent difference. In the same figure,
the response for Run R2, with 56 elements is observed
to lie below the curve for Run R1, showing the effect of
mesh refinement. In this run, the maximum number of iter-
ations was specified as 400 and it was found to predict a
collapse pressure of 6.2 C_{uo}; again at the termination
of the run the stiffness had reduced to less than 1/32 of
the original elastic stiffness. Had the run been terminated
at 200 iterations, it would have predicted 6.0 C_{uo} as
collapse pressure, which is 3 percent less than that for
I_{max} = 400. Also, since only a comparitive study is
attempted herein, this accuracy is sufficient and so the
value of I_{max} was kept at 200 or 300 in subsequent runs.
Also, it was observed that for 100 iterations, the
computing time in DEC 1090 Computer was more than 2 minutes
and the analysis with I_{max} = 400 required about double
the time required for I_{max} = 200, for fairly close load
increments; and so the compromise had to be made.

Incidentally, the collapse pressure predicted by slip line method for circular footing is 5.69 C_u. The predicted value from the present analysis is 6.2 C_u (Run R1). The slip line solution (Chen (29)) uses Tresca yield criterion, with some more simplifying assumptions regarding stresses (Harr-von Karman hypothesis), where-as von-Mises criterion has been used in the present analysis. So the small difference may be due to different assumptions and approximations in both the methods.

It was observed that the load deformation response obtained by the present analysis with 56 parabolic elements almost coincided with analysis by Biondi et al (12), who have used about 600 triangular elements for the same problem. The mesh 2S, is similar to mesh used near the tip of pile in the analysis of pile and piled circular footing. The results obtained using mesh 2S are in satisfactory agreement with the results obtained using a refined mesh (Run R 2). This shows the adequacy of meshes 2P and 2M near the pile tip.

4.4.2.2 Central column load:

This type of load has been referred as concentrated load in this thesis (Sec. 2.2.1). The load-settlement response for this loading ($d_c/d = 4$), is shown in Figs. 4.7 and 4.8. Runs R3 and R4 have been made with mesh 1, without

interface elements and hence they correspond to fully
adhesive contact. Run R3 is for K_R = 100 and Run R4 is
for K_R = 1. It can be observed that the load-settlement
curves from both runs tend to approach the same ultimate
pressure equal to 110 C_u (Average collapse pressure = 6.9 C_u).
This shows that the flexibility of the footing does not
have significant effect on the collapse load for the range
of K_R values between 1 and 100, which may normally occur
in practice.

From Fig. 4.7, for Run R5 (without refinement near the
edge) with joint element simulating rough interfaces, the
collapse pressure obtained is 120 C_u. This mesh was rather
coarse near the raft edge than previous one and hence the
difference in predicted collapse load. With mesh refined
near the edge (Mesh 2 RM and Run R7 shown in Fig. 4.8), the
corresponding collapse pressure falls to 104 C_u. This
difference indicates the effect of mesh refinement near the
edge, where there is stress concentration. With the same
mesh (Run R8), for smooth contact the numerical collapse
pressure is 96 C_u (Average pressure is 6.0 C_u). It may
be noted that this value is close to the collapse load
obtained for u.d.l. over circular area previously (Sec.4.2.2.1).
The value was 6.0 C_u and 6.2 C_u for I_{max} = 200 and 400
respectively. This shows that the bearing capacity is not

significantly different for u.d.l. on a completely flexible footing and loading on rigid footing (K_R = 100).

The effect of adhesive contact is to increase the collapse load by about 8 % (comparing Run R7 and R8). The effect of such adhesive contact on collapse load, predicted by slip line method is about 6 % (Chen (29)). It is to be noted that pressure distribution at failure, predicted by slip line method for smooth contact is completely different, from that predicted by finite element method. In the former case, pressure is maximum near the centre (Chen (29)) and in the latter case, the pressure tends to become uniform near failure (Fig. 4.14).

In Fig. 4.8, it may be observed that for smooth contact also, as previously observed for rough contact, the collapse load for K_R = 1 and 100, approach the same value (comparing Run R8 and R.10 - Fig. 4.8). It is of interest to note that for K_R = 0 (completely flexible footing, with central column loading), the collapse load would reduce to one sixteenth of the value for rigid footing, for the geometry and loading used in this analysis.

For non-homogeneous soil considered (For smooth contact) the collapse load obtained is 104 C_{uo} (Run R9 and Fig. 4.8), as against 96 C_{uo} for homogeneous soil.

Since the load-settlement curve is observed to rise further for non-homogeneous soil and the run was terminated after 200 iterations, the actual collapse load may be slightly more and hence the difference may also be slightly more. This also indicates that for non-homogeneous soil with stiffness and strength increasing with depth, for the same convergence criterion, larger value of I_{max} is to be specified for obtaining satisfactory collapse prediction and hence the present numerical technique may be more expensive for such soil condition, than homogeneous soil. Similar observations have been made by Griffiths (66), in the analysis of strip footing.

Small tensile stresses were induced near the ground level at locations away from the footing. These tensile stresses were found to vanish as failure takes place, for smooth contact. Also it was found that these stresses were so small that they would tend to become compressive, when a small surcharge, which would normally be present in practical cases, is considered.

Bending moments and contact pressures have been plotted in Fig. 4.14. It can be observed that the contact pressures (non-dimensional) tend to become uniform near

collapse, both for rigid and fairly flexible and both
for homogeneous and non-homogeneous soil. The bending
moment (non-dimensional) decreases slightly for rigid
footing (K_R = 100) and this decrease is about 10 percent
for smooth contact and about 5 percent for adhesive contact
(Runs R7 and R8 in Fig. 4.14). For fairly flexible footing
(K_R = 1), the value of bending moment increases by about
10 percent as collapse is approached (Fig. 4.14 and Run R10).

Spread of plastic zones for Run R7 to R.10, has been
shown in Figs. 4.15 to 4.18. Figs. 4.15 and 4.16 show the
spread of plastic zones for rough and smooth contact for
a rigid footing subjected to central column loading. In
both cases, yielding starts near the edge of the footing.
For rough contact, soil below the centre of the footing
does not become plastic with loading equal to 104 C_{uo}, whereas
for smooth contact with loading equal to 96 C_{uo}, the
complete zone below footing becomes plastic. Another
observation that can be made from these figures is that
the spread of plastic zones in the horizontal direction
is slightly more for rough contact. The effect of
rigidity of the footing on the spread of plastic zones
can be assessed from Figs. 4.16 and 4.18. Significant

difference for $K_R = 1$, compared to $K_R = 100$, is that the yielding starts from below the centre. But the plastic zones tends to be similar for $K_R = 1$ and $K_R = 100$, for loads near failure ($q_u \approx 96\ C_{uo}$). The effect of nonhomogeneity of soil on the spread of plastic zones can be seen in Figs. 4.16 and 4.17. For both homogeneous and non-homogeneous soils considered, yield starts near the edge. For non-homogeneous soil, the plastic zone tends to extend upto a shallower depth;but tends to move horizontally to greater extent near the surface, compared to homogeneous soil.

4.4.3 Single Pile

Details of computer runs made for single pile are given in Table 4.2.

4.4.3.1 Collapse load

Figs. 4.9 and 4.10 show the load deformation response of single pile for different soil conditions. It would be worthwhile to compare the finite element results with conventional values of collapse load.

In the conventional method (Static formula-Bowles(14)), the bearing capacity of single pile under undrained condition is calculated as

$$Q_{ult.} = \pi\ dL\ \alpha_a C_u + 9\ C_u\ \pi d^2/4 \qquad (4.1)$$

where

$Q_{ult.}$ = ultimate bearing capacity of pile

α_a = adhesion factor

d = diameter of pile

L = length of pile

C_u = undrained cohesion of soil.

For calculation in the case of non-homogeneous soil, in which C_u increases linearly with depth, the value of C_u at tip has been used for second term in Eq. 4.1 and the average value of C_u at mid length of pile has been used for first term in Eq. 4.1. The values of bearing capacity obtained using Eq. 4.1 is termed as value from conventional method in subsequent discussion. For the parameters used in the analysis of single pile, these values (collapse pressure) work out to be 41 C_{uo} for adhesion factor ($\alpha_a = C_a/C_{uo}$) equal to 1 and 25 C_{uo} for $\alpha_a = 0.5$, for homogeneous soil. For non-homogeneous soil considered, the collapse load from Eq. 4.1 works out to be 66 C_{uo}.

Runs P1 and P2, have been made without interface elements and hence these results correspond to complete adhesion at the interface and failure can take place in the soil mass adjacent to interface. The collapse pressure obtained is 56 C_{uo} (Fig. 4.9) for Run P1, which

is about 35 percent more than conventional value for adhesion factor equal to 1. This difference could partly be due to non-failure of interface and failure at locations away from the interface and partly due to coarseness of the mesh near the tip of the pile. The collapse pressure obtained from Run P2 is 96 C_{uo} (Fig. 4.9), which is about 70 percent more compared to Run P1. This shows the effect of enlargement of base (d_b = 2d, where d_b is the diameter of enlarged base). As collapse is approached small tensile stresses were observed in a small zone adjacent to and above enlarged base even when weight of the soil was considered. The maximum magnitude of these tensile stresses was found to be of the order of magnitude of the value of C_u.

Runs P3 and P4 were made with the same mesh as used for Run P1, but with joint elements at the interfaces. The collapse pressures obtained (Fig. 4.9) are 50 C_{uo} and 36 C_{uo} for α_a equal to 1 and 0.5 respectively. There is an overprediction of about 20 percent compared to conventional method. Since this overprediction may be mainly due to coarseness of the mesh near the tip, where there is stress concentration, the mesh was refined near the tip and rest of the runs were made using this refined

it was observed that pile material did not fail anywhere.

Run P9 (Fig. 4.10) made assuming soil to be non-homogeneous, shows a collapse pressure of 72 C_{uo}, where as the value calculated using conventional method is 66 C_{uo}. The difference would have been less, had the soil been treated as no tension material, as in the case of Runs P6 and P10.

In general the collapse load obtained from conventional method and finite element elasto-plastic analysis do not differ much for both homogeneous and non-homogeneous soil condition. However, finite element method can be used for the determination of collapse load for problems involving more complicated geometry, sequence of construction/installation and complicated material behaviour. Also, the load settlement response in the intermediate stages, is also obtained.

4.4.3.2 Load transferred by end bearing

In Fig. 4.19(a), it can be observed that the percent load transmitted by the tip (PTL) increases as skin friction failure takes place for all the runs. It can also be observed that the tip load tends to the same value for K = 1500 and K = 100 near collapse.

4.4.3.3 Spread of plastic zones

The spread of plastic zone has been shown in Figs. 4.20 to 4.23, for different runs. It can be observed that the skin friction failure at interface is faster for K = 1500 compared to K = 100 (comparing Runs P5 and P7 in Figs. 4.20 and 4.21); but the plastic zones are similar near collapse, for both values of K (Pile stiffness factor). For fairly compressible pile (K = 100) with adhesion factor equals 0.5, the skin friction failure starts both from top and bottom (Fig.4.22), contrary to other cases where the skin friction failure was observed to start from bottom and extend upwards. Plastic zones near collapse can be seen to be similar for both values of adhesion factors (comparing Runs P8 and P7 in Figs. 4.21 and 4.22). The effect of soil non-homogeneity on the spread of plastic zones, is to reduce its extent slightly (comparing Runs P9 and P5 in Figs. 4.20 and 4.23).

Two runs were made assuming smooth and rough interface between pile tip and soil respectively. It was observed from these runs, that the failure zones and collapse loads were not significantly affected by the interface conditions between tip of pile and soil. This may be because the end bearing part of bearing capacity

(from conventional method) is small (less than 25 %) and
the effect of rough contact is also small as observed in
Sec. 4.4.2.2., for circular footing.

4.4.4 Piled Circular Footing

Details of computer runs made for piled circular
footing are given in Table 4.3.

4.4.4.1 Collapse load:

Load-deformation response of piled circular footing
has been shown in Figs. 4.11 to 4.13, for different cases.
Runs PR1, PR2 and PR3 have been made without joint elements
and hence they correspond to fully adhesive contact. The
collapse pressure obtained from Run PR1 (for K_R = 100) and
Run PR2 (for K_R = 1) are equal to 130 C_{uo} (Fig. 4.11). It
can also be observed from Fig. 4.11, that the results
taken with 26 increments and 13 increments coincide with
each other, indicating that the results are not very
sensitive to increment size. Since these runs were made
with coarse mesh and runs were terminated after 200
iterations, these results are not very accurate. However,
they indicate the effect of mesh   refinement
and effect of base enlargement. The collapse
load obtained for piled circular footing with

enlarged base ($d_b = 2d$, where d_b is the diameter of the enlarge base), is 170 C_{uo}, which is about 30 percent more than the value for uniform section (Fig. 4.11). As collapse is approached, small tensile stresses were observed in a small zone adjacent to and above the enlarged base, even when weight of the soil was considered. The maximum magnitude of these tensile stresses was found to be of the order of the value of C_{uo}, occurring adjacent to enlarged base, as observed in the case of single pile in Sec. 4.4.3.1.

Runs PR4, PR5 and PR6, have been made with joint element and with mesh refinement near the tip of pile. For these runs, the shear strength of all interfaces, (both footing-soil and pile-soil) have been assumed to be equal to C_{uo} or 0.5 C_{uo}. From runs PR4 (for $K_R = 100$) and PR6 (for $K_R = 1$), it can be observed Fig. 4.12 that the value of collapse load approaches the same value of 138 C_{uo}, indicating that the footing flexibility does not have any significant effect on the collapse load. The collapse load obtained for adhesion factor = 0.5, is 126 C_{uo} (Fig.4.12). Since these results were taken without refinement near the footing edge, they are less accurate than subsequent runs discussed herein.

Runs PR7 to PR11, have been made using mesh 2M, with joint elements and with refinement both near pile tip

and footing edge. These results have been presented in
Fig. 4.13. In all these runs the footing base and pile
tip have been assumed to be smooth, and vertical pile
soil interface has been assumed to have finite shear
strength. The collapse load obtained (for $K_R = 100$) from
Run PR7, is about 132 C_{uo}. The sum of the bearing capacity
of annular footing (with inner diameter equal to one fourth
outer diameter) and bearing capacity of single pile,
(computed based on the values obtained in Sec. 4.4.2. and
Sec. 4.4.3., for circular footing and single pile), comes to
134 C_{uo}. Similarly, the collapse pressure for $\alpha_a = 0.5$,
(Run PR8) from analysis of piled circular footing is 126 C_{uo}
and the sum of the bearing capacities of footing and pile,
as assessed previously comes to 116 C_{uo}. Hence the bearing
capacity of piled circular footing in undrained soil
condition, may be assumed to be equal to the sum of the
bearing capacity of pile and annular portion of the footing
in contact with soil.

Runs PR9 and PR.10, were made assuming $E_P/E_{SO} = 100$
and $K_R = 1$. The numerical collapse loads obtained are
approximately equal to those from Runs PR7 and PR8(for
$E_P/E_{SO} = 1500$ and $K_R = 100$), indicating that the pile
compressibility and footing flexibility do not have

significant effect on the collapse load, for the range
of parameters considered. In these runs, the value of
shear strength of footing and pile material was assumed
to be 100 times that of soil and nowhere failure of pile or
footing material was indicated.

Run PR11 was made assuming soil to be non-homogeneous
with strength and stiffness increasing linearly with depth,
as explained in Sec. 4.3.1. The collapse load obtained
from this run is 174 C_{uo} (Fig. 4.13). The sum of the
bearing capacities of footing and pile as assessed earlier,
works out to be 170 C_{uo}. Hence for non-homogeneous soil
condition considered herein also, the bearing capacity of
piled circular footing can be seen to be approximately
the sum of the bearing capacities of pile and annular footing.

4.4.4.2 Percentage pile load (PPL)

The value of PPL, in general, reduces as collapse is
approached (Fig. 4.24(b)). It can be observed from
Fig. 4.24(b), that the curves for Runs PR8 and PR10 (for
$\alpha_a = 0.5$) tend to merge with each other and curves for
Run PR7 and PR9 (for $\alpha_a = 1$) tend to merge, near collapse.
Hence, it can be inferred that near collapse, the value of
PPL tends to be idependent of pile compressibility and footing
flexibility, for a given value of adhesion factor.

The percentage load transmitted though the tip (PTL), tends to increase initially and then decreases as collapse is approached (Fig. 4.19(b). This effect is more pronounced for adhesion factor equal to 0.5, than adhesion factor equal to 1. Again, near collapse the value of percentage load transmitted by tip approaches the same value, for a given value of adhesion factor, irrespective of pile compressibility and footing flexibility (comparing Runs PR7 and PR9 for $\alpha_a = 1$ and Runs PR8 and PR10 for $\alpha_a = 0.5$, in Fig. 4.19(b)).

4.4.4.3 Footing bending moment.

From Fig. 4.24(a), it can be observed that the footing bending moment (non-dimensional) increases as collapse is approached for all the cases considered. This increase is more for $K_R = 1$ and $K = 100$ than for $K_R = 100$ and $K = 1500$ (comparing Runs PR7 and PR9). For Run PR9 ($K_R = 1$ and $K = 100$), the increase in bending moment is about 50 percent. This increase is about 13 percent and 24 percent for Run PR7 ($K_R = 100$, $K = 1500$ and $\alpha_a = 1$) and Run PR8 ($K_R = 100$, $K = 1500$ and $\alpha_a = 0.5$) respectively. This increase in bending moment is slightly more for non-homogeneous soil considered than homogeneous soil.

4.4.4.4 Spread of plastic zones

Development of plastic zones have been shown in Figs. 4.25 to 4.29. Shear failure of interface starts with loads as small as one fourth of the ultimate bearing capacity in all the cases considered. The plastic zones, in general, start developing near pile-tip and footing edge and these zones spread simultaneously as load is increased. Comparison of Run PR7 (adhesion factor = 1.0) and Run PR8 (adhesion factor = 0.5) shows that spread of skin friction failure as well as soil failure is faster for $\alpha_a = 0.5$ than for $\alpha_a = 1.0$ (Figs. 4.25 and 4.26). For the range of parameters considered, the plastic zones around tip and around footing are observed to be distinct. The zone near pile-footing interface is least prone to failure and these zones fail only near complete collapse.

Comparison of Run PR8 and PR10 (Figs. 4.26 and 4.28) shows that the plastic zones near collapse are similar for both the cases, even though the spread of failure is faster for Run PR10 (Fig. 4.28). This shows that the collapse behaviour is similar, irrespective of pile compressibility and footing flexibility, for the range of parameters considered.

Fig. 4.29 shows the spread of plastic zones for non-homogeneous soil condition. The spread of plastic

zone for this run (Run PR11), compared to homogeneous soil
case (Run PR7, Fig.4.25), is similar except that in the
non-homogeneous case the plastic zones spreads to shallower
depth both below the footing and pile. Top portion of pile
is less prone to skin friction failure in non-homogeneous
case than homogeneous case.

Compared to unpiled footing, in the case of piled
footing, the plastic zones, in general, spread to greater
depth below footing. Compared to single pile also, the
plastic zones spread to greater depth below pile, in the
case of piled circular footing, for the cases considered.
The reason for this may be that in the case of single
pile, once complete skin friction failure occurs, the soil
is free to move, whereas in the piled circular footing
it is not so.

For adhesion factor (α_a) equal to 0.5 (Runs PR8 and PR10),
it can be observed in Figs. 4.26 and 4.28, that the plastic
zone below footing and that around pile tip, do not meet
each other, whereas for $\alpha_a = 1.0$, they meet each other near
the collapse. This may be the reason for the difference
in bearing capacity of piled circular footing compared
to the sum of bearing capacities of annular footing and

single pile observed previously (Sec. 4.4.4.1) for $\alpha_a = 1.0$

and $\alpha_a = 0.5$. (For $\alpha_a = 1.0$, Numerical Collapse pressure $= 132\ C_{uo}$.

The sum $= 134\ C_{uo}$. For $\alpha_a = 0.5$, Numerical collapse pressure

$= 126\ C_{uo}$. The sum $= 116\ C_{uo}$).

4.4.4.5 Drained behaviour of piled footing

The study taken up here is confined to undrained response of piled circular footing. Study of drained response of the same would be worthwhile. However, some indications of drained behaviour are available from the model tests performed by Palk and Naborczyk (101), Akinmusuru (2), and Knabe (79), on piled footing set in sandy soil. From these works, it has been observed that the bearing capacity of piled footing set in sandy soil is considerably more (about 30 percent more in some cases), than the sum of bearing capacity of footing and single pile. It is of interest to note that from the present analysis, it is observed that in the case of saturated undrained clay the bearing capacity of piled circular footing is roughly equal to this sum.

Some studies made using Tresca and Drucker -Prager yield criteria and associated computation difficulties have been presented in Appendix D.

4.5 COMPARISON OF COMPUTING TIME

The CPU time required for some runs, has been compared in Table 4.4. It can be observed that the CPU time increases as the number of increments and/or the maximum number of iterations specified increases. From the trend of load-settlement curve for single pile (Fig. 4.10), for circular footing (Fig. 4.8) and for piled circular footing (Fig.4.13), it is observed that the maximum number of iterations that may be specified to asses the collapse satisfactorily is less for single pile and more for piled circular footing and circular footing. Hence elasto-plastic analysis, by the present procedure, may require considerably more CPU time than analysis of single pile. This may be because the failure is rather sudden in the case of single pile and fairly gradual in the case of circular footing and piled circular footing considered.

4.6 CONCLUSIONS

1. Using six noded interface elements to model interface behaviour and parabolic isoparametric elements to model the material behaviour, the load-deformation response, spread of plastic zones and collapse load can be determined satisfactorily by means of 'initial stress' finite element elasto-plastic

analysis, for any complicated geometry of the problem.

2. The bearing capacity of a circular footing, subjected to central column loading is not sensitive to footing flexibility in the range of $K_R = 1$ and $K_R = 100$.

3. Bending moment (Non-diaml.) reduces for rigid footing and increases for fairly flexible footing, subjected to central column loading, as collapse is approached. However, these effects are small (about 10 percent).

4. The effect of adhesion between footing and soil on the numerical collapse load, is not substantial (less than 10 %).

5. In the case of single pile, small tensile mean normal stress zone develops near the pile tip, as collapse is approached. However, it may not influence the results significantly.

6. The bearing capacity of circular footing and single pile, computed from finite element elasto-plastic analysis, agrees satisfactorily with conventional solutions. However, finite element method can be used for studying the complete progressive failure mechanism and also for determining collapse load for problems involving more complicated geometry and/or

material behaviour, which cannot be solved by
other methods.

7. The bearing capacity of piled circular footing in
saturated clay in undrained condition, may be approx-
imately assumed to be equal to the sum of the bearing
capacity of pile and footing in contact with soil.
The bearing capacity of piled circular footing is not
significantly affected by footing flexibility and
pile compressibility for the range of parameters
considered.

8. The bearing capacity of single pile and piled circular
footing can be significantly increased by enlarging
the tip of the pile.

9. Provision of pile in a circular footing is more
advantageous in the case of non-homogeneous soil,
in which the shear strength increases with depth,
than homogeneous soil, in increasing the bearing
capacity.

10. As collapse is approached the footing bending moment
increases in the case of piled circular footing and
this effect is more for compressible pile and flexible
footing.

11. Plastic zones around tip of pile, plastic zones below the footing and skin friction failure of pile-soil interface, spread simultaneously, as load is increased in the case of piled circular footing. For the shallow pile considered, the failure zones around pile tip and footing base are fairly distinct.

TABLE 4.1   CIRCULAR FOOTING

(Details of Computer Runs)

n No.	Loading	K_R	K	Interface	Mesh	Soil type
	udl	O	⊢	⊢	2S	Homo.
	' '	O	⊢	⊢	2R(udl)	Homo.
	Central Column	100	1500	Adhesive (No joint)	1	Homo.
	' '	1	1500	' '	1	Homo.
	' '	100	1500	Rough	2R	Homo.
	' '	100	1500	Smooth	2R	Homo.
	' '	100	1500	Rough	2RM	Homo.
	' '	100	1500	Smooth	2RM	Homo.
	' '	100	1500	Smooth	2RM	Non-Homo.
	' '	1	1500	Smooth	2RM	Homo.

TABLE 4.2   SINGLE PILE
(Details of Computer Runs)

n No.	K	Interface	Mesh	Soil type	Adhesion factor (C_a/C_u)
I	1500	Adhesive (No joint element)	1P	Homo.	∞
2	1500		1P (Enlarged base)	''	∞
3	1500	Finite shear strength at interface	1PJ	''	1.0
·	1500		1PJ	''	0.5
:	1500		2P	''	1.0
:	1500		2P	''	0.5
·	100		2P	''	1.0
·	100		2P	''	0.5
·	1500		2P	Non-Homo.	1.0
O	1500		2P	Homo.	1.0

te: Only in Run No. P10 and P6 weight of soil has been considered and soil has been treated as no tension material.

TABLE 4.3   PILED CIRCULAR FOOTING
(Details of Computer Runs)

n No.	K_R	K	Interface	Mesh	Soil type	Adhesion Factor C_a/C_u
1	100	1500	Adhesive(No joint element)	1	Homo.	∞
2	1	1500		1	Homo.	∞
3	100	1500		1 (Enlarged base)	Homo.	∞
⊦	100	1500	Finite shear strength at interfaces.	2	Homo.	1.0
5	100	1500		2	Homo.	0.5
5	1	1500		2	Homo.	1.0
7	100	1500	Smooth raft and pile base.Finite shear strength at vertical pile-soil interface.	2M	Homo.	1.0
8	100	1500		2M	Homo.	0.5
)	1	100		2M	Homo.	1.0
O	1	100		2M	Homo.	0.5
1	100	1500		2M	Non-Homo.	1.0

TABLE 4.4   COMPARISON OF CPU TIME

Foundation Type	Run No.	No. of increments	Max. No. of iterations	CPU Time in DEC1090 Computer Min:Sec.
Circular Footing	R5	15	200	12:25
	R6	13	200	8:16
	R7	13	200	14:05
	R8	12	200	12:46
	R9	13	200	10:41
	R10	13	400	20:05
Single Pile	P9	18	151	6:44
	P10	21	51	4:11
Piled Circular Footing	PR4	23	200	21:49
	PR5	21	189	17:30
	PR8	21	300	37:40
	PR10	21	300	35:29

Fig.4·1   MESHES 1,1P and 1PJ

Labels within figure:

2d

d/2

q

Footing

16 d

L=8d
Pile

16 d

16 d   Rough rigid boundary

Smooth
boundary

MESH 1–For piled
footing and footing
only
68 Elements
235 Nodes

MESH 1P–For pile
only (Without inter-
face elements)
64 Elements
221 Nodes

MESH 1PJ–For pile
only (With interface
elements)
72 Elements
241 Nodes
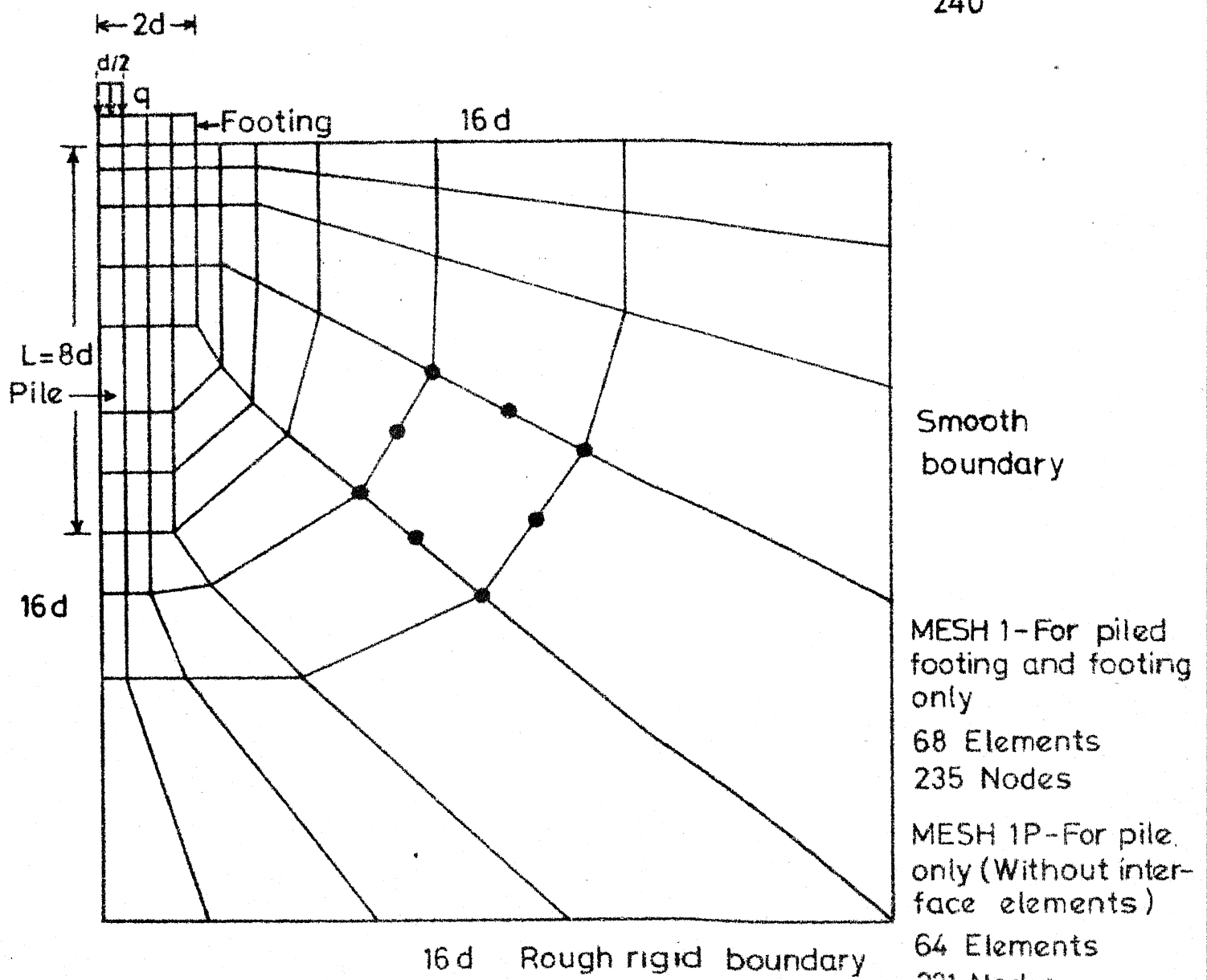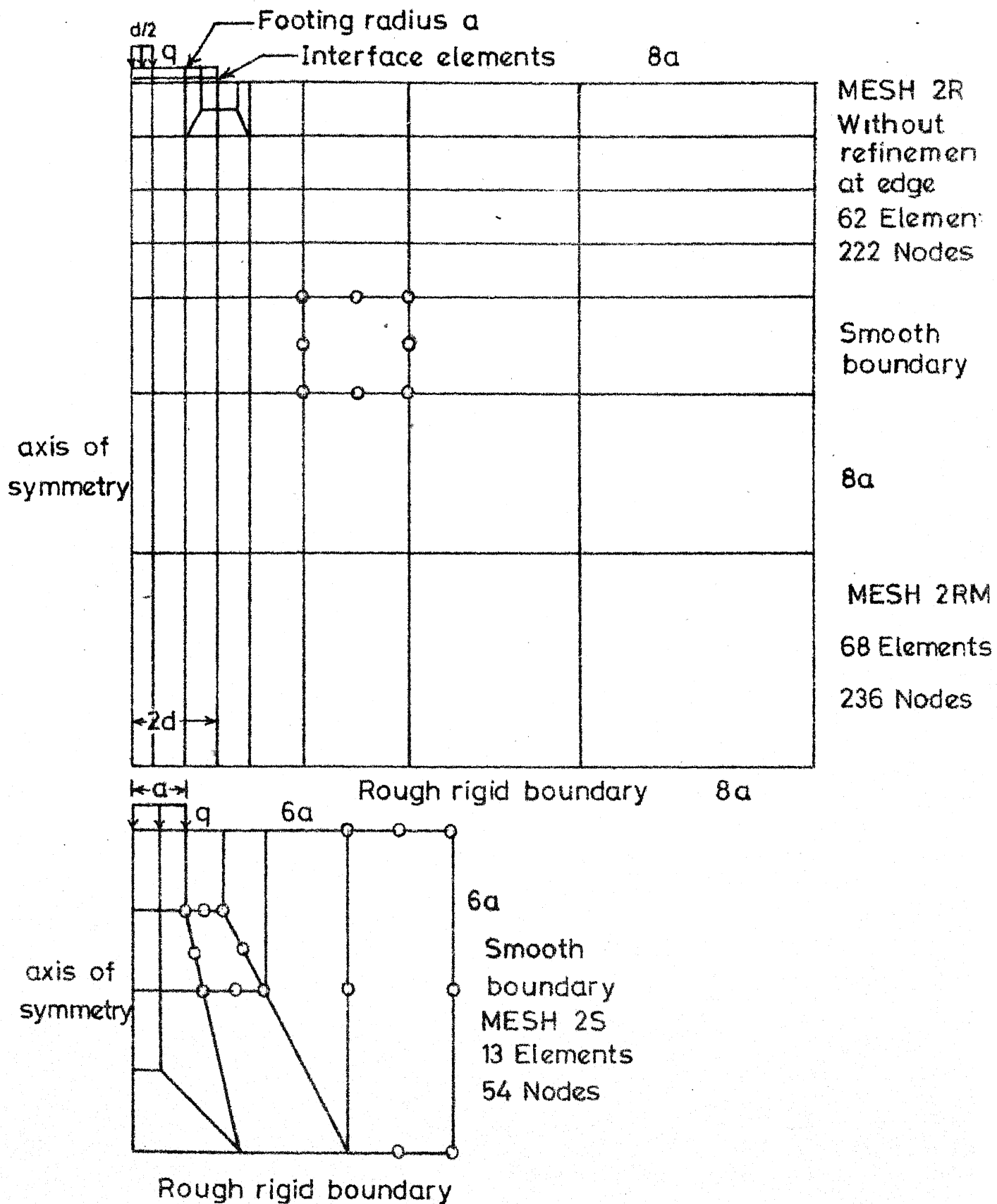
Fig.4·2
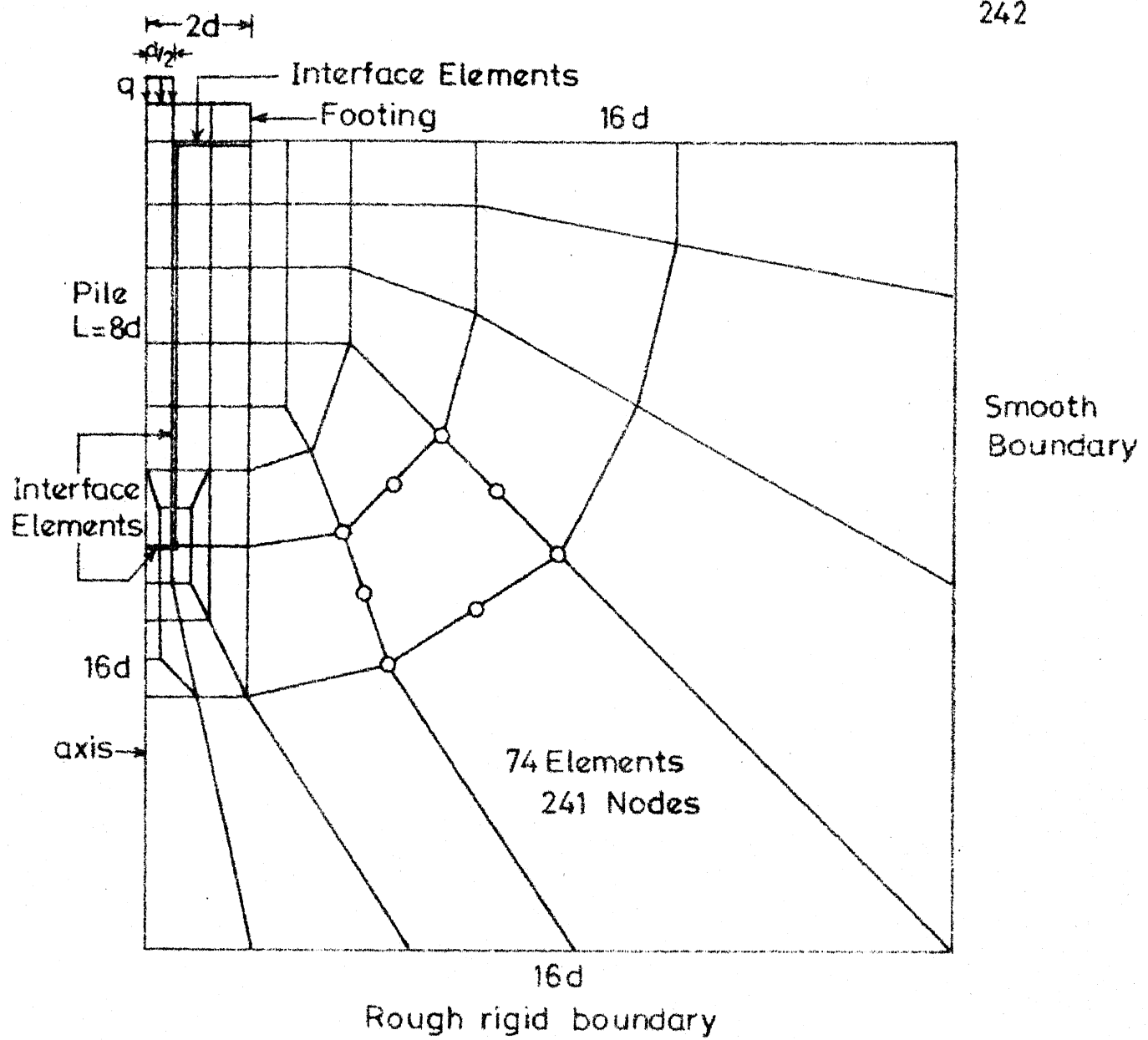
Fig.43   MESH 2
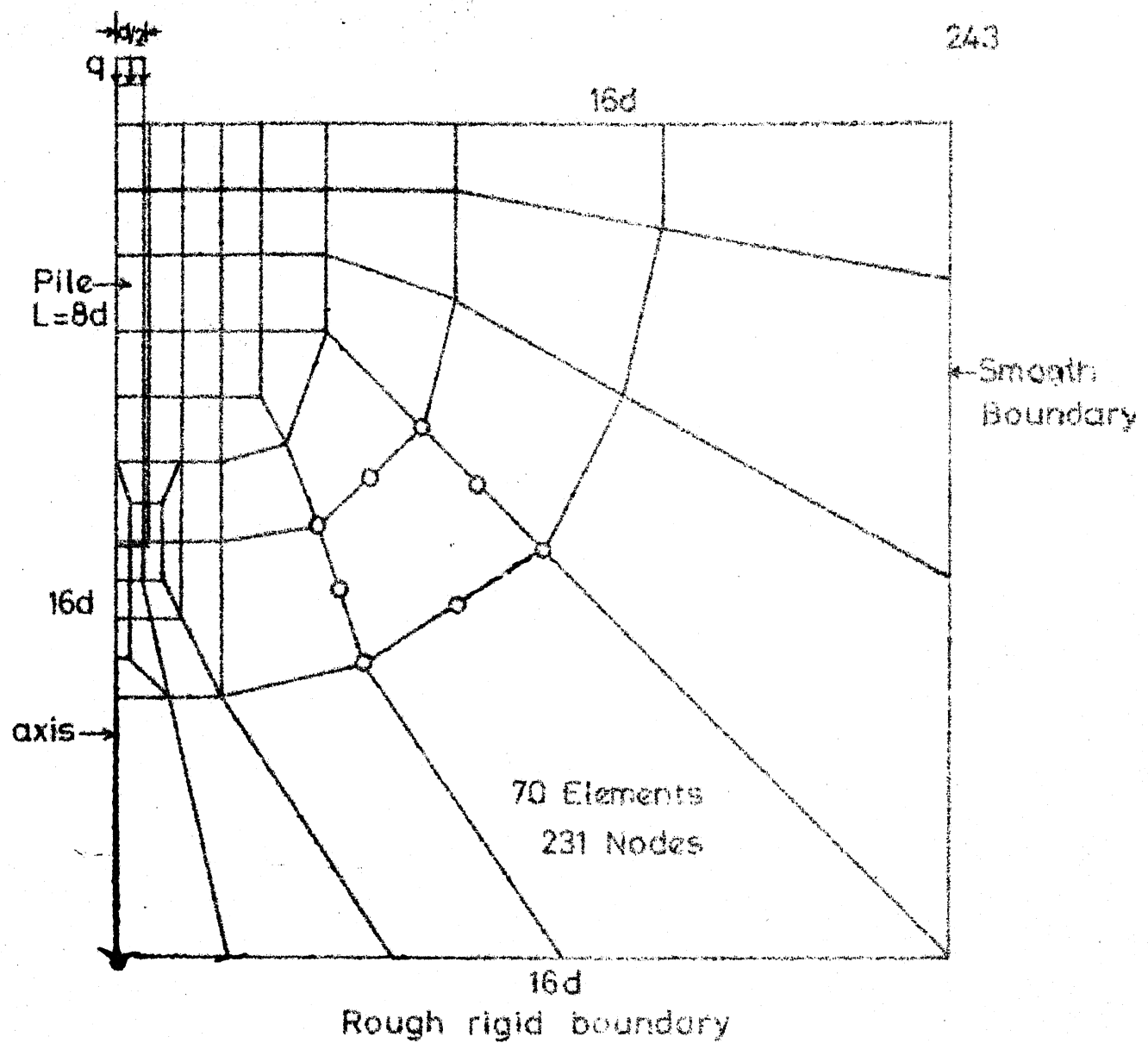
Fig. 4.4   MESH   2P
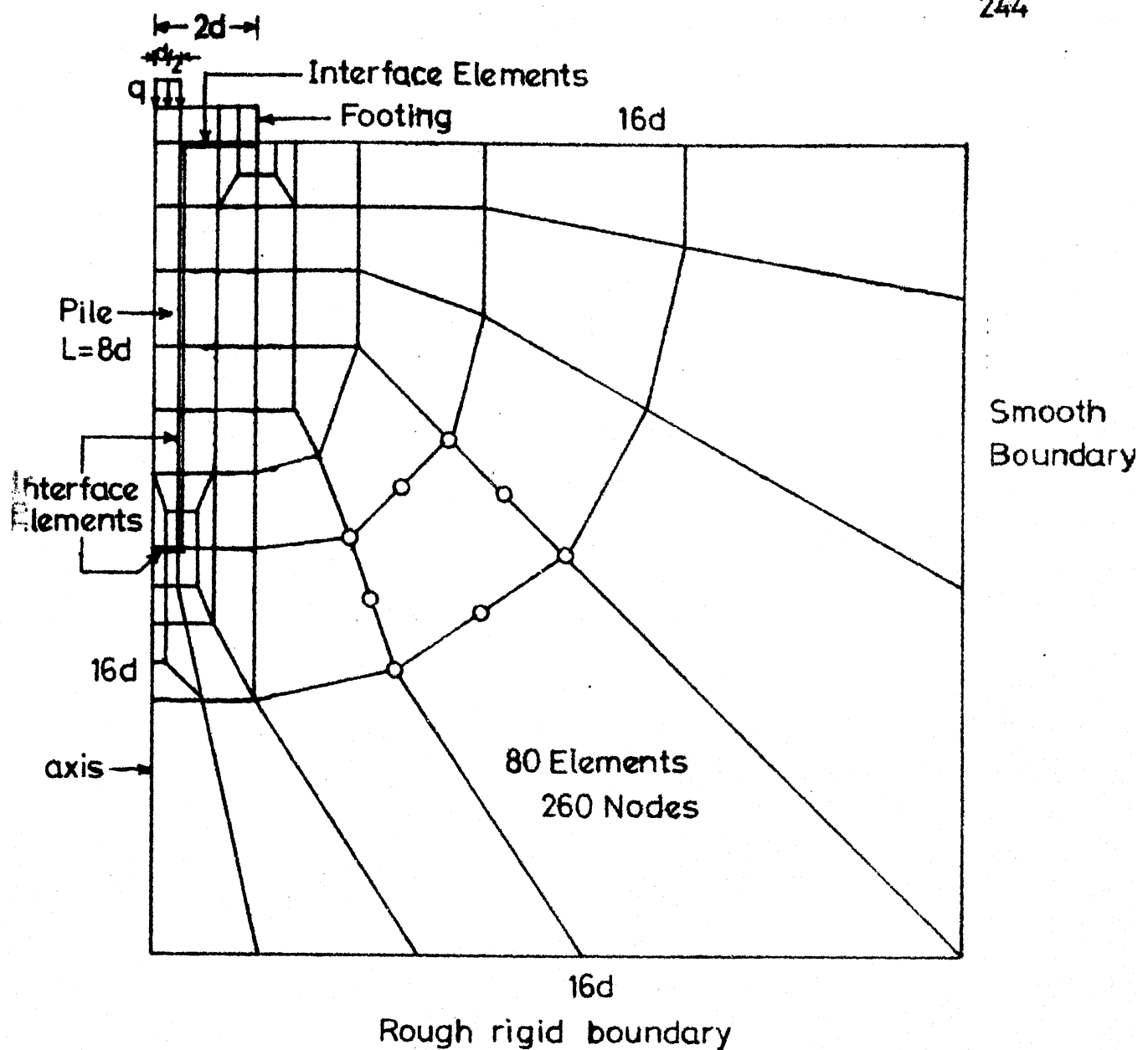
Fig. 4·5   MESH   2M
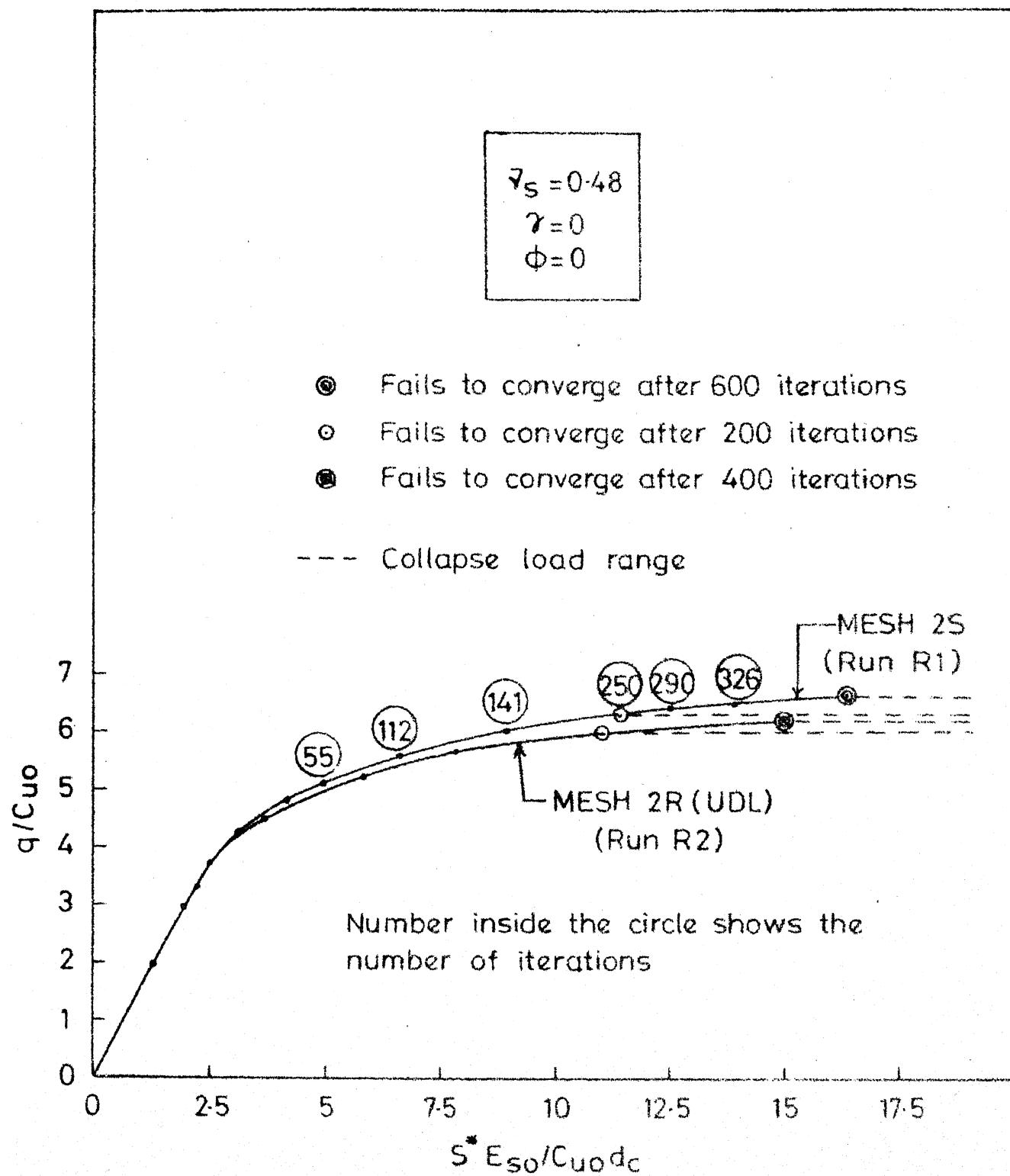
Fig.4·6   Circular Raft (UDL) Load-Displacement Curve
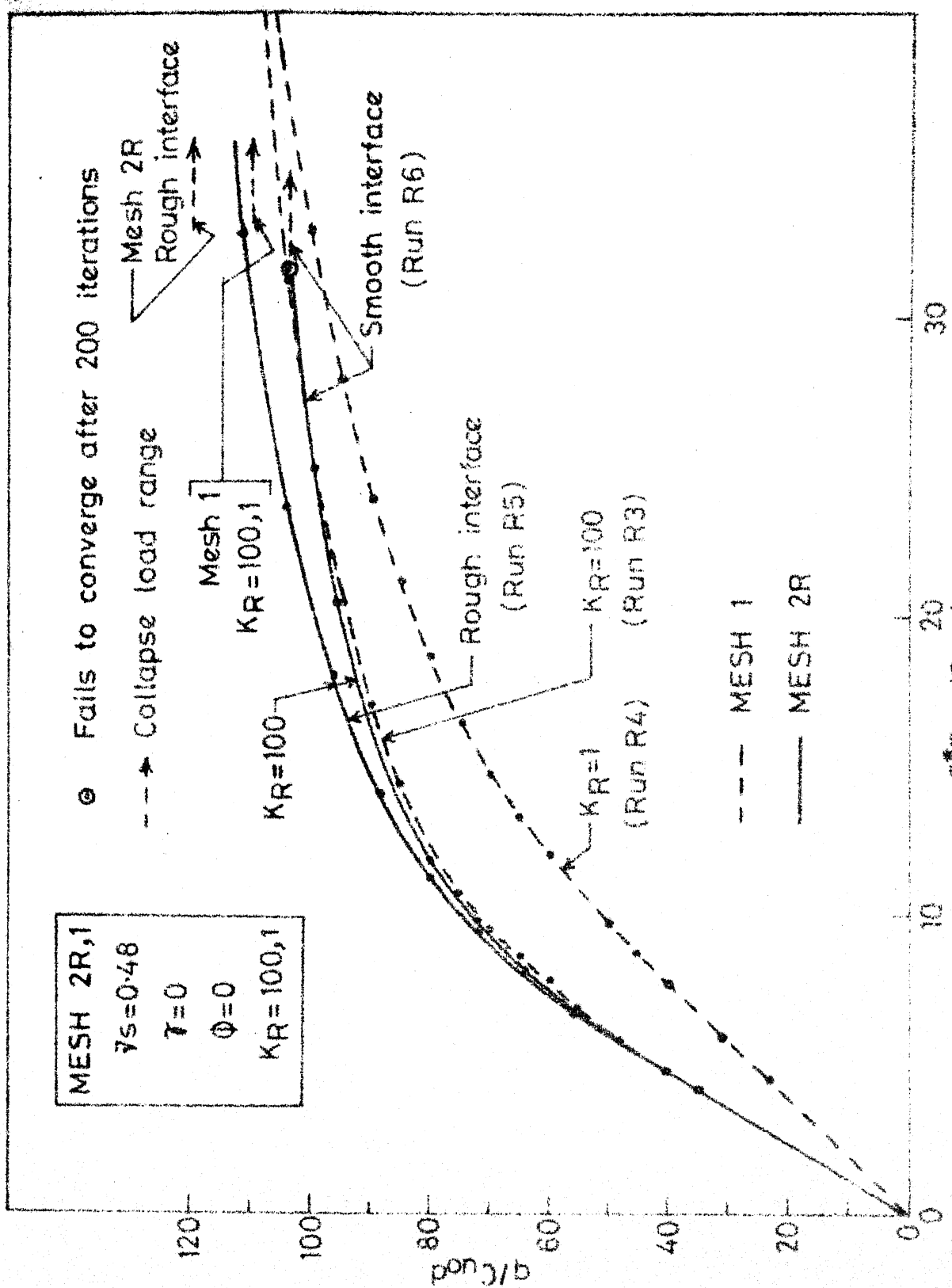
FIG 4.7   Circular footing load-displacement curve
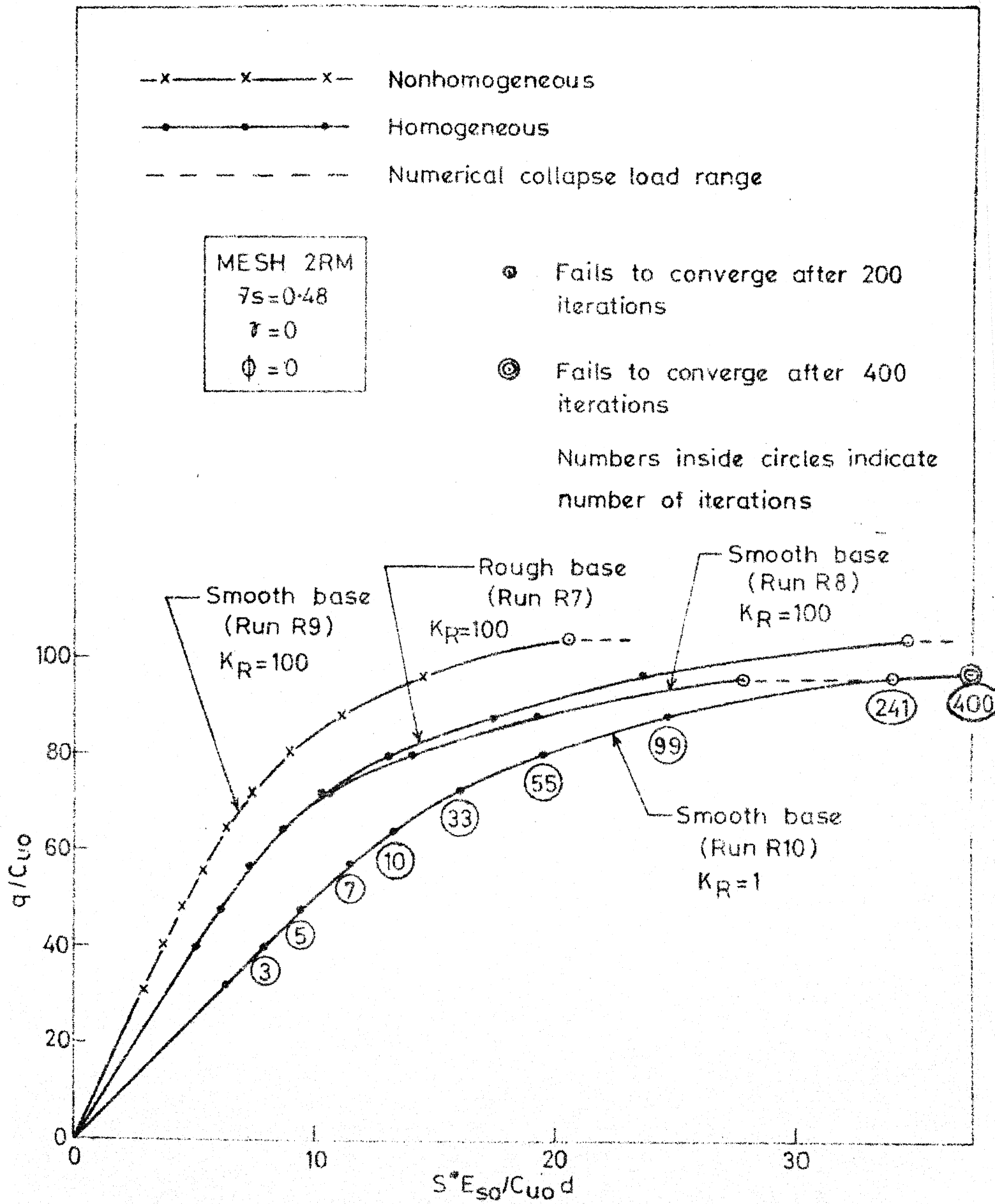
FIG.4·8   Circular footing load-displacement curve
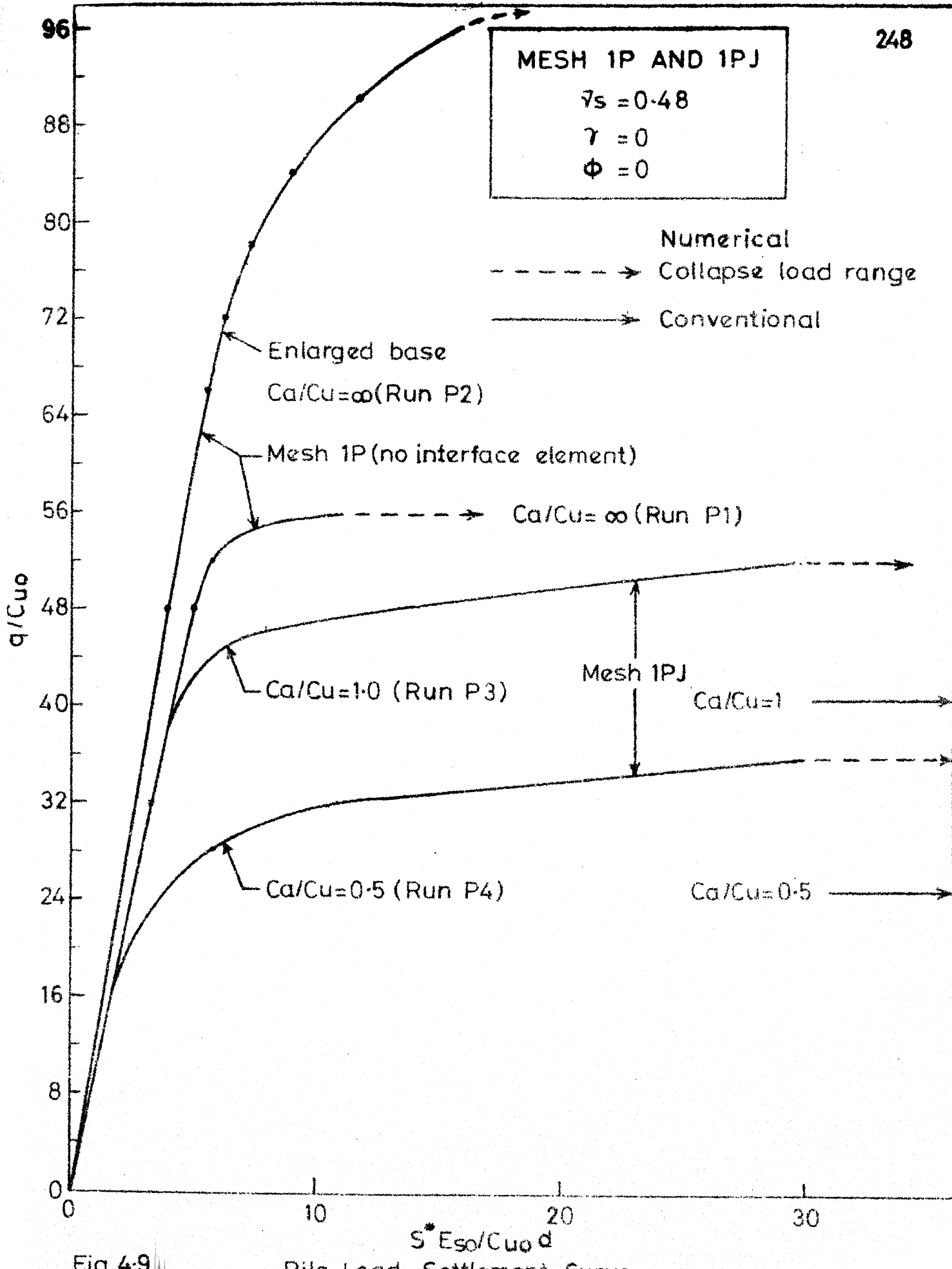
Fig. 4·9 Pile Load – Settlement Curve
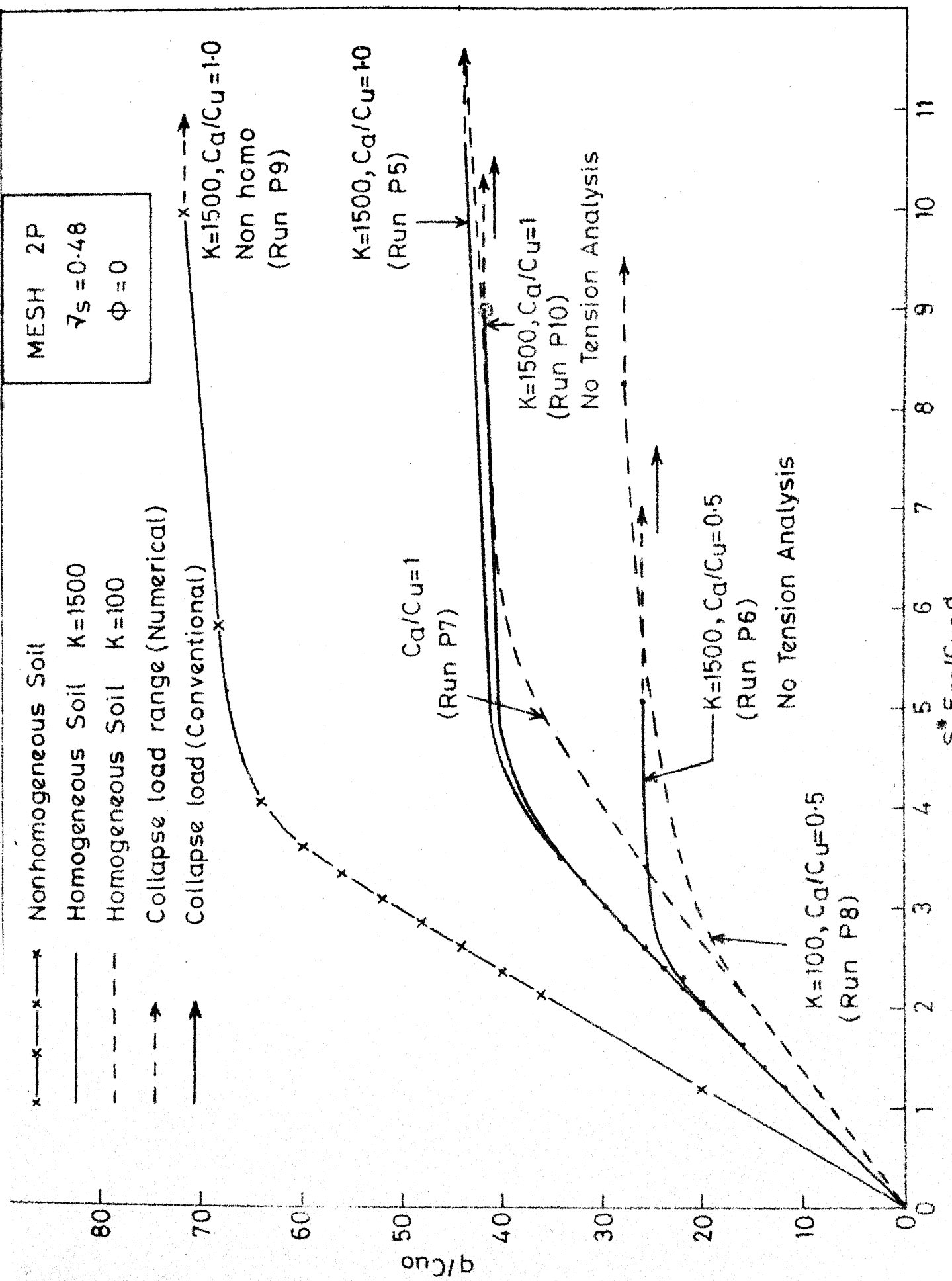
Fig. 4.10   Pile Load-Displacement Curve
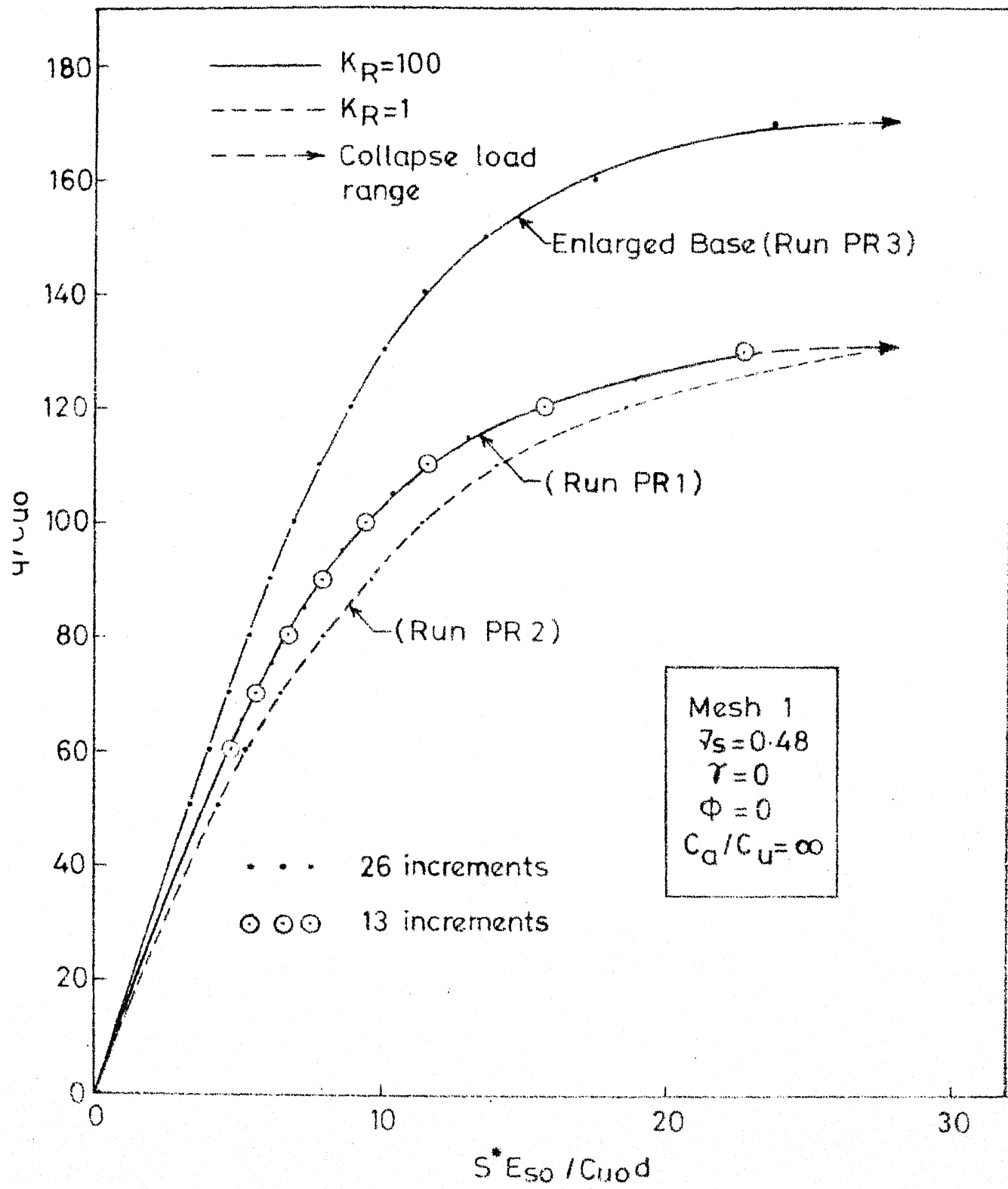
Fig. 4·11   Piled circular footing Load-Displacement Curve
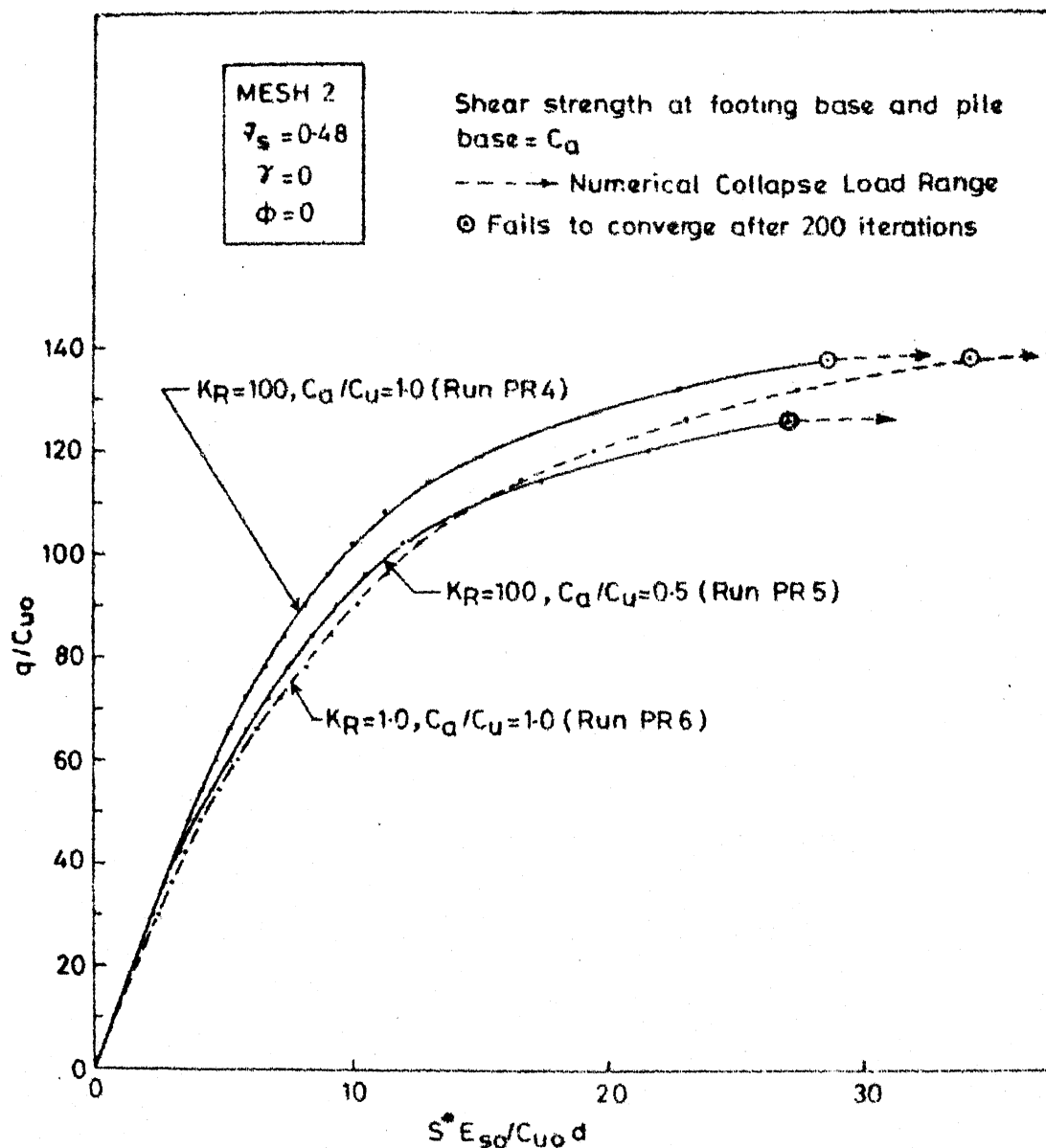
Fig. 4.12   Piled circular footing Load-displacement Curve
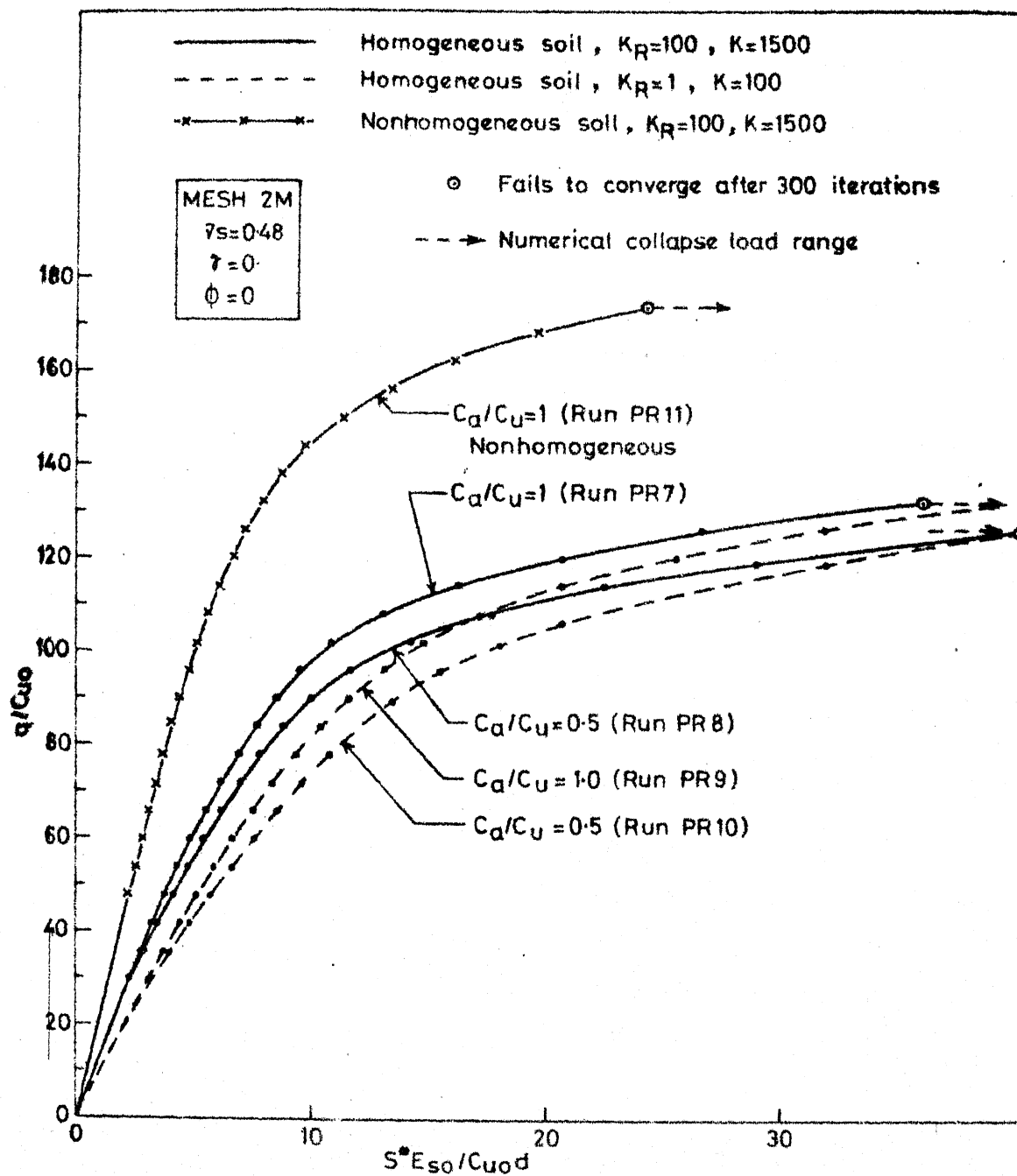
FIG.4·13   Piled circular footing load-displacement curve
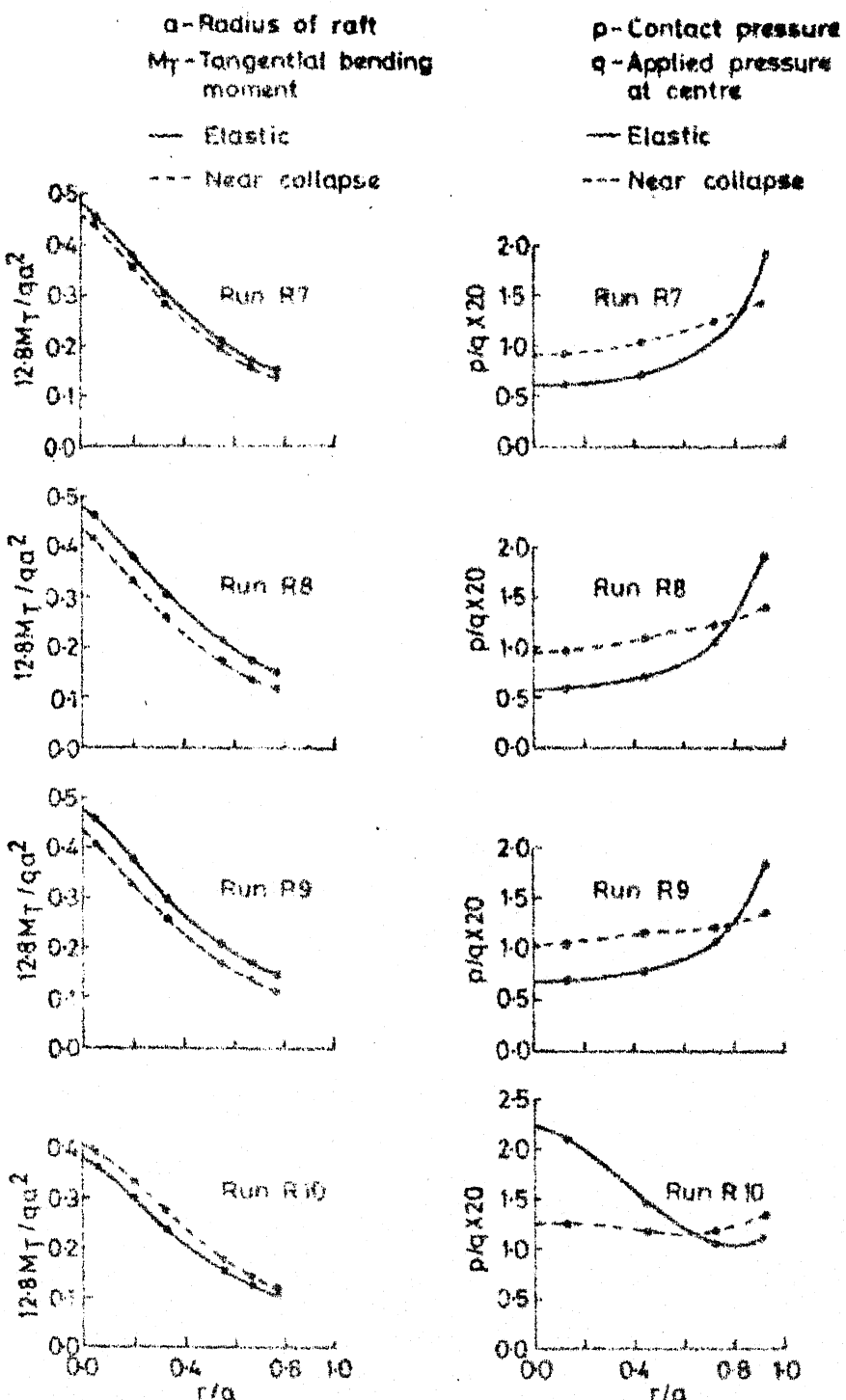
FIG.4.14 RAFT BENDING MOMENT AND CONTACT PRESSURE
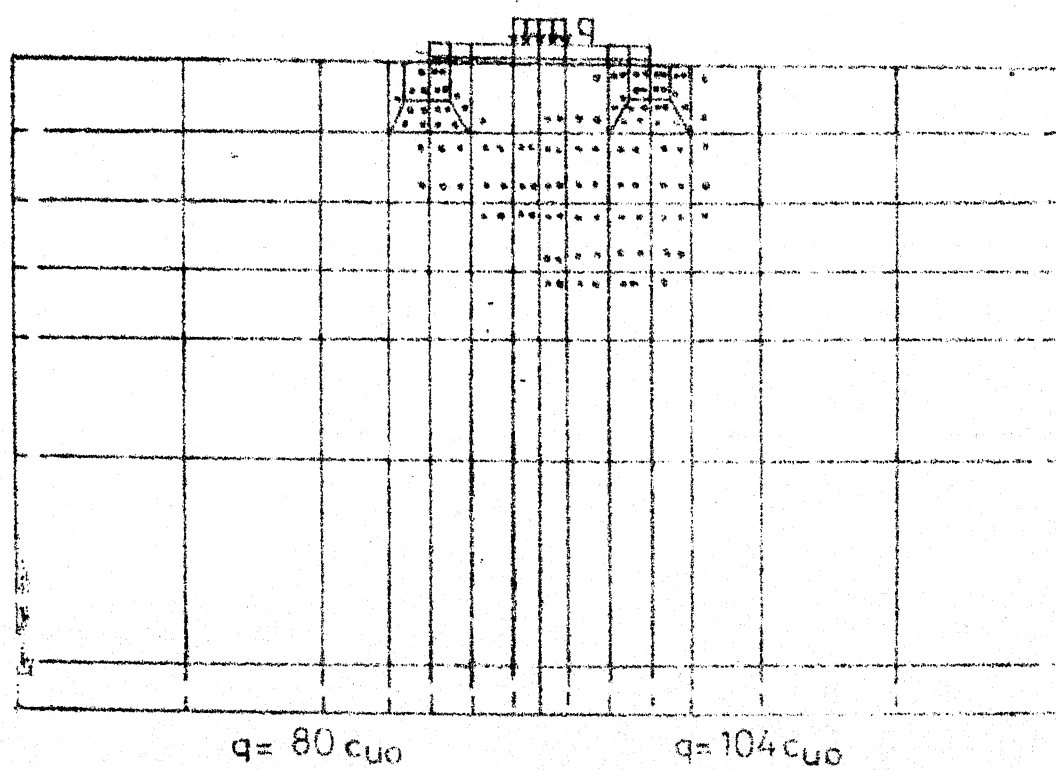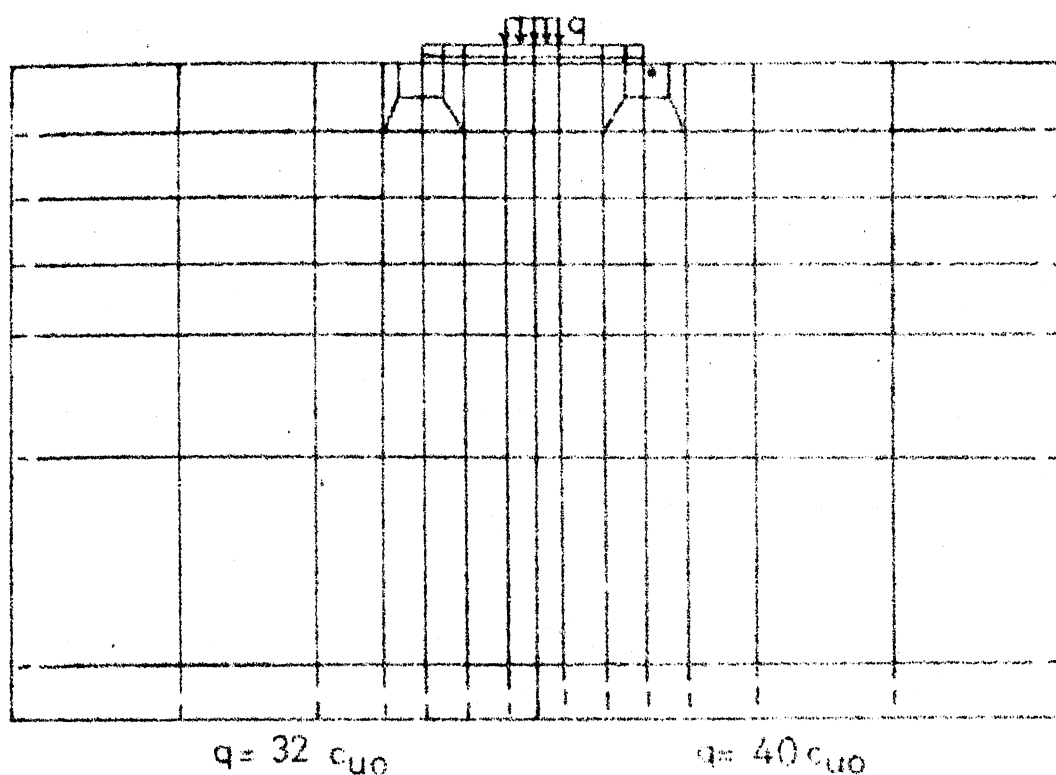
Fig. 4·15   SPREAD OF PLASTIC ZONE (RUN R7)

$q = 32\ c_{uo}$ $q = 40\ c_{uo}$

$q = 80\ c_{uo}$ $q = 96\ c_{uo}$
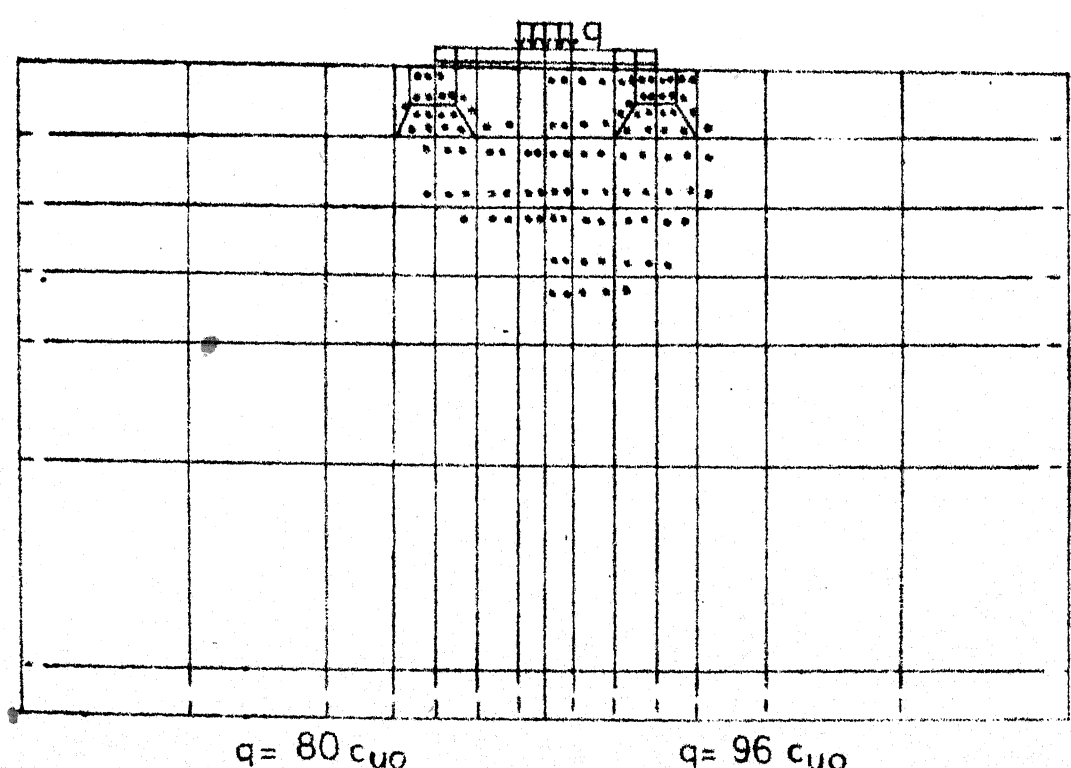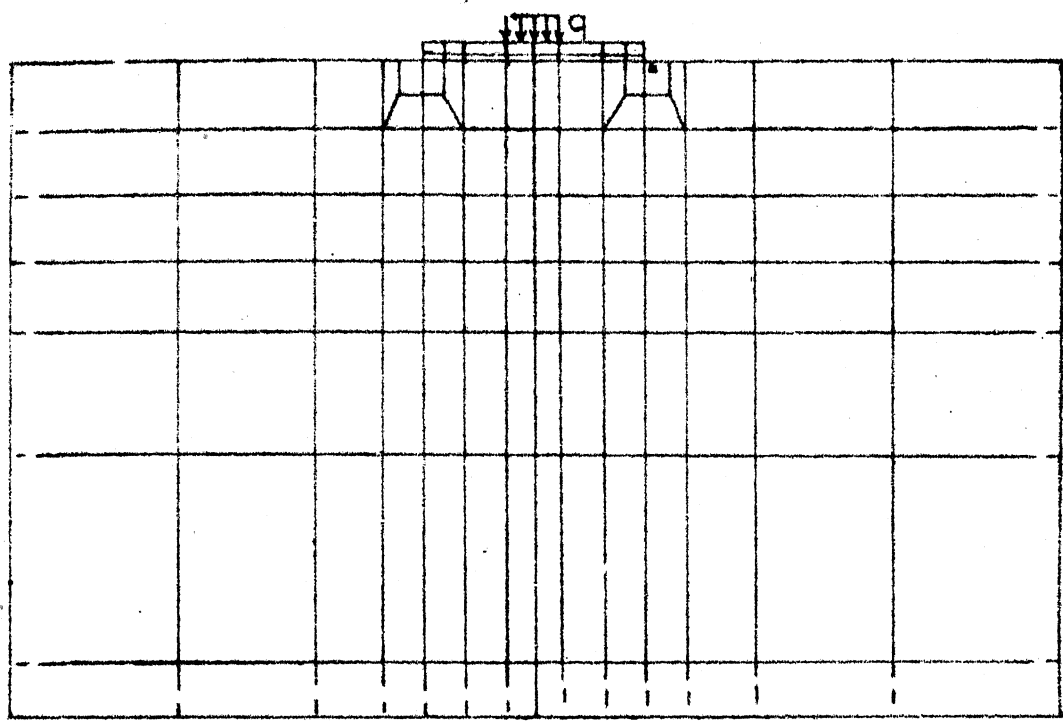
Fig.4·16   SPREAD OF PLASTIC ZONE (RUN R8)
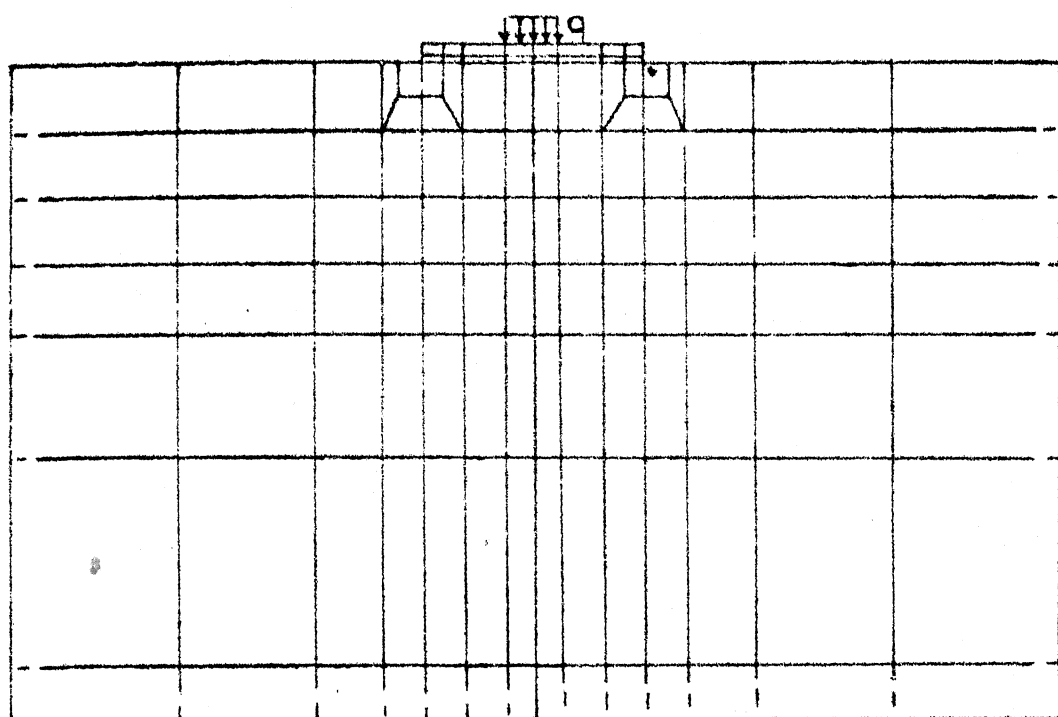
$q = 32\,c_{uo}$ $q = 40\,c_{uo}$
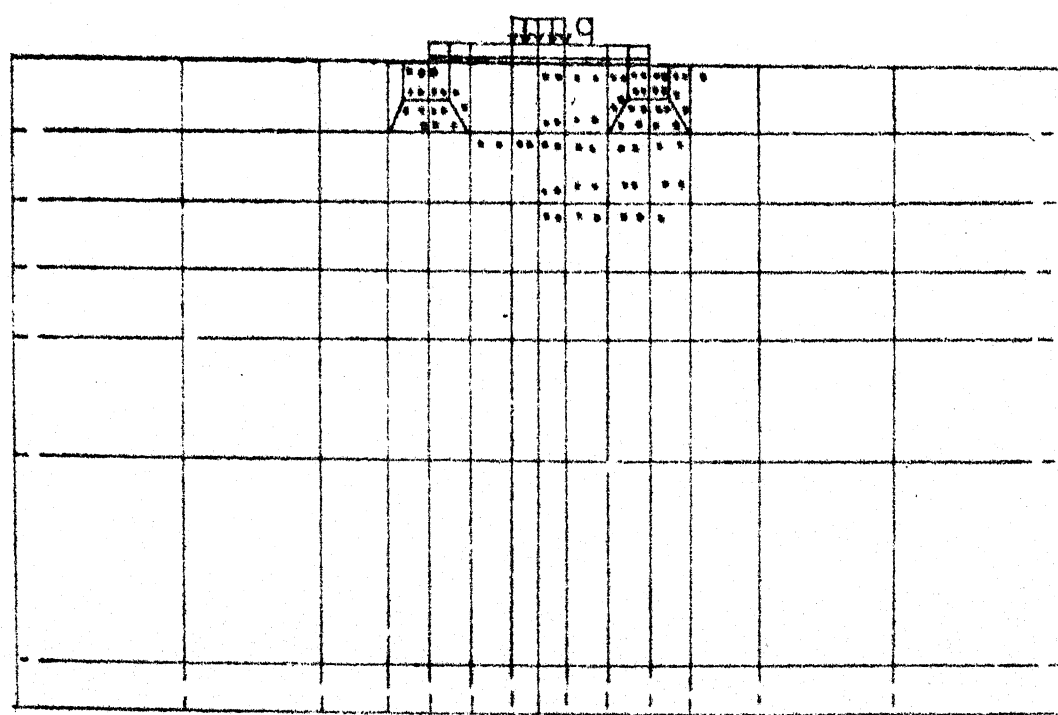
$q = 80\,c_{uo}$ $q = 104\,c_{uo}$

Fig. 4·17   SPREAD OF PLASTIC ZONE (RUN R9)

$$q = 32\ c_{uo} \qquad q = 40\ c_{uo}$$

$$q = 80\ c_{uo} \qquad q = 98\ c_{uo}$$
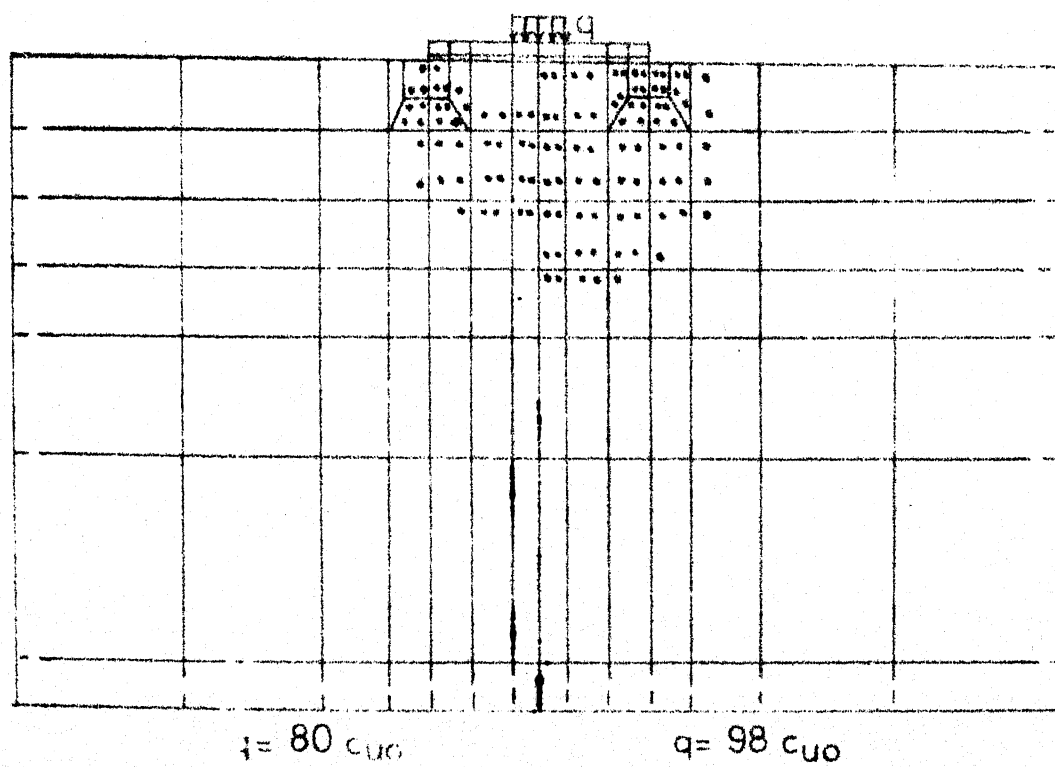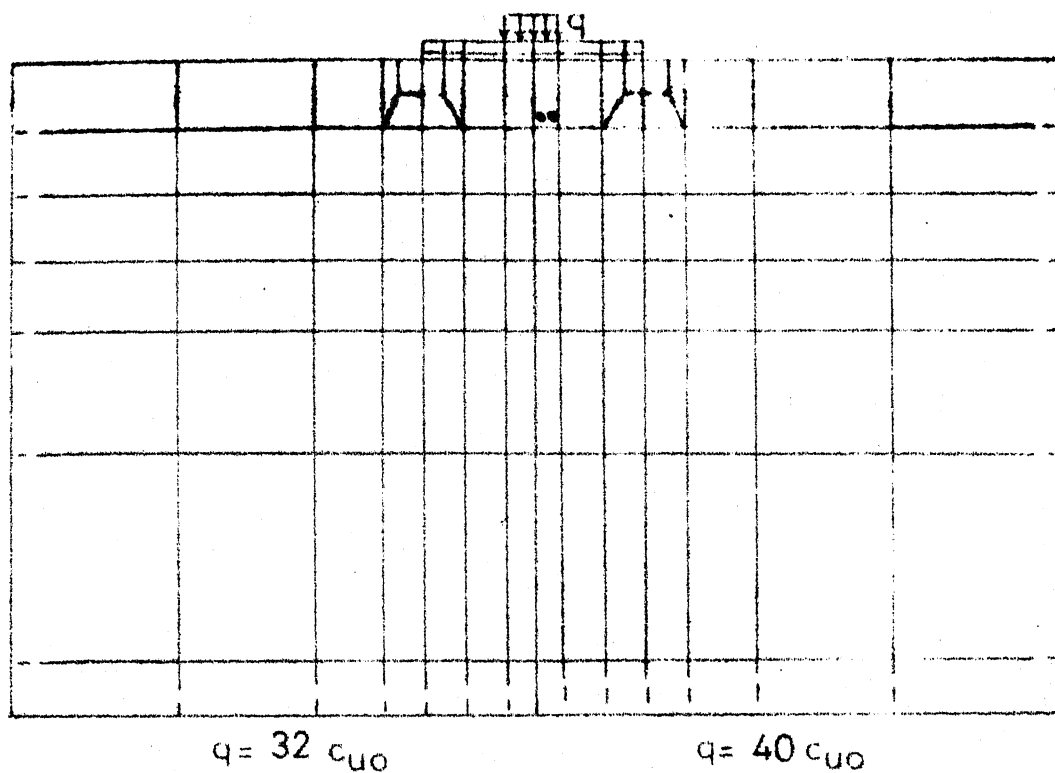
Fig. 4.18 SPREAD OF PLASTIC ZONE (RUN R10)
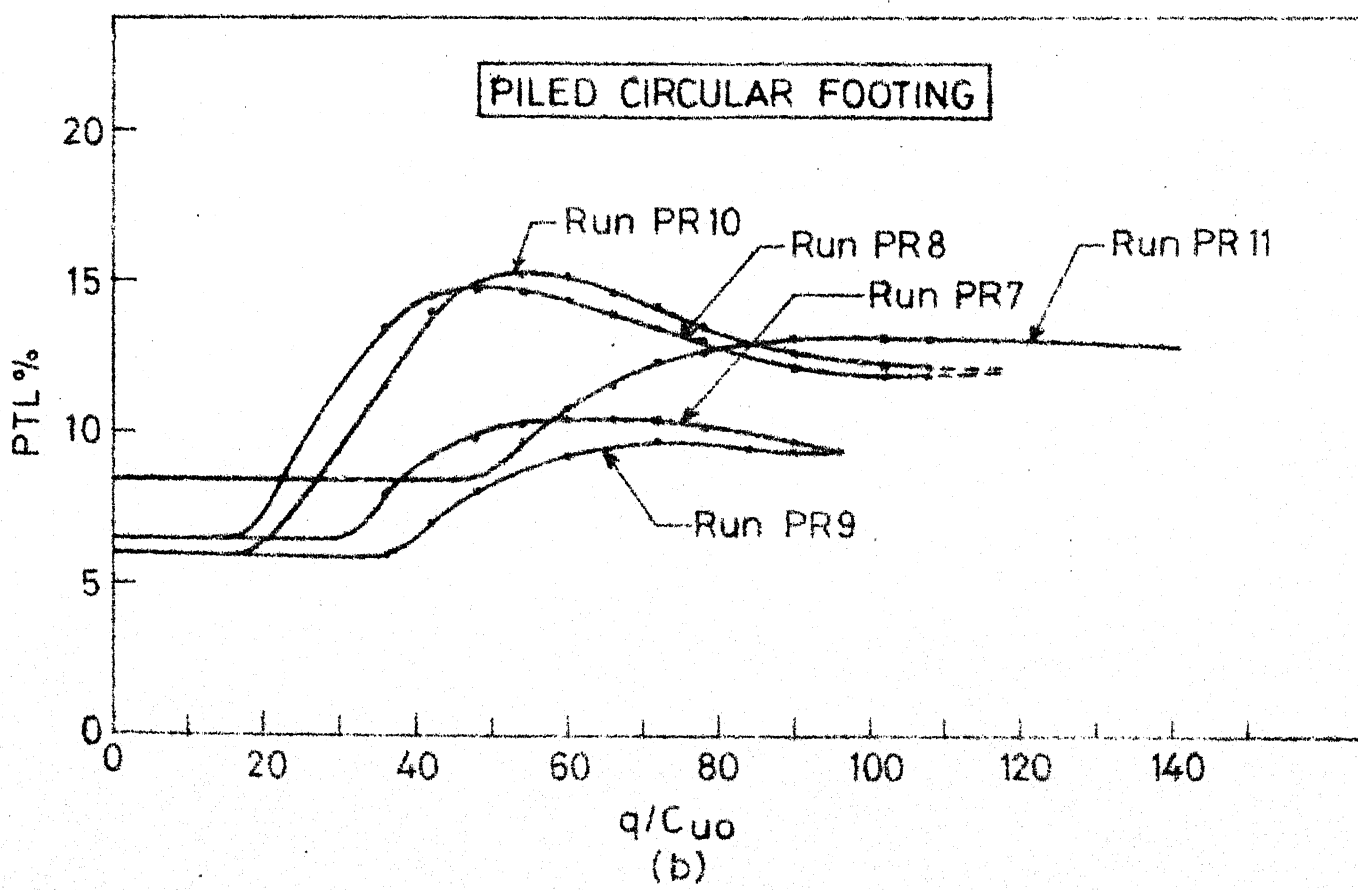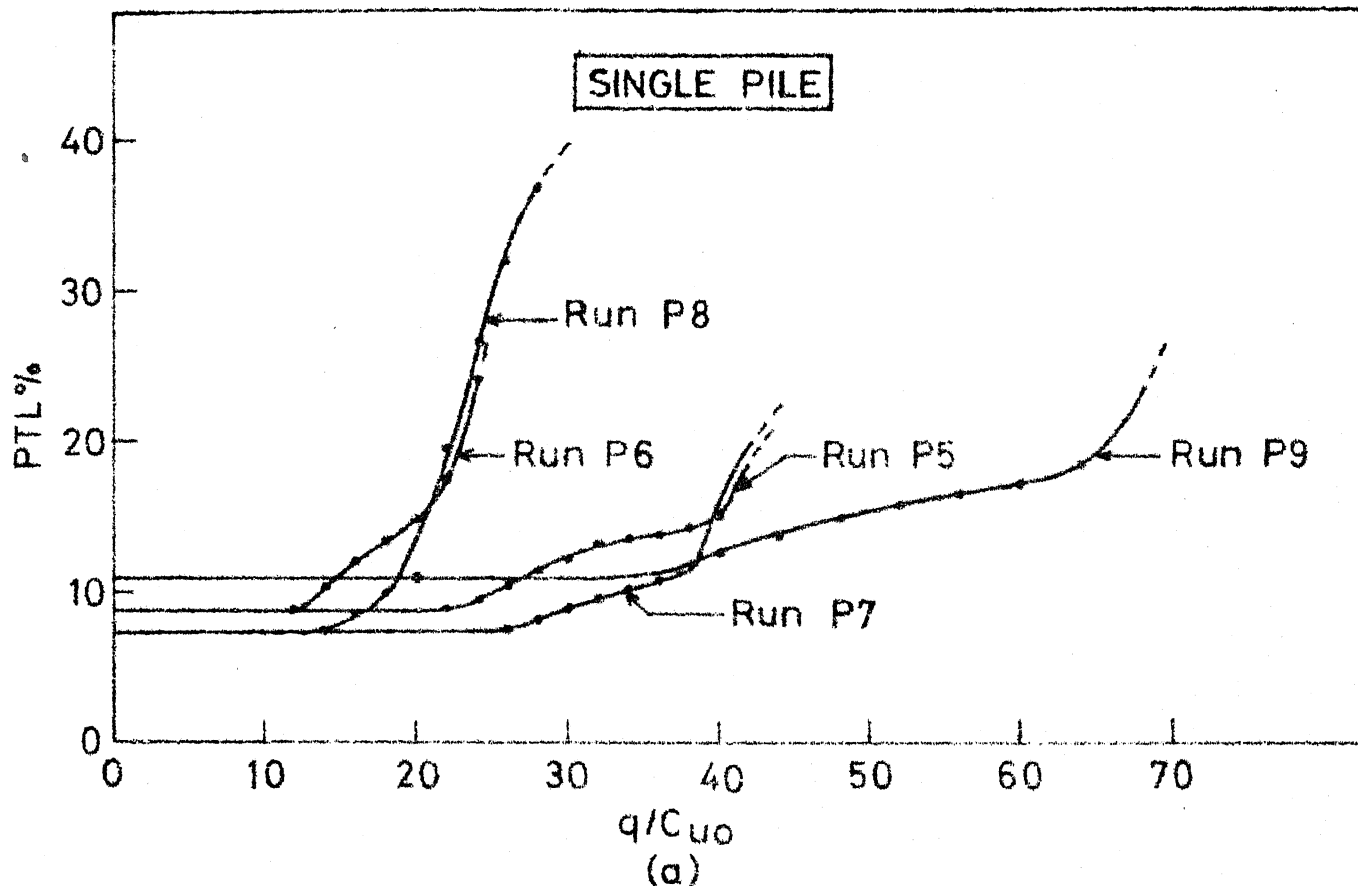
FIG. 4·19 (a) & (b)   Percentage tip load (PTL) Vs q/C_uo

q= 26 c$_{uo}$ q= 30 c$_{uo}$

• Yielding of soil

‡ Interface failure

q= 40 c$_{uo}$ q= 44 c$_{uo}$
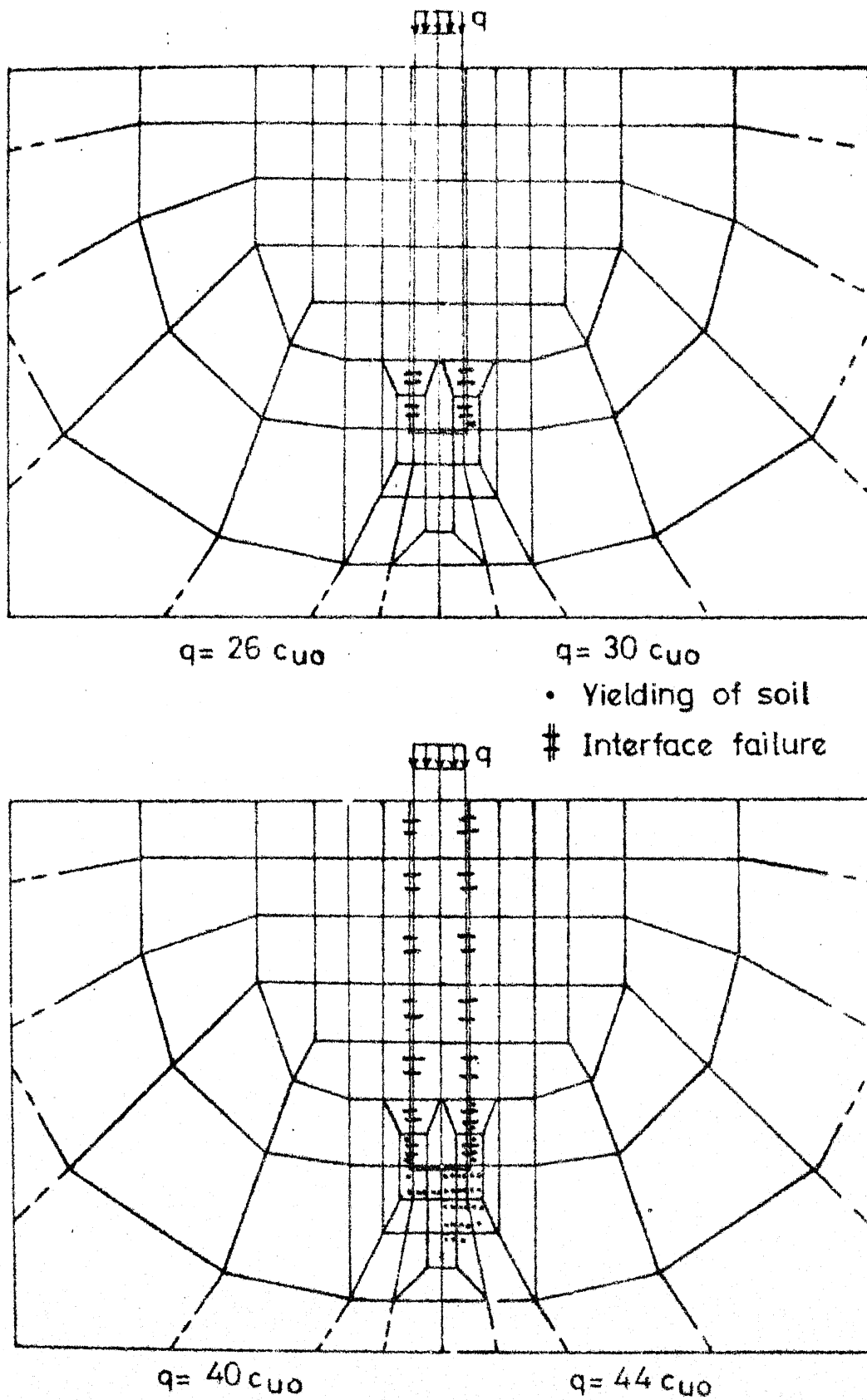
Fig. 4·20   SPREAD OF PLASTIC ZONE (RUN P5)
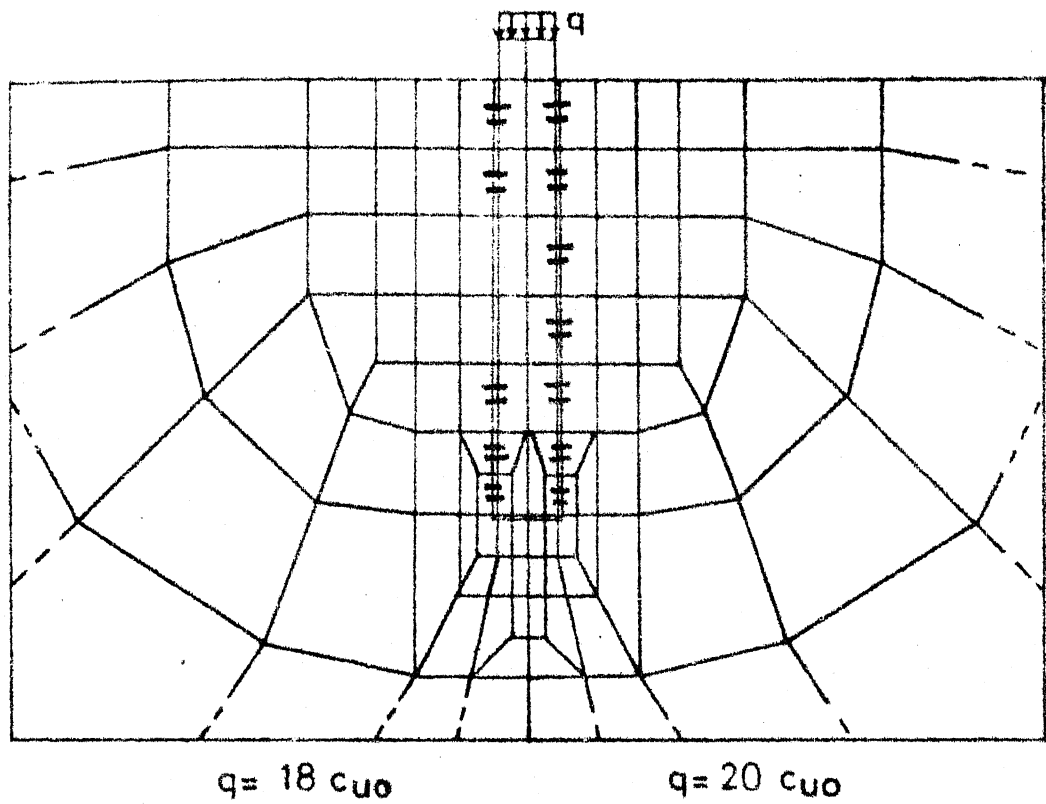
q= 18 c_uo   q= 20 c_uo
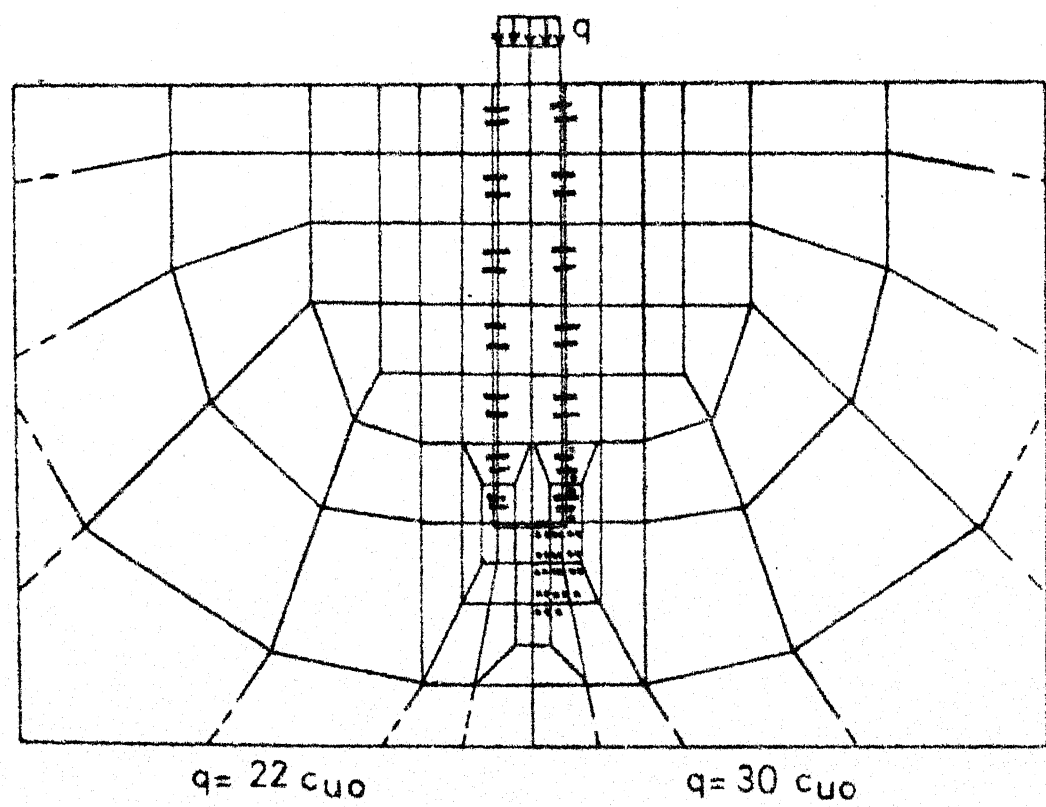
q= 22 c_uo   q= 30 c_uo

Fig. 4.22   SPREAD OF PLASTIC ZONE (RUN P8)

$q= 36\ c_{uo}$ $q= 40\ c_{uo}$
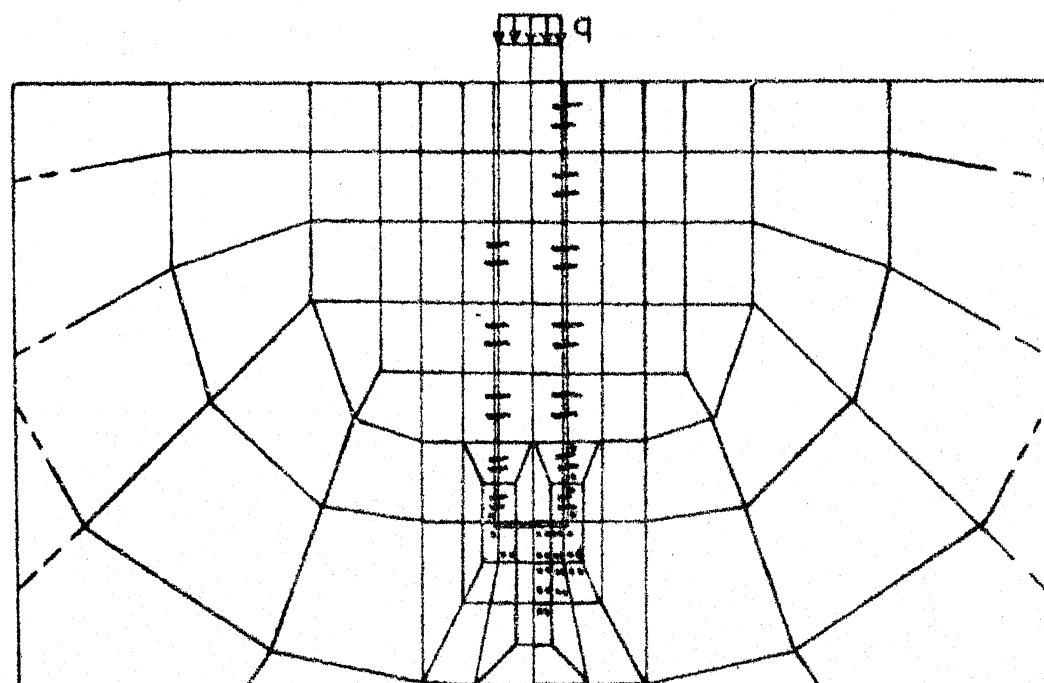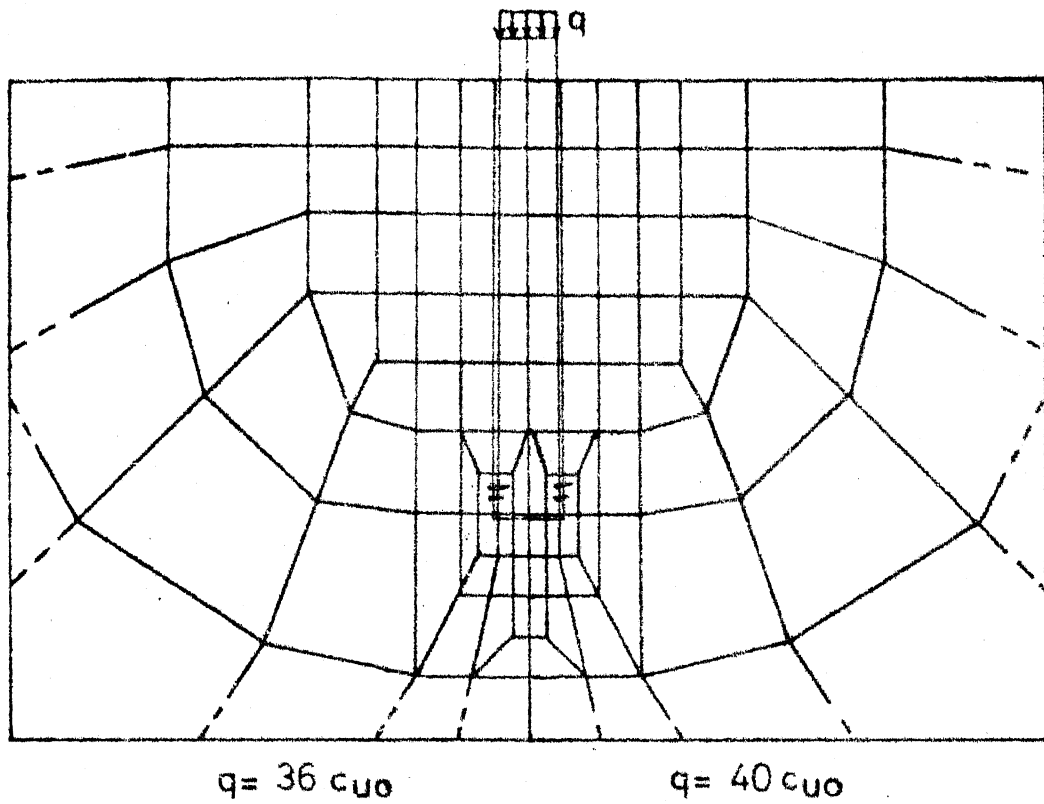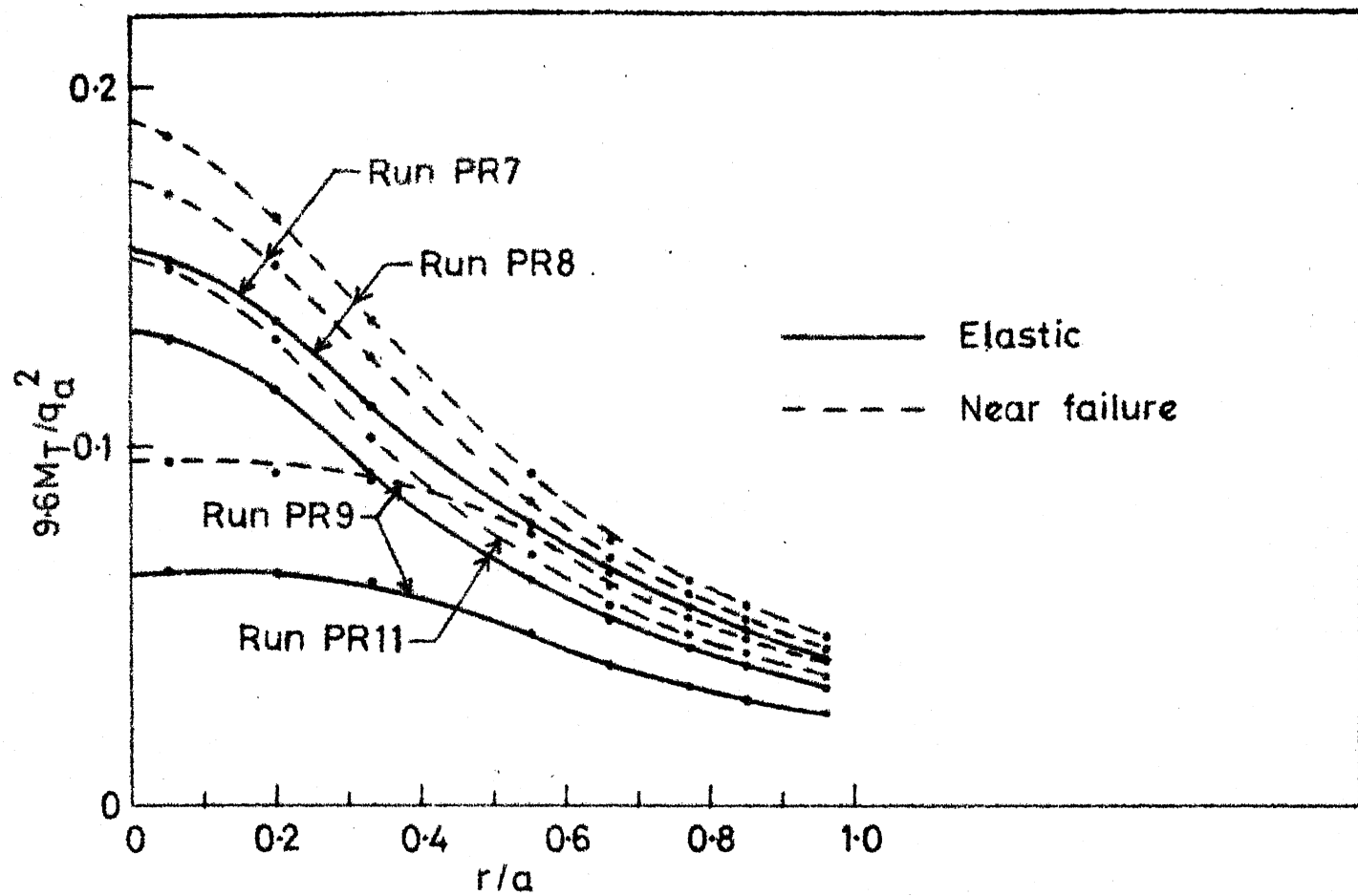
FIG.4·24(a)   Bending moment Vs r/a
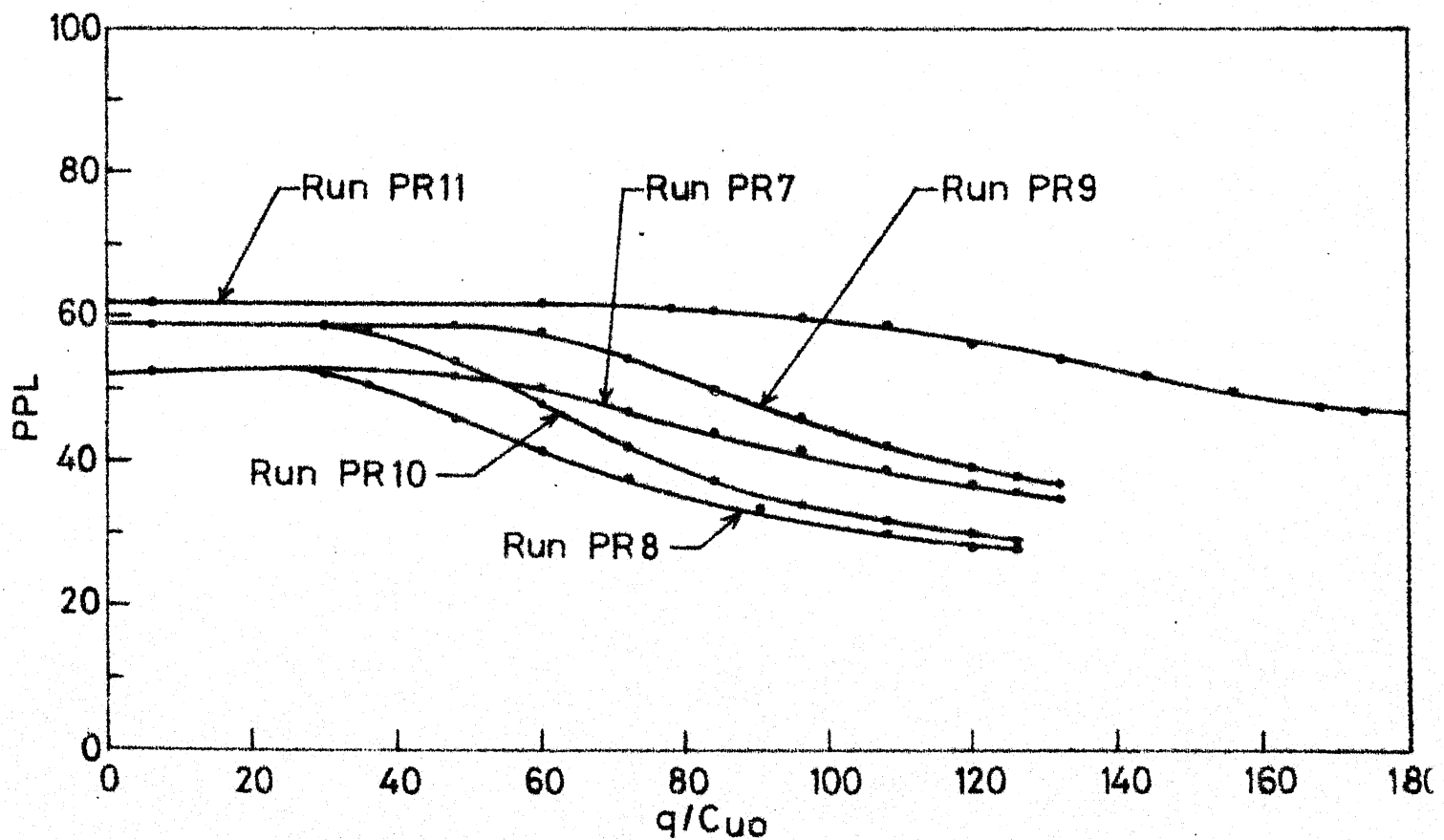
FIG.4·24(b)   Percent pile load (PPL) Vs applied pressure

$q = 36\ c_{uo}$ $q = 60\ c_{uo}$
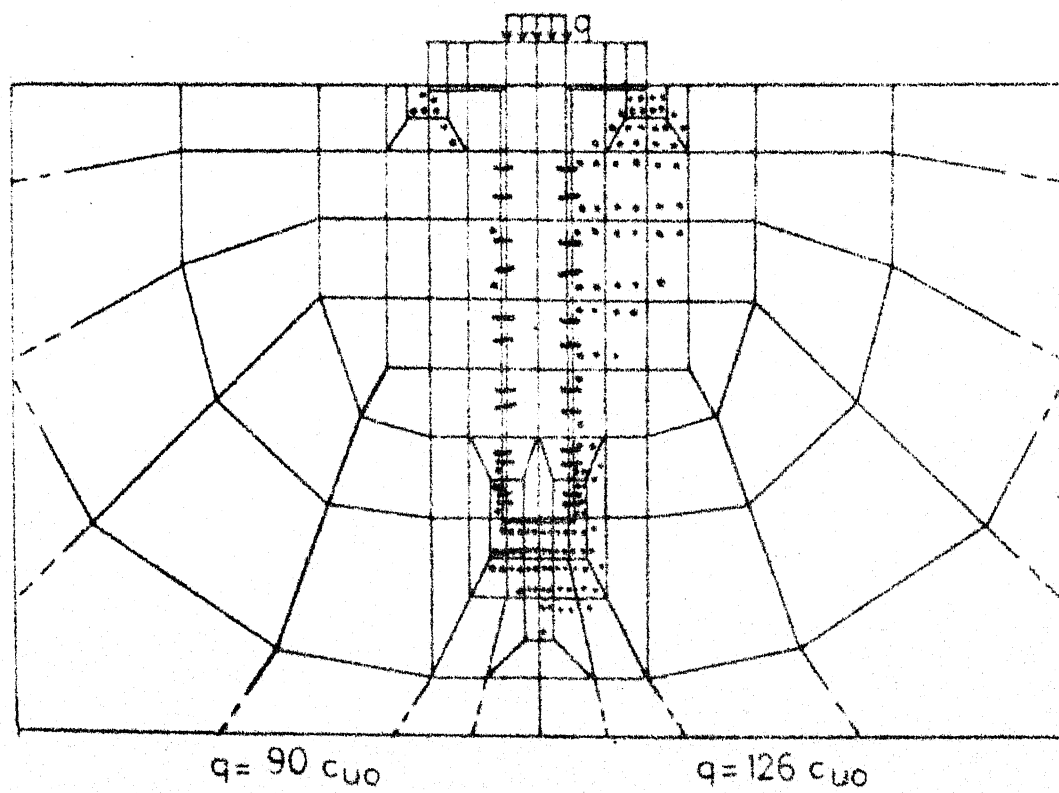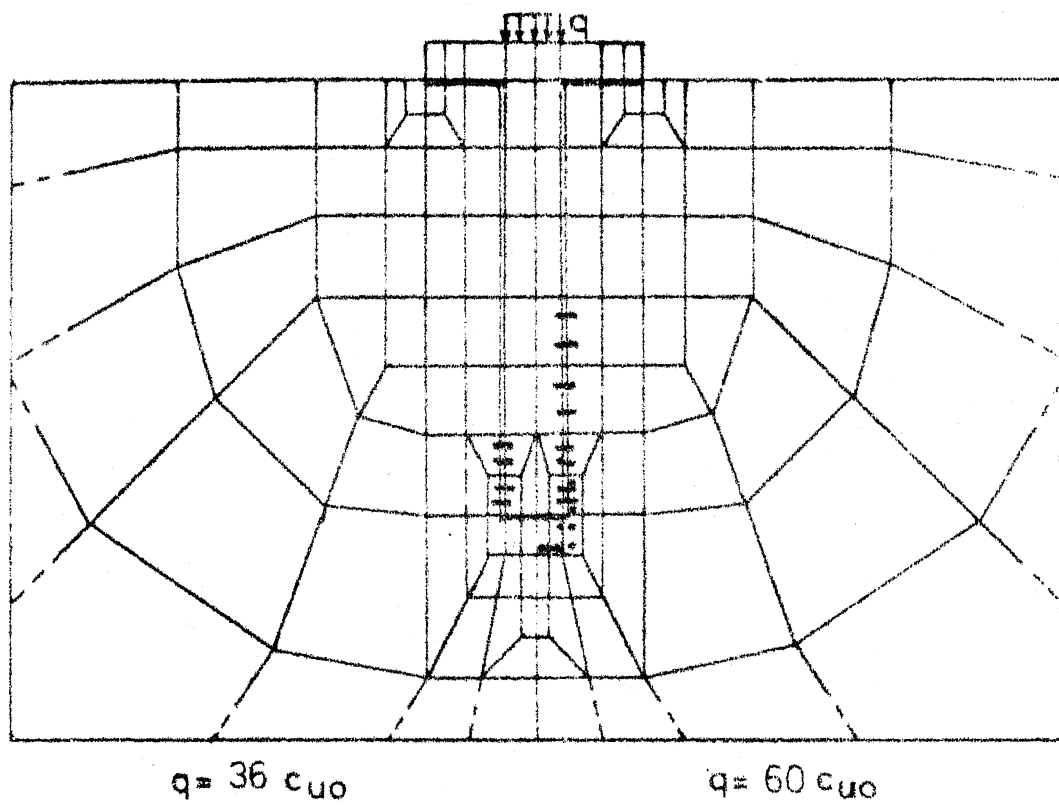
$q = 90\ c_{uo}$ $q = 126\ c_{uo}$

Fig. 4·25 SPREAD OF PLASTIC ZONE (RUN PR 7)
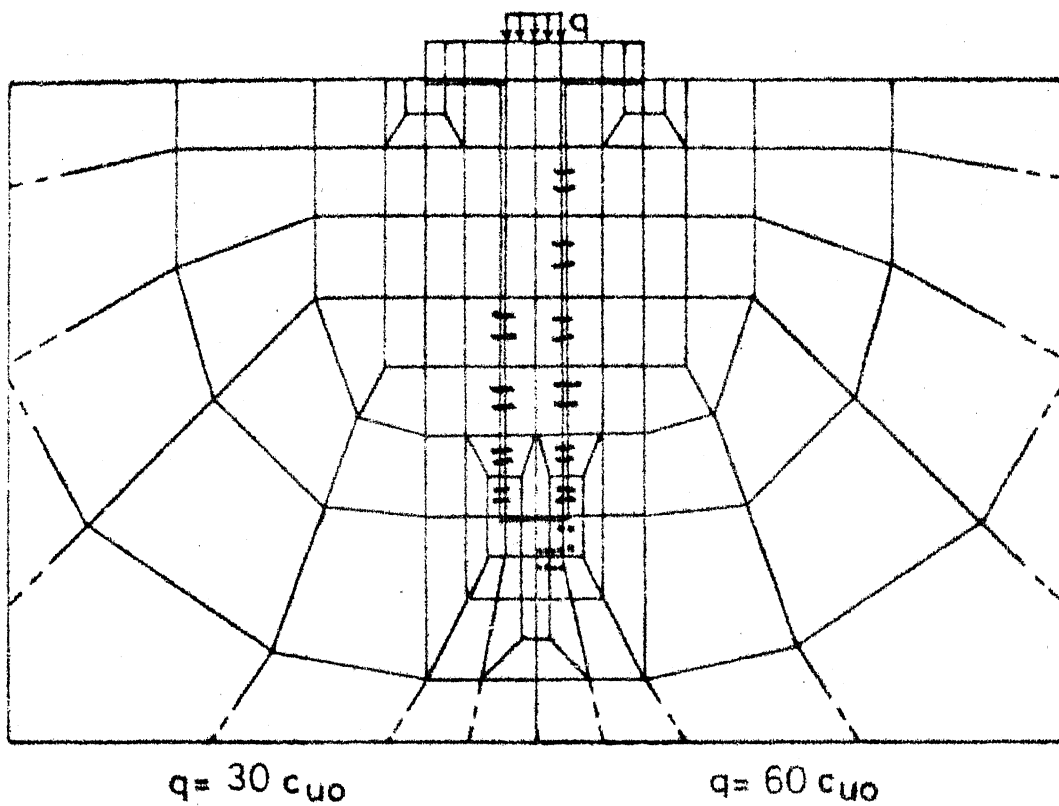
q= 30 c_{uo}   q= 60 c_{uo}
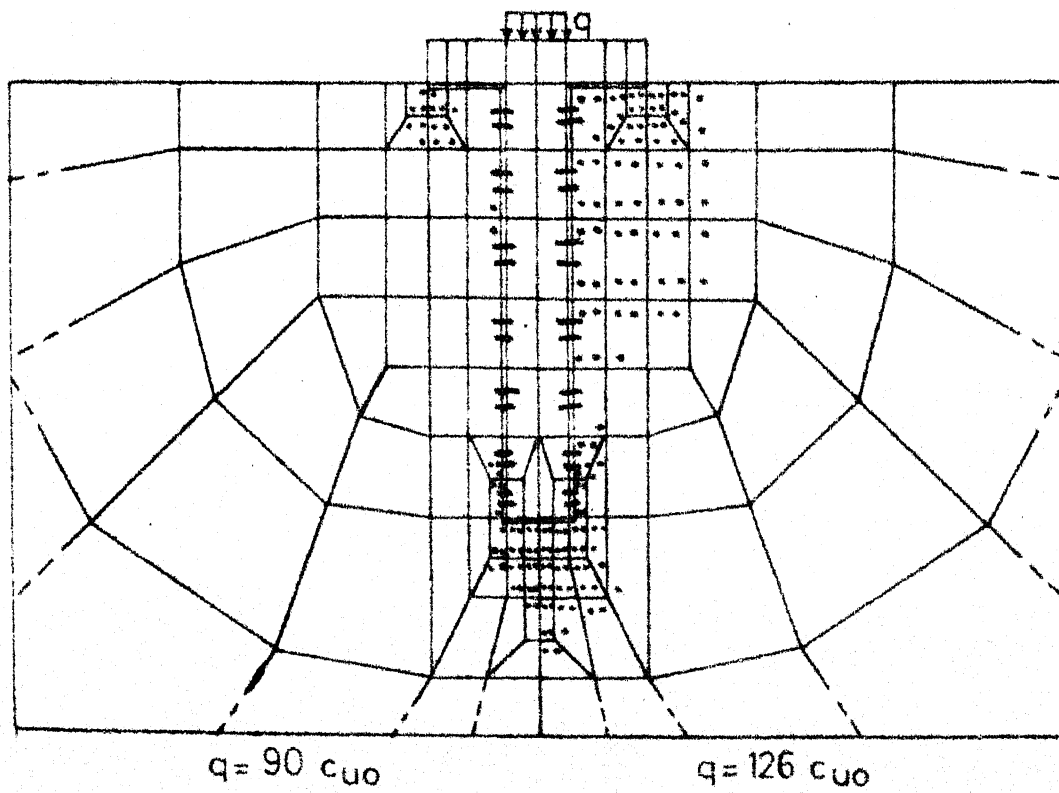
q= 90 c_{uo}   q= 126 c_{uo}

Fig. 4·26   SPREAD OF PLASTIC ZONE (RUN PR 8)
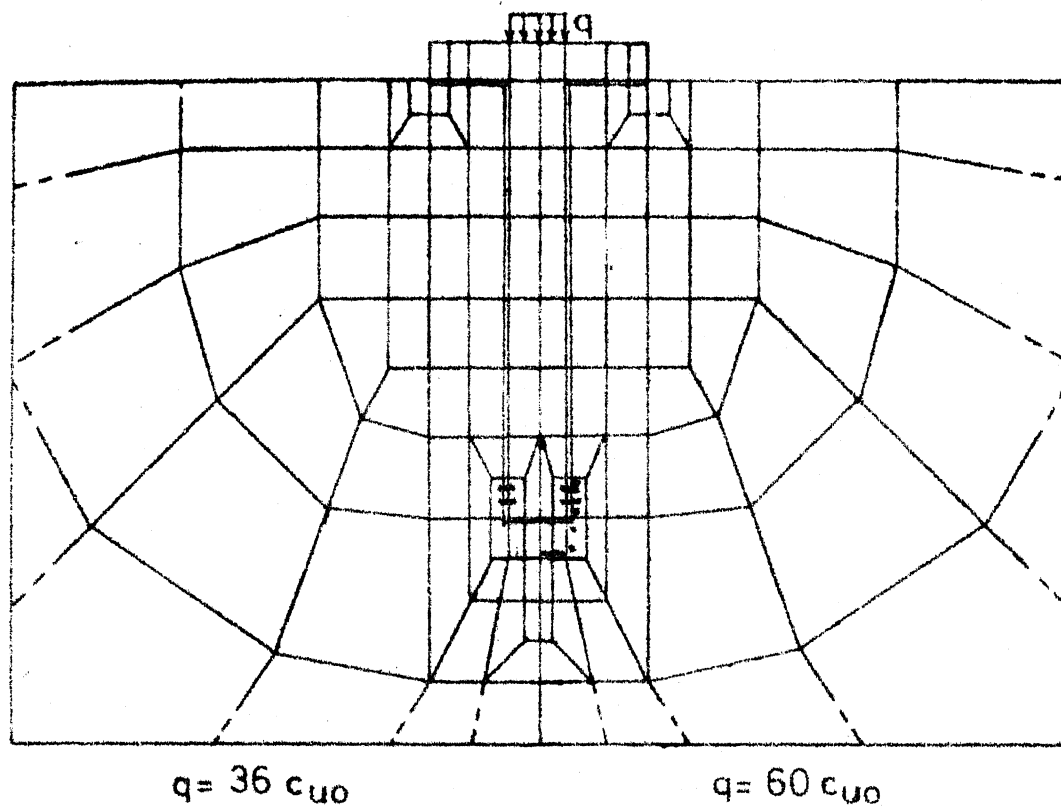
q= 36 c_uo   q= 60 c_uo
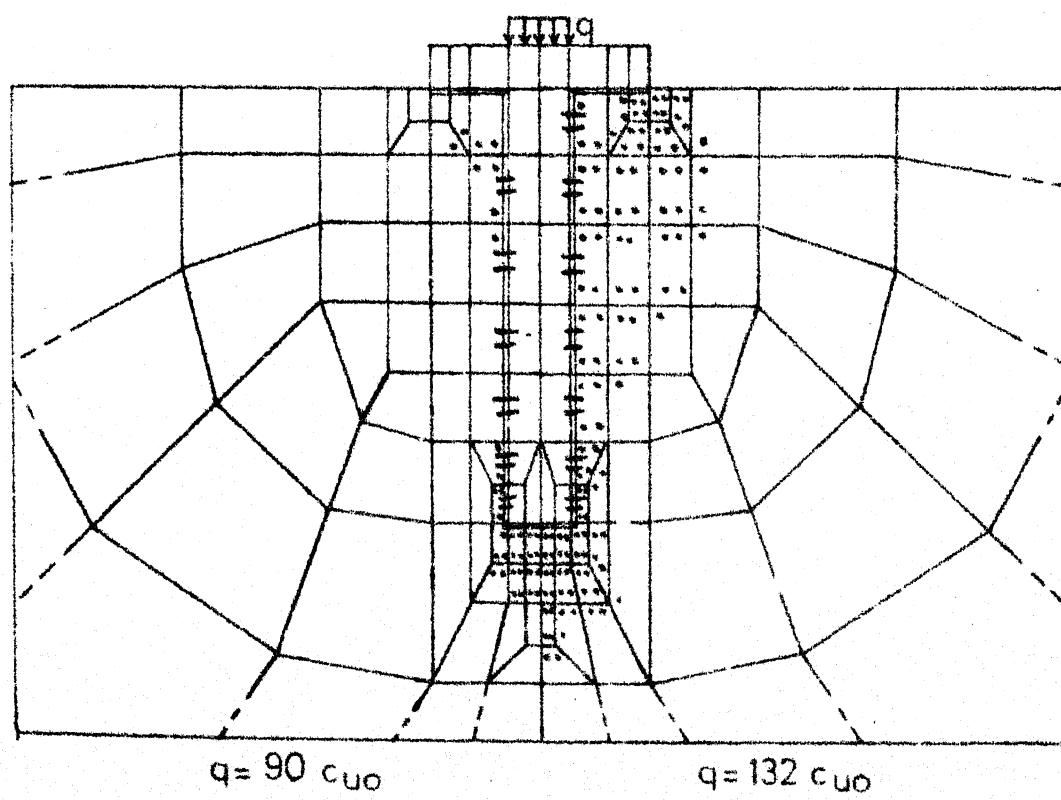
q= 90 c_uo   q= 132 c_uo

Fig. 4·27   SPREAD OF PLASTIC ZONE (RUN PR 9)
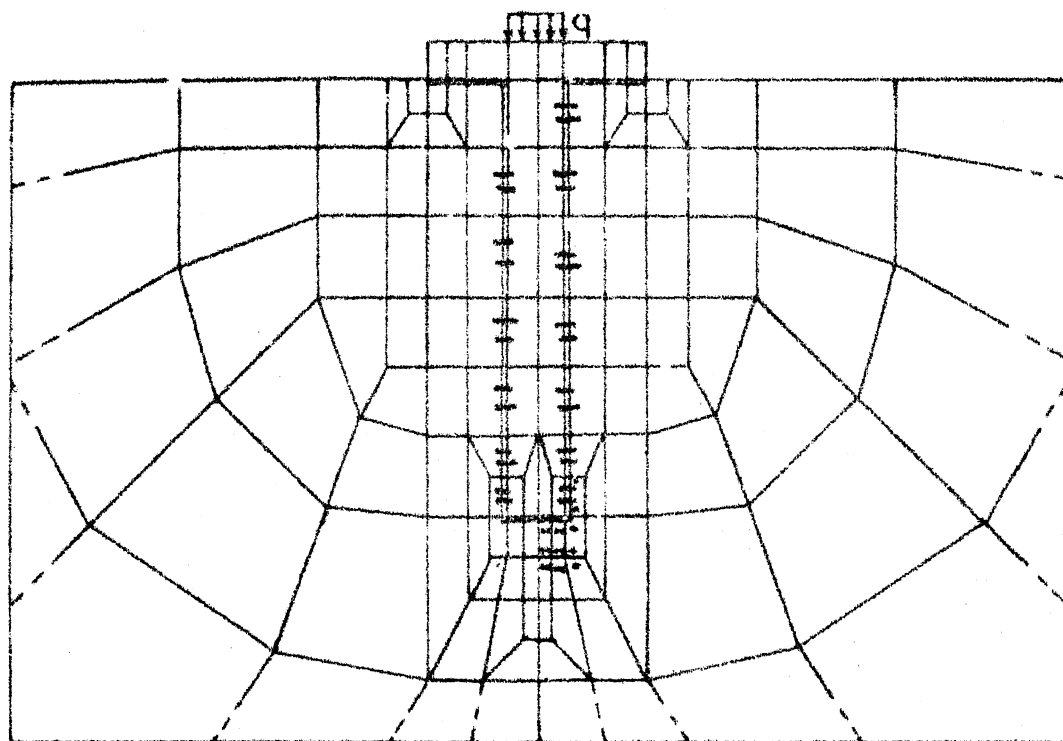
$q = 36\,c_{uo}$ $q = 60\,c_{uo}$
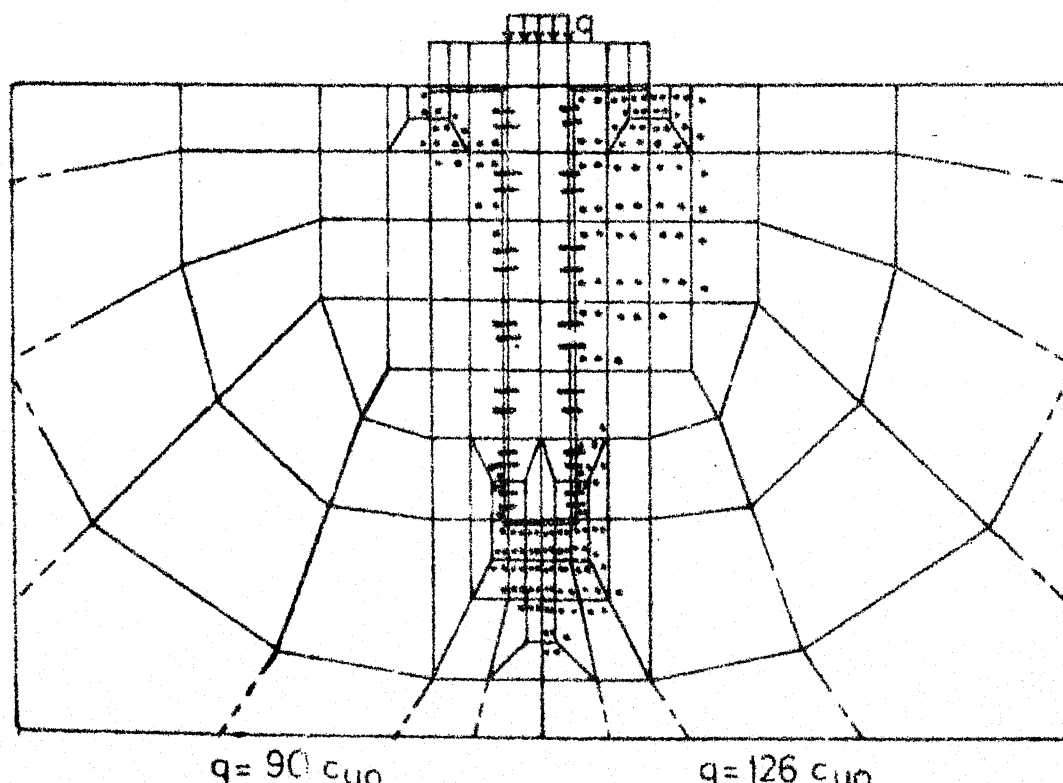
$q = 90\,c_{uo}$ $q = 126\,c_{uo}$

Fig. 4·28   SPREAD OF PLASTIC ZONE (RUN PR 10)

q= 60 c$_{uo}$ q= 90 c$_{uo}$

q=120 c$_{uo}$ q=174 c$_{uo}$
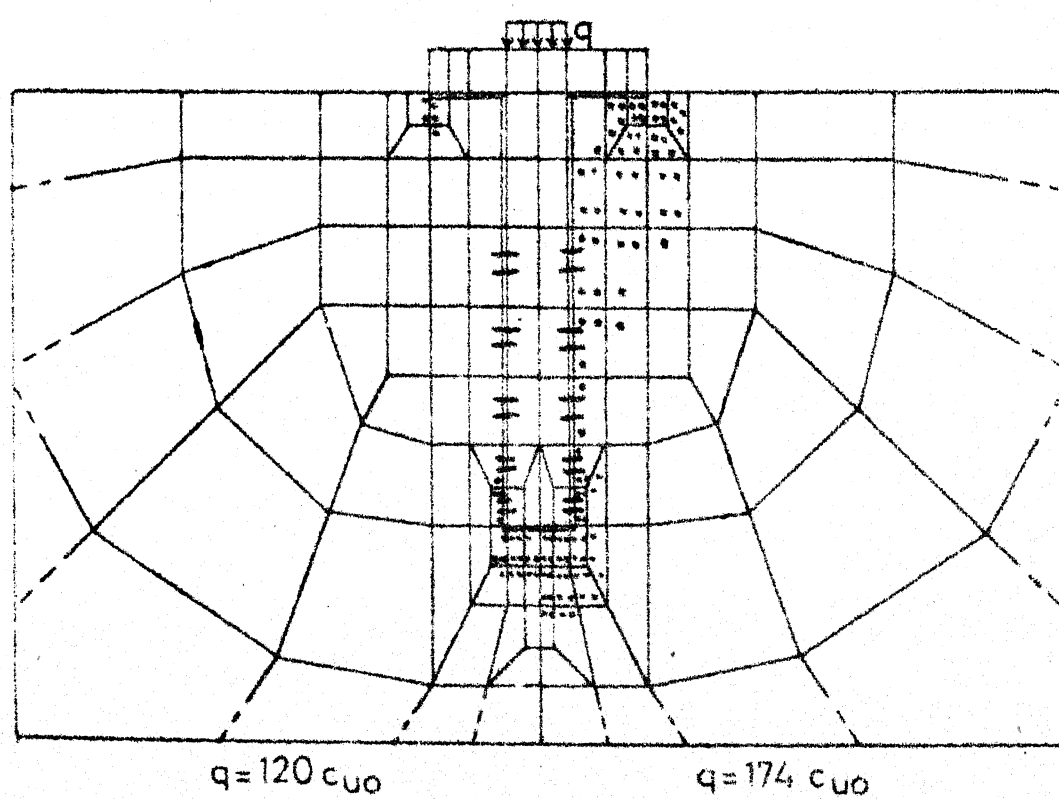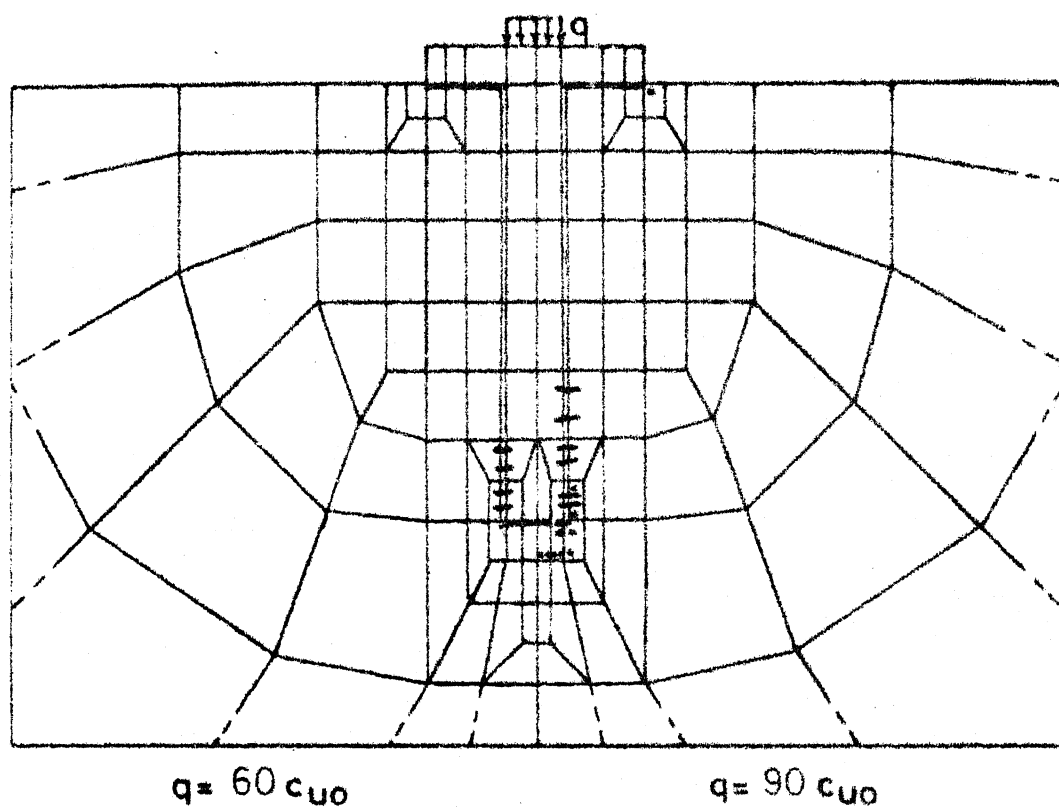
Fig.4·29   SPREAD OF PLASTIC ZONE (RUN PR11)

CHAPTER 5

SETTLEMENT ANALYSIS OF PILE GROUP AND PILE-RAFT

UNDER DIFFERENT SOIL CONDITIONS

5.1 INTRODUCTION

Methods available for determining the settlement of pile-raft (raft is in contact with the soil medium in addition to being a pile cap) and pile group (free standing), set in elastic continuum can be broadly listed as follows.

1. Three dimensional finite element analysis Ottaviani(98)).

2. Boundary element method (Butterfield and Banerjee (24), Banerjee (7), Banerjee and Butterfield (8), and Banerjee and Davies (9)).

3. Interaction factor method (Davis and Poulos (56), Poulos (108), and Poulos (109).

Three dimensional finite element analysis can be used to handle any complex situation in soil and/or foundation. But it is very expensive even if a linear analysis is attempted. Ottaviani (98), has done linearly elastic analysis of a small group of 3^2 piles and the computation time required was 200 minutes. Non-linear analysis may be prohibitively costly. Also, seperate analysis is required for each individual geometrical configuration of the system.

Boundary element method is limited for cases for which complete solutions are available for point load anywhere inside the medium. Also, if applied to pile group, this method requires seperate analysis, for each individual case as 3 dimensional finite element method. Accordingly this method may also be expensive if a number of cases are to be studied.

One of the relatively economical method is probably 'interaction factor method' (Poulos (107)). This method requires the determination of settlement of 'single unit' under unit load, which may be termed as 'Influence Coefficient (factor)'. For free standing pile groups, 'single unit' refers to single free standing pile and for pile-raft 'single unit' refers to single pile with a square or equivalent circular cap whose plan area is equal to square of the spacing(s) between the piles, for square arrangement of piles. Also, it requires the determination of 'interaction factors' between two such units. 'Interaction factor' denotes the additional settlement of the unit in question due to unit load on the other units. Influence factors and interaction factors have been discussed and results have been presented by Poulos and Davis (111), for wide range of parameters, for homogeneous isotropic elastic half space. These factors have also been presented by Poulos (109), for certain cases of soil non-homogeneity,

computed after making certain approximation for the case
of free standing piles. Approximate method of determining
the influence factors and interaction factors have also been
described by Randolph and Wroth (114), which can also be used
for problems concerning non-homogeneous soil. However, these
approximate methods of determining interaction factors, have
been used mainly for 'Gibson' type soils (Poulos (109),
Randolph and Wroth (114)). Banerjee and Davies (9) have
also solved some pile group problems for this type of soil.
Banerjee and Butterfield (8), have solved a particular case
of pile group in a multi-layered soil medium, using boundary
element method. The effect of cross-anisotropy does not
appear to have been studied for piled foundations. The
interaction factors have not been presented for pile-cap units
set in non-homogeneous or anisotropic soil.

If a pile-raft of any arbitrary geometry and stiffness
is to be analysed, it requires the determination of some more
interaction factors (Hain and Lee (68) and Wiesner and Brown
(144)). Knabe (80) has proposed a general method of analysis
of pile-raft system; but this method requires a number of
finite element analyses, for analysing a single case. However,
Knabes' (80) method can be used for analysing pile-raft set
in non-homogeneous and/or anisotropy soil. The above analys s

are likely to be expensive, compared to Poulos and Davis (111)
analysis, particularly so, if soil is arbitrarily layered
and/or anisotropic, as these methods would require a number of
finite element analyses for the determination of interaction
for each case, or would require three dimensional finite
element representation of soil (Hain and Lee (68)). For
square arrangement of piles, the procedure described by Davis
and Poulos (56) have been shown to be adequate if the cap is
perfectly rigid or perfectly flexible (for uniformly distri-
buted loading), if only settlements are required (Brown et al
(17)). So this method has been used for the analysis of pile-
raft herein. Two dimensional idealisation may be possible
for certain configuration of pile-raft. One such case has
been solved using axi-symmetric finite elements, in
Chapter 6.

In this Chapter linear interaction factor method of
analysis of Poulos and Davis (111) is extended to handle
any arbitrary layering of soil and/or any arbitrary variation
of modulus with depth and/or anisotropy, by combining finite
element method. Also, a 'non-linear interaction factor method
of analysis' is described. A number of cases of pile groups
and pile-rafts with square arrangement of piles, set in
different types of soil (homogeneous, non-homogeneous and

transversely isotropic) have been solved by the proposed methods. Comparison has been made with available solutions in some cases. Effect of different parameters, on the behaviour of pile group and pile-raft has been discussed in detail.

5.2 METHOD OF ANALYSIS

5.2.1 Linear Elastic Analysis

5.2.1.1 Interaction factor:

The interaction factor (I_{ij}) is defined as follows.

I_{ij} = settlement of ith unit due to unit load on jth unit (Fig. 5.6).

When $i = j$, I_{ij} equals the influence factor.

(I_{ij} may be more correctly called as interaction coefficient. Since interaction factor is more familiar term, it has been used throughout. However interaction coefficient can be converted into interaction factor (α) readily by dividing it by the settlement of single unit due to unit load).

The above definition of interaction factor is slightly different from that of Poulos and Davis (111), who have defined interaction factor based on two equally loaded units. Cooke et al.(36) have used the present definition of interaction factors successfully in their experimental investigation.

It is assumed in this work that the presence of piles can be ignored, while computing the interaction fac-tors. Hence the interaction factor at any distance r can be computed from the settlement of soil at radial distance r, due to unit load on the unit in question. So the values of I_{ij}, can be determined from an axisymmetric finite element analysis of single unit or from field test of single unit (as in Fig. 5.1(c)). Interaction factors have also been computed using finite element analysis, neglecting the presence of piles as done herein, by Randolph (154)* also, in the case of piles subjected to lateral loading. The error due to this assumption is likely to be more for closer spacing of piles than for larger spacing as pointed out by Cooke (34), who has made same assumption and has used field load test data for the assessment of interaction factors.

Since a condensation procedure described in Appendix A was used, the influence factors and interaction factors were obtained for capped units of different cap rigidities subjected to different loading and also for single free standing pile from the same run. The essential advantage

----

* This reference appeared when this part of work of thesis was completed.

of the present method of computing the interaction factors
is that computation for non-homogeneous and/or anisotropic
soil condition does not pose any special problem.

5.2.1.2 Method of analysis

Once influence factors and interaction factors are
determined the computation of settlement of pile group and
pile-raft can be done as described by Poulos and Davis (111).
The computation procedure is briefly described below.

The load-settlement relation can be written as

$$[I_{ij}] \{P_i\} = \{\delta_i\} \qquad (5.1)$$

$$\sum_{i=1}^{M} P_i = P \qquad (5.2)$$

where $[I_{ij}]$ = influence and interaction factor matrix
                (flexibility matrix)

   $\{P_i\}$ = the load vector

   $\{\delta_i\}$ = settlement vector.

Equations 5.1 and 5.2 can be solved to determine the settle-
ment vector for either perfectly rigid or perfectly flexible
cap condition. In the former case the vector $\{\delta_i\}$ contains
equal terms δ_0 and vector $\{P_i\}$ unknown.   In the latter
case $\{P_i\}$ is known and $\{\delta_i\}$ is unknown.

5.2.2 Non-linear Interaction Factor Method

5.2.2.1 General

In a pile group with rigid cap the load carried by edge piles are considerably more than the average load and the load carried by these piles may exceed its ultimate bearing capacity, even under working load conditions in some cases. This point has been observed in the theoretical results given by Poulos and Davis (111), as well as from the present analysis and also from field studies by Cooke et al (37,38). In a pile-raft, the applied load may be equal to or even more than the ultimate bearing capacity of free standing piles. Possibility of pile loads exceeding its bearing capacity is more for such pile-rafts. This necessitates non-linear settlement analysis of pile groups and pile-rafts. To make a rigorous non-linear analysis of pile groups and pile-rafts. 3-dimensional non-linear finite element analysis is required, which is very costly. Also due to uncertainty in the accuracy of the parameters determined from testing of small samples due to disturbance and difference in laboratory and field stress paths, such an expensive analysis may not always be justified. So a simplified non-linear interaction factor method of analysis is described below.

5.2.2.2 Assumptions

Influence factors and interaction factors are affected by failure of soil around the unit in question and not affected by the failure of soil near other units. This assumption is likely to be satisfied if the spacing is not close and failure takes place over a small zone around pile only. This assumption might be satisfied in most of the practical cases in the working load range. Davis and Poulos (56), have also made these assumptions in their analysis of pile-rafts, but they have used constant interaction factors (as per their definition), over the entire range of loading. They have varied the influence factors only, depending on load. In the proposed analysis, the interaction factors can also be varied depending on the load range.

Superposition is assumed to be valid and it is likely to be fairly satisfied for working load range, as the failure zones may be small compared to the overall continuum participating in transmitting the load. Davis and Poulos (56) have also made this assumption in their analysis of pile-raft and this assumption is unavoidable in such methods. Implication of this requires verification by model/field studies.

5.2.2.3 Determination of interaction factor

Determination of these factors is the most important part in the analysis and the subsequent computation part is

straight forward. These factors may be obtained either from field load tests or theoretically by elasto-plastic finite element analysis of single unit. Both of these procedures are described below.

After installing the group of piles, load tests may be performed in the field on a few representative units. (The unit may be single free standing pile or single pile with a square cap, which forms a typical unit of pile-raft system). Complete load-settlement curve of such units may be obtained from load tests. The settlement of other piles due to load on the pile in question may also be measured, from which the interaction factors for different load ranges can be assessed. It may be noted that the interaction factors for the actual pile reinforced continuum is obtained. The instruments developed recently, for the accurate determination of small displacements (Cooke et al (36)), may be very useful for such field measurements. Theoretically load test has to be carried out on each unit. Since soil is usually horizontally layered, by testing a few representative units at corner, middle of the edge and centre of the group, the different interaction factors can be assigned. For example, for a group of 4^2 piles, only 3 units need to be tested. The load settlement curves can be approximated into

multi-linear portions (as in Fig. 5.4). A tri-linear
approximation is expected to be sufficient for most of the
cases, as observed from the shape of load-settlement curve
of single unit, obtained by elasto-plastic finite element
analysis (Fig. 5.3). Corresponding to each linear portion,
the interaction factors I_{ij}, can be assigned, for different
units from the measured settlement of different piles, due to
load on other piles.

Alternately, the influence factors and interaction
factors for different loading ranges may also be obtained
from incremental elasto-plastic finite element analysis of
single unit. Part of the results of one such analysis is
shown in Fig. 5.3. The load settlement curve obtained can be
divided into multi-linear portions. The interaction
settlement curve for $r = 1.125 \, d_c$ (where r is the radial
distance from centre and d_c is the diameter of the cap),
is shown in this figure. Similar curves for required values
of r can be plotted. From these curves, the values of
I_{ij}, for different values of r can be computed, for different
load ranges, which can be used in a general non-linear
analysis explained subsequently.

However, a bilinear approximation was used herein to
illustrate the method, for pile-raft. The bilinear

approximation used is also shown in Fig. 5.3. The same bilinear approximation was used in the calculation of settlement of piled circular footing as explained in Chapter 2. Therein, the said approximation was arrived at from an approximate (excess load cut-off) elasto-plastic analysis. From Fig. 5.3, it is observed that the same approximation fits satisfactorily with the results of elasto-plastic finite element analysis, using von-Mises yield criterion. The details of this analysis has been explained in Chapter 4. From the interaction settlement curve, it is also seen that the same approximation is satisfactory for interaction factors also. Hence, it is assumed that the first linear portion extends upto a load of P^1_{max}.

where

$$P^1_{max} = (UBC + UBC/PPL)/2 \qquad (5.3)$$

in which

   UBC = ultimate bearing capacity of pile

   PPL = percentage load shared by pile.

The slope of the first portion corresponds to the elastic stiffness of pile-cap unit. The interaction factors also correspond to the elastic interaction factors of a single unit. The slope of the second portion corresponds to the elastic stiffness of circular raft. Interaction factors

for second portion also correspond to those of circular raft. These factors were obtained from elastic analysis of single unit and circular raft.

It can be observed from Fig. 5.3, that the interaction settlement does not increase as settlement of the unit does, for greater loads. Or in other words interaction is less as plastic zone spreads. This is because, as the soil fails, the settlement of the unit increases; but this effect is local. The effect at locations away from the unit is less pronounced. This aspect does not appear to have been considered in the non-linear interaction type analyses reported (Davis and Poulos (56), O'Neill et al (97) and Awoshika and Reese (4)).

Interaction factors can also be obtained from the field load test of single unit and measurement of settlement at different radial distances before the installation of the entire group of piles, ignoring the presence of other piles, as done in the theoretical method explained above.

5.2.2.4 Method of non-linear analysis

If the load settlement curve and interaction settlement curves are assumed to be multi-linear (with N linear portions), as in Fig. 5.4, the load settlement relation of

the system containing M units can be written as,

$$[I_1] \{P^1\} + [I_2] \{P^2\} \ldots [I_i] \{P^i\} \ldots$$
$$\text{MxM} \quad \text{Mx1} \qquad \text{MxM} \quad \text{Mx1} \qquad \text{MxM} \quad \text{Mx1}$$

$$\ldots + [I_N] \{P^N\} = \{\delta\} \qquad\qquad (5.4)$$
$$\text{MxM} \quad \text{Mx1} \qquad \text{Mx1}$$

where $\{P^i\}$ and $[I_i]$ are the load vector and interaction factor matrix, for the ith linear portion, respectively. Different terms in matrix $[I_i]$ can be obtained from inverse of slope of curves like those shown in Fig. 5.4, for the ith linear portion. For example, in $[I_i]$, I_{jj} is the inverse of slope of curve A, and I_{kj} is the inverse of the slope of curve B, in Fig. 5.4, $\{\delta\}$ is the settlement vector. Subscript j refers to the jth unit. $P^i_{j\ max}$ refers to the maximum load range for ith linear portion and for jth unit.

If the cap is assumed to be completely flexible, $\{P^T\}$ is known. Direct substitution of P^i_j, in equation 5.4 gives the settlement of different units. It may be noted, that $P^i_j \leq P^i_{jmax}$ and $P^T_j = P^1_{jmax} + P^2_{jmax} \ldots + P^i_j$, where P^T_j refers to the total load on jth unit.

If the cap is assumed to be perfectly rigid, the Eq.5.4 will have to be solved along with the following boundary conditions.

$$\{ \delta \} = \delta_o (11 \ldots 1)^T \tag{5.5}$$

$$\sum_{\substack{j=1,M \\ i=1,N}} (11 \ldots 1) \{ P_j^i \} = P \tag{5.6}$$

where P is the total applied load and δ_o is the settlement of rigid cap.

In this case $\{ P_j^i \}$ are unknowns. Solution is obtained by iteration as follows.

Initially all $\{ P_j^i \}$ except $\{ P_j^1 \}$ are made zero. Eq. 5.4, 5.5 and 5.6 are solved for δ_o and $\{ P^1 \}$. If P_j^1 exceeds $P_{j\ max}^1$, P_j^1 is made equal to P_{jmax}^1 and P_j^2 is treated as unknown. Again it is resolved to obtain new values of δ_o and $\{ P^i \}$. If any P_j^i exceeds P_{jmax}^i, P_j^i is made equal to P_{jmax}^i and P_j^{i+1} is treated as unknown. The iterations are continued till, all the values of P_j^i are less than or equal to P_{jmax}^i. Always there would be (M+1) unknowns, where M is the number of units (i.e. M number of unknown loads P_j^i and one value of δ_o).

By computing the settlements for different values of applied load P, it is also possible to trace the load-settlement response of pile group or pile-raft.

5.2.2.5 Bilinear analysis

The bilinear analysis used herein for illustration is a special case of general non-linear analysis described above

(where N = 2). A detailed description of computation procedure for this analysis is presented in Appendix E. Such analysis may be useful in the preliminary stage of design. For homogeneous soils, the relevent interaction factors have been given by Poulos and Davis (111), for pile-cap (Rigid) units for semiinfinite elastic continuum. The influence factors and interaction factors for circular raft, which are required to model the second portion of the bilinear idealisation (5.2.2.3) can be obtained from Poulos and Davis (110). For problems involving layered soil, modulus varying with depth, anisotropic soil etc., these factors can be obtained by axi-symmetric finite element analysis, as has been carried out in the present work (Sec. 5.2.2.3). For more rigorous analysis, interaction factors obtained from field load tests or from elasto-plastic analysis of single units, as explained earlier, may be used, in a tri-linear or multi-linear analysis.

5.2.2.6 Limitations and advantages

The limitation of the method described, in the case of pile-raft, is that the analysis requires the assumption of square arrangement of piles. Another limitation is, that the cap is assumed to be either perfectly rigid or flexible. However, if the cap is of finite rigidity, the problem can

be solved for the two extreme cases of perfectly rigid or flexible cap, which gives the bounds of the solution.

Essential advantages of the proposed method are,

1. It is economical, once the influence factors and interaction factors are determined, the computing cost is negligible, compared to 3-dimensional finite element analysis. It was observed that the bilinear analysis carried out, required only 2 or 3 iterations to get the results.

2. It is possible to use the actual field load test results rather than to rely on laboratory test results on small representative samples.

5.2.3 Computer Programs Developed

Three computer programs were developed for the analyses reported in this Chapter, with the following capabilities.

1. Linear 'interaction factor' analysis of pile group with rigid cap. (Program RIGPG).

2. Bilinear interaction factor analysis of pile-raft with rigid cap (Program RIGPR).

3. Bilinear interaction factor analysis of pile-raft with flexible cap (Program FLEXPR). In all the three programs, the influence factors and interaction factors are to be fed

as input data. The program interpolates the interaction factors for required values of r (radial distance) using the values at three points, so that the middle point is near r. Then the program computes the settlement of pile group/pile-raft, values of R_G and R_S and load shared by individual piles, for different pile group/pile-raft configurations.

5.3 FINITE ELEMENT ANALYSIS

Details of finite element analysis used to study the behaviour of piled circular footing, single pile and circular raft have been described in Chapter 2. Results concerning the behaviour of such units were discussed therein. From the same analysis, the interaction factors were also obtained for circular raft, single pile and piled circular footing, as explained in Sec. 5.2.2.3.

For analysis of pile-raft with rigid cap the interaction factors were taken from the analysis of circular raft and piled circular footing with $K_R = 100$ (K_R is the relative rigidity of the footing or raft as defined in Eq. 2.1 in Chapter 2). For analysis with flexible cap, the results from the analysis with $K_R = 0.1$ were used.

The details of elements used, mesh etc., have been presented in Chapter 2. It was found that satisfactory

results of interaction factors (By comparing with the factors given by Poulos and Davis (111)) can be obtained, if the right hand side boundary was kept at a distance of, at-least equal to twice the length of pile (For mesh, Fig. A.1 in Appendix-A). It was also found that if the layer depth is large compared to the right hand side boundary, the interaction factors are more sensitive to the type of right hand side boundary (free or restrained). In such cases, the interaction factors computed by taking average of values for free and restrained right hand side boundary was found to give satisfactory results. It was also observed that, when the right hand side boundary was restrained in the horizontal direction, the interaction factors near the right hand side boundary became negative. Due to these reasons the right hand side boundary was kept free at 50d from the centre line (d is the diameter of pile), as $L/d = 10$ and $L/d = 25$, have been considered, in the present work. The bottom rough rigid boundary was kept at 80d, from the ground level.

5.4 PARAMETERS CONSIDERED

5.4.1 General

Solutions have been obtained for pile group and pile-raft, consisting of square arrangement of piles with 2^2, 3^2, 4^2, 5^2 and 6^2 units, set in homogeneous, non-homogeneous

and cross-anisotropic soil medium. The geometry of the problem for a typical case of pile group and pile-raft consisting of 4^2 units are shown in Fig. 5.6. If s is the spacing of the units, the equivalent diameter (d_c) of single unit for pile-raft is given by,

$$s = \sqrt{\pi} \ \ d_c/2 \tag{5.7}$$

Following parameters were considered:

No. of units = 2^2, 3^2, 4^2, 5^2 and 6^2 for d_c/d = 5

No. of units = 2^2, 3^2 and 4^2 for d_c/d = 10

η = 0.5, 1 and ∞.

where η = ultimate bearing capacity of single pile/applied load per single unit.

(η can be equal to or even less than 1 for pile-raft, as raft may contribute substantial bearing capacity).

Poisson's ratios of pile and cap material ν_p = 0.15.

The group factors R_G and R_S (Poulos and Davis (111) are defined as follows.

Group reduction factor (R_G) = settlement of pile group or pile-raft/settlement of single free standing pile, under the same total load.

Settlement factor (R_S) = settlement of pile group or pile-raft/settlement of single free standing pile for the same average load as a pile in the group.

$$K_R = 100 \text{ (for rigid cap)}$$

$$K_R = 0.1 \text{ (for flexible cap).}$$

5.4.2 Homogeneous Soil

$$L/d = 10 \text{ and } 25$$

$$d_c/d = 5 \text{ and } 10$$

$$K = 1500 \text{ and } 200$$

$$\nu_S = 0, 0.3 \text{ and } 0.47.$$

5.4.3 Transversely Isotropic Soil

The definition of anisotropic parameters have been given in Sec. 2.2.2, in Chapter 2.

$$L/d = 10 \text{ and } 25$$

$$d_c/d = 5 \text{ and } 10$$

$$K = 1500 \text{ and } 200$$

For incompressible material:

$$\nu_{SV} = 0.5, \qquad \nu_{SH} = 1 - n/2$$

$$n = E_{SH}/E_{SV} = 1, 1.5, 2.5, 3.5 \text{ and } 3.98.$$

$$m = 0.38.$$

For drained condition:

$$\nu'_{SV} = 0, \qquad \nu'_{SH} = -0.55, \qquad m' = 0.76, \qquad n' = 3.$$

(These parameters approximately correspond to undrained case with n = 2.5, as explained in Sec. 2.2.2, Chapter 2).

5.4.4 Non-homogeneous Soil

Definition of non-homogeneity parameters and description of different types of non-homogeneity considered have been given in Sec. 2.2.2, Chapter 2.

5.4.4.1 Modulus linearly increasing with depth (Fig.5.22)

ψ (Eq. 2.1b, Chapter 2)   = 2.5 and 10

K = 1500

L/d = 10 and 25, ν_S = 0.3.

5.4.4.2 Layered soil

A two layer soil medium in which a softer soil underlies a stiffer soil is considered (Fig. 5.26).

$K = E_P/E_{ST} = 400$

E_{ST}/E_{SB} = 5 in most of the cases.

E_{ST}/E_{SB} = 3 and 10 in some cases.

h/L = 0.1, 0.4, 0.5, 1.0 and 1.5

where

E_{ST} = Young's modulus of top soil

E_{SB} = Young's modulus of bottom soil

h = thickness of top soil layer

L/d = 10 and 25, d_c/d = 5 and 10

ν_S = 0.3.

5.4.4.3 Non-homogeneity due to the effect of installation

Method of considering this type of non-homogeneity, definition of parameters, description of symbols used etc., have been explained in Sec. 2.2.2, Chapter 2.

Sandy Soil:

I_0 = homogeneous soil

I_3 = modulus as shown in Fig. 5.32(a).

$d_c/d = 5$, $L/d = 10$, $K = 1500$ and $\nu_S = 0.3$.

Clayey soil:

I_0 = homogeneous soil

I_1, I_2, I_4 and I_5 = modulus as shown in Fig. 5.32(b).

I_2 and I_5 = refers to soft clay which may become stiffer
         due to the installation of driven piles.

I_1 and I_4 = refers to stiff clay which may become softer
         due to the installation of bored piles.

   K = 1500 for soft clay

   K = 500 for stiff clay

   ν_S = 0.47, $L/d = 10$, $d_c/d = 5$.

5.5   COMPARISON OF RESULTS

Some of the results obtained for homogeneous soil condition are compared with solutions given by Poulos and Davis (111) in Figs. 5.1 and 5.2 and Tables 5.1 to 5.6. It is seen in Figs. 5.1(a) and 5.1(b), that the interaction

factors computed from the axi-symmetrical finite element
analysis are in close agreement with those reported by
Poulos and Davis (111), for both free standing piles and
pile-cap units, for L/d = 10 and L/d = 25, if H/L was kept
equal to 8 (L is the length of pile and H is the thickness
of the soil layer). For L/d = 25 and H/L = 3.5, there is
some difference between the results of both the analyses.
This difference may be attributed to the effect of finite
layer and compressibility of pile.

In Fig. 5.2, the values of settlement factors
R_S (Sec. 5.4.1), for different free standing pile groups
are compared, with those obtained by Poulos and Davis (111).
The agreement is good for H/L = 8. Since there is no
solution available for a combination of finite layer and
compressible pile, exact comparison could not be made, for
such cases.

It was found, from a seperate analysis, that the
computed loads carried by individual piles, are not very
sensitive to the finite layer thickness, if the layer depth
is considerably large, compared to pile length. Hence
comparison of computed pile loads can be made. This may
be a more rigorous test of accuracy than comparison of
settlement (R_S). The computed values of loads taken by

individual piles are presented in Tables 5.1 to 5.6. A comparison of these results reveal that there is less than 4 % difference in pile loads for a spacing of 5d, for both K = 200 and 1500 and for both L/d = 10 and 25. For a spacing of 2d also, the difference is small except for the piles carrying very small loads, which are highly sensitive to the values of interaction factors. Hence, it can be concluded that the present method of obtaining interaction factors from finite element analysis, gives results of comparable accuracy as that of Poulos and Davis (111).

For closer spacing of piles, the results from both the methods are likely to be less accurate than in the case of larger spacing, as the physical presence of the piles, at the locations of which interaction factors are computed, is neglected in the present analysis and the presence of piles is completely neglected by Poulos and Davis (111). The essential advantage of the present method of assessing the interaction factors is that this procedure can be used in a straight forward manner to layered soils, anisotropic soils etc.

In Fig. 5.5, the results of present analysis and Poulos and Davis (111) analysis are compared for pile-raft (Rigid) consisting of different number of units, in a

square configuration. The settlements (R_G) are in good agreement for both L/d = 10 and L/d = 25, if H/L is equal to 8. The small difference in the case of L/d = 25, K = 1500 and H/L = 3.2, may be attributed to the effect of finite layer and compressibility (In Poulos and Davis (111) analysis values of both K and H/L have been taken as ∞).

5.6 RESULTS AND DISCUSSION

5.6.1 Homogeneous Soil

For homogeneous soil condition the effect of different parameters on free standing pile groups, has been discussed extensively by Poulos and Davis (111). Hence, pile-raft analysis only is discussed for this soil condition.

5.6.1.1 Pile-raft with rigid cap

Effect of pile compressibility:

It can be observed in Figs. 5.5 and 5.7, the effect of pile compressibility on R_G is very small for L/d=10 and quite considerable for L/d = 25, for pile-raft (rigid), consisting of larger number of units. The effect in the latter case is about 30 % for larger group and about 13 % for single unit when R_G for K = 200 and K = 1500 are compared

Effect of Poisson's ratio of soil (ν_S):

The effect of ν_S, on the value of R_G, is found to be

appreciable (Fig. 5.7). From Fig. 5.7, it is observed that the value of R_G for $\nu_S = 0$ is about 25 % more than that for $\nu_S = 0.47$, for $L/d = 25$, $K = 1500$ and $d_c/d = 5$. The ratios of R_G ($\nu_S = 0$)/R_G ($\nu_S = 0.5$) computed from the present analysis are compared with the values computed by Poulos and Davis (111), for rigid raft-incompressible pile system in a semi-infinite mass of soil, in Table 5.7. The comparison reveals that there is good agreement. The ratio of R_G ($\nu_S = 0.3$)/R_G ($\nu_S = 0.5$) computed from the present analysis was also found to agree with the results of Poulos and Davis(111) approximation, assuming linear variation of R_G with ν_S. (These ratios were 1.1 and 1.09 respectively). This indicates that the corrections for ν_S suggested by Poulos and Davis (111), are not very sensitive to finite layer and compressibility of pile, in the range of parameters considered ($K = 1500$ and H/L 3.2).

Load carried by individual piles:

The loads carried by individual pile-normalised with ultimate bearing capacity of single pile-computed from elastic analysis for certain parameters have been tabulated in Table 5.8, for $\eta = 1$. It can be seen from these results that the corner piles will have to carry load of about double the ultimate bearing capacity of piles. The piles

in the interior carry very small loads. This shows the necessity for some kind of non-linear analysis. If the soil is assumed to be clay in undrained condition, the bearing capacity of pile-raft is approximately equal to the sum of bearing capacity of piles plus that of raft in contact with soil (Sec. 4.4.4.1 and Poulos and Davis (111)). For the parameters used, for the analysis reported in Table 5.8, using conventional theory (Bowles (14)) the factor of safety works out to be 2.5. Hence this situation can occur in practice.

Effect of failure of piles:

The effect of failure of piles can be assessed from the results of bilinear analysis reported, for $\eta = 0.5$ and 1.0, in Figs. 5.5 and 5.7. Such effect of failure of piles, is more in cases in which pile is more dominant in the system and the value of ν_S is small (as seen in Figs. 5.5 and 5.7). For $L/d = 10$, the effect of pile failure is small (less than 10 $\%$), as seen in Fig. 5.5, for the cases considered. For $L/d = 25$ and $\nu_S = 0$, the effect of failure of piles is considerable; for $\eta = 0.5$, the pile failure increases the value of R_G by more than 50 $\%$ for 2^2 units and by 25 $\%$ for 6^2 units (Fig. 5.7). The effect of pile failure decreases as group size increases.

It can also be seen that the approximation suggested by Davis and Poulos (56) (Eq. 5.7), to account for pile failure is in close agreement with the present bilinear analysis, for $\eta = 0.5$, except for single unit and 2^2 units. The present analysis differs from Davis and Poulos' (56) approximate analysis, as mentioned below.

1.   In Davis and Poulos' (56) approximation, the variable nature of load distribution among different units, has not been considered and settlement allowing for pile failure is calculated as follows.

$$S = R_G \times S_{1p} \times UBC \times M + I_{RR} \times (P-UBC \times M) \qquad (5.7)$$

where

   S_{1p} = settlement of single pile with unit load

   UBC = ultimate bearing capacity of single pile

   M   = number of units or piles

   P   = total load

   I_{RR} = settlement of raft (rigid) under unit load.

    In the present bilinear analysis, the variable nature of loads on individual piles, is considered.

2.   The load at which failure of piles occur is assumed to be equal to UBC of pile in Davis and Poulos' (56) approximation. In the present analysis, it is assumed to be

different for rigid raft-pile ($K_R = 0.1$) units, subjected to uniformly distributed load over the entire raft area. The difference between them is about 15 to 20 % . In Fig.5.8(a), it can be observed that the value of R_G computed using these interac-tion factors are not significantly different, for both values of K and at the centre as well as at edge. The difference is less than 5 % . The reason for such agreement, even though the influence and interaction factors are differing by as large as 20 % , could be due to the possibility of the errors in these factors balancing with each other. (It may be observed that the influence factor is over estimated and interaction factor is under estimated, when the values for $K_R = 100$ is used instead of the values for $K_R = 0.1$ (Fig. 5.8 (b)). It may be noted, that Brown et al (17), have compared the results obtained using Davis and Poulos' (56) method with those obtained using more rigorous 'plate on piles and continuum' approach (Hain and Lee (68)), for some cases of pile-raft. They have concluded that for very flexible cap with pile subjected to uniformly distributed load, results of settlement from Davis and Poulos' (56) approach, agree closely with more rigorous (Hain and Lee (68)) analysis. The reason for such agreement may be the balancing of errors as discussed above.

In the case of flexible pile-raft subjected to uniformly
distributed load, the possibility of pile failure is remote,
as only small percentage of load is transmitted by the pile.
In the present analysis also, it was observed that the
solutions were same for $\eta = 1.0$ (i.e. elastic) and $\eta = 0.5$.

5.6.1.3 Effect of smooth contact between cap and soil

The analysis reported in this chapter has been done
assuming adhesive contact between cap and soil, using the
interaction factors obtained from the analysis of single
unit assuming adhesive contact. To investigate the effect,
if the contact between cap and soil happens to be smooth,
the interaction factors were computed for a few cases,
from the analysis reported in Chapter 3, using interface
elements to model smooth contact. A few cases of pile-raft
with rigid cap was analysed using these interaction factors
and these results have been compared with adhesive contact
solutions in Fig. 5.9. For the value of ν_S equal to 0,
the effect of interface condition is expected to be
maximum, as the effect of interface condition, on the
settlement, was found to be maximum for this value of
Poisson's ratio of soil in Chapter 3. It can be observed
in Fig. 5.9, even for $\nu_S = 0$, the effect of smooth contact

on the computed values of settlement (R_G) is very small, for both L/d = 10 and L/d = 25. For L/d = 25, the values of R_G obtained for smooth and adhesive contact almost coincide. For ν_S = 0.47, the effect of smooth contact was found to be still less.

The actual interface condition in the field may be in between perfectly smooth and fully adhesive contact, at raft-soil interface, as partial interfacial slip may take place. Since the settlements computed for perfectly smooth contact and fully adhesive contact assumptions are in very close agreement with each other, assumption of either smooth or adhesive contact may give realistic values of settlement, for the range of parameters considered.

5.6.2 Transversely Isotropic Soil

A detailed description of transversely isotropic soil considered has been given in Chapter 2, Sec. 2.2.2. Definition of parameters and other details of analysis, have also been given therein.

5.6.2.1 Pile group

The computed values of interaction factors (α) for the cross-anisotropic soil considered have been plotted in Figs. 5.10 and 5.11. The corresponding values for isotropic soil have also been shown for comparison. It may be observed

from Fig. 5.10, for incompressible material, the effect of anisotropy is to reduce the interaction, for smaller values of r and increase the interaction at locations far away from the pile, for both $L/d = 10$ and $L/d = 25$. It may also be observed that the interaction factors are not significantly affected if the soil anisotropy is mild ($n = 1.5$) and the effect of anisotropy on α is small even for $n = 2.5$. As n increases beyond 2.5, its effect on α increases rapidly. For the cross anisotropic soil in drained condition the effect of cross-anisotropy is to increase the 'interaction' consistantly for all values of r (Fig. 5.11).

Computed values of R_G, for incompressible material, for different values of anisotropic parameters have been plotted in Figs. 5.12 and 5.13. It can be observed that the effect of cross anisotropy of incompressible material is not significant upto $n = 2.5$ (The effect is less than 5%). But for larger values of n, the effect of cross anisotropy on the values of R_G, becomes significant. This is consistant with the trend observed in the case of interaction factors discussed above (in **this** section) and also with the trend observed in the behaviour of single pile (Sec. 2.6.2). It may also be observed that for values of n nearly equal to 4, the value of R_G appears to tend to

isotropic soil value, as group size increases.

The effect of cross anisotropy (for drained parameters considered) is to increase the values of R_G. This effect is more for larger spacing than for smaller spacing, as observed in Fig. 5.14. Maximum effect (for s/d = 5 and L/d=10) observed is about 17 percent.

The loads carried by individual piles, for L/d = 10, have been tabulated in Tables 5.9 and 5.10, for 3^2 pile group and 5^2 pile group, set in incompressible soil. It can be observed that pile loads are not much affected upto n = 2.5. It may also be observed that there is large difference between the load taken by corner piles and centre piles for n = 1 and as n approaches the limiting value of 4, the loads tend to be distributed equally among all the piles.

5.6.2.2 Pile-raft

Pile-raft (with rigid cap): The values of interaction factors for different values of n have been plotted in Fig. 5.15, for some cases of pile-raft systems. For incompressible material ($v_s \simeq 0.5$), it can be observed in Fig. 5.15, that the interaction factors are not affected much, by cross anisotropy, for values of n upto 2.5 (comparing the values of α for n = 1, 1.5 and 2.5). It can also be observed that the effect of cross-anisotropy is to reduce the value of

α for smaller values of r and the vice-versa for larger values of r. This trend is similar to free standing piles discussed (Sec. 5.6.2.1) earlier. For values of n greater than 2.5, the values of α increase considerably as the value of r increases, compared to isotropic soil. For n = 3.98, the interaction factors appear to become independent of L/d. For the drained cross-anisotropic parameters considered, the effect of such anisotropy is to increase the values of interaction factors as observed in the case of free standing piles. This effect increases with r.

The computed values of R_G have been plotted in Figs. 5.16 to 5.19, for different parameters. It can be observed from these figures, that the effect of cross anisotropy on R_G is small, for values of n upto 2.5, for all the cases considered. For the value of n equal to 3.5, the effect of cross anisotropy is to reduce the value of R_G significantly. For n = 3.98, the effect for small groups is to increase the value of R_G compared to isotropic soil. For larger group, the value of R_G tends to that for isotropic soil. In general, the trends are similar to the trends observed previously (Sec. 5.6.2.1), in the case of free standing pile groups. When the pile failure is considered using bi-linear analysis (Sec. 5.2.2.5), the difference between the

values of R_G for n =1 and n = 2.5, is slightly more than linear analysis, as observed in Fig. 5.17, for η = 0.5.

The results of analysis using drained cross anisotropic parameters have been plotted in Fig. 5.19. The effect of cross anisotropy is to increase the values of R_G compared to isotropic case. This effect increases as the number of units increases. For 6^2 units, this increase is about 15 %. For η = 0.5, from the results of the bilinear analysis, (also shown in Fig. 5.19) it can be observed that the effect of cross anisotropy is slightly more than that in the linear analysis.

The loads carried by individual piles have been tabulated for a pile-raft (rigid) consisting of 5^2 units in Tables 5.11 and 5.12. It can be observed that as the value of n increases, the pile load decrease in general. The ratio of maximum load to minimum load has also been tabulated for different values of n. It is seen that this ratio decreases as n increases. Or in otherwords, the loads tend to be uniformly distributed among the units as the value of n tends to the limiting value of 4. Also the portion of load transmitted by the piles decreases as the value of n increases.

Pile-raft with completely flexible cap:

The results obtained assuming completely flexible cap
for a particular case is shown in Fig. 5.20(b), for n = 1
and n=2.5. It can be observed that the value of R_G is not
affected much by the anisotropy for n = 2.5. It is also
seen that the results obtained using the interaction factors
for K_R = 100 and K_R = 0.1 are also quite close to each other,
as observed in the case of isotropic soil (Sec. 5.6.1.2).

5.6.3 Non-homogeneous Soil

5.6.3.1 General

Three different types of non-homogeneities have been
considered as in the analysis of piled circular footing
(Chapter 2). They are, 1. modulus linearly increasing
with depth, 2. a two layer soil medium in which there is a
weaker soil below and 3. non-homogeneities arising due to the
effect of installation. The parameters used are same as
those used in Chapter 2 (Sec. 2.2.2) and have also been
listed earlier in this Chapter (Sec. 5.4.4).

5.6.3.2 Modulus linearly increasing with depth (Fig.5.22)

Pile group (rigid cap): The values of R_G obtained
from the present analysis have been plotted in Figs. 5.21
and 5.22. It can be observed in these figures that the values
of R_G substantially reduce, as the degree of heterogeneity

increases (i.e. as value of ψ decreases). This effect
is more for groups consisting of larger number of piles and
for larger spacing. This effect is found to be slightly
more for $L/d = 25$ than $L/d = 10$. The observed substantial
reduction in the value of R_G, may be due to the large
reduction in the values of interaction factors observed,
due to this type of soil non-homogeneity. Similar observ-
ations have been made by Banerjee (7) and Poulos (109),
for some other sets of parameters.

The loads carried by individual piles have been
tabulated in Table 5.13, for a 5^2 group with a spacing
of 5d. It can be observed that as the degree of non-homo-
geneity increases, the pile load tends to be distributed
more uniformly among the piles, for both $L/d = 10$ and
$L/d = 25$ (comparing the values for $\psi = \infty$, 10 and 2.5).

Pile-raft (rigid cap):

The interaction factors for some cases of pile-raft
(when the cap is rigid), have been shown in Fig. 5.23. It
can be observed that the interaction factors are substantially
reduced by the soil non-homogeneity (comparing the results
for $\psi = 10$ and 2.5 with those of homogeneous soil ($\psi = \infty$)).
The computed values of R_G have been plotted in Figs. 5.24 and
5.25, for $L/d = 10$ and $L/d = 25$ respectively. It can be

observed that the values of R_G are substantially reduced by the soil non-homogeneity. The reduction in the values of R_G is maximum for $L/d = 25$, $\psi = 2.5$ and for 6^2 group. This reduction is more than 50 percent, compared to homogeneous case.

The results for free standing pile group have also been plotted in Fig. 5.24. It can be observed that for homogeneous soil there is small difference between pile-raft and free standing pile group (with same spacing), indicating the effect of cap resting on ground; but for $\psi = 2.5$, (strongly non-homogeneous soil) the effect of such cap action becomes negligible and the results of free standing pile group analysis coincide with the pile-raft analysis, as seen in Fig. 5.24.

The results of bilinear analysis have also been shown in Figs. 5.24 and 5.25. It can be observed that the effect of pile failure is more for non-homogeneous soil of this type (for smaller groups particularly) than homogeneous soil (comparing $\psi = \infty$ and $\psi = 2.5$ for $\eta = 0.5$ and $\eta = \infty$). As the group size increases, the bilinear analysis curves for different values of ψ, are found to intersect with each other.

Pile-raft (completely flexible cap):

The results of analysis of a particular case of pile-raft in which raft is flexible, set in a strongly non-

homogeneous soil ($\psi = 2.5$) are shown in Fig. 5.20(a). The results using the interaction factors computed from the analysis of single unit with $K_R = 100$ and $K_R = 0.1$, have been compared. It is observed that the values of R_G are significantly different. The difference is about 25 percent. It may be recalled, for homogeneous soil a similar comparison was made between the values of R_G computed using interaction factors from analysis of single units with $K_R = 100$ and $K_R = 0.1$, and the difference was less than 5 percent (Sec. 5.6.1.2). Hence, for analysis of pile-raft with flexible cap, set in strongly non-homogeneous soil, use of interaction factors obtained from rigid pile-cap unit analysis, may significantly underestimate the settlement.

5.6.3.3 Layered soil:

A two layered soil medium with a stiffer soil overlying softer soil (Sec. 2.2.2, Fig.5.26) has been considered as in the case of piled circular footing (Chapter 2, Sec. 2.5.3). The ratio h/L (where h is the thickness of the top layer) was varied and its effect on the settlement behaviour of pile group and pile-raft, has been discussed in this section, for different cases.

Pile group (Rigid Cap):

The computed results for pile group have been presented in Figs. 5.26 and 5.27, for different values of

h/L, for L/d = 10 and L/d = 25, respectively. It can be observed that the values of R_G are fairly sensitive to the values of h/L. It can also be observed that the value of R_G is maximum for a particular value of h/L depending on parameters like L/d, s/d and number of piles in the group, for a given value of E_{ST}/E_{SB}, as seen in Figs. 5.26(b) and 5.27(a). In general, this maximum occurs near the value of h/L = 0.6. However for L/d = 10, it is observed in Fig. 5.27(a), that the value of R_G increases continuously with h/L for s/d=5. The values of R_G for E_{ST}/E_{SB} = 10 (for h/L = 1), have also been plotted in Fig. 5.27(b). This shows the sensitivity of R_G for the value of E_{ST}/E_{SB} (comparing the results for E_{ST}/E_{SB} = 10 and E_{ST}/E_{SB} = 5, for h/L = 1).

The computed values of the loads carried by individual piles, for some cases have been tabulated in Table 5.14. It can be observed that the difference between the maximum and minimum pile load, is maximum for an intermediate value of h/L (at h/L = 0.5 for L/d = 25 and at h/L =1 for L/d = 10). In such cases, the minimum pile load becomes negative. The pile loads for E_{ST}/E_{SB} = 3 and E_{ST}/E_{SB} = 10, have also been tabulated in the same table. It can be observed that the magnitudes of such negative loads increases for E_{ST}/E_{SB}= 10, compared to E_{ST}/E_{SB} = 5. It may also be noted, for

E_{ST}/E_{SB} = 3, no such negative pile loads occur. These trends are reverse of the trends observed in the case of modulus increasing with depth (Sec. 5.6.3.2).

Pile-raft (with rigid cap/raft):

The computed values of R_G, for pile-raft with rigid cap/raft, have been plotted in Fig. 5.28. It can be observed that the values of R_G are fairly sensitive to the value of h/L. It can also be observed that the effect of this type of non-homogeneity on R_G, increases as the group size becomes larger. For L/d = 10, the results for E_{ST}/E_{SB} = 3, 5 and 10, have also been plotted for h/L = 1. This shows the effect of stiffness ratio (of soil layers) on the values of R_G, for the two layer soil medium. In general, the value of R_G is found to be more around h/L = 1, for larger group.

In Fig. 5.29, the values of R_G have been plotted against h/L. It can be observed that for L/d = 25, the value of R_G is maximum in the range of h/L = 0.4 and h/L = 1, for both d_c/d = 5 and d_c/d = 10. It can also be observed that as group size becomes larger, the value of h/L at which R_G is maximum changes from 0.5 to 1.0. For L/d = 10, the value of R_G increases continuously as h/L increases for pile-raft consisting of more than 3^2 piles. These trends are in general similar to free standing pile group.

The effect of failure of piles can be assessed from the results of bilinear analysis, which have also been plotted in Fig. 5.29. It is observed that this non-linear effect is insignificant for $L/d = 10$ or $d_c/d = 10$. However, for $L/d=25$ and $d_c/d = 5$, in which case pile is some what dominant in the system, the effect of pile failure is significant. It is also observed that the difference between bilinear analysis and linear analysis is minimum when the value of R_G is maximum.

Comparison of results obtained from free standing pile group analysis (with same spacing as pile-raft) and pile raft analysis, has also been made in Fig. 5.29. It is seen that only when raft is fairly dominant in the pile-raft system ($d_c/d = 10$, $L/d = 25$), the difference between these analyses is significant.

In Fig. 5.30, the values of the ratio of settlement of pile-raft (rigid) to the settlement of raft (rigid with $K_R = 100$ also computed from the present analysis) (S_{PR}^*/S_R^*) have been plotted against h/L, for different parameters. This ratio is maximum in the range of $h/L = 0.4$ to $h/L =1$, as observed in the case of R_G before (Fig.5.29). It can be observed that this ratio is greater than 1, for some cases ($d_c/d = 10$ and $L/d = 25$, for $h/L = 0.7$). This shows that in such cases, provision of as many as 16 piles (with $L/d = 25$),

is futile and may even be counter-productive, as for as reduction in settlement is concerned. The results of free standing pile group analysis are also shown in the same figure. It can be observed that the results from free standing pile group analysis shows greater settlement and for $d_c/d = 10$ and $L/d = 25$, this ratio is about 1.06, for $h/L = 0.7$; or in other words provision of 16 piles increases the settlement by 6 % compared to free raft. This is because provision of piles may increase the stresses in the softer bottom layer in the two layer soil medium considered. Hence proper care has to be taken to avoid such situations, while designing piled foundations in layered soil with a softer layer below.

Pile-raft (with completely flexible cap/raft):

The results of analysis of pile-raft with flexible cap/raft, for $d_c/d = 10$ and $L/d = 25$, have been shown in Fig.5.31. It can be observed that the influence of h/L on the values of R_G is different from that for the rigid cap condition (comparing Figs. 5.29 and 5.31). It can also be observed that the results of analysis using the interaction factors obtained from the analysis of pile-cap unit with $K_R = 0.1$ and $K_R = 100$, agree with each other as observed in the case of homogeneous soil (Sec. 5.6.1.2).

5.6.3.4 Effect of installation of piles on the behaviour
of pile-raft:

Non-homogeneity arising due to the effect of install-
ation of piles have been considered in an approximate manner
by using different modulii for the disturbed zones and details
of the analysis have been given in Chapter 2 (Sec. 2.2.2).
From the same analysis interaction factors have been also
obtained and used in the analysis of pile-raft, with rigid
cap/raft herein. Since interaction factors obtained from the
analysis of single unit has been used in the present analysis,
implicit assumption is the soil disturbance away from the
pile does not affect the interaction significantly.

For a loose sandy soil, which may get compacted due to
the installation of driven pile, the results have been shown
in Fig. 5.32(a). It can be observed that the effect of
installation of piles, is to increase the values of R_G by
about 15 % , for the parameters considered.

The results of analyses pertaining to clayey soils
are shown in Fig. 5.32(b). The results for cases designated
as I_0 (K = 500), I_1 and I_4 correspond to a stiff clayey
soil, which may get softened due to the installation of
bored piles. In this case, it can be observed that the
effect of installation of piles is to reduce the values of
R_G upto about 25 % depending on the degree of disturbance

(comparing the curves for I_0 (K = 500), I_1 (moderate disturbance) and I_4 (strong disturbance)). Curves designated as I_0(K=1500), $I_{\sim}$ and I_5 correspond to a soft clay which may become stiffer during the installation of driven piles. In this case, there is an increase in the value of R_G to a magnitude similar to the previous case.

5.7 CONCLUSIONS

1. Interaction factor method of determining the settlement of free standing pile-group and pile-raft has been extended to solve problems related to any linearly elastic soil medium, using axisymmetric finite element analysis. It has been shown that this procedure gives sufficiently accurate results.

2. The need for a non-linear settlement analysis has been outlined. A 'non-linear' interaction factor method of analysis has been described. The proposed method can take into account the variable nature of interaction, which has been shown to occur in some cases. As some simplifying assumptions have been made, the effectiveness of the proposed method has to be tested by model tests or field tests.

3. The method of determining the interaction factors from the field load tests or from a finite element

analysis, have been described. A bi-linear analysis which may be used at the preliminary stages of design of pile-raft, has been proposed and used for the illustration of the method. Some cases of pile group and pile-raft set in different types of soils have been analysed and results discussed.

4. For certain cases, the approximate methods suggested by Davis and Poulos (56), for the analysis of pile-raft, have been found to be satisfactory. These are as follows.

(a) The results of present bilinear analysis and results from the approximate method proposed by Davis and Poulos (56), almost agree with each other in many cases.

(b) The correction factors for $\overset{\cdot}{\mathcal{V}}_S$, proposed by Davis and Poulos (56), also agree with those obtained from the present analysis.

(c) Results of analysis of pile-raft with completely flexible cap/raft using the interaction factors obtained from the analysis of rigid cap ($K_R = 100$) pile unit (as done by Davis and Poulos (56)), agrees well with the results of more accurate analysis using the results of flexible ($K_R = 0.1$) cap-pile unit analysis, in many cases.

5. The pile compressibility is found to affect the settlement of pile-raft significantly.

6. The effect of failure of piles on the value of R_G, as assessed from the present bi-linear analysis is considerable, if the piles are dominant in the system. The effect of failure of piles, is more for $\nu_S = 0$ than $\nu_S = 0.5$.

7. The effect of cross anisotropy on the values of R_G is small, for the values of n upto 2.5, in the case of incompressible material. However, for strongly anisotropic soil condition (n > 2.5), the effect of anisotropy becomes significant, for both pile group and pile-raft. The effect of cross anisotropy of incompressible material is to distribute the loads more uniformly among the piles, in the case of pile groups and pile-rafts.

8. The effect of modulus linearly increasing with depth on the behaviour of pile group and pile-raft is quite significant. The non-homogeneity of this kind tends to distribute the loads more uniformly among the pile's, in the case of pile-group with rigid cap. Analysis of pile-raft with flexible cap, set in strongly non-homogeneous soil of this kind, using interaction factor obtained from the analysis of rigid

pile-cap units may significantly underestimate the settlement.

9. For two layer soil medium in which a stiffer soil is overlying, the settlement of piled foundation may be more than the settlement of free raft, (due to higher stressing of bottom layer) indicating that provision of piles is counter-productive in such cases. For such a soil medium, the values of R_G are maximum for a particular value of h/L, in the range of 0.5 and 1.0, depending on different parameters, for pile group and pile-raft. In this range of h/L, the difference between the maximum pile load and minimum pile load, is maximum, in a pile group. The effect of cap resting on the ground, i.e. the difference between the values of settlements obtained from analysis as pile group and pile-raft, is significant only for a system in which raft/cap is of considerable dominance.

10. The effect of installation of piles is found to affect the values of R_G by about 15 to 25 % .

TABLE 5.1 LOAD ON PILES/AVERAGE LOAD

K = 1500   s/d = 5   L/d = 10 5^2 pile group

Pile No.(Fig.5.2)	Poulos and Davis(111) H/L = ∞	Present Analysis
1	1.77*	1.77
2	1.14	1.14
3	1.09	1.09 H/L=8
4	0.52	0.51
5	0.48	0.48
6	0.44	0.45

TABLE 5.2 LOAD ON PILES/AVERAGE LOAD

K = 1500   s/d = 2   L/d = 10 5^2 pile group

1	2.54	2.56
2	1.19	1.18
3	1.12	1.15
4	0.06	0.06 H/L = 8
5	0.09	0.09
6	0.10	0.13

TABLE 5.3 LOAD ON PILES/AVERAGE LOAD

K = 200   s/d = 5   L/d = 25 5^2 pile group

1	1.78	1.73
2	1.16	1.15
3	1.07	1.07 H/L=3.2
4	0.55	0.56
5	0.48	0.49
6	0.40	0.42

* Values interpolated from Poulos and Davis (111) are given in Tables 5.1 to 5.7

TABLE 5.4   LOAD ON PILES/AVERAGE LOAD

K = 200   s/d = 2   L/d = 25 5^2 pile group

Pile No.(Fig.5.2)	Poulos and Davis(111) H/L = $\alpha\infty$	Present Analysis H/L = 3.2
1	2.10	2.29
2	1.18	1.18
3	1.05	1.12
4	0.44	0.22
5	0.21	0.21
6	0.14	0.20

TABLE 5.5   LOAD ON PILES/AVERAGE LOAD

K = 1500   s/d = 5   L/d = 25 5^2 pile group

1	2.02	2.05
2	1.19	1.19
3	1.09	1.09
4	0.38	0.37
5	0.31	0.31
6	0.25	0.24

TABLE 5.6   LOAD ON PILE/AVERAGE LOAD

K = 1500   s/d = 2   L/d = 25 5^2 pile group

1	2.55	2.65
2	1.12	1.14
3	1.20	1.12
4	0.20 - -0.2	0.02
5	0.12 - 0.09	0.04
6	0.04 - 0.25	0.07

TABLE 5.7   GROUP REDUCTION FACTOR RATIO
$(R_G(\nu_S = 0) / R_G(\nu_S \simeq 0.5))$

$d_c/d = 5$ $L/d = 25$ $K = 1500$

No. of units	Poulos and Davis (111)	Present Analysis
5^2	1.22	1.26
4^2	1.21	1.25
3^2	1.18	1.22
2^2	1.15	1.20
1	1.11	1.05

TABLE 5.8 LOAD ON PILE/UBC OF PILE

$d_c/d = 5$ $L/d = 25$ $K = 1500$ $\nu_S = 0.47$

6^2 pile group-linearly elastic analysis

Pile No.	Load on Pile/UBC of pile ($\eta = 1.0$)
1	2.10
2	0.90
3	0.94
4	0.10
5	0.16
6	0.20

TABLE 5.9 PILE LOADS – 3^2 PILE GROUP
(Cross anisotropic soil)

s/d = 5   L/d = 10 $\nu_{SV} \simeq 0.5$ m = 0.38 $\nu_{SH} = 1-n/2$

Total load = 100 units

K	Pile No. (Fig.5.2)	n = 1	n=1.5	n = 2.5	n=3.5	n=3.98
1500	1	14.07	14.01	13.56	12.83	11.59
	2	9.69	9.72	9.95	10.30	10.90
	3	4.94	5.06	5.97	7.45	10.06
200	1	13.59	13.50	13.20	12.43	11.47
	2	9.93	9.98	10.13	10.50	10.96
	3	5.90	6.09	6.71	8.28	10.30

TABLE 5.10 PILE LOADS – 5^2 PILE GROUP (Cross anisotropic soil)

s/d = 5   L/d = 10 $\nu_{SV} \simeq 0.5,$ m = 0.38 $\nu_{SH} = 1-\frac{n}{2}$

Total load = 100 units

K	Pile No.	n = 1	n=1.5	n = 2.5	n=3.5	n=3.98
1500	1	7.09	7.04	6.58	5.80	4.37
	2	4.56	4.56	4.50	4.39	4.09
	3	4.35	4.35	4.30	4.22	4.07
	4	2.05	2.08	2.38	2.86	3.74
	5	1.94	1.96	2.24	2.71	3.72
	6	1.82	1.84	2.08	2.54	3.69
200	1	6.68	6.60	6.28	5.44	4.29
	2	4.53	4.52	4.47	4.34	4.07
	3	4.30	4.29	4.26	4.17	4.05
	4	2.32	2.38	2.58	3.10	3.80
	5	2.15	2.20	2.39	2.93	3.78
	6	1.98	2.02	2.20	2.75	3.74

TABLE 5.11   PILE LOADS - PILE-RAFT L/d = 10 (Cross anisotropic soil)

5^2 group, $d_c/d = 5$, $\nu_{SV} \simeq 0.5$,   m = 0.38, $\nu_{SH} = 1 - \frac{n}{2}$, K=1500

Pile No. (Fig.5.2)	n = 1	n = 1.5	n = 2.5	n = 3.5	n = 3.98
1	4.40	4.31	3.61	2.41	0.78
2	2.13	2.10	1.82	1.34	0.54
3	2.38	2.34	2.07	1.49	0.58
4	0.46	0.47	0.49	0.48	0.34
5	0.68	0.68	0.73	0.64	0.39
6	0.89	0.88	0.80	0.65	0.40
Max.pile load / Min.pile load	9.57	9.17	7.37	5.02	2.29

Total applied load = 100 units in Tables 5.11 and 5.12.

TABLE 5.12   PILE LOADS - PILE-RAFT L/d = 25 (Cross anisotropic soil)

group, $d_c/d = 5$,   K = 1500, $\nu_{SV} \simeq 0.5$,   m = 0.38 $\nu_{SH} = 1 - \frac{n}{2}$

Pile No. (Fig.5.2)	n=1	n=1.5	n = 2.5	n = 3.5	n = 3.98
1	7.02	6.88	5.98	4.27	1.28
2	3.09	3.04	2.71	2.17	0.87
3	3.43	3.37	3.14	2.49	0.95
4	0.28	0.31	0.38	0.57	0.55
5	0.60	0.62	0.80	0.90	0.63
6	0.88	0.89	0.95	0.94	0.65
Max.pile load / Min.pile load	25	22	15.7	7.5	2.30

TABLE 5.13 PILE LOADS - PILE GROUP

(Non-homogeneous soil)

s/d =5 5^2 group   K = 1500 ν_S = 0.3   L/d=10 and 25

Pile No. (Fig. 5.2)	$\psi = \infty$ (Homo.)	$\psi = 10$	$\psi = 2.5$
1	7.51[a]	6.49	5.90
	8.70[b]	7.22	6.17
2	4.58	4.45	4.38
	4.78	4.61	4.46
3	4.41	4.34	4.26
	4.42	4.33	4.24
4	1.77	2.38	2.76
	1.14	2.01	2.65
5	1.73	2.33	2.67
	0.98	1.82	2.45
6	1.67	2.27	2.58
	0.82	1.62	2.24

a - L/d = 10   b - L/d = 25

Total applied load = 100 units.

TABLE 5.14   PILE LOADS - PILE GROUP (LAYERED SOIL)

5^2 group, Total load = 100 units,   K = 400,   L/d = 25 and 10
s/d = 5

Pile No. (Fig.5.2)	h/L=0.1 E_{ST}/E_{SB}=5	E_{ST}/E_{SB}=5 h/L = 0.4[x] h/L = 0.5[y]	h/L = 1 E_{ST}/E_{SB} = 5	h/L=1.5 E_{ST}/E_{SB} = 5	h/L=1 E_{ST}/E_{SB} = 3	h/L=1 E_{ST}/E_{SB} = 10
1	9.80[a]	11.28	9.27	8.32	-	-
	7.80[b]	9.92	10.56	9.73	9.30	12.63
2	4.59	5.10	4.91	4.77	-	-
	4.56	4.68	4.99	4.94	4.85	5.21
3	4.72	4.44	4.35	4.35	-	-
	4.47	4.67	4.47	4.39	4.45	4.46
4	0.27	-0.20	0.93	1.42	-	-
	1.57	0.21	0.12	0.65	0.80	-0.97
5	0.75	-0.47	0.58	1.15	-	-
	1.63	0.59	-0.07	0.34	0.64	-1.19
6	1.15	-0.72	0.22	0.88	-	-
	1.57	0.95	-0.24	0.03	0.49	-1.38

a - L/d = 25   b - L/d = 10   (Negative sign indicates tensile load)

x - for L/d = 25   y - for L/d = 10.
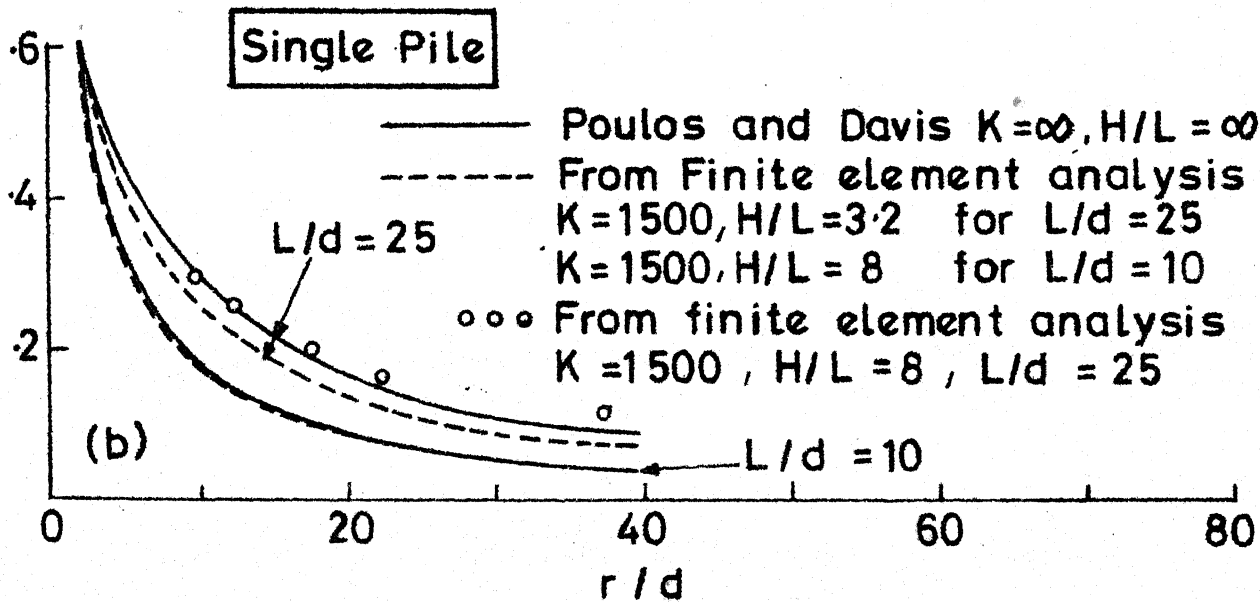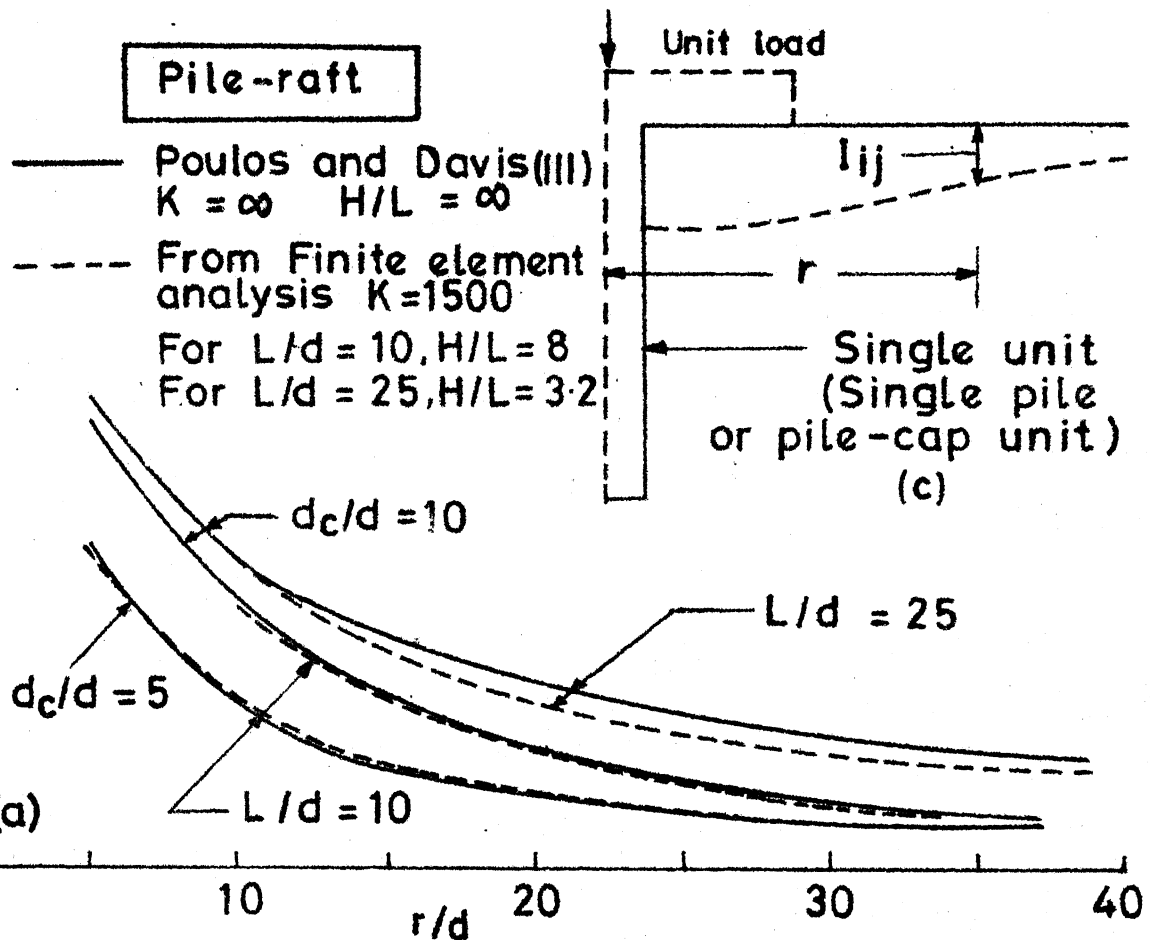
Fig.5.1(a) & (b) Interaction Factor Vs r/d
(c) Interaction Factor definition
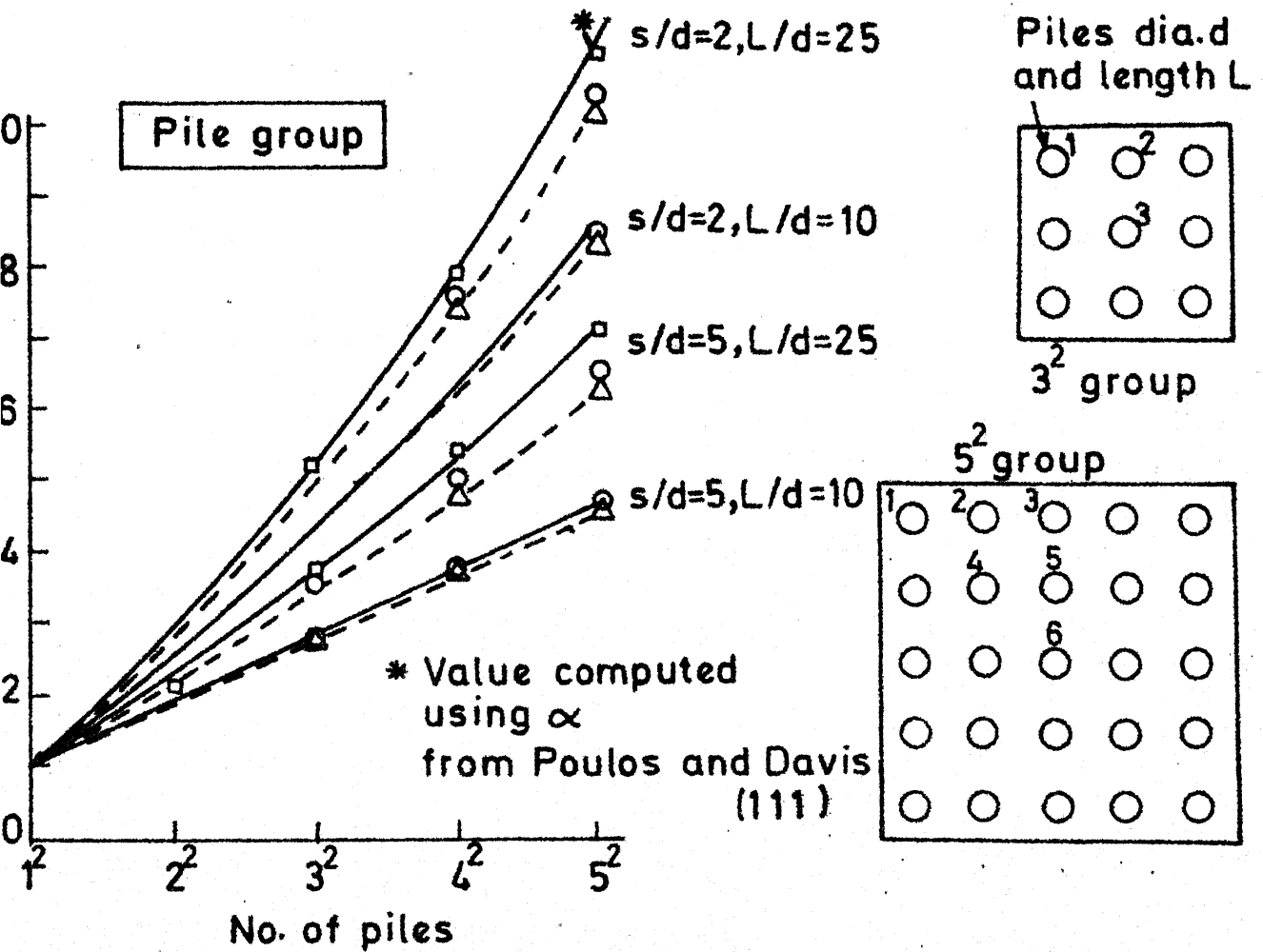
Fig.5·2 R_s Vs Number of Piles
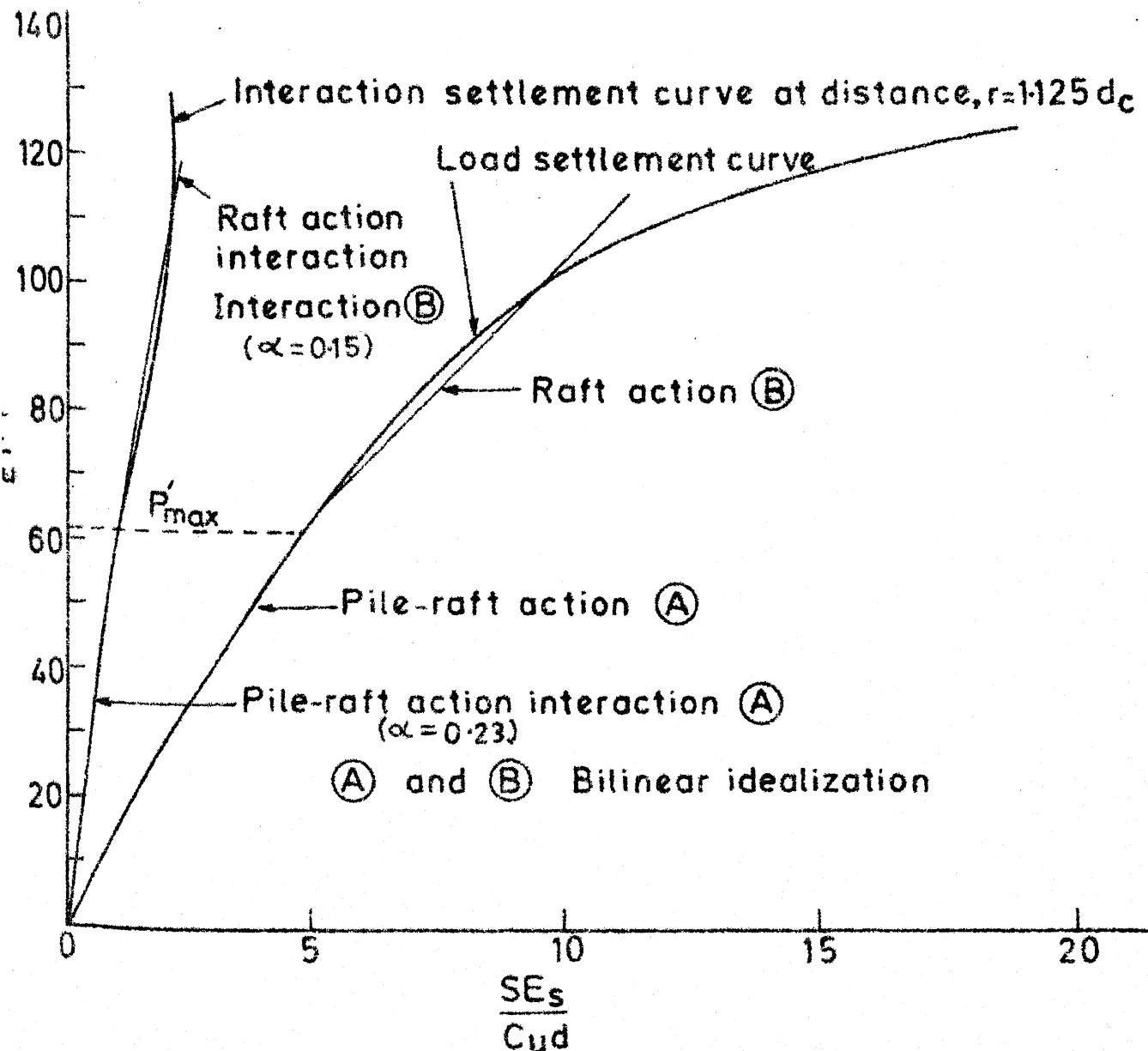
Fig. 5·3 Elasto-plastic (Von Mises) Analysis of piled circular footing

Fig. 5·4 Load-Settlement curve of jth unit and k^{th} unit with loading on j^{th} unit
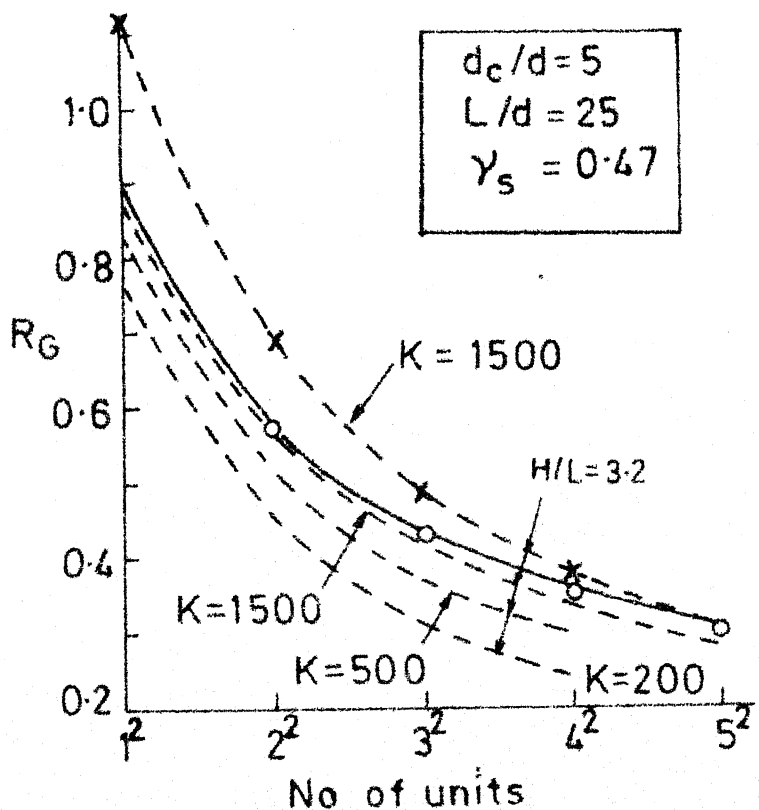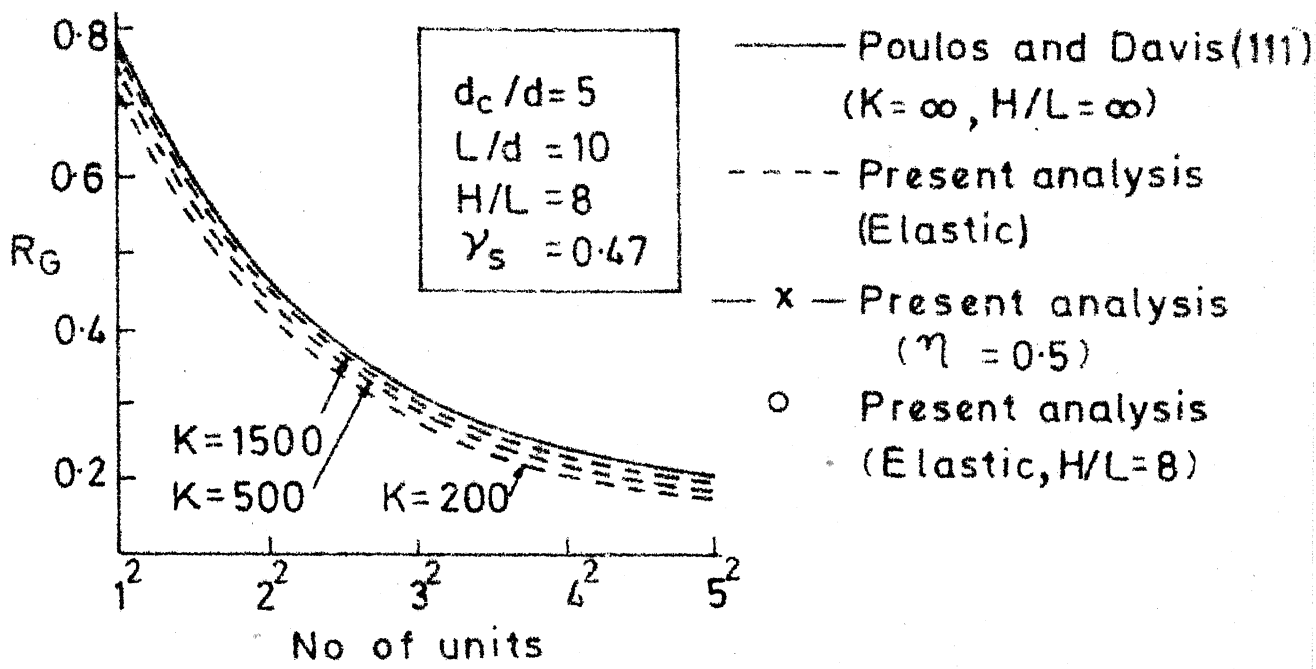
Fig. 5.5 R_G Vs No. of units (Pile rigid-raft)
Homogeneous soil
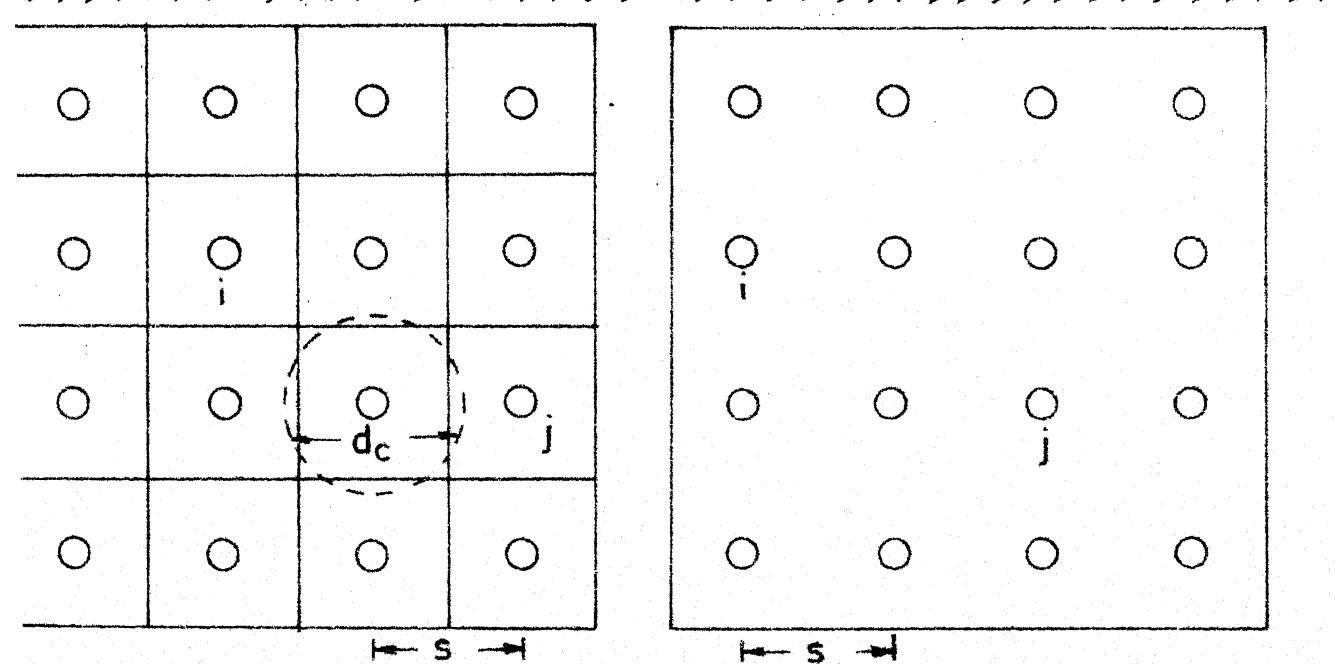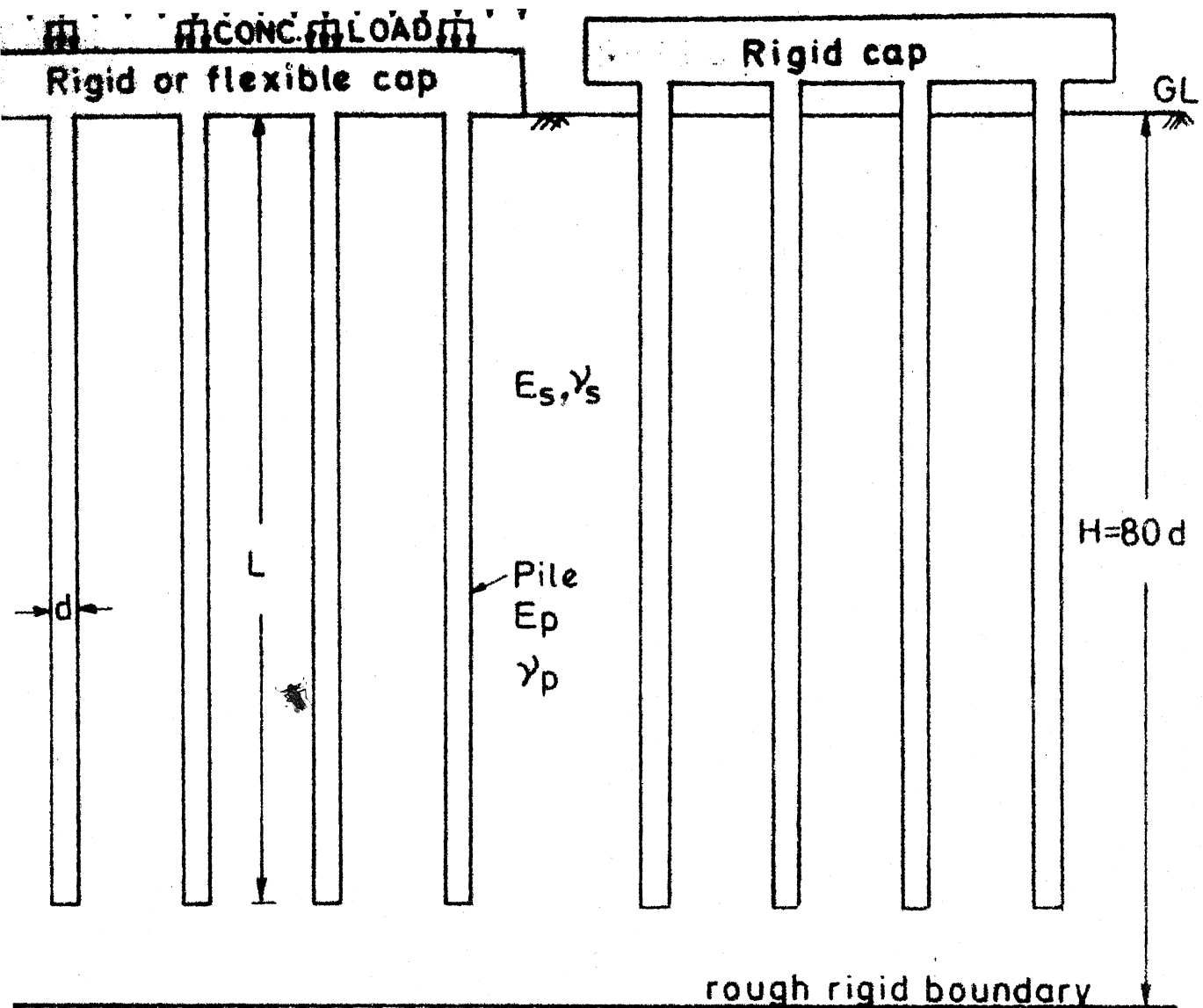
Fig. 5·6 Typical Pile group and Pile-raft
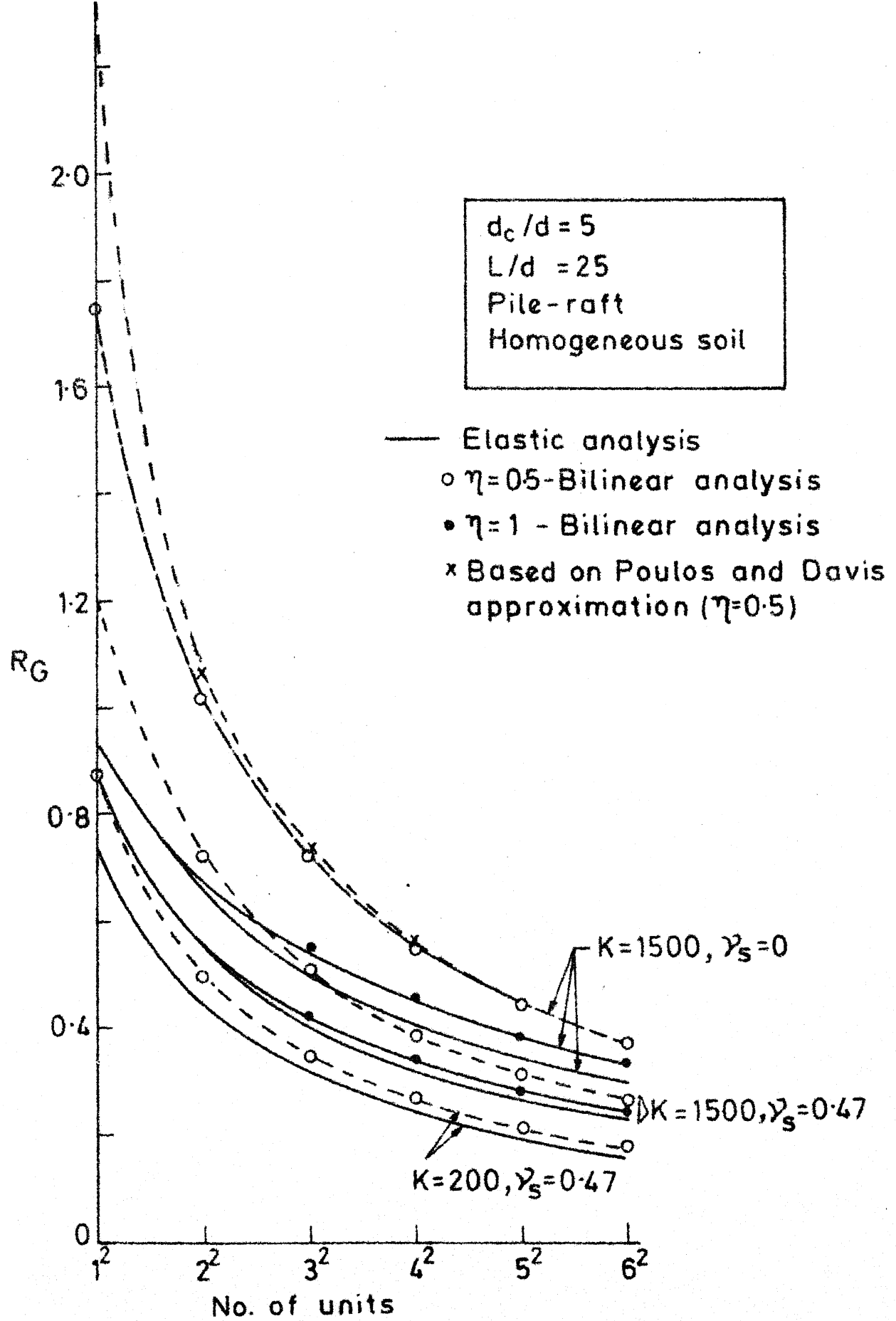
Fig.5·7 R_G Vs No of units (Rigid raft-pile)
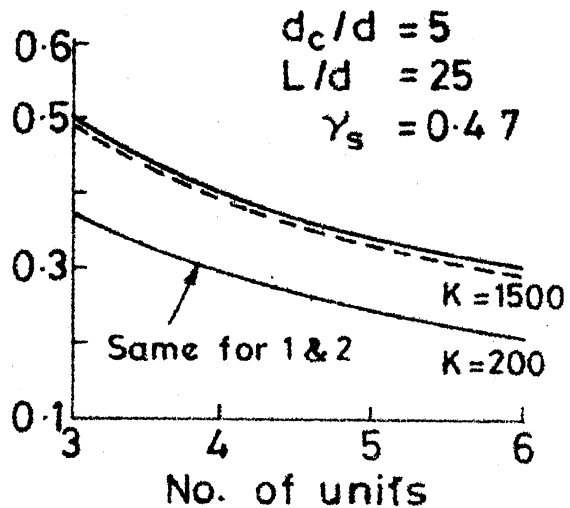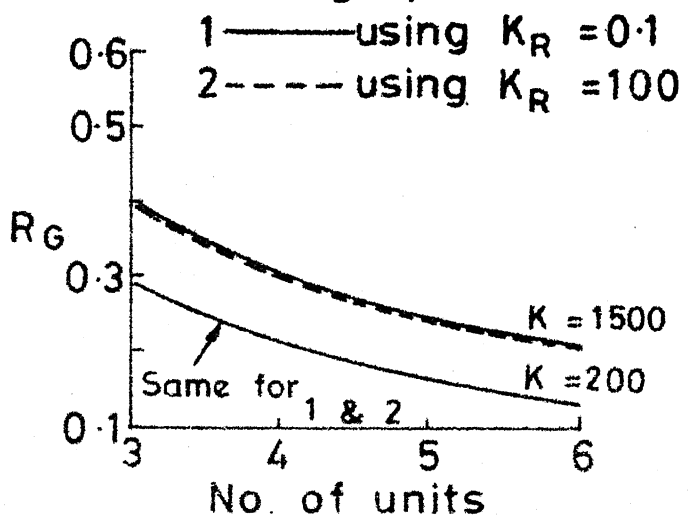
Fig. 5·8(a) R_G vs No. of units (Flexible Pile-raft
- Homogeneous soil)

Centre piles
$d_c/d = 5$
$L/d = 25$
$\gamma_s = 0·47$

R_G

$K = 1500$
Same for 1 & 2
$K = 200$

No. of units

Edge piles
1 ——— using $K_R = 0·1$
2 ----- using $K_R = 100$

R_G

$K = 1500$
$K = 200$
Same for 1 & 2

No. of units

For single unit

$R_G = 0·654$ for $K_R = 0·1$ (udl)

$R_G = 0·757$ for $K_R = 100$

$K = 200$
$L/d = 25$
$d_c/d = 5$
Homogeneous
soil
pile-raft

α

$K_R = 100$

$K_R = 0·1$ udl

r/d
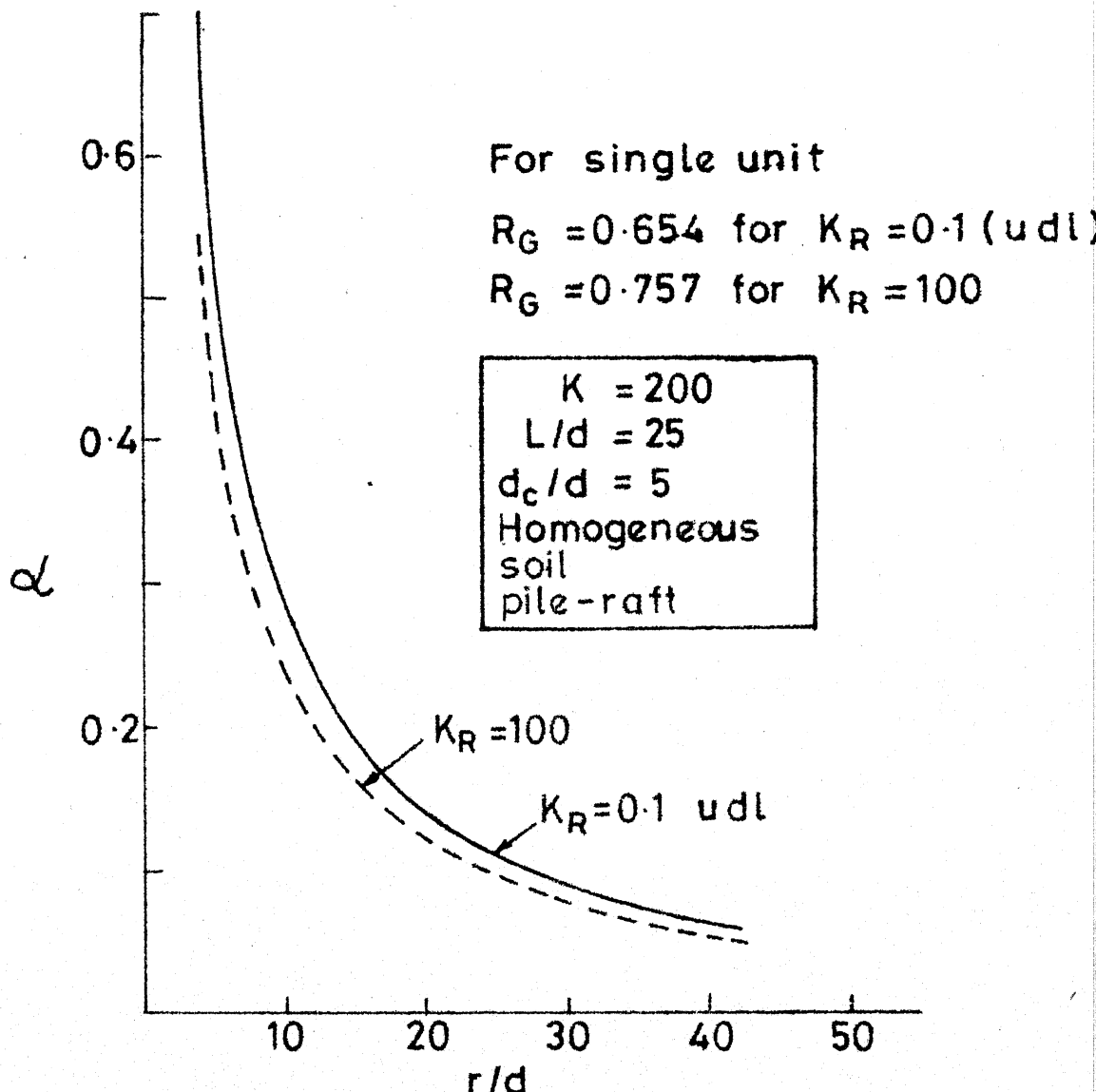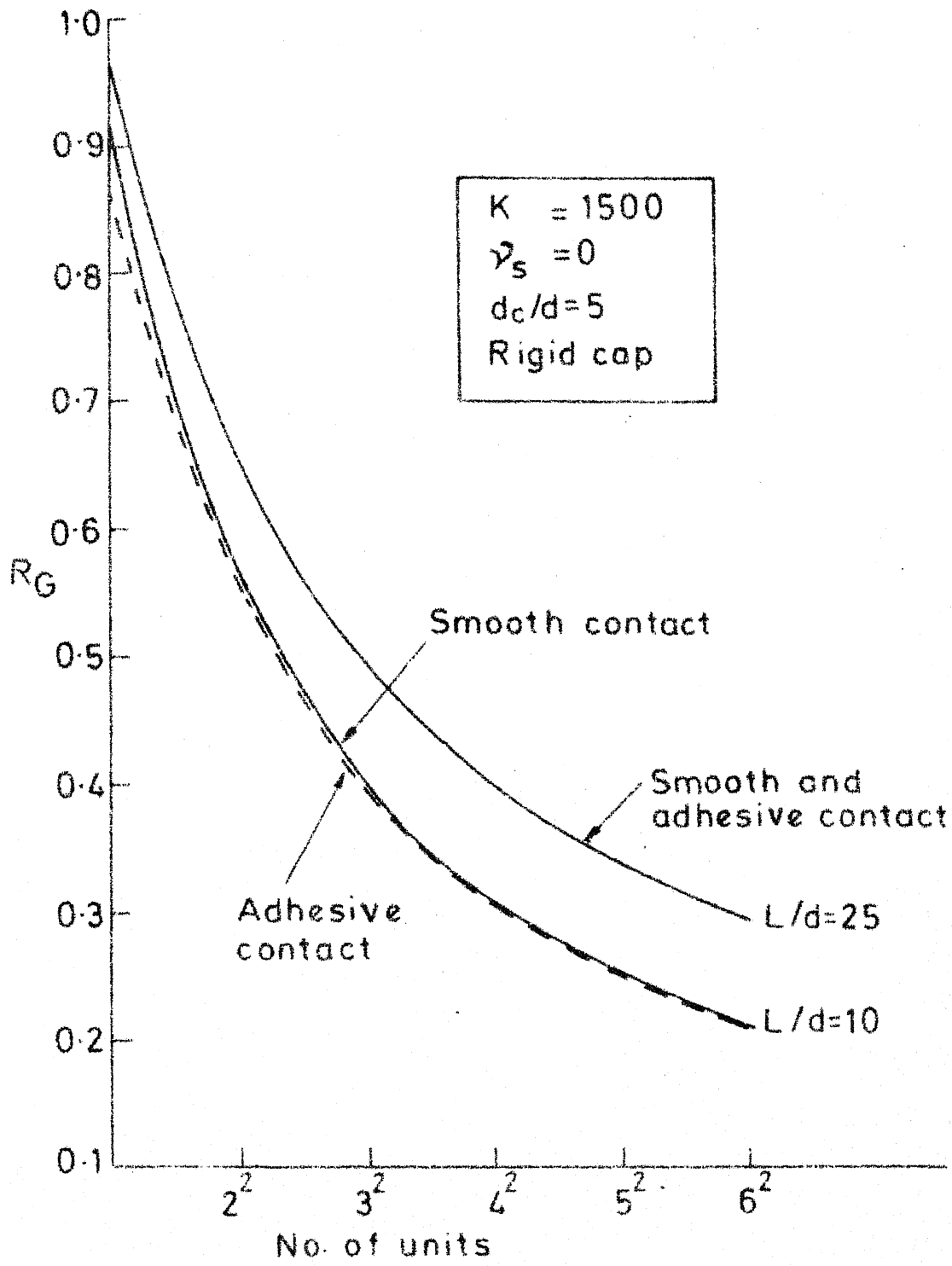
Fig.5·9 R_G Vs No. of units (Rigid pile-raft) For homogeneous soil
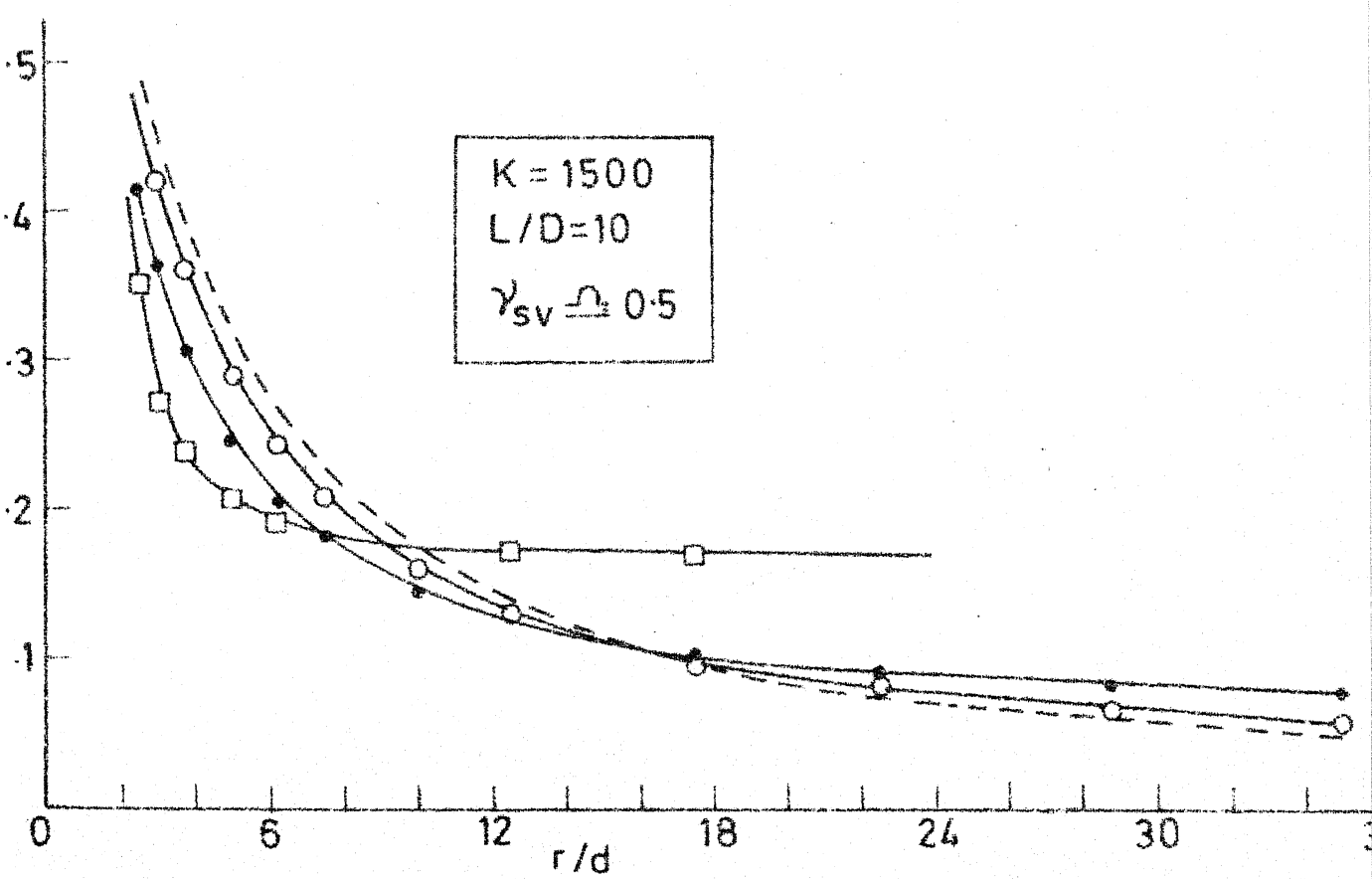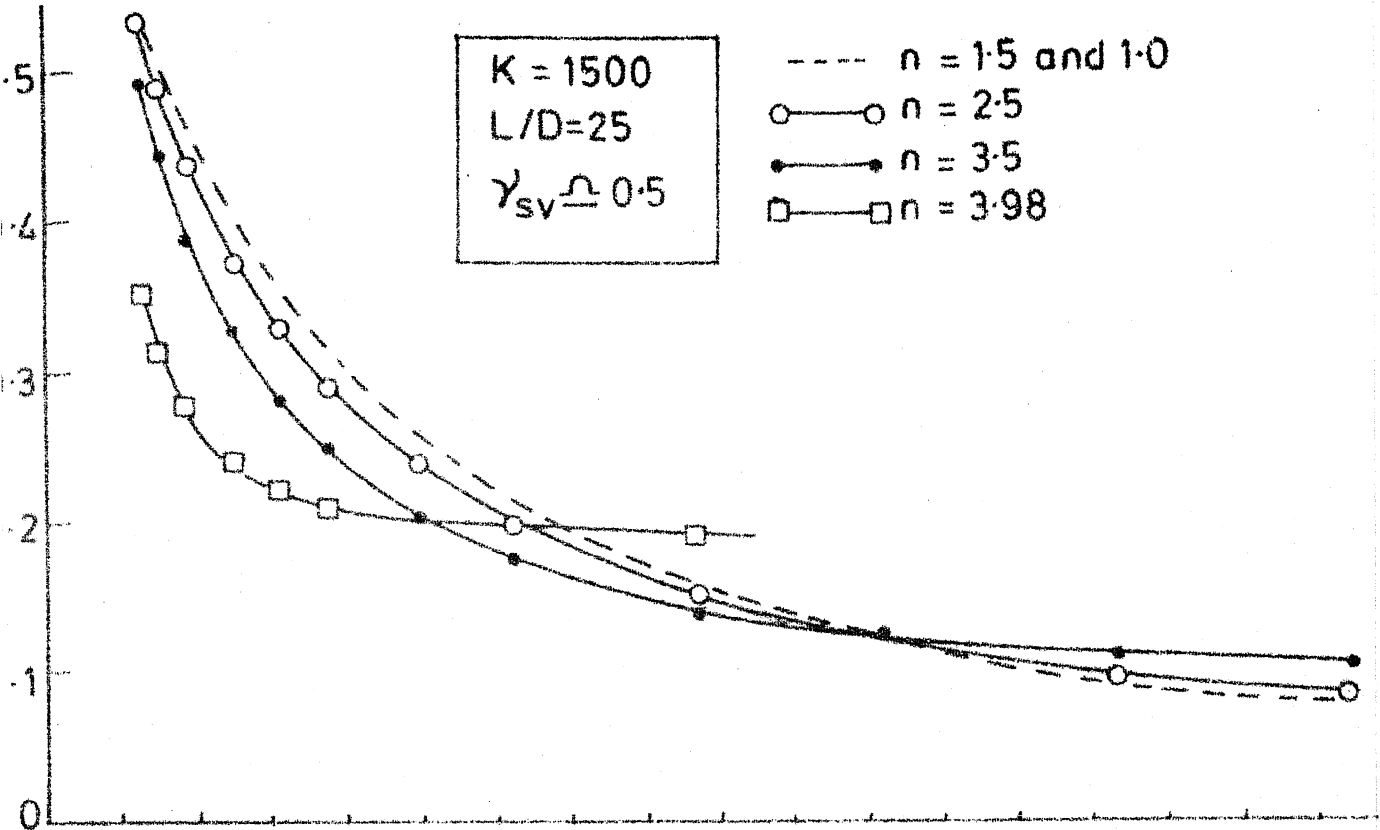
Fig.5.10 Interaction Factors Vs r/d (Pile group) Anisotropic so
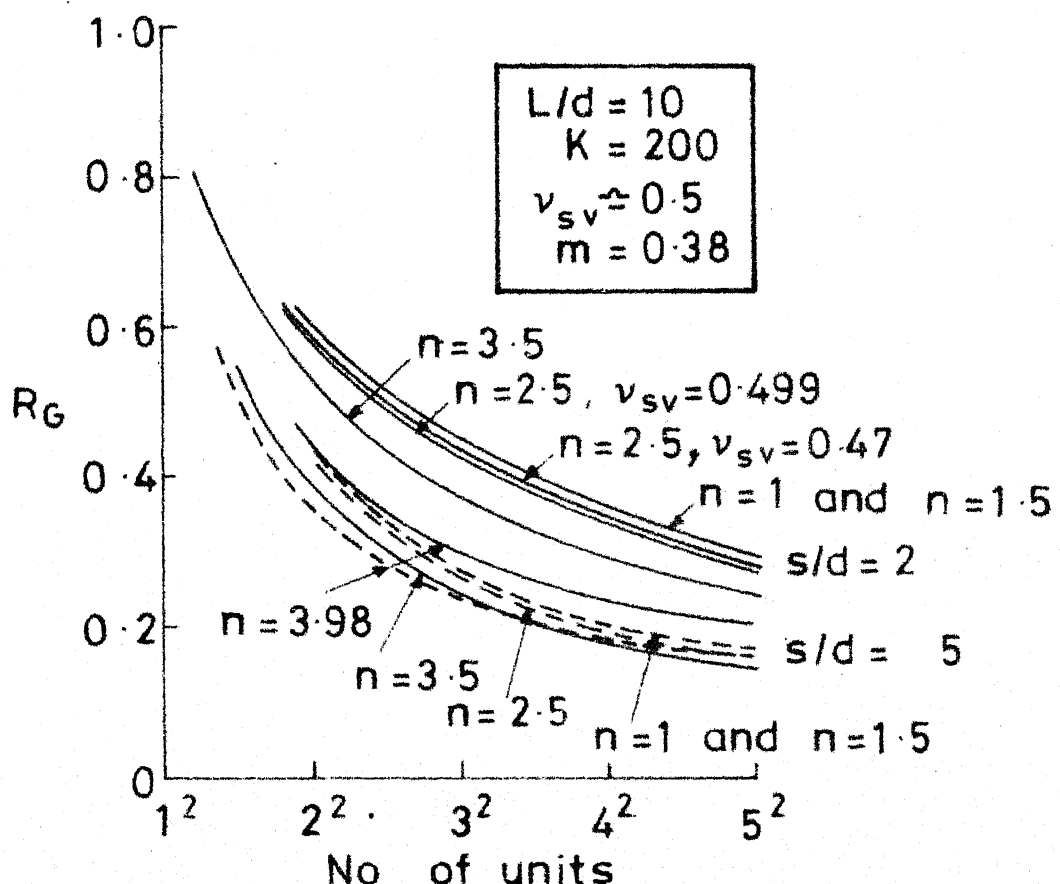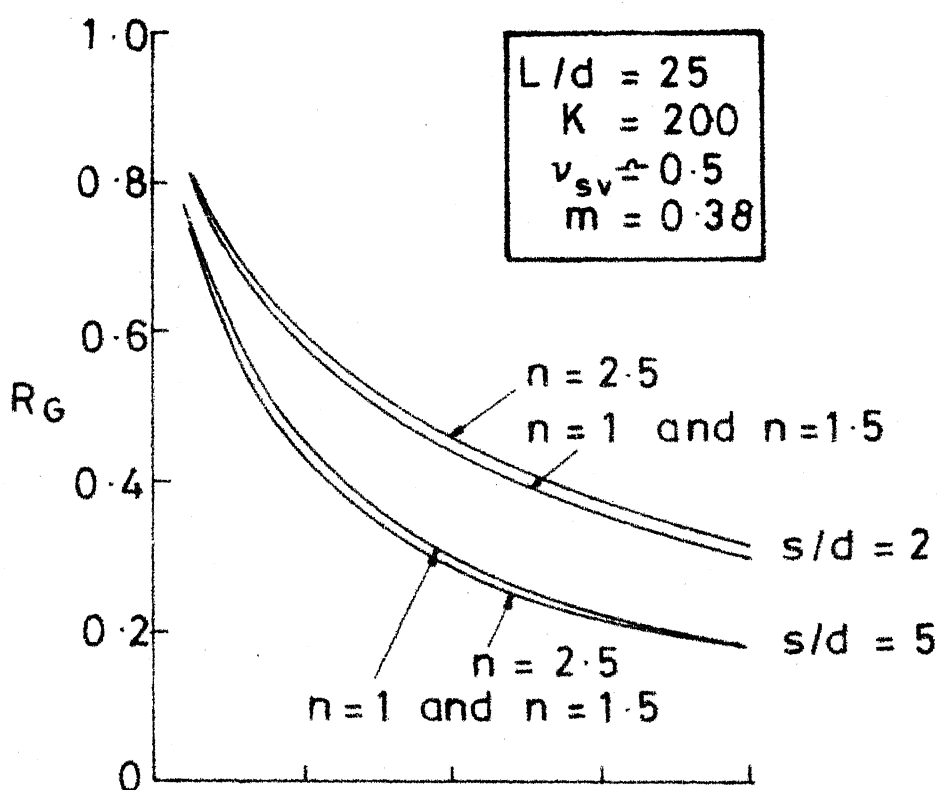
Fig. 5·12 R_G Vs   No. of units (Pile group)
-Anisotropic soil-
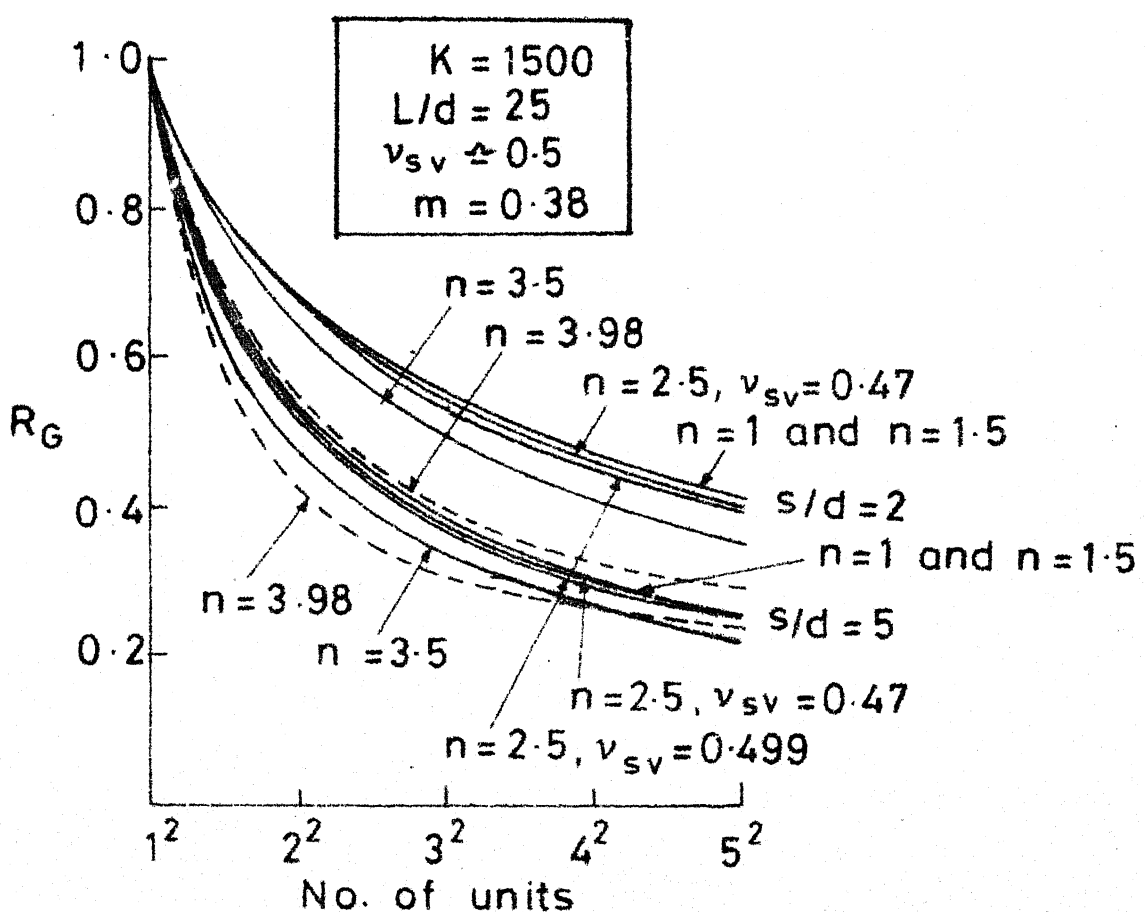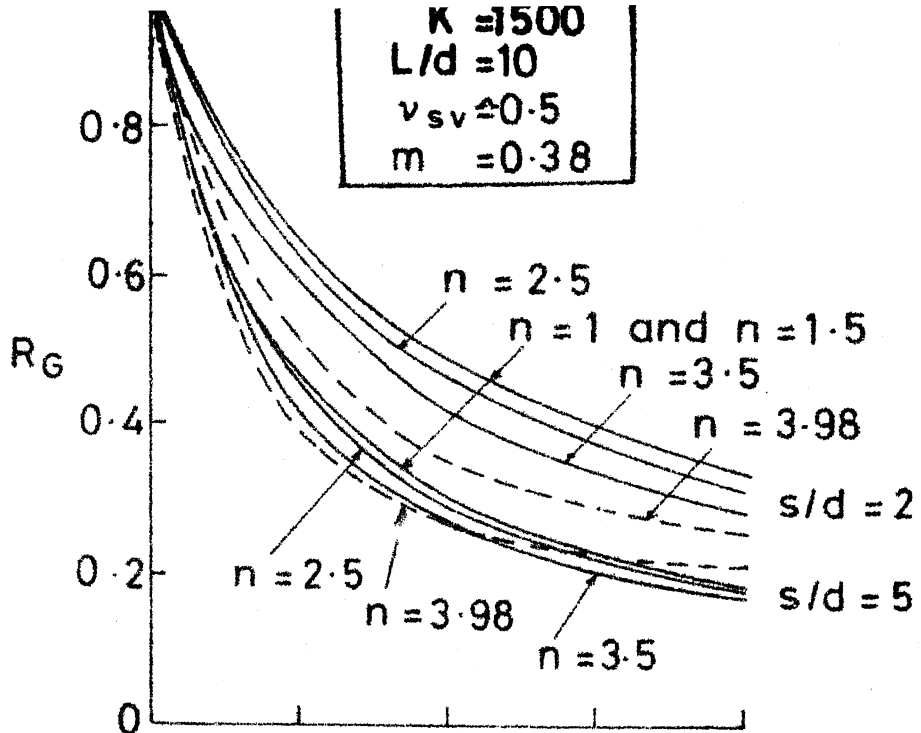
Fig. 5·13 R_G Vs   No. of units(Pile group)
For Cross-Anisotropic soil

$K = 1500$
$\gamma'_{SV} = 0$
$n' = 3 - \gamma_{SH} = -0.55, m' = 0.76$
$n' = 1 - \text{Isotropic}$

R_G

No. of units

$n' = 3$
$n' = 1, \ s/d = 2, L/d = 25$
$n' = 3$
$n' = 1, \ S/d = 2, L/d = 10$
$n' = 3$
$n' = 1, \ s/d = 5, L/d = 25$
$n' = 3$
$n' = 1, \ s/d = 5, L/d = 10$
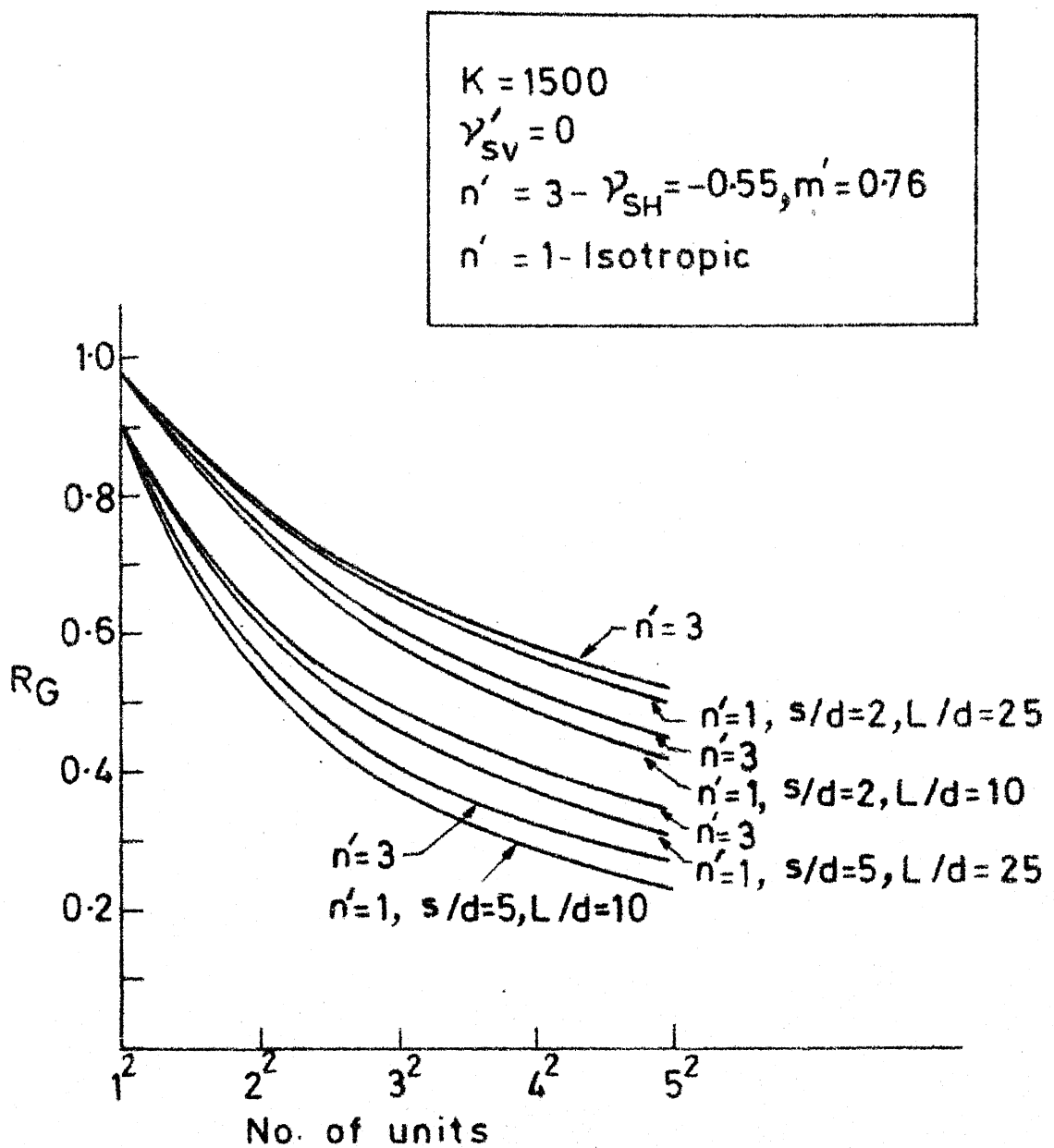
Fig. 5·14 R_G Vs No. of units (Pile group) for
Anisotropic soil

Fig. 5.15 Interaction Factors Vs r/dc (Pile-raft) Anisotropic soil
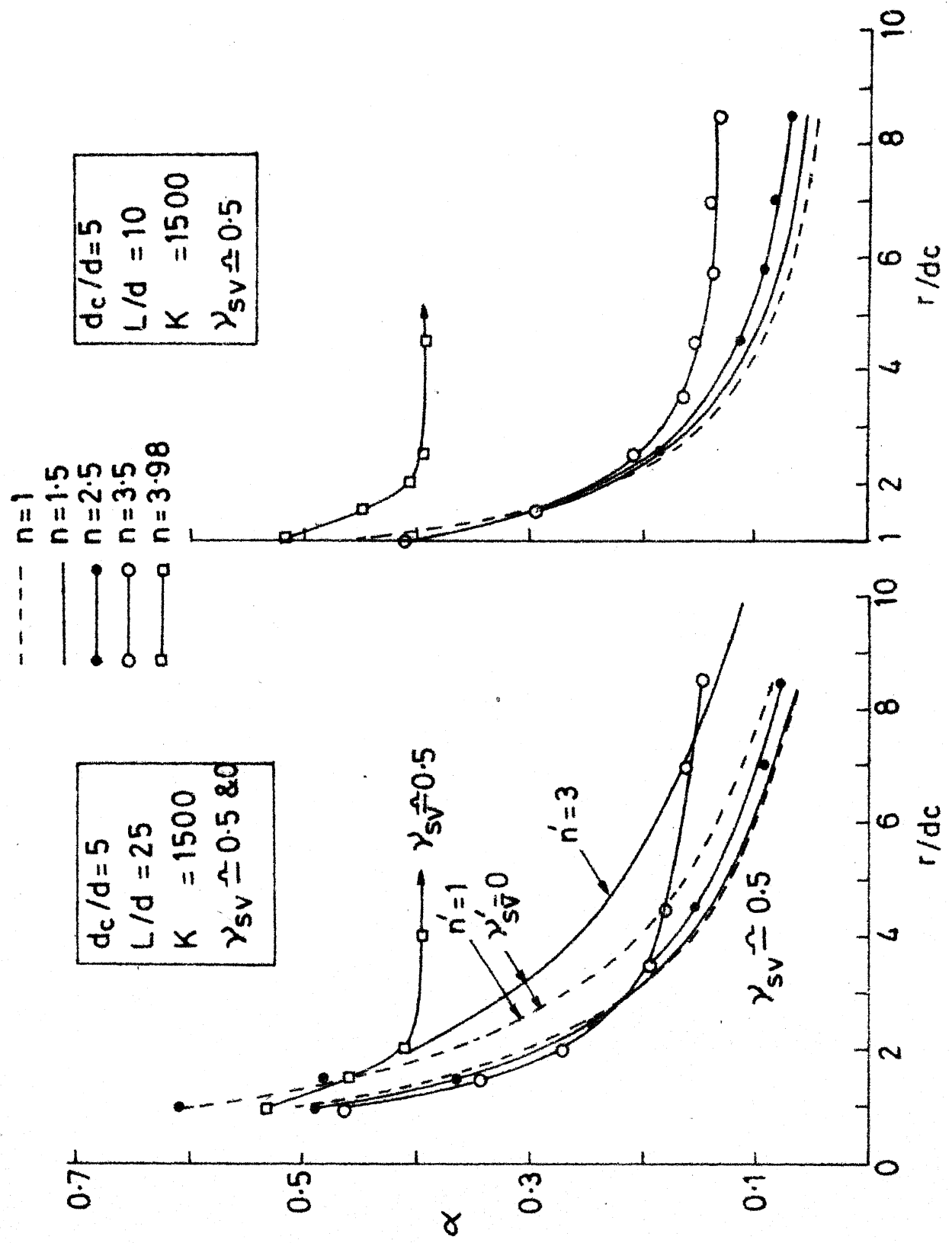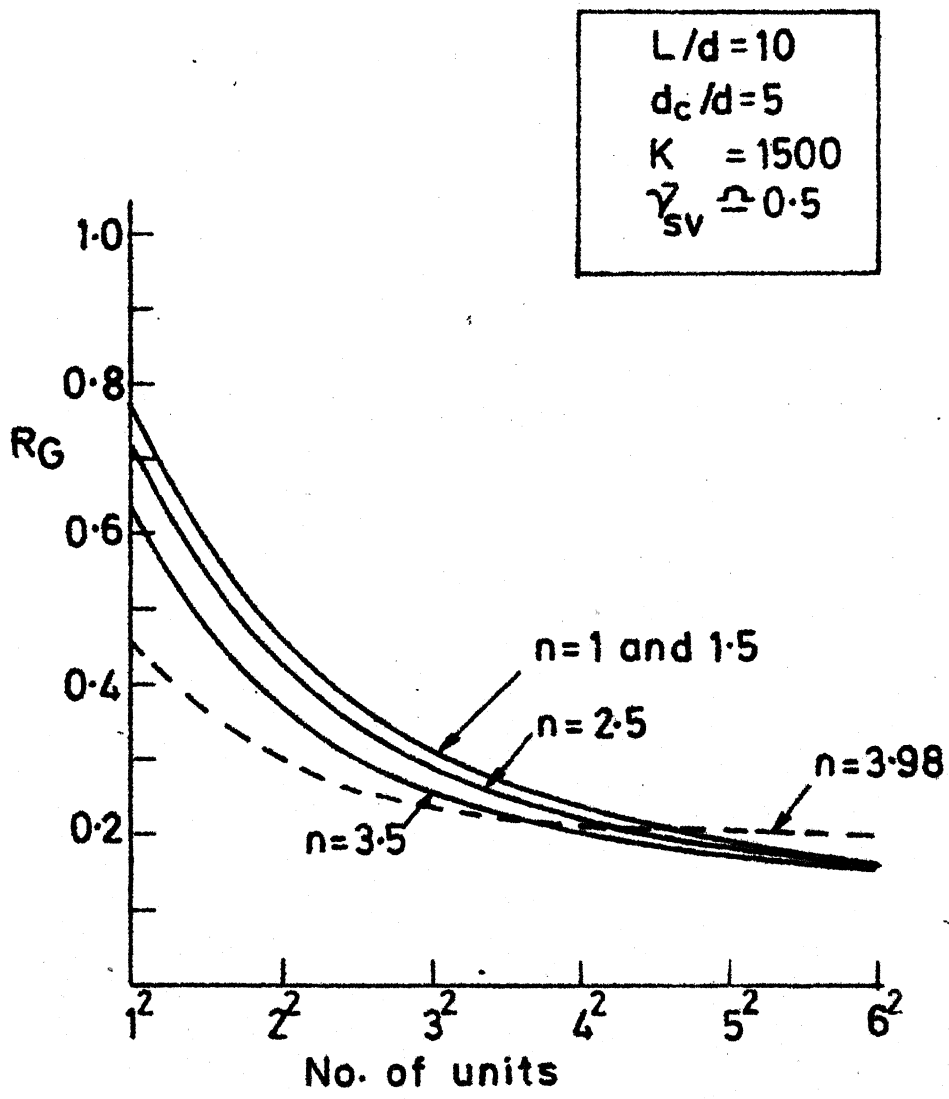
Fig. 5·16 R_G Vs No. of units (Rigid pile-raft) Anisotropic soil
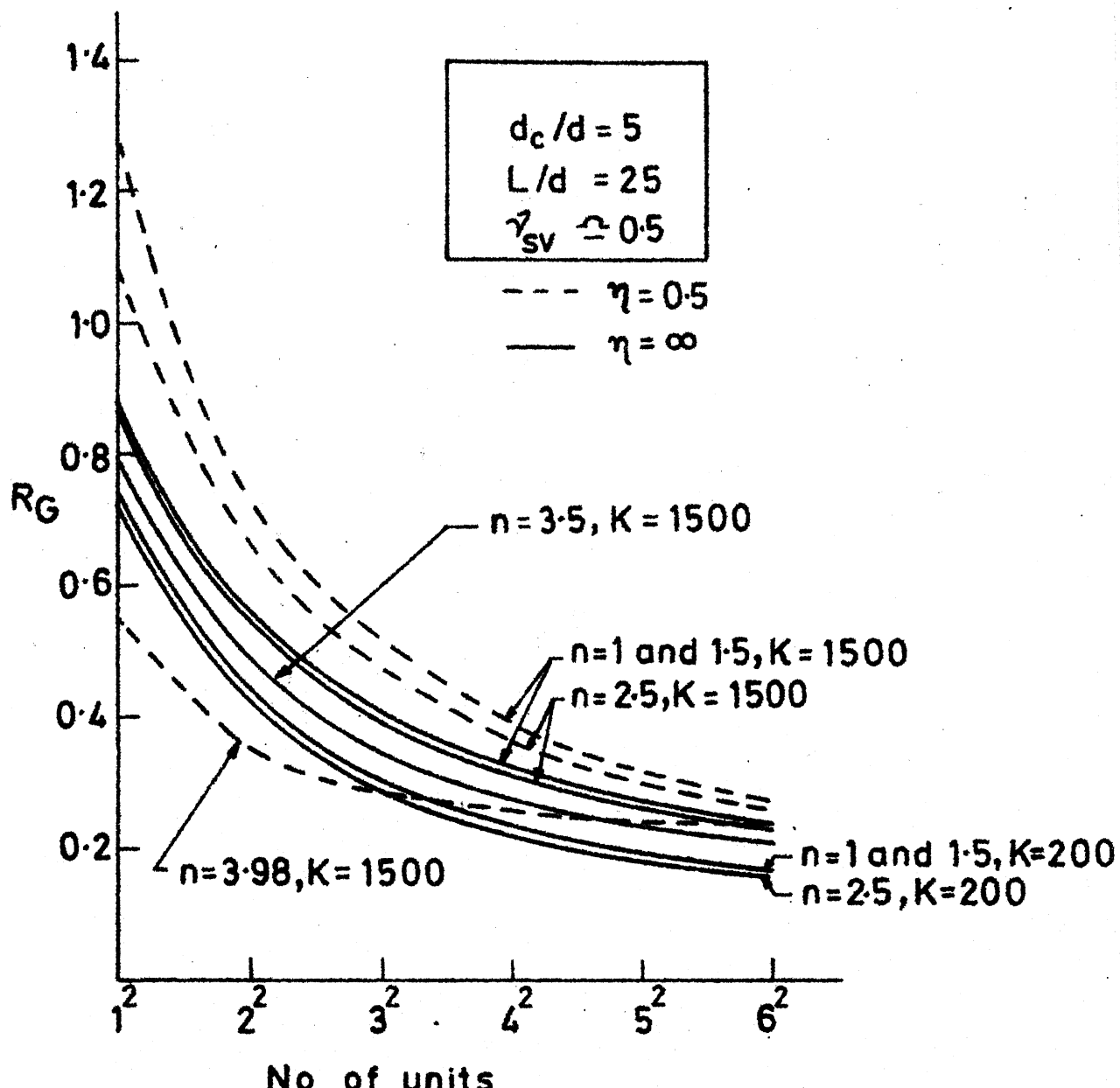
Fig. 5.17 R_G Vs No. of units (Rigid pile-raft) Anisotropic soil
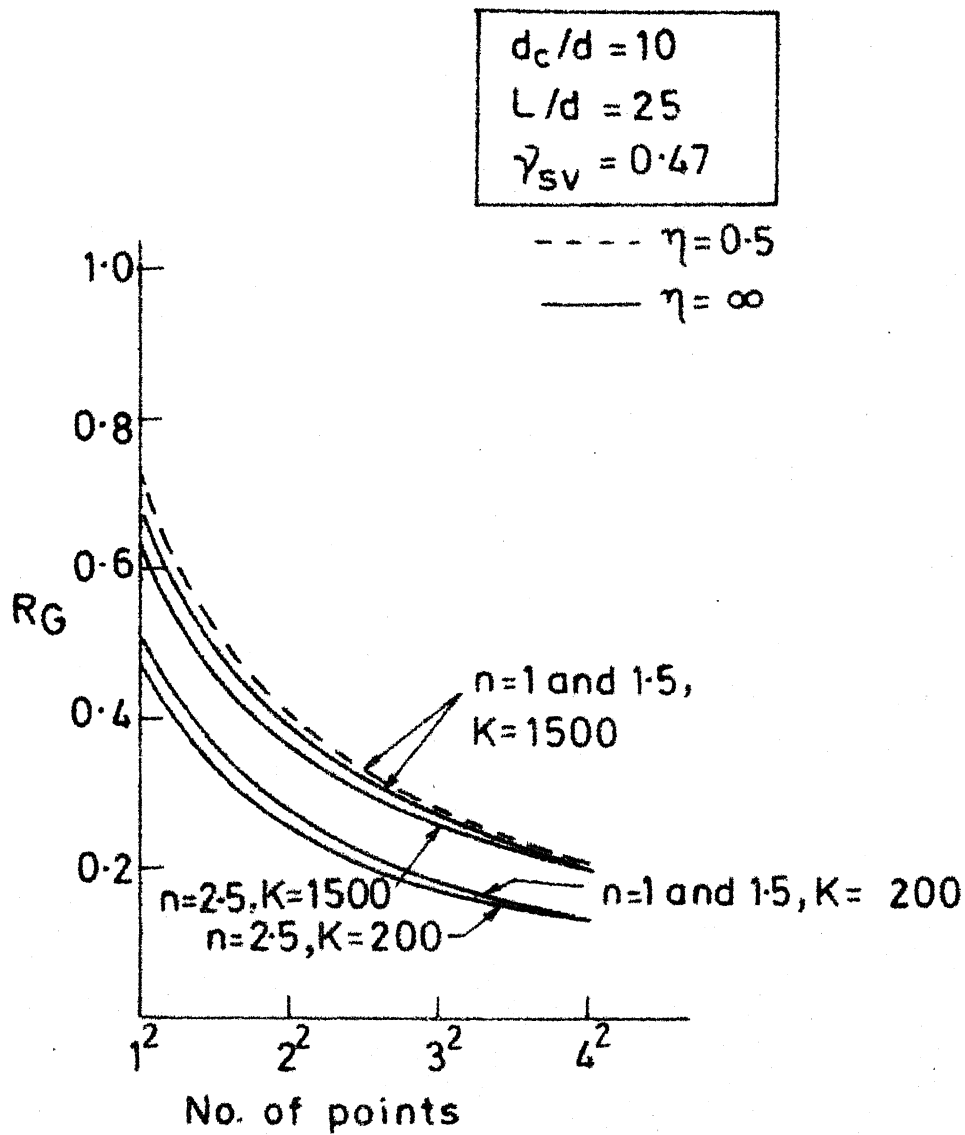
Fig. 5·18 R_G Vs No. of units (Rigid pile-raft) for Anisotropic soil
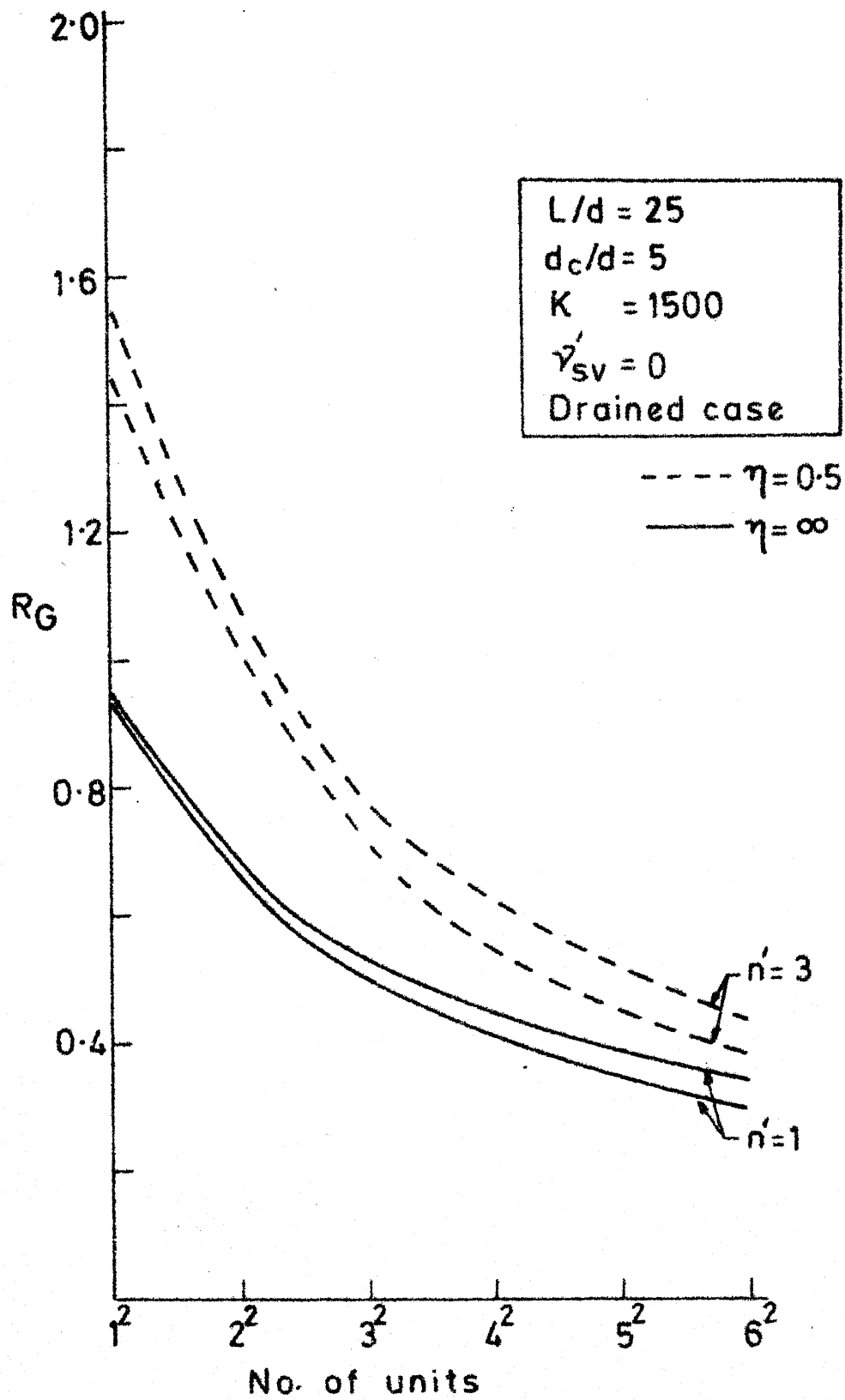
Fig. 5·19 R_G Vs No. of units (Rigid pile-raft)
- Anisotropic soil
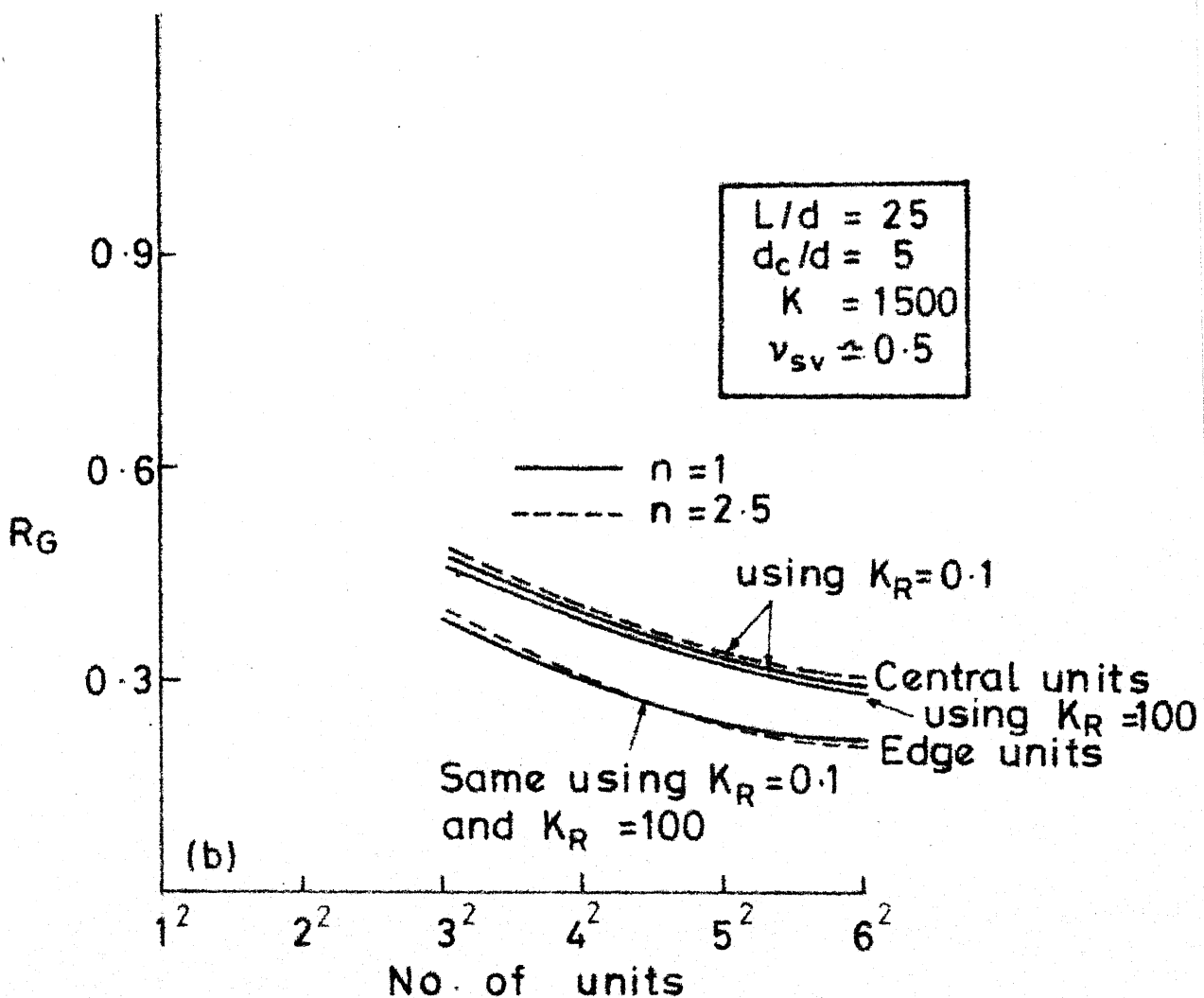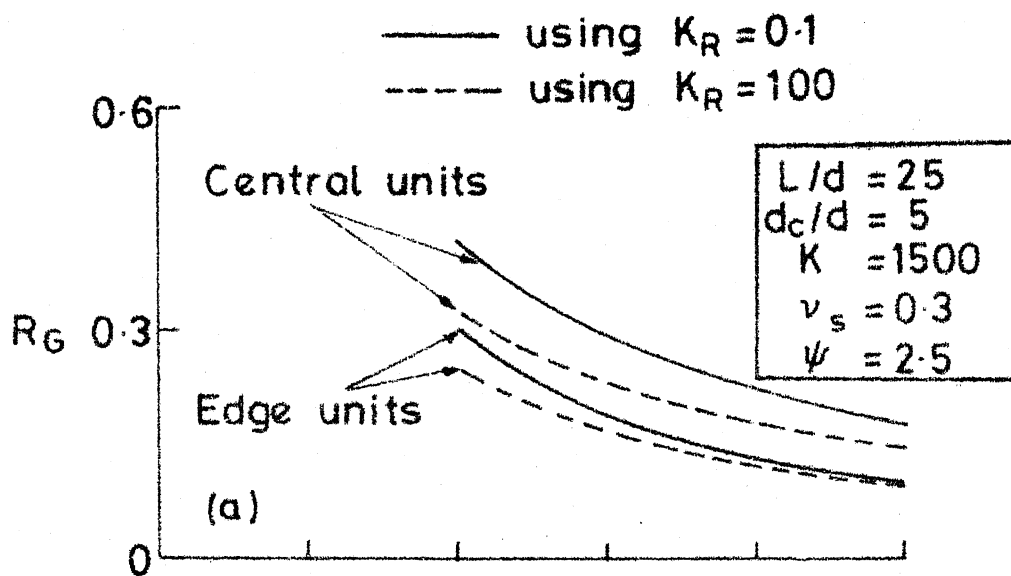
Fig. 5·20 R_G Vs No of units (Flexible Pile-raft)
(a) Non-homegene soil (b) Cross-Anisotropic soil
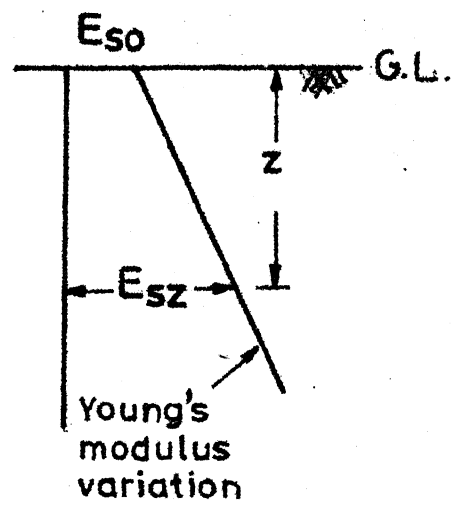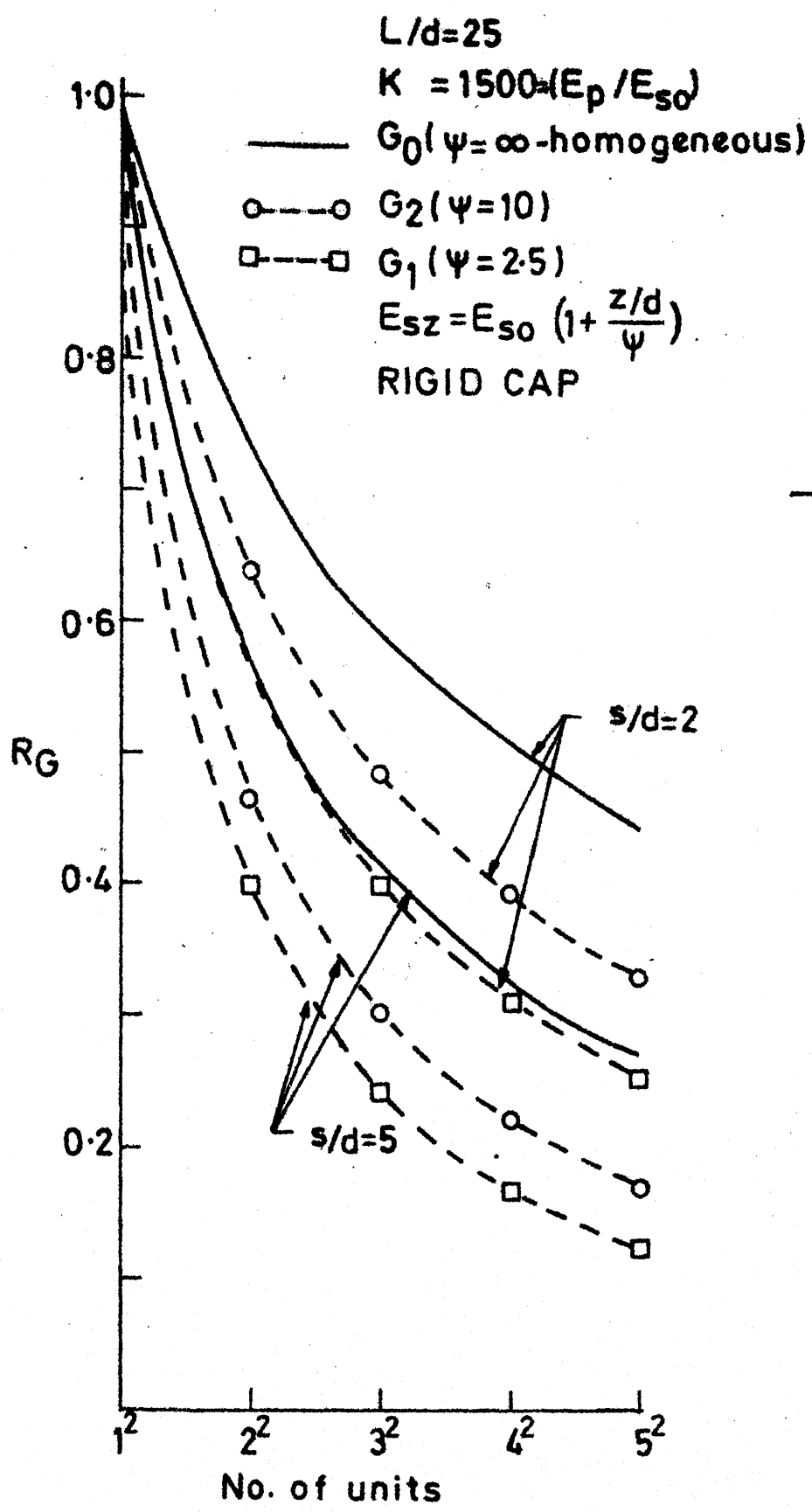
Fig. 5·21 R_G Vs No of units (Pile group)
Non-homogeneous soil
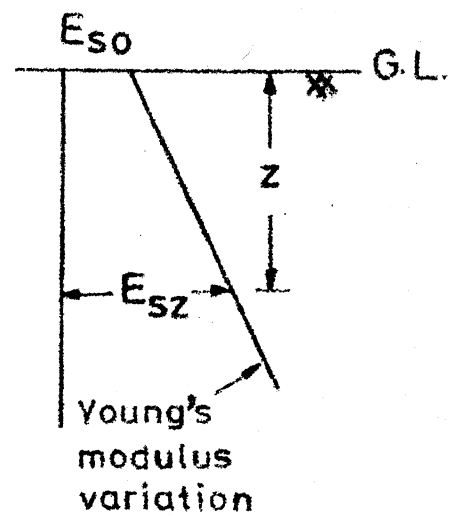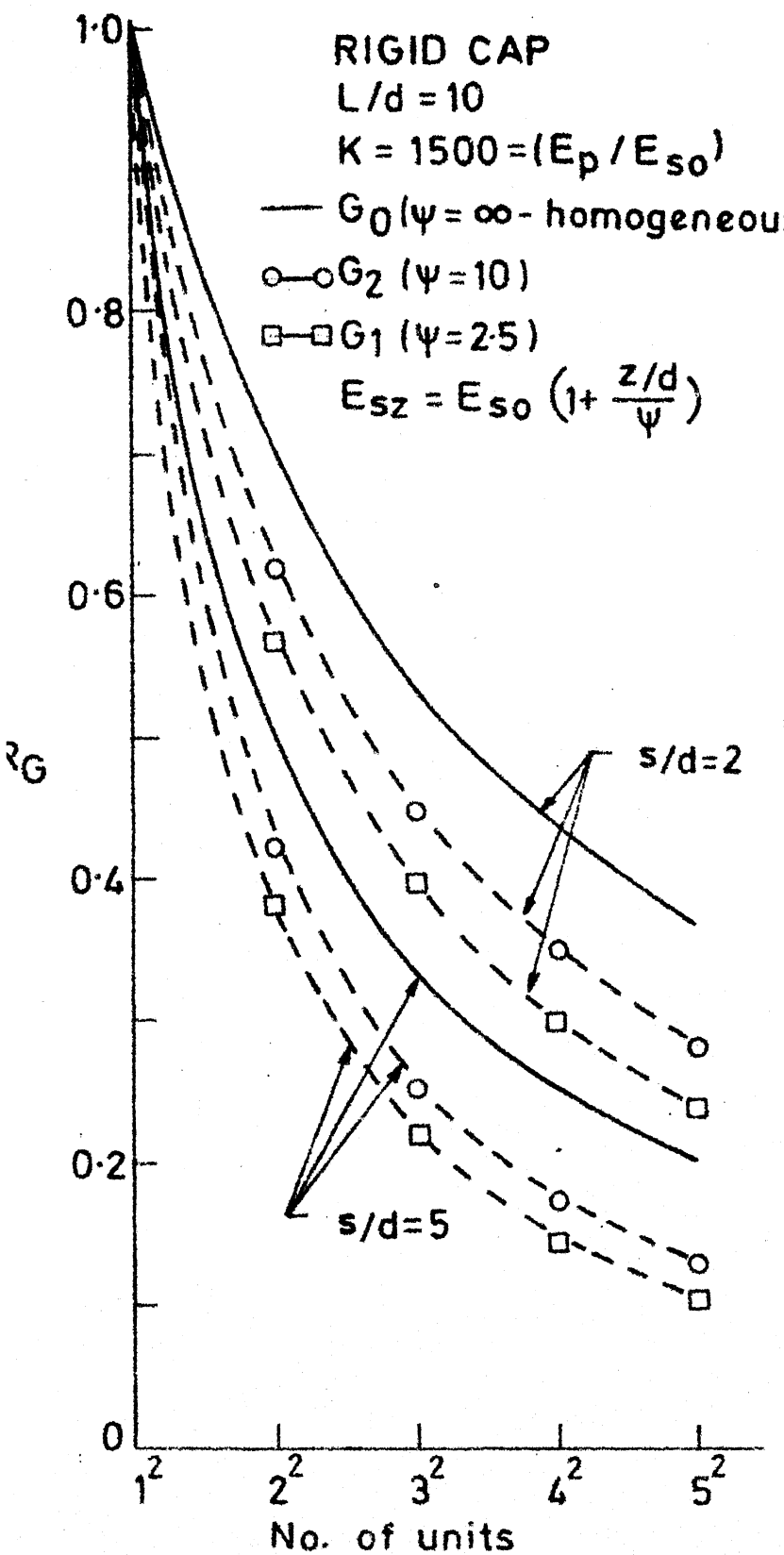
Fig. 5·22 R_G Vs No. of units (Pile group)
Non-homogeneous soil
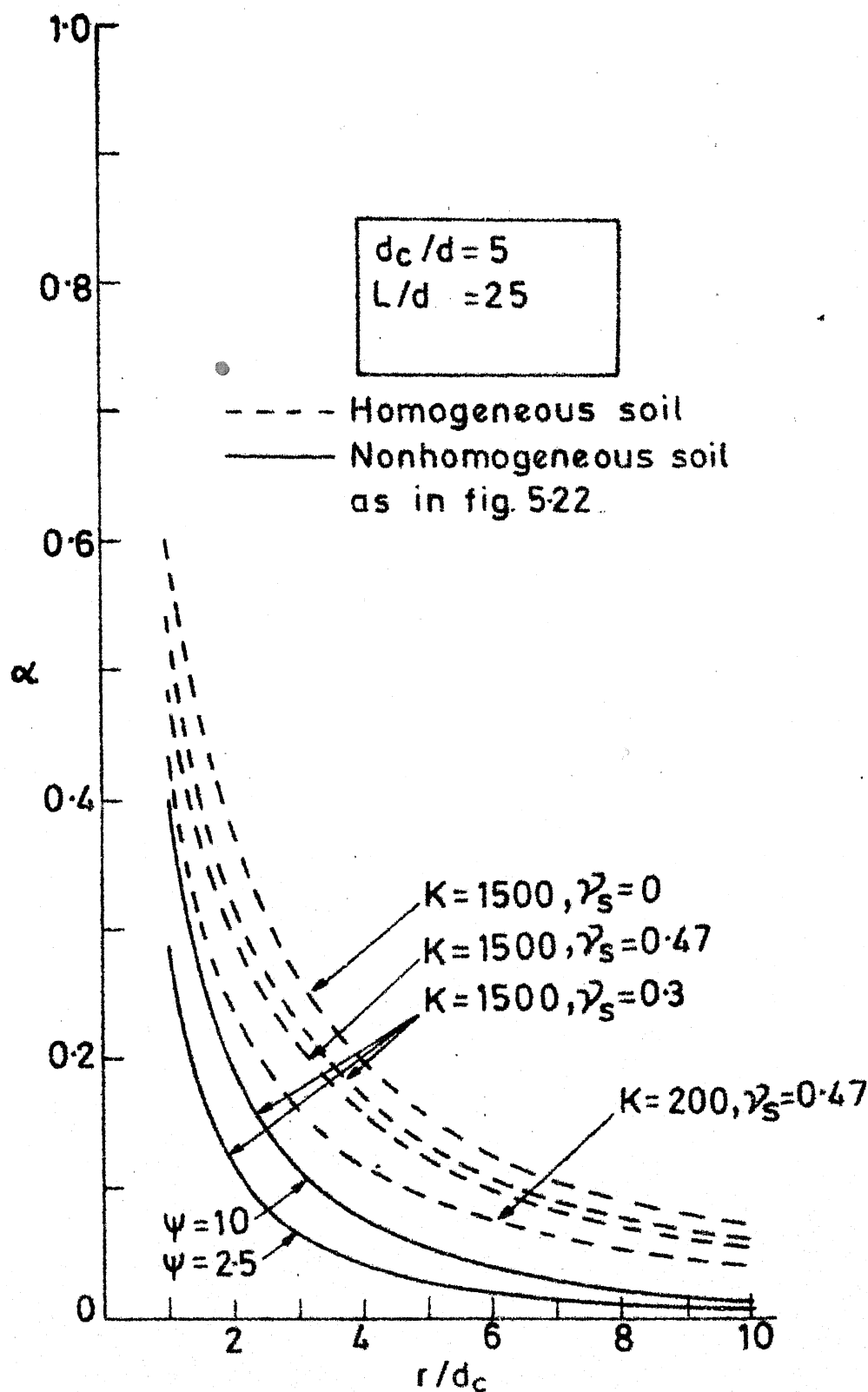
Fig. 5.23 Interaction Factor Vs r/d (pile-raft)
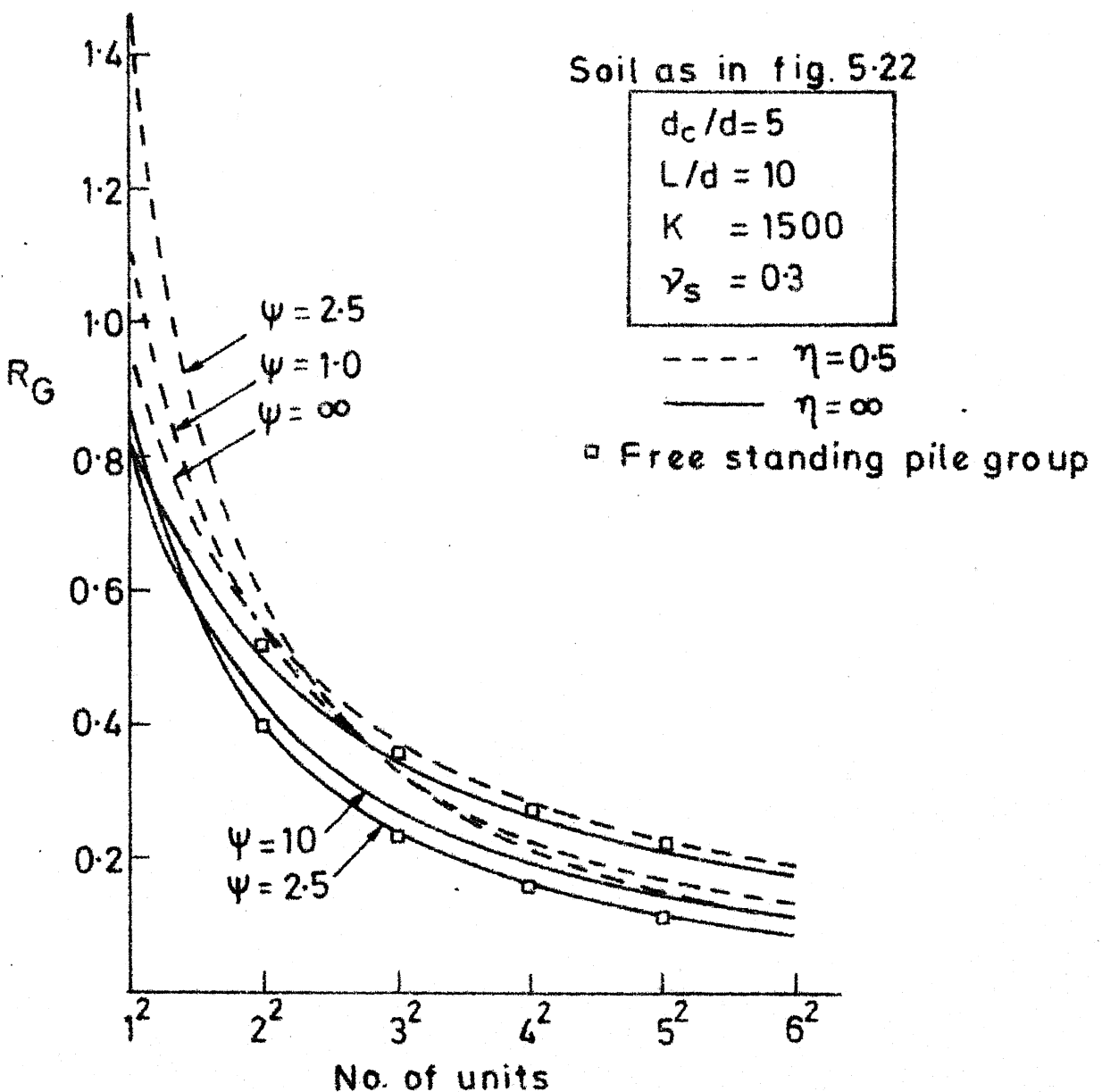
Fig. 5·24 R_G Vs No. of units (Rigid pile-raft)
-Non-homogeneous soil
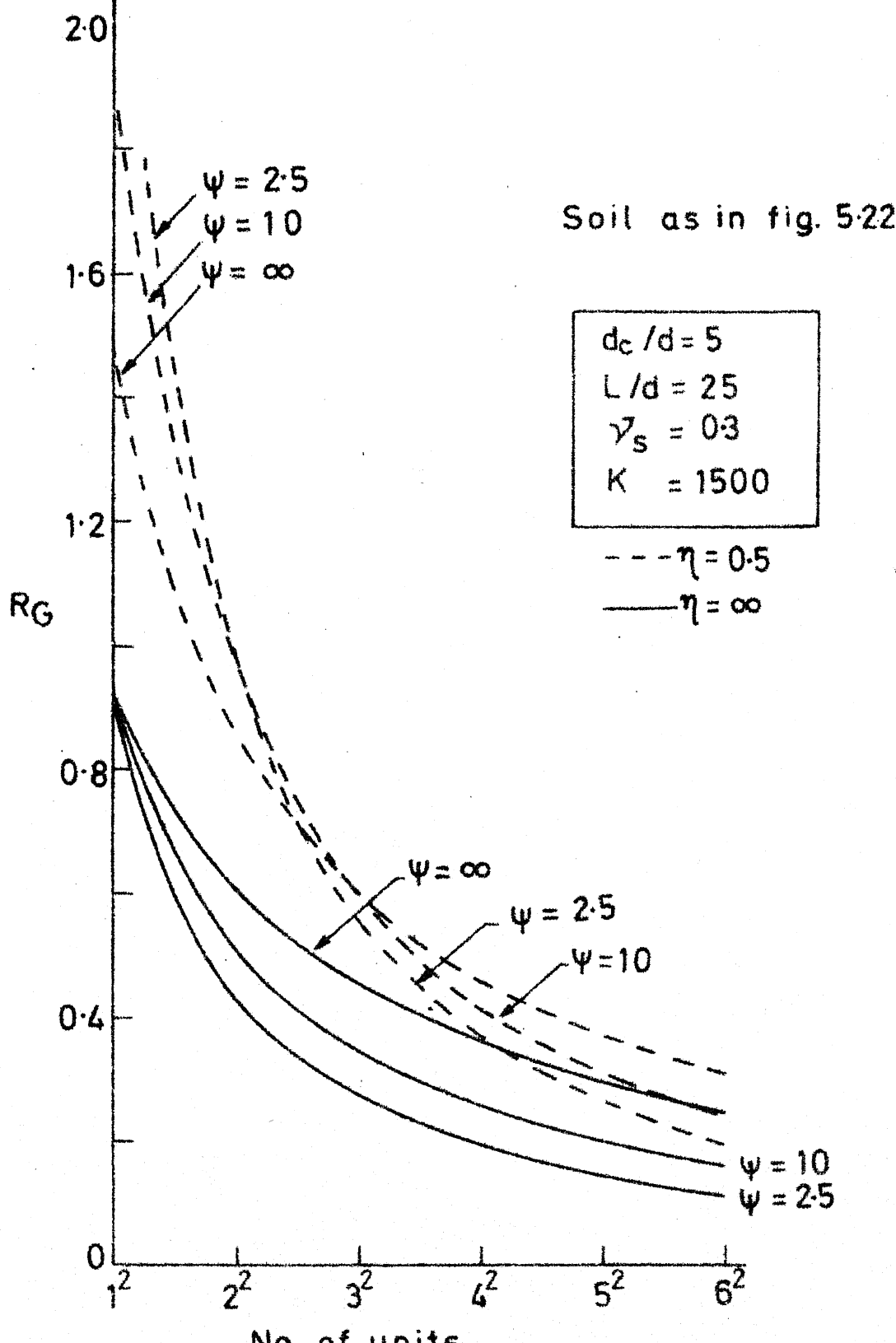
Fig.5·25 R_G Vs No. of units (Rigid pile-raft)
Non-homogeneous soil
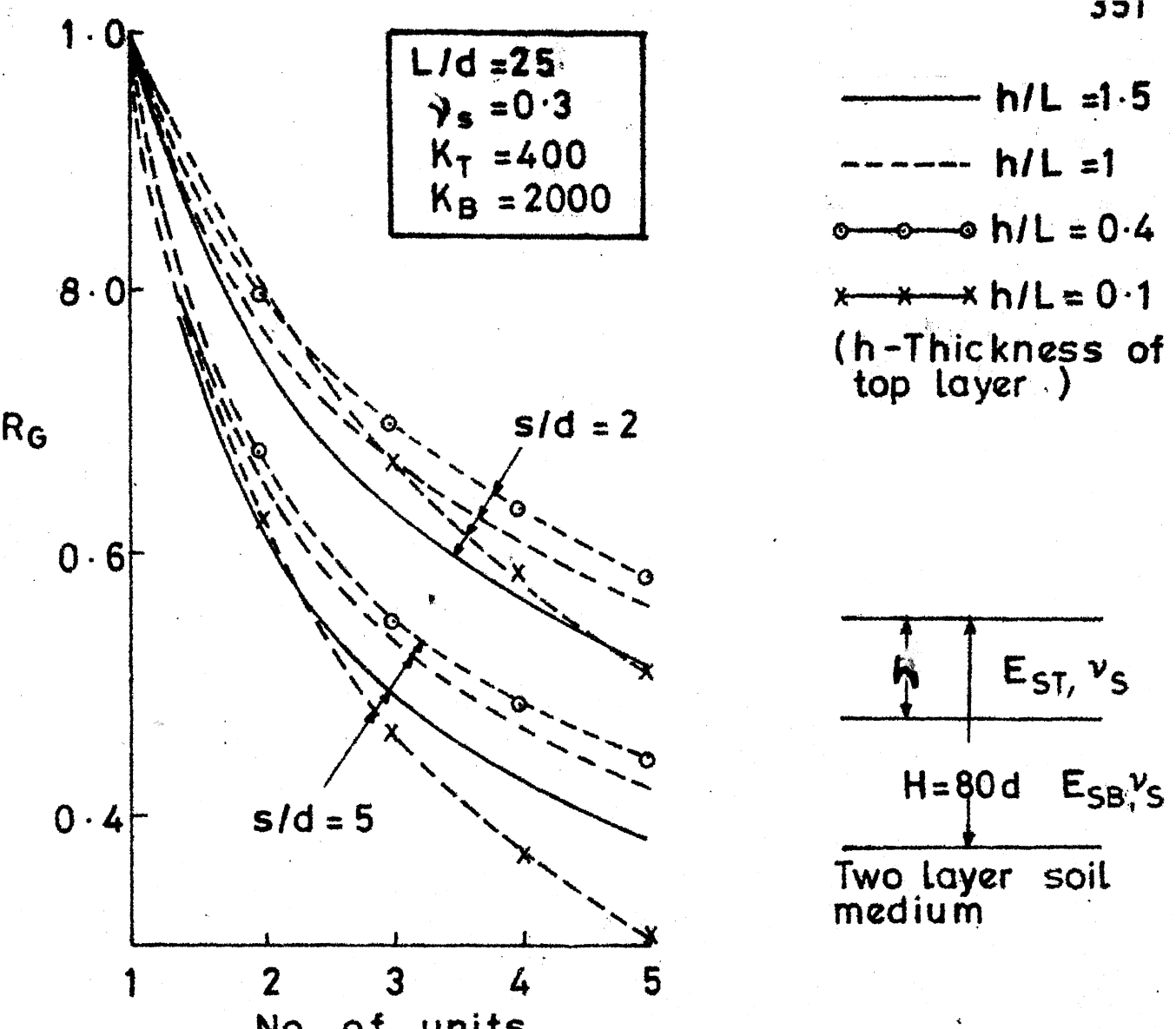
Fig. 5·26 (a) R_G Vs   No. of units (Pile group)
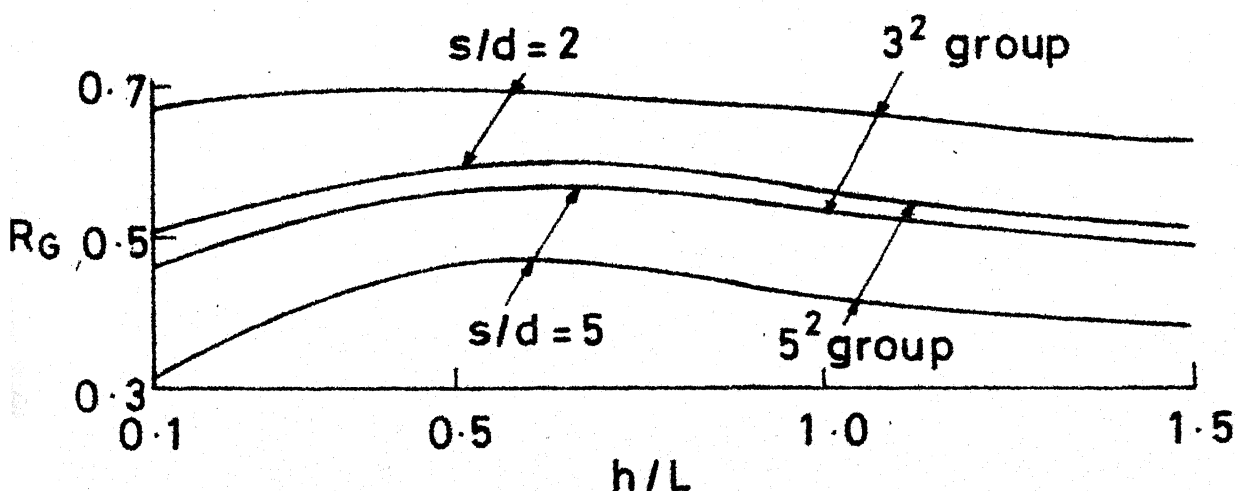
Fig. 5·26 (b) R_G Vs   h/L (Pile group)

Fig.5·27(a) R_G Vs h/L

Two layers soil medium
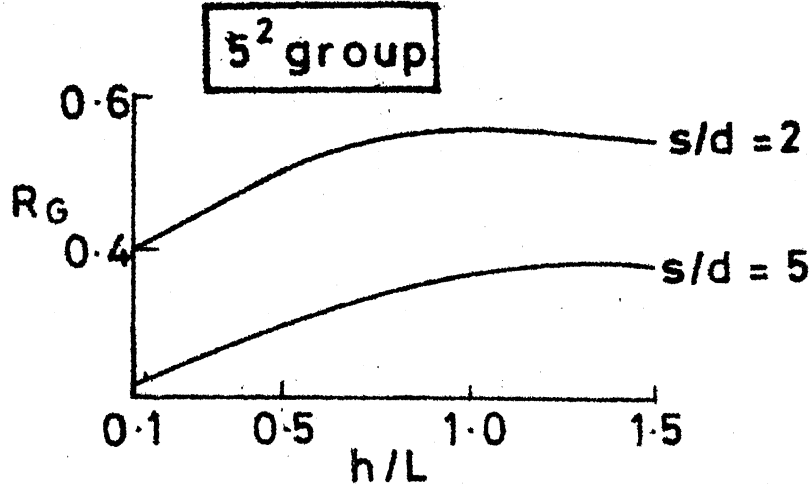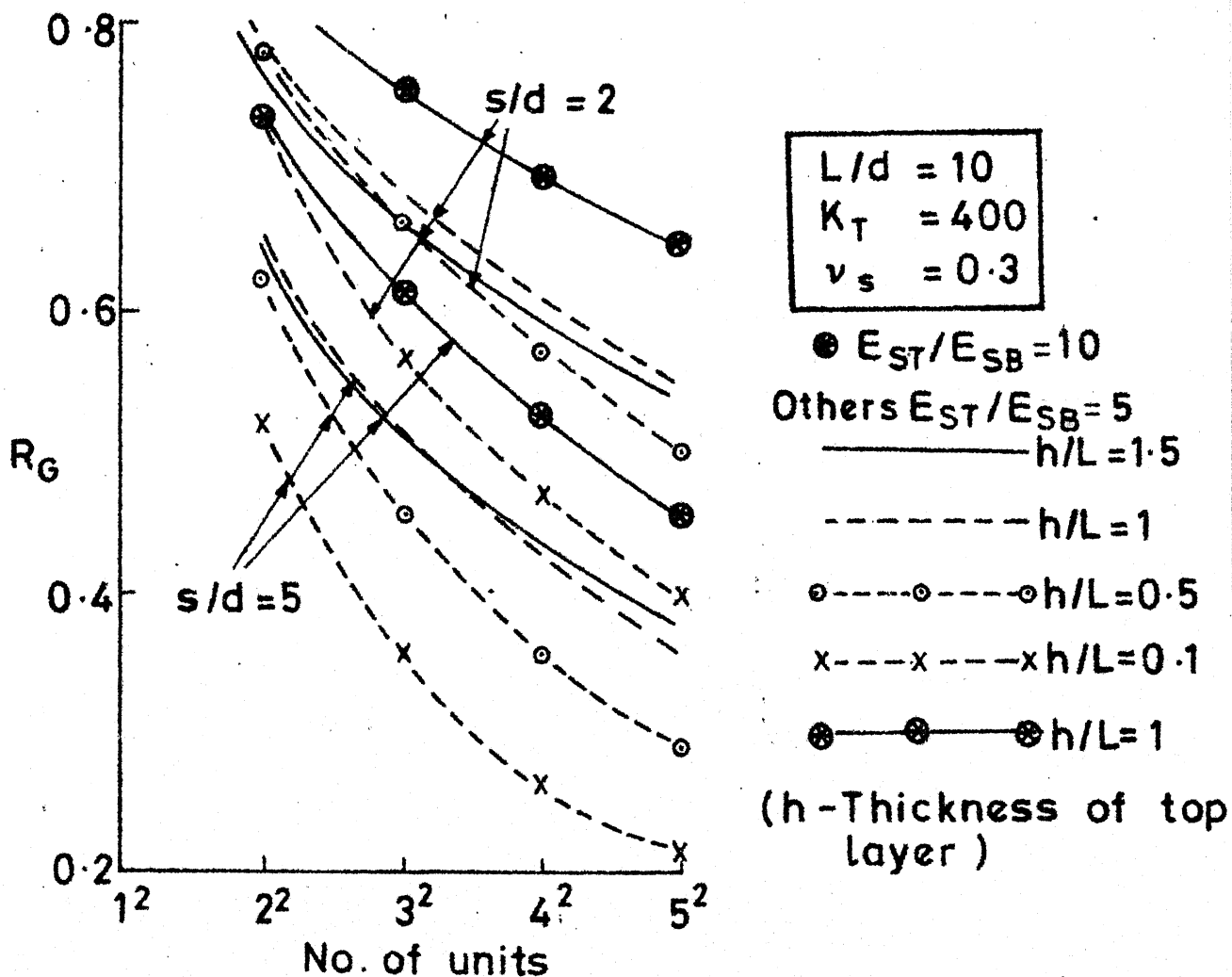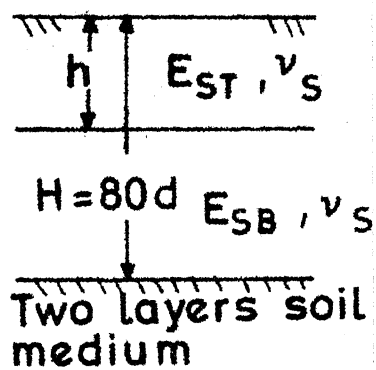
Fig.5·27(b) R_G Vs No. of units (Pile grou
- Layered soil
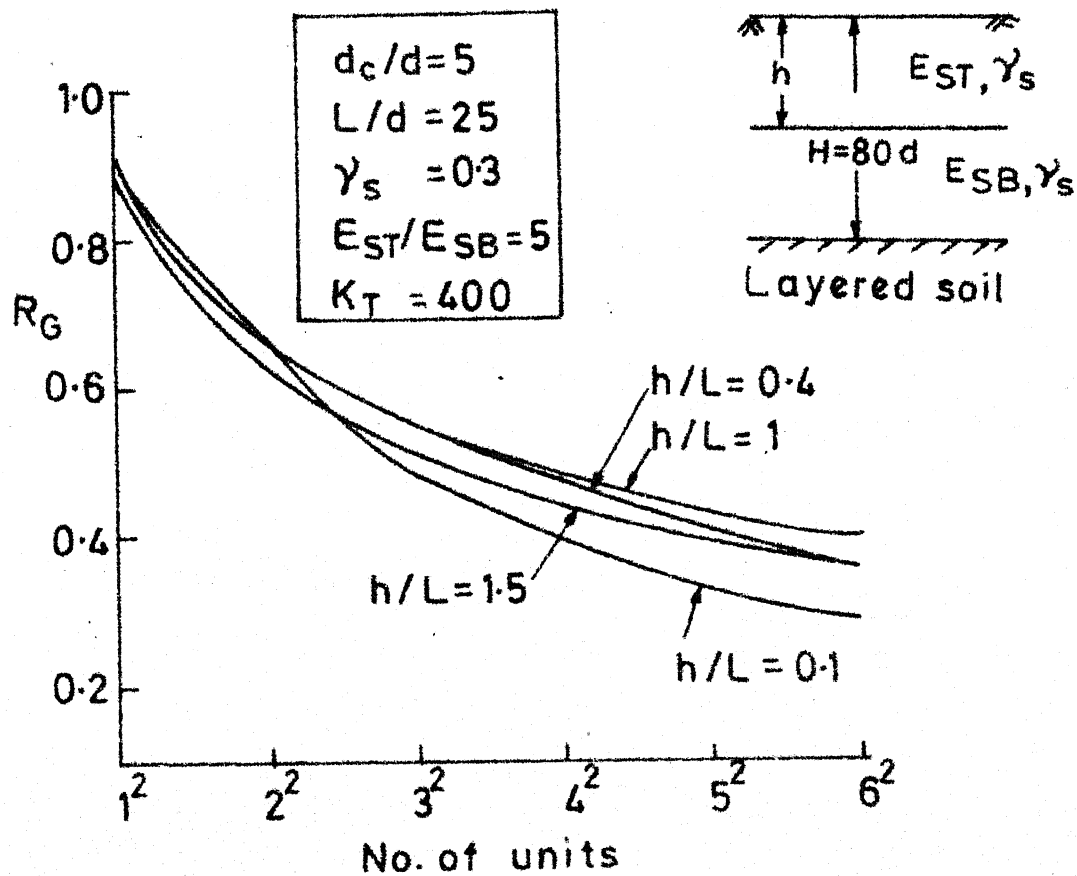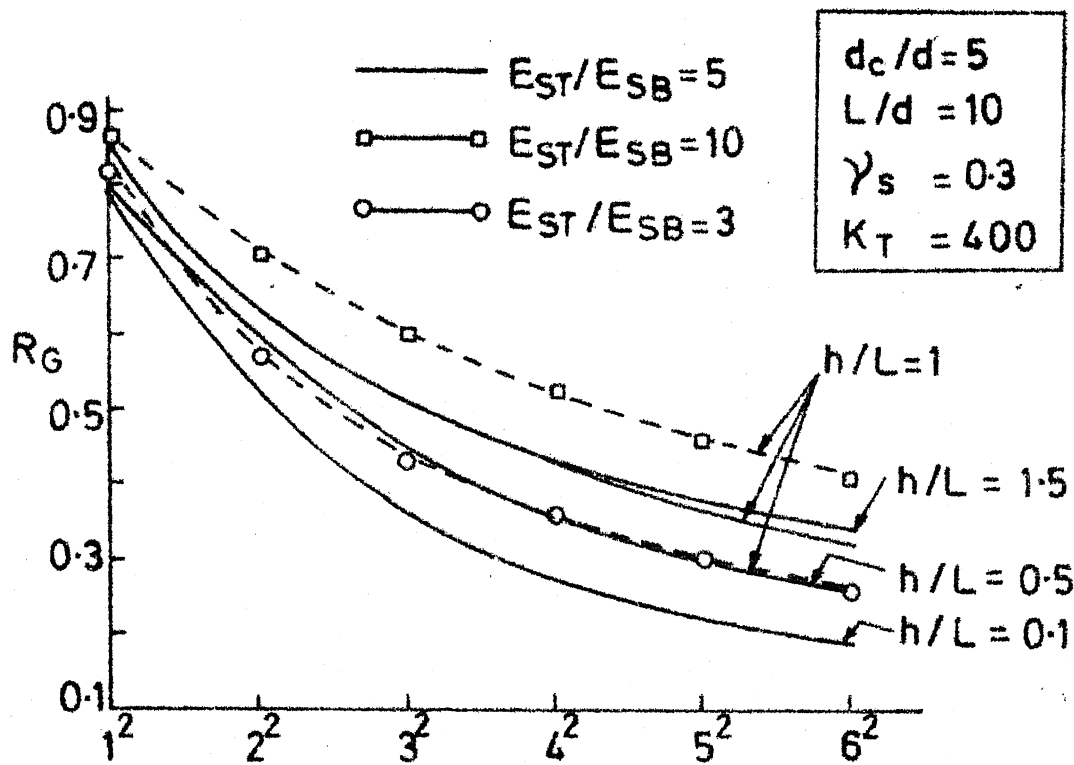
Fig. 5·28 R_G Vs No. of units (Rigid pile raft)
Layered soil
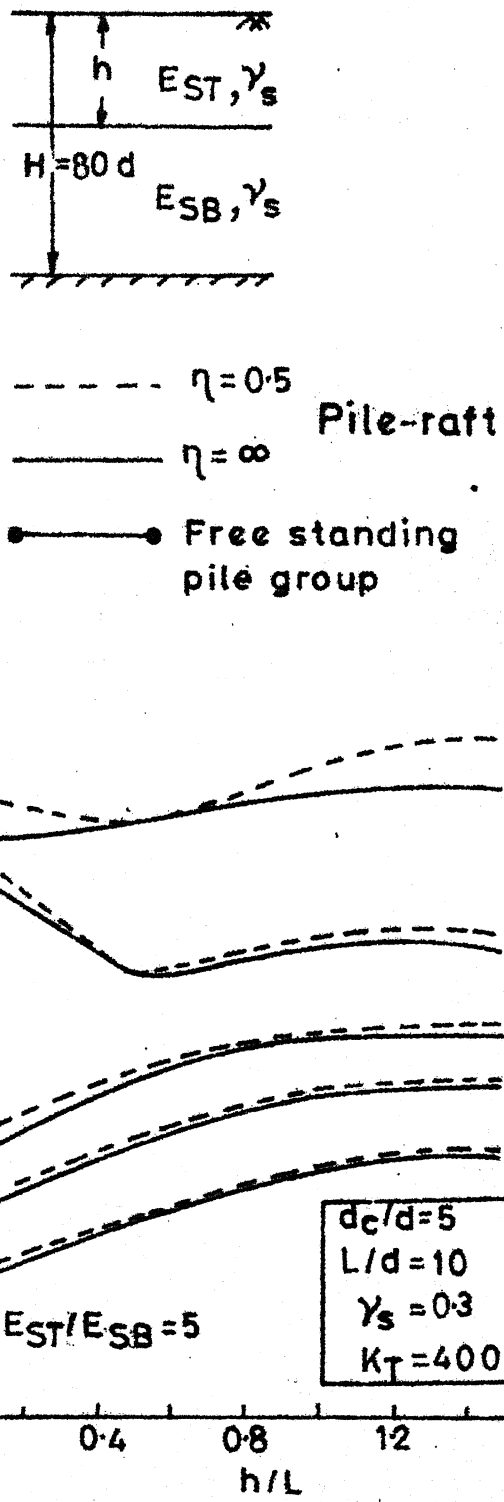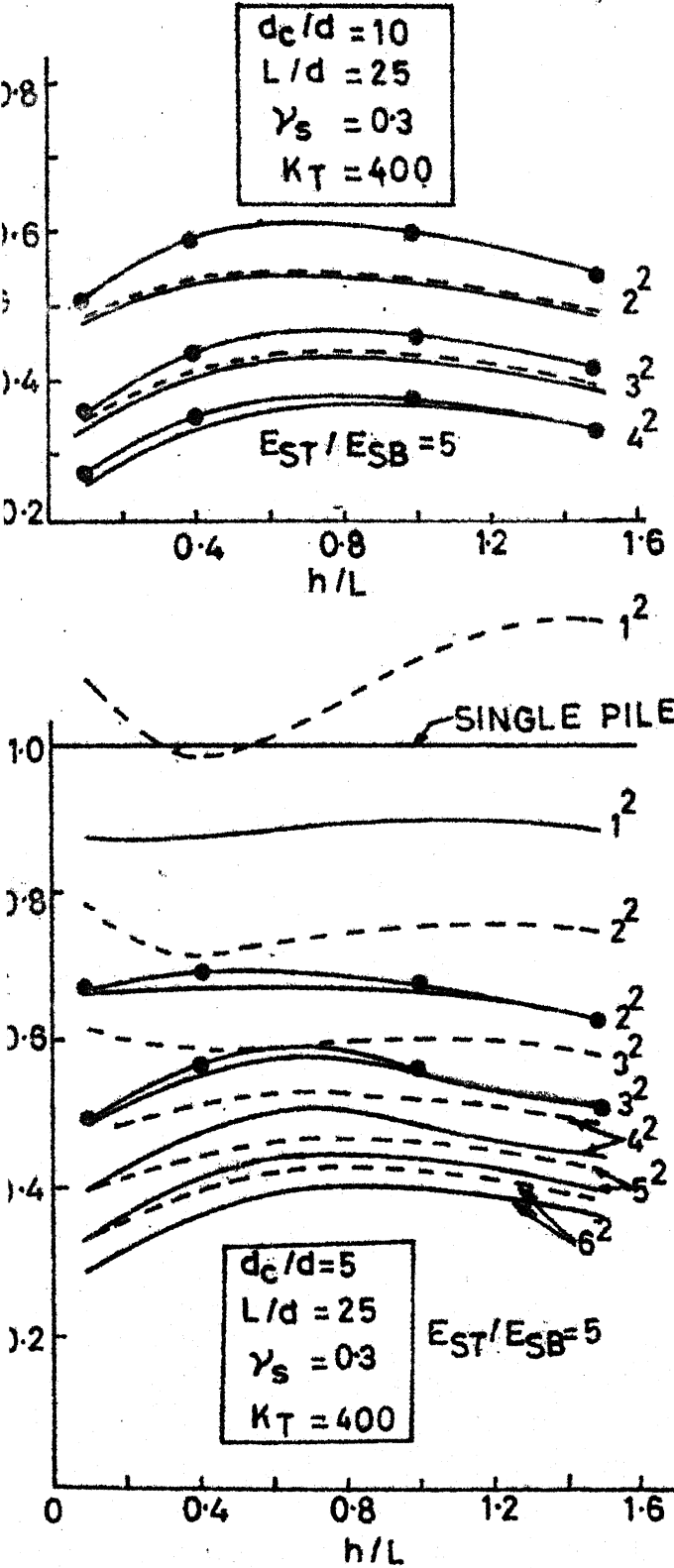
Fig. 5·29 R_G Vs   h/L   (Rigid Pile-raft) Layered soil
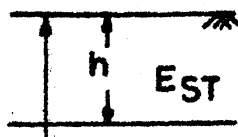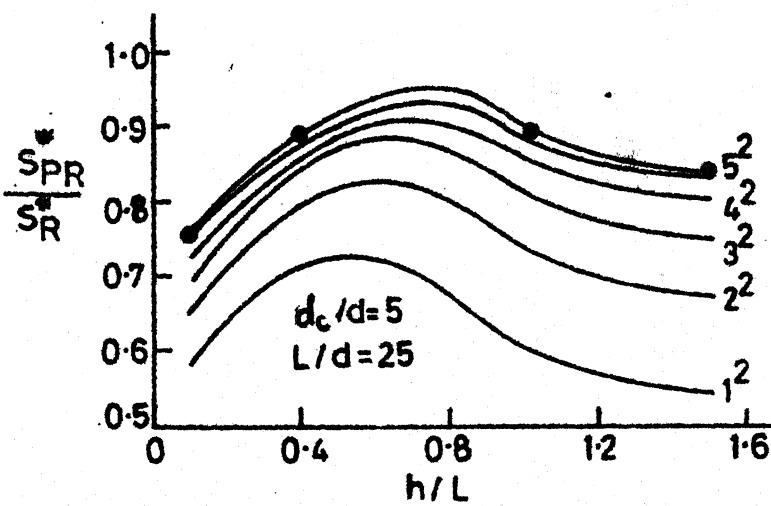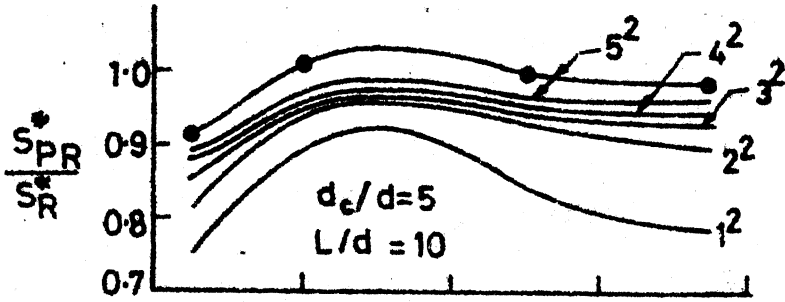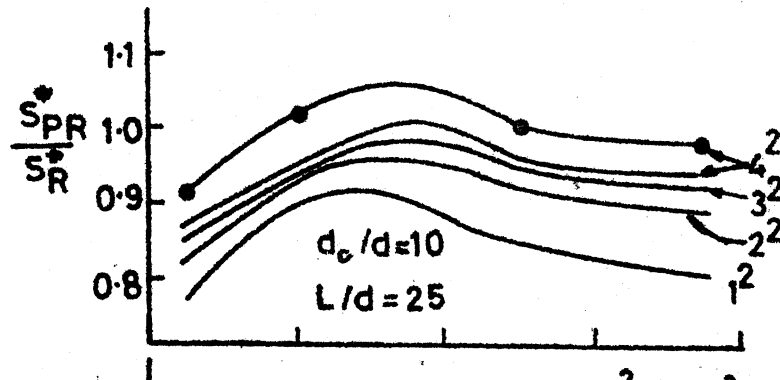
Fig. 5·30 S_{PR}^*/S_R^* Vs h/L (Rigid pile-raft)
Two layered soil medium
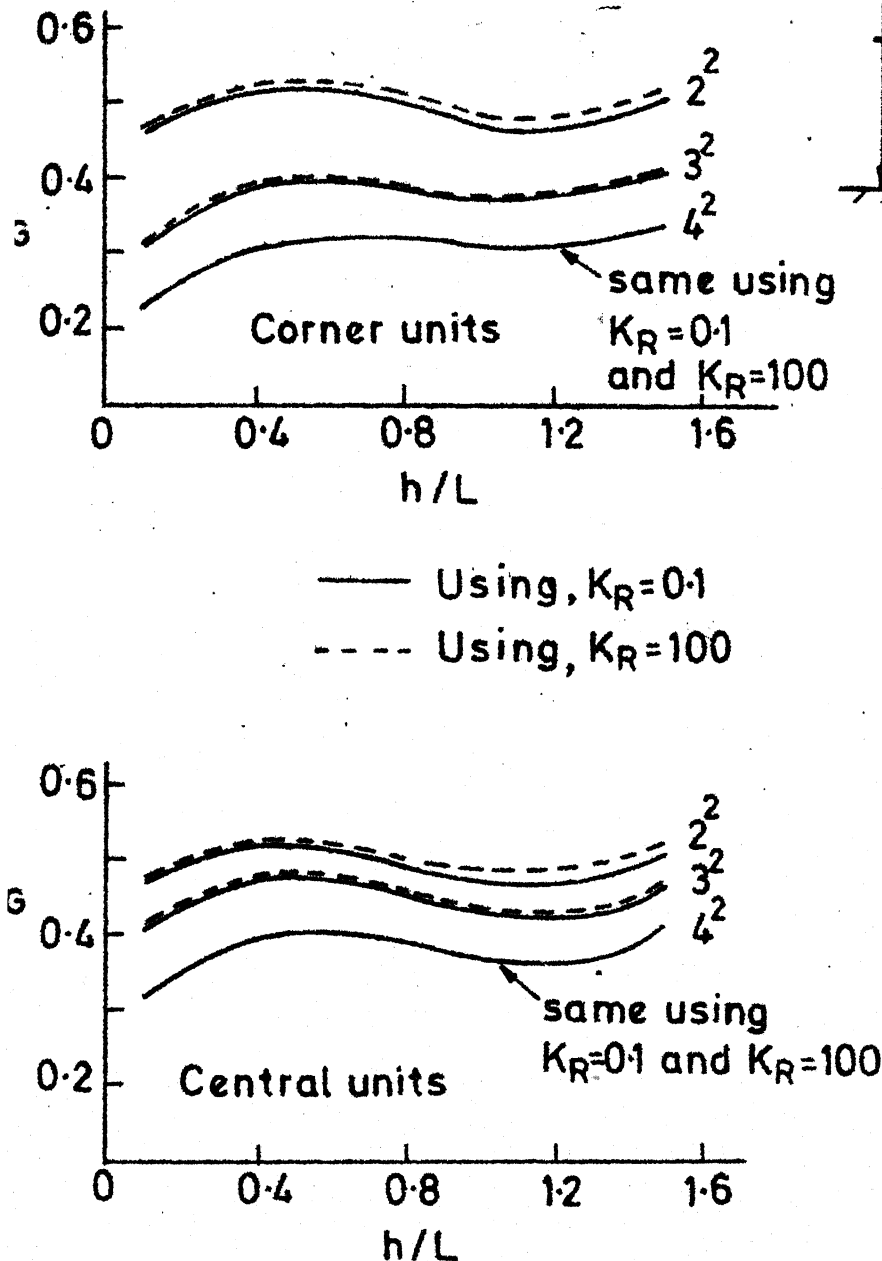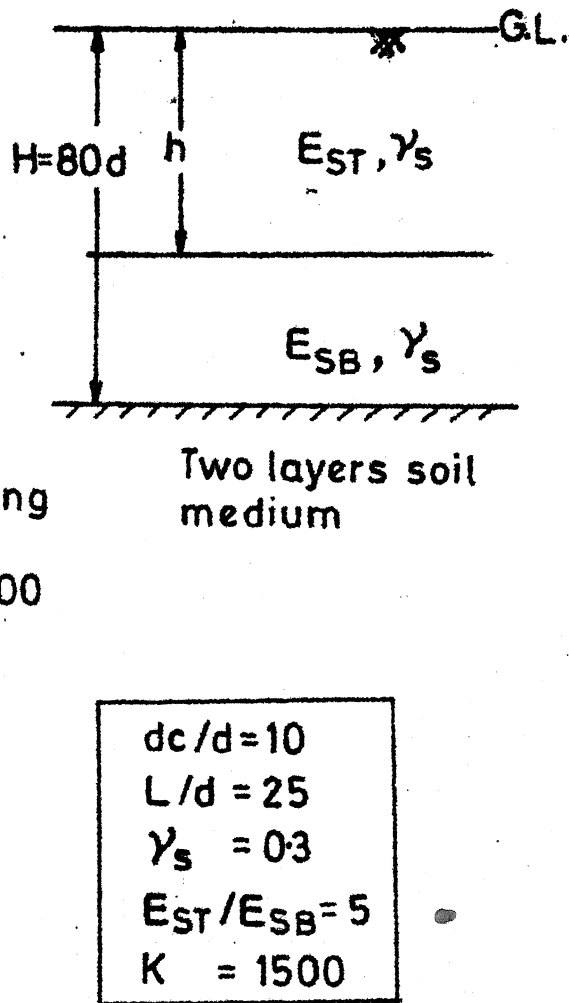
Fig.5.31 R_G Vs h/L (Pile-raft with flexible cap)
Layered soil
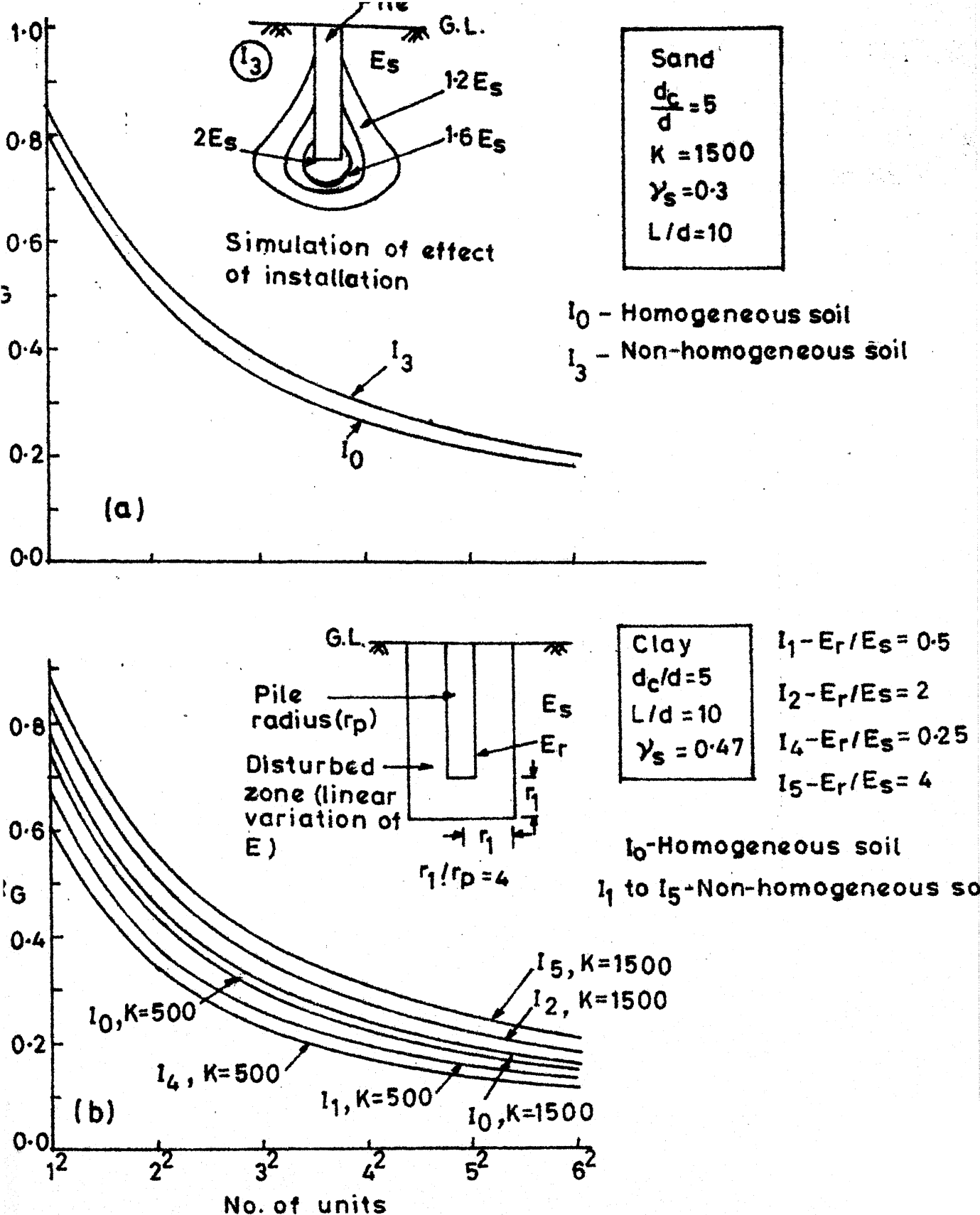
Fig. 5·32 R_G Vs No. of units (Rigid pile-raft)
(a) Loose sand (b) Clay

CHAPTER 6

INTERACTION OF SUPERSTRUCTURE WITH CIRCULAR

RAFT AND PILE RAFT

6.1 INTRODUCTION

Importance of the study of the mutual interaction of superstructure, foundation and soil has been recognised as early as 1947 (Meyerhof (90)). From then onwards several attempts have been made to improve the analytical technique for the analysis of such systems (e.g. Chamecki (26)). The availability of high speed computers and powerful finite element technique, have made a complete analysis of such systems possible. Most of the finite element analyses reported are pertaining to the interaction of plane frame with foundation-soil system (viz. Lee and Harison (86), Lee and Brown (85), Wiberg (142), King and Chandrasekaran (77) etc.) and interaction of space frame with foundation soil system (viz. Majid and Cunnel (87), King and Chandrasekaran (77), Lee (84), Buragohain et al (19), Wardle and Fraser (140) etc.). A number of references of the above analyses have been given by Hooper (75). Relatively few analyses have been reported on the influence of core-wall structures on the behaviour of foundation-soil system. Hooper (75) has analysed a core wall structure

assuming zero rotations at appropriate nodes of the raft mesh, without including the core wall structure in the analysis. Any rigorous analysis of walled structure-foundation-soil system would require discretisation of walls, which is likely to be computationally expensive, for building structures of even moderate size. However, for certain type of structures such as the one shown in Fig. 6.1, which may be used as storage structure, the analysis may not be expensive. An approximate way to include the effect of superstructure is to increase the thickness of the raft appropriately (Hooper (72)). Even though this approach may give satisfactory estimate of differential displacement, it may not give realistic value of bending moments (Hooper (75)).

Most of the analyses reported are pertaining to a particular case and are useful in indicating some of the parametric effects. Analysis by Brown (16), however, attempts to generate design charts for certain configuration of plane framed structures. In the present work attempt is made to present non-dimensional chart to design the foundation of the type of axisymmetrical structure analysed, for certain range of parameters, in addition to making extensive parametric studies.

Analysis of a particular case of a water tank
(a structure similar to one analysed herein), has been
reported by Smith (128). He has used annular plate bending
finite elements, to model the circular raft. In the same
analysis, it is possible to include the superstructure, but
the connection between the superstructure and raft will have
to be assumed as either hinged or fixed. Also, it would
be very difficult to satisfy complete compatibility between
raft and soil, by this formulation. Recently, Booker and
Small (13)*, have developed another analytical technique,
which in effect is similar to finite element method used
by Smith (128). Rowe et al (122)*, have extended this
method to handle soil non-homogeneity. The influence of
superstructure on the behaviour of pile-raft foundation
system, does not appear to have been studied.

For such type of structures, in which there is no
interaction of loads, hinged connection eliminates the
major effect of the interaction of superstructure, with
foundation-soil system; in this case foundation-soil system
can be analysed independently. If the connection between
superstructure and raft is assumed to be fixed, it is
possible to design the foundation accordingly, taking into
account the effect of superstructure. In some cases it

may be difficult to achieve full fixity in the actual construction. Alternately, if the superstructure and raft are modelled by continuum elements, as done in the present analysis, the actual elastic connection that may occur in the case of monolithic construction can be modelled (Singh et al (125)), and also complete compatibility can be satisfied.

Rigorous analysis of pile-raft systems require three dimensional analysis. However, the problem can be idealised as axisymmetrical (Hooper (72) and Knabe (80)) or plane strain (Desai et al (44)), if the piles are closely spaced in an annulus or lying in a plane in the longitudinal direction, respectively. In the present work, a solid annulus of certain stiffness has been used to represent an axisymmetrical arrangement of closely spaced piles or a solid skirt.

In this Chapter, the effect of a superstructure (Fig. 6.1) in completely adhesive connection with a circular raft-soil system and a circular raft-pile-soil system has been investigated. The effect of providing an annular arrangement of piles or skirt on the behaviour of circular raft is discussed. Detailed parametric study has been carried out to asses the influence of different parameters.

The analysis with and without superstructure have been compared and the results of the analysis for different loadings that may be relevent to this type of structures, are presented in the form of non-dimensional charts, which may be used in the design of foundation of such structures with certain geometry and material parameters. The effect of soil modulus increasing linearly with depth is discussed. The effect of variation of soil stiffness and superstructure stiffness is also indicated. The effect of adhesive contact has been discussed for certain cases. The conclusions drawn from this analysis are listed at the end.

6.2 FINITE ELEMENT ANALYSIS

The raft, superstructure, soil and also equivalent annulus of piles (Sec. 6.6) have been modelled by axi-symmetric parabolic isoparametric elements, as in the case of the analysis of piled circular footing, reported in Chapters 2, 3 and 4. The analysis was carried out assuming all the materials to be linearly elastic and isotropic. This simplification reduces the number of parameters and makes it possible to present the solutions for general use. The soil is assumed to be homogeneous in most of the cases and a particular case of soil non-homogeneity has al been considered. Though, for homogeneous soil condi

it would be more economical to represent the continuum by Mindlin's equation than finite element representation, the later was used as the former requires additional programming effort. Also, since a 'condensation procedure' explained in Appendix A, has been used, a number of cases, as many as 20, could be analysed in one run. If any specific field problem is to be studied, the non-linearity of soil and/or foundation material can be accounted for with the same program with some modifications. Interface condition can also be simulated using interface elements, as done in Chapters 3 and 4.

The connections between superstructure and raft, raft base and soil and also between pile head and raft have been assumed to be fully adhesive, for presentation of results. Solutions for circular raft presented for $\nu_s = 0.47$, also apply to smooth contact between raft base and soil (Hooper (73)) approximately. Assumption of adhesive contact between raft and pile head and between superstructure and raft models the elastic connections between them as mentioned earlier.

The computation of bending moments, in-plane stresses, shear force and load taken by piles was carried out as explained in Chapter 2, (Sec. 2.3) and Appendix A. An

equilibrium check was carried out by integrating the vertical stresses below the raft as mentioned in Chapter 2 (Sec. 2.3). The difference observed in such check, was less than 0.5 % and it was less than 0.1 % in most of the cases.

The mesh used is shown in Fig. 6.1. The mesh was refined at the connection between superstructure and raft by increasing the number of elements in that region by three times and it was found that the displacements were affected by less than 0.2 % and the bending moments by less than 2 %, except immediately below the superstructure. Similar observations were made, while refining the mesh above the pile head in the analysis of piled circular footing, which has been reported in Appendix B. The adequacy of one layer of elements for representing the circular raft for the geometrical parameters used in this analysis was confirmed from the analysis of a circular plate supported at the edge, subjected to different loading, reported in Appendix B. Since the maximum bending moment does not occur immediately below the superstructure, for the cases considered, and also since critical section for bending moment is adjacent to superstructure, the results of bending moments are reported from centre to a section near the superstructure-raft inter-connection (Section A in Fig. 6.1).

6.3 PARAMETERS AND LOADING CONSIDERED

6.3.1 Parameters Considered

Geometry of the structure considered is shown in Fig. 6.1 The outer radius of the superstructure is denoted as 'a'. The thickness of cylindrical and hemispherical portions of the superstructure has been assumed to be 0.1a. The clear projection of the circular raft beyond the superstructure is 0.1a. The raft is assumed to be resting on the surface of a thick layer of soil whose thickness is assumed to be 6.5a. The right hand side boundary was kept free, at a distance of 6.8a from the centre. The thickness of equivalent annulus (of piles)was assumed to be 0.1a, and it was assumed to lie vertically below the superstructure.

The following parameters were considerd:

$$\text{Relative rigidity } (K_R) = \frac{E_R}{E_{SO}} (1 - \nu_S^2)(t_R/a')^3 \qquad (6.1)$$

where K_R =   relative rigidity of the raft

      E_R =   Young's modulus of raft material

      E_{SO} =   Young's modulus of soil at ground level

      ν_S =   Poisson's ratio of soil

      t_R =   thickness of the raft

      a' =   Outer radius of the raft
             ($a' = 1.1a$, in the present case).

K_R = 0.1, 0.5, 2 and 10

E_R/E_{SO} = 1500 in most of the cases

E_R/E_{SO} = 300 in some cases

E_{SS}/E_R = 1 in most of the cases

where E_{SS} = Young's modulus of superstructure material.

E_{SS}/E_R = 1/5 in some cases

E_{peq}/E_S = 600   where E_{peq} = the equivalent modulus of solid annulus, representing piles. (Vide eq. 6.2)

Non-homogeneity factor $(\beta) = E_{Sa}/E_{SO}$

where E_{Sa} = Young's modulus at $Z = a$

E_{SO} = Young's modulus at $Z = 0$

Z = depth below ground level

β = 1 (Homogeneous) and 3 (Non-homogeneous) were considered.

ν_S = 0.47 and 0

L/a = 0, 1, 2 and 3 where L = length of piles.

6.3.2 Loading

Three types of loading have been considered as follows:

1.   A vertical u.d.l over a radius equal to a, acting on the raft surface, denoted as q_1 (Fig. 6.1).

2.   A vertical u.d.l. over an annulus of inner radius 0.9a and outer radius 'a', acting on the surface of the raft, denoted as q_2 (Fig. 6.1).

3.   A lateral pressure in the radial direction acting
      on the cylindrical portion of the superstructure;
      this lateral pressure is assumed to be linearly
      varying as shown in Fig. 6.12. This pressure is
      denoted as q_3.

Loading q_1 represents the loading due to the weight
of the material stored or the dead and live load that may
act, if the structure is used as some utility structure.

Loading q_2, represents the loading due to self weight
of the superstructure and any other load that may be trans-
mitted to the foundation through superstructure. It is
assumed that horizontal force and moment are not transmitted
to the base of the superstructure, for this loading. To
asses the implication of this assumption, a seperate analysis
was done imposing gravity load to the superstructure elements
and it was compared with analysis with loading q_2, the
magnitude of q_2 being equal to the pressure due to the
weight of the structure. It was found that analysis with
loading q_2 overestimated displacements, moments (of raft)
etc. by less than 5 % , compared to analysis with gravity
load. From the same analysis, it was also observed that
the gravity stresses were underestimated by about 2 % ,
probably due to discretisation error. Hence, the actual
difference would be less than 3 % . However, if one is

interested in the stresses and displacements in the super-structure, the analysis has to be done for gravity loading and other loadings, if any. For the purpose of comparison of analysis with and without superstructure, it is convenient to consider the loading (q_2) as assumed. Loading q_3 represents the lateral pressure exerted by the material stored (usually liquids or granular material) inside. In most of the practical cases, it is reasonable to assume a linear variation as shown in Fig. 6.12.

The solutions obtained for loading q_1 and q_2, are also valid for wide variation in the height of the cylindrical portion and/or variation in the shape of the roof portion. This point is discussed further subsequently. However, the solutions for loading q_3, is valid only for the particular geometry of the superstructure considered, as the behaviour depends on the height of the cylindrical portion, the type of connection between the roof portion and cylindrical portion and also the shape of the roof.

6.4 DISCUSSION OF RESULTS

6.4.1 General

The results of the analysis are plotted in Figs. 6.1 to 6.15 and some results are tabulated in Tables 6.1 to 6.6. In figures, 'Non-homogeneous' denotes the non-homogeneous

soil considered (Sec. 6.3.1) and results shown without any specific remark are for homogeneous soil with $E_R/E_{SO} = 1500$ and $E_{SS}/E_R = 1$. Notations used in figures and tables:

$S*$ = maximum settlement

S = settlement at any radial distance r from centre line, at the ground level

Δ = differential settlement

PPL = percent load shared by piles

$M*$ = maximum bending moment/unit length

M_R = radial bending moment/unit length at r

M_T = tangential bending moment/unit length at r.

Q = shear force at specified location/unit (arc) length.

r = radial distance from centre line

I_S = settlement influence factors

I_Δ = differential settlement influence factors

S_0 = denotes analysis without including superstructure (without superstructure elements in Fig. 6.1)

S_1 = denotes analysis considering superstructure (Fig.6.1)

I_{MR} = radial bending moment influence factors

I_{MT} = tangential bending moment influence factors

f_R^* = maximum radial in-plane stress

f_T^* = maximum tangential in-plane stress.

(Other notations have been explained in Sec. 6.3.1).

6.4.2 Settlement

For loadings q_1 and q_2, the effect of superstructure on maximum settlement is, in general, small as seen in Figs. 6.2 and 6.3, particularly when the raft is rigid ($K_R = 10$), for which case the effect of superstructure on settlement is insignificant for all the cases considered (comparing results for S_0 and S_1, which represent analyses without and with including the superstructure). As the value of K_R reduces, the effect of superstructure becomes significant; the maximum effect when $K_R = 0.1$ and $\nu_S = 0.47$ for loading q_1 on unpiled raft, is about 15 %. For $\nu_S = 0$, the effect is less than that for $\nu_S = 0.47$. This may be due to the adhesive contact assumed in this analysis. For pile-raft considered, the effect of superstructure is significantly less, compared to circular raft (Fig. 6.2 and 6.3). For loading q_2, the superstructure does not have any effect on the maximum settlement of pile-raft, for all values of L/a used. For $L/a = 0$ also, the effect of superstructure is less for this loading than q_1. For the particular case of non-homogeneous soil condition considered the effect of superstructure on maximum settlement shows similar trends to that in the case of homogeneous soil, even though the magnitude of settlement reduces by one third of homogeneous case.

The settlement due to loading q_3, was found to be in-significant compared to those due to loading q_1 and q_2. However, the differential settlement was found to be some what significant, for loading q_3 also. The complete results considering the superstructure, for homogeneous soil condition and $\nu_S = 0.47$, have been tabulated in Tables 6.1 and 6.2, for loadings q_1, q_2 and q_3 and for different values of L/a and K_R. Complete settlement profile, for any combination of these loadings can be obtained, by superposing these solutions and hence the differential settlement can also be computed.

It can be observed in Fig. 6.2 that the maximum settlement reduces by more than 50 %, when piles of length 3a are provided near the edge. This percentage reduction is more for $\nu_S = 0$ than $\nu_S = 0.47$. This may be because greater load is shared by piles when $\nu_S = 0$, and also settlement of pile is less for this value of ν_S, compared to $\nu_S = 0.47$. The reduction in settlement due to provision of piles is more for larger value of K_R, for loading q_1. For loading q_2, the maximum settlement is insensitive to the value of K_R, in the case of pile-raft, for all values of L/a considered. Increasing pile length, causes less than proportionate (comparing the results for $L/a = 0,1,2$ and 3, in Figs. 6.2 and 6.3) reduction in maximum settlement.

It appears that $L/a = 2$, may be cost effective.

6.4.3. Differential Settlement

6.4.3.1 Circular raft-without considering superstructure

When the superstructure is not considered, the effect of adhesive contact on differential settlement of circular raft can be assessed by comparing I_Δ $(= \Delta \, E_s /(1 - \nu_S^2) qa)$ for $\nu_S = 0.47$ and $\nu_S = 0$. (Δ can be obtained from Figs. 6.4 and 6.5). I_Δ is independent of ν_S for smooth contact for vertical loading. If $\nu_S = 0.5$, the adhesive contact effect is negligible (Hooper (73)). Hence, such comparison of I_Δ, for $\nu_S = 0.47$ and $\nu_S = 0$, indicates the effect of adhesive contact. For loading q_1, the effect of adhesive contact, assessed as mentioned above, is to reduce the differential settlement by about 40 %, for all values of K_R. For loading q_2, adhesive contact, increases the differential settlement, by about 40 %, for $K_R = 2$ and by about 17 % for $K_R = 0.5$. It is to be noted that the effect of adhesive contact is reverse and also decreases as K_R decreases, for this loading, compared to loading q_1.

6.4.3.2 Effect of superstructure on differential settlement of circular raft.

There is substantial reduction (more than 60 %) in differential settlement in the case of circular raft, when

the superstructure is considered as seen in Figs.6.4 and 6.5 (comparing S_0 and S_1), for both loading q_1 and q_2 and for both values of ν_S. It is of interest to note that the adhesive contact (for $\nu_S = 0$) reduces the differential settlement by about 40 % as discussed earlier and the superstructure effect further reduces Δ by about 60 % for $\nu_S = 0$, for loading q_1 (Fig. 6.4). For loading q_2, superstructure stiffness reduces the value of Δ by about 50 % .

As the value of K_R reduces the effect of superstructure in reducing the differential settlement reduces slightly.

6.4.3.3 Pile-raft

In the case of pile-raft, the effect of super-structure on Δ is less compared to that in the case of circular raft. Provision of piles, increases the differential settlement slightly in the case of loading q_1, when the superstructure is considered, whereas the differential settlement is substantially reduced, in the case of loading q_2, whether superstructure is considered or not. This reduction is substantially more for $\nu_S = 0$, compared to $\nu_S = 0.47$ (comparing the results for $L/a = 0$, 1, 2 and 3 in Figs. 6.4 and 6.5).

6.4.3.4 Effect of variation in soil/superstructure stiffness:

In the case of non-homogeneous soil considered also, there is substantial reduction in differential settlement,

For edge loading (q_2), it can be seen (Fig. 6.6) that the load is almost directly transmitted through piles. So a ring beam connecting the piles, instead of full circular raft-pile system may be highly economical, for this loading. Solutions of some of these cases for incompressible piles and rigid ring foundation has been given by Karmarkar (76).

The effect of soil non-homogeneity is to increase the values of PPL to the extent of about 5 % , for loading q_2 (Fig. 6.6). In the case of loading q_1, nonhomogeneity of soil slightly reduces the value of PPL for smaller values of K_R, and increases the value of PPL for rigid-raft (K_R=10). The presence of superstructure increases the value of PPL as K_R reduces for loading q_1, for both homogeneous and non-homogeneous soil conditions, the effect being slightly more for non-homogeneous soil (Fig. 6.6).

6.4.5 Bending Moment
6.4.5.1 General

The maximum bending moments vs K_R, have been plotted in Figs. 6.7 to 6.10, for loading q_1 and q_2, for different parameters. In the case of loading q_1 maximum positive moment always occurs near centre and maximum negative moment if any, occurs near the superstructure. In the case of loading q_2, maximum negative moment occurs

near the centre and maximum positive moment, if any, occurs near the superstructure.

6.4.5.2   Circular raft-without considering superstructure:

In the analysis of circular raft without superstructure, for any vertical loading, the values of bending moments are independent of the value of ν_S, for a given K_R, in the case of smooth contact between raft and soil. However, for rough contact, shear stresses develop at the interface for values of ν_S less than 0.5 and this reduces the positive bending moments and increases negative bending moments. This effect is maximum, when $\nu_S = 0$. The effect of adhesive contact for u.d.l. and parabolic loading has been discussed by Hooper (73) and the effect for central column loading has been discussed in Appendix A. The effect of adhesive contact on circular raft, subjected to loading near the edge (q_2) is of some importance, as this loading may occur when the storage structure is empty. The magnitude of this effect can be seen from Figs. 6.9 and 6.10, by comparing the values of maximum bending moments for $\nu_S = 0.47$ and $\nu_S = 0$, for L/a = 0 and 'S_0'. (The value of bending moment for $\nu_S = 0.5$, correspond to smooth contact value). For $K_R = 10$, the magnitude of maximum negative moment is about 50 % more for $\nu_S = 0$ than for $\nu_S = 0.47$. Hence, smooth

contact assumption would lead to an error of about 50 %,
on the unsafe side, if the contact happens to be perfectly
adhesive for $\nu_S = 0$. However, interfacial slip may
reduce this difference to some extent. It can also be seen
that there is large reduction in positive moment due to
adhesive contact, for this loading (q_2), which occurs near
the load (q_2) (comparing the values of bending moments for
$\nu_S = 0.47$ and $\nu_S = 0$, in Figs. 6.9 and 6.10).

6.4.5.3 Circular raft - The effect of superstructure for
          loading q_1

From Figs. 6.7 and 6.8, the following observations
can be made. The presence of superstructure in general
reduces positive bending moments and increases the magnitude
of the negative bending moments, in the case of loading q_1,
for both $\nu_S = 0.47$ and $\nu_S = 0$ (comparing S_0 and S_1
in Figs. 6.7 and 6.8). This effect is maximum in the range
of $K_R = 0.5$ to 2.0. For extremely rigid raft $K_R \gg 10$ and
extremely flexible raft $K_R = 0.1$, the effect of presence
of superstructure tends to reduce. For $K_R = 2$, the
reduction in positive bending moment, due to the superstructure
is about 50 %. For $\nu_S = 0.47$ (Fig. 6.7), if superstructure
is not considered, no negative bending moment occurs and
for $\nu_S = 0$, some negative moment occurs due to adhesive

contact, for this loading (Fig. 6.8). When the super-structure is included in the analysis, considerable negative bending moment occur for both values of ν_S. For very flexible raft, the magnitude of this negative moments are greater than the positive moments.

6.4.5.4   Circular raft - The effect of superstructure loading q_2

From Figs. 6.9 and 6.10, the following observations can be made. For loading q_2, the effect of superstructure on the positive and negative bending moments, is less pronounced than for loading q_1, for circular raft. (Comparing Figs. 6.7 and 6.8 with Figs. 6.9 and 6.10). For $K_R = 2$, the reduction in maximum negative bending moment due to superstructure stiffness is about 30 % . For this loading, increase in positive moment due to superstructure stiffness is large, as for loading q_1. For $K_R = 0.1$ the value of negative moment that occurs near the centre, is not affected by superstructure stiffness (Figs. 6.9 and 6.10). However, the values of positive moments that occur near the superstructure, are slightly affected by the superstructure stiffness, for $K_R = 0.1$ also.

6.4.5.5   Circular raft-non-homogeneous soil

The computed values of bending moments for non-homogeneous soil condition have also been shown in Figs. 6.7

and 6.9. From these figures following observations can be made. The bending moment values for circular raft (without superstructure) on non-homogeneous soil and homogeneous soil have been compared. The magnitudes of bending moments for non-homogeneous soil are significantly different from those for homogeneous soil (Figs. 6.7 and 6.9). The magnitude of positive moment reduces by about 20 %, for $K_R = 10$ and by 70 %, for $K_R = 0.1$, for loading q_1, compared to homogeneous soil. For loading q_2, the magnitude of maximum negative moment increases by 40 % for $K_R = 10$ and decreases by 10 % for $K_R = 10$ and decreases by 10 % for $K_R = 0.1$. For this loading, there is slight reduction in positive bending moment compared to homogeneous soil.

Effect of superstructure - loading q_1

The effect of superstructure on the positive bending moment is similar to homogeneous case (Fig. 6.7). There is about 50 % reduction in bending moment when superstructure stiffness is considered, for $K_R = 2$, and for stiffer or more flexible raft, this effect tends to decrease. The negative bending moments that develop due to the presence of superstructure, are less than those in the case of homogeneous soil, even though the trend is same.

Effect of superstructure - loading q_2: (Fig. 6.9)

The effect of superstructure on the negative bending moment is similar to that in the case of homogeneous

soil (comparing S_0 and S_1, for these soils). There is a reduction of about 30 % , for K_R = 2 and tends to reduce as K_R increases or decreases. The effect of super-structure on positive moments, is significantly more compared to homogeneous soil. There is about 100 % increase in this moment for K_R = 2, as against 50 % in the case of homogeneous soil, for the same value of K_R.

6.4.5.6 Pile-raft:

Homogeneous soil-loading q_1 : Provision of pile reduces the positive moment in general (Fig. 6.7) except for K_R = 10, for a particular case of L/a = 2 or 3, when the superstructure is not considered. (In this case, maximum bending moment is more than that for unpiled circular raft; or the provision of piles, increases the bending moment). For L/a = 1, the reduction in maximum positive moment is more than the reduction in the case of L/a = 2 and 3, particularly in the range of K_R = 2. So there appears to be an optimum length of pile, for which the maximum positive bending moment is minimum, for this loading. However, when superstructure is considered, the bending moment increases as L/a increases. The effect of super-structure stiffness on the maximum positive moment is in general smaller for pile-raft compared to raft.

Provision of piles, in general increases the negative bending moment, when superstructure is considered. This increase is quite large and maximum for $K_R = 10$ (Fig. 6.7), for all values of L/a.

Homogeneous soil - loading q_2: (Fig. 6.9). The magnitude of negative bending moments are substantially reduced by the provision of piles. For $L/a = 3$, the negative and positive bending moments become insignificant, compared to those for raft, and the effect of superstructure stiffness also becomes insignificant (Fig. 6.9). For $L/a = 1$, the maximum negative moment reduces by 50 % , compared to raft (Fig. 6.9). The effect of superstructure stiffness, is to reduce the negative bending moment by about 20 % , for $K_R = 10$. As K_R reduces to 0.1, the superstructure does not have any significant effect on bending moment.

Non-homogeneous soil: (Figs. 6.7 and 6.9). Non-homogeneity of soil does not have significant effect on maximum positive bending moment, for $K_R = 10$, compared to homogeneous soil, for loading q_1 and q_2 (Figs. 6.7 and 6.9). However, for $K_R = 0.1$, the non-homogeneity reduces the maximum positive moment by about 50 % , for loading q_1. For loading q_2, the superstructure does not have any significant effect on the bending moments, which are already small.

Effect of variation of superstructure stiffness and soil stiffness: These effects can be observed from *a, *b and *c, in Figs. 6.7 and 6.9. As the soil becomes stiffer and superstructure becomes more flexible, the solutions tends to solutions without considering superstructure.

6.4.5.7 Loading q_3

The results for this loading were taken only for the cases considering superstructure and all the results pertain to 'S_1'. Loading q_3 introduces, significant (Fig. 6.12(b)) negative bending moments in the raft, particularly for stiffer raft. As K_R approaches 0.1, this negative moments reduce to very small values. These negative moments are slightly more for $\nu_S = 0.47$ than for $\nu_S = 0$. The provision of piles, reduces the magnitudes of these moments slightly.

As stated earlier, the settlements due to this loading are very small; but the differential settlements are significant. The differential settlement is maximum in the range of $K_R = 0.5$ to 1 (Fig. 6.12(a)). The differential settlements are less, for $\nu_S = 0.47$ than for $\nu_S = 0$, for stiffer raft and the other way for flexible raft. However, Δ is more for $\nu_S = 0$, for all values of K_R.

6.4.6 Shear Force

The shear force values have been shown in Figs. 6.11 and 6.13. From these figures the following observations can be made.

The values of shear forces are not affected by the presence of superstructure for K_R=10, for both values of ν_S and for both loadings. For smaller values of K_R the superstructure stiffness increases the values of shear force marginally. This effect is less for pile-raft, than raft. The maximum increase in shear force due to superstructure stiffness is for raft, whose K_R = 0.1 (about 70 %). The effects for non-homogeneous soil are similar to those for homogeneous soil.

6.4.7 Contact Pressure

The contact pressures have not been plotted. However, from the computed results, following observations were made.

The contact pressures were found to be not affected much by the superstructure, for stiffer raft, for loading q_1 and q_2. For flexible raft the presence of superstructure was found to increase the contact pressure at the edge and reduce the contact pressures near the centre, for loading q_1 and it was found to be the other way for loading q_2. Due to loading q_3, tensile contact pressures were found to be

set up at some locations, and these tensile stresses were found to be insignificant compared to compressive stresses due to loading q_1 and q_2.

6.4.8 In-plane Stresses

For circular raft when superstructure is not considered, there are no significant in-plane stresses for $\nu_S = 0.5$, for vertical loading. However, the presence of superstructure introduces in-plane stresses, even for $\nu_S = 0.5$. These in-plane stresses develop due to elastic connections between superstructure and raft, between pile head and raft, and also between raft base and soil. The method of computing these in-plane stresses, for the present formulation, has been discussed in Chapter 2 (Sec. 2.4.8)

The computed values of in-plane stresses have been shown in Figs. 6.14 and 6.15, for different parameters. The in-plane stresses were found to be almost constant along the radial direction, for $\nu_S = 0.47$. Also, these stresses were almost equal in radial (f_R^*) and tangential (f_T^*) directions except in a small zone near the superstructure, wherein the tangential stresses were significantly more. The magnitude of these stresses in general, increases as K_R reduces, for all the cases considered.

For $\nu_S = 0$, in the case of circular raft, when the superstructure is not considered, the in-plane stresses are compressive, for both loading q_1 and q_2 (Fig. 6.15). The in-plane stresses due to the superstructure stiffness are tensile and compressive for loading q_1 and q_2 respectively. The net effect, due to the combined action of adhesion between raft base and soil and the elastic connection between superstructure and raft are small compressive and tensile stresses for loading q_2 and q_1 respectively.

Provision of piles slightly increases these stresses in the case of loading q_1. In the case of loading q_2, for S_1, the compressive in-plane stresses developed, increase substantially compared to unpiled raft as seen in Fig.6.15(b).

For $\nu_S = 0.47$, the values of f_R^* for the cases 'S_1' are shown in Figs. 6.14 and 6.15, for $L/a = 0$, 1, 2 and 3, for different loading and for different values of K_R. For loading q_2, provision of piles reduces the in-plane stresses and this reduction is more for longer piles. For loading q_1, the reduction in the values of in-plane stresses, is observed to be more for shorter piles ($L/a=1$). For loading q_3, provision of piles increases the in-plane stresses and these stresses are not sensitive to L/a, for $L/a \geq 1$.

The magnitudes of these in-plane stresses were found to be about 10 % to 20 % of the maximum bending stresses, for the cases considered, for loading q_1 and q_2. For loading q_3, the in-plane stresses are more and these stresses become dominant for flexible raft, or pile-raft.

6.5   COMPARISON WITH SIMPLIFIED ANALYSIS

Apart from the finite element analyses discussed so far, a simplified analysis was also carried out for a particular case of circular raft ($K_R = 2$, $\nu_S = 0.47$), with loading q_1 and q_2. In this analysis, the circular plate on finite elastic layer was analysed using finite difference method assuming thin plate theory and representing the soil by numerical integration of available solutions for finite elastic layer. For this simplified analysis the computer program developed by Karmarkar (76), was modified and used and detailed description of the procedure is also given by him. To include the effect of superstructure, a condition of zero slope was introduced at the location of superstructure raft connection. A similar approximate method has been used by Hooper (75), in his analysis of a rectangular raft, as mentioned in the section 6.1. The effect of superstructure assessed from the simplified analysis are compared with finite element analysis results, in Table 6.7.

From Table 6.7, it can be observed that the simplified analysis overpredicts the effect of superstructure on the maximum bending moments and this overprediction increases as the soil becomes stiffer or superstructure becomes more flexible, as the results of simplified analysis are independent of stiffness of the superstructure and soil, for a given value of K_R. In the case of differential settlement also the simplified analysis was found to overpredict the effect of superstructure as observed in the case of bending moment to similar extent. This study indicates the order of difference between simplified analysis and finite element analysis.

6.6 DESIGN CHARTS

The solutions obtained from the finite element analyses, for the particular geometry (Fig. 6.1), of the superstructure have been presented in Tables 6.1 to 6.6 and Figs. 6.1 to 6.15.

Solutions were also obtained for a circular raft (K_R=10) without hemispherical dome portion (with only cylindrical portion) and with height of cylindrical portion equal to 0.4a, 0.7a, a and 2a, for loading q_1 and q_2. It was found that the solutions for heights equal to a and 2a almost coincided with those obtained from the original analysis (with superstructure as in Fig. 6.1, the results of which

have been presented in Tables and Figures). For height
equal to 0.7a, the difference in bending moment and diff-
erential settlement compared with original analysis was
less than 3 % (settlement, pile load etc. are not very
sensitive to superstructure stiffness). Only in the case of
analysis with height of cylindrical superstructure equal to
0.4a, the difference was significant. Hence, the solutions
presented for loading q_1 and q_2, can be used for any height
of superstructure and for any shape of top cover, provided
height of superstructure is greater than 0.7a, for certain
range of other parameters.

From tables and figures, the values of settlements,
differential settlements, bending moments, maximum shear
force, the pile loads (if any) and maximum in-plane stresses
can be computed for circular raft with a cylindrical super-
structure whose thickness is 0.1a, founded on the surface of
a soil whose modulus is 1/1500 of the modulus of the raft/
superstructure material and also for a circular raft, with
closely spaced piles in an annulus or a circular raft with
a solid skirt, whose width is 0.1a, near the edge and
whose modulus (in the case of skirt) or equivalent modulus
E_{peq} (in the case of piles) is 600 times that of soil,
with different depths of embedment (L/a = 1, 2 and 3).

.The equivalent Young's modulus E_{peq} of annulus of area A containing piles whose total area of cross section is equal to A_p can be calculated as,

$$E_{peq} = \frac{E_p A_p + E_S (A - A_p)}{A} \qquad (6.2)$$

where E_p, E_S = Young's modulus of pile material and soil respectively.

It is to be noted that the loading q_1 (used in the analysis for presentation of results) is u.d.l. over a circular of radius 'a', which is the outer radius of the superstructure. For u.d.l. over '0.9a' (over the inner portion of the raft), the solutions can be obtained by subtracting the solution for q_2, from the solution for q_1. It is also to be noted that for loading q_3, the solutions presented apply to the particular geometry of the superstructure considered in the analysis. These solutions may be used for the analysis of the foundation for different conditions of the structure like the 'storage structure full' and 'empty', by superposing these solutions appropriately.

Since E_R/E_S has been assume to be equal to 1500, in most of the cases, these solutions may be useful in the case of such structures, founded on weak soil, in which case the differential settlement is likely to be more and the

same can be reduced by considering the superstructure stiffness and/or by the provision of piles or skirt. However, it is possible to generate design charts for wider range of parameters similar to the ones presented herein.

6.7 CONCLUSIONS

1. The problem of interaction of superstructure-foundation-soil system can be analysed, including the effect of in-plane stresses, using parabolic isoparametric finite elements.

2. In general, the maximum settlements are not very sensitive to the superstructure stiffness, particularly so for pile-raft. Provision of piles or skirt near the edge substantially reduces the settlement of circular raft.

3. For edge loading of circular raft founded on a soil whose $\nu_S = 0$, the adhesive contact at raft-soil interface, increases the magnitude of maximum negative bending moment and differential settlement by about 50 %, for fairly rigid raft.

4. Inclusion of superstructure in the analysis, appreciably (to the extent of 60 %) reduces the differential settlement in the case of circular raft of practical range of stiffness ($K_R = 1$ to 10).

Provision of piles or skirt reduces the differential settlement for edge loading (q_2), whereas for u.d.l. (q_1) there is slight increase in differential settlement, due to provision of piles. The effect of superstructure rigidity on the differential settlement are of similar extent for both homogeneous and non-homogeneous soil considered.

5. Piles carry significant percentage of load for both loadings q_1 and q_2. Particularly for loading q_2, almost entire load is taken by piles and the pile loads are insensitive to raft stiffness for this loading. Pile loads are significantly more for $\nu_S = 0$ than for $\nu_S = 0.47$.

6. The superstructure stiffness in general, reduces the positive bending moments (to the extent of 50-60 %) and increases the magnitudes of negative bending moments for u.d.l. (q_1), for practical range of values of raft stiffness. For edge loading (q_2), the effects are slightly less compared to u.d.l. (q_1). Such effect of superstructure stiffness on bending moments, is found to be in general, less in the case of pile-raft, than circular raft. The effect of superstructure stiffness on bending moment are of similar nature for both homogeneous and non-homogeneous soil

considered. Provision of piles reduces the positive bending moments and increases the negative bending moments, for loading q_1. For loading q_2, the magnitude of negative bending moments reduce substantially, due to the provision of piles.

7. In-plane stresses develop in the raft, due to the elastic connections between different components of the system (pile-raft-superstructure-soil). These stresses increase as K_R reduces. The magnitude of these stresses were found to be about 10 to 20 % of maximum bending stresses, for loading q_1 and q_2. For loading q_3, the in-plane stresses are larger and become dominant for flexible raft.

8. The simplified analysis to include the effect of superstructure, by assuming zero slope at super-structure-raft inter connection, overpredicts the effect of superstructure on bending moment and differential settlement. This overprediction increases considerably as the soil becomes stiffer and/or as the superstructure becomes more flexible.

9. The values of shear forces and contact pressures are not affected much by the presence of superstructure for both loading q_1 and q_2, in the case of fairly rigid raft ($K_R = 10$).

TABLE 6.1   SETTLEMENT INFLUENCE FACTORS - I_S

$$I_S = \frac{SE_S}{qa} \qquad (q = q_1 \text{ or } q_2 \text{ or } q_3)$$

$$\nu_S = 0.47, \qquad L/a = 0 \quad \text{and} \quad L/a = 1$$

r/a	q_1		q_2		q_3	
	$L/a = 0$	$L/a=1$	$L/a = 0$	$L/a = 1$	$L/a = 0$	$L/a=1$
1	2	3	4	5	6	7
0.0	0.9516[a]	0.7169	0.1771	0.1328	-0.02583	-0.02260
	0.9757[b]	0.7459	0.1743	0.1316	-0.04699	-0.03724
	1.0245[c]	0.8086	0.1669	0.1282	-0.05225	-0.03818
	1.1572[d]	0.9592	0.1469	0.1204	-0.03560	-0.02119
0.1	0.9514	0.7167	0.1771	0.1328	-0.02551	-0.02233
	0.9750	0.7451	0.1744	0.1317	-0.04645	-0.03684
	1.0225	0.8063	0.1671	0.1283	-0.05174	-0.03788
	1.1521	0.9536	0.1477	0.1207	-0.03557	-0.02140
0.2	0.9507	0.7159	0.1772	0.1329	-0.02457	-0.02155
	0.9729	0.7426	0.1746	0.1318	-0.04477	-0.03562
	1.0168	0.7994	0.1679	0.1287	-0.05016	-0.03693
	1.1375	0.9372	0.1498	0.1216	-0.03537	-0.02169
0.3	0.9497	0.7148	9.1773	0.1329	-0.02299	-0.02024
	0.9695	0.7386	0.1751	0.1320	-0.04198	-0.03359
	1.0077	0.7884	0.1692	0.1293	-0.04747	-0.03533
	1.1135	0.9106	0.1533	0.1231	-0.03491	-0.02223
0.4	0.9482	0.7132	0.1774	0.1330	-0.02075	-0.01838
	0.9649	0.7334	0.1755	0.1322	-0.03804	-0.03070
	0.9957	0.8741	0.1708	0.1300	-0.04356	-0.03290
	1.0819	0.8753	0.1580	0.1251	-0.03386	-0.02250

1	2	3	4	5	6	7
0.5	0.9465	0.7112	0.1776	0.1331	-0.01787	-0.01598
	0.9595	0.7271	0.1763	0.1326	-0.03293	-0.02693
	0.9816	0.7573	0.1728	0.1309	-0.03832	-0.02961
	1.0442	0.8333	0.1636	0.1273	-0.03195	-0.02250
0.6	0.9445	0.7090	0.1778	0.1332	-0.01437	-0.01308
	0.9535	0.7203	0.1770	0.1329	-0.02660	-0.02223
	0.9665	0.7394	0.1749	0.1318	-0.03158	-0.02518
	1.0037	0.7881	0.1698	0.1297	-0.02856	-0.02138
0.7	0.9423	0.7067	0.1780	0.1333	-0.01024	-0.00966
	0.9472	0.7134	0.1777	0.1332	-0.01902	-0.01661
	0.9515	0.7220	0.1770	0.1327	-0.02316	-0.01955
	0.9638	0.7440	0.1760	0.1320	-0.02312	-0.01890
0.8	0.9400	0.7044	0.1782	0.1334	-0.00528	-0.00546
	0.9412	0.7071	0.1783	0.1335	-0.01008	-0.00983
	0.9383	0.7073	0.1789	0.1334	-0.01279	-0.01223
	0.9310	0.7083	0.1811	0.1338	-0.01468	-0.01366
0.9	0.9378	0.7020	0.1784	0.1334	-0.00021	-0.00069
	0.9358	0.7019	0.1788	0.1337	-0.00017	-0.00174
	0.9287	0.6976	0.1798	0.1338	-0.00032	-0.00291
	0.9119	0.6892	0.1839	0.1347	-0.00236	-0.00483
1.0	0.9356	0.7003	0.1785	0.1335	0.00610	-0.00375
	0.9313	0.6987	0.1791	0.1338	0.01115	-0.00602
	0.9225	0.6936	0.1801	0.1339	0.01292	-0.00643
	0.9055	0.6855	0.1841	0.1348	0.01098	00.00510
1.1	0.9333	0.6986	0.1786	0.1336	0.01200	0.00883
	0.9265	0.6952	0.1792	0.1339	0.02200	0.01460
	0.9156	0.6892	0.1801	0.1339	0.02591	0.01643
	0.8955	0.6808	0.1831	0.1345	0.02359	0.01521

a - $K_R = 10$ b - $K_R = 2$ c - $K_R = 0.5$ d - $K_R = 0.1$

TABLE 6.2   SETTLEMENT INFLUENCE FACTORS - I_S

$$I_S = \frac{SE_S}{qa} \quad (q = q_1, q_2 \text{ or } q_3)$$

Tabulated values are $I_S \times 10$, $\nu_S = 0.47$, $L/a = 2$ and $L/a = 3$

r/a	q_1		q_2		q_3	
	L/a=2	L/a=3	L/a=2	L/a=3	L/a=2	L/a=3
1	2	3	4	5	6	7
0.0	5.4780[a]	4.3100	1.0055	0.7831	-0.2344	-0.2376
	5.8066[b]	4.6517	0.9998	0.7793	-0.3819	-0.3857
	6.5259[c]	5.4087	0.9839	0.7701	-0.3808	-0.3817
	8.1269[d]	7.0647	0.9502	0.7502	-0.1909	-0.1860
0.1	5.4752	4.3071	1.0056	0.7831	-0.2317	-0.2350
	5.7970	4.6418	1.0000	0.7794	-0.3780	-0.3818
	6.4997	5.3814	0.9845	0.7705	-0.3782	-0.3792
	8.0668	7.0026	0.9516	0.7510	-0.1936	-0.1888
0.2	5.4669	4.2984	1.0057	0.7832	-0.2240	-0.2272
	5.7691	4.6127	1.0006	0.7797	-0.3662	-0.3701
	6.4233	5.3020	0.9861	0.7714	-0.3697	-0.3710
	7.8918	6.8220	0.9554	0.7531	-0.1984	-0.1940
0.3	5.4535	4.2845	1.0060	0.7834	-0.2110	-0.2143
	5.7243	4.5660	1.0015	0.7802	-0.3464	-0.3503
	6.3008	5.1747	0.9887	0.7729	-0.3552	-0.3568
	7.6073	6.5284	0.9617	0.7567	-0.2068	-0.2030
0.4	5.4356	4.2658	1.0063	0.7835	-0.1924	-0.1957
	5.6651	4.5043	1.0026	0.7809	-0.3181	-0.3222
	6.1406	5.0083	0.9920	0.7748	-0.3331	-0.3351
	7.2307	6.1400	0.9699	0.7614	-0.2134	-0.2104

1	2	3	4	5	6	7
0.50	5.4138	4.2431	1.0068	0.7838	-0.1685	-0.1718
	5.5949	4.4312	1.0040	0.7816	-0.2811	-0.2854
	5.9530	4.8136	0.9958	0.7770	-0.3026	-0.3052
	6.7822	5.6776	0.9796	0.7670	-0.2181	-0.2160
0.60	5.3892	4.2173	1.0072	0.7840	-0.1397	-0.1430
	5.5184	4.3516	1.0054	0.7825	-0.2349	-0.2394
	5.7537	4.6068	0.9998	0.7793	-0.2609	-0.2639
	6.3006	5.1814	0.9898	0.7729	-0.2117	-0.2105
0.70	5.3631	4.1901	1.0077	0.7843	-0.1056	-0.1090
	5.4412	4.2714	1.0068	0.7832	-0.1794	-0.1840
	5.5605	4.4065	1.0036	0.7815	-0.2070	-0.2105
	5.8314	4.6983	0.9997	0.7785	-0.1916	-0.1913
0.80	5.3372	4.1632	1.0081	0.7845	-0.0637	-0.0671
	5.3707	4.1981	1.0081	0.7839	-0.1124	-0.1171
	5.3982	4.2384	1.0067	0.7832	-0.1357	-0.1396
	5.4516	4.3075	1.0073	0.7829	-0.1428	-0.1433
0.90	5.3105	4.1353	1.0082	0.7844	-0.0162	-0.0196
	5.3126	4.1379	1.0087	0.7842	-0.0320	-0.0369
	5.2923	4.1288	1.0083	0.7841	-0.0436	-0.0478
	5.2492	4.0996	1.0110	0.7850	-0.0563	-0.0571
1.00	5.2919	4.1160	1.0085	0.7846	0.0283	0.0248
	5.2773	4.1014	1.0092	0.7844	0.0453	0.0404
	5.2488	4.0842	1.0087	0.7842	0.0494	0.0452
	5.2107	4.0605	1.0111	0.7849	0.0428	0.0419
1.10	5.2731	4.0967	1.0091	0.7850	0.0789	0.0755
	5.2403	4.0636	1.0095	0.7846	0.1309	0.1260
	5.2039	4.0386	1.0086	0.7840	0.1490	0.1448
	5.1677	4.0196	1.0090	0.7832	0.1437	0.1429

a - K_R =10   b - K_R = 2   c - K_R = 0.5   d - K_R = 0.1

TABLE 6.3 BENDING MOMENT INFLUENCE FACTORS - I_{MR} AND I_{MT}

$$I_{MR} = M_R/qa^2, \quad I_{MT} = M_T/qa^2 \quad (q = q_1, q_2 \text{ or } q_3)$$

$$\nu_S = 0.47 \quad L/a = 0$$

r/a	q_1		q_2		q_3	
	$I_{MR} \times 1000$	$I_{MT} \times 1000$	$I_{MR} \times 1000$	$I_{MT} \times 1000$	$I_{MR} \times 1000$	$I_{MT} \times 1000$
1	2	3	4	5	6	7
0.0423	71.155[a]	71.599	-7.455	-7.514	-106.347	-106.321
	47.389[b]	47.793	-5.809	-5.865	- 37.151	-37.097
	32.338[c]	32.675	-4.467	-4.512	- 8.717	- 8.659
	16.595[d]	16.896	-2.411	-2.425	- 0.150	- 0.120
0.1577	68.010	69.668	-7.036	-7.257	-106.583	-106.485
	44.506	46.034	-5.418	-5.627	- 37.539	- 37.338
	29.977	31.233	-4.159	-4.323	- 9.121	- 8.907
	15.800	16.308	-2.312	-2.364	- 0.358	- 0.247
0.2423	64.669	68.126	-6.588	-7.529	-106.823	-106.577
	41.440	44.618	-5.015	-5.435	- 37.952	- 37.526
	27.475	30.077	-3.830	-3.435	- 9.553	- 9.107
	14.806	15.863	-2.212	-2.321	- 0.576	- 0.347
0.3577	56.760	64.512	-5.497	-6.562	-107.353	-106.767
	34.167	41.270	-3.974	-4.969	- 38.900	- 37.955
	21.346	27.286	-2.984	-3.793	- 10.567	- 9.572
	11.886	14.597	-1.858	-2.174	- 1.151	- 0.603
0.4423	49.580	61.121	-4.487	-6.095	-107.836	-107.057
	27.440	38.148	-3.020	-4.533	- 39.756	- 38.372
	15.717	24.920	-2.185	-3.435	- 11.488	- 10.006
	9.028	13.372	-1.497	-2.028	- 1.697	- 0.847

1	2	3	4	5	6	7
0.5577	37.000	55.089	-2.619	-5.226	-108.675	-107.636
	15.637	32.571	-1.236	-3.719	- 41.201	- 39.103
	5.459	19.958	-0.623	-2.744	- 13.070	- 10.765
	2.812	10.764	-0.585	-1.670	- 2.756	- 1.318
0.6422	26.395	50.290	-0.980	-4.525	-109.364	-107.778
	5.607	28.032	0.336	-3.037	-42.394	- 39.632
	-3.375	15.992	0.786	-2.146	-14.394	- 11.376
	-3.115	8.400	0.335	-1.330	- 3.712	- 1.726
0.7577	9.885	42.981	1.823	-3.378	-110.293	-107.668
	-10.189	20.977	3.071	-1.886	- 44.112	- 40.352
	-17.965	9.585	3.344	-1.089	- 16.360	- 12.286
	-14.400	3.977	2.351	-0.603	- 5.309	- 2.405
0.8211	0.106	37.420	3.611	-2.469	-110.846	-108.851
	-19.636	15.929	4.826	-1.064	-45.090	- 41.075
	-26.861	5.195	5.022	-3.557	-17.489	- 11.376
	-21.932	0.822	3.795	-0.060	- 6.296	- 2.877
0.8789	-9.132	30.259	5.513	-1.256	-111.436	-111.965
	-28.632	9.849	6.684	-0.085	- 45.956	- 42.229
	-35.471	0.231	6.824	0.482	- 18.480	- 13.709
	-29.730	- 2.750	5.450	0.586	- 7.208	- 3.406

a - K_R = 10   b - K_R = 2   c - K_R = 0.5   d - K_R = 0.1

TABLE 6.4 BENDING MOMENT INFLUENCE FACTORS - I_{MR} AND I_{MT}

$$I_{MR} = M_R/qa^2, \quad I_{MT} = M_T/qa^2 \quad (q = q_1, \ q_2 \ \text{or} \ q_3)$$

$$\nu_S = 0.47 \qquad L/a = 1$$

r/a	q_1		q_2		q_3	
	$I_{MR} \times 1000$	$I_{MT} \times 1000$	$I_{MR} \times 1000$	$I_{MT} \times 1000$	$I_{MR} \times 1000$	$I_{MT} \times 1000$
1	2	3	4	5	6	7
0.0423	79.508[a]	80.089	-3.764	-3.796	-88.231	-88.198
	55.375[b]	55.904	-2.762	-2.793	-27.062	-27.004
	38.884[c]	39.298	-2.073	-2.098	- 5.136	- 5.079
	18.652[d]	18.799	-1.044	-1.054	0.456	0.480
0.1577	75.390	77.555	-3.535	-3.655	-88.498	-88.374
	51.643	53.619	-2.547	-2.661	-27.470	-27.255
	35.981	37.524	-1.899	-1.992	- 5.533	- 5.322
	17.608	18.160	-0.973	-1.011	0.282	0.374
0.2423	71.017	75.554	-3.289	-3.543	-88.772	-88.488
	47.670	51.794	-2.317	-2.555	-27.903	-27.454
	32.894	36.108	-1.715	-1.906	- 5.954	- 5.516
	16.517	17.676	-0.900	-0.977	0.102	0.292
0.3577	60.504	70.799	-2.711	-3.279	-89.408	-88.745
	38.032	47.414	-1.773	-2.305	-28.934	-27.924
	25.185	32.619	-1.267	-1.701	- 6.981	- 5.985
	13.261	16.272	-0.695	-0.887	- 0.406	0.070
0.4423	50.871	66.284	-2.183	-3.029	-89.989	-89.055
	29.178	43.309	-1.273	-2.072	-29.870	-28.365
	18.037	29.358	-0.852	-1.511	- 7.923	- 6.420
	10.064	14.910	-0.495	-0.801	-0.894	- 0.143

Contd. Table 6.4

1	2	3	4	5	6	7
0.5577	33.490	58.049	-1.260	-2.585	-91.030	-89.656
	13.082	35.813	-0.395	-1.659	-31.532	-29.157
	4.636	23.267	-0.102	-1.166	- 9.636	- 7.210
	2.925	11.945	-0.084	-0.625	- 1.919	- 0.582
0.6422	18.547	51.513	-0.479	-2.234	-91.891	-89.938
	- 0.849	29.659	0.355	-1.318	-32.932	-29.785
	- 7.187	18.111	0.547	-0.874	-11.110	- 7.872
	- 3.977	9.239	0.297	-0.467	- 2.873	- 0.971
0.7577	-5.883	41.250	0.766	-1.698	-93.197	-90.180
	-23.891	19.738	1.545	-0.784	-35.145	-30.750
	-27.399	9.482	1.603	-0.403	-13.519	- 8.940
	-17.558	4.027	0.994	-0.184	- 4.648	- 1.680
0.8211	-20.890	33.026	1.521	-1.271	-93.999	-91.147
	-38.159	12.508	2.270	-0.411	-36.467	-31.492
	-40.168	3.469	2.253	-0.089	-14.958	- 9.662
	-26.798	0.249	1.452	0.012	- 5.811	- 2.182
0.8789	-36.197	21.898	2.215	-0.709	-94.956	-93.401
	-52.574	3.643	2.947	0.018	-37.877	-32.485
	-53.135	- 3.447	2.869	0.251	-16.520	-10.493
	-36.676	-4.110	1.906	0.224	- 7.082	- 2.768

a - K_R = 10   b - K_R = 2   c - K_R = 0.5   d - K_R = 0.1

TABLE 6.5   BENDING MOMENT INFLUENCE FACTORS - I_{MR} AND I_{MT}

$$I_{MR} = M_R/qa^2 \qquad I_{MT} = M_T/qa^2 \qquad (q = q_1, \; q_2 \; \text{or} \; q_3)$$

$$\nu_S = 0.47 \qquad L/a = 2$$

r/a	q_1		q_2		q_3	
	$I_{MR} \times 1000$	$I_{MT} \times 1000$	$I_{MR} \times 1000$	$I_{MT} \times 1000$	$I_{MR} \times 1000$	$I_{MT} \times 1000$
1	2	3	4	5	6	7
0.0423	89.890[a]	90.561	-1.725	-1.739	-87.736	-87.698
	62.582[b]	63.190	-1.235	-1.249	-26.379	-26.314
	43.458[c]	43.926	-0.910	-0.921	- 4.558	- 4.495
	19.938[d]	20.098	-0.442	-0.446	0.670	0.697
0.1577	85.133	87.634	-1.621	-1.675	-88.035	-87.894
	58.294	60.565	-1.138	-1.190	-26.842	-26.598
	40.170	41.918	-0.835	-0.875	- 5.004	- 4.767
	18.810	19.407	-0.413	-0.428	0.481	0.581
0.2423	80.079	85.319	-1.510	-1.624	-88.344	-88.025
	53.724	58.464	-1.035	-1.142	-27.333	-26.824
	36.677	40.313	-0.754	-0.838	- 5.477	- 4.986
	17.632	18.883	-0.383	-0.415	0.285	0.492
0.3577	67.968	79.834	-1.246	-1.505	-89.	-88.319
	42.672	53.435	-0.791	-1.030	-28.501	-27.356
	27.991	36.376	-0.556	-0.748	- 6.631	- 5.512
	14.123	17.369	-0.298	-0.377	- 0.266	0.251
0.4423	56.880	74.630	-1.004	-1.391	-89.719	-88.665
	32.524	48.727	-0.566	-0.925	-29.562	-27.856
	19.927	32.696	-0.374	-0.664	- 7.689	- 6.000
	10.687	15.902	-0.214	-0.341	- 0.795	0.019

1	2	3	4	5	6	7
0.5577	36.965	65.172	-0.580	-1.187	-90.890	-89.328
	14.165	40.161	-0.168	-0.739	-31.440	-28.751
	4.875	25.845	-0.044	-0.512	- 9.609	- 6.888
	3.480	12.724	-0.038	-0.267	- 1.904	- 0.455
0.6422	19.860	57.669	-0.220	-1.027	-91.861	-89.659
	- 1.692	33.130	0.172	-0.585	-33.025	-29.464
	- 8.373	20.049	0.244	-0.383	-11.261	- 7.629
	- 4.328	9.824	0.125	-0.200	- 2.935	- 0.877
0.7577	- 7.945	45.934	-0.355	-0.780	-93.338	-89.976
	-27.771	21.840	0.718	-0.341	-35.527	-30.559
	-30.876	10.391	0.718	-0.173	-13.955	- 8.825
	-18.782	4.261	0.425	-0.078	- 4.848	- 1.643
0.8211	-25.074	36.547	0.706	-0.583	-94.244	-91.003
	-43.885	13.652	1.053	-0.172	-37.025	-31.393
	-45.045	3.693	1.013	-0.033	-15.595	- 9.634
	-28.597	0.239	0.624	0.006	- 6.101	- 2.184
0.8789	-42.147	23.907	1.039	-0.395	-95.294	-93.334
	-59.983	3.688	1.372	0.024	-38.595	-32.495
	-59.310	- 3.959	1.300	0.118	-17.293	-10.562
	-39.033	- 4.381	0.827	0.097	- 7.459	- 2.813

a - $K_R = 10$ b - $K_R = 2$ c - $K_R = 0.5$ d - $K_R = 0.1$

TABLE 6.6 BENDING MOMENT INFLUENCE FACTORS - I_{MR} and I_{MT}

$$I_{MR} = M_R/qa^2 \qquad I_{MT} = M_T/qa^2 \qquad (q = q_1, q_2 \text{ or } q_3)$$

$$\nu_S = 0.47 \qquad L/a = 3$$

r/a	q₁		q₂		q₃	
	I_{MR}x1000	I_{MT}x1000	I_{MR}x1000	I_{MT}x1000	I_{MR}x1000	I_{MT}x1000
0.0423	93.798[a]	94.499	-0.968	-0.976	-87.629	-87.590
	65.207[b]	65.844	-0.703	-0.711	-26.232	-26.165
	45.163[c]	45.651	-0.525	-0.531	- 4.441	- 4.376
	20.582[d]	20.748	-0.251	-0.253	- 0.150	- 0.120
0.1577	88.819	91.437	-0.907	-0.939	-87.935	-87.790
	60.715	63.095	-0.647	-0.677	-26.706	-26.455
	41.731	43.555	-0.482	-0.505	- 4.897	- 4.654
	19.408	20.029	-0.235	-0.243	- 0.358	- 0.247
0.2423	83.522	89.011	-0.843	-0.909	-88.252	-87.924
	55.934	60.895	-0.587	-0.649	-27.209	-26.687
	38.085	41.879	-0.436	-0.484	- 5.381	- 4.878
	18.182	19.484	-0.220	-0.236	-00.576	- 0.347
0.3577	70.840	83.266	-0.691	-0.840	-88.988	-88.227
	44.380	55.634	-0.445	-0.584	-28.406	-27.233
	29.025	37.772	-0.323	-0.432	- 6.561	- 5.416
	14.537	17.910	-0.174	-0.216	- 1.151	- 0.603
0.4423	59.227	77.815	-0.550	-0.774	-89.660	-88.580
	33.768	50.711	-0.315	-0.523	-29.494	-27.745
	20.623	33.935	-0.217	-0.384	- 7.642	- 5.916
	10.981	16.388	-0.126	-0.196	- 1.697	- 0.847

Contd. Table 6.6

1	2	3	4	5	6	7
0.5577	38.409	67.921	-0.302	-0.655	-90.859	-89.257
	14.596	41.763	-0.082	-0.415	-31.420	-28.663
	4.967	26.803	-0.024	-0.296	- 9.603	- 6.822
	3.101	13.104	-0.023	-0.154	- 2.756	- 1.318
0.6422	20.540	60.072	-0.089	-0.562	-91.854	-89.599
	- 1.951	34.417	0.118	-0.325	-33.044	-29.393
	- 8.801	20.771	0.146	-0.221	-11.291	- 7.580
	-4.509	10.108	0.070	-0.116	- 3.712	- 1.726
0.7577	-8.452	47.816	0.255	-0.417	-93.368	-89.932
	-29.117	22.636	0.444	-0.180	-35.609	-30.517
	-32.143	10.735	0.430	-0.096	-14.043	- 8.802
	-19.379	4.374	0.247	-0.045	- 5.309	- 2.405
0.8211	-26.237	38.019	0.465	-0.299	-94.297	-90.972
	-45.888	14.106	0.645	-0.080	-37.144	-31.371
	-46.832	3.786	0.608	-0.013	-15.719	- 9.628
	-29.465	0.235	0.366	0.004	- 6.296	- 2.877
0.8789	-44.019	24.852	0.674	-0.137	-95.366	-93.319
	-62.584	3.753	0.842	0.036	-38.748	-32.496
	-61.587	- 4.139	0.784	0.077	-17.450	-10.575
	-40.168	- 4.511	0.489	0.058	- 7.208	- 3.406

a - $K_R = 10$ b $K_R = 2$ c - $K_R = 0.5$ d - $K_R = 0.1$

TABLE 6.7   COMPARISON WITH SIMPLIFIED ANALYSIS

Circular raft - $K_R = 2$, $H/a = 6.5$, $\nu_S = 0.47$

Superstructure - As in Fig. 6.1 Soil-Homogeneous

Effect when super-structure is considered	Loading	Finite element analysis $E_R/E_{SO}=1500$ $E_{SS}/E_R=1$ (Case 1)	Finite element analysis $E_R/E_{SO}=300$ $E_{SS}/E_R=1/5$ (Case 2)	Simplified analysis (same for Cas 1 and 2)
Percentage change in max. positive moment	q_1	50	17	65
Max. negative bending moment $M_R^*/q_1 a^2$	q_1	0.029	0.001	0.054
Percentage change in max. negative moment	q_2	30	8	40
Percentage change in max. positive moment	q_2	50	-	100
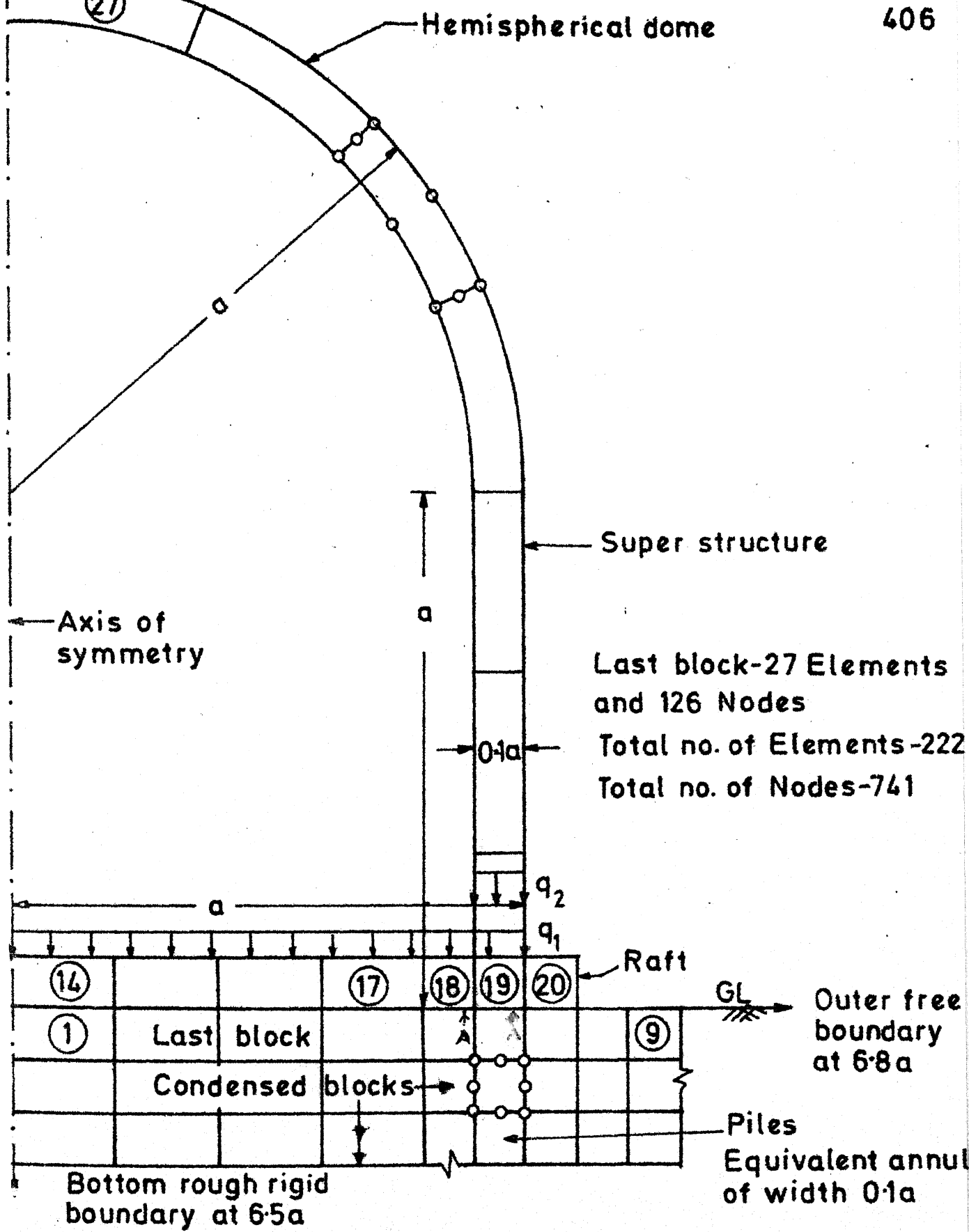
Fig.6·1 Mesh for superstructure-foundation-soil interaction

Text labels within the figure:

- Hemispherical dome
- Super structure
- Axis of symmetry
- Last block-27 Elements and 126 Nodes
- Total no. of Elements-222
- Total no. of Nodes-741
- Raft
- GL
- Outer free boundary at 6·8a
- Piles
- Equivalent annul of width 0·1a
- Last block
- Condensed blocks
- Bottom rough rigid boundary at 6·5a
- q_2
- q_1
- 0·1a
- a
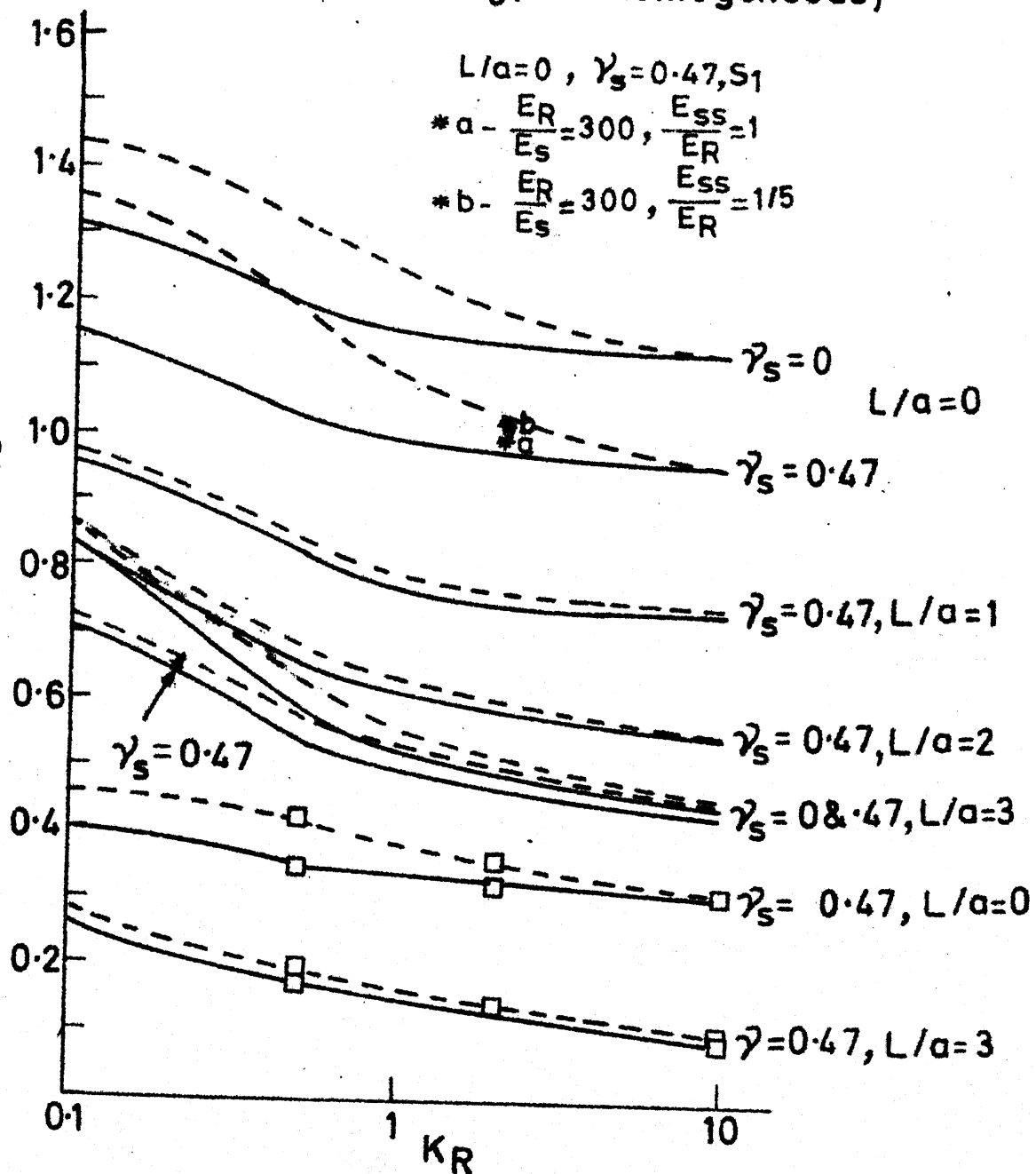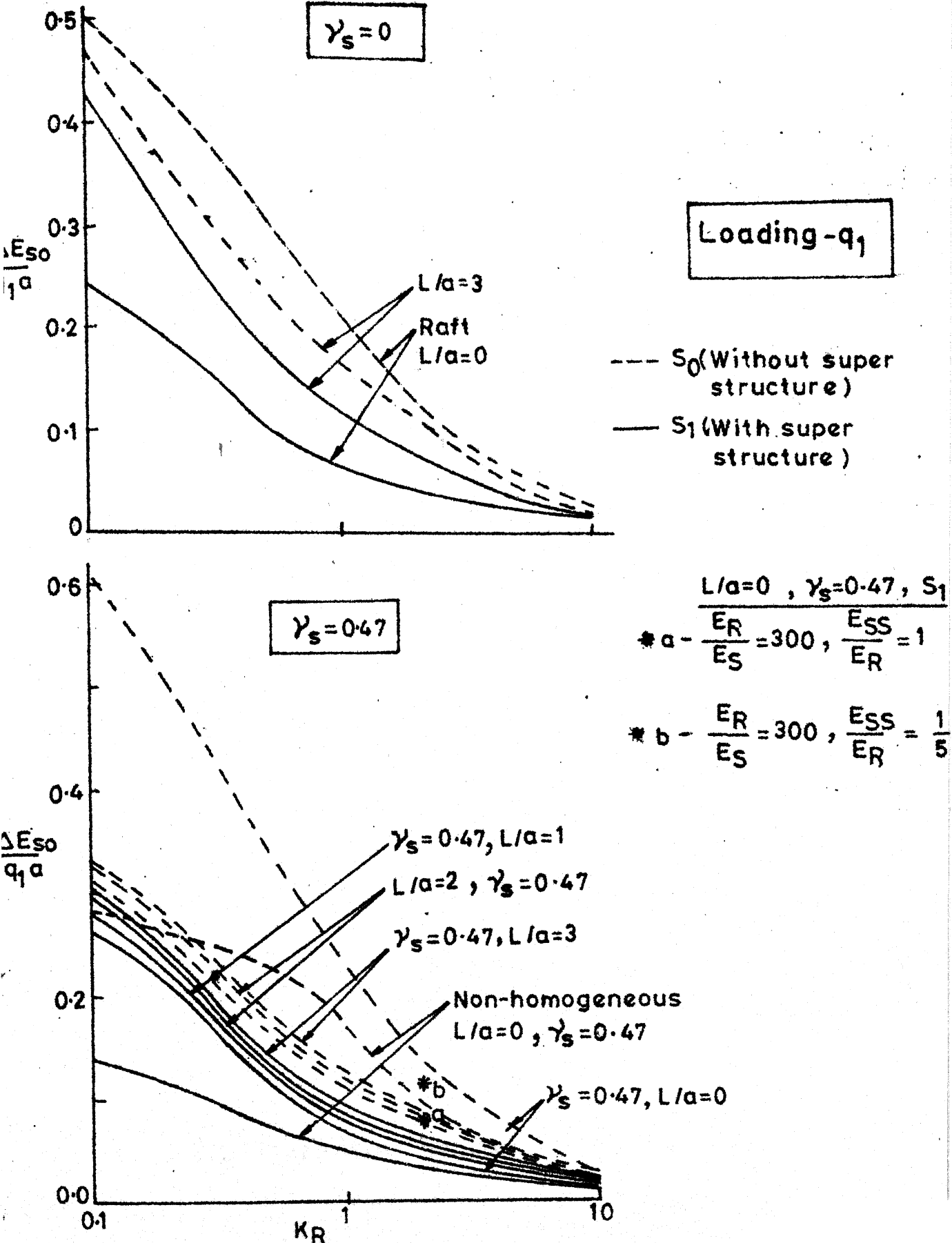
Fig. 6·2 Max. Settlement Vs K_R

Fig. 6·3 Max. Settlement Vs K_R

Fig. 6·4 Differential Settlement Vs K_R
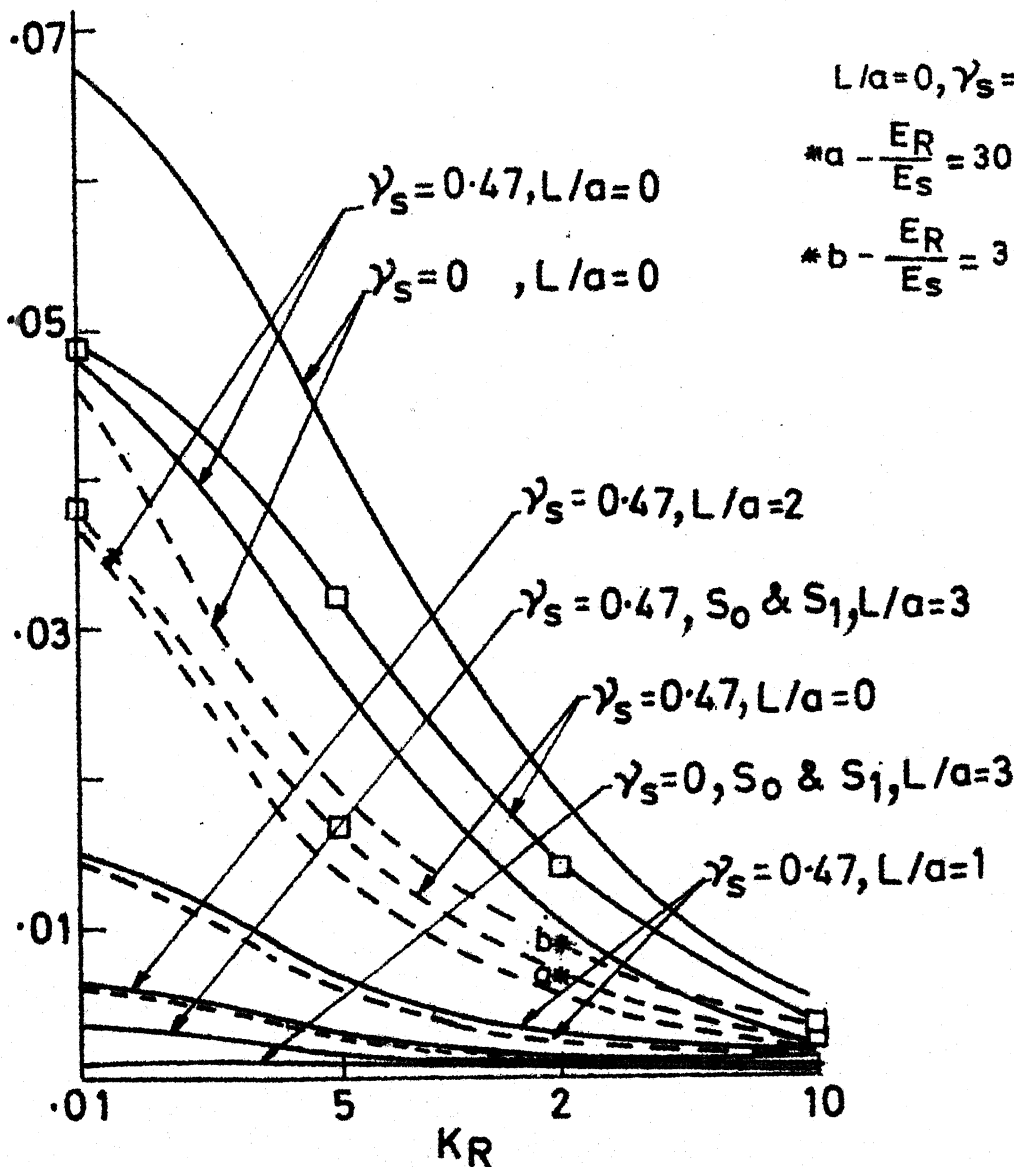
Fig.6·5 Differential Settlement Vs K_R
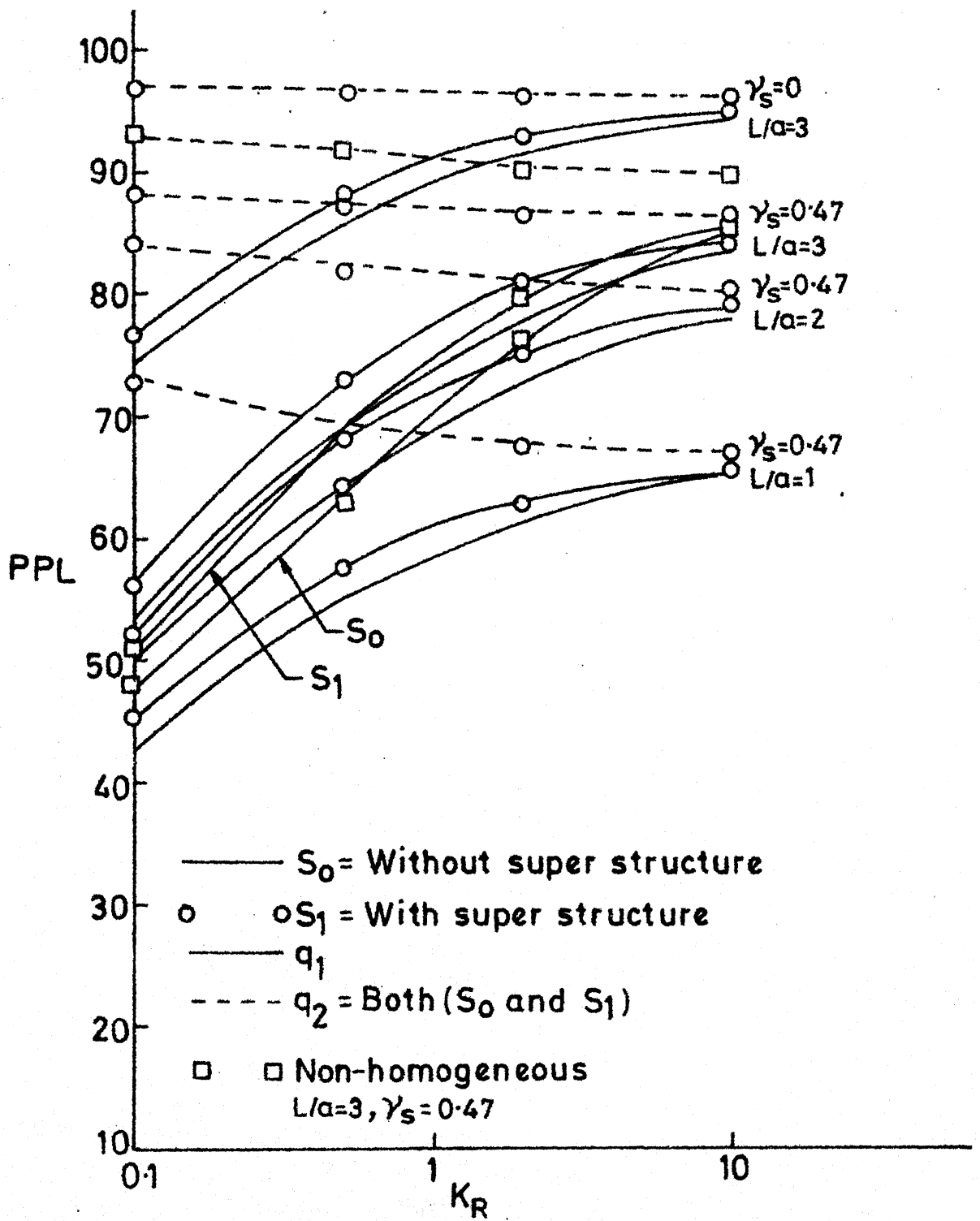
Fig. 6·6 Percent Pile Load Vs K_R
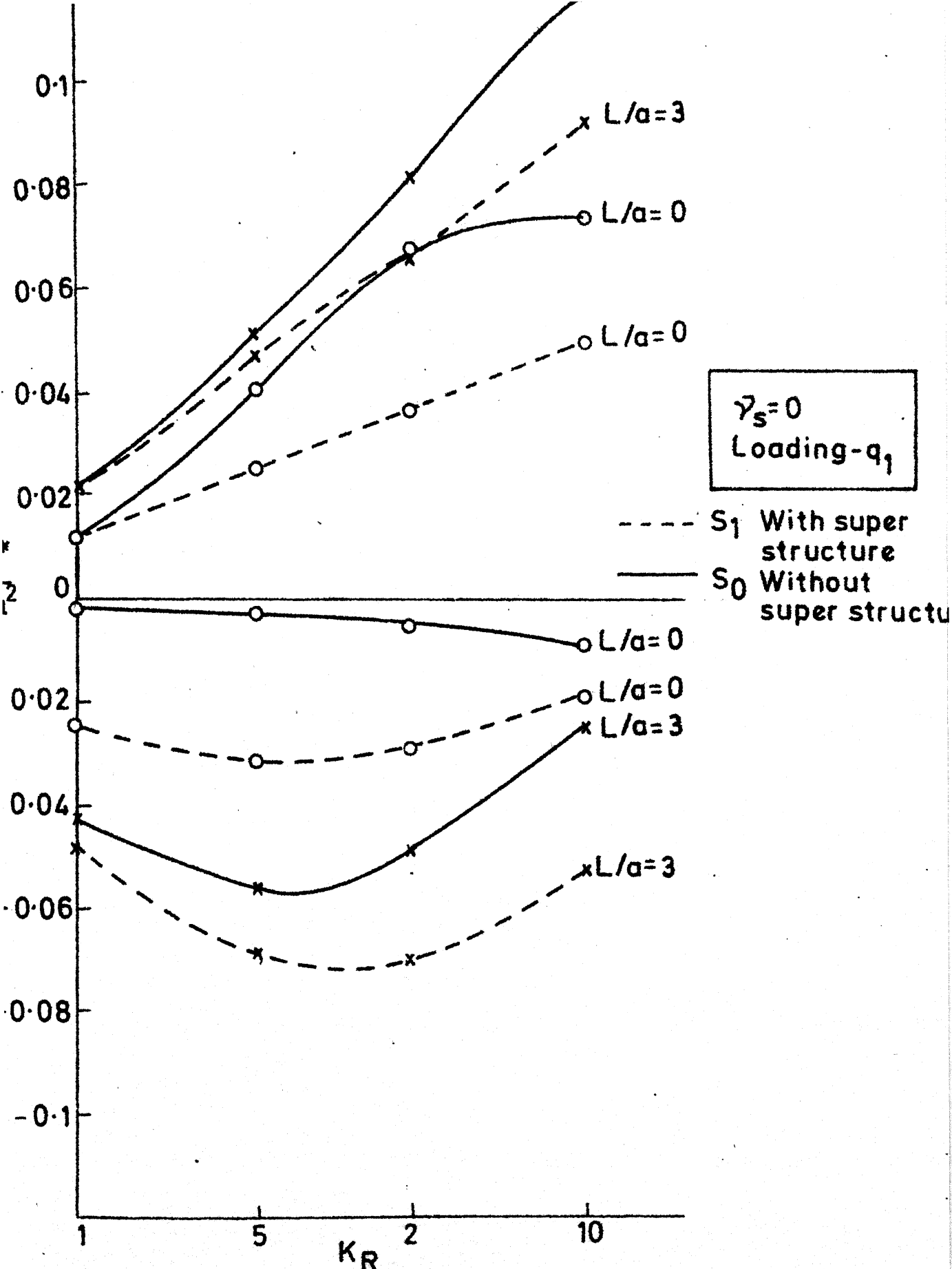
Fig.6·8 Max. Bending Moment Vs K_R
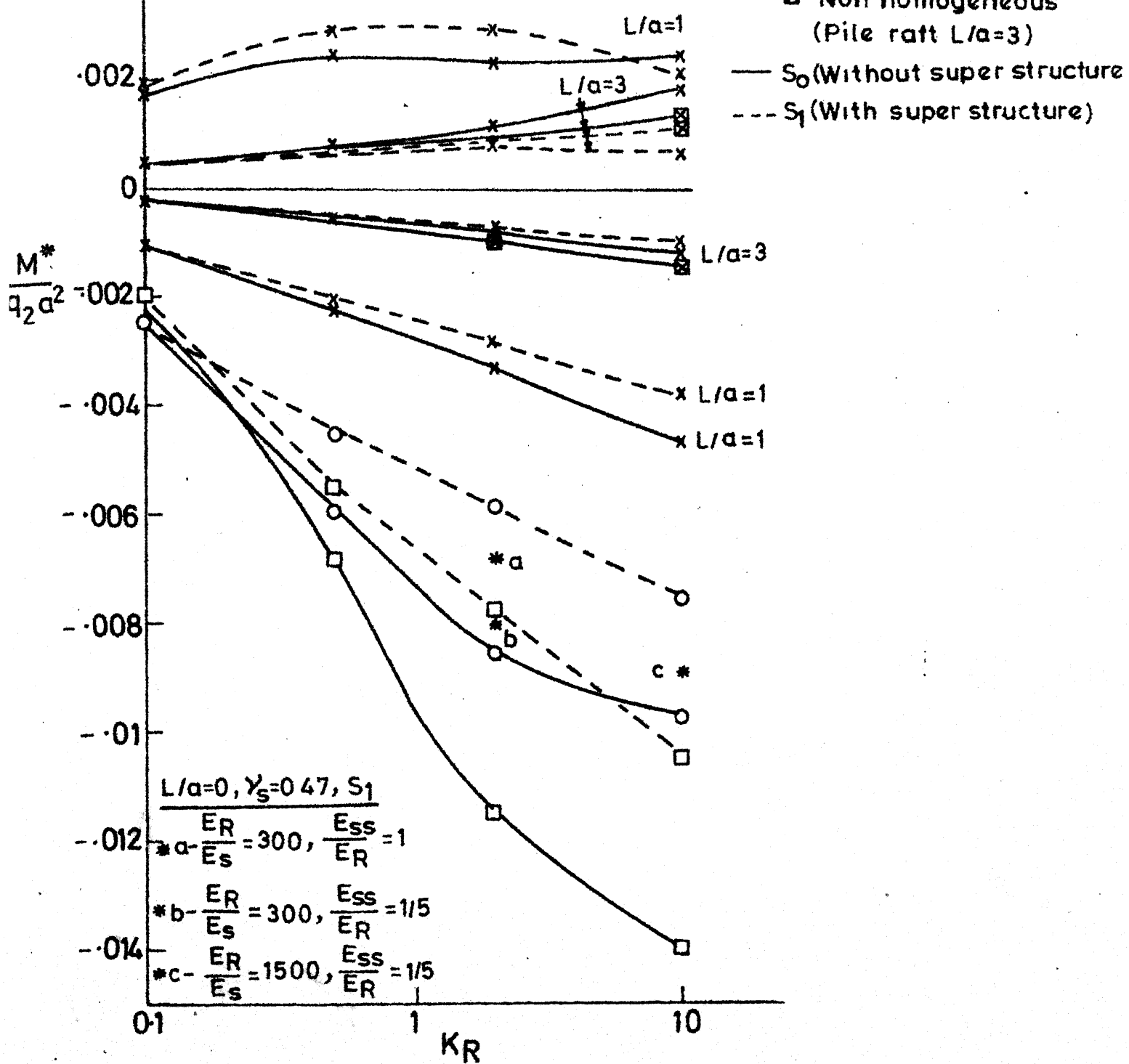
Fig. 6.9 Max. Bending Moment Vs K_R
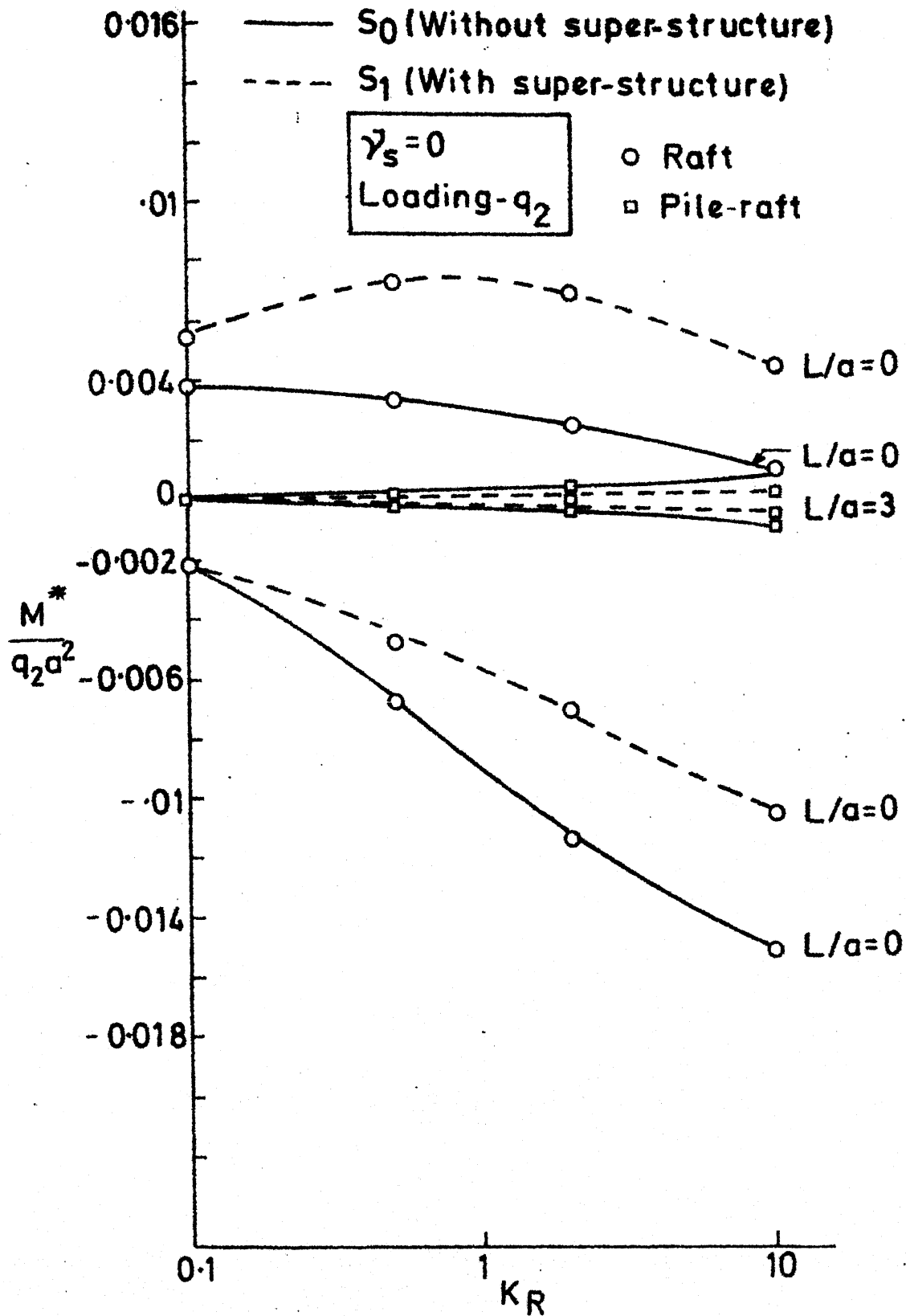
Fig. 6·10 Max. Bending Moment Vs K_R
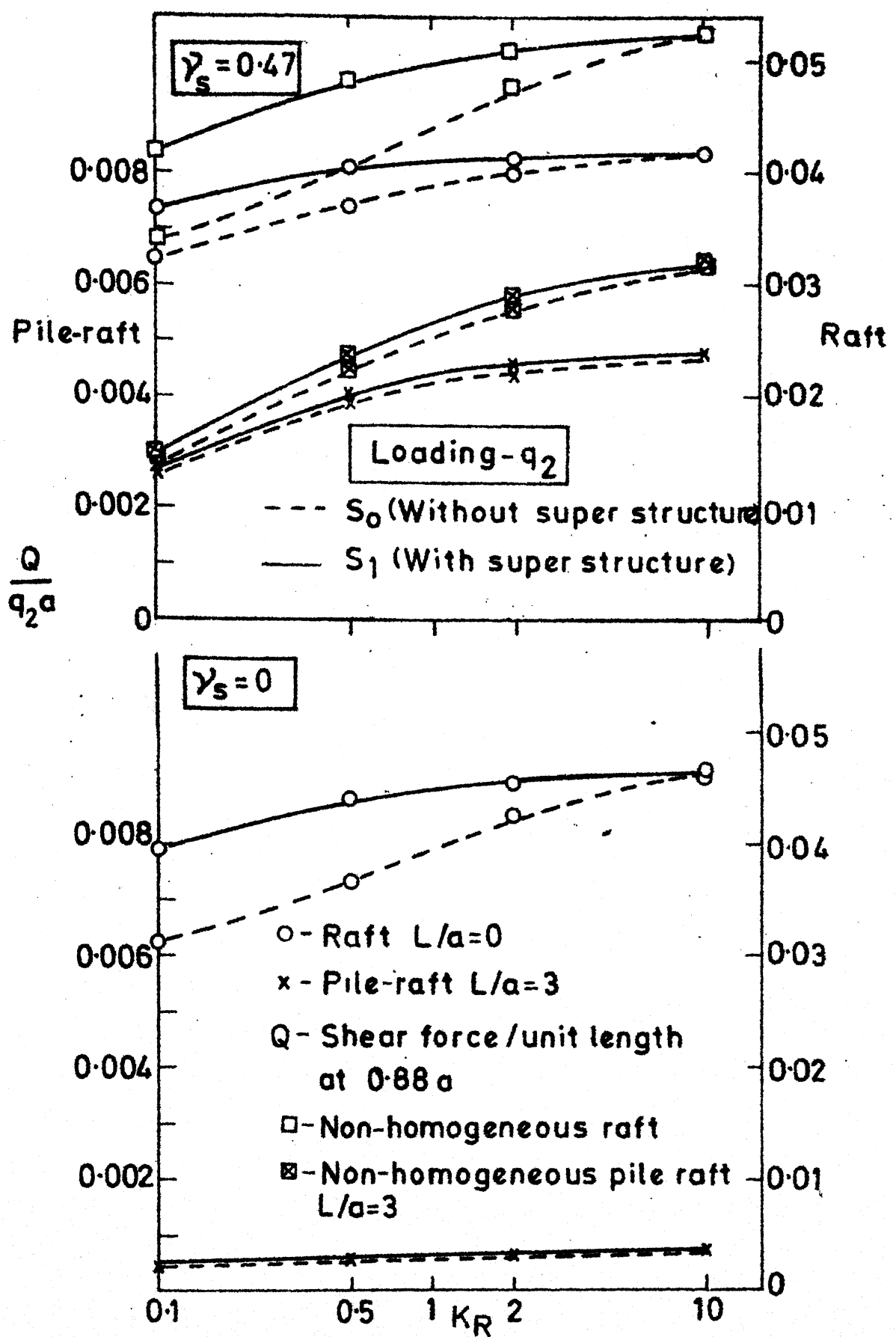
Fig.6·11 Shear force Vs K_R
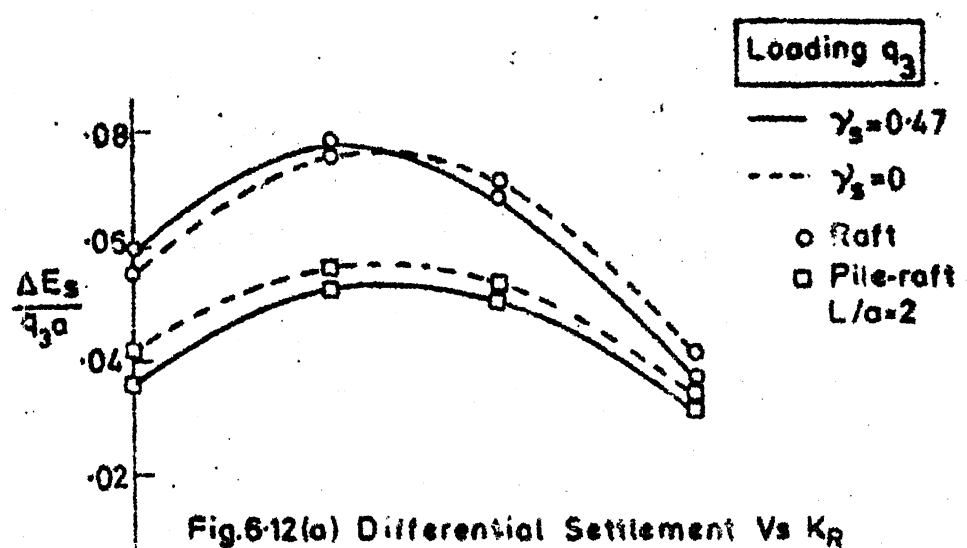
Fig. 6·12(a) Differential Settlement Vs K_R
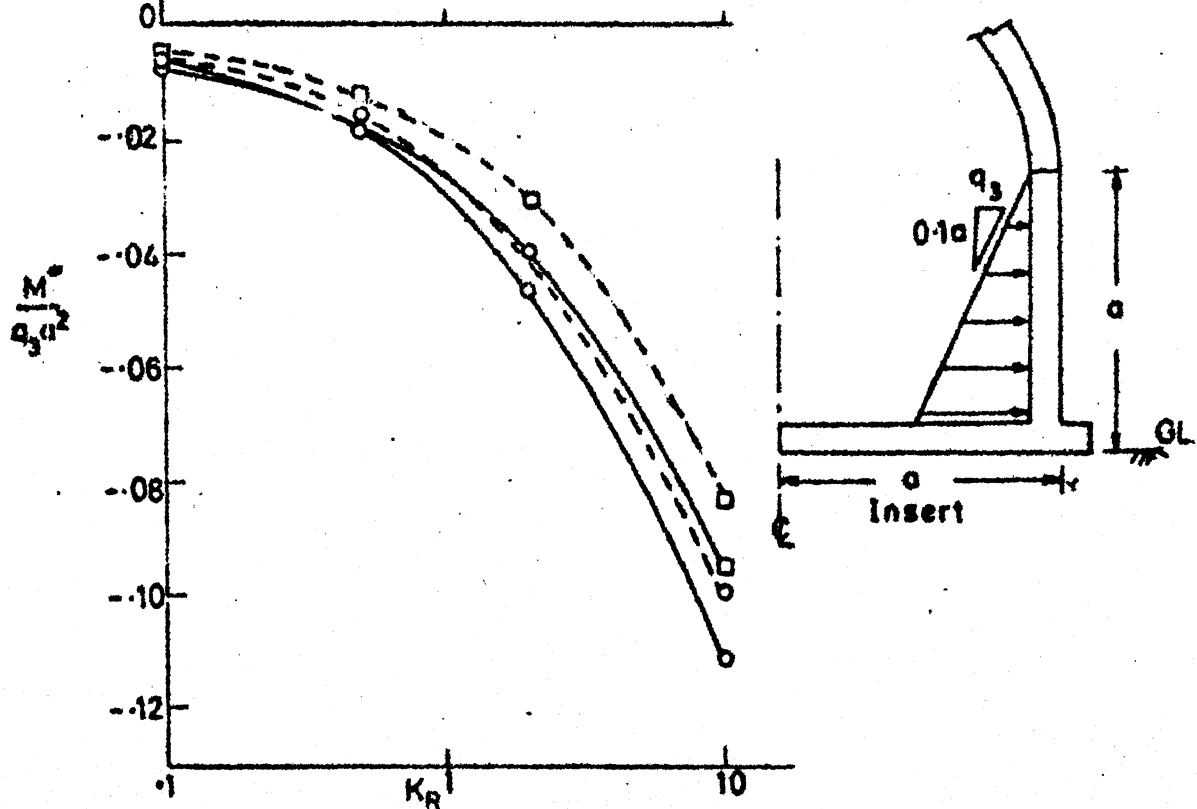
Fig. 6·12(b) Max. Bending Moment Vs K_R
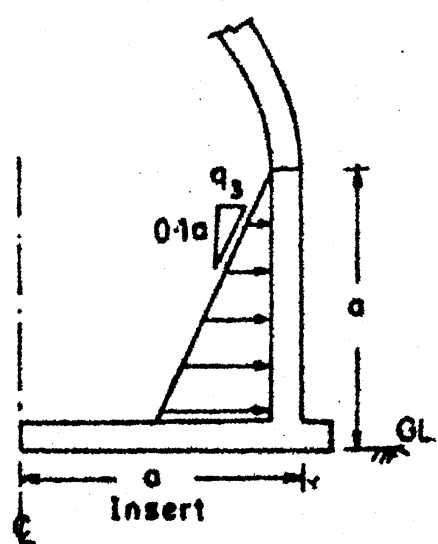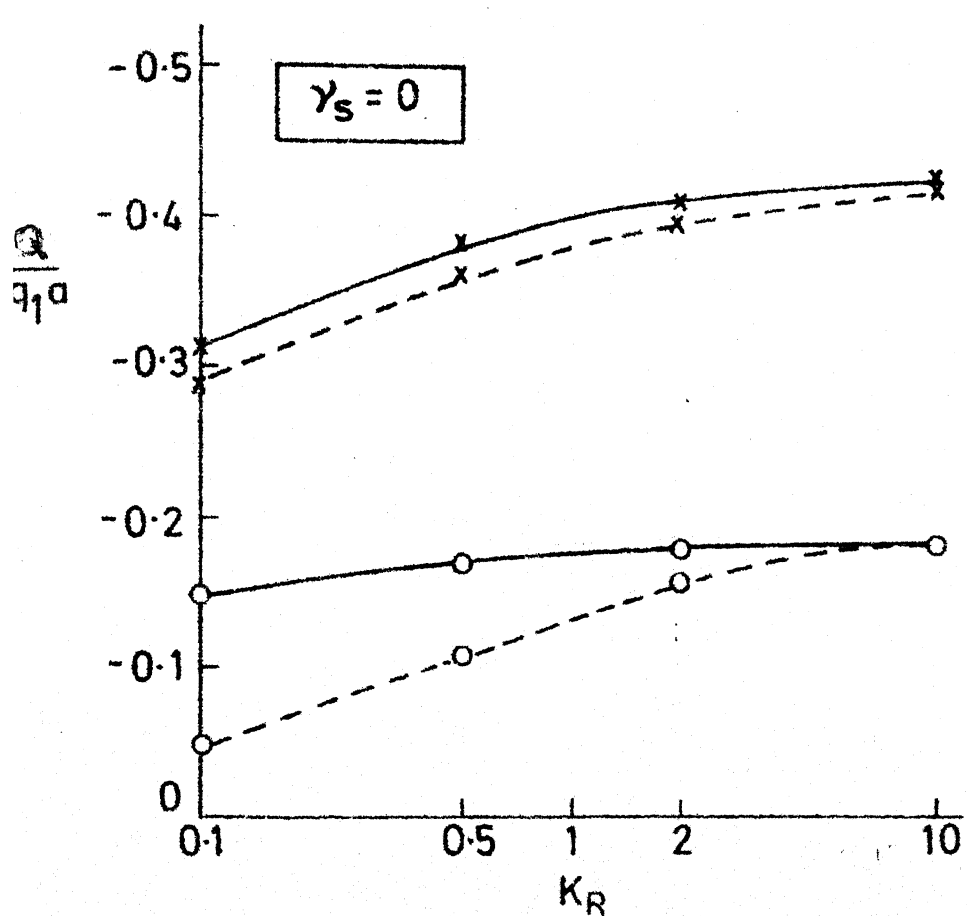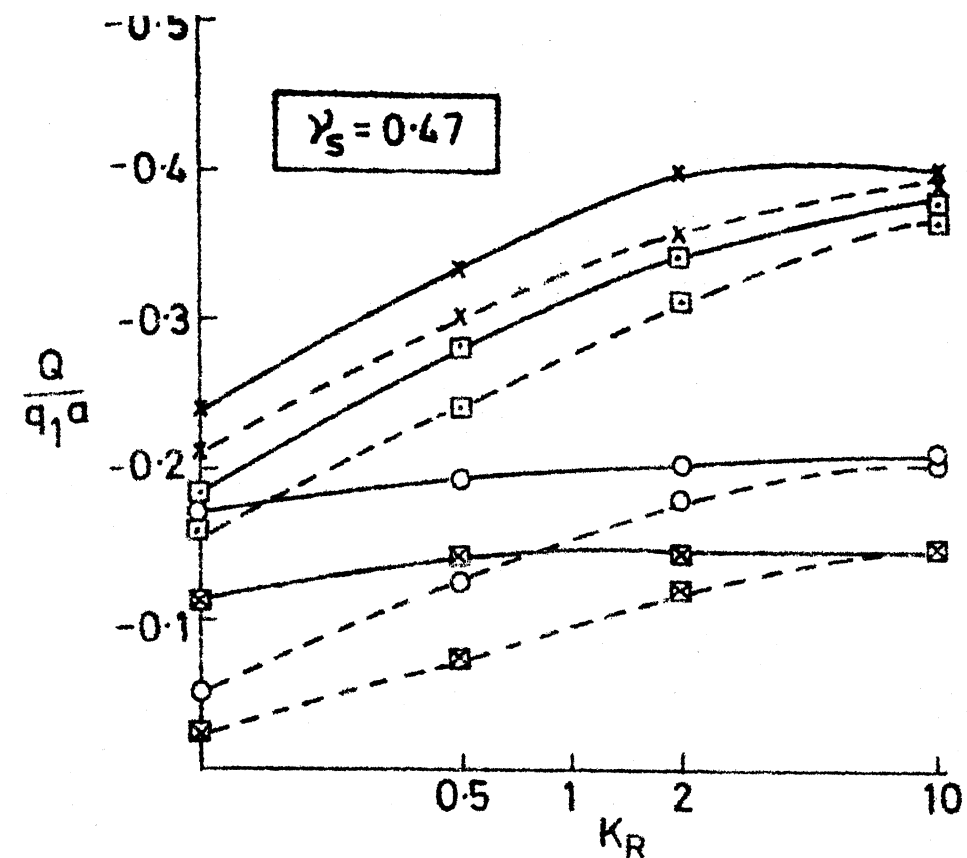
Fig. 6·13 Shear Force Vs K_R
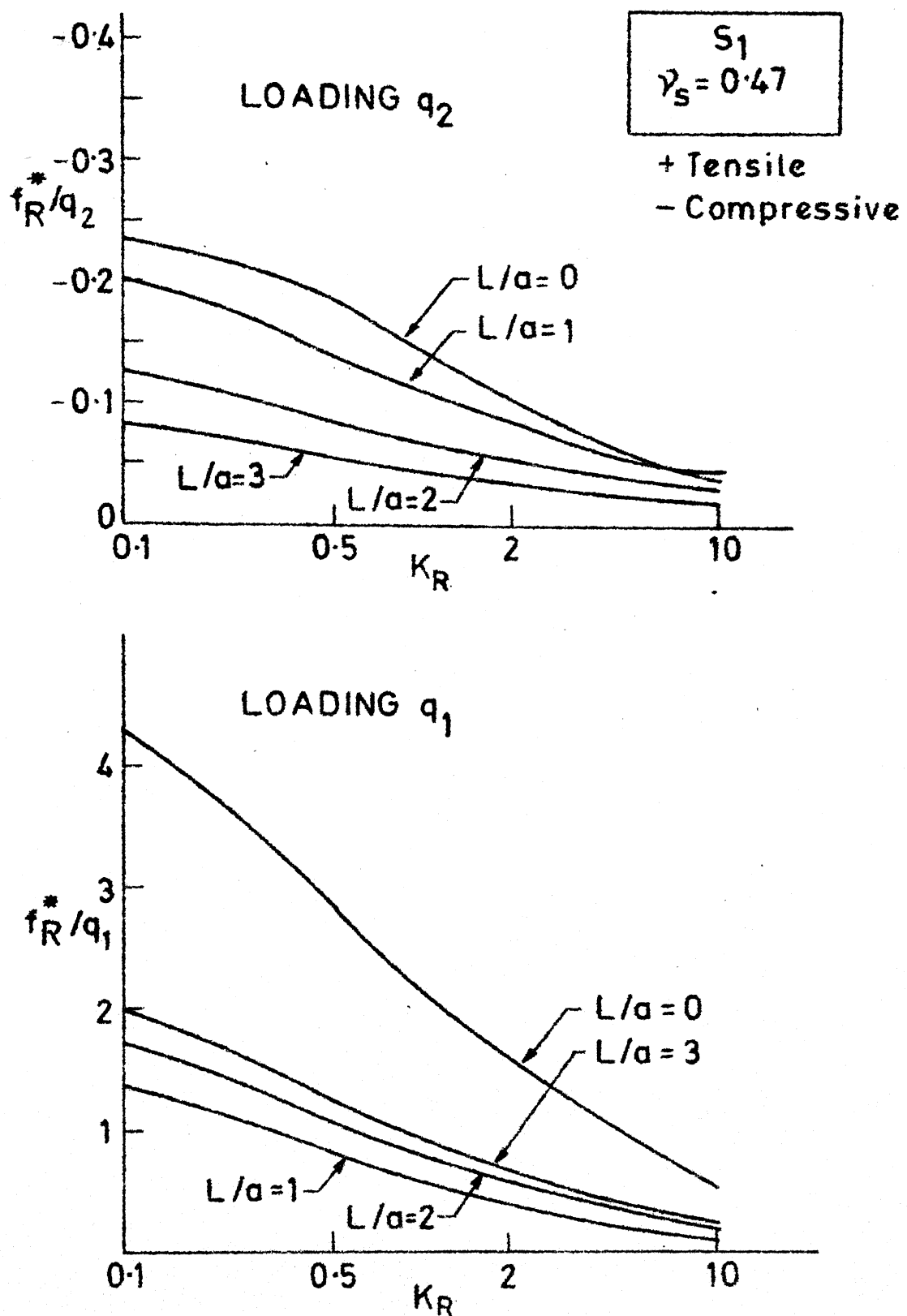
Fig. 6·14 Max. in-plane Stress Vs K_R
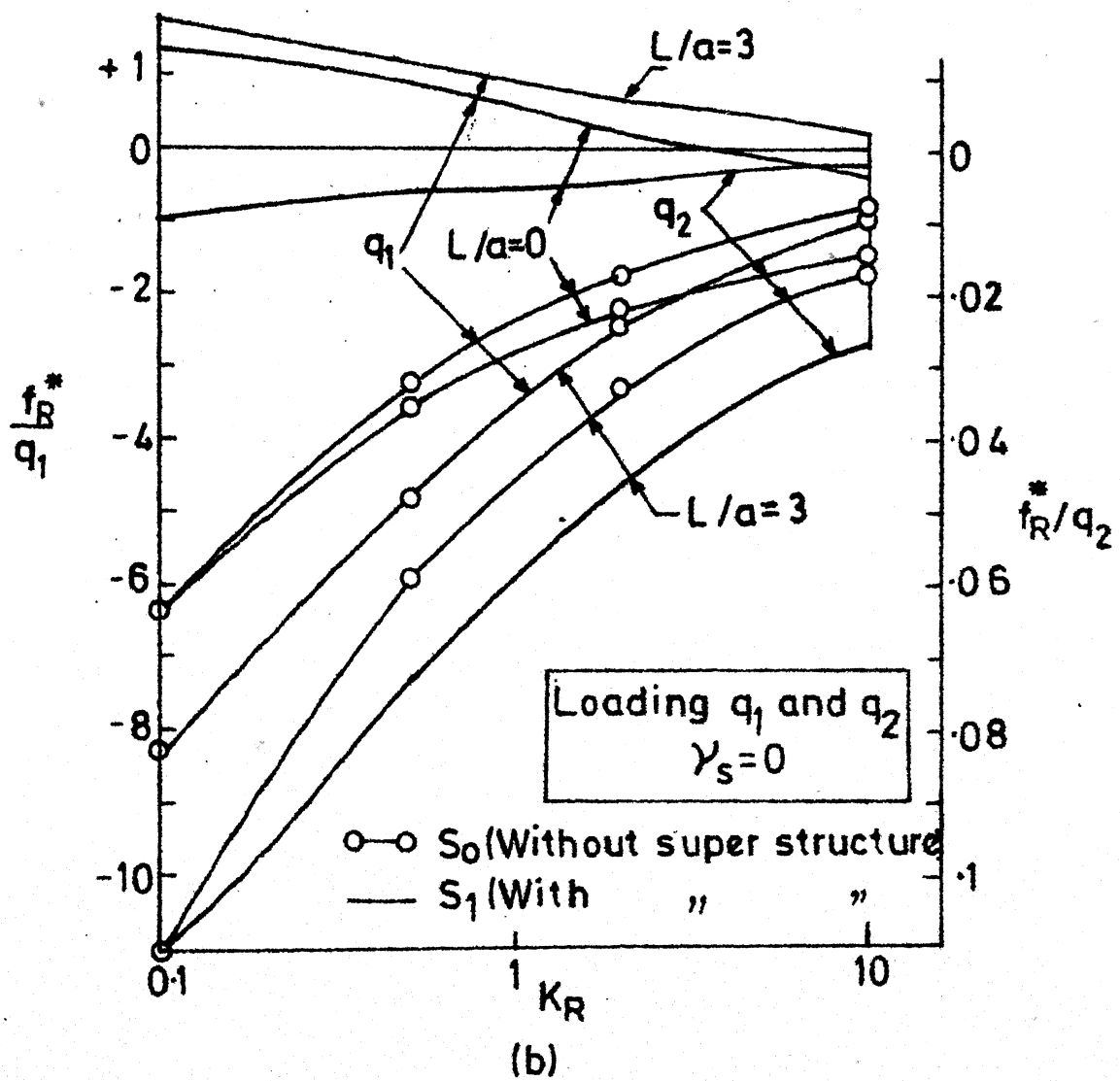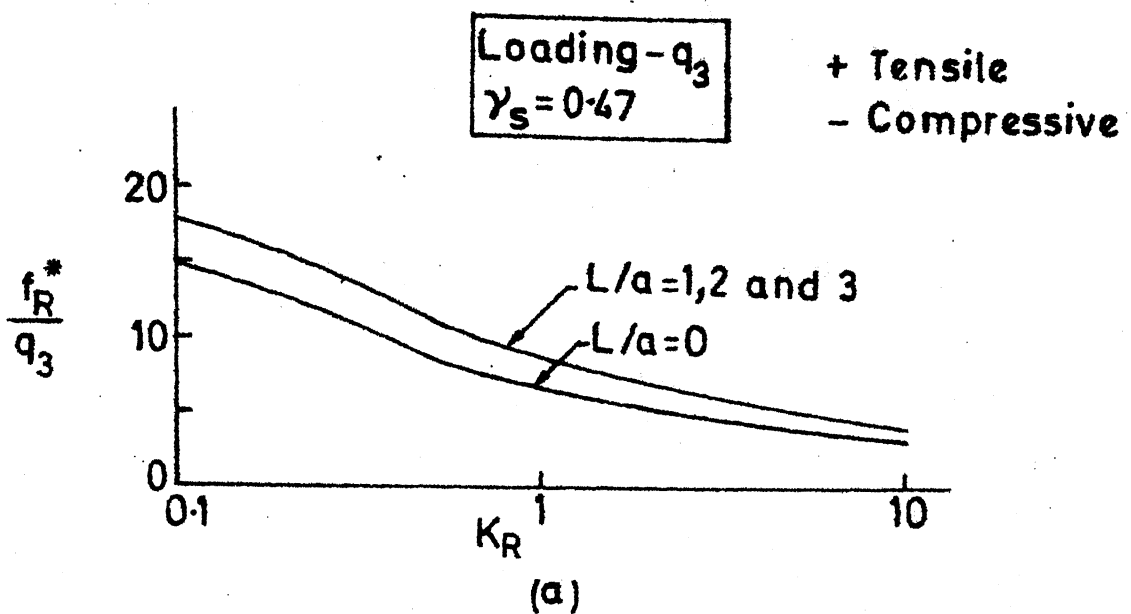
Fig. 6·15 Max. in-plane Stress Vs K_R

CHAPTER 7

CONCLUSIONS AND RECOMMENDATIONS

7.1 SUMMARY

Finite element technique has been used to present solutions for wide range of parameters for a piled circular footing of finite flexibility set in different types of soil, like homogeneous, non-homogeneous soils of different kinds and cross-anisotropic soils. Effect of different geometric and material parameters on the behaviour of the system has been discussed in detail. The effectiveness of piled circular footing compared to other types of foundations has been brought out by examples. An approximate method, for determining the settlement, in case of pile failure has been described. The effect of interface condition on the behaviour of the system has been studied and discussed in detail.

Elasto-plastic analysis has been carried out to study the undrained behaviour of circular footing, single pile and piled circular footing, using 'initial stress' finite element computation technique, with and without interface elements. The effects of parameters like, flexibility of footing, compressibility of pile, non-homogeneity of soil etc. on the behaviour of these foundations,

have been discussed. Some difficulties when this numerical technique is used for Tresca and Drucker-Prager material have been indicated.

A simple procedure, combining axisymmetric finite element analysis and interaction factor method, has been developed, for analysis of pile groups and pile-raft systems set in any linear elastic medium. Using this procedure settlement behaviour of pile groups and pile-rafts, consisting of different number of units in a square arrangement, set in different type of soil like, homogeneous, non-homogeneous (of different kinds) and cross anisotropic has been analysed. The effect of different parameters have been discussed in detail.

The necessity of a non-linear analysis with variable 'interaction' with load level is indicated. A simple 'non-linear interaction factor' method of analysis has been developed for this purpose. A particular case of this analysis, namely a 'bi-linear analysis', has been used for illustration of the method and for presentation of some results, in the case of pile-raft systems.

The effect of an axi-symmetrical superstructure on the behaviour of circular raft and piled circular raft have been studied using finite elements. Solutions have been

obtained with and without considering the superstructure and compared. The effect of different parameters like, flexibility of raft, length of pile and non-homogeneity of soil have been discussed in detail. The solutions have been presented in non-dimensional form for different loading conditions for which such structures may be subjected to.

Though analysis of piled foundation was the essential aim, some results taken for circular raft/footing and single pile, from which conclusions of some importance could be drawn, have been presented and discussed.

The numerical solutions obtained have been compared with available solutions in many cases, to ascertain the accuracy.

Most of the computer programs used for the above analyses were developed specially for this purpose. In some cases, some programs developed at IIT Kanpur were checked, modified to suit the present requirements and used.

Some useful conclusions could be drawn from these analyses and they have been listed at the end of each chapter. These conclusions have been summed up in the next section. This study has indicated a number of areas in which further work is needed. The scope for such future work is listed in Sec. 7.3.

7.2 CONCLUSIONS

7.2.1 Piled Circular Footing-Working Load Response

7.2.1.1 Homogeneous soil

(a) One of the important conclusions that could be drawn from the present work is that piled circular footing is an efficient type of foundation. This combination may be very effective in transmitting the load safely without excessive deformations in many cases.

(b) In the case of central column loading (concentrated load), the bending moments, shear force and differential settlement substantially reduce by the provision of pile to a circular footing. This shows the effectiveness of piled circular footing in the structural design point of view.

(c) When subjected to u.d.l., in the case of flexible footing with pile, there is an optimum value of K_R, at which the system is most efficient in reducing the settlement, compared to circular footing. For this loading, the values of bending moment, shear force and differential settlement increase compared to unpiled footing by appreciable amount.

(d) The values of bending moment in a piled circular footing are quite sensitive to the values of Poisson's ratio of soil. One of the reasons for this is that the load

shared by pile is sensitive to the values of ν_s.

(e) The footing flexibility in general and the pile compressibility for longer pile (L/d>10), affect the behaviour of piled footing significantly and hence it is expected to affect the behaviour of general pile-raft system also.

(f) The non-dimensional solutions presented and the approximate procedure suggested to account for pile failure, would be useful in the design of piled footing of wide range of geometric and material parameters.

7.2.1.2 Non-homogeneous soil condition
Soil stiffness linerly increasing with depth:

(a) Provision of a pile for reducing the settlement of circular footing, is significantly more effective for this type of soil than homogeneous soil, particularly when the footing is fairly flexible and loading is concentrated near the centre. In the case of flexible footing with pile subjected to u.d.l., there is an optimum value of non-homogeneity coefficient (ψ), at which provision of pile is most effective in reducing the settlement.

(b) The load shared by pile is fairly sensitive to this type of non-homogeneity, the sensitivity being more for rigid footing-pile system.

(c)   The values of maximum bending moment and differential settlement substantially reduce compared to those of homogeneous case, in the case of concentrated loading.

Two layer soil medium with stiffer top layer:

(a)   In general, provision of pile is less effective in reducing the settlement of circular footing for this type of non-homogeneity and its effectiveness is observed to be minimum in the range of values of h/L between 0.4 and 0.7 (where h is the thickness of top soil layer).

(b)   The percentage load shared by pile is minimum for h/L in the range of 0.4 and 0.7.

(c)   The values of bending moment and differential settlement are quite sensitive to this type of soil non-homogeneity. In general, maximum bending moment and differential settlement increase in the case of concentrated load and decrease in the case of u.d.l.

Effect of Installation of pile:

(a)   The values of settlement and load shared by pile are not very sensitive to this type of non-homogeneity, except when soil is highly sensitive to the installation of pile (Cases I_4 and I_5, Sec. 2.2.2).

(b)   The values of bending moment and differential settlement are fairly sensitive to this type of non-homogeneity, even if soil is moderately sensitive to the installation of pile (Cases I_1, I_2 and I_3 in Sec. 2.2.2).

7.2.1.3 Transversely Isotropic soil

(a)   The settlement of piled circular footing significantly reduces due to the cross-anisotropy, in the range of parameters considered. This reduction is considerably more in the case of undrained condition than drained condition. For values of n upto 2.5, the effectiveness of provision of pile in reducing the settlement of circular footing is not very much different from that for isotropic case.

(b)   The percentage load shared by pile is not significantly affected by cross-anisotropy for values of n ranging from 1 to 2.5. For the limiting value of n = 4, almost entire load is transmitted by footing.

(c)   The shear stress distribution in the top region of pile is significantly less in the case of piled circular footing, compared to single free standing pile, for both isotropic and cross-anisotropic incompressible material.

7.2.1.4 Effect of interface conditions

(a)   The settlement and percentage of load shared by piles are not significantly affected by the type of contact

(smooth or adhesive) between footing and soil and also between pile head and footing, in a piled circular footing.

(b)   The values of footing bending moments adjacent to the piles are significantly affected (about 20 to 30 %) by the type of contact between footing - pile - soil . The differential settlement is also affected by similar amount by the type of contact.

(c)   The effect of type of contact between footing and pile becomes insignificant near the edge of the footing. on bending moment. The effect of the type of contact between footing and soil is maximum for $\nu_s = 0$ and this effect is maximum near footing edge.

7.2.2   Piled Circular Footing - Progressive Deformation Upto Collapse

(a)   The bearing capacity of piled circular footing in saturated clay in undrained condition may be approximately assumed to be equal to the sum of the bearing capacity of pile and footing in contact with soil.

(b)   The bearing capacity of piled circular footing in saturated clay in undrained condition, is not significantly affected by the footing flexibility and pile compressibility for the range of parameters considered.

(c)   The bearing capacity of piled circular footing
can be significantly increased by enlarging the tip of
the pile.

(d)   There is significant increase in bearing capacity
of piled circular footing in the case of soil whose stiffness
and strength increase with depth, compared to homogeneous
soil.

(e)   As collapse is approached the footing bending moments
(non-dimensional) increase. The plastic zones around pile
and footing and also the extent of skin friction
failure of pile-soil interface, spread simultaneously for
the piled footings considered.

7.2.3 Circular Footing/Raft

7.2.3.1 Elasto-plastic analysis

(a)   The bearing capacity of circular footing subjected
to central column loading is not significantly affected
by the rigidity of the footing (K_R in the range of 1 to 100),
for the value of $d_c/d = 4$ (d = diameter of loaded area).

(b)   The bending moments (non-dimensional) in a circular
footing with central column loading are not affected much
(less than 10 %) as collapse is approached.

(c)   The effect of adhesive contact on the collapse load
of circular footing is small (about 8 %   increase compared
to smooth contact).

7.2.3.4 Elastic analysis

(a)   The effect of adhesive contact on maximum bending moment of circular footing is small (less than 8 percent), if the loading is concentrated near the centre.

(b)   The effect of adhesive contact on maximum bending moment of circular footing subjected to edge loading, is to increase the magnitude of negative bending moments by large amount (about 50 %).

7.2.4   Single Pile

7.2.4.1 Elasto-plastic analysis

(a)   As collapse is approached small tensile stresses develop near the tip of the shallow pile considered. However, it does not influence the ultimate bearing capacity of pile significantly.

(b)   Compressibility of pile does not influence the collapse load of the pile significantly for the cases considered.

7.2.4.2 Elastic analysis

(a)   The effect of installation of single free standing pile, on the settlement, decreases with increasing values of L/d.

(b)   The effect of cross-anisotropy on the settlement of single pile reduces with increasing L/d and this effect

is fairly independent of the values of K for the values of n ranging from 1 to 3.5.

(c)   The cross-anisotropy of incompressible soil significantly affects the values of mean normal stress (σ_m) around pile.

7.2.5 Pile Group and Pile-raft

(a)   The 'interaction factors' may be computed from finite element analysis of single pile or single pile-cap units, using which settlement of pile-group/pile-raft set in non-homogeneous and/or anisotropic soil, can be computed in a straight forward manner.

(b)   A 'non-linear interaction factor method' which considers the non-linear nature of interaction, which has been shown to occur in some cases, is proposed. This analysis can also be carried out using field pile load test data.

(c)   The effect of cross-anisotropy on the settlement of pile group and pile-raft (unless piles are insignificant in the system) is not much for values of n in the range of 1 to 2.5, in the case of incompressible material. However for strongly anisotropic (n > 3) incompressible material, the effect of cross-anisotropy is significant,

for both pile groups and pill-rafts and in such cases the loads tend to get distributed more uniformly among the piles (with rigid cap/raft).

(d)   The effect of modulus linearly increasing with depth on the behaviour of pile group and pile-raft is quite significant. The non-homogeneity of this kind tends to distribute the loads more uniformly among the piles in the case of pile group with rigid cap.

(e)   In the case of two layer soil medium in which a stiffer soil is overlying, the settlement of piled foundation may be more than the settlement of free raft, for certain parameters, indicating that the provision of piles is counter-productive. For such soil medium the value of R_G is maximum for a particular value of h/L in the range of 0.5 to 1.0, depending on different parameters, for both pile group and pile-raft.

(f)   The effect of installation of piles is found to affect the values of R_G by about 15 to 25 % .

7.2.6 Effect of Superstructure

(a)   In general, the maximum settlement of circular raft and circular raft-pile system is not very sensitive to the superstructure stiffness, particularly so for pile-raft. Provision of piles(skirt)near the edge of circular raft

substantially reduces the settlements.

(b)   Inclusion of the superstructure in the analysis of a circular raft appreciably (to the extent of 60 %) reduces the differential settlement for practical range of raft rigidities (K_R = 1 to 10).

(c)   The superstructure stiffness in general reduces the positive bending moment (to the extent of 50-60 %) and increases the magnitudes of negative bending moments for practical range of values of raft stiffness, in the case of u.d.l. For edge loading this effect is less compared to u.d.l.

(d)   Such effect of superstructure stiffness on bending moment is less in the case of pile-raft than in the case of circular raft.

Provision of piles near the edge of a circular raft substantially reduces the values of negative bending moments, for edge loading.

(e)   Piles, when provided near the edge, carry substantial percent of load for both loading (u.d.l. and edge loading). In the case of edge loading almost the entire load is carried by piles.

soil system, is very useful for studies of the kind attempted in this work. For a given soil profile, results for as many as 24 cases were taken in a single run. Since the elements representing the soil are condensed, it becomes very economical in such cases where the foundation/interface/ superstructure is to be modified and solved repeatedly for a given soil profile.

(b)   The parabolic isoparametric elements can model the various components of the systems like footing, raft, pile, soil and superstructure satisfactorily. Also using these elements compatibility can be satisfied throughout and adhesive elastic connections between different components of the system can be modelled in a straight forward manner. In such parabolic isoparametric elements, the computation of bending moments can be conveniently done by integrating the stresses. Such integration by Gauss quadrature technique amounts to just addition of moments of Gauss point stresses which are already calculated and hence it becomes computationally efficient.

(c)   By using 6 noded interface elements of zero thickness the interface behaviour including the stresses in the vicinity of and at the interface can be computed to sufficient accuracy. However, the values of stiffnesses (k_n and k_s)

have to be chosen for a given situation carefully,
particularly when Poisson's ratio of soil is near 0.5.

(d)   The 'initial stress' computation technique for
elasto-plastic finite element analysis is satisfactory,
for the problems analysed. However, it is quite expensive,
particularly when the system is stiff (e.g. CPU time
required for C-$\emptyset$ soil is more than that for C soil. CPU
time required for piled footing is more than that required
for single pile).

(e)   The conventional 'initial stress' finite element
technique (using quadratic isoparametric axisymmetric
elements with reduced integration) fails for Tresca yield
criterion, even though the same technique gives satisfactory
results when von-Mises or Drucker-Prager yield criterion is
used, for the problems analysed herein.

7.3 RECOMMENDATIONS FOR FUTURE WORK

7.3.1 Piled Circular Footing

(a)   The analysis of piled circular footing carried out in
the present work is limited to static vertical axisymmetrical
loads and it is found to be an efficient type of foundation.
It is likely to be equally or more effective for moment
loading and dynamic or siesmic loading. Analysis for such
loading may be very useful.

(b)   In the present work, comparisons of this type of foundations with other types of foundations were made in terms of volume of the material. More sophisticated cost analysis coupled with optimization technique would be highly useful in arriving at economical design of such foundations.

(c)   In the case of elasto-plastic analysis slip at interfaces were simulated by assigning an arbitrary low value of shear stiffness, which does not appear to have sound physical basis (Desai (46)). Improved modelling of the interfaces may be achieved in the line of research being presently carried out (Desai (46)).

(d)   A comprehensive study may be carried out to over come the difficulties mentioned in Appendix D, when Mohr-Coulomb type yield criterion is used. The analysis of piled circular footing for $C-\emptyset$ material may be carried out. Since this type of foundation is likely to be efficient in bearing capacity point of view also, for such soils, such work may be useful.

(e)   Model/field tests on such foundation would be very useful in indicating the applicability of the approximate procedure suggested for taking into account the pile failure.

7.3.2 Pile Groups and Pile-Raft

(a) Field or model tests may be carried out on pile and pile-cap units and using these results the settlements may be computed by the proposed 'non-linear interaction factor method' and compared with the actual behaviour of pile groups and pile-raft systems, for different geometries to asses the effectiveness of the proposed method.

(b) Pile-raft system may be an ideal combination in some cases. Optimization study on such systems would be highly useful in arriving at economical design, satisfying both bearing capacity and permissible settlement requirements.

7.3.3 Effect of Superstructure

(a) Solutions were presented for certain range of parameters for the design of foundation of a simple type of axisymmetrical structure. The possibility of presentation of some correction factors for variations in soil and superstructure stiffness for generalisation may be explored.

(b) The superstructure-foundation-soil system analysis for some typical structures like framed, walled etc.,

using three-dimensional quadratic isoparametric elements may be carried out and compared with results using plate and beam elements for modelling foundation and superstructure to indicate the effect of different assumptions like hinged, fixed and elastic connections at the location of interfaces.

APPENDIX - A

A CONDENSATION PROCEDURE FOR LARGE FINITE ELEMENT PROBLEMS

A.1 INTRODUCTION

In geotechnical engineering problems, often it is required to discretise the soil continuum, when finite element method is used. When continuum of a large horizontal and vertical extent is discretised, the computer storage required is very high, particularly so for three dimensional problems. If the continuum is homogeneous, infinite elements (Buragohain (21)) can be used to overcome this difficulty. However, in the case of arbitrarily non-homogeneous cases discretisation of the continuum will have to be done. If the available active storage capacity in the computer is not sufficient, the common procedure is to assemble in blocks, and solve using block solution routine (Wilson et al (145)). This requires writing in tape and reading from tape, which increases the computing time. Also it involves programming complications. A simple 'condensation' procedure for solving large finite element problems using banded storage and solution technique, without use of tape or auxiliary storage is described in this Appendix. The present procedure is similar to 'physical blocking' described by Christian Meyer (32). Even if the available core is more, the saving in core used, would be of some significance in the systems in which the computing charges are based on both core used and time.

Some solutions obtained for flexible circular footing in adhesive contact with deep elastic soil layer and single pile in elastic soil, using the above procedure are given. Results so obtained by finite element method are compared with available solutions, to ascertain the adequacy of mesh used, for the analysis of circular footing and single pile. For the present finite element formulation different numerical techniques for computing bending moment and shear force are compared.

The 'condensation procedure' and the method of computation of contact pressure, bending moment and shear force, described herein was implemented in the computer program developed (PRELAN) and was used for the analyses reported in Chapters 2, 3, 5, and 6. The meshes similar to one used in the analysis reported herein, were used in the analyses reported in Chapters 2, 3, 5 and 6.

A.2 DESCRIPTION

The procedure described is similar to 'substructure technique' (Prezemienicki (112)), but here it is done by mere matrix manipulation without physically seperating the various parts of the assembly. The mesh is divided into NT blocks (10 blocks in the case illustrated in Fig.A.1). The size of each block must be such that it can be assembled

and solved with the available computer storage. The lines
(or planes in the case of three dimensional problems), which
separate the blocks must traverse the entire domain. If the
problem is very large or the storage available is very small,
it is possible to solve by the present procedure if at least
one row of elements (or one slice of elements in the case
of three dimensional problems) can be assembled and solved with
the available storage.

The first block is assembled and condensed by partial
inversion (simple Gaussian elimination for banded symmetrical
matrix (Desai and Abel (45)) was used), upto the equation
NEE in Fig. A.2a. NEE are the equations eliminated
corresponding to nodes which are not common to block 1 and
block 2. (N-NEE) are the equations corresponding to nodes
which are common to block 1 and block 2, where N is the
total number of equations for block 1. The matrix B
(Fig. A.2a) obtained after partial inversion represents the
effect of the elements in block 1 on the nodes which are
common to block 1 and block 2. The numbering of nodes is
to be done such that the last set of nodes in the Mth
block are the first set of nodes in the (M + 1)th block.
The matrix B is added to the stiffness matrix of the second
block while initialising (Fig. A.2b). This is continued

upto (NT-1)th block, i.e. (NT-1) blocks are condensed. The last block (10th block in Fig. A.1) alone is solved for displacements, stresses etc. If the problem is to be solved for different modifications in the NTth block (for example, for different thicknesses of foundation, as used in the case of analyses reported in Chapters 2 and 3, or different modifications in the foundation and or superstructure, as used in the analyses reported in Chapter 6), this procedure is particularly advantageous. The matrix B can be stored in the active storage and the last block alone can be solved repeatedly. If the problem is to be solved for different loading conditions, the right hand side can be modified and solved as usual. (This technique was used in the analyses reported in Chapters 2, 3 and 6). Schematic diagram of the procedure is given in Fig. A.3.

Analyses of piled circular footing, circular footing, single pile, circular raft and circular pile-raft under different soil conditions have been carried out using this procedure, the results of which have been discussed in Chapters 2 to 6. Some results for a circular raft and single pile are presented in this Appendix. These results show the adequacy of the mesh for circular raft and single

pile and hence it is expected to be adequate for the
analysis of piled circular footing analysed in Chapter 2
and 3.

The mesh used (Fig. A.1) contains 371 eight noded
isoparametric elements in axisymmetric form, used for modell-
ing soil, footing and pile. The mesh has been so arranged
that the same mesh can be used for different lengths of pile.
The active computer storage required was high (about 300 K),
if one step assembly and solution were to be performed. The
mesh was divided into 10 blocks. Nine blocks were condensed
by the procedure described. Each of the nine blocks condensed
contained 3 rows of elements. The band width was 88 and the
number of equations per block was 300. The active storage
required was only 30 K. Since the problem was required to
be solved for six different footing thicknesses (for different
rigidities of footing), the 10th block alone was assembled
and solved for displacements, contact pressures, bending
moments etc. repeatedly. The problem was solved for two
different loading conditions in most of the cases. Hence
the results for a number of cases (11 to 24) were obtained
in one run. The CPU time in DEC 1090 Computer was about
2 minutes 15 seconds. The CPU time was compared by solving
a smaller problem by single step solution and present
procedure. The present procedure required slightly less

time. This may be because, back substitution was done only for the last block, when using the present procedure.

The limitation of this procedure is that the complete solution can be obtained only for nodes and elements in the last block. Since in most of the soil-foundation inter- action problems the settlement, stresses etc. are required near the foundation only, this procedure can be conveniently used for the linear analysis. For nonlinear analysis, the portion of the continuum which may not exhibit nonlinearity can be condensed by this procedure. If the displacements, stresses etc. are required in the blocks which have been condensed, the reduced matrices will have to be saved in tape and back substitution will have to be done block by block. Even in that case this procedure may be economical than a general block assembly and block solution procedure (Wilson et al (145)). It is assumed that there is no externally applied load or specified displacement in the blocks condensed. If there are any, the right hand side vector after condensation, may be added to the next block while initialising, as done for stiffness matrix. The geometrical boundary conditions, do not pose any special problem.

A.3 ANALYSIS OF CIRCULAR FOOTING

A.3.1 General

The mesh used is shown in Fig. A.1. Two types of vertical loading were considered namely uniformly distributed load (q) over the entire footing area (termed as udl) and uniformly distributed load (q) over a small circle of diameter d, at the centre (termed as concentrated load). The solutions were obtained for different values of relative rigidities (K_R - as defined by equation 2.1a in Chapter 2) of the footing.

A.3.2 Comparison of Settlement

The computed settlements for u.d.l. have been shown in Fig. A.4. Brown's (15) solutions for circular footing subjected to u.d.l., for smooth contact between footing and soil have also been shown in the same figure. As fully adhesive contact has been assumed in the present work, the present solution and Brown's solution must agree for incompressible material (Poisson's ratio (ν_S) of soil = 0.5), in which case the shear stresses at the interface becomes nearly equal to zero (Hooper (73)). In the present analysis a ν_S value of 0.47 was used to avoid any numerical difficulty. A close agreement of settlement (S_R^*) values can be seen in Fig. A.4. It was found that the agreement

was also good in the case of differential settlement. The contact pressure was obtained by taking the average of vertical stresses at 4 Gauss points in each element immediately below the footing and was found to be in good agreement with the values obtained by Brown (15).

A.3.3 Computation of Bending Moment

Since continuum elements were used to model the footing, direct output of bending moments could not be obtained. Alternately if annular plate bending finite elements (Paramasivam (102) and Pardoen (103)) are used, it is possible to obtain the values of bending moments and shear forces directly; but the limitations are as follows:

1. It is difficult to solve adhesive contact problems.

2. It is difficult to satisfy compatibility at the interface.

3. The connection between pile head and raft and between superstructure and raft will have to be assumed either hinged or fixed. By the present formulation, it is possible to model a compatible elastic connection between the pile head, raft and superstructure.

For computing the bending moments, two procedures were compared, one with known displacements to solve for bending moments using thin axisymmetrical plate equation

(Timoshenko et al (131)) by finite difference method, and the second by integrating the moments of radial and tangential stresses, over the entire thickness i.e.

Radial bending moment (M_R) = $\int_{-t/2}^{t/2} \sigma_R \, ZdZ$ $\qquad$ (A.1)

Tangential bending moment (M_T) = $\int_{-t/2}^{t/2} \sigma_\theta \, ZdZ$ $\qquad$ (A.2)

in which

σ_R = radial stress

σ_θ = tangential stress

t = thickness of raft

Z = vertical distance.

The computed values of maximum bending moment (M_R^*) have been shown in Fig. A.6. It can be observed that the first procedure completely failed when the plate is very thick $(K_R = 100)$. This may be due to the additional deformation due to shear stresses, which is particularly significant for thick plates. The results of the second procedure are found to agree well with Brown's solution (Brown(15)). Th results obtained by numerical integration of equation A.1 and A.2 with 2 and 3 point Gauss quadrature were compared and the difference was negligible. Hence 2-point Gauss

quadrature has been used throughout for computing bending moments. The shear force was also computed by integrating the shear stresses (τ_{rz}) over the entire thickness. It was found that 2-point Gauss quadrature was adequate for integration.

A.3.4 Circular Footing with Central Column Loading

The problem of circular raft in adhesive contact with deep elastic layer, subjected to u.d.l. and parabolic loading has been discussed by Hooper (73). Since circular footing subjected to central column loading (termed as concentrated load herein) is of practical significance, some results for this problem are presented in Figs. A.5 and A.7. Fig. A.5 shows the settlement influence factors for different ratios of diameter of footing (d_c) to diameter of loaded area (d) with uniform pressure q, for values of $\nu_S = 0$, 0.3 and 0.47 and for different values of K_R. Fig. A.7 shows the maximum bending moment (M*) for u.d.l. and for concentrated load with $d_c/d = 5$. It can be observed that the maximum bending moment reduces by about 50 % (for $K_R = 100$, u.d.l) for $\nu_S = 0$, compared to $\nu_S = 0.47$. When the value of $\nu_S = 0.5$ the solutions have to be same whether contact is smooth or adhesive at least for rigid raft. Also the smooth contact solutions

are independent of the values of ν_s. Hence the said reduction of 50 % for u.d.l. is the effect of adhesive contact for $\nu_s = 0$. It can be observed in Fig. A.7, that the corresponding reduction in maximum bending moments for concentrated load is less than 8 percent. However it was observed that the values of bending moment near the edge of the footing, where they are minimum, are substantially affected by adhesive contact.

A.4 ANALYSIS OF SINGLE PILE

The results of settlement obtained using the same mesh (Fig. A.1) for the analysis of different cases of single pile are presented in Table A.1. The values of settlement computed using charts presented by Poulos and Davis (110,111) are also given for comparison.

It can be observed in Table A.1, that the agreement between settlement obtained from the present analysis and settlement calculated using Poulos and Davis(110,111) charts are close for L/d = 10. For L/d = 25, the differences between the finite element (average) and Poulos and Davis (110, 111) values, increase as the compressibility of pile increases and also as ν_s reduces.

The calculations using Poulos and Davis (111), charts were performed as follows

is presented. This procedure is particularly economical, if a number of different foundations and (or) superstructure are to be analysed for a given soil profile.

The bending moment can be determined to acceptable accuracy by integrating the moment of stresses at the cross section using parabolic displacement continuum elements. The effect of adhesive contact on the maximum bending moment of circular footing reduces considerably when the loading is concentrated over a small area at the centre.

The solutions obtained using the mesh shown in Fig. A.1, agree well with the available solutions both in the case of circular footing and single pile. Hence the mesh is expected to be adequate for the analysis of piled circular footing, which is a combination of both.

TABLE A.1 COMPARISON OF SETTLEMENT OF SINGLE PILE

Length of Pile (L)/ diameter of pile (d) L/d	Young's modulus of pile material E_p / Young's modulus of soils	Present Analysis			Results using Poulos and Davis(110, (111)	% difference between 6 and 5
		RRHS	FRHS	AVERAGE		
1	2	3	4	5	6	7
10	1500	105.0^a	111.0	108.0	110.0	1.85
		90.5^b	91.2	90.9	91.3	0.44
	500	112.0	116.0	114.0	115.0	0.88
		96.1	97.0	96.7	95.8	0.93
	200	122.0	127.0	124.5	125.0	0.40
		108.0	109.0	108.5	106.0	2.30
25	1500	56.7	61.7	59.2	56.8	4.05
		49.4	50.3	49.9	49.0	1.80
	500	68.1	73.2	70.7	66.0	6.65
		61.3	62.0	61.7	56.0	9.24
	200	89.5	94.7	92.1	80.8	11.96
		82.6	83.4	83.0	70.3	15.66

a - $S^* E_S/qd$ x 1000 for $\nu_S = 0.47$ RRHS - Restricted right hand side boundary

b - $S^* E_S/qd$ x1000 for $\nu_S = 0$ FRHS - Free right hand side boundary
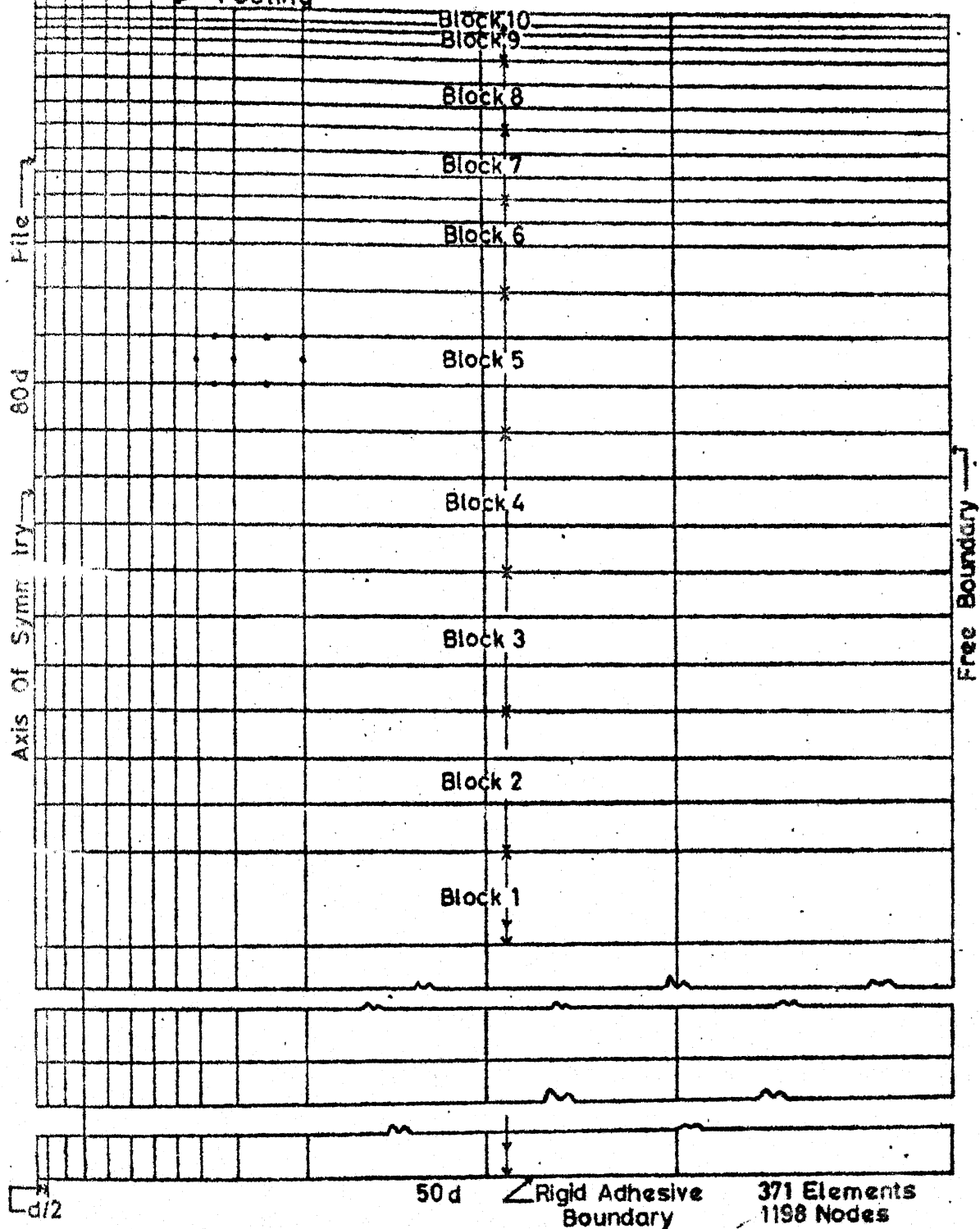
Fig.A-1 Typical Mesh
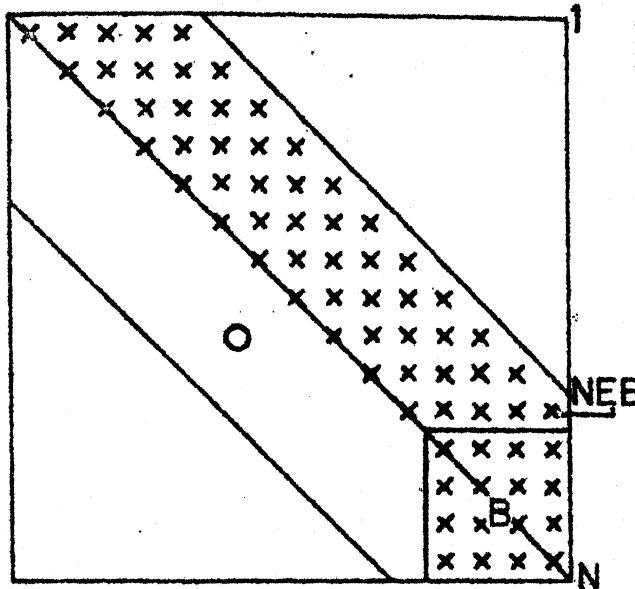
Fig. A.2(a)
M^{th} block after
condensing
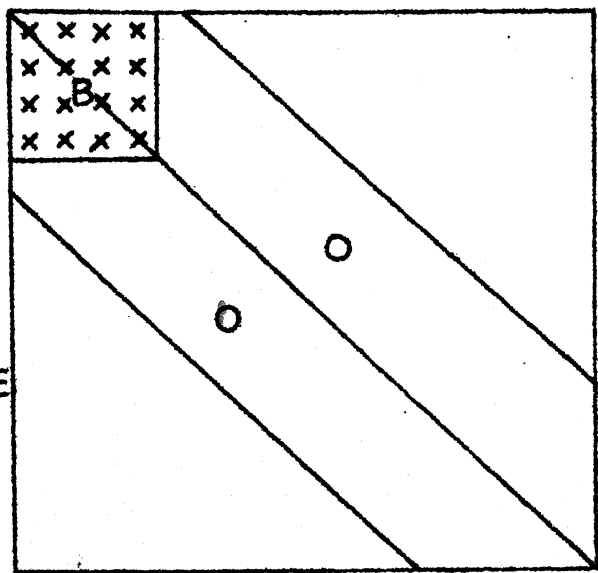
Fig. A.2(b)
$(M+1)^{th}$ block after
adding [B] and
initialising

Fig. A3 SCHEMATIC DIAGRAM
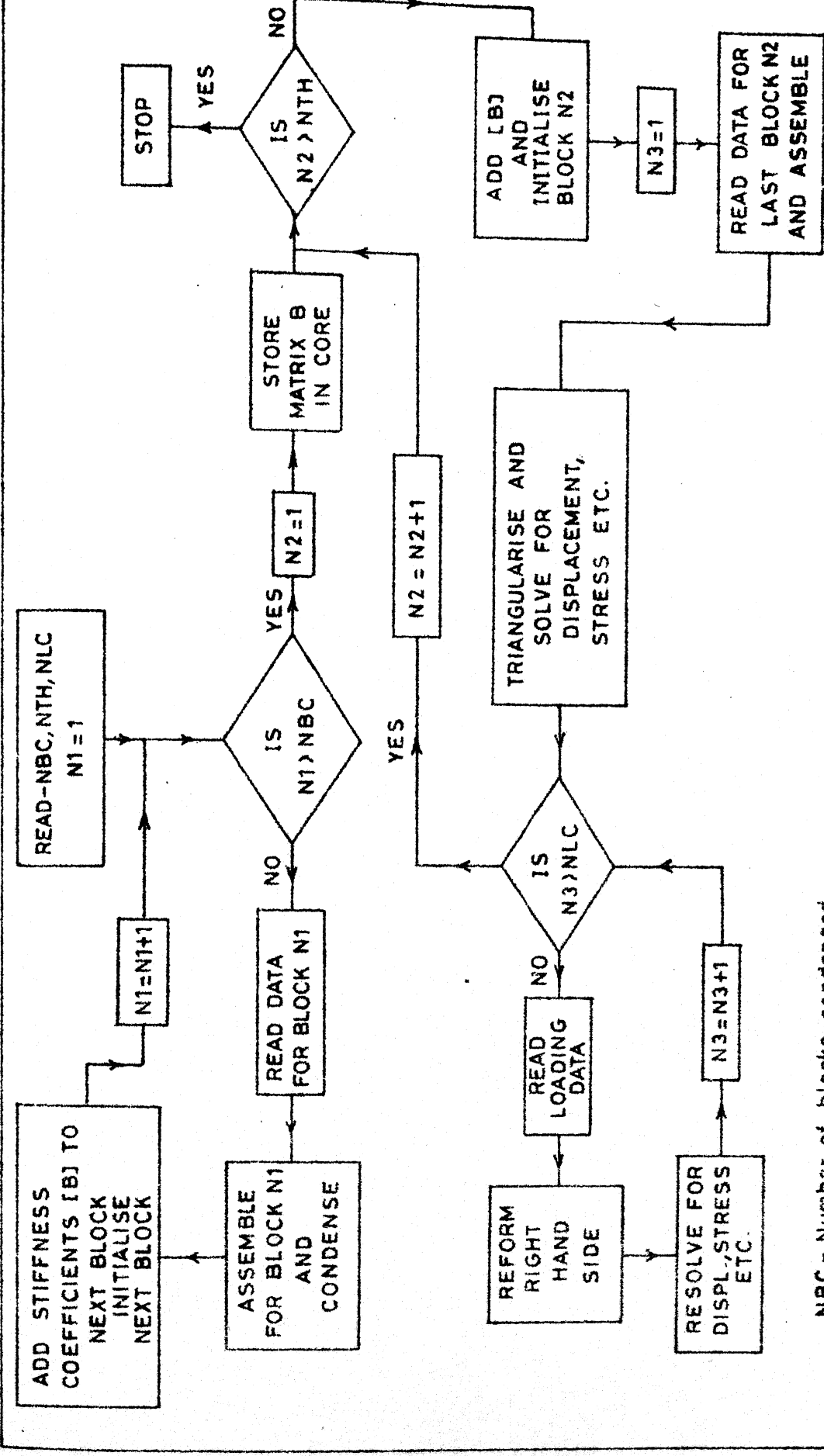
NBC - Number of blocks condensed

NTH - Number of different last blocks

NLC - Number of load cases for each last block
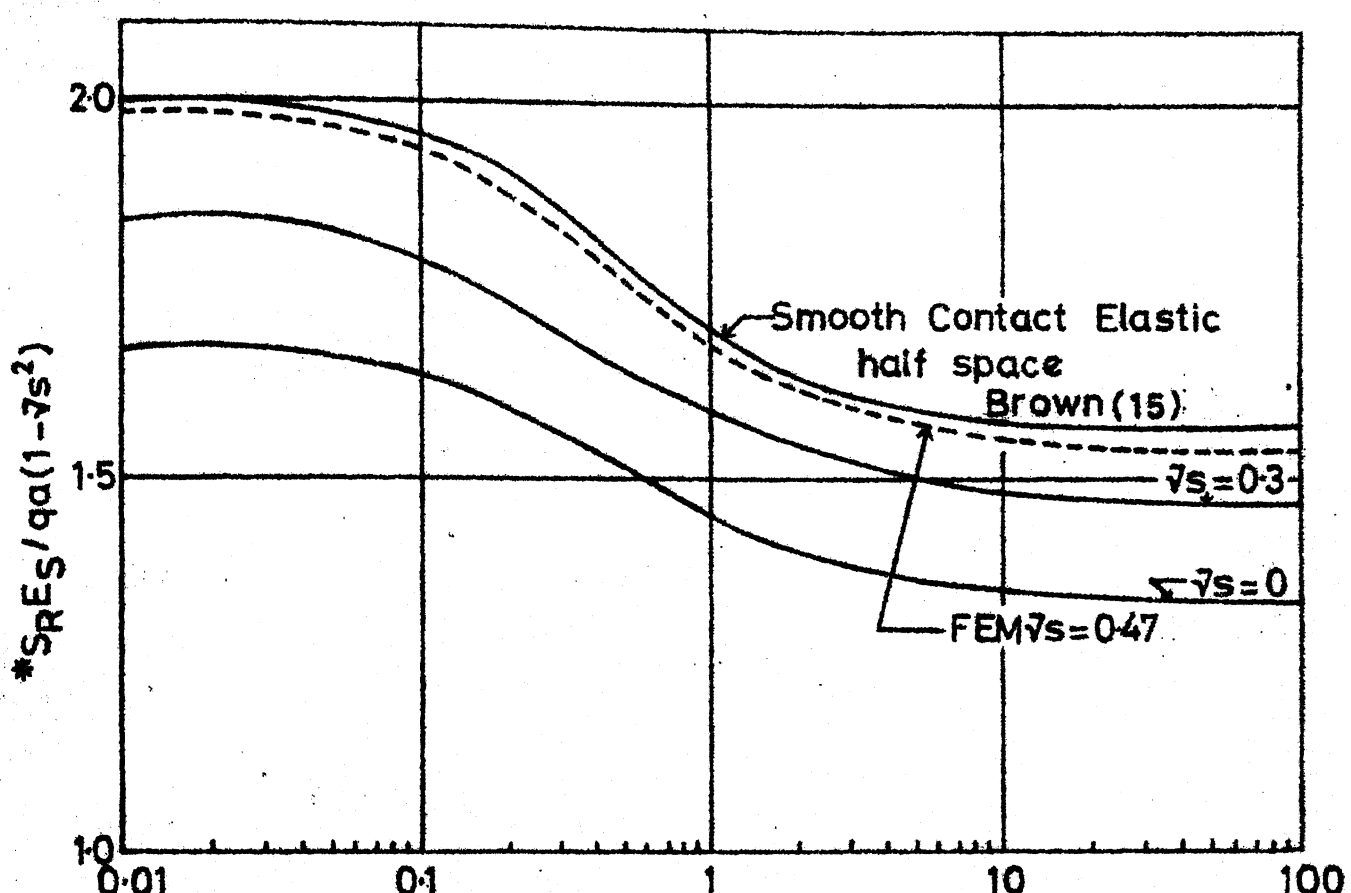
Fig.A·4   Raft   Settlement (udl) Vs K_R
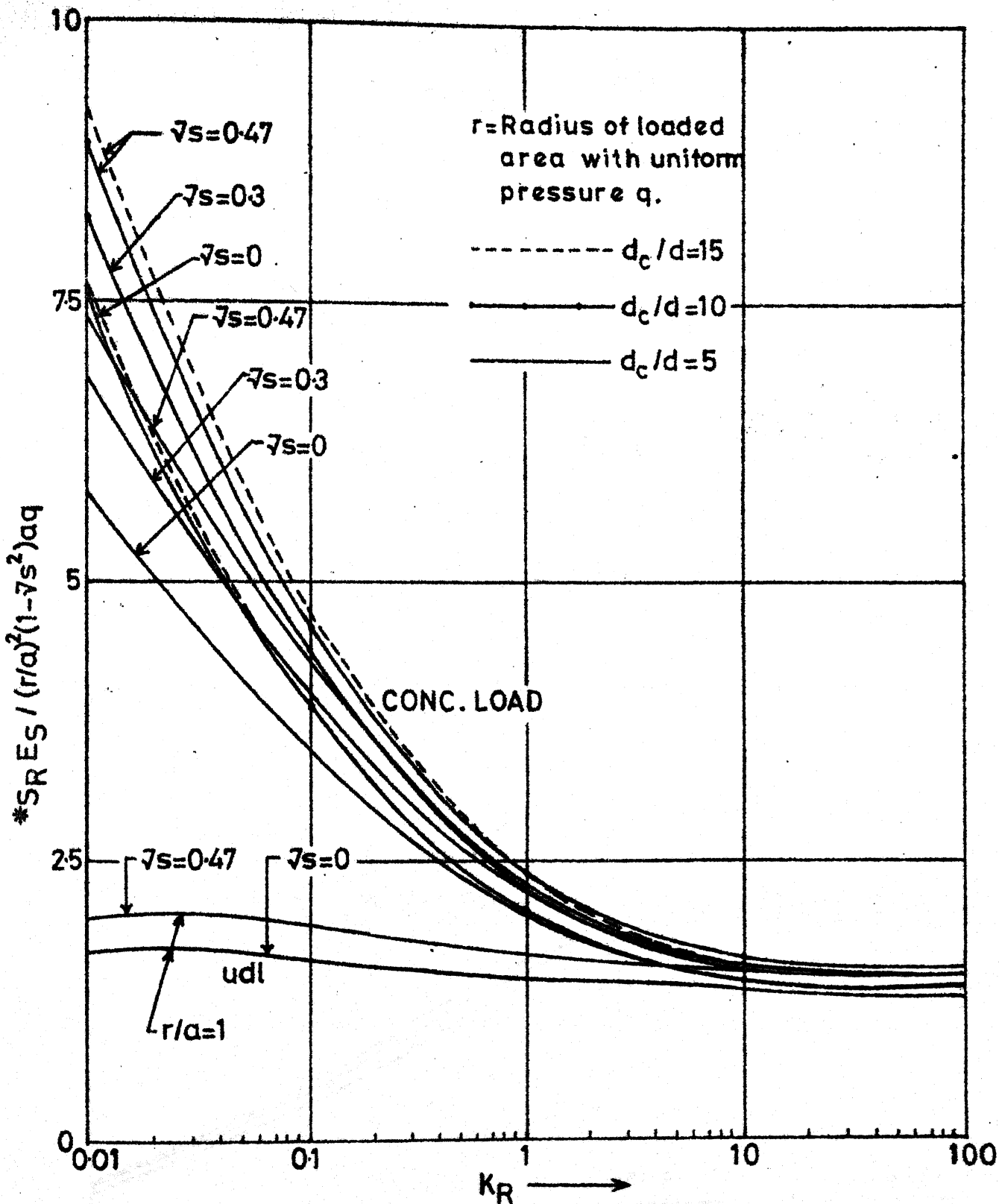
Fig.A·5   Raft Settlement Vs K_R
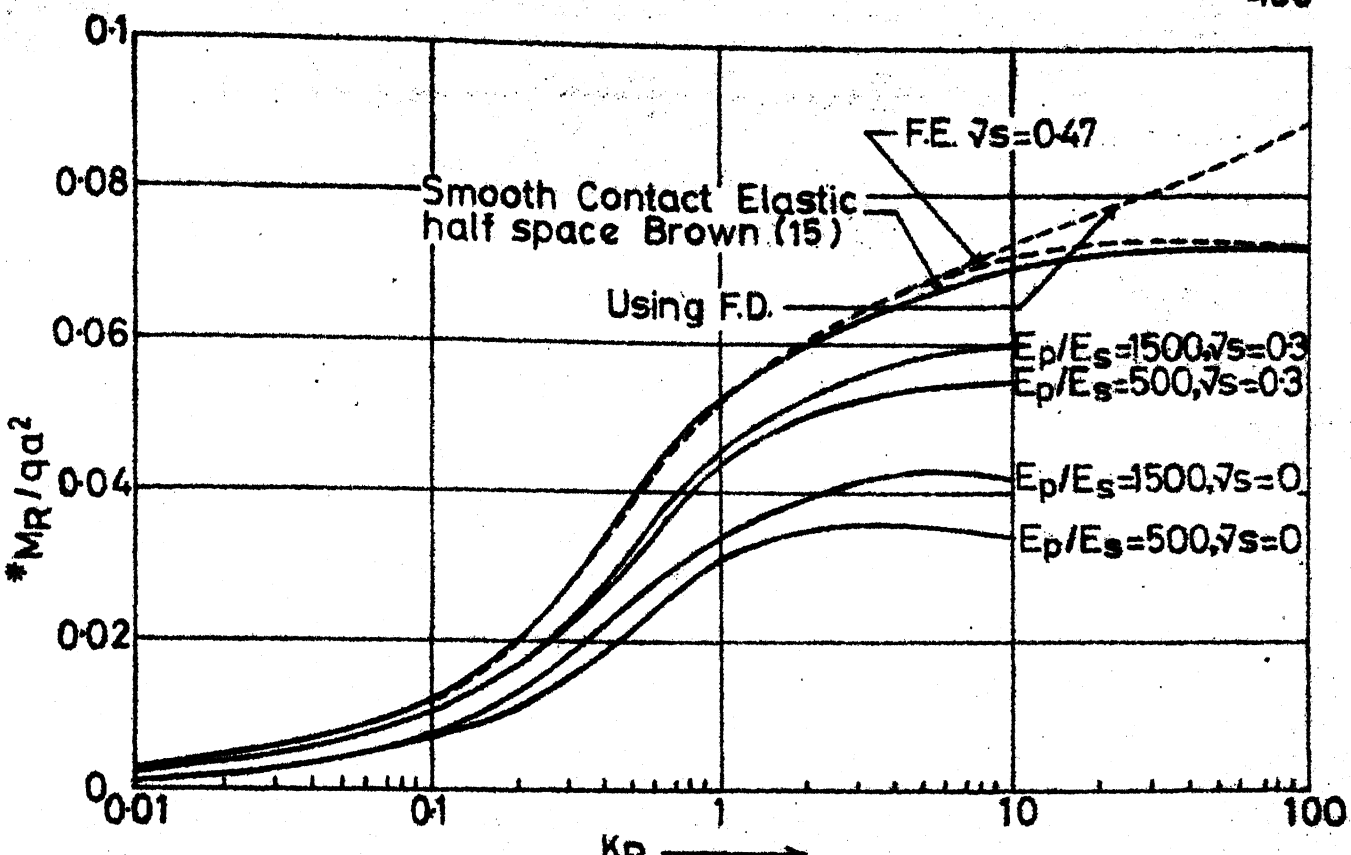
Fig.A·6 Raft Bending Moment (udl) Vs K_R

a – Radius of footing

r – Radius of loaded area with uniform pressure q.

M* – Maximum bending moment
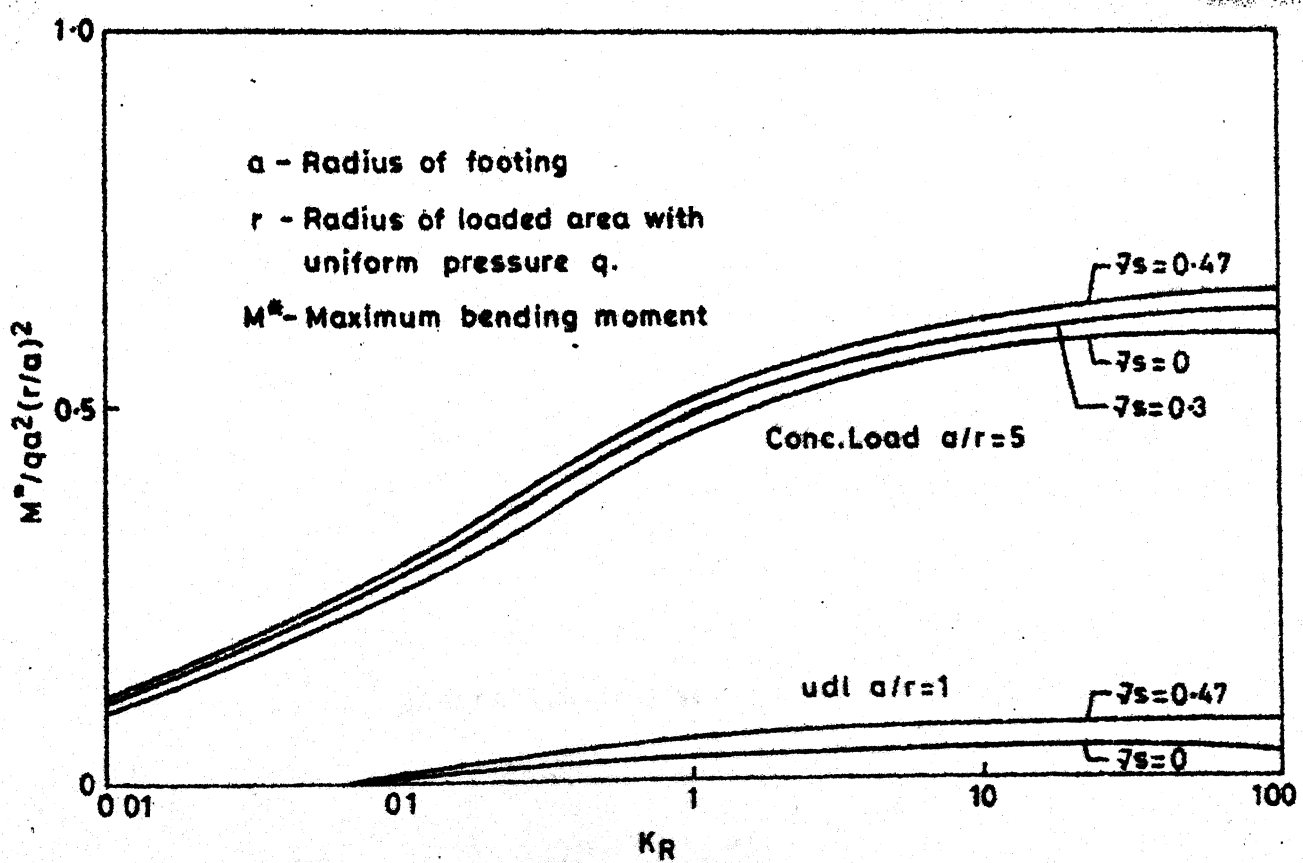
Fig.A7 Bending moment Vs K_R

SOME STUDIES ON EIGHT NODED ISOPARAMETRIC ELEMENTS IN BENDING

B.1 INTRODUCTION

Since eight noded isoparametric elements in axisymmetrical form have been used to represent the footing or raft in most of the work reported in this thesis, a study has been carried out to asses their performance in bending. Different types of loading, that footing may be subjected to in the problems solved in Chapters 2, 3, 4 and 6, have been considered. The range of aspect ratios within which these elements, give satisfactory results is investigated, considering a simple problem of a circular plate supported at the edge. The effect of mesh refinement in the footing portion in a piled circular footing is also studied.

B.2 ANALYSIS OF CIRCULAR PLATE

A circular plate is discretised in three different ways as shown in Fig. B.1a (Meshes 1T, 2T and 3T). Different types of loading considered have also been shown. The results obtained using mesh 1T and 2T, with one layer of elements representing the plate, are given in Table B.1. Different ratios of thickness to radius of plate (t/a), have been used, ranging from 0.02 to 0.4. These are the range of values of t/a that has been used in most of the work reported in other chapters. Discretisation as shown in Fig. B.1a, gives

rise to different aspect ratios (vertical dimension (1)/ horizontal dimension (b)), as given in Table B.1. These are the range of aspect ratios used for piled circular footing, pile-raft systems and raft problems. The values of maximum deflection and maximum radial bending moment computed, for Load case 1 (udl) and Load case 2 (concentrated load) are given in Table B.1. The calculated values using thin plate theory (Timoshenko et al (131)) are also given for comparison. For thick plates only values of bending moments are compared. It can be observed that the agreement is good, except for very thin plate ($t/a = 0.02$), when aspect ratio is 1/10 and very thick plate. The difference is less than 2 % in all cases except those underlined. Even in underlined cases the difference in bending moment is less than 6 % . Comparison of settlement and bending moment for the same t/a with different aspect ratios, also reveals that there is very good agreement except for $t/a = 0.02$ and 0.4, as previously observed. In these cases of t/a also, the agreement is satisfactory for concentrated load (difference less than 6 %). The settlement of piled circular footing and circular footing are less sensitive to plate stiffness for very thick or thin plate and so satisfactory results can be obtained even for cases with these aspect ratios. Since for $t/a = 0.4$ the results of settlement obtained with aspect ratio of 2/1

and 4/1, differ by about 12 %, further check using two layers of elements (Mesh 3T) was carried out and compared with results of settlement obtained using one layer of elements (Mesh 1T), in Fig. B.1(b). It can be observed that the agreement is close, showing that one layer of elements with aspect ratio 2/1 is adequate, for this value of t/a also, for both cases of loading. Hence it can be concluded that one row of about 5 elements with aspect ratio in the range of 1/5 to 2/1 may satisfactorily model the circular footing with normal value of t/a (0.02 to 0.4). For thin plates paralinear elements (Agarwala et al (1), Buragohain and Shah (21)) is as good or a better alternative.

Due to adhesive contact between footing and soil and elastic connections between footing and pile/superstructure, shear stresses are transmitted to the footing surface. To assess the adequacy of one layer of elements, under this loading, some results were taken with uniform shear stress over the entire plate surface (Load case 3 in Fig. B.1a) and shear stress and vertical stress over the central portion (Load case 4 - in Fig. B.1a). The values of bending moment obtained using one layer of elements (Mesh 2T) and two layers of elements (Mesh 3T), are compared in Fig. B.1(c). The results obtained using both the meshes almost coincide

showing that for shear loading also, one layer of elements
is adequate for getting satisfactory results. Good agreement
was observed in the case of displacements also.

B.3 ANALYSIS OF PILED CIRCULAR FOOTING

In the case of piled circular footing analysed in
Chapter 2, 3 and 4, adhesive elastic connections have been
assumed. To asses the adequacy of the meshes used in those
analyses, the effect of meshrefinement   was studied using
the 3 meshes shown in Fig. B.2(a). (Only portion of mesh
near footing is shown in the figure and the rest of the
portion is similar to Fig. A.1 in Appendix A). Mesh 1 PCF
and Mesh 3 PCF have been used in the analyses reported in
Chapter 3 and Chapter 2 respectively. Mesh 2 PCF is
similar to mesh 1 PCF, but with two layers of elements
representing the plate. The results of bending moment
obtained using these three meshes are compared in Fig. B.2(b)
(for udl) and Fig. B.2(c) (for concentrated load) for a
particular case of piled circular footing (details given
in Fig. B.2). It can be observed that there is very good
agreement between the values obtained using the three
meshes. It was observed that the values of bending moment
vertically above the pile differed upto about 7 %. The
values of maximum settlement and percent pile load computed

using these 3 meshes were found to agree very closely.
The computed values of differential settlement is shown in
Table B.2, for these 3 meshes. The agreement is good.
Hence it can be concluded that one layer of element as in
mesh 1 PCF or Mesh 2 PCF, is adequate. The results of bending
moment obtained using meshes 1 PCF and 3 PCF for another
case of piled circular footing are compared in Fig. B.3.
There is good agreement in this case also.

TABLE B.1 COMPARISON OF RESULTS - CIRCULAR PLATE

(Data as in Fig. B.1)

a - Load case 1 (udl)   q = 1   b - Load case 2 (concentrated load)

Thickness/ Radius t/a	Aspect ratio l/b (Fig.B.1)	$S^* E_p/200$ Max. deflection qa		M^*/qa^2 Max. bending moment (Radial)	
		Present analysis	Thin plate theory(131)	Present analysis	Thin plate Theory(131)
0.02	1/10	551.47[a]	512.80	0.2078	0.1970
		50.87[b]	47.84	0.0295	0.0284
	1/5	505.35	512.80	0.2021	0.1970
		47.21	47.84	0.0294	0.0284
0.04	1/5	63.92	64.10	0.1965	0.1970
		5.97	5.98	0.0286	0.0284
	1/2.5	63.75	64.10	0.1958	0.1970
		5.95	5.98	0.0284	0.0284
0.1	1/2	4.132	4.104	0.1970	0.1970
		0.387	0.383	0.0287	0.0284
	1/1	4.135	4.104	0.1969	0.1970
		0.387	0.383	0.0285	0.0284
0.2	1/1	0.5332	-	0.1973	0.1970
		0.0502	-	0.0290	0.0284
	2/1	0.5380	-	0.1972	0.1970
		0.0502	-	0.0287	0.0284
0.4	2/1	0.0837	-	0.1981	0.1970
		0.0073	-	0.0301	0.0284
	4/1	0.0936	-	0.1979	0.1970
		0.0076	-	0.0293	0.0284

TABLE B.2   COMPARISON OF DIFFERENTIAL SETTLEMENT

$$d_c/d = 5 \qquad L/d = 10 \qquad \nu_S = 0$$

$$K = 1500$$

K_R	MESH (Fig. B.2)		
	1 PCF	2 PCF	3 PCF
10	51.0^a	51.2	50.4
	12.7^b	12.8	12.7
1	214.5	214.4	213.7
	61.5	62.0	61.1

$$a - udl - \frac{\Delta E_S}{qa} \times 1000$$

$$b - conc.\ load - \frac{\Delta E_S}{qa} \times 10000.$$
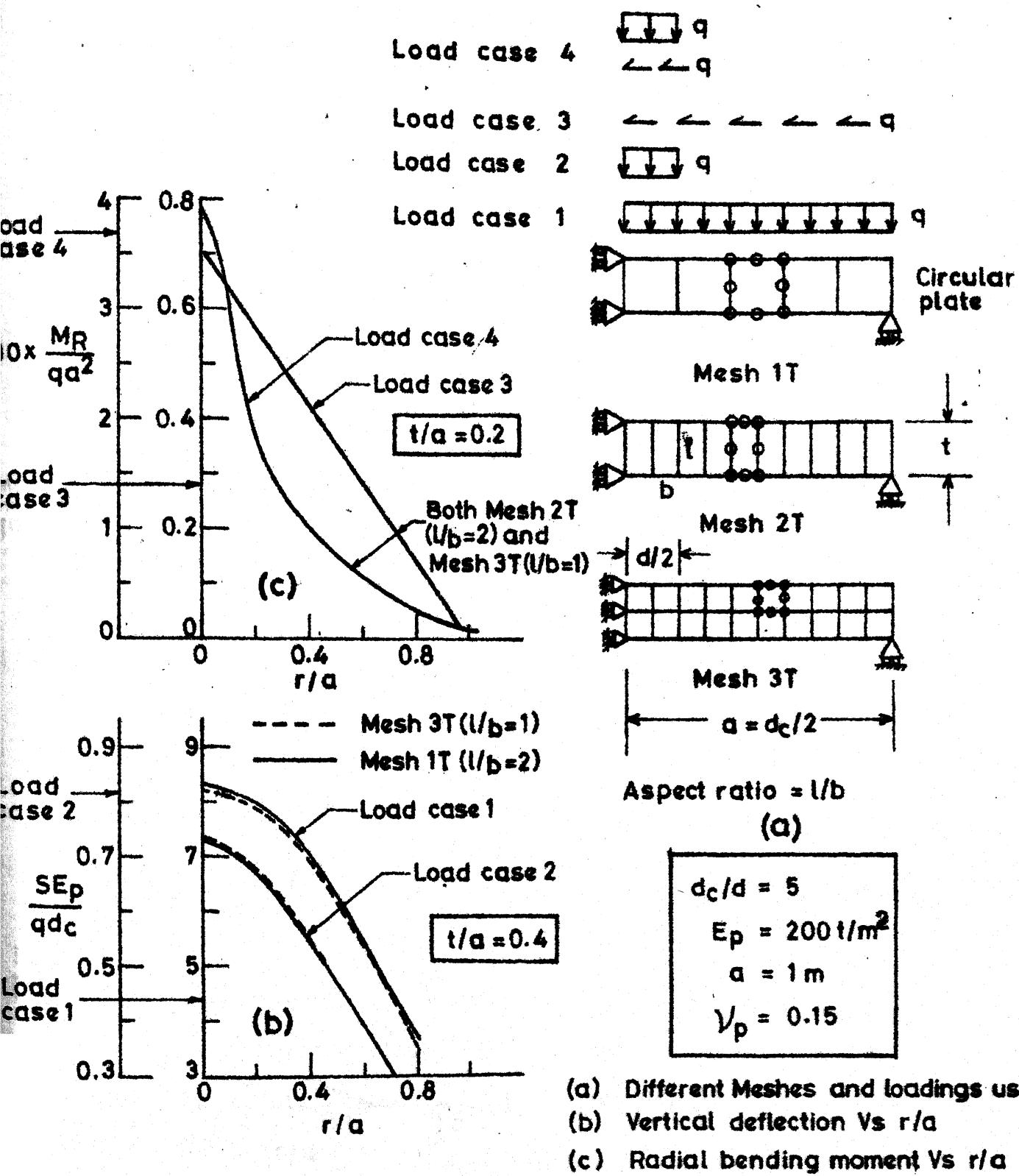
Fig. B.1 Circular plate supported at edge.

Fig. B.2   Comparison of meshes

Legend:
- ———— Mesh 1 PCF
- – – – – Mesh 2 PCF
- o o o Mesh 3 PCF

Graph (c): $\frac{M_R}{q a^2} \times 100$ vs r/a, labeled "Conc. load", with curves $K_R = 10$, $K_R = 1$, "both Mesh 1 PCF and Mesh 2 PCF"

Graph (b): $\frac{M_R}{q a^2}$ vs r/a, labeled "udl", with curves $K_R = 10$, $K_R = 1$, "both Mesh 1 PCF and Mesh 2 PCF"

Parameters box:
$d_c / d = 5$
$L/d = 10$
$\nu_S = 0$
$K = 1500$

(a) Meshes and loadings
(b) M_R Vs r/a (u.d.l.)
(c) M_R Vs r/a (conc. load)
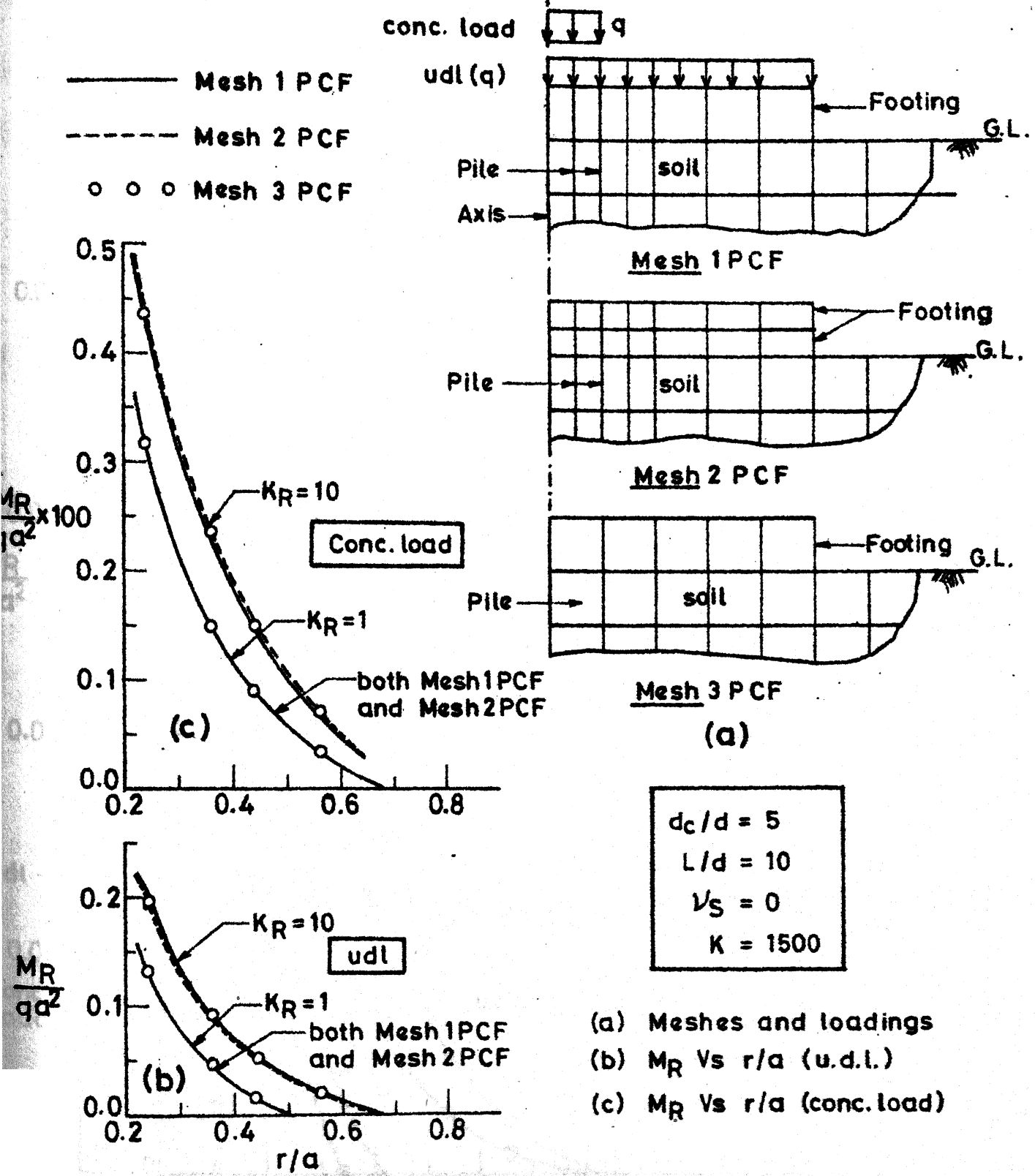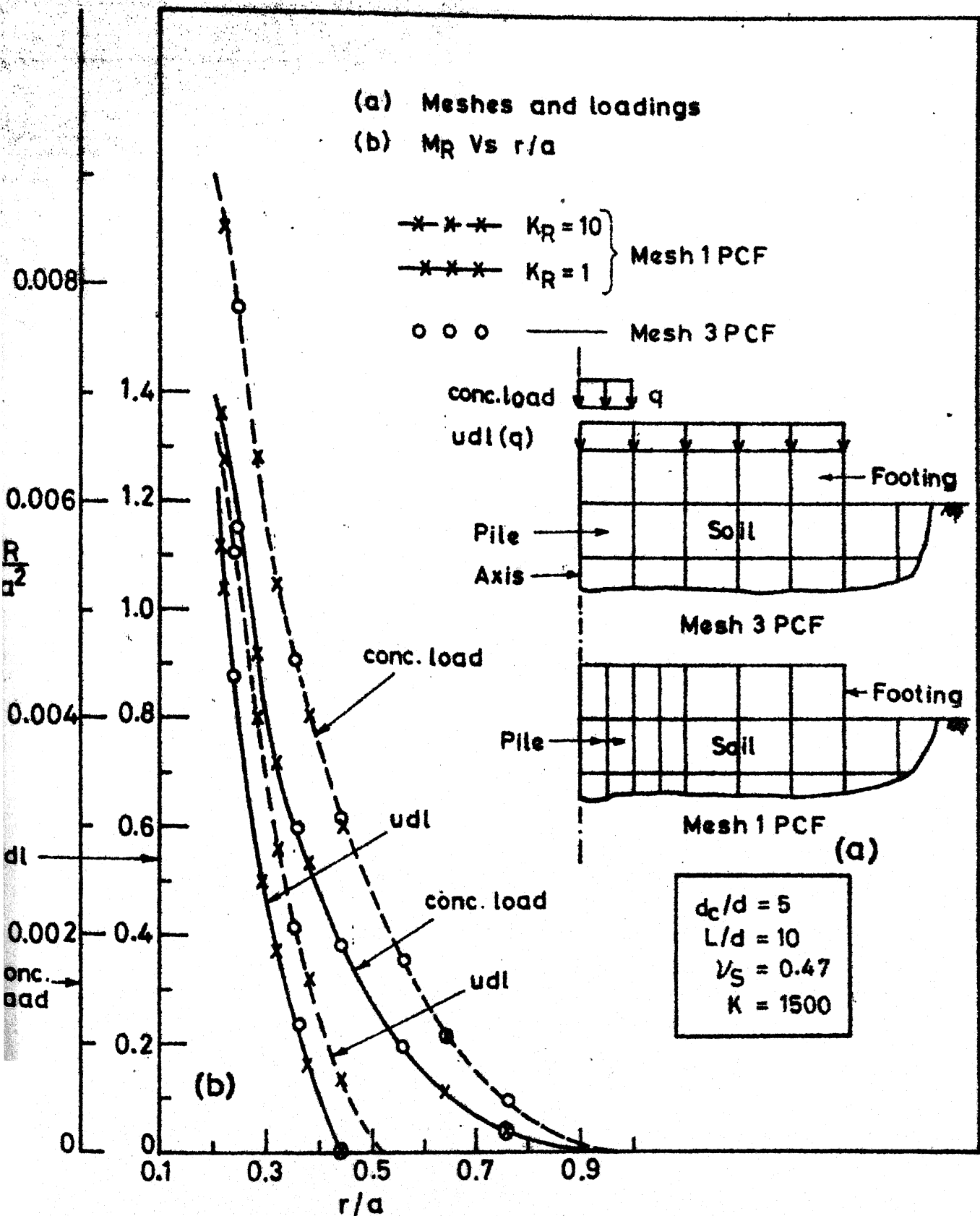
Fig. 8.3   Comparison of Meshes.

APPENDIX - C

PERFORMANCE OF SIX NODED INTERFACE ELEMENTS

C.1 INTRODUCTION

Some details of six noded interface element (Buragohain (20)) has already been discussed in Chapters 3 and 4. More details about this element and explicit expressions for the stiffness matrix for straight sided element, have been given by Vijayan (138). These expressions were checked and implemented in the computer program developed for elastic analysis and also in the computer program developed for elasto-plastic analysis, which have been used in Chapters 3 and 4 respectively, so as to model vertical or horizontal interfaces. In the elastic analysis reported in Chapter 3, this element has been used to model smooth contact between pile head and footing or smooth contact between footing base and soil, in a piled circular footing. In the elasto-plastic analysis, in addition to modelling smooth contact, this element has been used to permit slip or separation at any interface, where the stress exceeds the strength. In the elastic analysis normal stiffness (k_n) is to be assigned an arbitrary large value and shear stiffness (k_s) any arbitrary small value, to model smooth contact. In

elasto-plastic analysis both k_n and k_s have to be assigned
arbitrary large values initially and if at any load increment
stress at the interface exceed the strength, the correspond-
ing stiffness has to be reduced to an arbitrary low value to
permit slip or separation. If a lower (than appropriate)
value is assigned for k_n or k_s initially (excessive) seper-
ation or slip would occur, involving error in computed
quantities. If very high value is assigned for these
stiffnesses, numerical ill-conditioning and (or) excessive
round off error may arise. Hence arriving at appropriate
values of k_n and k_s for these elements requires a separate
study for any problem and for a given computer (Desai (46)).
Such a study has been carried out in this Appendix to asses
the performance of these elements and also to ascertain the
values of k_n and k_s which give satisfactory results, for
the parameters used in Chapters 3 and 4.

C.2 CASES CONSIDERED

Results of analysis using interface   elements can
be checked on the basis of some known results. For example
the computed values of settlement, bending moment, and
contact pressure must be almost same for smooth as well as
adhesive contact for Poisson's ratio   (ν_s) = 0.5, in the
case of a circular footing. The results of bending moment

and contact pressure for smooth contact must be independent
of the values of ν_s. When no such known results are avail-
able for example in the case of piled circular footing, the
following checks may be performed.

1.   The solutions obtained without interface elements
       must agree closely with those obtained with interface
       elements, simulating fully adhesive contact by using
       large value of k_n and k_s.

2.   The computed error from an equilibrium check (as
       detailed in Section 2.3) must be small.

3.   Another check is that the displacements of two
       nodes (with same coordinates) attached to both
       portions must agree to as many decimals as possible
       for adhesive contact.

       For performing the above checks the following cases
were considered.

       Mesh used is similar to Fig. A.1 in Appendix A, but
with two columns of elements (Fig. B.1a - Mesh 1PCF)
representing pile and slight modification in the horizontal
direction, keeping the boundaries same. The computation
procedure has been described in Appendix A.

Circular Footing:

Case 1   - Without using interface elements simulating
             a fully adhesive contact.

Case 2 - Using interface elements to simulate fully
adhesive contact. ($k_n = 10^7$, $k_s = 10^9$).

Case 3 - Using interface elements to simulate smooth
contact ($k_n = 10^7$, $k_s = 10^{-4}$).

Case 4 - Using interface elements to simulate smooth
contact ($k_n = 10^9$, $k_s = 10^{-4}$)

Piled Circular Footing:

Case 1 and 2, mentioned above were considered.
In Case 2, $k_n = 10^9$ and $k_n = 10^7$ were used for footing-pile
interface and for footing soil interface respectively.
$K_s = 10^9$ was used for all interface elements.

C.3 RESULTS AND DISCUSSION

The computed results of maximum settlement,
maximum bending moment and contact pressure near the
centre have been tabulatd for different cases considered
for circular footing in Table C.1. Checks as explained
earlier in Sec. C.2 are performed as follows.

It can be observed that the results for Case 1
and Case 2 agree very closely for both values of ν_s
and for all values of K_R considered. The valuesof k_n
and k_s were varied and it was found, with increasing

values of these stiffnesses, the error from equilibrium check increased. It can be observed that the results for Case 3 and Case 4 also agree well with results for Case 1 and Case 2, for $\nu_S = 0.47$. The difference in the values of bending moment is upto about 5 %, which may be due to the value $\nu_S = 0.47$ used instead of 0.5. The values of bending moment and contact pressures for cases $\nu_S = 0.47$ and $\nu_S = 0$ agree well for smooth contact (Case 3 and Case 4). It was found that the results for smooth contact was almost same when $k_S = 10^{-2}$ and 10^{-4} were used, showing that the results are not very sensitive to k_S, provided it is sufficiently low. (Since there is no problem of ill-conditioning/roundoff error in using low value, even zero can be used). Incidentally the computed quantities for smooth contact are in satisfactory agreement with the solutions given by Brown (15).

The results of percentage error computed for different cases have been tabulated in Table C.2. It can be observed that the error slightly increases when interface elements are used (comparing Case 1 with other Cases). In general, the error is less than 0.5 percent, except for $\nu_S = 0.47$ in case 4. This shows that

for $\nu_S = 0.47$, if $k_n = 10^9$ (Case 4) is used the error increases, which indicates ill-conditioning and (or) roundoff error.

In the case of piled circular footing the error was found to be still more if high value of k_n is used for $\nu_S = 0.47$. Hence for modelling smooth contact between footing and soil, $k_n = 10^7$ and $k_S = 10^{-4}$ was used for the analysis reported in Chapters 3 and 4.

The results obtained for Case 1 and Case 2 , for piled circular footing have been shown in Table C.3. It can be observed that the results for Case 1 and Case 2 are in good agreement showwing that the values of k_n and k_S used may give satisfactory results. The error from equilibrium check was found to be less than 0.5 % for all the case of piled circular footings considered in Chapters 3 and 4, using interface elements.

The displacements for nodes with same coordinates in the cases of adhesive contact agreed upto at least five decimals for the cases reported. If higher values of k_n or k_S are used the agreement was upto larger number of decimals but the error from equilibrium check increased.

C.4   CONCLUSIONS

Using six noded interface elements in conjunction
with solid elements the interface can be modelled satis-
factorily. The stresses adjacent to the interface
(as contact pressure and bending moment) can also be
obtained to acceptable accuracy.

The use of very high value of k_n or k_s increases the
round-off error and or illconditioning for values of ν_s
nearly equal to 0.5. The values of k_n and k_s that may
be used for getting satisfactory results ih the analysis
of piled circular footing, for the parameters and computer
used, have been indicated.

TABLE C.1 COMPARISON OF RESULTS USING 6 NODED INTERFACE ELEMENTS - CIRCULAR RAFT

$E_S = 200 t/m^2$, $d_c = 2 m$, $H/a = 32$, $E_p/E_S = 1500$,

$d_c/d = 5$ Free right hand side boundary

Loading	Description	Without joint element (fully adhesive)	With joint element $k_n=10^7$ $k_s = 10^9$ (fully adhesive)	With joint element $k_n = 10^7$ $k_s = 10^{-4}$ (smooth)	With joint element $k_n=10^9$ $k_s =10^{-4}$ (smooth)
		CASE 1	CASE 2	CASE 3	CASE 4
1	2	3	4	5	6
	Poisson's ratio of soil (ν_S) = 0.47				
u.d.l. (q)	Max. Settlement x 1000 (m)	5.94[a] 6.01[b] 6.55[c]	5.94 6.01 6.54	5.96 6.03 6.58	5.92 6.00 6.54
	Max. Bending moment x 100 (tm/m)	7.59 7.50 5.41	7.59 7.50 5.41	8.01 7.66 5.49	7.96 7.64 5.46
	Contact pressure near centre (t/m^2)	0.49 0.51 0.69	0.49 0.51 0.69	0.49 0.52 0.70	0.49 0.52 0.69
Concentrated load (udl q over circle dia. d at centre)	Max. Settlement x 10000 (m)	2.39 2.54 3.60	2.39 2.54 3.60	2.40 2.55 3.62	2.38 2.53 3.60
	Max. Bending moment x 100 (tm/m)	2.45 2.33 1.94	2.45 2.33 1.94	2.47 2.34 1.95	2.47 2.34 1.95

1	2	3	4	5	6
onc. load udl q over ircle dia. at centre)	Contact pressure near centre x 10 (t/m^2)	0.20 0.25 0.65	0.20 0.25 0.65	0.20 0.26 0.67	0.20 0.26 0.67

Poisson's Ratio of Soil (ν_S) = 0

1	2	3	4	5	6
udl (q)	Max. settlement x 1000 (m)	6.84 6.90 7.31	6.830 6.880 7.30	7.54 7.65 8.37	7.55 7.66 8.39
	Max. Bending Moment x 100 (tm/m)	2.66 4.53 4.00	2.63 4.52 4.00	8.25 7.91 5.63	8.20 7.87 5.62
	Contact pressure near centre (t/m^2)	0.53 0.55 0.69	0.53 0.55 0.69	0.49 0.51 0.70	0.49 0.51 0.70
Concentrated load (udl q over circle dia. d at centre)	Max. Settlement x 10000 (m)	2.76 2.91 3.58	2.75 2.90 3.59	3.04 3.23 4.62	3.04 3.24 4.62
	Max. bending moment x 100 (tm/m)	2.23 2.18 1.77	2.23 2.17 1.76	2.46 2.35 1.95	2.46 2.35 1.95
	Contact pressure near centre x 10 (t/m^2)	0.22 0.28 0.71	0.22 0.28 0.69	0.20 0.26 0.70	0.20 0.26 0.70

a - K_R = 100 b - K_R = 10 c - K_R = 1

TABLE C.2   RESULTS OF EQUILIBRIUM CHECK USING 6 NODED
INTERFACE ELEMENTS - CIRCULAR RAFT
(Data and Cases as in Table C.1)
Percentage error from equilibrium check

Loading	Case 1	Case 2	Case 3	Case 4
u.d.l. ($\nu_S = 0.47$)	0.06^a 0.07^b 0.10^c	0.10 0.09 0.20	0.15 0.13 0.21	0.79 0.64 0.82
Concentrated ($\nu_S = 0.47$)	0.06 0.07 0.12	0.10 0.10 0.22	0.15 0.13 0.22	0.79 0.65 0.87
u.d.l. ($\nu_S = 0$)	0.13 0.14 0.18	0.32 0.31 0.22	0.38 0.28 0.41	0.34 0.17 0.13
concentrated ($\nu_S = 0$)	0.13 0.14 0.19	0.32 0.32 0.23	0.38 0.29 0.46	0.34 0.18 0.18

a - $K_R = 100$ b - $K_R = 10$ c - $K_R = 1$

TABLE C.3   COMPARISON OF RESULTS - PILED CIRCULAR FOOTING

$d_c/d = 5$, $K_R = 100$ (Other data and cases as in Table C.1)

Description	u.d.l.		concentrated load	
	Case 1	Case 2	Case 1	Case 2
Max.Settlement x 1000 (m)	6.31^a 4.25^b	6.31 4.24	2.53 1.70	2.53 1.70
Max.footing bending moment x 100 (tm/m)	7.40 13.84	7.20 13.87	0.97 6.86	0.97 6.85
Percentage pile load	27.77 48.70	27.80 48.77	28.33 49.49	28.37 49.56

a - L/d = 2.5, $\nu_S = 0$ b - L/d = 10, $\nu_S = 0.47$

SOME STUDIES USING TRESCA AND DRUCKER-PRAGER YIELD CRITERIA IN ELASTO-PLASTIC ANALYSIS

D.1 INTRODUCTION

Elasto-plastic finite element analysis using von Mises yield criterion was discussed in Chapter 4. Some computer runs were made using Mohr- Coulomb and **Drucker** - Prager yield criterion also. The original computer programme developed for (Vijayan (138)) elasto-plastic analysis using Mohr-Coulomb yield criterion was modified to handle Drucker-Prager criterion also. The initial stress computation technique and other details of analysis, are same as those used in Chapter 4. The results obtained for smooth rigid circular footing ($K_R = 100$) subjected to central column loading are discussed here. The purpose of this Appendix is to present some difficulties met with in the conventional initial stress elasto-plastic finite element analysis, when Tresca criterion is used and also to compare the computing time for such analysis in the case of frictional soil with that in the case of purely cohesive soil.

D.2 DETAILS OF COMPUTER RUNS

Details of four computer runs, which are discussed herein, are given in Table D.1. All the runs pertain to

smooth rigid circular footing (K_R = 100) subjected to central column loading (concentrated loading). The smooth contact was simulated using interface elements. The mesh used for these analyses is Mesh 2RM (Fig. 4.2, Chapter 4). In all cases fully associated perfect plasticity has been assumed.

D.3 UNDRAINED ANALYSIS

The results of undrained analysis using Drucker-Prager yield criterion (Run D_1) is shown in Fig. D.1a. For $\emptyset$ = 0, Drucker-Prager yield criterion reduces to von Mises criterion. Hence the results are same as the results reported in Chapter 4, for von-Mises criterion (Fig. 4.8). This checks the program developed for Drucker-Prager criterion. It can be observed that the trend of the load settlement curve shows a collapse pressure of about 104 C_u, which is in satisfactory agreement with commonly used value (from Winter Corn and Fang (146)) which is 99.2 C_u, for the parameters used in the present work. The result obtained (Run D_2) using Tresca yield criterion is also shown in Fig. D.1a. It can be observed that for pressure greater than 96 C_u, the load-settlement curve rises almost linearly without indicating any collapse. The same trend was observed when Tresca criterion was used in the analysis of flexible circular

footing with u.d.l. and also in the analysis of piled circular footing. Similar difficulties have been reported by different authors and different remedial measures have been suggested by them, as follows.

1.   Davis and Booker (55), has reported that no collapse load could be obtained in the case of strip footing using Mohr-Coulomb (associated) criterion. They advocate checking the sign of the rate of plastic work and ensuring positive rate of work throughout. Rowe and Davis (123), have obtained satisfactory results in the case of circular footing incorporating the above checks. They have used quadrilaterals consisting of 4 constant strain triangles in their analysis.

2.   Toh and Sloan (132) could not obtain collapse load, using Tresca criterion and linear isoparametric quadrilaterals, by conventional displacement elasto-plastic formulation. They advocate mixed variational principle.

3.   Sloan and Randolph (127), have shown (based on the work of Nagtegaal et al (94)) theoretically that only 15 noded cubic strain triangle is to be used for getting satisfactory results for incompressible material loaded by circular footing and lower order

elements may not give realistic results. They have also shown that satisfactory results can be obtained by using such higher order elements, for Tresca material. However, they have mentioned that reduced integration in the case of other lower order elements like parabolic one may improve the results; but they have not made any studies on its effectiveness. The present analysis throws some light on the effectiveness of such reduced integration. In the present analysis, reduced integration (2 x 2 Gauss quadrature) was used. For von Mises criterion, the present analysis indicates the collapse load satisfactorily; but for Tresca material it has completely failed. So it appears that the type of yield surface has got some thing to do with the performance of these elements in elasto-plastic analysis and further work is required to study this aspect.

As stated above three completely different approaches are presented in the literature to overcome the difficulty in the case of Tresca material. Comparative merits require to be studied.

D.4 DRAINED ANALYSIS

The results of analysis using inner cone (Run D_3) and outer cone (Run D_4) of Drucker -Prager yield criterion

(Zienkievicz(149)) are shown in Fig. D.1b. The trend of the load-settlement curve is such that it may indicate collapse, had the load increment be continued. However, since the maximum number of iterations was specified as 600, the run got terminated at applied pressure of 288 Cu. For predicting collapse load satisfactorily it requires much more number of iterations than 600. It is of interest to compare Run D_3 and Run D_1. Run D_1 (undrained case) required maximum iterations of about 300 and CPU time of about 22 minutes and has predicted collapse load satisfactorily. Run D_3 (Drained case), with maximum iterations specified as 600, has consumed CPU time of about 50 minutes and it appears that it requires much more CPU time to satisfactorily predict collapse. Further, Run D_3 has been made with larger load increments than Run D_1. (Collapse has been approached in 13 equal increments in Run D_1 and 6 equal increments in Run D_3). It can be observed that when outer cone (Run D_4) of Drucker-Prager criterion is used, it appears that it may require more CPU time than analysis with inner cone (Run D_3), for predicting collapse satisfactorily. So, it can be concluded that drained analysis using yield criterion like Drucker-Prager's is substantially more expensive than undrained analysis, when elasto-plastic finite element technique is used. Modification of the

stiffness matrix after each load increment (Zienkiewicz(152))
and allowing limited number of iterations within each incre-
ment may improve the situation. However comparative cost
and accuracy of this approach requires to be studied.

TABLE D.1   DETAILS OF COMPUTER RUNS

Common data for all runs:

$d_c/d = 4$, unit wt. of soil = 0, $E_S/C_u = 400$, $K_R = 100$

Run No.	Yield Criterion	$\emptyset$	ν_S	Max. No. of iterations specified	No. of increments	CPU Time min.
D_1	Drucker-Prager (von Mises)	0	0.48	300	13	22
D_2	Mohr-Coulomb (Tresca)	0	0.48	300	20	–
D_3	Drucker-Prager Inner Cone	30°	0.30	600	6	49
D_4	Drucker-Prager Outer Cone	30°	0.30	300	14	50

No. of iterations ⟶ ②②②②

Outer cone

Drucker-Prager
$\phi = 30°$
$E_S/C_u = 400$
$\nu_S = 0.3$
$T = 0$

Inner cone
Outer cone

Mohr-coulomb

Inner cone

- Fails to converge after 300 iterations
- Fails to converge after 600 iterations

} Collapse load range

(b)

$S^* E_S / C_u d$

Tresca

Drucker-Prager ($\phi = 0$)
(von Mises)

$\nu_S = 0.48$
$T = 0$
$\phi = 0$

o Fails to converge after 300 iterations
⟶ Collapse load range
⇢ Becomes linear-no collapse load is indicated

(a)

$S^* E_S / C_u d$

Fig. D.1 Load-settlement curve (Tresca and Drucker-Prager criteria)

APPENDIX - E

BILINEAR INTERACTION FACTOR METHOD - COMPUTATION PROCEDURE

The load settlement relations with boundary conditions, for a pile-raft with a rigid cap can be written as

$$[I_{PR}] \{P_{PR}\} + [I_R] \{P_R\} = (1 \ 1 \dots \ 1)^T \ \delta_0 \qquad \text{(E.1)}$$
$$\underset{M\times M}{\ } \quad \underset{M\times 1}{\ } \quad \underset{M\times M}{\ } \quad \underset{M\times 1}{\ } \quad \underset{M\times 1}{\ }$$

$$(1 \ 1 \dots \ 1) \{P_{PR}\} + (1 \ 1 \dots \ 1) \{P_R\} = P \qquad \text{(E.2)}$$
$$\underset{1\times M}{\ } \quad \underset{M\times 1}{\ } \quad \underset{1\times M}{\ } \quad \underset{M\times 1}{\ }$$

where $[I_{PR}]$ = flexibility matrix of the system for pile-raft action

  $[I_R]$ = flexibility matrix for raft action.

  ($[I_{PR}]$ and $[I_R]$ can be generated using influence coefficients (factors) and interaction coefficients (factors) for pile-cap units and unpiled raft units respectively or from field data).

  $\{P_{PR}\}$ = loads transmitted by pile-raft action by different units.

  $\{P_R\}$ = loads transmitted by raft action by different units.
  δ_0 = settlement of rigid cap, P = total applied load,
  M = number of pile-cap units.

- -

$(1 \ 1 \dots \ 1)^T$ - unit column vector

$(1 \ 1 \dots \ 1)$ - unit row vector.

Initially the entire load is assumed to be transmitted by pile-raft action.

Hence Eqs. E.1 and E.2 become,

$$[I_{PR}] \; \{P_{PR}\} = (11 \; .... \; 1)^T \; \delta_0 \qquad (E.3)$$

$$(11 \; .... \; 1) \; \{P_{PR}\} = P \qquad (E.4)$$

From Eq. E.3

$$\{P_{PR}\} = [I_{PR}]^{-1} \; (11 \; .... \; 1)^T \; \delta_0 \qquad (E.5)$$

Multiplying Eq. E.5 by unit row vector and from Eq. E.4.

$$P = (111 \; .... \; 1) \; \{P_{PR}\} = (11 \; .... \; 1) \; [I_{PR}]^{-1} (11....1)^T \delta_0$$

$$\qquad\qquad (E.6)$$

STEP 1 : Eq. E.6 can be solved for δ_0. Substituting the value of δ_0 in Eq. E.5, $\{P_{PR}\}$ can be obtained. (This gives the results for linear analysis).

The limiting load on any unit (P_{max}^1) for pile-raft action is given by

$$P_{max}^1 = (UBC + \frac{UBC}{PPL} \times 100)/2 \qquad (E.7)$$

where

UBC = ultimate bearing capacity of single pile

PPL = percentage load shared by pile.

STEP 3 : Eq. E.11 can be solved for δ_O. The value of δ_O can be substituted in Eq. E.10 to obtain $\{P_U\}$. If any P_U corresponding to pile-raft action (i.e. the corresponding $P_K = 0$), exceeds P^1_{max} corresponding rows and columns of $[I_U]$ and $[I_K]$ are interchanged. The corresponding P_K is made equal to P^1_{max}. Step 3 is repeated till all values of P_U corresponsing to pile-raft action (i.e. the corresponding $P_K = 0$), do not exceed P^1_{max} in which case the final results are obtained.

DETAILS OF COMPUTER PROGRAM FOR ELASTO-PLASTIC ANALYSIS

The Program ELAPLA described in this Appendix is the modified version of original Computer Program developed at IIT, Kanpur (Vijayan (138)). The program can be used for axi-symmetrical elasto-plastic analysis using von Mises yield criterion. Eight noded quadratic isoparametric elements are used to discretise the different components of the system such as soil, footing and pile. Six noded interface elements model the interface behaviour. 'Initial stress' method has been used for the computation of the non-linear problem. Assembly and solution are performed in core.

Most of the computation steps are carried out in various sub-routines of the program as described below. Flow charts for MAIN, ASEMBL, STRESS and JOISTR are presented in Figs.F.1 to F.4.

MAIN   Reads and prints the title of the problem.

        Calls DATAIN, ASEMBL, CHOLES, STRESS and JOISTR

        Calls PRINTR to print final results. Checks for tension failure and if there is any tension failure makes JCOUNT = JCOUNT + 1 checks whether stiffness of

the system has reduced to the specified fraction of the original elastic stiffness.

DATAIN   Reads and prints maximum number of increments, maximum number of interations, convergence criterion, material type, material properties, interface data and surface traction data. It also generates and prints nodal point and element data.

ASEMBL   1.   Initialises global stiffness matrix, and total displacement vector.

         2.   Assembles load vector.

         3.   Calls ISO8PL and JOI6PL and assembles global stiffness matrix.

         4.   Calls GEOMBC

            For first increment and first iteration, it performs 1, 2, 3 and 4. If number of iteration is equal to 1, it performs 2.

If JCOUNT is not equal to 0 (i.e. there is inter-face or tension failure), it performs 3 and 4.
If JCOUNT is equal to 0 (i.e. there is no interface or tension failure), it performs 4.

ISO8PL Initialises element stiffness matrix and forms
        stress-strain matrix.
        Calls SHAPE to form elements of strain displacement
        matrix (B) and Jacobian determinant matrix and
        Jacobian determinant for all integration points
        in all elements and stores B matrix and determi-
        nant of Jacobian for all integration points in
        all elements.

JOI6PL calculates the element stiffness matrix for
        straight sided 6 noded interface elements.

SHAPE   calculates shape function, X and Y derivatives
        of shape function and determinant of Jacobian for
        8 noded elements.

GEOMBC applies prescribed boundary conditions at nodes.

JOISTR computes stresses at interfaces. Checks whether
        stresses exceed permissible value and if so,
        reduces corresponding joint stiffness to small
        value and makes JCOUNT = JCOUNT +1 . Prints
        stresses at interface, results of equilibrium
        check, percentage pile load, percentage tip
        load and percentage load transmitted by footing.

CHOLES   carries out triangularisation of the banded
symmetric matrix by Cholesky decomposition for
INCR = 1 and ITER = 1 and also if JCOUNT is not
equal to zero. Solves for displacements by back
substitution for all iterations.

STRESS   initialises the total stress and strain vector or
assigns initial stresses due to gravity loads.
Selects incremental nodal displacements and
calculates incremental strains and stresses (unless
there is any tension failure). Calculates yield
stress at integration points and checks for yielding
at these points. Calls ELPLAS if element has
yielded. Computes correction stress vector if
yielded and forms residual load vector.
Checks for convergence and calls PRINTR once solution
converges.

ELPLAS   calculates elasto-plastic matrix for the current
stress values at each integration point using
von Mises model.

PRINTR   prints load increment, number of iterations
performed, applied load, total and incremental
displacements at nodal points.

Prints co-ordinates of integration points,
condition of the point (elastic or plastic)and
stresses.

Calculates percentage load shared by pile if any
and bending moments and prints the same.
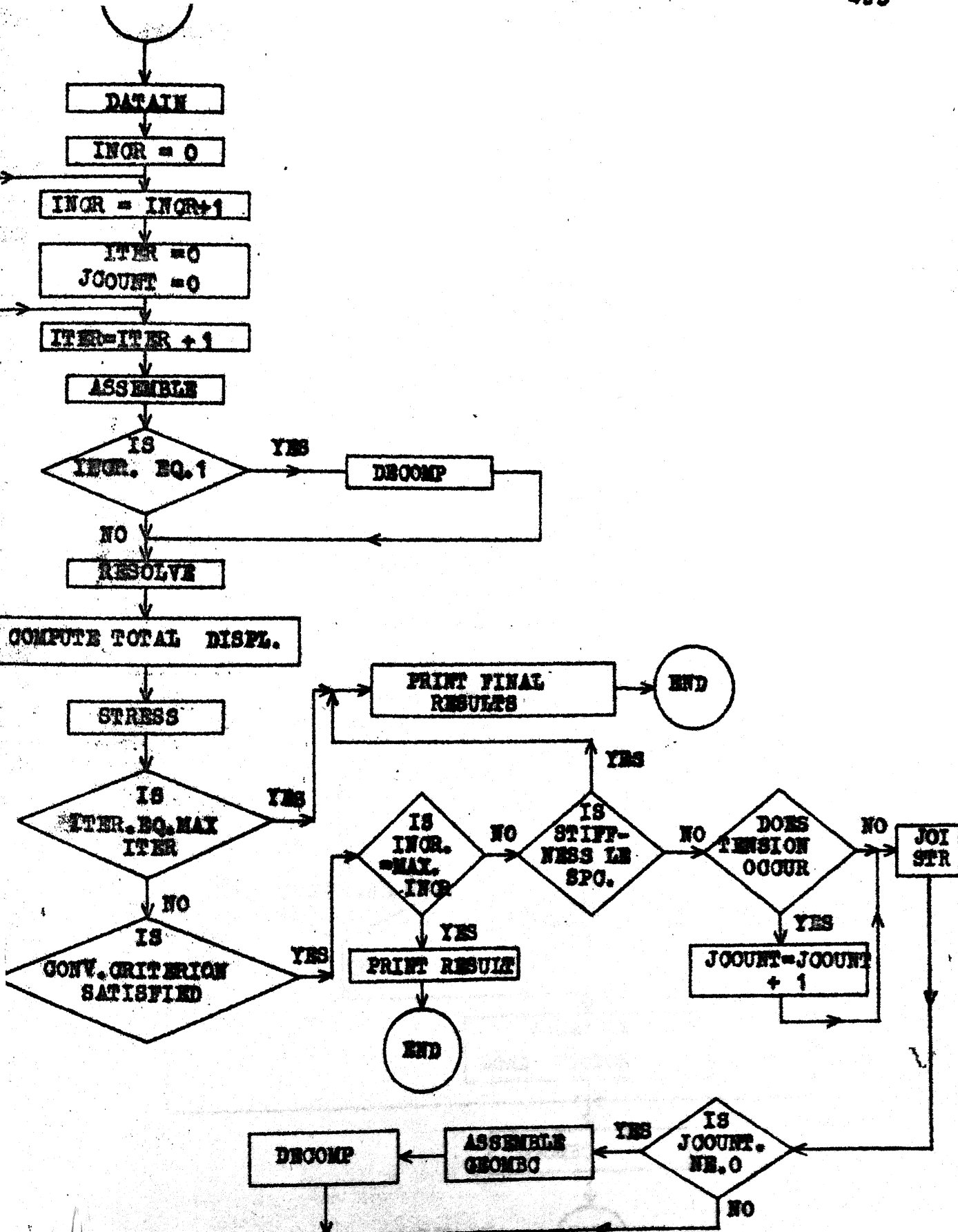
Fig. F.1   MAIN
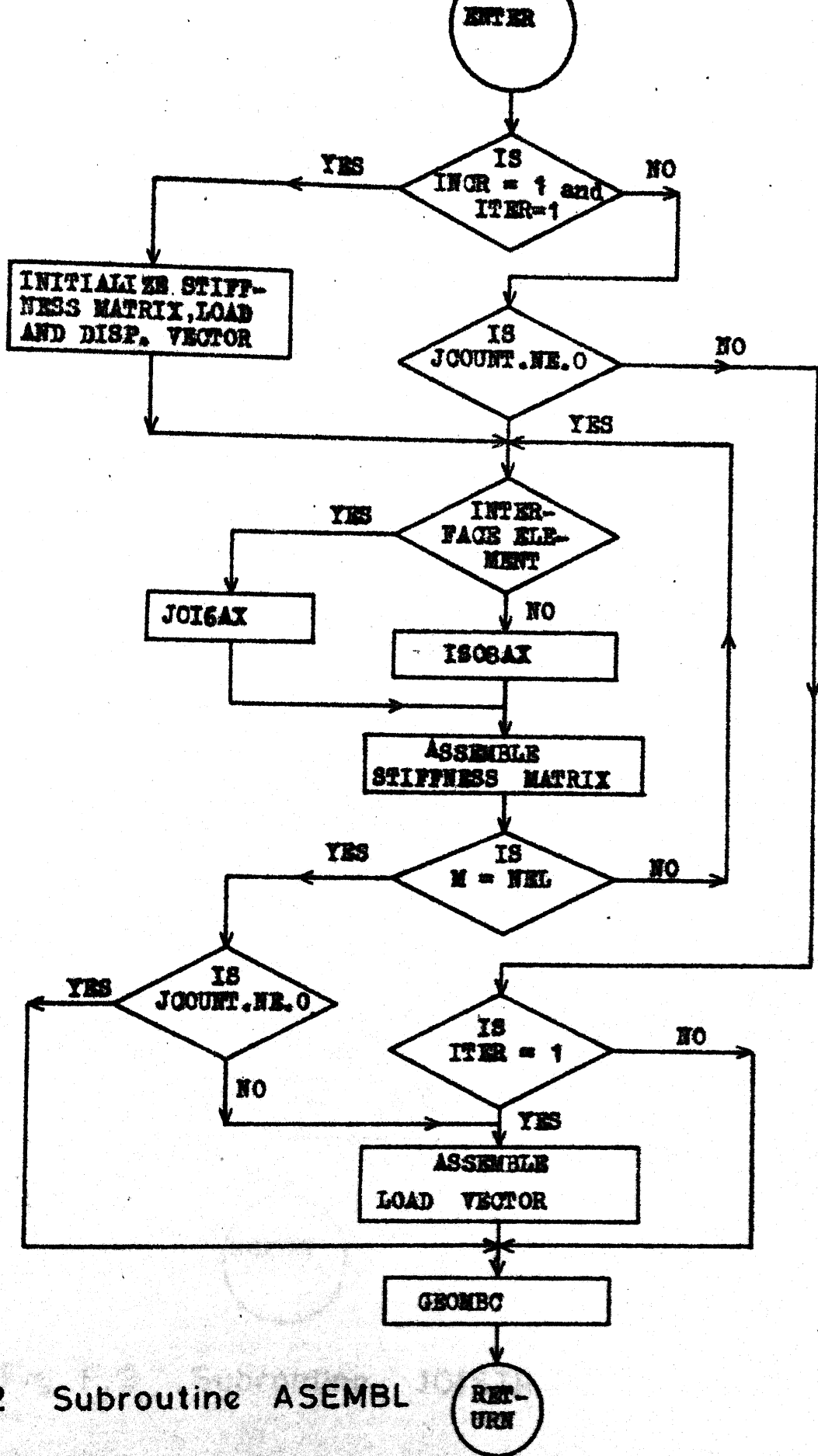
Fig. F.2 Subroutine ASEMBL
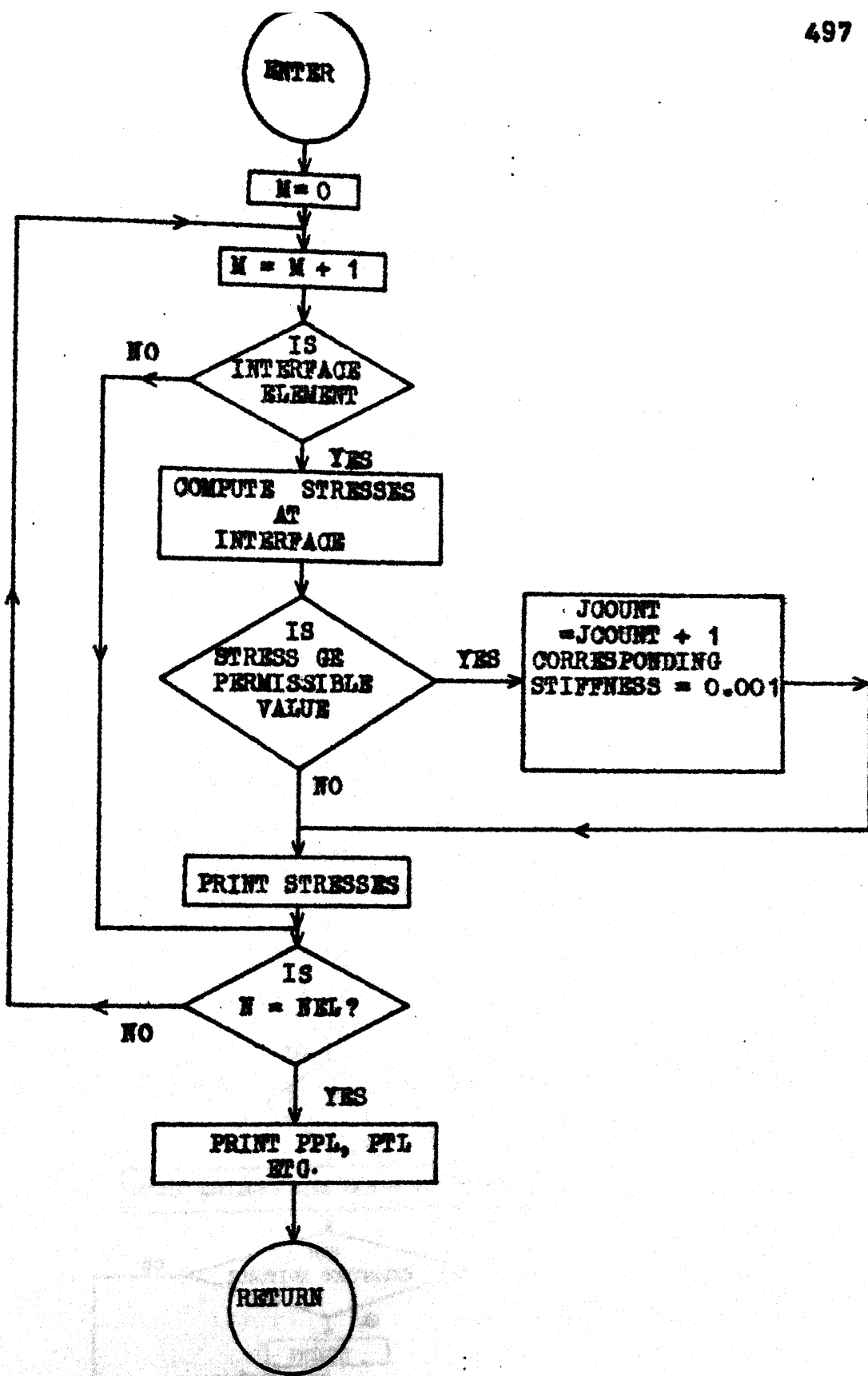
Fig. F.3   Subroutine   JOISTR

ENTER

INITIALISE TOTAL
STRESS AND STRAIN
VECTOR ← YES ← INCR=1
ITER=1

NO

COMPUTE INCREMENTAL STRAINS AND STRESSES AT INT. POINT

COMPUTE TOTAL STRAINS AND STRESSES AT INT. POINT

IS
THERE TENS-
ION FAILURE
?

YES

NO

COMPUTE YIELD STRESS AT INT. POINT

HAS
POINT YIELDED

NO

YES

ELPLAS

COMPUTE CORRECTION STRESSES
COMPUTE RESIDUAL LOAD VECTOR
ADD TO GLOBAL VECTOR

IP = 4 → NO

YES

M = NEL → NO

YES

CHECK RESIDUAL LOAD VECTOR FOR CONVER.

HAS
SOLUTION CONVERGED

NO

YES

PRINTR

RETURN

Fig. F. 4 Subroutine STRESS

APPENDIX-G

REFERENCES

1. Agarwala, S.K., Nayak, G.C., and Arya, A.S. (1979).
   Analysis for interacting thin and thick shell structures,
   Proc. of Int. Conf. on Computer Methods in Civil Engg.,
   Roorkee, India, pp. 147-150.

2. Akinmusuru, J.O. (1980). Interaction of piles and cap
   in piled footings, J. Geotech. Div., ASCE, pp. 1263-1268.

3. Arora, K.R. (1981). Soil-structure interaction analysis
   of the strip and circular footings on sand, Ph.D. Thesis,
   IIT, Delhi, India.

4. Awoshika, K. and Reese, L.C. (1977). Non-linear analysis
   of a foundation consisting of a group of pile, Proc. of
   9th Int. Nat. Conf. on S.M. and F.E., Tokyo, Spec. Sess.
   No. 12.

5. Balaam, N.P., Booker, J.R., Poulos, H.G. (1976).
   Analysis of granular pile behaviour using finite elements
   School of Civil Engg., Univ. of Sydney, Aust. Res. Rep.
   No. 295.

6. Balaam, N.P., Poulos, H.G. and Booker, J.R. (1974).
   Finite element analysis of the effects of installation
   on pile load-settlement behaviour, School of Civil Engg.,
   Univ. of Sydney, Res. Rep. No. 246.

7. Banerjee, P.K. (1978). Analysis of axially and laterally
   loaded pile groups, Developments in Soil Mechanics-1,
   Edited by Scott, C.R., Applied Science Publishers Ltd.,
   London, pp. 317-346.

8. Banerjee, P.K., and Butterfield, R. (1977). Boundary
   element methods in Geomechanics, Finite Elements in
   Geomechanics, Edited by Gudhes, John Willey and Sons,
   pp. 529-570.

9. Banerjee, P.K., and Davies, T.G. (1977). Analysis of
   pile groups embedded in Gibson soil, Proc. 9th Int. Conf.
   SMFE, Tokyo, pp. 381-386.

10. Banerjee, P.K. and Davies, T.G. (1979). Analysis of some reported case histories of laterally loaded pile groups, Instn. of Civil Engineers, Numerical Methods in Offshore Piling, ICE, London, pp. 83-90.

11. Bathe, K.J. and Wilson, E.L. (1978). Numerical methods in finite element analysis, Prentice Hall India Pvt. Ltd., New Delhi.

12. Biondi, P., Manufredini, S., Martinetti, R., Ribacehi, and Riccioni, R. (1976). Limit load of a foundation in a foundation in a strain softening soil, Num. Methods in Geomech., Edited by Desai, C.S., Published by ASCE, pp. 591-598.

13. Booker, J.R. and Small, J.C. (1981). The analysis of liquid storage tanks on deep elastic foundations, School of Civil Engg. and Mining Eng., Univ. of Sydney, Aust., Res. Rep. No. 403.

14. Bowles, J.E. (1977). Foundation analysis and design, McGraw-Hill Kogakusha, Ltd., (Second Edition), Tokyo.

15. Brown, P.T. (1969). Numerical analysis of uniformly loaded circular raft on deep elastic foundation, Geotechnique, 19, No. 3, pp. 399-404.

16. Brown, P.T. (1975). Settlement analysis of structural foundation systems, Proc. 2nd Australia - NZ Conf. Geomech., Brisbane, pp. 79-82.

17. Brown, P.T., Poulos, H.G. and Wiesner, T.J. (1976). Piled raft foundation design, School of Civil Engg., Univ. of Sydney, Aust., Res. Rep. No. R 299.

18. Brown, P.T., and Wiesner, T.J. (1975). Behaviour of uniformly loaded piled strip foundation, Soils and foundation, Vol. 15, No. 4, pp. 13-21.

19. Buragohain, D.N., Raghavan, N. and Chandrasekaran, V.S. (1977). Interaction of frames with pile foundations, Proc. Int. Symp. Soil, Struct. Interaction, Roorkee, India, pp. 237-243.

20. Buragohain, D.N. and Shah, V.L. (1977). Curved Interface elements for interaction problems, Proc. of Int. Symp. on soil struct. Interaction, Roorkee, India, pp. 197-201.

21. Buragohain, D.N. and Shah, V.L. (1979). 3-D interactive finite element analysis of foundation structures, Proc. of Int. Conf. on Computer applications in Civil Engg., Roorkee, India, pp. 275-284.

22. Burland, J.B. and Cooke, R.W. (1974). The design of bored piles in stiff clay, Ground Engg., 7(4), 28-30, pp. 33-35.

23. Butterfield, R., and Banerjee, P.K. (1971). The problem of pile group and pile cap interaction, Geotechnique, Vol. 21, No.2, pp. 135-142.

24. Butterfield, R. and Banerjee, P.K. (1971). The elastic analysis of compressible piles and pile groups, Geotechnique, Vol. 21, No.1, pp. 43-60.

25. Butterfield, R. and Ghosh, N., (1980). A linear elastic interpretation of model tests on single piles and group of piles in clay, Institution of Civil Engineers. Numerical methods in Offshore Piling, London, pp.109-118.

26. Chamecki, S. (1956). Structural rigidity in calculating settlements, Jl. S.M. and F. Div., ASCE, 82, SM1,pp.1-19.

27. Chang, C.Y. and Duncan, J.M. (1970). Analysis of soil movements around a deep excavation, J.S.M. and F. Div., ASCE, 96, SM-5, pp. 1655-82.

28. Chaw, Y.K. and Smith, I.M. (1982). Static/dynamic analysis of an axially loaded pile, Proc. of Int. Conf. on N.M. in Geomechanics, Edmonton, Canada, Vol.2, pp. 819-824.

29. Chen, W.F. (1975). Limit analysis and soil plasticity, Developments in Geotech. Eng. Vol.7 Elsevier Scientific Publishing Co., Newyark, pp. 333-340.

30. Christian, J.T. and Desai, C.S. (1977). Constitutive laws for geologic media, Numerical Methods in Geotechnical Engg., Edited by Desai, C.S. and Christian, J.T., McGraw-Hill Book Company, pp. 66-115.

31. Christian, J.T., Hagmann, A.J. and Marr, W.A. (1977). Incremental Plasticity analysis of frictional soil, Int. J. Num. Maths. in Geomechanics, Vol.4, pp.343-375.

32. Christian Meyer (1975). Special problems related to linear equation solvers, Jl. of Struct. Div., ASCE, pp. 869-890.

33. Clough, G.W. and Duncan, J.M. (1971). Finite element analysis of retaining wall behaviour, J.S.M. and F. Div., ASCE, Vol. 97, SM-12, pp. 1657-1673.

34. Cooke, R.W. (1975). The settlement of friction pile foundations, B.R.E., U.K., Current paper, CP 12/75.

35. Cooke, R.W. (1978). The design of piled foundations, Developments in soil mechanics-1, Edited by Scott, C.R., Associated Science Publishers Ltd., London, pp. 275-315.

36. Cooke, R.W., Prince and Tarr, (1979). Jacked piles in London clay a study of load transfer and settlement under working conditions, Geotechnique, 29,(2), pp.113-147.

37. Cooke, R.W., Price, G. and Tarr, K. (1980). Jacked pile in London clay interaction and group behaviour under working conditions, Geotechnique, 30, pp.97-136.

38. Cooke, R.W., Smith, Cooch and Sillet (1981). Some observations of the foundation loading and settlement of multi-storeyed building on a pile-raft foundation in London clay, Proc. of Instn. of Engrs., London, August.

39. Dunlop, P. and Duncan, J.M. (1970). Development of failure around excavated slopes, J.S.M. and F. Div., ASCE, Vol. 96, pp. 471-493.

40. Duncan, J.M. and Clough, G.W. (1971). Finite element analysis of Port Allen Lock, J.S.M. and F. Div., ASCE Vol. 97, SM 8, pp. 1053-1068.

41. Duncan, J.M. and Chang, C.Y. (1970). Nonlinear analysis of stress and strain in soils, J.S.M. and F. Div., ASCE, Vol. 96 No. SM5, pp.1629-1653.

42. Desai, C.S. and Reese, L.C. (1970). Analysis of circular footings on layered soils, J.S.M. and F. Div., ASCE, 96, SM 4, pp. 1289-1310.

43. Desai, C.S., Phan, H.V. and Sture, S. (1981). Procedure, selection and application of plasticity models for a soil, Int. Jl. for Num. Anl. Methods in Geomechanics, pp.295-312.

44. Desai, C.S., Johnson, L.D. and Hargett, C.M. (1974). Analysis of pile-supported gravity lock, J.Geotech. Eng. Div., ASCE, Vol.100, No.GT 9, pp.1009-1029.

45. Desai, C.S. and Abel, J.F. (1972). Introduction to the finite element method - A numerical method for engineering analysis.(East-West Edition) Affiliated East-West Press Pvt. Ltd., New Delhi.

46. Desai, C.S. (1981). Behaviour of interfaces between structural and geologic media, Int. Nat. Conf. on Recent Advances in Geotechnical Earthquake Eng. and Soil Dynamics, St. Louis, MO, Vol.II, pp.619-638.

47. Desai, C.S. (1978). Effect of driving and subsequent consolidation on behaviour of driven piles, Int. Jl. for Num. and Anl. Methods in Geomechanics, pp. 283-301.

48. Desai, C.S. (1977). Soil structure interaction and simulation problems, Finite Elements in Geomechanics, Edited by Gudhes, G., John Wiley and Sons, pp.209-250.

49. Desai, C.S. (1974). Numerical design analysis of piles in sands, J. Geotech., Div., ASCE. Vol.100. GT 6, pp. 613-635.

50. Desai, C.S. (1971). Non-linear analysis using spline functions, J. S.M.F. Div., ASCE, Vol. 98, No. SM9, pp. 967-971.

51. DeMellow, V.B.F. (1969). Foundations of buildings in clay, State of the Art Volume, Proc. 7th Int. Conf. Soil Mech. Found. Engg., Mexico, pp. 49-136.

52. D'Appolonia, D.J., Poulos, H.G. and Ladd, C.C. (1971). Initial settlement of structures on clay, Jl. of S.M. and F. Div., ASCE, Vol. 97, SM10, pp. 1359-1377.

53. Das, S.C. and Gangopadhyay, C.R. (1978), Undrained stresses and deformations under footings, J.Geotech. Div., ASCE, Vol. 104, No.GT1, pp. 11-25.

54. Davidson, H.L. and Chen, W.F. (1977). Non-linear response of undrained clay to footings, Computers and Structures, Vol.7, pp. 539-546.

55. Davis, E.H. and Booker, J.R. (1974). The significance of the rate of plastic work in elasto-plastic analysis, School of Civil Engg., Univ. of Sydney, Aust., Res. Rep. No. R 242.

56. Davis, E.H. and Poulos, H.G. (1969). The analysis and design of pile-raft systems, School of Civil Eng., Univ. of Sydney, Aust., Res. Rep. No. R122.

57. Davis, E.H. and Poulos, H.G. (1972). The analysis of pile-raft systems, Aust. Geomechanics Jl., Vol. G2, No.1, pp. 21-27.

58. Ellison, R.D., D'Appolonia and Theirs (1971). Load deformation mechanism of bored piles, J.S.M. and F. Div., ASCE, Vol. 97, SM 4, pp. 661-677.

59. Fernandez, R.M. and Christian, J.T. (1971). Finite element analysis of large strains in soils, NASA Research Report, R71-37.

60. Frank, R., Guenot, A. and Humbert, P. (1982). Numerical analysis of contacts in Geomechanics, Proc. of Int. Conf. on Num. Methods in Geomechanics, Edmonton, Canada, Vol. 1, pp. 37-46.

61. Gazetas, G., (1981). Variational estimation of the settlement of a circular raft on anisotropic soil, Soils and foundation, Vol. 21, No.4, pp.654-660.

62. Gazetas, G. (1982). Stresses and displacements in cross anisotropic soils, J. Geotech., Engg. Div., ASCE, Vol. 108, No. GT4, pp. 532-533.

63. Gerrard, C.M. and Harrison, W.J. (1970). Circular loads applied to a cross-anisotropic half-space, C.S.I.R.O. Aust. Div. App. Geomech. Tech. Pap. No. 8.

64. Girijavallaban, C.V. and Reese, L.C. (1968). FEM for problems in soil mechanics, J.S.M. and F. Div. ASCE, Vol. 94, SM 2, pp. 473-496.

65. Goodman, R.E., Taylor, R.L. and Brekke, T.L. (1968). A model for the mechanics of jointed rocks, J.S.M.F. Div., ASCE, Vol. 94, No. SM3, pp. 637-659.

66. Griffiths, D.V. (1982). Computation of bearing capacity in layered soil, Proc. of 4th Int. Conf. on Num.Methods in Geomechanics, Edmonton, Canada, Vol. 1, pp.163-170.

67. Hagmann, A.J. (1971). Prediction of stresses and strains under drained loading conditions, M.I.T., Mass., Dept. of Civil Engg., Report, R71-3.

68. Hain, S.J. and Lee, I.K. (1978). The analysis of flexible raft-pile systems, Geotechnique, 28, No.1, pp. 65-83.

69. Hoeg, K. (1972). Finite element analysis of strain softening clay, J.S.M.F. Div., ASCE, Vol.98, No.SM1, pp. 43-58.

70. Hoeg, K., Christian, J.T. and Whitman, R.V. (1968). Settlement of strip load on elastic-plastic soil, J.S.M.F. Div., ASCE, Vol. 94, No.SM2, pp.431-445.

71. Honglandaromp, T., Chen, N. and Lee, S. (1973). Load distribution in rectangular footings on piles, Geotechnical Engrg., 4, No.2, pp. 77-90.

72. Hooper, J.A. (1973). Observations on the behaviour of a piled-raft foundation on London clay, Proc. of Instn. of Engineers, London, Vol. 55, pp. 855-877.

73. Hooper, J.A. (1974). Analysis of a circular raft in adhesive contact with a thick elastic layer, Geotechnique, 24, No.4, pp. 561-580.

74. Hooper, J.A. (1975). Elastic settlement of a circular raft in adhesive contact with a transversely isotropic medium, Geotechnique, 25(4), pp. 691-711.

75. Hooper, J.A., (1978). Foundation interaction analysis, Developments in soil mechanics 1, Edited by Scott, C.R., Associated Science Publishers Ltd., London, 149-211.

76. Karmarkar, R.S. (1982). Settlement analysis of annular footings, Ph.D. Thesis, IIT Kanpur, India.

77. King, G.J.W. and Chandrasekaran, V.S. (1975). An assessment of interaction between a structure and its foundation, Settlement of Structures, Pentech Press, London, pp. 368-383.

78. King, G.J.W. and Chandrasekaran, V.S. (1977). Interactive analysis using a simplified soil model, Proc. of Int. Symp. Soil Struct. Interaction, Roorkee, India, pp. 93-99.

79. Knabe, W. (1976). Model test on piled foundations(Polish), Rozprawy Hydrotechnizne, pp. 75-131.

80. Knabe, W. (1977). Interaction of a soil medium and a piled foundation (Polish), Arch. Hydrotech., 38, pp.3-64.

81. Kondner, R.L. (1963). Hyperbolic stress-strain response, Cohesive soils, J.S.M. and F. Div., ASCE, Vol. 89, No.SM1, pp. 115-143.

82. Kulhawy, F.H. Duncan, J.M. and Seed, H.B. (1972). Stresses and movements in Oroville dam, J.S.M. and F.Div., ASCE, Vol. 98, SM-7, pp. 653-665.

83. Law, K.T. (1982). Numerical analysis of pile loading and pulling tests, Proc. 4th Int. Conf. on Num. Methods in Geomechanics, Edmonton, Canada, Vol.2, pp.825-834.

84. Lee, I.K. (1975). Structure-foundation-supporting soil interaction analysis, Soil Mechanics-Recent Developments, Edited by Valliappan, S., Hain, S. and Lee, I.K., pp. 255-294.

85. Lee, I.K. and Brown, P.T. (1972). Structure-foundation interaction analysis, J.Struct. Div., ASCE, Vol. 98, ST 11, pp. 2413-2431.

86. Lee, I.K. and Harrison, H.B. (1970). Structure and foundation interaction theory, J. Struct. Div., ASCE, Vol. 96, ST2, pp. 177-197.

87. Majid, K.I. and Cunnell, M.D. (1976). A theoretical and experimental investigation into soil-structure interaction, Geotechnique, 26, (2), pp.331-350.

88. Marti, J. and Cundall, P. (1982). Mixed discretization Procedure for accurate modelling of plastic collapse, Int. Jl. for Num and Anl. Methods in Geomech., pp.129-141.

89. Matsumoto, T. and Ko, H.Y. (1982). Finite element analysis of strain softening clay, Proc. of 4th Int. Conf. on Num. Methods in Geomechanics, Edmonton, Canada, Vol.1, pp. 213-222.

90. Meyerhof, G.G. (1947). The settlement analysis of building frames, Struct. Engr. 25(9), pp. 369-409.

91. Meyerhof, G.G. (1959). Compaction of sands and bearing capacity of piles, Jl. S.M. and F. Div., ASCE, Vol. 88, SM 6, pp. 1-29.

92. Meyerhof, G.G. (1976). Bearing capacity and settlement of pile foundations, J.Geotech. Engg. Div., ASCE, 102, GT 3, pp. 195-228.

93. Mitchell, J.K. and Gardner, W.S. (1971). Analysis of load bearing fills over soft soils, J.S.M. and F. Div., ASCE, Vol. 97, SM-11, pp. 1549-1572.

94. Nagtegaal, J.C., Parks, D.M. and Rice, J.R. (1974). On numerically accurate finite element solutions in the fully plastic range, Computer Methods in App. Mech. and Eng., 4, pp. 153-177.

95. Nayak, G.C. and Zienkiewicz, O.C. (1972). Elasto-plastic stress analysis - A generalisation for various constitutive relations including strain softening. Int. J. Num. Methods in Engg., Vol. 5, pp. 669-685.

96. Nayak, G.C. and Zienkiewicz, O.C. (1972). Convenient forms of stress invariants for plasticity, J. Struct. Div., ASCE Vol. 98, pp. 949-954.

97. O'Neill, M.W., Ghazzaly, O.I., and Ha., H.B. (1977). Analysis of 3-dimensional pile groups with non-linear soil response and pile-soil-pile interaction, Proc. of 9th Offshore Tech. Conf., Vol. 2, pp. 245-256.

98. Ottaviani, M., (1975). Three dimensional finite element analysis of vertically loaded pile group, Geotechnique, 25, pp. 159-174.

99. Ottaviani, M. and Marchetti, (1979). Observed and predicted test pile behaviour, Int. J. Num. and Anl. Methods in Geomechanics, April-June, pp. 131-144.

100. Ozawa, Y. and Duncan, J.M. (1976). Elasto-plastic finite element analyses of sand deformations, Numerical Methods in Geomechanics, Edited by Desai, C.S., ASCE Publication, Vol. 1, pp. 243-263.

101. Palk, J. and Naborczyk, T. (1977). Bearing Capacity of piles with the spot footing, Proc. of 9th Int. Nat. Conf. on S.M. and F.E., Tokyo, pp. 683-686.

102. Paramasivam, V. (1974). Finite element analysis of axi-symmetric plates, Int. Conf. on FEM in Eng., C I T., Coimbatore, India, pp. 198-213.

103. Pardoen, G.C. (1973). Static, Vibration and buckling analysis of axi-symmetric circular plates using finite elements, Computer and Structures, Vol.3, pp.355-375.

104. Pande, G.N. and Sharma, K.G. (1979). A Non-linear Elastic/Visco plastic model by a two stage time stepping scheme, Proc. 3rd Int. Conf. on Num. Methods in Geomechanics, Aachen, pp.59-66.

105. Pande, G.N. and Sharma, K.G. (1979). On joint/interface elements and associated problems of numerical ill conditioning, Int. J. Num. Anl. Methods in Geomechanics, pp. 293-300.

106. Poulos, H.G. (1968). The influence of a rigid cap on the settlement behaviour of an axially loaded pile, Civil Engg. Trans. Instn. of Engrs., Aust. Vol. CE 10, No. 2, pp. 206-208.

107. Poulos, H.G. (1968). Analysis of the settlement of pile groups, Geotechnique, 18, (4), pp. 449-471.

108. Poulos, H.G. (1976). Estimation of pile group settlements, School of Civil Engg., Univ. of Sydney, Aust., Res. Rep. No. R 288.

109. Poulos, H.G. (1979). Group factors for pile deflection estimation, School of Civil Engg., Univ. of Sydney, Aust., Res. Rep. No. 351.

110. Poulos, H.G. and Davis E.H. (1974). Elastic solutions for soil and rock mechanics, John Wiley and Sons.

111. Poulos, H.G., and Davis, E.H. (1980). Pile foundation analysis and design, John Wiley and Sons, Series in Geotechnical Engg.

112. Przemienicki, J.S. (1968). Theory of matrix structural analysis, McGraw-Hill Kogakusha Ltd.

113. Randolph, M.F. and Wroth, C.P. (1978). Analysis of deformation of vertically loaded piles, J. Geotech. Div., ASCE, pp. 1465-1485.

114. Randolph, M.F., and Wroth, C.P. (1979). An analysis of the vertical deformation of pile groups, Geotechnique, 29, pp. 423-439.

115. Rao, N.B.S. (1982). Studies on empirical modelling of Soil behaviour, Ph.D. Thesis, IIT Kanpur, India.

116. Reese, L.C., O'Neill, M.W., and Smith (1970). Generalized analysis of pile foundation, J.S.M.F. Div., ASCE, Vol. 96, SM 1, pp. 235-251.

117. Roscoe, K.H. (1970). The influence of strains in soil mechanics, Tenth Rankine Lecture, Geotechnique, Vol. 20, No.2, pp. 129-170.

118. Roscoe, K.H., and Burland, J.B. (1968). On the genera-lised stress strain behaviour of 'wet' clay, Engineering Plasticity, Cambridge Univ. Press, London, pp. 535-609.

119. Roscoe, K.H., Schofield, A.N., and Thurairajah, A. (1963). Yielding of clays in states wetter than critical, Geotechnique, Vol. 13, No.3, pp. 211-240.

120. Roscoe, K.H., Schofield, A.N., and Wroth, C.P.(1958).
On the yielding of soils, Geotechnique, Vol.8, No.1,
pp. 22-53.

121. Rowe, P.K., Booker, J.R. and Balaam, N.P. (1978).
Application of initial stress method to soil structure
interaction, Int. J. for Num. Methods in Engg., Vol.12,
pp. 873-882.

122. Rowe, R.K., Booker, J.R. and Small, J.C. (1982).
The influence of soil non-homogeneity upon the perfor-
mance of liquid storage tanks, Proc. of 4th Int. Conf.
on Num. Methods in Geomechanics, Edmonton, Canada,
pp. 757-766.

123. Rowe, R.K. and Davis, E.H. (1977). Application of the
finite element method to the prediction of collapse
loads, School of Civil Engg., Univ. of Sydney, Aust.,
Res. Rep. No. R 310.

124. Schofield, A., and Wroth, C.P. (1968). Critical state
soil mechanics, McGraw Hill, New Yark.

125. Singh, K.K., Prakash, A, and Jain, O.P. (1979). Finite
element analysis of intze tanks, Proc. Int. Conf. on
Computer Applications in Civil Engg., Roorkee, India,
pp. 239-244.

126. Skempton, A.W. (1959). Cast in situ bored piles in
London clay, Geotechnique, 9, No. 4, pp. 153-173.

127. Sloan, S.W. and Randolph, M.F. (1982). Numerical
predictions of collapse loads using finite element
methods, Int. Jl. for Num. and An. Methods in
Geomechanics, Vol. 6, No.1, pp. 47-76.

128. Smith, I.M. (1970). A finite element approach to elastic
soil structure interaction, Canadian Geotech., Jl., Vol.7,
No.2, pp. 95-105.

129.   Sture, S. and Ko, H.Y. (1976).   Stress analysis of
       Strain softening clay,   Num. Methods in Geomechanics,
       Edited by Desai, C.S. Published by ASCE, Vol. 1,
       pp. 580-590.

130.   Swamisaran, Pande, G.N. and Zienkiewicz, O.C. (1977).
       Shallow foundation problems, Int. Symp. on Soil Struct.
       Interaction, Roorkee, India, pp. 223-230.

131.   Timoshenko, S.P. and Kriegar, S.W. (1959).   Theory of
       Plates and Shells, McGraw-Hill Kogakusha Ltd., pp.51-62.

132.   Toh, C.T. and Sloan, S.W. (1980).   Finite element analysis
       of isotropic and anisotropic cohesive soil with a view
       to correctly predict collapse load,   Int. J. for Num.
       and An. Methods in Geomech., Jan.-March, pp. 1-23.

133.   Valliappan, S. (1975).   Application of finite element
       method to soil deformation, Soil Mechanics Recent
       Development Edited by Valliappan, Hain and Lee,
       Unisearch Ltd. Aust., pp.113-142.

134.   Varadarajan, A. and Arora, K.R. (1979).   An interactive
       study of strip footing sand bed system, Proc. Third Int.
       Conf. on Num. Methods in Geomechanics, Aachen, Germany,
       pp. 1041-1051.

135.   Varadarajan, A. and Arora, K.R. (1982).   Interaction
       of circular footing sand bed system, Proc. of 4th Int.
       Conf. on Num. Methods in Geomechanics, Edmonton, Canada,
       Vol. 2, pp. 945-953.

136.   Varadarajan, A. and Singh, R.B., (1982).   Analysis of
       tunnels by coupling FEM and BEM, Proc. of 4th Int.Conf.on
       Num. Methods in Geomechanics, Edmonton, Canada, Edited
       by Eisenstein, Vol.2, pp. 611-618.

137.   Varadarajan, A. and Yudhbir (1975).   Analysis of active
       earth pressure problems by FEM, J. Geotech. Div., ASCE,
       Vol. 101, GT 7, pp. 601-614.

138. Vijayan, C. (1981). Finite element analysis of strip and circular plate anchors. Ph.D. Thesis, Dept. of Civil Engg., IIT Kanpur, India.

139. Wardle, L.J. (1977). A computer program for the analysis of multiple complex circular loads on layered anisotropic media. User's manual CSIRO-Div. Appl. Geomech. Program Circly. Geomech. Computer Program No.2.

140. Wardle, L.J. and Fraser, R.A. (1975). Methods for raft foundation design, including soil-structure interaction, Proc. Symp. Raft Foun. Perth, Aust., pp.1-11.

141. Ward, W.H., Samuels, S.G. and Butter, M.E.(1959). Further studies on the properties of London clay, Geotechnique, 9, No.2, pp. 33-58.

142. Wiberg, N.E. (1982). Soil structure interaction in plane frame stability analysis, Proc. of 4th Int. Conf. on N.M. in Geomechanics, Edmonton, Canada, pp.781-786.

143. Wiesner, T.J. and Brown, P.T. (1975). Behaviour of piled strip footing subjected to concentrated loads, Civil Engg. Deptt., Univ. of Sydney, Aust., Res. Rep. No. R 275.

144. Wiesner, T.G. and Brown, P.T. (1980), Laboratory tests on model piled-raft foundations, J. Geotech. Eng. Div. ASCE, July, pp. 767-788.

145. Wilson, E.L., Bathe, Kaus-Jurgen and Doherty, W.P. (1974). Direct solution of large system of linear equations, Computer and Structures, Vol.4, pp.363-372.

146. Winter Corn, H.F. and Fang, H.Y. (1975). Foundation Engineering Hand Book, Van Nostrand Reinhold Company.

147. Withiam, J.L. and Kulawy, E.H. (1979). Analytical model for drilled shaft foundation, Proc. 3rd Int. Conf. on Num. Methods in Geomechanics, Aachen, Vol.2, pp. 1115-1122.

148. Yudhbir, Jain, K.K. and Rao, N.B.S. (1981), 'Path dependent constitutive laws for soft clays', Proc. of of Symp., Implementation of Computer Procedures and Stress-strain Laws in Geotech. Engg., New York.

149. Zienkiewicz, O.C. and Humpheson, C. (1977). Viscoplasticity: A generalized model for description of soil behaviour, Numerical Methods in Geomechanics, Edited by Desai and Christian, McGraw Hill Co., pp.116-147.

150. Zienkiewicz, O.C., Humpheson, C., and Lewis, R.W. (1977). A unified approach to soil mechanics problems (including plasticity and visco-plasticity). Finite elements in Geomechanics, Edited by Gudhes, G., John Wiley and Sons, pp. 151-178.

151. Zienkiewicz, O.C., and Naylor, D.J. (1972). The adoption of critical state soil mechanics for use in finite elements, Proc. Roscoe memorial Symp., Cambridge, pp. 537-547.

152. Zienkiewicz, O.C. (1977). The finite element method, (The third, expanded and revised edition), Tata McGraw-Hill Publishing Co. Ltd., New Delhi.

153. Zienkiewicz, O.C., Valliappan, S., and King, I.P. (1969). Elasto-plastic solutions of engineering problems-'initial stress' finite element approach, Int. J. of Num. Math. in Engg., Vol.1, 1969, pp. 75-100.

154. Randolph, M.F. (1981). The response of flexible piles to lateral loading, Geotechnique, 31, pp. 247-259.

Following papers have been published from part of the work reported in Chapter 2 (homogeneous soil condition) and Appendix A.

1. 'A condensation procedure for finite element analysis', Proceeding of the 4th International Conference on Numerical Methods in Geomechanics, Vol. 1, Edmonton, Canada, May - June 1982, pp. 87-92.

2. 'Finite element analysis of piled circular footings', Proceeding of the 4th International Conference on Numerical methods in Geomechanics, Vol. 2, Edmonton, Canada, May-June 1982, pp. 843-852.